Ramesh S. Chaughule
Rajesh Dashaputra *Editors*

Advances in Dental Implantology using Nanomaterials and Allied Technology Applications

Springer

Advances in Dental Implantology using Nanomaterials and Allied Technology Applications

Ramesh S. Chaughule • Rajesh Dashaputra
Editors

Advances in Dental Implantology using Nanomaterials and Allied Technology Applications

Springer

Editors
Ramesh S. Chaughule
Department of Chemistry
Ramnarain Ruia Autonomous College
Matunga, Mumbai, India

Rajesh Dashaputra
Department of Dentistry
Bhabha Atomic Research Center Hospital
Mumbai, India

ISBN 978-3-030-52206-3 ISBN 978-3-030-52207-0 (eBook)
https://doi.org/10.1007/978-3-030-52207-0

This Springer imprint is published by the registered company Springer Nature Switzerland AG
The registered company address is: Gewerbestrasse 11, 6330 Cham, Switzerland

Foreword

I am glad to write a foreword for this book "Advances in Dental Implantology using Nanomaterials and Allied Technology Applications" to be published by Springer, USA, that focuses on the use of nanotechnology in dentistry and particularly in the field of implants. This book, edited by Drs. Ramesh S. Chaughule and Rajesh Dashaputra, presents a collection of topics from eminent authors across the globe on the use of nanobiomaterials for implantology and their clinical applications.

Nanotechnology is a new field that has enormous scope in the dental science. One can make use of it in understanding and achieving cell-specific functions. Nanoscale surface morphology augments the surface area and thus provides an increased implant surface area that can react to the biologic environment. The composition of dental implants, surface energy, and roughness and topography can be improved for better osseointegration, and cellular activities and tissue responses occurring at the bone–implant interface can be altered by nanoscale modifications and can result in better treatment outcomes.

Nanosurface modification changes chemical as well as biological interactions of the implant, due to changed implant surface interaction with ions, biomolecules, and cells. This change in interactions in turn favorably influences molecular and cellular activities, leading to altered osseointegration. Numerous methods have been tried to enhance the osteointegration property by promoting the attachment, proliferation, and differentiation of bone-forming cells on the implant surface. Graphene and their products may provide excellent coating strategies for dental implants to improve osteointegration. Nanotechnology offers therapeutic methods for esthetic dentistry. Teeth that undergo treatment, such as fillings or crowns, will be restored with natural biological materials in a manner that is indistinguishable from natural dentition.

In recent years, there have been numerous publications appearing in the nanotechnology in dentistry. Developments in clinical applications are likely to accelerate in future. All the authors led by Dr. Chaughule should be congratulated to present a comprehensive and timely book to produce a useful and comprehensive text on nanobiomaterials and their clinical applications in dental implants.

C. N. R. Rao
Jawaharlal Nehru Centre for Advanced Scientific Research
Bangalore, India

Foreword

I am delighted to be asked to write a foreword for the second book in dentistry 'Advances in Dental Implantology Using Nanomaterials and Allied Technology Applications' to be published by Springer, USA.

Endo-osseous dental implants have revolutionised how clinicians manage patients with failing dentitions. Patient demand has driven the need for shorter treatment times necessitating quicker healing and rapid reconstructions leading to a search for newer technologies. Whilst a number of textbooks have been written, there are very few bringing together the application of nanotechnology across the field of implantology. This book builds on the concepts of nanotechnology, already covered in the first book 'Dental Applications of Nanotechnology' published by Springer, and its impact on the provision of dental implant treatment. The authors, led by Dr. Chaughule, have done an excellent job in succinctly putting together ways in which nanotechnology can influence and has influenced the provision of implant treatment from surgery to prosthetic reconstruction and post-treatment biological complications. The second section on 'Applications' of such new technologies in the field of implantology gives this book a unique feature by bringing science and technology into clinical application.

The book is aimed at experienced clinicians and those new to dental implantology as well as students, researchers and scientists. It is well written and structured making it easy for the reader to follow the difficult notions at the nano level as applied to implantology. In my 20 years of experience in implantology, this is a much needed book which provides useful and relevant content to readers and can serve as a general textbook or a reference book. I commend the efforts of the authors in producing this comprehensive book, which closes an important gap in an ever-changing field.

Ulpee Darbar
Eastman Dental Hospital & Institute
London, UK
Royal College of Surgeons, Edinburgh
Edinburgh, UK

Foreword

As a clinician fascinated by scientific backgrounds and as a passionate reader from early childhood on, I always feel excited when I open a new book. This one over exceeded my expectations.

There are books that have more footnotes and references than text, which is great help for a small group of researchers, but the majority of clinicians would close the book as quickly as a flash. Then there are books in dentistry that look more like picture books: nice to turn pages, but nothing to underline. And finally, there are books like this one: valuable information, a good read, text parts to be underlined, literature references inviting for further study and images from clinical work excellently illustrating the topics at hand.

The editors of the book, "Advances in Dental Implantology using Nanomaterials and Allied Technology Applications", Professor Ramesh S. Chaughule and Dr. Rajesh Dashaputra, together with many prestigious contributors across the globe, collected research and clinic in the best way possible. This provides us with comprehensive information on the expanding fields of nanotechnology as well as the latest developments in materials science, engineering and technology applied in dentistry. This book is quite essential to valuable research and a natural sequel to their numerous published papers and the book: "Dental Applications of Nanotechnology".

It is the unique combination of clinician-researcher-teacher-mentor-author-speaker features with IT understanding, which enables one to write such a comprehensive work.

Nanotechnology and its application in dentistry are hot topics. This book covers aspects ranging from research to the clinic, providing a complete framework and knowledge base. Nanotechnologies are increasingly used for surface modifications of dental implants. This book explains why nanometer-controlled implant surfaces may ultimately direct the nature of peri-implant tissues and improve their clinical success rate.

Students, researchers and clinicians who want to learn more about nanomaterial utilization in bone regeneration, prosthetic rehabilitation, biofilm and peri-implantitis control, bone grafting and tissue engineering will benefit from the solid footing in this compilation.

The second part of the book is the sum of accumulated knowledge about the newest developments in dentistry. And it is more than just an update. It provides an overview of the current state of knowledge, valuable clinical protocols for CAD/CAM technology, modelling and impressions in implants, printing in dentistry, maxillofacial reconstruction, 3D impressions in maxillofacial surgery and zygomatic implants. As an oral surgeon, periodontist and implantologist, I find this book to be a comprehensive professional reference that bridges the gap between fundamental materials science and medicine.

This book is laying the foundation for further publications that I am looking forward to read.

Snehjena Pohl
Department of Oral Medicine and Periodontology,
Medical Faculty,
University of Rijeka,
Rijeka, Croatia

Preface

The term nanotechnology is widely attributed to the American Nobel Laureate Dr. Richard Feynman. It is mainly concerned for the creation of functional materials, devices, and systems through control of matter in 1–100 nm length scale exploiting physical, chemical, and biological properties. Nanotechnology is a relatively newer field of science that is finding enormous scope in dental and medical science. This field is useful in multitude of applications, including dental diagnosis, materials, surface treatments of dental implants, and improving orthopedic implant devices. The changes in chemistry or topography of implant surface can occur due to nanoscale modification which can alter the implant surface interaction with ions, biomolecules, and cells leading to create surfaces with controlled topography and chemistry. Nanobiomaterials used in dental applications have superior abrasion resistance, lower shrinkage, and enhanced optical and esthetic properties due to their enhanced surface-to-volume ratio as compared to their bulk materials. Thus, they are used in light polymerizable composites, impression materials, ceramics, and dental implant coatings. Nanotechnology offers engineers and biologists new ways of interacting with relevant biological processes. Moreover, it has provided means of understanding and achieving cell-specific functions. The elucidation of bone healing physiology has driven investigators to engineer implant surfaces that closely mimic natural bone characteristics. Thus, the field of nanotechnology has bright prospects as it offers the possibility of great advances and improvement in the field of dentistry with an extrapolation of current resources to a new scale.

In modern dentistry, dental implant plays most viable role in the replacement of missing teeth. Implant restores not only form and function but also esthetics of the patients. Dental implants are manufactured from materials such as pure titanium, surgical stainless steel, and titanium alloys. The long-term survival of implants primarily depends on seamless osseointegration with bone and can get compromised by the inflammatory condition that causes peri-implantitis and loss of supporting bone. Osseointegration at the bone–implant interface and the amount of bacterial colonization around the implants have to be looked into carefully. The enhancement of bone formation at the bone–implant interface has been achieved through the modulation of osteoblasts adhesion and spreading, induced by structural modifications

of the implant surface, particularly at the nanoscale level. In this context, traditional chemical and physical processes find new applications to achieve the best dental implant technology.

The use of nanotechnology has been tested on a wide range of materials (such as metals, ceramics, polymers, and composites), either nanostructured surface features or constituent nanomaterials including grains, fibers, or particles with at least one dimension from 1 to 100 nm. The osteointegration of the orthopedic implants could improve the biocompatibility and the life span of the implants. The ideal implants should be made by materials easily colonized by bone-forming cells (osteoblasts), which can synthesize new bone matrix. The implant surfaces can alter cellular and tissue responses that may promote osseointegration. Some implant materials are not often compatible with osteoblasts, but rather promote the formation of soft connective tissue. Surface coatings using nanohydroxyapatite and calcium phosphate (CaP) particles make the new implants more acceptable as these materials enhance the integration of nanocoatings resembling biological materials to the periodontal tissues. Furthermore, osteoconductive nanoparticles induce a chemical bond with bone to attain good biological fixation for implants. Bioactive CaP nanocrystals deposited on titanium implants are resorbable and stimulate bone apposition and healing. Future nanometer-controlled surfaces may ultimately direct the nature of peri-implant tissues and improve their clinical success rate. Surface modification of implants using antibacterial properties can also decrease the potential for infection, and certainly improves clinical outcomes.

We are pleased to introduce this second book "Advances in Dental Implantology using Nanomaterials and Allied Technology Applications" to aspiring and working scientists, dental practitioners, and as a ready reference for the dental students to understand the principles of nanotechnology, its applications, and latest techniques. The first book "Dental Applications of Nanotechnology" was very well received by all the interested readers. The present second book covers primarily two sections. The first section covers **Nanobiomaterials** in implant applications, in bone regeneration, prosthetic rehabilitation, to control biofilm and peri-implantitis, bone grafting and tissue engineering. The second section covers implant stability, peri-implantitis, lasers, CAD/CAM technology, impressions, 3D printing, reconstruction with bone grafts, and zygomatic implants under **Applications**.

Nanotechnology assists in understanding and achieving cell-specific functions and thus critical steps in osseointegration can be modulated by nanoscale modification of the implant surface. It is possible to mimic bone formation process occurring at nanoscale level to achieve better osseointegration and higher implant surface ratio. Praveena et al. discuss in their chapter about the role of nanotechnology in the various methods and techniques of imparting nanoparticle-coated implants for the improvement of osseointegration using nanosurface features of dental implants and their antimicrobial activity. The application of nanomaterials in craniofacial bone regeneration is a newly advancing field which holds great capabilities for enhancing conventional therapeutic methods. Chapter by Hosseinpour et al. highlights the applications of nanobiomaterials as bone scaffolds, delivery systems, and barrier membranes for craniofacial bone regeneration. Maxillofacial reconstruction is complicated

due to the etiology and nature of the tissue injury. Nanobiomaterials in prosthetic rehabilitation of maxillofacial defects play an important role. Sybil et al. have shown in their chapter that the restoration of soft tissues like skin, cartilage, and mucosa without the support of the underlying bony architecture is possible with prosthesis. Graphene-based materials have gained extensive attention in the field of dentistry. Rokaya et al. have summarized the basic properties of graphene and the latest progress based on current knowledge. Minimizing biofilm formation and peri-implantitis is a great concern. Petrini et al. have discussed the novel materials and surfaces that could decrease early failure and improve long-term success in implantology. Reconstruction of craniofacial defects poses a challenging task for craniofacial surgeons. Bone grafting is the standard technique employed for bone reconstruction. However, with the advent of novel biomaterials as bone substitutes for grafting procedures, attractive alternatives have unlocked for surgeons. Kalluri and Duan have focused on the various biomaterials that are currently used as bone substitutes in craniofacial bone regeneration along with an update of the active research among each class of biomaterials going on in this area. For damaged tissues and organs affected by trauma, a regenerative medicine is required. Advanced nano-functional biomaterials can promote cellular adhesion, proliferation, differentiation, and morphogenesis in a controlled spatiotemporal manner. Midha et al. discuss about the importance of nanobiomaterials in tissue engineering and biological interaction with stem cells. In implants, a direct relationship seems to exist between the primary stability and bone density. Polyurethane foam has been proposed for in vitro tests to simulate the consistency and the density of the bone. Chapter by Tumedei et al. emphasizes the role of polyurethane foam as a model to study primary implant stability.

Peri-implant diseases, such as peri-implant mucositis and peri-implantitis, correspond to former periodontal conditions—gingivitis and periodontitis, and, analogically, are considered serious and chronic conditions jeopardizing the undertaken rehabilitation treatment using implant. Peri-implantitis, which is defined as a pathologic condition of all tissues supporting dental implant, can lead to its loss, if not recognized and treated on time. Porenczuk and Gorski in their chapter discuss to bring closer prevalence and risk factors of peri-implantitis along with prevention and treatment methods. The use of laser has increased rapidly in the last couple of decades. Their use in implant dentistry has seen an upsurge in the past years. At present, wide varieties of procedures are carried out using lasers. Laser can be classified based on the wavelengths and tissue on which it acts. The chapter by Miglani and Patro highlights the various types of lasers and their various applications at different stages of dental implantology. Proper diagnosis and appropriate treatmesnt planning is paramount to achieve the best long-term prognosis in implant dentistry. Computer-aided implant surgery has dramatically improved the quality of surgical procedures used for dental implant bed preparation and implant placement. The three-dimensional assessment of the restorative goal using cone beam computerized tomography (CBCT), radiographic template, and implant design programs allows realistic planning and optimized positioning of implants using surgical guides. D'Souza and Aras in their chapter explain the applications of CAD/CAM technology in dental implant

planning and implant surgery. Accurate replication of the clinical situations in a physical or virtual mode is required before and during the treatment for the planning or execution of the prosthetic phase by the laboratories. Impression making and modelling tools form a vital segment in the armamentarium of implantologists and so also the techniques need high level of skill development. Chapter by Dashaputra et al. explores all the techniques and critical steps essential in both the forms of modelling and impression making for accurate replications and success. The dental field is embracing the trend of digital dentistry. 3D printers and 3D scanners designed for dental applications can now help dentists offer a better and more personalized service to patients while offering substantial cost reductions and simplifying complex dental appliances production workflows. Implant dentistry was one of the first disciplines to experience 3D printed guides for predictable surgeries. A revolution in materials and technologies has resulted in further evolution, including the printing of prosthodontic frameworks, dentures, and implant components. Kalman discusses the exciting advancement of 3D printing and its applications to industry and medicine, with an in-depth presentation of its application to dentistry. Maxillofacial reconstruction using bone grafts, dental implants, and bone tissue engineering approach is a complex and exciting topic and poses significant challenges to oral and maxillofacial surgeons. Advances in the field of bone tissue engineering over the past few decades offer promising new treatment alternatives using biocompatible scaffold materials, autologous mesenchymal stem cells, and growth factors. Guastaldi et al., in their chapter, focus on the reconstruction of the maxilla and the mandible. The prime objective of the 3D impression-taking process in oral surgeries is obtaining a high-quality copy of one or several implants. This requires structures, healthy adjacent and antagonist teeth and other maxillofacial regions, establishing a proper interocclusal relationship and then converting this information into accurate replicas of the missing or abnormal implanted structures. Chapter by Irfan addresses the technical aspects and applications of digital impressions in maxillofacial surgeries. On severely resorbed maxilla the limitations for the installation of conventional implants require alveolar reconstructive procedures with the use of autogenous bone grafts harvested from iliac intraoral donor sites or autologous bone graft, increasing morbidity and cost of the treatment. As an alternative to the use of large bone reconstruction, zygoma bone can be used as anchorage for long implants supporting prosthetic rehabilitation. Chapter by Soares et al. discusses the importance of technology and virtual planning to correctly disseminate the masticatory forces on these implants.

The editors wish to thank all the distinguished and expert contributors for their enthusiastic participation in this endeavor and also some contributors who did the job at last hour. We are confident that the book will serve as a valuable guide for researchers and students of dentistry, materials engineering, bioengineering, and medicine. Dr. Chaughule wishes to thank Dr. Suhas Pednekar, Vice Chancellor, Mumbai University, Dr. Anushree Lokur, Principal, Ramnarain Ruia Autonomous College, and his family members for all the supports. Dr. Dashaputra wishes to thank his mentor Dr. Chaughule first to give the opportunity to be a coeditor. He too wishes to thank his wife and family for the support during this book preparation.

Special thanks are also due to Dr. Snigdha Patki-Chitnis, oral and maxillofacial surgeon, who did a very difficult but meticulous job of moderating a difficult chapter on zygoma implants originally written by non-English authors. Last but not least, the editors sincerely thank Springer staff for their support from time to time.

Mumbai, India

Ramesh S. Chaughule
Rajesh Dashaputra

Contents

Contributors

Adwait Aphale Dental Implants and Smile Rehabilitation Center, Kolhapur, India

Dental Implants and Smile Rehabilitation Center, Pune, India

Meena Ajay Aras Department of Prosthodontics, Crown and Bridge, Goa Dental College and Hospital, Bambolim, Goa, India

Andrea Castilho SENAC Trainee Program on Oral and Maxillofacial Surgery, São Paulo, Brazil

Ramesh S. Chaughule Department of Chemistry, Ramnarain Ruia Autonomous College, Matunga, Mumbai, India

Anjali Chauhan Special Center for Nanoscience, Jawaharlal Nehru University, New Delhi, India

Snigdha Chitnis Oral and Maxillofacial Surgeon, Pune, India

Luca Comuzzi Private Practice, Conegliano, TV, Italy

Rajesh Dashaputra Department of Dentistry, Bhabha Atomic Research Center Hospital, Mumbai, India

Simonetta D'Ercole Department of Medical, Oral and Biotechnological Science, University G. d'Annunzio of Chieti, Chieti, Italy

Kathleen Manuela D'Souza Department of Prosthodontics, Crown and Bridge, Goa Dental College and Hospital, Bambolim, Goa, India

Yuanyuan Duan Department of Biomedical Materials Science, University of Mississippi Medical Center, Jackson, MS, USA

Bartłomiej Górski Department of the Periodontology and Oral Diseases, Medical University of Warsaw, Warsaw, Poland

Fernando P. S. Guastaldi Skeletal Biology Research Center, Department of Oral and Maxillofacial Surgery, Massachusetts General Hospital, Harvard School of Dental Medicine, Boston, MA, USA

Walter C. Guralnick Department of Oral and Maxillofacial Surgery, Massachusetts General Hospital, Harvard School of Dental Medicine, Boston, MA, USA

Satyabodh Guttal SDM College of Dental Sciences and Hospital, Dharwad, India

Sepanta Hosseinpour School of Dentistry, The University of Queensland, Brisbane, QLD, Australia

Giovanna Iezzi Department of Medical, Oral and Biotechnological Sciences, University of Chieti-Pescara, Chieti, Italy

Irfan Kachwala Diplomate American Board of Prosthodontics, Mumbai, India

Lohitha Kalluri Department of Biomedical Materials Science, University of Mississippi Medical Center, Jackson, MS, USA

Les Kalman Department of Restorative Dentistry, Schulich School of Medicine and Dentistry, Western University, London, ON, Canada

Chang Lei Australian Institute for Bioengineering and Nanotechnology, The University of Queensland, Brisbane, QLD, Australia

Baboucarr Lowe School of Dentistry, The University of Queensland, Brisbane, QLD, Australia

Joseph P. McCain Jr Skeletal Biology Research Center, Department of Oral and Maxillofacial Surgery, Massachusetts General Hospital, Harvard School of Dental Medicine, Boston, MA, USA

Swati Midha Special Center for Nanoscience, Jawaharlal Nehru University, New Delhi, India

Sanjay Miglani Department of Conservative Dentistry and Endodontics, Faculty of Dentistry, Jamia Millia Islamia, New Delhi, India

Irfan Mohammed School of Dentistry, Federal University of Pelotas, Pelotas, RS, Brazil

Joao L. G. C. Monteiro Skeletal Biology Research Center, Department of Oral and Maxillofacial Surgery, Massachusetts General Hospital, Harvard School of Dental Medicine, Boston, MA, USA

Ashwin Nanda School of Dentistry, The University of Queensland, Brisbane, QLD, Australia

R. S. Neelakandan Meenakshi Ammal Dental College and Research Centre, Chennai, India

Swadheena Patro Department of Conservative Dentistry and Endodontics, Kalinga Institute of Dental Sciences, Bhubaneswar, Odisha, India

Morena Petrini Department of Medical, Oral and Biotechnological Science, University G. d'Annunzio of Chieti, Chieti, Italy

Adriano Piattelli Department of Medical, Oral and Biotechnological Science, University G. d'Annunzio of Chieti, Chieti, Italy

Biomaterials Engineering, Universidad Catolica de San Antonio de Murcia, Murcia, Spain

Fondazione Villa Serena per la Ricerca, Città S. Angelo, Italy

Serena Pilato Department of Pharmacy, University G. d'Annunzio of Chieti, Chieti, Italy

Alicja Porenczuk Restorative Dentistry Department, Medical University of Warsaw, Warsaw, Poland

Channamsetty Praveena Department of Prosthodontics, Malla Reddy Institute of Dental Sciences, Hyderabad, Telangana, India

Jiaqian Qin Metallurgy and Materials Science Research Institute, Chulalongkorn University, Bangkok, Thailand

Milena Radunovic Laboratory for Microbiology, School of Dental Medicine, University of Belgrade, Belgrade, Serbia

Dinesh Rokaya Research Unit of Herbal Medicine, Faculty of Dentistry, Chulalongkorn University, Bangkok, Thailand

Vinicius Rosa Oral Sciences, Faculty of Dentistry, National University of Singapore, Singapore, Singapore

Janak Sapkota Institute of Polymer Processing, Department of Polymer Engineering and Science, Montan Universitaet Leoben, Leoben, Austria

K. V. Satyanarayana Department of Periodontics, Rainbow Super Speciality Dental Hospital, Hyderabad, Telangana, India

Antonio Scarano Department of Medical, Oral and Biotechnological Science, University G. d'Annunzio of Chieti, Chieti, Italy

Claudia Caminero Soares Prosthodontics and Periodontist, Osteogenesis Research Institute, São Paulo, Brazil

Marcelo Melo Soares Osteogenesis Research Institute, São Paulo, Brazil

Oswaldo Cruz Hospital, São Paulo, Brazil

SENAC Trainee Program on Oral and Maxillofacial Surgery, São Paulo, Brazil

Viritpon Srimaneepong Department of Prosthodontics, Faculty of Dentistry, Chulalongkorn University, Bangkok, Thailand

Deborah Sybil Faculty of Dentistry, Jamia Millia Islamia, New Delhi, India

Toru Takusagawa Skeletal Biology Research Center, Department of Oral and Maxillofacial Surgery, Massachusetts General Hospital, Harvard School of Dental Medicine, Boston, MA, USA

Pasutha Thunyakitpisal Research Unit of Herbal Medicine, Faculty of Dentistry, Chulalongkorn University, Bangkok, Thailand

Department of Anatomy, Faculty of Dentistry, Chulalongkorn University, Bangkok, Thailand

Maria J. Troulis Skeletal Biology Research Center, Department of Oral and Maxillofacial Surgery, Massachusetts General Hospital, Harvard School of Dental Medicine, Boston, MA, USA

Walter C. Guralnick Distinguished Professor of Oral and Maxillofacial Surgery, Massachusetts General Hospital, Harvard School of Dental Medicine, Boston, MA, USA

Margherita Tumedei Department of Medical, Oral and Biotechnological Sciences, University of Chieti-Pescara, Chieti, Italy

Chun Xu School of Dentistry, The University of Queensland, Brisbane, QLD, Australia

Qingsong Ye School of Dentistry, The University of Queensland, Brisbane, QLD, Australia

Nanotechnology in Implant Dentistry

Channamsetty Praveena, Ramesh S. Chaughule, and K. V. Satyanarayana

Abstract Recent advancements in engineering tools and techniques coupled with the extrapolation of nanotechnology in the field of dentistry have rendered dental implant therapy as the most reliable treatment option for replacement of missing natural dentition. Nanotechnology has driven dental implants to a newer level. It assists in understanding and achieving cell-specific functions, and thus critical steps in osseointegration can be modulated by nanoscale modification of the implant surface. It is possible to mimic bone formation process occurring at nanoscale level to achieve better osseointegration and higher implant surface ratio. This review chapter also discusses the various methods and techniques of imparting nanoparticle-coated implants for the improvement of osseointegration using nanosurfaced features of the dental implants and their antimicrobial activity.

Keywords Nanotechnology · Osseointegration · Nanoscale · Implant surface ratio · Surface treatment · Nanotopography

C. Praveena (✉)
Department of Prosthodontics, Malla Reddy Institute of Dental Sciences, Hyderabad, Telangana, India

R. S. Chaughule
Department of Chemistry, Ramnarain Ruia Autonomous College, Matunga, Mumbai, India

K. V. Satyanarayana
Department of Periodontics, Rainbow Super Speciality Dental Hospital, Hyderabad, Telangana, India

R. S. Chaughule, R. Dashaputra (eds.), *Advances in Dental Implantology using Nanomaterials and Allied Technology Applications*,
https://doi.org/10.1007/978-3-030-52207-0_1

1 Introduction

Dental implants have been in the market place for a long period of time for restoring or replacing teeth. The challenges faced by dental surgeons during dental implantation are controlling the high chances of infections and achieving osseointegration. Many studies have been attempted to enhance the osseointegration of implants by various surface modifications. The aim of dental manufacturers is to provide dental implants with surface biological properties for the adsorption of proteins, the adhesion and differentiation of cells, and tissue integration. These biological properties are allied to chemical composition, wettability, and roughness of metal implants surfaces. However, the control of these surface properties at the protein and cell levels, thus in the nanometer range, remains a potential challenge for researchers and dental implants manufacturers [1].

Modern science and technology has undergone a major revolution with the evolution of nanotechnology and hence has been assimilated into various medical disciplines including dentistry. Bulk material when reduced to nanoscale, there is significant change in the optical, thermal, and antimicrobial properties [2]. This alteration of the desired physicochemical properties of nanomaterials has led to the conceptual development of "**nanodentistry.**" The continuous ongoing quest for the introduction of newer materials for promoting better oral health has led to the discovery of various nanobiomaterials, advanced clinical tools, and better treatment modalities.

With the advent of hybrid science named nanobiotechnology, nanomaterials have noteworthy applications in implant dentistry [3]. The application of "nano" to implants, abutments, and bone substitutes drastically changed their biologic response. Nanotechnologies generate surfaces with controlled topography and chemistry that would aid in understanding biological interactions and developing novel implant surfaces with predictable tissue-integrative properties [4].

In this chapter, the biomedical applications of nanoparticles and nanopatterned surfaces in implant dentistry, including the recent nanocoated implant materials and technologies which are responsible for tuning the cell-specific interactions and promoting osseointegration, are discussed. The sequence of biological events in relation to the surface is related. Mechanisms of interaction with blood, platelets, and mesenchymal stem cells on the surface of implants are described.

1.1 Nanotechnology Definition

While many definitions of nanotechnology exist, the most widely used is from the US Government's National Nanotechnology Initiative (NNI). According to the NNI, nanotechnology is defined as: "Research and technology development at the atomic, molecular and macromolecular levels in the length scale of approximately 1–100 nm range, to provide a fundamental understanding of phenomena and materials at the nanoscale and to create and use structures, devices and systems that have novel properties and functions because of their small and/or intermediate size" [5].

Nanotechnology or molecular engineering is the production of functional materials and structures in the range of 0.1–100 nm-nanoscale by various physical or chemical methods [6]. The term "nano" is derived from "***nanos***," the Greek word for "***dwarf***." A nanometer is 10^{-9} a meter or one-billionth of a meter [7]. In simple terms, it is engineering at the atomic and molecular scale. It is a highly multidisciplinary field and cuts across many disciplines, including colloidal science, chemistry, applied physics, and biology.

1.2 Historical Review

Nanotechnology is not a new term. Although nanotechnology has been around since the beginning of time, the discovery of nanotechnology is widely attributed to the American Physicist and Nobel Laureate, Dr. Richard Phillips Feynman [7]. The first use of the word "nanotechnology" has been attributed to Taniguchi in 1974. In 1986, Eric Drexler introduced and popularized the term "nanotechnology" in his book "Engines of Creation" [5]. Dr. Robert A. Fretias Jr. is one among the pioneer scientists who has written about nanomedicine, nanodentistry, and their future changes [5]. It was introduced into dentistry as nanocomposites in the year 2002 by Filtek Supreme [8].

1.3 Classification of Nanomaterials

Siegel has classified nanomaterials [6, 9] based on dimensions as shown in Table 1.

1.4 Approaches in Nanotechnology

The fabrication techniques of the nanoscale materials can be divided into the following three approaches [7, 8]:

(a) Larger to smaller (top-down approach)

Table 1 Classification of nanomaterials based on dimensions

Dimension	Characteristics	Examples
Zero	Clusters/powders	Atomic clusters, filaments, and cluster assemblies
One	Multilayers	Nano thin film
Two	Ultrafine grained over-layers	Nanotubes, Nanofibers, and Nanowires
Three	Nanophase materials consisting of equiaxed nanometer-sized grains	Nanoparticles, Nanopowders, Dendrimers, Fullerences, Quantum dots, Nanostructures, Nanocapsules, and Nanopores

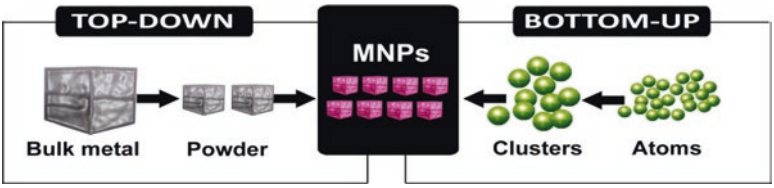

Fig. 1 Top-down and bottom-up approaches

Table 2 Examples of top-down and bottom-up approach

Top-down approach examples	Bottom-up approach examples
1. Salivary diagnostics	1. Inducing local anesthesia
2. Laser plasma application for periodontia	2. Hypersensitivity cure
3. Nanotechnology-based root-end sealant	3. Tooth repair
4. Nano needles	4. Nanorobotic dentifrice (dentifrobots)
5. Nano bone fibers	5. Orthodontic nanorobots
6. Nanocomposites	6. Dental durability and cosmetics
7. Nanotechnology for GIC	7. Nanotech floss
8. Nanoceramic technology	8. Photosensitizers and carriers
9. Nanobond	9. Diagnosis and treatment of oral cancer
10. Nanosolutions	
11. Coating agents	
12. Nanotechnology for impression materials	
13. Nanocomposite denture teeth	
14. Nanoparticles as antimicrobial agents	
15. Implants surface coatings	
16. Nano bone replacement materials	

Top-down fabrication reduces large pieces of materials all the way down to the nanoscale (Fig. 1). This approach requires larger amounts of materials and can lead to waste if excess material is discarded. Here, larger materials are patterned and carved down to make nanoscale structures in precise patterns. Materials reduced to the nanoscale can suddenly show very different properties, enabling unique applications (Table 2).

(b) Simple to complex (bottom-up approach)
The bottom-up approach to nano-manufacturing creates products by building them up from atomic and molecular-scale components, which can be time-consuming (Fig. 1). This begins by designing and synthesizing custom-made molecules that have the ability to self-assemble or self-organize into higher-order structures.

(c) Functional approach
In this approach, components of the desired functionality are developed without regard to how they might be assembled.

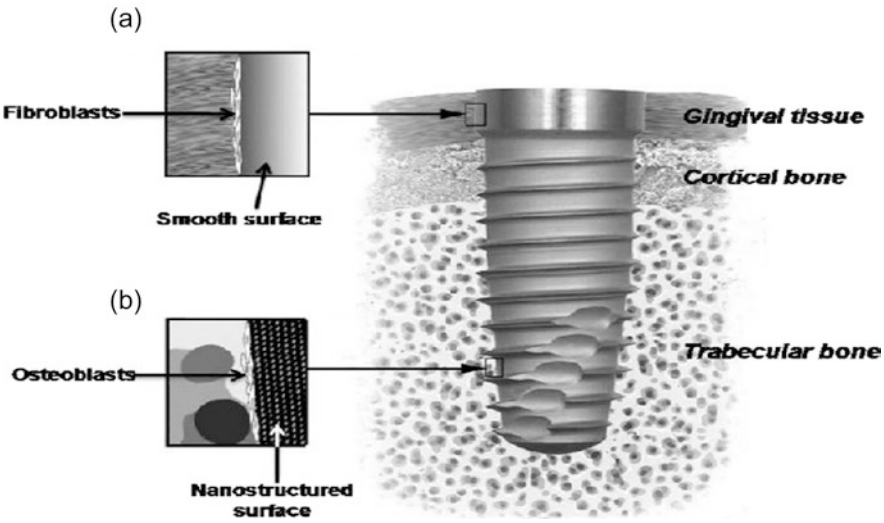

Fig. 2 Osseointegration. (**a**) Intimate contact with gingival tissue. (**b**) Contact osteogenesis

2 Concept of Osseointegration

Modification of dental osseous implants at nanoscale level produced by various techniques can alter biological responses that may improve osseointegration and dental implant procedures. The high success rates for endosseous implants have resulted from many research approaches with the aim of enhancing and accelerating bone anchorage to the implant, thereby providing optimal support for the intraoral prosthetic devices. This innovatory breakthrough has first emerged from the research efforts of the Branemark group in the late 1960s by pioneering the placement of machined screw-type commercially pure titanium (cpTi) implants with minimum surgical trauma. The bone bonding ability, termed as "osseointegration" by Brånemark et al. (1977), of this machined implant was principally the result of the proper surgical technique providing macrostability to the implant and the biocompatible nature of the bulk titanium [10].

Osseointegration of dental implants was earlier characterized as a structural and functional connection between newly formed bone and the implant surface, which became a synonym for the biomechanical concept of secondary stability [11]. Osseointegration comprises a cascade of complex physiological mechanisms similar to direct fracture healing (Fig. 2). The drilling of an implant cavity resembles a traumatic insult to bony tissue leading to distinct phases of wound healing [12]. New bone generates from the borders of the drill hole (distance osteogenesis) or by osteogenic cells on the surface of the implant (contact osteogenesis). In distance osteogenesis, osteoblasts migrate to the surface of the implant cavity, differentiate, and lead to the formation of new bone. Thus, bone grows in an appositional manner

towards the implant. In contact osteogenesis, osteogenic cells migrate directly onto the implant surface and generate *de novo* bone [13].

After decades of research, better designs and materials have evolved, with increase in survival rate and low failure rate. The most frequent cause for failure is insufficient bone formation around the implant surface. In this, the implant surface and tissue interface play a critical role [14]. Implant surface composition, surface energy, surface roughness, and topography are the four material-related factors which can influence biological events at the bone–implant interface. Macro, micro, and nano are the three types of surface structures. Current surface structures are controlled, at best, at the micron level, but tissue response is mainly dictated by processes controlled at the nanoscale. Surface profiles of implants in the nanometer range play an important role in the adsorption of proteins and adhesion of osteoblastic cells, promote osteogenic differentiation, and may improve the osseointegration of the implants [15]. Hence, we need strategies to improve the current metallic dental implants, through surface modifications of the implant either by applying novel ceramic coatings or by patterning the implant's surfaces.

3 Interactions of Surface Dental Implants with Blood

The first biological event after the implantation is blood–implant contact [16]. Immediate response is adsorption of platelets and interaction of plasma proteins with the implant surface (Fig. 3). Plasma proteins with other substances such as glucose, amino acids, and various ions influence the wettability of implant surface

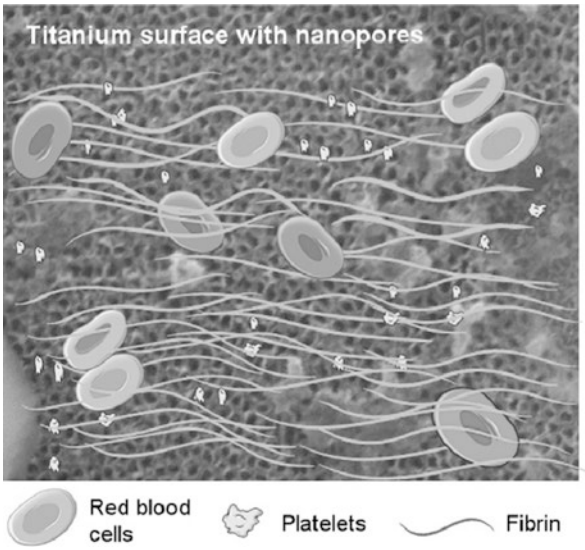

Fig. 3 Interactions of the surface of implant with blood

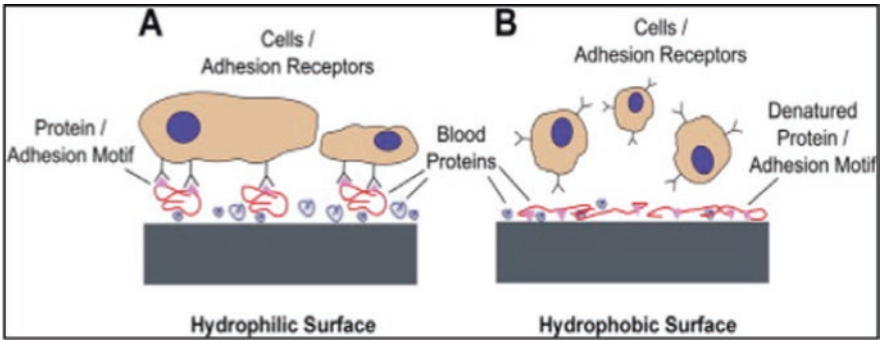

Fig. 4 Cellular interactions of hydrophilic surface (**a**) and hydrophobic surface (**b**)

which can be altered by its surface modifications [17]. It is assumed that Vroman effect will be observed around the implant surface in which the highest mobility proteins generally arrive first and are later replaced by less mobile proteins that have a higher affinity for the surface which enhance osseointegration [18]. As it has been proven that hydrophilic surface exhibits better blood coagulation and osseointegration than a hydrophobic surface, modern implants are emerging with high hydrophilic and rough implant surfaces (Fig. 4) [19].

Fibronectin and vitronectin help in cell attachment by cell-binding RGD domain (arg-gly-asp tripeptide). RGD chain interacts with cell membrane [20] integrins, which in turn play a vital role in adhesion of many cell lineages.

3.1 Role of Macrophage Cells

Macrophage lineage depends on its phenotype, i.e., if the stimulus is for proregenerative (M2) macrophage phenotype, more number of M2 will be in that vicinity compared to proinflammatory (M1) phenotype [16]. Dominant proregenerative (M2) macrophage phenotype which aids in tissue regeneration forms the bone around the implant, by stimulating the osteogenic differentiation of osteoprogenitor cells and suppressing the inflammatory response [16].

3.2 Interactions Between Surfaces and Mesenchymal Stem Cells

Blood coagulation is followed by various cell interactions. After migration of mesenchymal stem cells (MSCs) to the implant site by chemokine stimulus from surrounding tissues, it invades the three-dimensional microporous structure that allows diffusion of regulatory factors [21, 22] and helps in the migration, proliferation, and

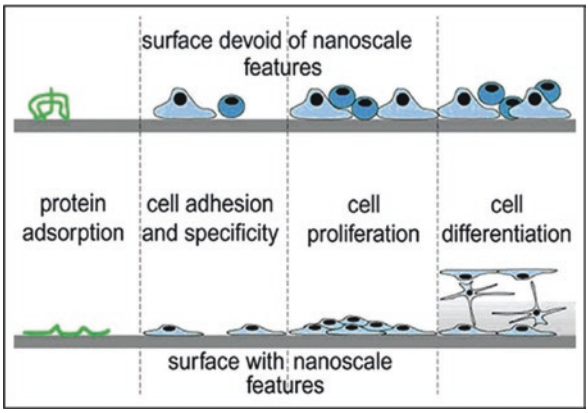

Fig. 5 Depiction of cell interactions on surfaces with and without nanoscale features

differentiation of MSCs. Once the MSC recruitment in the injured site is completed, it adheres on the local extracellular matrix as well as on the implant surface beginning an extensive proliferation in order to build up new tissue. Surface modification of implant surface at nano level helps in the adhesion of MSCs (Fig. 5).

Here MSCs can be differentiated into either fibroblastic or osteoblastic based on the stimulus. If the stimulus is for fibroblast cells, it initiates fibrous capsule formation obstructing the bond between implant and bone by forming collagen and thus results in an implant failure [23]. At the same time, it is desired to have more fibroblastic proliferation near gingival part of implant. Studies have revealed less fibroblast proliferation at nanosurface than conventional surface which facilitates better osseointegration [24].

Increased levels of alkaline phosphatase and calcium are observed in cell layers on nanosized materials after 21 and 28 days [25, 26]. Nanorough Ti and nanostructured Ti showed better results compared to nanosmooth surfaces [27, 28] and greatly enhanced osseointegration has been observed with micro- and nanopore surfaces [29, 30]. Adhesion, proliferation, and differentiation of MSCs depend on local chemical environment, surface topography of implant, and its surface tension for predictable regeneration.

3.3 Nanosurface and Bacterial Proliferation

It is noted that a profound decrease in bacterial colonization on nanostructured TiO_2 and ZnO regardless of the surface [31]. These observations need further research on biofilm formation and peri-implantitis around implants.

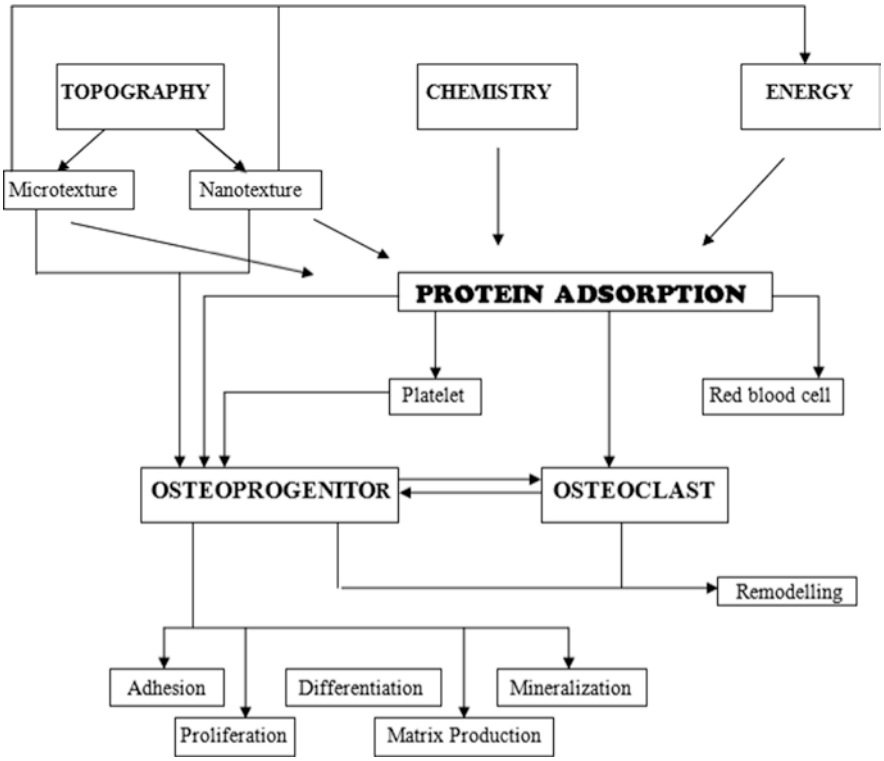

Fig. 6 Effect of surface characteristics of the implant on the osteogenic response

4 Surface Functionalization for Enhanced Osseointegration

The surface of a titanium implant plays a central role in determining the biological response of the host bone for several reasons (Fig. 6).

The surface characteristics of an implant regulate the healing mechanisms at the bone–implant interface since it is the only region contacting the bone. Surface functionalization had gained the interest of many manufacturers for enhancing the biomechanical anchorage and osseointegration of the implant at the histological level. Commonly used techniques [14] to alter surface properties of titanium are as follows (Table 3).

All these modifications regulate the morphology, physicochemical composition, and surface energy of the implant surface. Two categories of surface properties are commonly suggested for affecting the tissue response to the implant: surface topography and physicochemical composition.

4.1 Topographical Features of Titanium Surfaces

The fate of an implant after implantation is decided by the adsorption of biomolecules and the consequent interactions of cells on the implant surface. Rough topography increases the surface area of the implant and cell adhesion, thereby achieving higher bone-to-implant contact and better biomechanical integrity [32]. It has been shown that moderate roughness (Ra, between 1 and 2 μm) and complex microtopographies are important for the enhanced osseointegration of titanium implants [33]. Implants with rough surfaces exhibited greater bone–implant interface compared to smooth surfaces [34].

Table 3 Methods for creating nano-features on dental implants

S. no.	Method	Characteristics
I.	**Ceramic coatings**	Thin layer of bioactive ceramics is applied on the implant surface and form a carbonated apatite layer on the implant surface through dissolution and precipitation. **Advantages:** – Faster healing time – Enhanced bone formation – Firmer implant-bone attachment – Reduction of metallic ion release
II.	**Self-assembly of monolayer**	These are ordered organic films in supramolecular chemistry formed by chemisorptions of an active organic coating on a solid surface
III.	**Physical approaches**	
	(a) Plasma spraying	Charged metallic ions or plasma are deposited on the surface by kinetic energy. Widely used for calcium phosphate coatings (HA) deposition. **Advantages:** – Increased osteoblastic density. – Greater bone-implant contact **Drawbacks:** – Long-term stability of implants affected – Lack of adherence of the coating can result in health hazards
	(b) Sputtering	Thin films of bioceramics are deposited by high-energy bombardment of high-energy ions. **Advantages:** Improved healing response and initial fixation. **Drawbacks:** Very slow deposition rate
	(c) Ion deposition	This method enables injection of elements on the near-surface region of the substrate using a beam of high-energy (10 keV) ions.

(continued)

Table 3 (continued)

S. no.	Method	Characteristics
IV.	**Chemical methods**	
	(a) Anodic oxidation	With the help of this technique, the smooth surface of titanium implants can be transformed into nano tubular structures of less than 100 nm diameter.
	(b) Acid treatment	By combining strong acids or bases and oxidants nano pits networks (pit diameter 20–100 nm) can effectively be generated on Titanium, Ti6Al4V, CrCoMoalloys, and Tantalum.
	(c) Alkali treatment	In this method, the titanium implant is immersed in either sodium or potassium hydroxide followed by heat treatment at 800 °C for 20 min that is followed by rinsing in distilled water. **Advantages:** Results in the growth of a nanostructured and bioactive sodium titanate layer on the dental implant surface.
	(d) Combination of anodization and chemical treatment	A combination of hydrothermal treatments and sodium hydroxide has been employed to titanium to create a wide variety of unique nanostructures. **Advantages:** Improved biological properties
	(e) Hydrogen peroxide treatment	H_2O_2 leads to oxidation and chemical dissolution of the titanium surface. The reaction between hydrogen peroxide and titanium dental surfaces leads to the formation of Titanium peroxy gels. **Advantages:** Immersion of treated dental implants in simulated body fluid leads to the development of thicker layers of titania gel which is beneficial for deposition of apatite crystals
	(f) Sol-gel treatment	This method leads to the formation of a uniform suspension of submicroscopic oxide particles in liquid (sol) by the procedure of controlled hydrolysis and condensation. **Advantages**: Leads to early bone healing and enhanced mechanical interlocking with bone. Sol-gel coating process improves dental implant surfaces by nanoscale surface modifications
	(g) Chemical vapor deposition	Nonvolatile compounds are deposited on the implant surface by a chemical reaction between implant surface and chemicals present in the gas. **Advantages:** By the process of chemical vapor deposition, metallic surface properties can be modified at the nanoscale level.
	(h) Combination of chemical vapor and sol-gel method	With the help of these techniques Niobium oxide and diamond-like carbon nano topographies have been deposited on titanium and other substrates which improve the bioactivity of implantable metals. **Advantages:** Metallic surface properties can be improved

(continued)

Table 3 (continued)

S. no.	Method	Characteristics
V.	**Nanoparticle deposition**	
	(a) Sol-gel	Creates a thin film of controlled chemical characteristics. Atomic-scale interactions display strong physical interactions
	(b) Discrete crystalline deposition	Superimposes a nanoscale surface topographical complexity on the surface.
	(c) Lithography and contact printing technique	Many different shapes and materials can be applied over the surface. Approaches are labor intensive and require considerable development prior to clinical translation and application on implant surface

Cellular interactions are affected by the surface topography. Surface roughness in the range from 1 to 10 μm influences the interface biology. Only limited studies documented better cellular proliferation on surfaces with microrough topography. Mustafa et al. [35] blasted the machined titanium surfaces with different microtopographies and found an insignificant increase in cell proliferation parallel to increasing roughness. However, numerous other studies demonstrated a negative correlation between surface microroughness and cell proliferation [36]. In the study done by Boyan et al. [37] it has been shown that on surfaces with rough microtopographies, osteoblasts secrete factors, such as osteoprotegerin (OPG), receptor activator of nuclear factor kappa B ligand (RANKL), prostaglandins (PGE1 and PGE2), and TGF-β1, that enhance osteoblast differentiation while decreasing osteoclast formation and activity [38]. These results reveal that on rough surfaces osteoblasts demonstrate a more differentiated phenotype, although the proliferation is negatively affected.

4.2 Physicochemical Composition of Titanium Surfaces

The surface chemistry, wettability, and charge are the other important parameters that affect the extent of bone response besides the surface topographical features [39]. Due to high affinity to oxygen, a very thin oxide film is formed on the titanium interacting surface when exposed to air [40]. Titanium dioxides have properties similar to ceramics. The chemical stability and corrosion resistance of its dense and protective oxide film determine the biocompatibility of titanium [41]. The crystal structure of this film is believed to be imperative for the success of implant integration. Anatase or rutile surfaces showed enhanced cellular proliferation and mineralized nodule formation, compared with amorphous ones [42]. Preliminary studies demonstrated that hydrophilic nature of titanium surfaces positively influences the cell differentiation and growth factor production [43, 44]. There are also differing results from other studies. Culture test of MSCs done by Bauer et al. [45] on nanotubular titanium surfaces having unlike wettability characteristics has shown

improved cellular adhesion on superhydrophobic surfaces compared with superhydrophilic surfaces. It is difficult to state that the hydrophilicity of surface is the only basis for enhanced outcomes with the current availability of uncertain results. The microtopography, the local chemical environment, and wettability altogether must be taken into consideration for eliciting the predictable results.

4.3 Nanotopographical Modification of Titanium Surfaces

After implantation, osteoblasts in the human body encounter various nanostructures during their cellular and tissue interactions creating an imperative need to produce better implant materials having also nanometer roughness. Several studies have recommended that nanophase materials formed from various chemistries such as metals, polymers, composites, and ceramics enhanced cellular activities when compared with conventional microrough materials [46]. Nanobiomaterials with nanoscale surface topography possess an increased percentage of atoms and crystal structures and higher surface area with high surface energy than the conventional ones leading to increased initial protein adsorption which is very crucial in regulating the cellular interactions on the implant surface. Webster et al. [47] reported increased osteoblast adhesion on nanophase materials. It has been proved that osteoblasts cultured on nanophase biomaterials exhibited improved osteogenic behavior than on conventional materials [48].

Although several methods are developed to produce nanoscale structures on titanium surface, the electrochemical anodization of titanium is the most popular and novel technique to produce controlled structures on implant surfaces for load-bearing approaches [49]. The titania nanotube arrays are the most promising type of titanium nanosurfaces for dental implantology [50]. Several studies have verified that cells cultured on these nanotubular surfaces showed better adhesion, proliferation, ALP activity, and bone matrix deposition [51]. Nanotubular surfaces drastically improved bone bonding strength by almost ninefold compared with grit blasted surfaces. The histological analysis showed greater bone–implant contact and collagen type I expression [52]. Cellular responses are considerably influenced by the nanomorphological features such as length, diameter, and wall thickness of titania nanotubes [53]. Although nanotubular structures on titanium offer a suitable infrastructure for better osseointegration [54, 55], still there is a need for further studies that would optimize the production of nanotubes for improved bioactivity.

5 Implant Coatings

In many cases, the failure occurs at the tissue–implant interface, which may be due to the implant material weakening its bond with the natural material. To overcome this, implants are often coated with a biocompatible material to increase their

adherence properties and produce a greater surface area to volume ratio for the highest possible contact area between the implant and natural tissue.

In addition to the higher surface areas and improved adhesion properties of the nanoparticle coatings, improved coating techniques are also being developed. While high temperature processes such as plasma spray can melt ceramic particles and reduce their surface area and adhesion properties, new low temperature processes with electromagnetic fields can maintain the nanomaterial properties. This provides the maximum possible contact area between the implants and bone surface to improve the potential for ingrowth in the host bone.

Nanotechnology brings a variety of new high surface area biocompatible nanomaterials and coatings to increase the adhesion, durability, and life span of implants. Nanostructure modification of dental implants improves osseointegration through enhanced biomimicry of host structures. Ceramic materials such as calcium phosphate (hydroxyapatite or HA) and calcium carbonate are the available calcium derivative nanoparticles (Table 4).

The composition of HA simulates the composition of the bone and teeth. HA like tricalcium phosphate does not undergo any resorption. Due to its chemical property

Table 4 Range of materials added to calcium phosphate for the production of nanocomposite coatings and their advantages and concerns

Material	Advantages	Concerns
Carbon nanotubes (CNT)	• Excellent mechanical properties • Used to reinforce the HA	• Nonbiodegradable. • Possible transfer of internal organs after the degradation of the matrix. • Free graphite is difficult to disperse homogeneously.
Nano-crystalline diamond	• Act as a selective protective barrier between implant and human environment, preventing release of metallic ions. • Resistance to bacterial colonization • Antioxidant and anticarcinogenic	• Limited studies documenting improved bone–implant interface
Bioactive glass	• Increased surface bioactivity. • Improves the bioactivity of metallic dental implants.	• Special attention is needed to control the surface reactivity rates.
Al_2O_3 nanoparticles	• Improved osseointegration • Good mechanical and strength properties • No adverse effect on cellular activity	
TiO_2 nanoparticles	• Capable of inducing cell growth and enhances osteoblastic activity.	• Crystallinity control is required.
Silica	• Alters the surface and interfacial properties of HA composites	• Long-term adhesion and reliability
Collagen	• Improved osteogenic effects and formation of new bone tissue without encapsulation.	

and ability to form crystals with inorganic components of teeth, it can build chemical bonds and make sure the immediate integration of titanium implants with the teeth and tissues around it. Nanoscale hydroxyapatite (HA)-coated implant surface will accelerate osseointegration and improve its quality relative to that of non-coated implants. The nanomechanical properties of the surrounding bone are evaluated by nanoindentation which shows the tissue quality significantly improving around HA-coated implants. Nano-hydroxyapatite is used as a single coating or in a combination with collagen, bioglass, or titanium dioxide in a composite coating to imitate the bio-environment of native bones [56].

Calcium carbonate is the other calcium derivative nanoparticle well known for its biocompatibility and osseoconduction. A direct contact has been reported between bone and calcium carbonate without any soft tissue interface.

5.1 Nanoparticle Coatings with Antimicrobial Activity

Dental implants are prone to failure as a result of bacterial biofilm accumulation. Implant surface designing should support the attachment of target tissue cells and prevent bacterial adhesion. Increasing the antibacterial ability and decreasing the bacterial compatibility of implant surfaces limits the biofilm formation. Zhao et al. [57] reviewed the in vitro and in vivo investigations for antibacterial coatings on Ti-based implants. Although progress has been made regarding antibacterial coating of implants, still there is no wide clinical utilization and in vivo information of antibacterial coating of implants.

Several studies reported that using antimicrobial medicines as nanoparticles-coated Ti can show sustained release pattern and improved antimicrobial efficiency (Table 5) [58].

Table 5 Nanomaterial coatings with antimicrobial activity

Type of material	Advantages
Ag nanoparticles	Enhanced antimicrobial effect, superior biocompatibility, and noncytotoxicity.
ZnO nanoparticles	Enhanced antimicrobial effect and good biocompatibility
CuO nanoparticle	Enhanced antimicrobial effects (significant inhibitory zones)
Quercitrin-	1. Increased collagen mRNA levels, decreased matrix metalloproteinase-1/tissue inhibitor of metalloproteinase-1 mRNA ratio, and decreased proinflammatory prostaglandin E2 release under basal and inflammatory conditions. 2. Ability to improve soft tissue integration, and therefore to increase dental implants success, anti-inflammatory properties.
Chlorhexidine (CHX)	Sustained release of CHX and improved antimicrobial efficiency and reduced subsequent colonization of the bacteria

5.1.1 Silver Nanoparticles

Silver ion (Ag^+) is a strong antibacterial agent with reasonable stability and broad spectrum antimicrobial effects. The size, shape, surface charge, concentration, and colloidal state are the most critical physicochemical parameters that affect the antimicrobial potential of silver nanoparticles (AgNPs). Nano-silver is comparatively less reactive than silver ions and therefore well suited for therapeutic and clinical applications [59]. AgNPs exhibit their antimicrobial potential through multifaceted mechanisms. The most prominent modes of antimicrobial action are through adhesion of AgNPs to microbial cells followed by penetration inside the cells and subsequently releasing reactive oxygen species (ROS) and free radicals for modulation of microbial signal by transduction pathways [60]. According to Bressan et al., silver-containing materials could inhibit bacterial attachment onto the dental implants. Studies demonstrated excellent biocompatibility of silver-containing implants without genotoxicity or cytotoxicity and reported no local or systemic side effects [61]. Various techniques can be used to prepare silver-containing coatings.

Ion implantations prepared by micro arc oxidation (MAO) provide a porous biofunctional TiO_2 coating with good adhesion to the surface of titanium implants [62]. Zhang et al. proved enhanced antimicrobial effect with superior biocompatibility and noncytotoxicity by coating TiO_2 implants with silver nanoparticles using MAO method [62].

5.1.2 Zinc Oxide (ZnO) Nanoparticles

ZnO nanoparticles have been reported to show antibacterial activity against both gram-positive and gram-negative bacteria, as well as against the spores which are resistant to high temperature and high pressure [63]. The proposed mechanisms for ZnO nanoparticles are the generation of hydrogen peroxide as well as the accumulation of the particles on the bacteria surface due to the electrostatic forces. In addition, ROS generation on the surface of the particles, zinc ion release, membrane dysfunction, and nanoparticle internalization could also be taken into account as the possible reasons of the antimicrobial activity of these nanoparticles. Memarzadeh et al. [63] observed that a 75/25% ratio of ZnO/nano-hydroxyapatite coated substrates deposited by electrohydrodynamic atomization (EHDA) could lead to enhanced osteoblast growth and produced a more biocompatible, osseoconductive, and antimicrobial implant. Their results also proved minimal toxicity for UMR-106 cells exposed to ZnO nanoparticles with no release of TNF-a and IL-6 cytokines for MG-63 cells cultured on ZnO substrates. According to proliferation and differentiation studies, the substrate exclusively coated with ZnO nanoparticles showed more efficiency than that with composite surface coatings.

5.1.3 Copper Oxide (CuO) Nanoparticles

The exploitation of copper oxide nanoparticles (CuO) has increased rapidly over the past decade because of their unique attributes to combat biofilm formation. The size, stability, and concentration determine the bactericidal activity of CuO nanoparticles [58]. CuO nanoparticles control the bacterial growth by passing through nanometric pores existing on bacterial cell membranes. CuO nanoparticles demonstrated high antibacterial activity while maintaining less cytotoxicity. Anu et al. [64] concluded that CuO nanoparticle-coated substrates deposited by standard slurry dipping method and chemical synthesis efficiently suppressed the dental infections. The results showed no inhibitory zones for uncoated materials, while the CuO nanoparticle-coated titanium dental implants showed significant inhibitory zones. Proliferation, adhesion, and spread of cells are markedly influenced by the formation of oxidation layer on Ti as per their hypotheses.

5.1.4 Quercitrin-Nanocoated Implants

Quercitrin is a natural yellow color flavonoid obtained from tartary buckwheat and from the bark of oak trees. Quercitrin has the inherent ability of enhancing both hard and soft tissue integration around the implant, thereby increasing the dental implant success and decreasing the risk of peri-implantitis. It is also hypothesized that quercitrin-coated dental implants show an inhibitory effect on osteoclastogenesis and thus can accomplish delayed bone resorption while promoting bone formation, producing more bony tissue just before the remodeling phase. Gomez-Florit et al. proved the soft tissue regeneration potential of quercitrin-nanocoated titanium surfaces by increased human gingival fibroblasts attachment. The anti-inflammatory properties are evaluated by mimicking the anti-inflammatory situation using interleukin-1-beta. The anti-inflammatory results showed increased collagen mRNA levels, decreased matrix metalloproteinase-1/tissue inhibitor of metalloproteinase-1 mRNA ratio, and decreased proinflammatory prostaglandin E2 release under basal and inflammatory conditions [65].

5.1.5 Chlorhexidine (CHX) Nanoparticles

Chlorhexidine (CHX) is a broad antimicrobial and antifungal spectrum. In a research work by Barbour et al., CHX-coated surface can reduce the growth of Streptococcus gordonii, but the CHX is rapidly depleted, leading to a short-term antimicrobial effect [66]. Wood et al. investigated the use of CHX hexametaphosphate (HMP) nanoparticles as a porous aggregating coating on titanium dental implants. The prepared CHX–HMP nanoparticle-coated Ti showed sustained release of CHX and improved antimicrobial efficiency. According to their microbiological results, colony-forming units (CFUs) in the wells containing the CHX–HMP nanoparticle-coated Ti decreased as a function of time, whereas CFUs in the uncoated Ti remained

constant. Also, their results revealed the existence of more live bacteria on uncoated Ti than on nanoparticle-coated Ti after 24 and 48 h [67].

5.2 Vitamin D3 Nanoparticle Coatings

According to currently available data, there is a great interest among dental surgeons and implantologists in analyzing relationships between vitamin D3 and the osseointegration process. Besides a known role of vitamin D3 in bone metabolism, D3 is also very relevant for the normal functioning of the immune system, which is of particular importance for a successful integration of a dental implant in surrounding bone tissue. Based on the results of a combined electrochemical–theoretical study conducted by Jozefina et al. [68], bioactive vitamin D3 coating created the dental implant surface more osseoinductive and simultaneously more corrosion resistant during exposure to aggressive media (oral cavity fluids).

6 Tissue Regeneration Scaffolds

Nanostructures are being researched for the preparation and improvement of tissue regeneration scaffolds. Research areas include the ability to develop molecular sensitive polymers using the optical properties of nanoparticles as a control system, manipulating the stiffness and strength of scaffolds using hybrid nanostructures, and the use of nanotechnology to prepare molecular imprints to maximize long-term viability and function of cells on scaffold surfaces [5].

Some nanomaterials and nanotechnology fabrication techniques that are being investigated as tissue regeneration scaffolds that provide improved structures are as follows:

(a) Nanoscale polymers such as Poly-vinyl alcohol (PVA) are being molded into heart valves and seeded with fibroblasts and endothelial cells.
(b) Polymer nanocomposites are being researched for bone scaffolds.

Scientific challenges related to a better understanding of molecular/cell biology and fabrication methods for producing large three-dimensional scaffolds are among the many obstacles yet to be overcome.

Nanostructures are also being used to study the fundamental properties of implanted tissues. In areas of in vivo analysis, nanostructures are used as tracers for implanted cells and to study the response of the host to implanted tissues.

7 Structural Implant Materials and Bone Repair

Nanotechnology in implant dentistry restricts itself not only to implant surface modifications but also to other biomaterials used in this field that can be used as implants or temporary bioresorbable structures. Bone is a high strength material that is used as both weight-bearing and non-weight-bearing. Bones are more than just structural materials as they also contain interconnected pores that allow body fluids to carry nutrients and permit interfacial reactions between hard and soft tissues. In the case of bone fractures, graft disorders, and dental applications, bones may require repair or replacement [5].

A variety of natural materials are used as bone substitutes. These include autografts from the patient's pelvis, allograft from another human, bovine material, or coral blocks. Natural materials tend to be brittle and can lose mechanical strength during sterilization. They can also cause inflammation, pain at the pelvis graft site, and potentially transmit disease. Bone cavities can also be filled with synthetic bone cement. C. Martin et al. have shown that nanostructured synthetic alloplasts fused with collagen promoted bone ingrowth compared to other materials, which could be a promising material to regenerate bone in severe bone defects due to atrophy after tooth/teeth loss [69]. Current bone cements containing polymethylmethacrylate (PMMA) act as filler or grout, which is injected as flowable paste and then hardens in vivo. While PMMA cement can offer adequate mechanical properties and bonding, it is typically recommended only for non-weight-bearing bones. PMMA has also been linked to tissue damage, nerve root pain, and other side effects.

High strength nanoceramic materials, such as calcium phosphate appetite (CPA) and hydroxyapatite (HA), can be made into flowable, moldable nanoparticle paste that can confirm to and interdigitate with bone. As natural bone is approximately 70% by weight CPA including hydroxyapatite (HA), biocompatibility is thought to be extremely high with minimal side effects. As its dense surface and tight three-dimensional crystalline structures will allow for superior compressive strength to PMMA, nanoceramics may be suitable for both weight-bearing and non-weight-bearing bones [5].

7.1 Bioresorbable Materials

Bioresorbable polymers are currently being used in degradable medical applications such as sutures and orthopedic fixation devices. With new production methods, nanostructures are being fabricated which could be used as temporary implants. Bioresorbable implants will be biodegradable and do not have to be removed in subsequent operation. Nanostructured implants are being designed to degrade at a rate that will slowly transfer load to a healing bone that it is supporting. Thus, it is possible in the near future to have nanomaterials used in the body to exceed current human performance on multiple dimensions and beyond current human limitations [8].

8 Conclusion

The futuristic view of multiple treatment opportunities offered by nanotechnological advances may sound unlikely, implausible, or even heretic. Yet, the theoretical and applied research to turn them into reality is progressing rapidly. Nanotechnology is still advancing and needs much more testing before appreciating its maximum potential in implant dentistry. Several nanosurface modification methods are widely being developed to enhance surface properties of titanium dental implant that result in rapid osseointegration and faster bone healing. Many in vitro and animal studies have shown that nanometer-controlled surfaces have a great effect on healing after implant placement. It affects the adsorption of proteins, blood clot formation, and cell behaviors occurring upon implantation. The techniques and methods developed should be applicable to clinical practice. Nanotechnology opens a new spectrum of possibilities for advancement in implant dentistry.

References

1. Lavenus S, Louarn G, Layrolle P. Nanotechnology and dental implants. Int J Biomater. 2010;2010:915327. https://doi.org/10.1155/2010/915327.
2. Wang W, Liao S, Zhu Y, Liu M, Zhao Q, Fu Y. Recent applications of nanomaterials in prosthodontics. J Nanomaterials. 2015; https://doi.org/10.1155/2015/408643.
3. Saji VS, Choe HC, Young KWK. Nanotechnology in biomedical applications—a review. Int J Nano Biomater. 2010;3:119–39.
4. Lavenus S, Ricquier I-C, Louarn G, Layrolle P. Cell interaction with nanopatterned surface of implants. Nanomedicine. 2010;5:937–47.
5. Subramani K, Ahmed W. Emerging nanotechnologies in dentistry, vol. 78–97. Amsterdam: Elsevier; 2012. p. 322–89.
6. Mitra SB, Holmes BN. An application of nanotechnology in advanced dental materials. J Am Dent Assoc. 2003;134:1382–90.
7. Sree L, Balasubramanian, Deepa. Nanotechnology in dentistry—a review. Int J Dent Sci Res. 2013;2:40–4.
8. Satyanarayana TSV, Rai R. Nanotechnology: the future. J Interdiscip Dent. 2011;1(2):93–100.
9. Siegel RW. Synthesis and processing of nanostructured materials. In: Nastasi M, Nastasi M, Parkin DM, Gleiter H (editors) Textbook of Mechanical properties and deformation behavior of materials having ultrafine microstructures, NATO-ASI, vol E233. Kluwer Academic, Dordrech; 1993. p. 508–36.
10. Brånemark PI, Hansson BO, Adell R, Breine U, Lindström J, Hallén O, Ohman A. Osseointegrated implants in the treatment of the edentulous jaw. Experience from a 10-year period. Scand J Plast Reconstr Surg Suppl. 1977;16:1–132.
11. Albrektsson T, Jacobsson M. Bone-metal interface in osseointegration. J Prosthet Dent. 1987;57(5):597–607.
12. von Wilmowsky C, Moest T, Nkenke E, Stelzle F, Schlegel KA. Implants in bone: part I. A current overview about tissue response, surface modifications and future perspectives. Oral Maxillofac Surg. 2014;18(3):243–57.
13. Junker R, Dimakis A, Thoneick M, Jansen JA. Effects of implant surface coatings and composition on bone integration: a systematic review. Clin Oral Implants Res. 2009;20(Suppl 4):185–206.

14. Gupta A, Singh G, Afreen S. Application of nanotechnology in dental implants. IOSR J Dent Med Sci. 2017;16(11):77–81.
15. Le Guehennec L, Soueidan A, Layrolle P, Amouriq Y. Surface treatments of titanium dental implants for rapid osseointegration. Dent Mater. 2007;23(3):844–54.
16. Park JW, Han SH, Hanawa T. Effects of surface nanotopography and calcium chemistry of titanium bone implants on early blood platelet and macrophage cell function. Biomed Res Int. 2018;2018:1362958. https://doi.org/10.1155/2018/1362958.
17. Khosravi N, Maeda A, DaCosta RS, Davies JE. Nanosurfaces modulate the mechanism of peri-implant endosseous healing by regulating neovascular morphogenesis. Commun Biol. 2018;1:72. https://doi.org/10.1038/s42003-018-0074-y.
18. Miller R, Guo Z, Vogler EA, Siedlecki CA. Plasma coagulation response to surfaces with nanoscale chemical heterogeneity. Biomaterials. 2006;27(2):208–15.
19. Sawase T, Jimbo R, Baba K, Shibata Y, Ikeda T, Atsuta M. Photo-induced hydrophilicity enhances initial cell behavior and early bone apposition. Clin Oral Implants Res. 2008;19(5):491–6.
20. Balasundaram G, Sato M, Webster TJ. Using hydroxyapatite nanoparticles and decreased crystallinity to promote osteoblast adhesion similar to functionalizing with RGD. Biomaterials. 2006;27(14):2798–805.
21. Catelas I, Sese N, Wu BM, Dunn JCY, Helgerson S, Tawil B. Human mesenchymal stem cell proliferation and osteogenic differentiation in fibrin gels in vitro. Tissue Eng. 2006;12(8):2385–96.
22. Schildhauer TA, Seybold D, Gebmann J, Muhr G, Koller M. Fixation of porous calcium phosphate with expanded bone marrowcells using an autologous plasma clot. Mater Werkst. 2007;38(12):1012–4.
23. Hobkirk JA. Progress in implant research. Int Dent J. 1983;33(4):341–9.
24. Eisenbarth E, Meyle J, Nachtigall W, Breme J. Influence of the surface structure of titanium materials on the adhesion of fibroblasts. Biomaterials. 1996;17(14):1399–403.
25. Meirelles L. On nano size structures for enhanced early bone formation. Gothenburg: Gothenburg University; 2007.
26. Colon G, et al. Increased osteoblast and decreased Staphylococcus epidermidis functions on nanophase ZnO and TiO2. J Biomed Mater Res A. 2006;78:595–604.
27. Puckett S, Pareta R, Webster TJ. Nano rough micron patterned titanium for directing osteoblast morphology and adhesion. Int J Nanomedicine. 2008;3(2):229–41.
28. Yao C, Slamovich EB, Webster TJ. Enhanced osteoblast functions on anodized titanium with nanotube-like structures. J Biomed Mater Res A. 2008;85(1):157–66.
29. Frosch KH, et al. Growth behavior, matrix production, and gene expression of human osteoblasts in defined cylindrical titanium channels. J Biomed Mater Res A. 2004;68(2):325–34.
30. Oh SH, Finones RR, Daraio C, Chen LH, Jin S. Growth of nano-scale hydroxyapatite using chemically treated titanium oxide nanotubes. Biomaterials. 2005;26(24):4938–43.
31. Thakral GK, Thakral R, Sharma N, Seth J, Vashisht JP. Nanosurface—the future of implants. J Clin Diagn Res. 2014;8(5):ZE07–10.
32. Cooper LF. A role for surface topography in creating and maintaining bone at titanium endosseous implants. J Prosth Dent. 2000;84(5):522–34.
33. Abrahamsson I, Zitzmann NU, Berglundh T, Wennerberg A, Lindhe J. Bone and soft tissue integration to titanium implants with different surface topography: an experimental study in the dog. Int J Oral Maxillofac Implants. 2001;16(3):323–32.
34. Al-Nawas B, Groetz KA, Goetz H, Duschner H, Wagner W. Comparative histomorphometry and resonance frequency analysis of implants with moderately rough surfaces in a loaded animal model. Clin Oral Implants Res. 2008;19(1):1–8.
35. Mustafa K, Wennerberg A, Wroblewski J, Hultenby K, Lopez BS, Arvidson K. Determining optimal surface roughness of TiO_2 blasted titanium implant material for attachment, proliferation and differentiation of cells derived from human mandibular alveolar bone. Clin Oral Implants Res. 2001;12(5):515–25.

36. Sader MS, Balduino A, Soares GA, Borojevic R. Effect of three distinct treatments of titanium surface on osteoblast attachment, proliferation, and differentiation. Clin Oral Implants Res. 2005;16(6):667–75.
37. Boyan BD, Batzer R, Kieswetter K, Liu Y, Cochran DL, Szmuckler-Moncler S, Dean DD, Schwartz Z. Titanium surface roughness alters responsiveness of MG63 osteoblast-like cells to 1 alpha,25-(OH)2D3. J Biomed Mater Res. 1998;39(1):77–85.
38. Lossdorfer S, Schwartz Z, Wang L, Lohmann CH, Turner JD, Wieland M, Cochran DL, Boyan BD. Microrough implant surface topographies increase osteogenesis by reducing osteoclast formation and activity. J Biomed Mater Res A. 2004;70(3):361–9.
39. Elias CN, Oshida Y, Lima JMC, Muller CA. Relationship between surface properties (roughness, wettability and morphology) of titanium and dental implant torque. J Mech Behav Biomed Mater. 2008;1(3):234–42.
40. Kasemo B, Gold J. Implant surfaces and interface processes. Adv Dent Res. 1999;13:8–20.
41. Healy KE, Ducheyne P. The mechanisms of passive dissolution of titanium in a model physiological environment. J Biomed Mater Res. 1992;26(3):319–38.
42. Li LH, Kong YM, Kim HW, Kim YW, Kim HE, Heo SJ, Koak JY. Improved biological performance of Ti implants due to surface modification by micro-arc oxidation. Biomaterials. 2004;25(14):2867–75.
43. Rausch-fan X, Qu Z, Wieland M, Matejka M, Schedle A. Differentiation and cytokine synthesis of human alveolar osteoblasts compared to osteoblast-like cells (MG63) in response to titanium surfaces. Dent Mater. 2008;24(1):102–10.
44. Zhao G, Raines AL, Wieland M, Schwartz Z, Boyan BD. Requirement for both micron- and submicron scale structure for synergistic responses of osteoblasts to substrate surface energy and topography. Biomaterials. 2007;28(18):2821–9.
45. Bauer S, Park J, Mark KV, Schmuki P. Improved attachment of mesenchymal stem cells on super-hydrophobic TiO_2 nanotubes. Acta Biomater. 2008;4(3):1576–82.
46. Gutwein LG, Webster TJ. Increased viable osteoblast density in the presence of nanophase compared to conventional alumina and titania particles. Biomaterials. 2004;25(18):4175–83.
47. Webster TJ, Schadler LS, Siegel RW, Bizios R. Mechanisms of enhanced osteoblast adhesion on nanophase alumina involves vitronectin. Tissue Eng. 2001;7(3):291–301.
48. Price RL, Gutwein LG, Kaledin L, Tepper F, Webster TJ. Osteoblast function on nanophase alumina materials: influence of chemistry, phase, and topography. J Biomed Mater Res A. 2003;67(4):1284–93.
49. Oh S, Daraio C, Chen LH, Pisanic TR, Fiñones RR, Jin S. Significantly accelerated osteoblast cell growth on aligned TiO_2 nanotubes. J Biomed Mater Res A. 2006;78(1):97–103.
50. Sjostrom T, Dalby MJ, Hart A, Tare R, Oreffo RO, Su B. Fabrication of pillarlike titania nanostructures on titanium and their interactions with human skeletal stem cells. Acta Biomater. 2009;5(5):1433–41.
51. Popat KC, Eltgroth M, Latempa TJ, Grimes CA, Desai TA. Decreased Staphylococcus epidermis adhesion and increased osteoblast functionality on antibiotic-loaded titania nanotubes. Biomaterials. 2007;28(32):4880–8.
52. Bjursten LM, Rasmusson L, Oh S, Smith GC, Brammer KS, Jin S. Titanium dioxide nanotubes enhance bone bonding in vivo. J Biomed Mater Res A. 2010;92(3):1218–24.
53. Brammer KS, Oh S, Cobb CJ, Bjursten LM, van der Heyde H, Jin S. Improved bone-forming functionality on diameter-controlled TiO_2 nanotube surface. Acta Biomater. 2009;5(8):3215–23.
54. Aninwene GE, Yao C, Webster TJ. Enhanced osteoblast adhesion to drugcoated anodized nanotubular titanium surfaces. Int J Nanomedicine. 2008;3(2):257–64.
55. Balasundaram G, Yao C, Webster TJ. TiO_2 nanotubes functionalized with regions of bone morphogenetic protein-2 increases osteoblast adhesion. J Biomed Mater Res A. 2008;84(2):447–53.
56. Choi AH, Ben-Nissan B, Matinlinna JP, Conway RC. Current perspectives: calcium phosphates nanocoatings and nanocomposite coatings in dentistry. J Dent Res. 2013;92:853–9.
57. Zhao L, Chu PK, Zhang Y, Wu Z. Antibacterial coatings on titanium implants. J Biomed Mater Res B Appl Biomater. 2009;91:470–80. https://doi.org/10.1002/jbm.b.31463.

58. Feridoun P, Javad Y, Vahid J, Solmaz MD. Overview of nanoparticle coating of dental implants for enhanced osseointegration and antimicrobial purposes. J Pharm Pharm Sci. 2017;20:148–60.
59. Hamouda IM. Current perspectives of nanoparticles in medical and dental biomaterials. J Biomed Res. 2012;26:143–51.
60. Maleki DS. Preparation and study of vitamin A palmitate microemulsion drug delivery system and investigation of co-surfactant effect. J Nanostruct Chem. 2013;3:1–6.
61. Bressan E, et al. Silver nanoparticles and mitochondrial interaction. Int J Dent. 2013;2013:01–8. https://doi.org/10.1155/2013/312747.
62. Zhang P, Zhang Z, Li W. Antibacterial TiO2 coating incorporating silver nanoparticles by microarc oxidation and ion implantation. J Nanomater. 2013;2013:2.
63. Memarzadeh K, Sharili AS, Huang J, Rawlinson SC, Allaker RP. Nanoparticulate zinc oxide as a coating material for orthopedic and dental implants. J Biomed Mater Res A. 2015;103:981–9.
64. Anu K, Maleeka Begum S, Rajesh G, Renuka Devi K. Wet biochemical synthesis of copper oxide nanoparticles coated on titanium dental implants. Int J Adv Res Sci Eng Technol. 2016;3:1191–4.
65. Gomez-Florit M, Pacha-Olivenza MA, Fernández-Calderón MC, Córdoba A, González-Martín ML, Monjo M, Ramis JM. Quercitrin-nanocoated titanium surfaces favour gingival cells against oral bacteria. Sci Rep. 2016;6:1–7.
66. Barbour ME, Maddocks SE, Wood NJ, Collins AM. Synthesis, characterization, and efficacy of antimicrobial chlorhexidine hexametaphosphate nanoparticles for applications in biomedical materials and consumer products. Int J Nanomedicine. 2013;8:3507–19.
67. Wood NJ, Jenkinson HF, Davis SA, Mann S, O'Sullivan DJ, Barbour ME. Chlorhexidine hexametaphosphate nanoparticles as a novel antimicrobial coating for dental implants. J Mater Sci Mater Med. 2015;26:1–10.
68. Katic J, Saric A, Despotovic I, Matijakovic N, Petkovic M, Petrovic Z. Bioactive coating on titanium dental implants for improved anticorrosion protection: a combined experimental and theoretical study. Coatings. 2019;9:612–24.
69. Jimbo R, Andersson M, Vandeweghe S. Nano in implant dentistry. Int J Dent. 2014;2014:1–2.

Nanobiomaterials in Craniofacial Bone Regeneration

Sepanta Hosseinpour, Ashwin Nanda, Chang Lei, Baboucarr Lowe, Qingsong Ye, and Chun Xu

Abstract Reconstruction of oral and craniofacial bone defects has been a challenging issue for maxillofacial surgeons, periodontists, and scientists. The application of nanomaterials in craniofacial bone regeneration is a newly advancing field which holds great capabilities for enhancing conventional therapeutic methods. Nanomaterials mimicking the nanostructure of bone tissue and representing distinctive smart functions are requisite for better bone regeneration in craniofacial region. In addition, nanobiomaterials can immobilize and deliver various bioactive molecules including small molecular drugs, growth factors and genes under a controlled manner, which promotes osteogenesis and angiogenesis. Several nanoparticle-based approaches such as nanohybrid scaffolds and nano-modified membranes were used to enhance bone regeneration for dental implant therapy, maxillary and mandibular bone reconstruction, and periodontal regeneration. Despite our knowledge in nanobiomaterials is rapidly growing, there are still concern regarding their standardization, safety, and efficacy for clinical applications. In this chapter, we highlight the applications of nanobiomaterials as bone scaffolds, delivery systems, and barrier membranes for craniofacial bone regeneration. The key challenges and future directions of nanomaterials for craniofacial bone regeneration are also discussed.

Keywords Nanomaterials · Biomaterials · Tissue engineering · Craniofacial bone reconstruction · Drug delivery · Nanotechnology · Scaffolds · Nanofibers

S. Hosseinpour (✉) · A. Nanda · B. Lowe · Q. Ye · C. Xu (✉)
School of Dentistry, The University of Queensland, Brisbane, QLD, Australia
e-mail: a.ye@uq.edu.au; chun.xu@uq.edu.au

C. Lei
Australian Institute for Bioengineering and Nanotechnology, The University of Queensland, Brisbane, QLD, Australia

R. S. Chaughule, R. Dashaputra (eds.), *Advances in Dental Implantology using Nanomaterials and Allied Technology Applications*,
https://doi.org/10.1007/978-3-030-52207-0_2

1 Introduction

Bone defects in craniofacial area caused by trauma, infections, congenial deformity, etc., are common and compromise the functions and aesthetics [1]. Various bone grafting materials [2, 3] have been applied to restore the structure and functions. Application of autologous bone grafting is the current gold standard in both orthopedic and cranio-maxillofacial bone repair [4, 5]. The autogenous bone grafts are obtained from surrounding tissues of the bone defects' site or from distant anatomical sites such as iliac crest or rib. However, autogenous bone grafts have limited supply and may cause nerve injury, pain, discomfort, and postoperative wound infections in the donor sites [6, 7]. In addition, failure in the long-term outcome can also be observed as massive resorption of the transplanted autogenous bone [8]. Allogenic bone grafts and various biomaterials such as hydroxyapatite (HA), tricalcium phosphate (TCP), and bioactive glass (BG) are receiving an increasing attention due to their large supply and no disease transmission. The traditional solid bioceramics are less satisfied due to their low bioactivities.

Nanomaterials with designed structures at the size range of several to several hundred nanometers (nm) present distinctive physical, chemical, and biological characteristics which are different from conventional bulk materials, and attract great attention in bone regeneration. For example, nanoparticles have been used for tracking mesenchymal stem cells (MSCs) [9, 10], and also for enhancing osteogenic differentiation towards various cells [11]. Nano-engineered scaffolds which mimic the structure of natural bone consist of a unique combination of hierarchical nano to macro structures that are designed and applied for craniofacial bone repairing. For example, by manupulating the designing of nanostructures, the mechanical properties of nanomaterials including their strength and stiffness can be turned to mimic natural bone structures [12]. In addition, various forms of nanomaterials such as nanofibers, nanotubes, and nanoparticles have recently emerged in the field of bone regeneration to improve the performance [13, 14].

In the stem cell-based therapy for bone tissue engineering, nano-/microscale interactions with different components of extracellular matrix showed a source of passive mechanical forces which can be influenced by a small-scale technology (Fig. 1). Nanotechnology fabricates a bio-inspired platform for regulating stem cell differentiation through advanced material design and/or smart drug delivery systems [12]. In the ensuing parts of this chapter, we will discuss nanomaterials incorporated scaffolds, nano-delivery systems, and nano-modified membranes for bone tissue engineering in craniofacial region.

2 Biological Mechanism of Bone Repair

Bone tissue is naturally structured with a unique pattern of collagen type one nanofibers and hydroxyapatite nanocrystals (Fig. 2). During bone regeneration process, assembly of these organic nanofibers with nano-inorganic crystals (biomineralization)

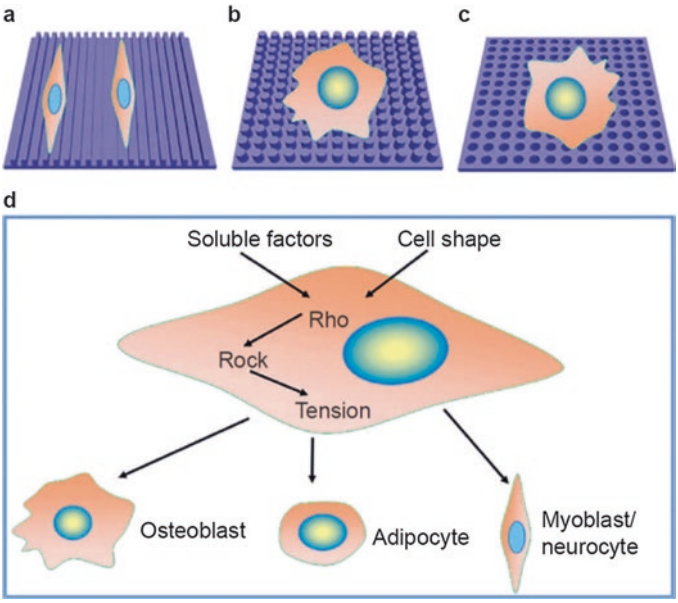

Fig. 1 Schematic shows the geometries of representative nanotopography. Stem cells can react to the passive forces by nanoscale design of materials (**a**–**c**). This "extracellular factors" can also alter the cell differentiation (**d**)

is essential. In vivo biomineralization is dependent on extracellular matrix for initiation (nucleation), growth, and determining the nanocrystals' orientations. Osteoblasts form osteoids by creating natural nanocomposites and secreting collagen fibrils [15].

Bone healing is a complex process that usually involves two process primary or secondary bone repair. Primary process only remodels lamellar bone in a correct anatomical reduction of bone, which may take months to years. Secondary process is the most common form of bone repair that occurs in bone defects or fractures, which consists of the following steps:

(a) Hematoma formation in the defect site that brings various growth factors and stem cells.
(b) Acute inflammation that recruits macrophages and neutrophils, and activates osteoprogenitor cells.
(c) Granulation tissue formation with active stem cell proliferation, extracellular matrix secretion, and angiogenesis.
(d) Biomineralization and differentiation of osteoprogenitor cells into osteoblasts, vascularization, and woven bone formation.
(e) Remodelling of the newly formed bone and formation of the Haversian system and osteoclasts [16].

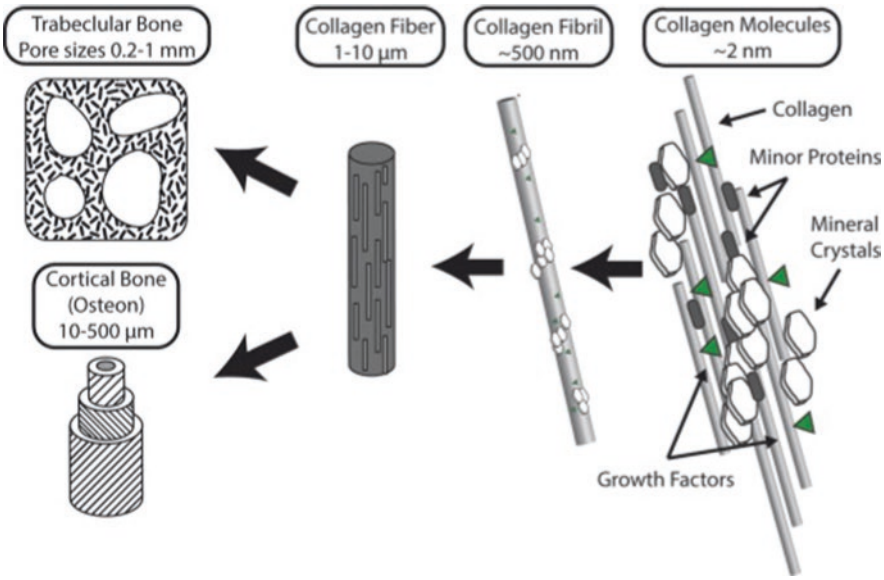

Fig. 2 Schematic nanostructure of bone tissue. Natural bone tissue consists of nanostructured oriented collagen fibers within an appetite nanocrystals structure

During these well-orchestrated cascades of biological events, numerous intra/extracellular signalling pathways and cell types participate to regenerate bone and rehabilitate the functions [17, 18]. It has been shown that platelet-derived growth factors (PDGF), transforming growth factors (TGF), and fibroblast growth factor (FGF) play important roles in the initiation and development of bone regeneration. PDGF and TGF-β are released immediately after bone injury by osteoblasts and chondrocytes [19, 20]. These growth factors have vital roles in the natural proliferation and differentiation of osteoprogenitor cells, and abnormal growth factor expressions can cause impaired healing [21].

3 Nanobiomaterials for Craniofacial Bone Regeneration

3.1 Nanobiomaterials-Based Bone Substitutes

Natural bone is made of organic constituents including collagen, glycoproteins, and glycosaminoglycan (GAGs) and inorganic phase mainly consisting of HA ($Ca_{10}(PO_4)6(OH)_2$) [22]. The presence of other elements such as silicon, magnesium, sodium, and potassium is also important for the physical property of the bone. To repair a bone defect, calcium in combination with phosphates forms the framework and other elements such as silicon helps in initial remineralization process. A wide diversity of bone substitute materials has been used in craniofacial bone regen-

eration, such as calcium phosphate, calcium carbonate, and calcium sulfate. Calcium phosphates show greater resistance to resorption when compared to calcium carbonates and calcium sulfates; hence calcium phosphates are more widely used as scaffold materials [23]. Calcium phosphate such as HA, biphasic ceramics, TCP, and bioactive glass (calcium with phosphates linked to silica glass) are added with small molecular drugs, growth factors, and genes for bone tissue regeneration [12]. HA is the most widely used bone repair materials and for the design of HA, In vitro studies demonstrated that HA with smaller size (nano-HA, 67 nm size) remarkably promoted osteoblast adhesion comparing to conventional HA with size of 179 nm. This may attribute to the high adsorption of vitronectin (a protein that promotes adhesion) on nano-HA ceramics [24]. Nano-HA were also applied for bone regeneration in sinus floor elevation surgery [25], where nano-HA showed similar bone repairing performance to freeze-dried allografts in vivo [26]. Although the application of nano-HA in extraction sockets showed hard tissue and soft tissue regeneration [27], nano-HA is brittle and its low mechanical strength is considered as a major limitation for its applications in bone regeneration. In this regard, many composite materials including PCL, PLA, and PLGA combined with nano-HA to improve their mechanical properties [28]. In fact, nanobiomaterials opened a new horizon for designing the most appropriate scaffolds for specific applications [28]. Based on the clinical purposes, they can generate specific characteristics, for instance, metallic nanomaterials including titanium and silver can be used in high-pressure areas [29, 30]. Ceramic nanomaterial scaffolds provide both metallic and nonmetallic properties [31], and composite nanomaterials often demonstrated a combination of dual functionality and biocompatibility with desired mechanical properties [32].

Nanomaterials in combination with drugs, genes, and proteins/enzymes initiate, accelerate, and configure bone regeneration in the body. Currently, researchers are stressing on their property of growth factors and enzyme delivery and sustained release in the affected site. They can be broadly classified as nanocomposite scaffolds, nanofibers scaffold, and nanoparticle incorporated in the scaffold [33].

3.1.1 Nanocomposite Scaffolds

Nanocomposites for bone repairing usually refer to a combination of polymers and inorganic nanoparticles that have been applied for bone regeneration due to their appropriate mechanical strength and good biocompatibility [34]. The new generation of materials can synergistically combine the advantages of polymers (e.g., lightweight, biocompatibility, and resilient) with the bioactive properties of inorganic nanoparticles [35]. The idea behind the application of nanomaterials is that, same scale materials to the bone infrastructure can improve materials' surfaces and bonding with surrounding bone tissues (Fig. 3) [36]. Previous studies demonstrated bioactivity of various nanoparticles including HA, TCP, and BG in a polymeric matrix which can be originated from polyethylene, polycaprolactone, and poly(ether ketone) in bone tissue engineering [34, 35].

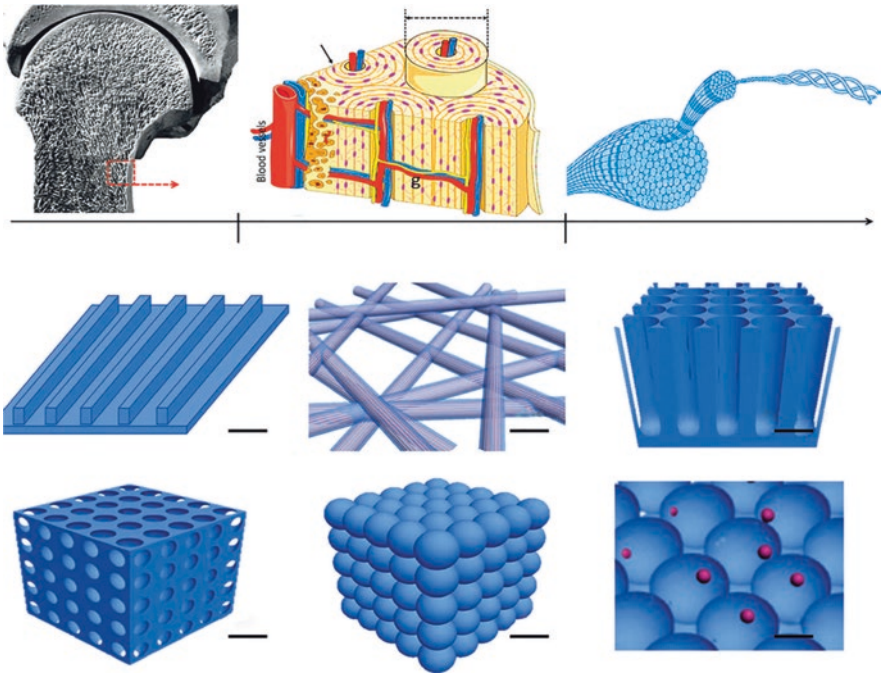

Fig. 3 The structure of natural bone at different scales and various nanostructured materials used in bone regeneration

3.1.2 Nanofiber Scaffolds

Nanofibrous incorporated scaffolds commonly consisted of fiber bundles (usually 10–500 nm) resembling collagen fiber bundles in the extracellular matrix. High surface-to-total-volume ratio improves cell adhesion, proliferation, and differentiation in these bone substitutes [37]. In fact, it has been shown that these nanofibrous scaffolds adsorb high amount of proteins and interact more properly with the cells which significantly increase osteoblasts attachments [38]. It was shown that the presence of nanofibers had a good impact on cell shaping and cell growth [39]. In vivo studies showed more bone formation after using nanofibrous scaffolds in comparison to solid bone substitutes [34, 40].

Fabrication of nanofiber scaffold is done by three methods: electrospinning, self-assembly, and phase separation. The electrospinning can be used for both synthetic and natural polymers. In the dentistry, gelatin membrane made by electrospinning has been used for periodontal tissue regeneration. Self-assembly is an autonomously forming process where components are arranged into a specific structure such as fibers. Some proteins can self-assemble to form complicated fibrous structures such as collagen, the main extracellular matrix in bone tissue. Phase separation is a process of quenching a single-phase polymer solution and separating the polymer into

a polymer-rich phase and a solvent-rich phase. The separation is thermodynamically preferred as the separated phases have lower free energy in the system [41]. With this method, nanofibers with a size of 100 nm can be formed and allow the fabrication of heterogeneous structures. Various designs of nanofibers scaffolds aim to mimicking the collagen fibers of natural bones. These architectural characteristics of nanofibers also enable the transport of cellular substances such as nutrients and signalling molecules [37].

3.1.3 Nanoparticle Incorporation in Scaffolds

Nanoparticles also can act as a bioactive component in scaffolds which enhance bone regeneration via sustained release [42]. Calcium- and silica-based nanoparticles have been shown to promote osteogenesis and angiogenesis which lead to a significant amount of newly regenerated bone [34]. In addition, they can deliver other bioactive molecules such as growth factors and provide a prolonged releasing period [43]. The addition of nanoparticles to polymer scaffolds mimics the deposition of apatite crystals onto the bone matrix, enhancing the cell response for regeneration [44]. In addition, nanoparticles embedded in scaffolds can improve the mechanical properties for bone tissue engineering applications [45].

3.2 Nano-Based Delivery Systems for Bone Regeneration

Nanotechnology and nano-based delivery systems are applied for bone regeneration and provide additional advantages compared to traditioanl delivery systems. Over past decades, nanotechnology has rapidly been developing in order to fabricate various nanocarriers including micellar formulations [46], polymer-drug incorporation [47], liposomal nanocarriers [48, 49], and inorganic nanoparticles [50] for delivery therapeutic agents [51, 52].

Nanomaterials with designed size and surface properties can carry small molecule drugs, nucleic acids, and proteins such as growth factors and antibodies [53]. In addition, recent investigations are working on “smart” nanoparticle-based delivery by adding some features to make them to be responsive in their biological environment. For instance, there are several nano-based delivery systems that are reacting to enzyme, pH, or redox levels alteration [54–56]. Figure 4 shows the current approaches for controlled release in nanocarriers.

Although the direct application of various bioactive molecules has been increasing for bone regeneration, direct administration has limitations such as non-specificity, low cellular uptake, and fast degradations [53]. These limitations lead to the usage of supra-physiological dosage which increased the risk of adverse effects and low efficiency. Nanoparticle-based carriers can able us to handle pharmacokinetics of the agents including protecting them from biodegradation. Nanoparticles as controlled drug delivery systems can enhance the efficacy by targeting specific cells and tissues

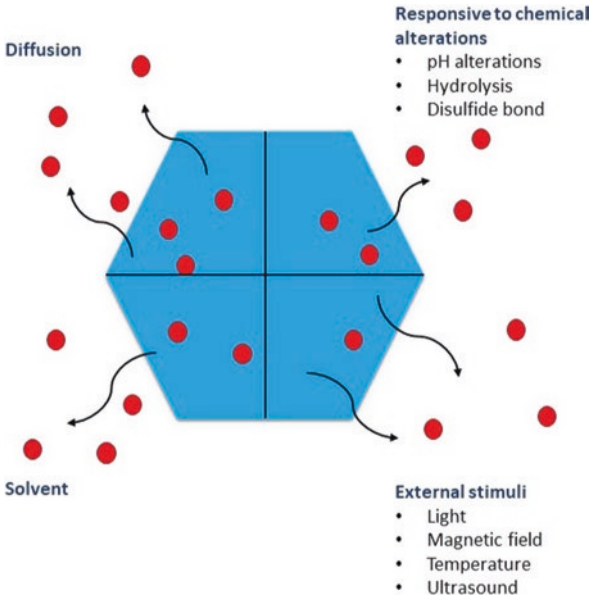

Fig. 4 Various mechanisms of controlled release systems of nanocarriers. Compared to simple diffusion, various responsive delivery systems are designed according to chemical or physical stimuli

[57], and improve transport properties by allowing more efficient deep penetration of therapeutic agents [58]. Nanoparticle-based delivery systems have several benefits in comparison to other approaches which include lower immune reaction, flexibility of designing to provide smart and low toxicity materials, and safety [59]. However, they often have low transfection efficiency [60]. On the other hand, there are various designing methods which can ameliorate this problem. In addition, their nano-dimensions cause a remarkable distinct physiochemical property that changes their fundamental characteristics including diffusivity, solubility, immunogenicity, and toxicity [57]. Several types of nanobiomaterials as delivery systems have been studied in bone regeneration. Silica nanoparticles (nS) because of their structure can carry high drug loadings and have the capacity of various surface modifications [61]. Several in vitro and in vivo studies showed no toxicity of silica particles (reviewed in [61]), and also FDA classified silica as "Generally Recognized as Safe" [61]. Clinical investigations demonstrated higher osteoinductivity and biocompatibility in silica nanoparticles incorporated bone substitutes [62–65]. In addition, silica nanoparticles inhibited bacteria adhesion and the unwanted inflammatory reaction [66, 67]. It has been shown that PLGA nanoparticles (nPLGA) can be used for target-specific and controlled delivery of drugs, antibodies, peptides, and growth factors (reviewed in [68]). In addition, nPLGA illustrated very little or no toxicity on cells and human organs [69, 70]. In the ensuing paragraphs, we will discuss the influencing physical factors, current applications of nanocarriers in bone regeneration, and existing challenges and future directions.

3.2.1 Physical Influential Factors

An effective nanocarrier not only should target specific cells and tissues, and efficient cellular uptake [71], but also avoid rapid clearance and immunogenic reactions [71, 72]. For instance, shape and size of these particles can determine their circulation time, the ability to pass through biological barriers, degradation, and drug release kinetics by affecting surface-to-volume ratio [73].

3.2.1.1 Shape and size

Nanoparticles' shape affects many delivery characteristics including cellular uptake, toxicity, and biodistribution [74]. For instance, in comparison to sphere shape, nonspherical shapes have higher specific surface area that can provide more feasible modifications opportunity for delivery systems. On the other hand, nonspherical shapes delineated decreased cellular uptake and biodistribution, and increased immunogenicity [74]. In addition to cell uptake, biodistribution of nanoparticles can be significantly influenced by their diverse geometry (rods, quasi-hemispherical, cylinder, etc.). Decuzzi and Ferrari reported that among silica nanoparticles with four different shapes (spherical, discoidal, quasi-hemispherical, and cylindrical), cylindrical shape particles mostly accumulated in the liver, whereas spherical silica nanoparticles mainly collected in the reticuloendothelial system [75]. Recent studies revealed that nanoparticles shape also modulates immune responses. Kumar et al. represented that rod-shaped polystyrene nanoparticles stimulate Th1 cells to produce antibody while spherical nanoparticles induced Th2 cells antibody expressions [76]. Moreover, ellipsoidal PLGA nanoparticles showed significant induction of CD-8^+ cells compared to spherical similar particles both in vitro and in vivo [77]. These phenomena can be explained by different antigen presentations to immune cells which caused different immune reactions, but the exact mechanism of this process is still unknown.

The other important physical factor of nanocarriers is their size [78, 79]. Zhang et al. demonstrated that size rather than shape can influence toxicity and biodistribution of nanogold particles. In fact, they showed that nanogold particles are distributed in different organs based on their sizes [80]. Moreover, cell uptake efficacy can be significantly altered by nanoparticles size. For instance, Mou et al. exhibited that mesoporous silica nanoparticles (MSNs) with 50 nm diameter had the best cellular uptake efficiency among a range of 30–280 nm MSNs particles [81]. Nanotechnology also facilitates controlling delivery efficacy of nanoparticles by using various designing methods. For instance, Fig. 5 demonstrated a nanolithographical method for the preparation of a nanostructured surface with nanogold particles to bind with BMP-2 [82]. In this technique, the size of gold nanoparticles can be exactly determined which offers a molecular-level controlling capability for growth factors delivery.

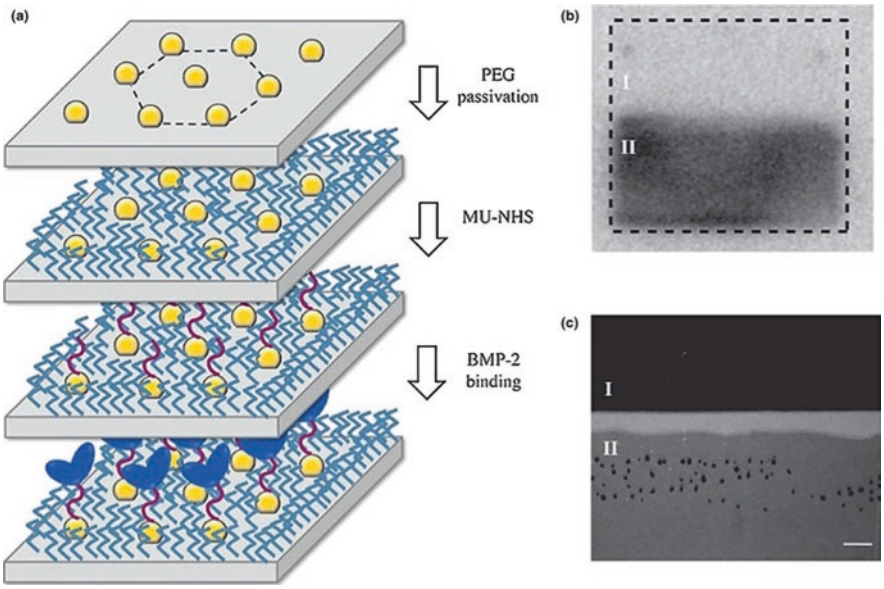

Fig. 5 Preparation of a nanostructured surface with nanogold particles to bind with bone morphogenic protein-2 (BMP-2) [82]. In this approach, polyethylene glycol (PEG) was used to inhibit unspecific adhesion of biological products and BMP-2 immobilized on the surface by binding covalently to the amines linkers (**a**). Phosphor imaging and fluorescent results confirmed the specific binding of BMP-2 to the functionalized nanomaterial surface (**b, c**)

3.2.1.2 Surface Modifications and Surface Roughness

Recently, surface-modified nanoparticles are becoming attractive drug carriers. In this regard, mostly natural or synthetic polymers are used to prepare nanoparticles [83]. The surface characteristics of nanoparticles are more important in comparison to the core due to the direct contact of this layer with cells, extracellular matrix, and fluids. In this regard, nanoparticles can be coated by various hydrophilic polymers for longer circulation in the body or can be conjugated with specific ligand proteins in order to site-specific delivery.

Lin et al. demonstrated that the transmembrane transport of MSNs is closely related to their surface zeta potentials and thus MSNs with positive charged surface can enter the cells more effectively than negatively charged similar nanoparticles [84]. Many surface modifications including polyethylenimine (PEI), amino group, and poly-L-lysine [85, 86] have been introduced to enhance cell uptake. But usually, cationic additive groups cause cytotoxicity and poor bio-stability [87].

Another physical factor is the surface roughness, which can improve protein adsorption capacity. Previous studies have shown that surface roughness can enhance cellular uptake in solid nanoparticles [88, 89]. Although it can influence cell uptake, it has a little contribution to lysosomal or endosomal escape and mostly surface modifications such as hydrophobic surface modification can improve these processes [90].

3.2.2 Current Application of Nanocarriers in Bone Regeneration

Nanomaterials commonly were applied for the delivery of growth factors, drugs, and nucleic acids (gene delivery) in bone tissue engineering [91]. In the following paragraphs, we discuss the concept of nanoparticle-based delivery systems for each of these categories. In addition, some of the most frequent nanocarriers and their applications in bone regeneration are summerized.

Growth factors, especially bone morphogenic proteins (BMPs), mainly regulate the bone repair process [92]. A multitude of approaches have been investigated to deliver and immobilize these factors to the bone substitutes or dental implants [93]. One possiblity is to incorporate growth factors into nanoparticles [94, 95]. In this regard, nanoscale materials are offering a advantage of molecular-level immobilization of scaffolds [80]. For instance, Cao et al. prepared a chitosan nanoparticle incorporated hydrogel loaded with BMP-2 and revealed that this combination increases cell proliferation, and adhesion in vitro, and bone regeneration in rabbits' radial critical-sized defects [96]. In addition, chitosan nanoparticle BMP-2 loaded hydrogel showed a significantly higher amount of new bone formation and bone marrow cavity consolidation in comparison to BMP-2 loaded hydrogel. Another improvement that can be done by nanoparticles is the sequential growth factor delivery. Previously BMP-2 and BMP-7 co-delivery were achieved by nanocarriers that constituted two different polymers (PLGA and poly(3-hydroxybutyrate-co-3-hydroxyvalerate) (PHBV)) with different biodegradation periods. In comparison to simultaneous delivery, this approach significantly enhanced the proliferation and differentiation of MSCs [97].

Another application of nanocarriers is for local drug delivery systems in bone tissue engineering [98]. One of the most common drugs that were used in bone regeneration is dexamethasone [88, 91]. Oliveira et al. produced a dexamethasone loaded dendrimer NPs and they have shown that these pH-responsive drug-loaded dendrimers enhanced ectopic bone formation in rat models [99–101] (Fig. 6). These evidences confirm that nanoparticles can provide a preprograming capability of delivery systems for bone tissue regeneration.

Another application of nanocarriers in bone regeneration is gene delivery. Although viral vectors have shown great transduction efficacy, there are some limitations to their clinical applications due to the potential safety and immunogenicity concerns [102]. Nonviral vectors such as nanocarriers have been applied to transport genes in a safer way in comparison to their viral counterparts [103]. Nanoparticles with rational design can pass through the cell membrane and escape from endosome/lysosome [91]. Kim et al. applied amine-modified MSNs for delivering BMP-2 DNA into rat MSCs [104]. The functionalization of MSNs with amine groups and enhanced its transfection ability up to 18%, and totally 66% of MSCs were transfected after 7 days. In another study, Santos et al. used PAMAM dendrimers for BMP-2 transfection which also demonstrated an efficient way of gene delivery for bone regeneration [105]. Other small nucleotide sequences such as microRNAs and small interfering RNAs which regulate several biological mechanisms post-transcriptionally also can be delivered by nanoparticles. For instance,

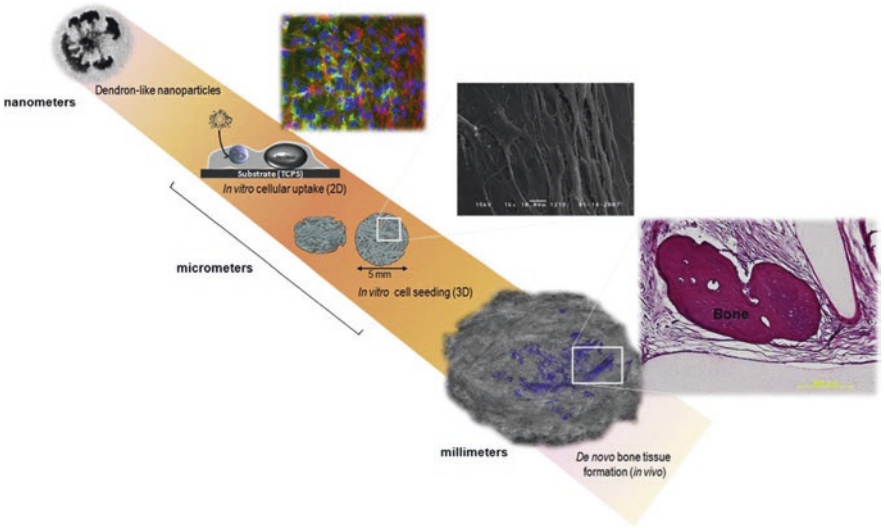

Fig. 6 Schematic diagram of Oliveira's approach for using Dendron-like nanoparticles for dexamethasone delivery in bone defects [99]. In this approach, dendritic nanoparticles were internalized into the stem cells and after that seeded on the scaffolds to enhance bone regeneration in vivo

microRNA-148b was transferred by a photoactivated delivery system by Qureshi et al. [106]. They designed a nano-silver delivery system and loaded microRNA via photocleavable links. They confirmed the osteogenic induction of adipose-derived stem cells in vitro and in vitro controlled by light [107].

Nanoparticles with various compositions are now available for preclinical research and clinical applications to deliver desired drug, growth factors, or bioactive molecules (Fig. 7). The most common nanoparticles that are being applied as a delivery system in bone tissue engineering consist of two major categories, organic or inorganic particles, and are discussed in the following part.

3.2.2.1 Liposomes

Liposomes are vesicles of mono- or bilayer of natural phospholipids which are commonly used as vehicles for drug delivery. For fabricating liposome carriers, genetic molecules are incorporated inside the liposome that can be done with two potential methods based on the hydrophobic or hydrophilic nature of the desired molecules [108]. Liposomes are biodegradable and biocompatible. In addition, technically it is feasible to functionalize liposome to react to light, pH, and other stimuli which made them the most frequent clinically applied nanoscale delivery system with many commercialized types [110].

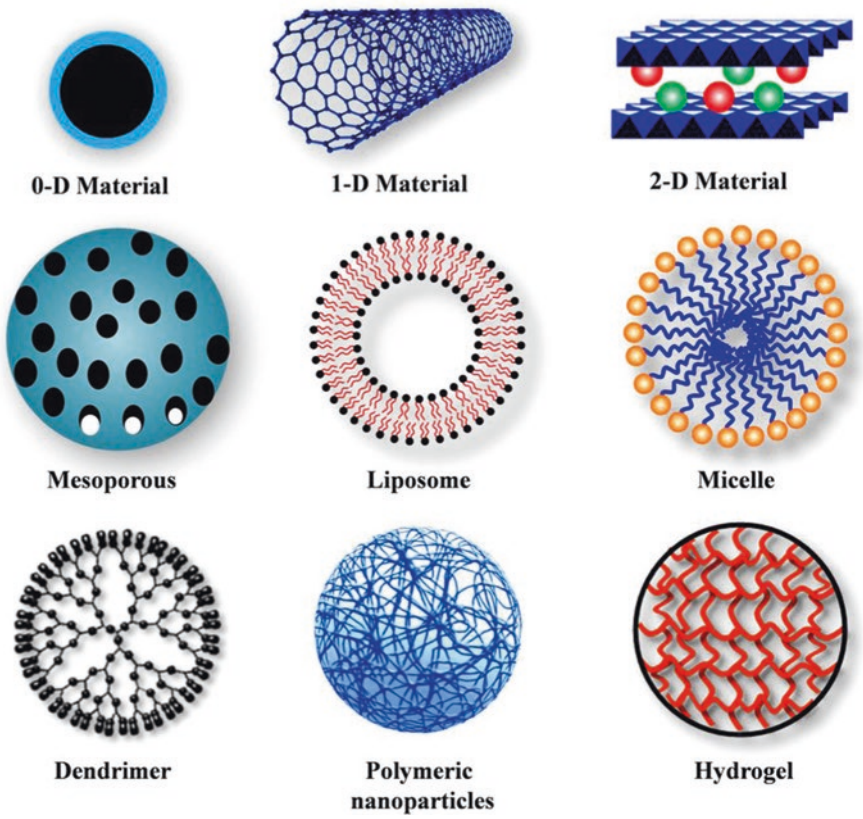

Fig. 7 Different types of nanocarriers used as controlled delivery vehicles

3.2.2.2 Dendrimers

Dendrimers are nanoparticles made of polymers with tree-like structures. These nanoparticles are usually biocompatible and biodegradable [111]. Its inner site commonly includes amine or other molecules with multiple reaction sites [112], and the surrounding functional groups provide a unique physicochemical property. These nanocarriers are also able to be responsive to various stimuli such as ionic condition, temperature, light, and pH [113]. Dendrimers are frequently used for target delivery with reliably reproducible results and appropriate pharmacokinetics in clinical applications [114].

3.2.2.3 Polymeric Nanoparticles

Nowadays, polymeric nanoparticles have been attracting attention due to their unique physical properties, various molecular architecture, biodegradability, and biocompatibility. In addition, their fabrication methods are flexible and various functionalization

techniques are available [116]. Commonly polymeric nanoparticles are of spherical shape with 100 nm diameter that can modify according to their applications. Polymeric micelles, spherical nanoparticles (Nanocapsules), and nanofibers are the most frequent type of these categories. Polymeric nanoparticles have a great loading capacity of various inorganic or organic molecules which can be dispersed, dissolved, or covalently linked with their monomers [116]. Hence, they are currently applied as a delivery system in cancer treatment, vaccination, inflammatory diseases, and tissue engineering [116–118]. Similar to other nanocarriers, polymeric nanoparticles can be functionalized with different methods generally based on the size of the ligand. Small ligand can be added to them before or after formation [119, 120]. However, larger molecules including polysaccharides, antibodies, or growth factors usually denature during fabrication; therefore, preferably they are linked at the surface of nanocarriers [121].

3.2.2.4 Nanofibers

Incorporating bioactive molecules directly into the materials is a novel strategy of smart delivery systems. But the incorporation of molecules especially proteins directly into scaffold is technically hard to procedure due to the desired molecules that may denature during fabrication procedure or cannot be released after scaffold forming. In this regard, nanofibers gained increasing attention because of their ability to mimicking natural extracellular matrix structures with high encapsulation efficiency of bioactive molecules [122, 123]. These nanofibers exhibited a gentle release pattern of different molecules without the initial burst release [95, 124]. Nanofibers can act as delivery vehicles with encapsulating desired molecules at specific sites and releasing them with various mechanisms such as erosion or degradation of fibers, and diffusion of factors. Figure 8 showed a specific designing of nanofiber scaffold for co-delivery of Dex and BMP-2 that gradually released by degradation of nanofibers and enhanced bone regeneration in an animal model [95].

3.2.2.5 Silica and Mesoporous Silica Nanoparticles

Silica is a biocompatible and chemically stable material used in various medical applications including drug delivery [125]. According to their application silica nanoparticles can be synthesized as mesoporous silica nanoparticles (MSNs), bulk silica nanoparticles, or core/shell silica nanoparticles. For controlled drug release usage, usually MSNs are applied because of their distinct pore size and structure, various morphologies, their resistance to heat, pH, and mechanical stress, and their low toxicity and ease of fabrication [126, 127]. Considering their pore size and volume that can precisely control during fabrication, they can be loaded by various numbers of molecules including small molecular drugs and growth factors [128].

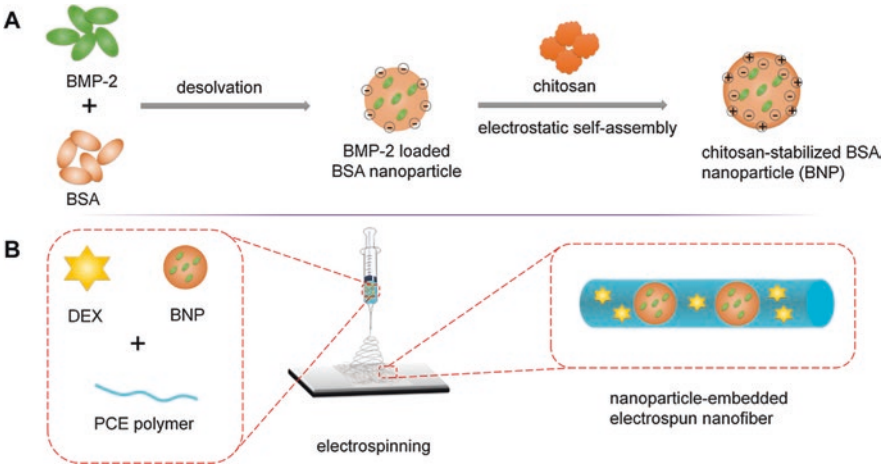

Fig. 8 Schematic illustration of the nanofiber loading process. (**a**) The formation of chitosan nanoparticles with BMP-2 loaded BSA. (**b**) Electrospinning of nanoparticle-embedded copolymer nanofibers [95]

3.2.2.6 Ceramic and Glass Nanoparticles

Bioceramic nanoparticles have been applied for enhancing scaffolds' physical properties, and also controlled delivery of various bioactive molecules [129, 130]. Despite that the synthesis of some of the bioceramic nanoparticles, especially bioactive glasses, is not simple, they attracted a lot of attention due to their advantages [131, 132]. Both natural and synthetic nanoscaled molecules can also add to them to produce a nanostructure delivery system [133, 134]. In addition, calcium phosphate nanoparticles have been previously used for gene delivery system in bone defect. DNA-functionalized calcium phosphate nanoparticles effectively delivered BMP-2 genes over 10 days [135].

3.2.2.7 Carbon Nanotubes

After the discovery of carbon nanotubes in the 1990s, they have been used in a wide variety of fields including microscopy, biosensing, reinforcing materials, and drug delivery systems [136]. These materials are graphitic tubular structures which are made of carbon atoms with a very high chemical and physical stability. Given their tubular molecular structure, they can be functionalized from inside and outside which provide a great opportunity for fabricating different delivery systems [137]. However, for clinical applications it is still needed to perform deeper toxicity tests due to the fact that several variables including diameter, charge, purity, etc., influence carbon nanotube's cytotoxicity [138].

3.2.2.8 Metallic Nanoparticles

Metallic nanoparticles demonstrated distinct properties, and are different from bulk nanoparticles due to the quantic effect [139]. Gold nanoparticles among metallic nanoparticles have been applied for many purposes, such as bioimaging, biosensing, and drug delivery [140–142]. This versatility is due to their several surface modifications, optical properties, and biocompatibility [143]. Gold nanoparticles are synthesized with various shapes including rods, spheres, cages, and star-like [91]. These nanoparticles were used to deliver bisphosphonate drugs previously [144, 145]. For instance, recently alendronate (a common bisphosphonate) is successfully delivered by gold nanoparticles in animal models and human [146].

3.2.2.9 Magnetic Nanoparticles

This group of nanocarriers consists of metallic or metallic oxide cores and inorganic or polymer coating [147]. Similar to the aforementioned nanoparticles, they can be functionalized for target drug release. Application of magnetic nanoparticles as drug delivery systems provided the opportunity to control specific target locations with an external magnetic field. Some of these materials have been successfully administered in bone regeneration for growth factors and gene delivery [122].

3.3 Nano-Modified Membrane Barriers for Guided Bone Regeneration

Generally, the growth speeds of connective tissue are faster than bone tissue. As a result, the invasion of fibrous tissue occurs in bone defect sites resulting in a barrier that prevents the growth of new bone [148, 149]. This invasion of connective tissues leads to anatomical aberrations and may need additional surgery for removal [150, 151]. Guided tissue/bone regeneration (GTR or GBR) is a well-established method that utilizes a barrier membrane against connective tissue invasion and promotes osteogenesis or bone augmentation forming (Fig. 9) [152–154]. Recent studies showed that membranes with drug delivery system could promote the periodontal ligament and alveolar bone regeneration (Fig. 9) [147, 149–151]. Currently, this method is widely used for periodontal regeneration and dental implants [149, 155].

Many researchers have tried to fabricate and modify GTR/GBR membranes by mixing synthetic and natural components by various techniques including film casting [156–158], dynamic filtration [159], and spinning [160]. In addition, these membranes can be prepared with drug and growth factors [156, 157, 161]. However, a material with appropriate degradability, biological, and mechanical properties is still requisite for in vivo GBR. Although these methods showed some major advancement, their application in clinical settings is still limited due to difficulty in handling and non-homogenous degradation rate [162]. Recent advances in nano-

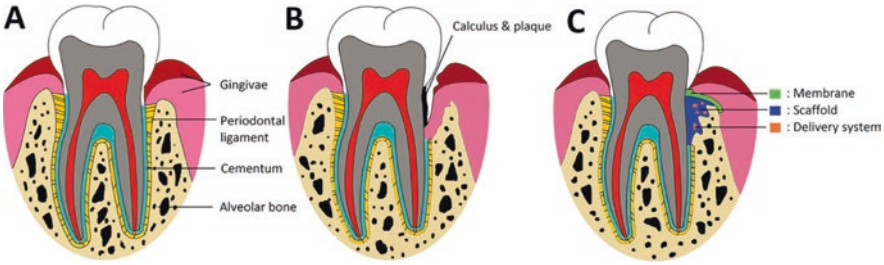

Fig. 9 A schematic illustration illustrating the normal periodontal tissues (**a**); injured periodontium in periodontitis (**b**); and forms of nanobiomaterials applied for periodontal regeneration (**c**)

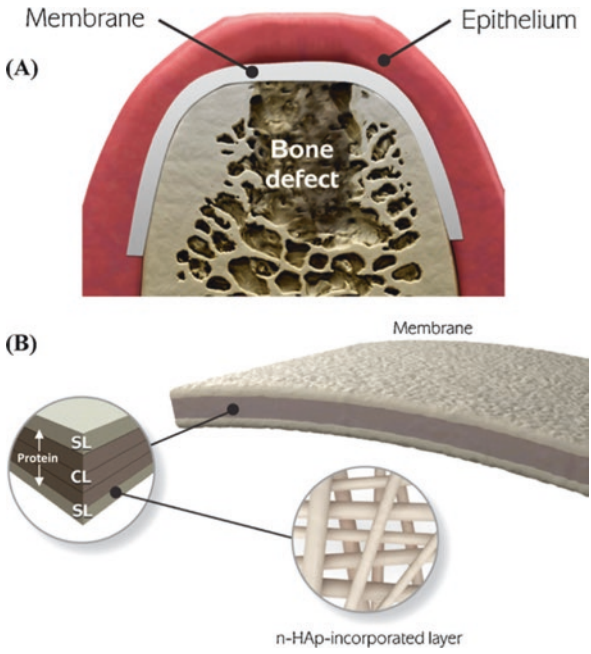

Fig. 10 Schematic demonstration of the spatially designed membrane (**a**), and its different layer with nano-hydroxyapatite incorporation (**b**)

technology increased the chance of fabricating biomimetic multifunctional membranes for periodontal GBR. Figure 10 showed a sample of these novel fabrications with the usage of nano-HA.

In a study by Wu et al. (2017), surface-modified chitosan nanofibrous membrane was applied in GBR of a critical-sized calvaria model in rats. The nanofibrous chitosan membrane was initially generated by electrospinning and surface modified using a butyrylation method. The process of surface modification proved advantageous in creating desirable fibrous morphology, increase in mechanical stability, reduced rapid swelling, attracted the adhesion and proliferation of fibroblast, and promoted regeneration [163]. The mechanical property of the GBR regenerative membrane strongly influences the nature of clinical applicability [164]. For example, in another study, a ratio (60:40 wt%) of nano-β-TCP particles and polycaprolactone,

respectively, yields a high bending property suitable for regeneration of large mandibular defect [165].

An approach to synchronize mechanical property and regenerative function inspires the development of multiple layered barrier membranes. The combination of carbonated nHA/PLGA using biomimetic and casting techniques can create porous and smooth surfaces on opposite sides of the membrane. This approach can control membrane flexibility, mechanical strength, and rate of biodegradation, altogether enhancing the biocompatibility and osteoconductivity function of the HA nanoparticles [157]. The nanoparticles can mimic the mineral crystals of the body and induce a significant change in the mechanical properties and regenerative quality of the membrane [166]. The fabrication of a robust regenerative membrane with bioactive compounds to support adequate regeneration of osteoporotic bone remains a major clinical challenge. In a recent study, functionalized nHA/carbon nanotubes with graphene oxides promoted osteointegration and regenerative bioactivity essential for the repair of osteopenic bony defects [167].

The use of electrospinning to fabricate the bilayered GBR membrane is an ideal option to enhance flexibility and mechanical strength. The biocompatible polyester (PCL) and polyglycerol sebacate (elastomeric polymer) are ideal candidates for this method. The bioactivity of the membrane can be further enhanced by the incorporation of β-TCP nanoparticles, which is osteoconductive and resorbable to support successful regeneration of bony defect [168]. For the same purpose, bilayered silk fibroin/PCL-PEG-PCL electrospun membranes were combined with nanocalcium phosphate. The synthesis of nanocalcium phosphate was done using a distinct approach, using a flame spray pyrolysis method. In this method, synthetic precursors of the calcium phosphate (liquid form) are pumped through a nozzle, dispersed by oxygen, ignited with methane and oxygen premixed gases. The nanoparticles are further collected on glass fiber filter above the flame and incorporated into the electrospun polymeric matrix. The membrane attracted apatite nucleation, induced mineralization, and enhanced osteoconductivity. Furthermore, the tensile strength of the membrane increased with the two-layered polymeric matrices maintaining stable coherent phases [169].

In another approach, the GBR membrane can be fabricated using a solution casting method with biocompatible, naturally derived polymeric microsphere. In this method, chitosan microspheres are initially generated and blended with a slurry of nHA particles using a wet chemical precipitation method and casted. An in situ biomimetic method can generate nHA/chitosan composite microsphere applicable in fabricating a GBR membrane. The incorporation of the microsphere can significantly enhance the mechanical property of the membrane. Meanwhile, microsphere-containing membrane has the advantage of maintaining space, improving biomimetic function, and promoting effective regeneration of bony defects [170]. The regenerative function of the GBR with antimicrobial properties can accelerate healing and regeneration of bony defects. The strategy to generate these kinds of membrane takes into consideration microbial control and efficient recapitulation of the extracellular matrix [171]. Additionally, GBR membranes are fabricated to release drugs, serve as regenerative barrier, and guide bone regeneration. In this direction, Tang et al. (2016) fabricated a GBR membrane comprising a PLGA/HA (core) and collagen/amoxicillin (shell) via coaxial electrospinning

method. The core-shell nanofiber adequately prevented the invasion of fibroblast into the area of the bony defect, due to the small pores of the membrane, together with its hydrophobic property. The in vitro results confirmed the nanofibrous membrane having the capacity to induce apatite nucleation and efficiently release the drug (amoxicillin) [172]. The functional behavior of polymeric membrane can be decorated, by the addition of silica nanoparticles and osteoconductive polymeric surfaces. First, the silica nanoparticles are synthesized to achieve mono-sized units via a sol-gel Stöber's method [173] to overcome particle aggregation, and poor interaction between polymeric interfaces, before electrospinning [174]. It is worth noting that the GBR membrane might have different properties, in terms of structure, regenerative performance, and degradability. However, the membrane must be sufficient in stiffness and biocompatibility to prevent collapse and avoid soft tissue invasion into the defect area. As such, these key properties will define an ideal membrane: (1) biocompatibility, (2) space-making, (3) cell occlusiveness, (4) tissue integration, and (5) resorbability [175].

4 Current State and Challenges of Nanobiomaterials Application

While promising results are demonstrated using nanomaterials for craniofacial bone regeneration, several challenges and prerequisites need to be addressed prior to translation to clinical settings. The first challenge is to optimize the biocompatibility and mechanical properties. For instance, nanomaterial-based hydrogel demonstrated a perfect cell proliferation during bone regeneration, but its mechanical properties are not suitable for some bone defects. On the other hand, the application of nanopolymers can strengthen hydrogel scaffold, however decrease its cellular biocompatibility [176]. In order to enhance cell viability, although novel scaffold fabrication techniques including electrospinning and 3D printing have been presented, until now, these methods have not been applied for nanomaterial-based craniofacial bone regeneration [176]. The second important issue is the immunogenic properties of the nanomaterials. Despite a bone substitute may totally mimic natural bone structure or even show superior cell viability, it may also cause some severe immune response in some individuals [177].

The other issue is nanomaterials' long-term potential side effects and toxicity. The ultra-small size of nanoparticles allows them to interact with normally unreachable substrates for their bigger counterparts [178]. Those particles' toxicity relies on numerous variables, such as particle size, surface charge, shape, administration manner etc. [179]. For instance, nanoparticles applied in oral cavity may enter into liver and spleen via bloodstream through the gastrointestinal route [178, 180]. In this regard, the systemic distribution of nanoparticles by the gastrointestinal tract and bloodstream demonstrated its neurotoxicity in zebra fish [179, 181]. In addition, most data about nanomaterial toxicity is based on in vitro dose-response assays in vitro [182]. More in vitro evaluating tests are needed to facilitate their further safe administrations.

5 Conclusion and Future Direction

The development of nanotechnology in bone tissue engineering presents greater diversity in designing scaffolds for enhancing proliferation, adhesion, and differentiation. Nanobiomaterials, by mimicking the nanostructure of natural bone tissue, represented promoted osteoblasts functions in comparison to their microstructured counterparts. Several studies have delineated the potential of nanoparticles for improving drug delivery and membrane barriers in bone regeneration. These materials showed a precise and smart immobilization of various growth factors in order to improve vascularization. In addition, nanofibers resemble the native extracellular matrix to provide a better microenvironment for bone regeneration.

Although there is still a need for further knowing the mechanisms and finding practical ways especially investigating in vivo long-term safety, for applying them in the craniofacial region, it is hoped this rapidly growing field will help us to reach efficient therapeutic approaches for craniofacial defects.

References

1. Dimitriou R, Jones E, McGonagle D, Giannoudis PV. Bone regeneration: current concepts and future directions. BMC Med. 2011;9(1):66.
2. Giannoudis PV, Dinopoulos H, Tsiridis E. Bone substitutes: an update. Injury. 2005;36(Suppl 3):20–7.
3. Giannoudis PV, Einhorn TA. Bone morphogenetic proteins in musculoskeletal medicine. Injury. 2009;40(Suppl 3):S1–3.
4. Nauth A, Lane J, Watson JT, Giannoudis P. Bone graft substitution and augmentation. J Orthop Trauma. 2015;29:S34–S8.
5. Piitulainen JM, Kauko T, Aitasalo KM, Vuorinen V, Vallittu PK, Posti JP. Outcomes of cranioplasty with synthetic materials and autologous bone grafts. World Neurosurg. 2015;83(5):708–14.
6. Lee JH, Hutzler LH, Shulman BS, Karia RJ, Egol KA. Does risk for malnutrition in patients presenting with fractures predict lower quality measures? J Orthop Trauma. 2015;29(8):373–8.
7. Reddy S, Khalifian S, Flores JM, Bellamy J, Manson PN, Rodriguez ED, et al. Clinical outcomes in cranioplasty: risk factors and choice of reconstructive material. Plast Reconstr Surg. 2014;133(4):864–73.
8. Iaccarino C, Viaroli E, Fricia M, Serchi E, Poli T, Servadei F. Preliminary results of a prospective study on methods of cranial reconstruction. J Oral Maxillofac Surg. 2015;73(12):2375–8.
9. Rosen AB, Kelly DJ, Schuldt AJ, Lu J, Potapova IA, Doronin SV, et al. Finding fluorescent needles in the cardiac haystack: tracking human mesenchymal stem cells labeled with quantum dots for quantitative in vivo three-dimensional fluorescence analysis. Stem Cells. 2007;25(8):2128–38.
10. Wang C, Cheng L, Xu H, Liu Z. Towards whole-body imaging at the single cell level using ultra-sensitive stem cell labeling with oligo-arginine modified upconversion nanoparticles. Biomaterials. 2012;33(19):4872–81.
11. Yi C, Liu D, Fong C-C, Zhang J, Yang M. Gold nanoparticles promote osteogenic differentiation of mesenchymal stem cells through p38 MAPK pathway. ACS Nano. 2010;4(11):6439–48.
12. Gong T, Xie J, Liao J, Zhang T, Lin S, Lin Y. Nanomaterials and bone regeneration. Bone Res. 2015;3:15029.

13. McMahon RE, Wang L, Skoracki R, Mathur AB. Development of nanomaterials for bone repair and regeneration. J Biomed Mater Res B. 2013;101(2):387–97.
14. Chen CS, Mrksich M, Huang S, Whitesides GM, Ingber DE. Geometric control of cell life and death. Science. 1997;276(5317):1425–8.
15. Li Y, Liu C. Nanomaterial-based bone regeneration. Nanoscale. 2017;9(15):4862–74.
16. Loi F, Córdova LA, Pajarinen J, Lin T-H, Yao Z, Goodman SB. Inflammation, fracture and bone repair. Bone. 2016;86:119–30.
17. Einhorn TA. The cell and molecular biology of fracture healing. Clin Orthop Relat Res. 1998;355(Suppl):S7–21.
18. Cho TJ, Gerstenfeld LC, Einhorn TA. Differential temporal expression of members of the transforming growth factor beta superfamily during murine fracture healing. J Bone Miner Res. 2002;17(3):513–20.
19. Fei Y, Gronowicz G, Hurley MM. Fibroblast growth factor-2, bone homeostasis and fracture repair. Curr Pharm Des. 2013;19(19):3354–63.
20. Giganti MG, Tresoldi I, Masuelli L, Modesti A, Grosso G, Liuni FM, et al. Fracture healing: from basic science to role of nutrition. Front Biosci. 2014;19:1162–75.
21. Wang Q, Yan J, Yang J, Li B. Nanomaterials promise better bone repair. Mater Today. 2016;19(8):451–63.
22. Nisbet D, Forsythe JS, Shen W, Finkelstein D, Horne MK. A review of the cellular response on electrospun nanofibers for tissue engineering. J Biomater Appl. 2009;24(1):7–29.
23. Rezwan K, Chen Q, Blaker J, Boccaccini AR. Biodegradable and bioactive porous polymer/inorganic composite scaffolds for bone tissue engineering. Biomaterials. 2006;27(18):3413–31.
24. Zhang L, Webster TJ. Nanotechnology and nanomaterials: promises for improved tissue regeneration. Nano Today. 2009;4(1):66–80.
25. Ghanaati S, Lorenz J, Obreja K, Choukroun J, Landes C, Sader RA. Nanocrystalline hydroxyapatite-based material already contributes to implant stability after 3 months: a clinical and radiologic 3-year follow-up investigation. J Oral Implantol. 2014;40(1):103–10.
26. Sadeghi R, Najafi M, Semyari H, Mashhadiabbas F. Histologic and histomorphometric evaluation of bone regeneration using nanocrystalline hydroxyapatite and human freeze-dried bone graft. J Orofac Orthop. 2017;78(2):144–52.
27. Reichert C, Wenghoefer M, Kutschera E, Götz W, Jäger A. Ridge preservation with synthetic nanocrystalline hydroxyapatite reduces the severity of gingival invaginations—a prospective clinical study. J Orofac Orthop. 2014;75(1):7–15.
28. Li G, Zhou T, Lin S, Shi S, Lin Y. Nanomaterials for craniofacial and dental tissue engineering. J Dent Res. 2017;96(7):725–32.
29. Dhivya S, Ajita J, Selvamurugan N. Metallic nanomaterials for bone tissue engineering. J Biomed Nanotechnol. 2015;11(10):1675–700.
30. Tevlin R, McArdle A, Atashroo D, Walmsley G, Senarath-Yapa K, Zielins E, et al. Biomaterials for craniofacial bone engineering. J Dent Res. 2014;93(12):1187–95.
31. Padovani GC, Feitosa VP, Sauro S, Tay FR, Durán G, Paula AJ, et al. Advances in dental materials through nanotechnology: facts, perspectives and toxicological aspects. Trends Biotechnol. 2015;33(11):621–36.
32. Choi A, Ben-Nissan B, Matinlinna J, Conway R. Current perspectives: calcium phosphate nanocoatings and nanocomposite coatings in dentistry. J Dent Res. 2013;92(10):853–9.
33. Kim K, Fisher JP. Nanoparticle technology in bone tissue engineering. J Drug Target. 2007;15(4):241–52.
34. Gera S, Sampathi S, Dodoala S. Role of nanoparticles in drug delivery and regenerative therapy for bone diseases. Curr Drug Deliv. 2017;14(7):904–16.
35. Sahoo NG, Pan YZ, Li L, He CB. Nanocomposites for bone tissue regeneration. Nanomedicine. 2013;8(4):639–53.
36. Sato M, Webster TJ. Nanobiotechnology: implications for the future of nanotechnology in orthopedic applications. Expert Rev Med Dev. 2004;1(1):105–14.

37. Smith L, Ma P. Nano-fibrous scaffolds for tissue engineering. Colloid Surf B. 2004;39(3):125–31.
38. Woo KM, Chen VJ, Ma PX. Nano-fibrous scaffolding architecture selectively enhances protein adsorption contributing to cell attachment. J Biomed Mater Res A. 2003;67(2):531–7.
39. Tuzlakoglu KN, Bolgen AJ, Salgado ME, Gomes EP, Reis RL. J Mater Sci Mater M. 2005;16:1099–104.
40. Woo KM, Chen VJ, Jung H-M, Kim T-I, Shin H-I, Baek J-H, et al. Comparative evaluation of nanofibrous scaffolding for bone regeneration in critical-size calvarial defects. Tissue Eng Part A. 2009;15(8):2155–62.
41. Gupte M, Ma P. Nanofibrous scaffolds for dental and craniofacial applications. J Dent Res. 2012;91(3):227–34.
42. Quaglia F. Bioinspired tissue engineering: the great promise of protein delivery technologies. Int J Pharm. 2008;364(2):281–97.
43. Vo TN, Kasper FK, Mikos AG. Strategies for controlled delivery of growth factors and cells for bone regeneration. Adv Drug Deliv Rev. 2012;64(12):1292–309.
44. Smith I, Liu X, Smith L, Ma P. Nanostructured polymer scaffolds for tissue engineering and regenerative medicine. Wiley Interdiscip Rev Nanomed Nanobiotechnol. 2009;1(2):226–36.
45. Hasan A, Morshed M, Memic A, Hassan S, Webster TJ, Marei HE-S. Nanoparticles in tissue engineering: applications, challenges and prospects. Int J Nanomed. 2018;13:5637.
46. Jeong JH, Kim SW, Park TG. Molecular design of functional polymers for gene therapy. Prog Polym Sci. 2007;32(11):1239–74.
47. Pasut G, Veronese F. Polymer–drug conjugation, recent achievements and general strategies. Prog Polym Sci. 2007;32(8–9):933–61.
48. Samad A, Sultana Y, Aqil M. Liposomal drug delivery systems: an update review. Curr Drug Deliv. 2007;4(4):297–305.
49. Torchilin VP. Recent advances with liposomes as pharmaceutical carriers. Nat Rev Drug Discov. 2005;4(2):145.
50. Duncan R. The dawning era of polymer therapeutics. Nat Rev Drug Discov. 2003;2(5):347.
51. Obeid MA, Al Qaraghuli MM, Alsaadi M, Alzahrani AR, Niwasabutra K, Ferro VA. Delivering natural products and biotherapeutics to improve drug efficacy. Ther Deliv. 2017;8(11):947–56.
52. Miele E, Spinelli GP, Miele E, Di Fabrizio E, Ferretti E, Tomao S, et al. Nanoparticle-based delivery of small interfering RNA: challenges for cancer therapy. Int J Nanomedicine. 2012;7:3637.
53. van Rijt S, Habibovic P. Enhancing regenerative approaches with nanoparticles. J R Soc Interface. 2017;14(129):20170093.
54. Liu D, Yang F, Xiong F, Gu N. The smart drug delivery system and its clinical potential. Theranostics. 2016;6(9):1306.
55. Song Y, Li Y, Xu Q, Liu Z. Mesoporous silica nanoparticles for stimuli-responsive controlled drug delivery: advances, challenges, and outlook. Int J Nanomedicine. 2017;12:87.
56. Ding C, Tong L, Feng J, Fu J. Recent advances in stimuli-responsive release function drug delivery systems for tumor treatment. Molecules. 2016;21(12):1715.
57. Patra JK, Das G, Fraceto LF, Campos EVR, del Pilar R-TM, Acosta-Torres LS, et al. Nano based drug delivery systems: recent developments and future prospects. J Nanobiotechnol. 2018;16(1):71.
58. Arayne MS, Sultana N, Qureshi F. Nanoparticles in delivery of cardiovascular drugs. Pak J Pharm Sci. 2007;20(4):340–8.
59. Suri SS, Fenniri H, Singh B. Nanotechnology-based drug delivery systems. J Occup Med Toxicol. 2007;2(1):16.
60. Curtin CM, Castaño IM, O'Brien FJ. Scaffold-based microRNA therapies in regenerative medicine and cancer. Adv Healthc Mater. 2018;7(1):1700695.
61. Watermann A, Brieger J. Mesoporous silica nanoparticles as drug delivery vehicles in cancer. Nano. 2017;7(7):189.

62. Arcos D, Vallet-Regí M. Sol–gel silica-based biomaterials and bone tissue regeneration. Acta Biomater. 2010;6(8):2874–88.
63. Madhumathi K, Kumar PS, Kavya K, Furuike T, Tamura H, Nair S, et al. Novel chitin/nanosilica composite scaffolds for bone tissue engineering applications. Int J Biol Macromol. 2009;45(3):289–92.
64. Hesaraki S, Alizadeh M, Borhan S, Pourbaghi-Masouleh M. Polymerizable nanoparticulate silica-reinforced calcium phosphate bone cement. J Biomed Mater Res B. 2012;100(6):1627–35.
65. Wu C-J, Gaharwar AK, Schexnailder PJ, Schmidt G. Development of biomedical polymer-silicate nanocomposites: a materials science perspective. Materials. 2010;3(5):2986–3005.
66. Cousins B, Allison H, Doherty P, Edwards C, Garvey M, Martin D, et al. Effects of a nanoparticulate silica substrate on cell attachment of Candida albicans. J Appl Microbiol. 2007;102(3):757–65.
67. Besinis A, De Peralta T, Handy RD. The antibacterial effects of silver, titanium dioxide and silica dioxide nanoparticles compared to the dental disinfectant chlorhexidine on Streptococcus mutans using a suite of bioassays. Nanotoxicology. 2014;8(1):1–16.
68. Mir M, Ahmed N, ur Rehman A. Recent applications of PLGA based nanostructures in drug delivery. Colloid Surf B. 2017;159:217–31.
69. Trif M, Florian PE, Roseanu A, Moisei M, Craciunescu O, Astete CE, et al. Cytotoxicity and intracellular fate of PLGA and chitosan-coated PLGA nanoparticles in Madin–Darby bovine kidney (MDBK) and human colorectal adenocarcinoma (Colo 205) cells. J Biomed Mater Res A. 2015;103(11):3599–611.
70. Alqahtani S, Simon L, Astete CE, Alayoubi A, Sylvester PW, Nazzal S, et al. Cellular uptake, antioxidant and antiproliferative activity of entrapped α-tocopherol and γ-tocotrienol in poly (lactic-co-glycolic) acid (PLGA) and chitosan covered PLGA nanoparticles (PLGA-Chi). J Colloid Interface Sci. 2015;445:243–51.
71. Caldorera-Moore M, Guimard N, Shi L, Roy K. Designer nanoparticles: incorporating size, shape and triggered release into nanoscale drug carriers. Expert Opin Drug Deliv. 2010;7(4):479–95.
72. Ferrari M. Cancer nanotechnology: opportunities and challenges. Nat Rev Cancer. 2005;5(3):161.
73. Dunne M, Corrigan O, Ramtoola Z. Influence of particle size and dissolution conditions on the degradation properties of polylactide-co-glycolide particles. Biomaterials. 2000;21(16):1659–68.
74. Jindal AB. The effect of particle shape on cellular interaction and drug delivery applications of micro-and nanoparticles. Int J Pharm. 2017;532(1):450–65.
75. Decuzzi P, Ferrari M. The receptor-mediated endocytosis of nonspherical particles. Biophys J. 2008;94(10):3790–7.
76. Kumar S, Anselmo AC, Banerjee A, Zakrewsky M, Mitragotri S. Shape and size-dependent immune response to antigen-carrying nanoparticles. J Control Release. 2015;220:141–8.
77. Sunshine JC, Perica K, Schneck JP, Green JJ. Particle shape dependence of CD8+ T cell activation by artificial antigen presenting cells. Biomaterials. 2014;35(1):269–77.
78. Blank F, Stumbles PA, Seydoux E, Holt PG, Fink A, Rothen-Rutishauser B, et al. Size-dependent uptake of particles by pulmonary antigen-presenting cell populations and trafficking to regional lymph nodes. Am J Respir Cell Mol Biol. 2013;49(1):67–77.
79. Joshi VB, Geary SM, Salem AK. Biodegradable particles as vaccine delivery systems: size matters. AAPS J. 2013;15(1):85–94.
80. Zhang J, Nie X, Ji Y, Liu Y, Wu X, Chen C, et al. Quantitative biokinetics and systemic translocation of various gold nanostructures are highly dependent on their size and shape. J Nanosci Nanotechnol. 2014;14(6):4124–38.
81. Lu F, Wu SH, Hung Y, Mou CY. Size effect on cell uptake in well-suspended, uniform mesoporous silica nanoparticles. Small. 2009;5(12):1408–13.

82. Schwab EH, Pohl TL, Haraszti TS, Schwaerzer GK, Hiepen C, Spatz JP, et al. Nanoscale control of surface immobilized BMP-2: toward a quantitative assessment of BMP-mediated signaling events. Nano Lett. 2015;15(3):1526–34.
83. Choi SW, Kim WS, Kim JH. Surface modification of functional nanoparticles for controlled drug delivery. J Dispers Sci Technol. 2003;24(3–4):475–87.
84. Igor S, Brian GT, Victor S-YL. J Am Chem Soc 2006;128(46):14792–14793.
85. Manzano M, Aina V, Arean C, Balas F, Cauda V, Colilla M, et al. Studies on MCM-41 mesoporous silica for drug delivery: effect of particle morphology and amine functionalization. Chem Eng J. 2008;137(1):30–7.
86. Xia T, Kovochich M, Liong M, Meng H, Kabehie S, George S, et al. Polyethyleneimine coating enhances the cellular uptake of mesoporous silica nanoparticles and allows safe delivery of siRNA and DNA constructs. ACS Nano. 2009;3(10):3273–86.
87. Jackson DA, Juranek S, Lipps HJ. Designing nonviral vectors for efficient gene transfer and long-term gene expression. Mol Ther. 2006;14(5):613–26.
88. Niu Y, Yu M, Hartono SB, Yang J, Xu H, Zhang H, et al. Nanoparticles mimicking viral surface topography for enhanced cellular delivery. Adv Mater. 2013;25(43):6233–7.
89. Massignani M, LoPresti C, Blanazs A, Madsen J, Armes SP, Lewis AL, et al. Controlling cellular uptake by surface chemistry, size, and surface topology at the nanoscale. Small. 2009;5(21):2424–32.
90. Niu Y, Yu M, Meka A, Liu Y, Zhang J, Yang Y, et al. Understanding the contribution of surface roughness and hydrophobic modification of silica nanoparticles to enhanced therapeutic protein delivery. J Mater Chem B. 2016;4(2):212–9.
91. Vieira S, Vial S, Reis RL, Oliveira JM. Nanoparticles for bone tissue engineering. Biotechnol Prog. 2017;33(3):590–611.
92. Reddi AH. Morphogenetic messages are in the extracellular matrix: biotechnology from bench to bedside. London: Portland Press Limited; 2000.
93. Luginbuehl V, Meinel L, Merkle HP, Gander B. Localized delivery of growth factors for bone repair. Eur J Pharm Biopharm. 2004;58(2):197–208.
94. Zhang S, Kucharski C, Doschak MR, Sebald W, Uludağ H. Polyethylenimine–PEG coated albumin nanoparticles for BMP-2 delivery. Biomaterials. 2010;31(5):952–63.
95. Li L, Zhou G, Wang Y, Yang G, Ding S, Zhou S. Controlled dual delivery of BMP-2 and dexamethasone by nanoparticle-embedded electrospun nanofibers for the efficient repair of critical-sized rat calvarial defect. Biomaterials. 2015;37:218–29.
96. Cao L, Werkmeister JA, Wang J, Glattauer V, McLean KM, Liu C. Bone regeneration using photocrosslinked hydrogel incorporating rhBMP-2 loaded 2-N, 6-O-sulfated chitosan nanoparticles. Biomaterials. 2014;35(9):2730–42.
97. Yilgor P, Hasirci N, Hasirci V. Sequential BMP-2/BMP-7 delivery from polyester nanocapsules. J Biomed Mater Res A. 2010;93(2):528–36.
98. Buckley L, Humphrey MB. Glucocorticoid-Induced Osteoporosis. N Engl J Med. 2018;379(26):2547–56.
99. Oliveira JM, Sousa RA, Malafaya PB, Silva SS, Kotobuki N, Hirose M, et al. In vivo study of dendronlike nanoparticles for stem cells “tune-up”: from nano to tissues. Nanomedicine. 2011;7(6):914–24.
100. Oliveira JM, Sousa RA, Kotobuki N, Tadokoro M, Hirose M, Mano JF, et al. The osteogenic differentiation of rat bone marrow stromal cells cultured with dexamethasone-loaded carboxymethylchitosan/poly (amidoamine) dendrimer nanoparticles. Biomaterials. 2009;30(5):804–13.
101. Oliveira JM, Kotobuki N, Tadokoro M, Hirose M, Mano J, Reis R, et al. Ex vivo culturing of stromal cells with dexamethasone-loaded carboxymethylchitosan/poly (amidoamine) dendrimer nanoparticles promotes ectopic bone formation. Bone. 2010;46(5):1424–35.
102. Yin H, Kanasty RL, Eltoukhy AA, Vegas AJ, Dorkin JR, Anderson DG. Non-viral vectors for gene-based therapy. Nat Rev Genet. 2014;15(8):541.

103. Lu C-H, Chang Y-H, Lin S-Y, Li K-C, Hu Y-C. Recent progresses in gene delivery-based bone tissue engineering. Biotechnol Adv. 2013;31(8):1695–706.
104. Kim TH, Kim M, Eltohamy M, Yun YR, Jang JH, Kim HW. Efficacy of mesoporous silica nanoparticles in delivering BMP-2 plasmid DNA for in vitro osteogenic stimulation of mesenchymal stem cells. J Biomed Mater Res A. 2013;101(6):1651–60.
105. Santos JL, Oramas E, Pêgo AP, Granja PL, Tomás H. Osteogenic differentiation of mesenchymal stem cells using PAMAM dendrimers as gene delivery vectors. J Control Release. 2009;134(2):141–8.
106. Qureshi AT, Monroe WT, Dasa V, Gimble JM, Hayes DJ. miR-148b–Nanoparticle conjugates for light mediated osteogenesis of human adipose stromal/stem cells. Biomaterials. 2013;34(31):7799–810.
107. Qureshi AT, Doyle A, Chen C, Coulon D, Dasa V, Del Piero F, et al. Photoactivated miR-148b–nanoparticle conjugates improve closure of critical size mouse calvarial defects. Acta Biomater. 2015;12:166–73.
108. Gulati M, Grover M, Singh S, Singh M. Lipophilic drug derivatives in liposomes. Int J Pharm. 1998;165(2):129–68.
109. Al-Jamal WT, Kostarelos K. Liposomes: from a clinically established drug delivery system to a nanoparticle platform for theranostic nanomedicine. Acc Chem Res. 2011;44(10):1094–104.
110. Hu X, Liu G, Li Y, Wang X, Liu S. Cell-penetrating hyperbranched polyprodrug amphiphiles for synergistic reductive milieu-triggered drug release and enhanced magnetic resonance signals. J Am Chem Soc. 2014;137(1):362–8.
111. Menjoge AR, Kannan RM, Tomalia DA. Dendrimer-based drug and imaging conjugates: design considerations for nanomedical applications. Drug Discov Today. 2010;15(5–6):171–85.
112. Tomalia DA. Birth of a new macromolecular architecture: dendrimers as quantized building blocks for nanoscale synthetic polymer chemistry. Prog Polym Sci. 2005;30(3–4):294–324.
113. Kojima C. Design of stimuli-responsive dendrimers. Expert Opin Drug Deliv. 2010;7(3):307–19.
114. Milhem O, Myles C, McKeown N, Attwood D, D'Emanuele A. Polyamidoamine Starburst® dendrimers as solubility enhancers. Int J Pharm. 2000;197(1–2):239–41.
115. Mecke A, Majoros IJ, Patri AK, Baker JR Jr, Banaszak Holl MM, Orr BG. Lipid bilayer disruption by polycationic polymers: the roles of size and chemical functional group. Langmuir. 2005;21(23):10348–54.
116. Nicolas J, Mura S, Brambilla D, Mackiewicz N, Couvreur P. Design, functionalization strategies and biomedical applications of targeted biodegradable/biocompatible polymer-based nanocarriers for drug delivery. Chem Soc Rev. 2013;42(3):1147–235.
117. Hu X, Liu G, Li Y, Wang X, Liu S. Cell-penetrating hyperbranched polyprodrug amphiphiles for synergistic reductive milieu-triggered drug release and enhanced magnetic resonance signals. J Am Chem Soc. 2015;137(1):362–8.
118. Hu X, Hu J, Tian J, Ge Z, Zhang G, Luo K, et al. Polyprodrug amphiphiles: hierarchical assemblies for shape-regulated cellular internalization, trafficking, and drug delivery. J Am Chem Soc. 2013;135(46):17617–29.
119. Thamake SI, Raut SL, Gryczynski Z, Ranjan AP, Vishwanatha JK. Alendronate coated poly-lactic-co-glycolic acid (PLGA) nanoparticles for active targeting of metastatic breast cancer. Biomaterials. 2012;33(29):7164–73.
120. Verderio P, Bonetti P, Colombo M, Pandolfi L, Prosperi D. Intracellular drug release from curcumin-loaded PLGA nanoparticles induces G2/M block in breast cancer cells. Biomacromolecules. 2013;14(3):672–82.
121. Xie Z, Su Y, Kim GB, Selvi E, Ma C, Aragon-Sanabria V, et al. Immune cell-mediated biodegradable theranostic nanoparticles for melanoma targeting and drug delivery. Small. 2017;13(10). https://doi.org/10.1002/smll.201603121
122. Li Y, Ye D, Li M, Ma M, Gu N. Adaptive materials based on iron oxide nanoparticles for bone regeneration. ChemPhysChem. 2018;19(16):1965–79.

123. Maity D, Agrawal DC. Synthesis of iron oxide nanoparticles under oxidizing environment and their stabilization in aqueous and non-aqueous media. J Magn Magn Mater. 2007;308(1):46–55.
124. Zhou X, Feng W, Qiu K, Chen L, Wang W, Nie W, et al. BMP-2 derived peptide and dexamethasone incorporated mesoporous silica nanoparticles for enhanced osteogenic differentiation of bone mesenchymal stem cells. ACS Appl Mater Interfaces. 2015;7(29):15777–89.
125. Tang Y, Zhao Y, Wang X, Lin T. Layer-by-layer assembly of silica nanoparticles on 3D fibrous scaffolds: enhancement of osteoblast cell adhesion, proliferation, and differentiation. J Biomed Mater Res A. 2014;102(11):3803–12.
126. Slowing II, Vivero-Escoto JL, Wu CW, Lin VS. Mesoporous silica nanoparticles as controlled release drug delivery and gene transfection carriers. Adv Drug Deliv Rev. 2008;60(11):1278–88.
127. Yang KN, Zhang CQ, Wang W, Wang PC, Zhou JP, Liang XJ. pH-responsive mesoporous silica nanoparticles employed in controlled drug delivery systems for cancer treatment. Cancer Biol Med. 2014;11(1):34–43.
128. Xu C, Lei C, Yu C. Mesoporous silica nanoparticles for protein protection and delivery. Front Chem. 2019;7:290.
129. Madhumathi K, Sampath Kumar TS. Regenerative potential and anti-bacterial activity of tetracycline loaded apatitic nanocarriers for the treatment of periodontitis. Biomed Mater (Bristol, England). 2014;9(3):035002.
130. Choi B, Cui ZK, Kim S, Fan J, Wu BM, Lee M. Glutamine-chitosan modified calcium phosphate nanoparticles for efficient siRNA delivery and osteogenic differentiation. J Mater Chem B. 2015;3(31):6448–55.
131. Pina S, Oliveira JM, Reis RL. Natural-based nanocomposites for bone tissue engineering and regenerative medicine: a review. Adv Mater (Deerfield Beach, Fla). 2015;27(7):1143–69.
132. Yao Q, Li W, Yu S, Ma L, Jin D, Boccaccini AR, et al. Multifunctional chitosan/polyvinyl pyrrolidone/45S5 Bioglass(R) scaffolds for MC3T3-E1 cell stimulation and drug release. Mater Sci Eng C Mater Biol Appl. 2015;56:473–80.
133. Ji L, Wang W, Jin D, Zhou S, Song X. In vitro bioactivity and mechanical properties of bioactive glass nanoparticles/polycaprolactone composites. Mater Sci Eng C Mater Biol Appl. 2015;46:1–9.
134. Leite ÁJ, Caridade SG, Mano JF. Synthesis and characterization of bioactive biodegradable chitosan composite spheres with shape memory capability. J Non-Cryst Solids. 2016;432:158–66.
135. Tenkumo T, Vanegas Saenz JR, Takada Y, Takahashi M, Rotan O, Sokolova V, et al. Gene transfection of human mesenchymal stem cells with a nano-hydroxyapatite-collagen scaffold containing DNA-functionalized calcium phosphate nanoparticles. Genes Cells. 2016;21(7):682–95.
136. Zhang Y, Bai Y, Yan B. Functionalized carbon nanotubes for potential medicinal applications. Drug Discov Today. 2010;15(11–12):428–35.
137. Balasubramanian K, Burghard M. Chemically functionalized carbon nanotubes. Small. 2005;1(2):180–92.
138. Liu Y, Zhao Y, Sun B, Chen C. Understanding the toxicity of carbon nanotubes. Acc Chem Res. 2013;46(3):702–13.
139. Zhao P, Li N, Astruc D. Review. Coord Chem Rev. 2013;257(3–4):638–65.
140. Vial S, Nykypanchuk D, Yager KG, Tkachenko AV, Gang O. Linear mesostructures in DNA—nanorod self-assembly. ACS Nano. 2013;7(6):5437–45.
141. Zhang YS, Wang Y, Wang L, Wang Y, Cai X, Zhang C, et al. Labeling human mesenchymal stem cells with gold nanocages for in vitro and in vivo tracking by two-photon microscopy and photoacoustic microscopy. Theranostics. 2013;3(8):532–43.
142. Guo R, Zhang L, Qian H, Li R, Jiang X, Liu B. Multifunctional nanocarriers for cell imaging, drug delivery, and near-IR photothermal therapy. Langmuir. 2010;26(8):5428–34.

143. Yeh YC, Creran B, Rotello VM. Gold nanoparticles: preparation, properties, and applications in bionanotechnology. Nanoscale. 2012;4(6):1871–80.
144. Cenni E, Avnet S, Granchi D, Fotia C, Salerno M, Micieli D, et al. The effect of poly(d,l-lactide-co-glycolide)-alendronate conjugate nanoparticles on human osteoclast precursors. J Biomater Sci Polym Ed. 2012;23(10):1285–300.
145. Fanord F, Fairbairn K, Kim H, Garces A, Bhethanabotla V, Gupta VK. Bisphosphonate-modified gold nanoparticles: a useful vehicle to study the treatment of osteonecrosis of the femoral head. Nanotechnology. 2011;22(3):035102.
146. Lee D, Heo DN, Kim HJ, Ko WK, Lee SJ, Heo M, et al. Inhibition of osteoclast differentiation and bone resorption by bisphosphonate-conjugated gold nanoparticles. Sci Rep. 2016;6:27336.
147. Sun C, Lee JS, Zhang M. Magnetic nanoparticles in MR imaging and drug delivery. Adv Drug Deliv Rev. 2008;60(11):1252–65.
148. Hunter KT, Ma T. In vitro evaluation of hydroxyapatite–chitosan–gelatin composite membrane in guided tissue regeneration. J Biomed Mater Res A. 2013;101(4):1016–25.
149. Xu C, Lei C, Meng L, Wang C, Song Y. Chitosan as a barrier membrane material in periodontal tissue regeneration. J Biomed Mater Res B. 2012;100(5):1435–43.
150. Gottlow J, Nyman S, Dahlin C, Linde A, et al. Healing of bone defects by guided tissue regeneration. Plast Reconstr Surg. 1988;81(5):672–6.
151. Fiorellini J, Howell T, Cochran D, Malmquist J, Lilly LC, Spagnoli D, Tolijaric J, Jones A, Nevins M. Randomizes study evaluation rhBMP-2 for extraction socket augmentation. J Periodontol. 2005;76(4):605–13.
152. Kim HS, Kim JT, Jung YJ, Ryu SC, Son HJ, Kim YG. Preparation of a porous chitosan/fibroin-hydroxyapatite composite matrix for tissue engineering. Macromol Res. 2007;15(1):65–73.
153. Ueyama Y, Ishikawa K, Mano T, Koyama T, Nagatsuka H, Suzuki K, et al. Usefulness as guided bone regeneration membrane of the alginate membrane. Biomaterials. 2002;23(9):2027–33.
154. Ignatius AA, Ohnmacht M, Claes LE, Kreidler J, Palm F. A composite polymer/tricalcium phosphate membrane for guided bone regeneration in maxillofacial surgery. J Biomed Mater Res. 2001;58(5):564–9.
155. Veríssimo DM, Leitão RF, Figueiró SD, Góes JC, Lima V, Silveira CO, et al. Guided bone regeneration produced by new mineralized and reticulated collagen membranes in critical-sized rat calvarial defects. Exp Biol Med. 2015;240(2):175–84.
156. Liao S, Watari F, Zhu Y, Uo M, Akasaka T, Wang W, et al. The degradation of the three layered nano-carbonated hydroxyapatite/collagen/PLGA composite membrane in vitro. Dent Mater. 2007;23(9):1120–8.
157. Liao S, Wang W, Uo M, Ohkawa S, Akasaka T, Tamura K, et al. A three-layered nano-carbonated hydroxyapatite/collagen/PLGA composite membrane for guided tissue regeneration. Biomaterials. 2005;26(36):7564–71.
158. Milella E, Barra G, Ramires PA, Leo G, Aversa P, Romito A. Poly(L-lactide)acid/alginate composite membranes for guided tissue regeneration. J Biomed Mater Res. 2001;57(2):248–57.
159. Teng SH, Lee EJ, Yoon BH, Shin DS, Kim HE, Oh JS. Chitosan/nanohydroxyapatite composite membranes via dynamic filtration for guided bone regeneration. J Biomed Mater Res A. 2009;88(3):569–80.
160. Bottino MC, Thomas V, Janowski GM. A novel spatially designed and functionally graded electrospun membrane for periodontal regeneration. Acta Biomater. 2011;7(1):216–24.
161. Kikuchi M, Koyama Y, Yamada T, Imamura Y, Okada T, Shirahama N, et al. Development of guided bone regeneration membrane composed of beta-tricalcium phosphate and poly (L-lactide-co-glycolide-co-epsilon-caprolactone) composites. Biomaterials. 2004;25(28):5979–86.
162. Bottino MC, Thomas V, Schmidt G, Vohra YK, Chu TM, Kowolik MJ, et al. Recent advances in the development of GTR/GBR membranes for periodontal regeneration—a materials perspective. Dent Mater. 2012;28(7):703–21.

163. Wu C, Su H, Karydis A, Anderson KM, Ghadri N, Tang S, et al. Mechanically stable surface-hydrophobilized chitosan nanofibrous barrier membranes for guided bone regeneration. Biomed Mater. 2017;13(1):015004.
164. Fujihara K, Kotaki M, Ramakrishna S. Guided bone regeneration membrane made of polycaprolactone/calcium carbonate composite nano-fibers. Biomaterials. 2005;26(19):4139–47.
165. Kikuchi M, Koyama Y, Yamada T, Imamura Y, Okada T, Shirahama N, et al. Development of guided bone regeneration membrane composed of β-tricalcium phosphate and poly (L-lactide-co-glycolide-co-ε-caprolactone) composites. Biomaterials. 2004;25(28):5979–86.
166. Yang F, Both SK, Yang X, Walboomers XF, Jansen JA. Development of an electrospun nano-apatite/PCL composite membrane for GTR/GBR application. Acta Biomater. 2009;5(9):3295–304.
167. Oliveira FC, Carvalho JO, Gusmão SBS, de Sousa GL, Mendes LMS, Freitas SAP, et al. High loads of nano-hydroxyapatite/graphene nanoribbon composites guided bone regeneration using an osteoporotic animal model. Int J Nanomedicine. 2019;14:865.
168. Rad MM, Khorasani SN, Ghasemi-Mobarakeh L, Prabhakaran MP, Foroughi MR, Kharaziha M, et al. Fabrication and characterization of two-layered nanofibrous membrane for guided bone and tissue regeneration application. Mater Sci Eng C. 2017;80:75–87.
169. Türkkan S, Pazarçeviren AE, Keskin D, Machin NE, Duygulu Ö, Tezcaner A. Nanosized CaP-silk fibroin-PCL-PEG-PCL/PCL based bilayer membranes for guided bone regeneration. Mater Sci Eng C. 2017;80:484–93.
170. Huang D, Niu L, Li J, Du J, Wei Y, Hu Y, et al. Reinforced chitosan membranes by microspheres for guided bone regeneration. J Mech Behav Biomed Mater. 2018;81:195–201.
171. Jin S, Li J, Wang J, Jiang J, Zuo Y, Li Y, et al. Electrospun silver ion-loaded calcium phosphate/chitosan antibacterial composite fibrous membranes for guided bone regeneration. Int J Nanomedicine. 2018;13:4591.
172. Tang Y, Chen L, Zhao K, Wu Z, Wang Y, Tan Q. Fabrication of PLGA/HA (core)-collagen/amoxicillin (shell) nanofiber membranes through coaxial electrospinning for guided tissue regeneration. Compos Sci Technol. 2016;125:100–7.
173. Diba M, Wang H, Kodger TE, Parsa S, Leeuwenburgh SC. Highly elastic and self-healing composite colloidal gels. Adv Mater. 2017;29(11):1604672.
174. Castro AG, Diba M, Kersten M, Jansen JA, van den Beucken JJ, Yang F. Development of a PCL-silica nanoparticles composite membrane for guided bone regeneration. Mater Sci Eng C. 2018;85:154–61.
175. Caballé-Serrano J, Munar-Frau A, Ortiz-Puigpelat O, Soto-Penaloza D, Peñarrocha M, Hernández-Alfaro F. On the search of the ideal barrier membrane for guided bone regeneration. J Clin Exp Dent. 2018;10(5):e477.
176. Orciani M, Fini M, Di Primio R, Mattioli-Belmonte M. Biofabrication and bone tissue regeneration: cell source, approaches, and challenges. Front Bioeng Biotechnol. 2017;5:17.
177. Shajkumar A. Future of nanotechnology in tissue engineering. In: Nanotechnology applications for tissue engineering. Amsterdam: Elsevier; 2015. p. 289–306.
178. Pietroiusti A, Stockmann-Juvala H, Lucaroni F, Savolainen K. Nanomaterial exposure, toxicity, and impact on human health. Wiley Interdiscip Rev Nanomed Nanobiotechnol. 2018;10(5):e1513.
179. Yildirimer L, Thanh NT, Loizidou M, Seifalian AM. Toxicology and clinical potential of nanoparticles. Nano Today. 2011;6(6):585–607.
180. Ganguly P, Breen A, Pillai SC. Toxicity of nanomaterials: exposure, pathways, assessment, and recent advances. ACS Biomater Sci Eng. 2018;4(7):2237–75.
181. Powers CM, Levin ED, Seidler FJ, Slotkin TA. Silver exposure in developing zebrafish produces persistent synaptic and behavioral changes. Neurotoxicol Teratol. 2011;33(2):329–32.
182. Bergin IL, Witzmann FA. Nanoparticle toxicity by the gastrointestinal route: evidence and knowledge gaps. Int J Biomed Nanosci Nanotechnol. 2013;3(1–2). https://doi.org/10.1504/IJBNN.2013.054515

Nanomaterials in Prosthetic Rehabilitation of Maxillofacial Defects

Deborah Sybil, Satyabodh Guttal, and Swati Midha

Abstract Maxillofacial reconstruction is complicated due to the etiology and nature of the tissue injury. The complexity of the facial structures adds to the difficulty of rehabilitation both functionally and esthetically. Skeletal reconstruction is by far the easiest part of the rehabilitation. Restoration of soft tissues like skin, cartilage, and mucosa without the support of the underlying bony architecture is possible with prosthesis. Silicone is the most commonly used prosthetic material for maxillofacial rehabilitation. Nanomaterials play an important role in bestowing color compatibility and interface stability in the prosthesis.

Keywords Maxillofacial prosthesis · Nanomaterials · Orbital defect · Nasal defect · Auricular defect · Maxillofacial reconstruction

1 Introduction

The structure of any part of the body corresponds to its function and so is it with the face. This part of the body supports numerous functions such as vision, hearing, breathing, mastication, and speech apart from its esthetic value. Out of the five sense organs that humans have, four are exclusively located in the maxillofacial region. The maxillofacial skeleton is therefore a unique combination of bony architecture. It comprises 14 bones, 6 of which are paired and 2 unpaired [1]. The facial skeleton is universally divided into three parts: the upper face comprising mainly of the forehead, the midface comprising 13 bones, and the lower face comprising the mandible.

D. Sybil (✉)
Faculty of Dentistry, Jamia Millia Islamia, New Delhi, India

S. Guttal
SDM College of Dental Sciences and Hospital, Dharwad, India

S. Midha
Special Center for Nanoscience, Jawaharlal Nehru University, New Delhi, India

R. S. Chaughule, R. Dashaputra (eds.), *Advances in Dental Implantology using Nanomaterials and Allied Technology Applications*,
https://doi.org/10.1007/978-3-030-52207-0_3

Mandible is the largest and the strongest bone of the face and is the only movable bone in the maxillofacial region. It is connected to the rest of the skull by two temporomandibular joints which are unique, as these are the only joints in the body which function exclusively simultaneously. Structurally, mandible is in the shape of a parabola, the vertex of which houses the chin, which is a unique esthetic feature of humans. Like other bones in the body, mandible has a medullary core with a cortical rim but unlike any other bone in the body, maxilla and mandible have multiple sockets in their alveolar processes for teeth. Maxilla is a paired bone and constitutes majority of the midface. Apart from supporting the teeth, which occlude with those in the mandible, maxilla forms part of the palate, lower part of the nose, and supports the eye. It houses the maxillary sinus which is an air-filled cavity within bone, and humidifies inhaled air, lightens the skull, adds resonance to voice, and produces protective mucus. The zygomatic buttress of maxilla is a thick extension of dense bone from maxilla towards zygomatic bone, the main function of which is to transmit occlusal forces to the cranium.

Various conditions affect the maxillofacial skeleton ranging from infections to malignancies. A list of the most common conditions affecting maxilla and mandible is given in Table 1. Barring a few such as arthritis, Garre's osteomyelitis, and osteoporosis, almost all of these conditions require one or the other form of surgery. Treatment of these conditions requires surgeries like fracture fixation, cyst enucleation, tumor resection, ankylosis release, contouring, etc. The extent of surgery

Table 1 List of some common conditions affecting maxillofacial skeleton [1]

Infections	**Cysts**	**Benign tumors**	**Bone lesions**
Osteomyelitis Suppurative Non-suppurative Garre's Infantile Arthritis	Odontogenic cysts Radicular OKC Periodontal Dentigerous Calcifying odontogenic ABC	Odontogenic tumors Ameloblastoma CEOT AOT Non-odontogenic Hemangioma Osteoma Chondroma Fibroma	Fibro-osseous lesions Paget's disease Cherubism Fibrous dysplasia Ossifying fibroma Giant cell lesions CGCG Cemento-ossifying lesions
Malignant tumors	**Congenital**	**Others**	**Conditions specific to maxillofacial region**
SCC Malignant odontogenic tumor Osteosarcoma Ewing's sarcoma	Aplasia Atresia Syndromic hypoplasia Cleft alveolus Hemifacial microsomia Osteogenesis imperfecta	Fracture AV malformations TMJ ankylosis Osteoradionecrosis Osteoporosis	Garre's osteomyelitis Cherubism Ameloblastoma Dental cysts Cemento-ossifying lesions Cleft deformities

OKC odontogenic keratocyst, *ABC* aneurysmal bone cyst, *CEOT* calcifying epithelial odontogenic tumor, *AOT* adenomatoid odontogenic tumor, *CGCG* central giant cell granuloma, *SCC* squamous cell carcinoma, *AV* arteriovenous, *TMJ* temporomandibular joint

depends on the extent and severity of the condition. Because of the nature of the disease, malignant lesions and certain locally aggressive lesions such as ameloblastoma and odontogenic keratocyst require resection of a rim of normal bone along with the lesional tissue. The residual deformity due to such resections, if not treated, can cause serious esthetic and functional problems. Reconstruction of the defects caused by jaw lesions and related surgeries may be done immediately or as a second stage procedure but has to be definitely addressed if one wishes to provide an acceptable quality of life to the patient.

2 History of Maxillofacial Skeletal Reconstruction

Most of the walled defects of the jaws such as bony cavities secondary to cyst enucleation heal physiologically. Larger defects of this kind may need particulate or granular bone grafts. Alloplastic grafts are osteoconductive which means that these grafts act as a scaffold for new bone formation. Osteoinduction is a process where osteogenesis is induced by recruitment and stimulation of immature cells. Addition of growth factors into alloplastic materials makes them osteoinductive. These two properties are considered adequate for new bone formation in bony cavities. Therefore, alloplastic grafts alone or in combination with growth factors, are sufficient for large bony cavities where physiologic healing is expected. Table 2 gives a list of grafts currently used in treatment of small defects of the jaws.

Reconstruction of defects secondary to resection is not as simple. Grafts used in such reconstruction must have osteogenic potential which is the ability of a graft to form new bone by the action of vital osteoblasts. For long, the only grafts which had osteogenic potential were autografts. A number of autografts have been used to reconstruct maxilla and mandible along with associated soft tissue (Table 3).

The gold standard of skeletal reconstruction in maxillofacial region is still autogenous bone: vascularized or nonvascularized. Segmental defects of 4–5 cm in size can be reconstructed with nonvascularized free bone grafts whereas defects larger than 5 cm require vascularized free flaps. This is because bone remodeling within a graft prerequisites adequate vascular supply especially to the core of the graft. Bone cells within a graft survive on diffusion from the margins during the first 5 days. The central parts of large nonvascularized bone grafts become necrotic and are revascularized within weeks to months depending on the vascularity of the donor site and

Table 2 Grafts currently used for small defects of the jaws [1]

Autogenous corticocancellous grafts	Commercially available allografts	Growth factors
Iliac Symphysis Tibial head Calvarium	Hydroxyapatite Tricalcium phosphate Bioactive glass Calcium sulfate	Bone morphogenetic protein Platelet-rich plasma Platelet-rich fibrin Interferon alpha

Table 3 Currently used maxillofacial reconstructive methods [1]

Graft	History	Disadvantages
Local soft tissue flaps		Insufficient for large defects Not applicable for composite defects Donor site morbidity
1. Tongue flap 2. Masseter flap 3. Buccal fat pad	Guerrero-Santos and Altamirano (1996) [3] Tiwari (1987) [4] Egyedi (1977) [5]	
Regional soft tissue flaps		Limited size of graft Not applicable for composite defects Donor site morbidity Compromised esthetics
1. Nasolabial flap 2. Temporalis flap 3. Forehead flap 4. Deltopectoral flap	Cohen and Edgerton (1971) [6] Lentz (1895) [7] McGregor (1963) [8] McGregor and Jackson (1970) [9]	
Regional composite flaps		Limited size of graft Donor site morbidity Compromised esthetics Difficult to adapt to recipient site
1. Sternocleidomastoid 2. Trapezius flap 3. Pectoralis major flap 4. Platysma flap 5. Latissimus dorsi flap 6. Submental flaps 7. Infrahyoid flaps	Jiano (1908) [10] Conley (1972) [11] Ariyan (1979) [12] Futrell et al. (1978) [13] Quillen et al. (1978) [14] Martin et al. (1993) [15] Wang et al. (1986) [16]	
Free nonvascularized bone grafts		Limited size of graft Necrosis of graft Donor site morbidity
1. Iliac crest 2. Rib 3. Calvarium	Taylor (1982) [17]	
Free vascularized grafts		Donor site morbidity Increased intraoperative time Need for microvascular surgical skills
1. Fibular grafts 2. Radial forearm grafts 3. Iliac crest grafts 4. Scapular grafts 5. Dorsalis pedis grafts	Ueba and Fujikawa (1983) [18], O'Brien and Morrison (1987) [19] Soutar et al. (1983) [20] Taylor (1982) [17] dos Santos (1984) [21] McCraw and Furlow (1975) [22]	
Allograft and xenograft		Infections Disease transmission Immunogenicity
1. Freeze-dried bone graft 2. Decellularized FDBG		
Implants		Inadequate reconstruction No functional rehabilitation Implant rejection Implant breakage or exposure Impedes growth in children Allergy
1. Stainless steel 2. Titanium 3. Vitallium 4. Silicon 5. Acrylic resins		

the structure of the grafted bone. The sources of newly formed bone are perivascular osteoprogenitor cells and undifferentiated mesenchymal cells which enter the graft accompanying the proliferating vessels [2]. However, in vascularized grafts, remodeling takes place across the whole graft at a time and therefore, grafts as large as 15–20 cm have high level of viability for the majority of bone forming cells inside the graft survive through the established blood supply. The primary perfusion of the grafted bone also sustains resistance against infections allowing survival of the graft independently from the donor site complications [2]. Because of these considerations, free vascularized bone grafts are currently the most suitable for reconstructing large segmental defects of the jaws.

3 Drawbacks in Present Reconstructive Options

The most commonly used vascularized graft for mandibular segmental defects are the fibula and iliac crest. The fibular graft has the advantage of adequate length, good stability, and adaptability to the recipient site. The disadvantages are patient immobility postoperatively, reduced height of graft for dental rehabilitation, and donor site morbidity. The iliac crest is a curved piece of mainly cancellous bone that allows three-dimensional carving into the shape of hemimandible but has the disadvantage of great deal of postoperative pain, gait disturbances, nerve injuries, hernia, and paresthesia [23]. Both the grafts need prolonged intraoperative time to harvest and reshape the bone to adapt to the recipient site and for donor site management. Moreover, such a reconstructive procedure does not completely restore jaw function. Functional dental rehabilitation requires restoration of mandible to near normal which is clinically difficult. Figure 1 shows the inadequacy of a vascularized fibula graft for a hemimandibulectomy defect in restoring the height and width of mandible [1].

The inability to replicate complex facial contours is another major drawback. For instance, reconstruction of segmental defects in the anterior mandible is challenging due to the geometry of bone in this region. Restoring its horseshoe shape to achieve proper contour and adequate function with the limitations of autogenous bone grafts

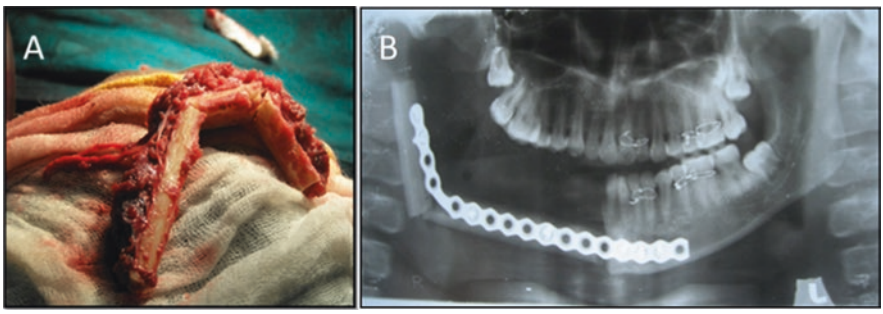

Fig. 1 (**a**) Harvested vascularized fibula graft. (**b**) Radiograph of mandible with vascularized graft in situ

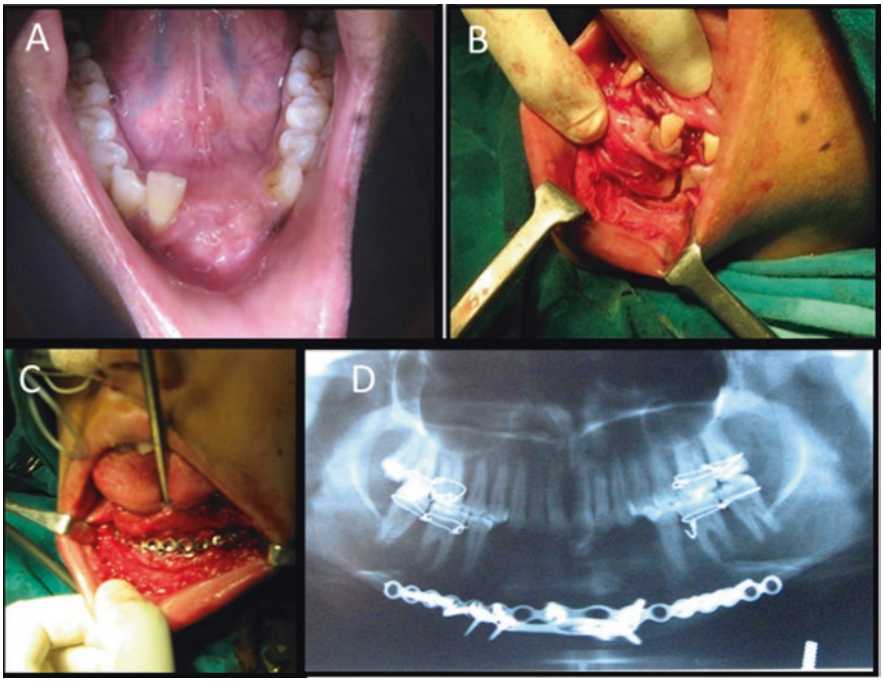

Fig. 2 Management of segmental defect in anterior mandible. (**a**) Clinical photograph of ameloblastoma in anterior mandible. (**b**) Intraoperative photograph of resection of ameloblastoma. (**c**, **d**) Photograph and radiograph of mandible after implant reconstruction

is difficult. Figure 2 shows a case of segmental resection in the anterior mandible and the problems associated with its reconstruction [1].

The midface poses a greater challenge because of its intricate anatomy and multiple interlacing and communicating spaces. Before the development of more sophisticated reconstructive techniques, prosthetic appliances were the only modality available to address the functional and esthetic requirements of such a complex defect. Free tissue transfers have made autologous maxillary reconstruction possible but functional and esthetic results are far from optimal.

4 Maxillofacial Prosthesis

Maxillofacial prostheses fabricated by a skilled prosthodontist or an anaplastologist provide an unparalleled reproduction of the lost facial form. It is of utmost importance that the prostheses be fabricated with optimal esthetics while maintaining an adequate appearance over its service lifetime. Modern materials for maxillofacial prostheses include vinyl plastisols, polymethylmethacrylates, polyurethanes, latex, and silicone elastomers. Properties like chemical inertness, strength, durability, and ease of manipulation make silicone elastomers the material of choice in

maxillofacial prostheses. Silicone elastomers used for the fabrication of maxillofacial prostheses have individual physical and mechanical properties; however, clinical problems such as gradual deterioration of color in a service environment and degradation of physical, static, and dynamic mechanical properties are common for all. In the chemical industry, during the past 10 years, research has been devoted to the development of a new industrial process that incorporates nanoparticles into a polymeric matrix, providing a new class of polymeric materials that offers the strength of nano-oxides, with the flexibility of the organic polymer matrix. The nano-sized material particles result in the optimization of individual material particle characteristics and control of biological, mechanical, electrical, magnetic, and optical characteristics as well. Nano-sized rutile TiO_2 and ZnO are known to have a high ultraviolet (UV) absorbing and scattering effects that result in protection from UV light. Nano-sized SiO_2, TiO_2, and ZnO are characterized by their small size, large specific area, active function, and strong interfacial interaction with the organic polymer. Therefore, one can improve the physical properties and optical properties of the organic polymer, as well as provide resistance to environmental stress-induced aging. Little has been reported in the literature on how the addition of these particles to a maxillofacial elastomer could affect its properties. Han et al. evaluated the effect of nano-sized oxides of various compositions in different concentration on the mechanical properties of a commercially available silicone elastomer. They determined that incorporation of Ti, Zn, or Ce nano-oxides at a concentration of 2.0% improved the overall mechanical properties of silicone A-2186 maxillofacial elastomer [24].

5 Case Reports

5.1 CASE 1: Nasal Prosthesis for a Patient with Mammalian Bite Injury [25]

A 32-year-old male patient reported with destructed nasal cartilage caused by a bear bite injury (Fig. 3a). Composite skin grafting was done in the upper lip and forehead region and a temporary nasal prosthesis was fabricated for the patient post-surgery which was retained with white surgical tape. Various prosthetic treatment modalities ranging from acrylic resin nasal prosthesis to implant-retained silicon prostheses were explained to the patient. The patient chose a spectacle retained nasal prosthesis made of acrylic resin due to economic constraints.

The boundary for the impression was outlined on the face. Light petrolatum was applied on the eyebrows and eyelashes. While taking care not to distort the nasal remnants/tissues by packing moist gauze into the defect, rolled modeling wax was used to confine the impression material. Facial moulage was made using an irreversible hydrocolloid material (Fig. 3b) reinforced with gauze and dental plaster and the impression poured in type III dental stone (Fig. 3c). The wax pattern of the nose with developed esthetic contours was sculpted on the master cast and the

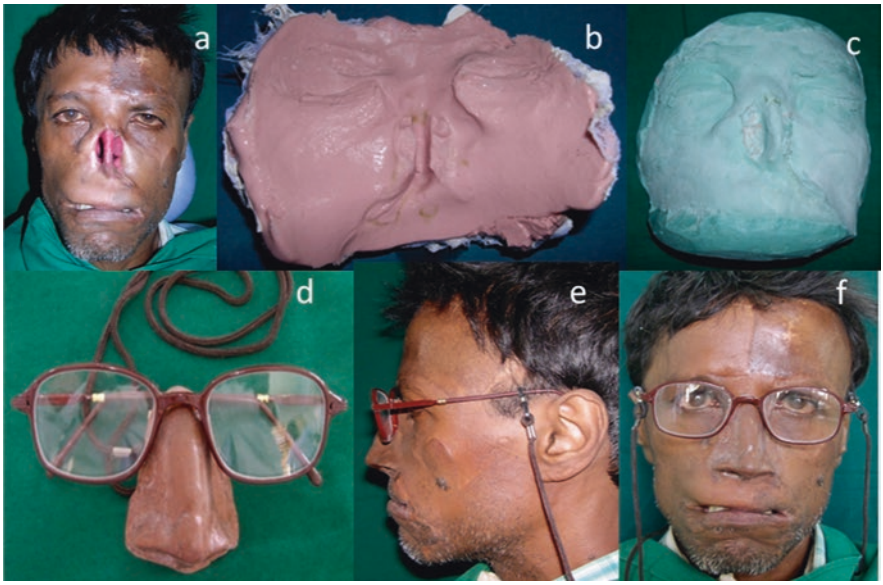

Fig. 3 Spectacle retained nasal prosthesis. (**a**) Patient's appearance after surgery. (**b**) Irreversible hydrocolloid impression. (**c**) Master cast. (**d**) The final prosthesis. (**e**, **f**) Prosthesis in situ

morphology of the wax prosthesis accomplished as per visual knowledge, previous photographs of the patient, and discussions with his relatives. The position of the wax pattern was further verified with clinical try-in. After marginal adaptation and confirmation of contours, the wax pattern was sealed on the master cast and molding procedures were carried out. Heat polymerizing clear acrylic resin with incorporation of intrinsic coloring using an acrylic-based paint to match the basic skin tone was packed and processed. The margins of the final prosthesis (Fig. 3d) were blended as close as possible with the skin contours. The spectacle frame was aligned on the bridge of the nose and attached using autopolymerizing resin. Extrinsic coloring was done to make it more esthetically acceptable (Fig. 3e, f).

5.2 CASE 2: Prosthetic Rehabilitation of a Midfacial Defect Resulting from Lethal Midline Granuloma [26]

A 22-year-old male patient with lethal midline granuloma, presented with severe destruction of midfacial structures including the nose, palate, and the paranasal sinuses along with inflamed right eye and adjacent soft tissues (Fig. 4a). Rehabilitation for both intra-orally with a prosthetic palate and extra-orally with the nasal prosthesis was planned for the patient. However, he only opted for the extra-oral nasal prosthesis for his facial disfigurement and exposed defect. A heat-polymerizing acrylic resin nasal prosthesis was planned. The boundary for the

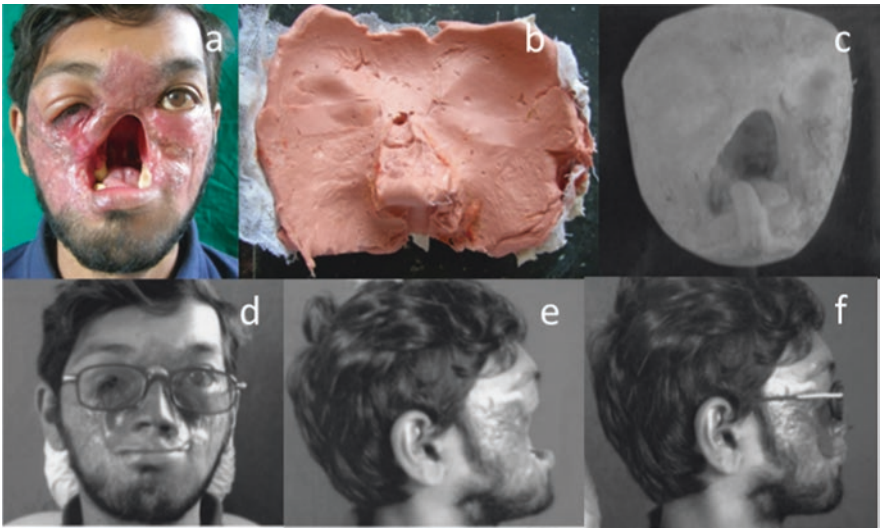

Fig. 4 Rehabilitation of midface defect. (**a**) Patient's photograph with the defect. (**b**) Irreversible hydrocolloid impression. (**c**) Stone cast. (**d**) Prosthesis in situ. (**e**) Lateral Profile before treatment. (**f**) Lateral profile after treatment

impression was outlined on the face. Rolled modeling wax was used to confine the impression material. Moist gauze was packed to prevent the flow of material into the undesired areas of the defect. Facial moulage was made using an irreversible hydrocolloid material reinforced with gauze and dental plaster under sedation (Fig. 4b). The impression was boxed and poured (Fig. 4c) in type III dental stone. The wax carving of the nose and the upper lip was carried out on the master cast. Patient's previous photographs and the references from his first circle relatives were taken as a guide to carve the wax prosthesis. Clinical trial was performed and the margins were flushed properly with the contours of the skin. Spectacle frame was also tried to check for the alignment and position to attach it for the final prosthesis. The prosthesis was processed using heat polymerizing clear acrylic resin with color incorporated to match the basic skin color of the patient. An acrylic-based paint was used for this purpose. The prosthesis was finished, the borders of the prosthesis rounded and eyeglass frame was properly aligned, and attached to the prosthesis using a cyanoacrylate adhesive. The attachment was reinforced with autopolymerizing acrylic resin at the bridge of the nose. The prosthesis gained retention with the help of this glass frame, and the proprioceptive input of an intact functioning lower lip aided in balancing and stabilizing the prosthesis. The upper lip was relined with soft resilient liner, thus giving a feeling of resiliency to the lower lip. The extrinsic coloring was performed. This enhanced the esthetics and resulted in a better appearance (Fig. 4d–f).

5.3 CASE 3: Orbital Prostheses in Patients with History of Carcinoma [27]

(a) A 45-year-old female patient complained of facial disfigurement due to loss of left eye. A history of carcinoma of the left eye followed by exenteration was recorded. As a result of altered facial esthetics, the patient suffered severe emotional trauma in terms of social acceptance.
(b) A 58-year-old female patient complained of missing right orbital contents following the surgery due to adenoid cystic carcinoma (Fig. 5a).

Both the patients were seeking an artificial orbital replacement. On examination, there was no anatomical undercut in the defect that could be utilized for retention. A custom-made ocular and orbital prosthesis was planned and the treatment procedure explained to the patient. Identical methods were employed to verify the reliability of the results in both patients.

Impression of the orbital defect was made using irreversible hydrocolloid reinforced with dental plaster and the cast poured in dental stone (Fig. 5b). The stone cast was duplicated with silicone duplicating material in a metal flask. After the duplicating material set, the master cast was separated and stone cast poured in the

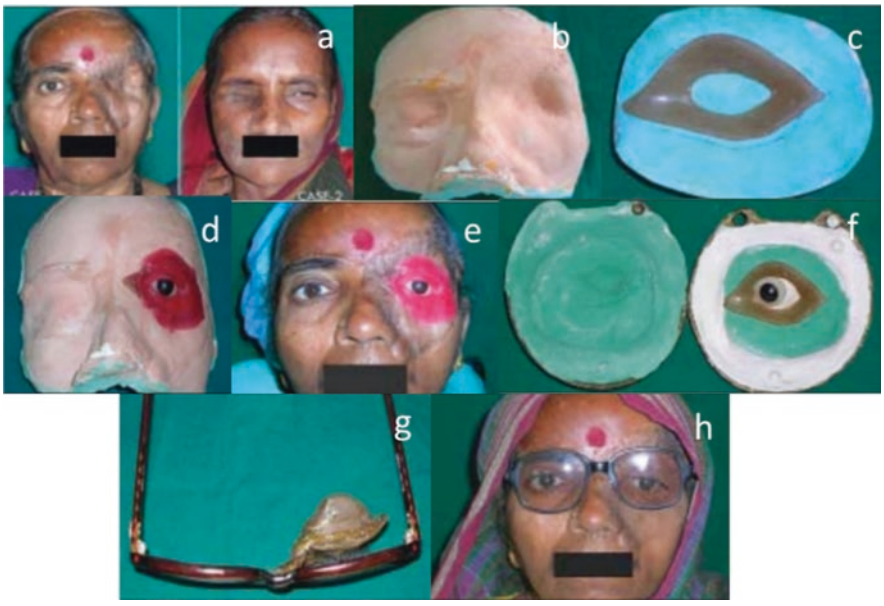

Fig. 5 Orbital prosthesis for exenteration defect. (**a**) Frontal view of patient with orbital defect. (**b**) Facial moulage. (**c**) Fit of acrylic resin base checked on cast. (**d**) Wax pattern of the orbital prosthesis with the medial margin of acrylic resin base exposed. (**e**) Trial of the wax pattern done and the position of medial extension of acrylic resin base evaluated. (**f**) Primer application for bonding with silicone following wax elimination. (**g**) Silicone orbital prosthesis attached to the eyeglass frame. (**h**) Fabricated prosthesis in situ

mold. Wax pattern for the acrylic resin base was made in a circumferential design adapting it to the perimeter of the defect. The pattern was sealed to the cast and invested. After wax elimination, heat-polymerizing acrylic resin was packed. Intrinsic coloring was applied to match the skin color around the defect. The resin base was retrieved, finished, and polished after curing. The fit of the base was checked on the cast (Fig. 5c). The wax pattern for the orbital prosthesis was prepared and the acrylic resin base embedded in it. The acrylic resin base was exposed only at the bridge of the nose for attachment to the eyeglass frame (Fig. 5d). Try-in (Fig. 5e) of the waxed-up prosthesis was done. At this stage, the eyeglass frame was selected and tried on the patient, and close approximation of the eyeglass frame to the resin base was checked. The wax pattern was sealed to the cast, flasking carried out, and wax eliminated (Fig. 5f). Primer was applied to the acrylic resin base for bonding with silicone. The silicone was packed. Intrinsic coloring was produced to match the patient's skin tone and cured at room temperature. The eyeglass frame was placed in situ. The silicone layer found on the medial extension of the resin base was cut to expose for felicitation of the attachment of the eyeglass frame to the resin base. With both the eyeglass frame and prosthesis placed in situ, the glass frame was attached to the acrylic resin base with the help of cyanoacrylate resin adhesive. The attachment was reinforced with autopolymerizing acrylic resin (Fig. 5g). Finally, the silicone orbital prosthesis retained by the eyeglass frame was placed in situ (Fig. 5f).

5.4 CASE 4: Orbital Prosthesis in Patient with Rhabdomyosarcoma [28]

A 45-year-old male patient complained of facial disfigurement due to loss of left eye (Fig. 6a). History revealed exenteration of orbit a year ago for eradication of rhabdomyosarcoma. Extra-orally, no definite bony or soft tissue undercut to aid in the retention of the prosthesis. After evaluation and inspection of the defect, the iris and pupil diameter were measured using calipers and impression with irreversible hydrocolloid was made reinforced with quick setting dental plaster (Fig. 6b–d). A cast was poured in dental stone type II which was duplicated and modeling wax adapted to fabricate shim (Fig. 6e). This waxed up shim was processed using heat polymerizing clear acrylic resin (Fig. 6f). Measurements were made from the patient's facial midline to the center of the pupil and from the inner canthus of the eye to the nasal bridge (Fig. 6g). The measurements were then transferred on the cast to help in positioning of the orbital prosthesis. A stock ocular prosthesis was selected closely matching the color, size, and shape of the iris and sclera of the other eye. The acrylic shim was exposed only at the bridge of the nose for attachment to the eyeglass frame. The eye was then secured in position on a bed of modeling wax according to the position gained using measurements of the other eye. The antero-posterior position was adjusted and verified on the patient when observed from profile and from the top of the head. Once the position was confirmed, the eyelids and the remaining portion was sculpted in wax (Fig. 6h) and tried in the patient's orbital defect. Consent from the patient regarding the appearance of the prosthesis

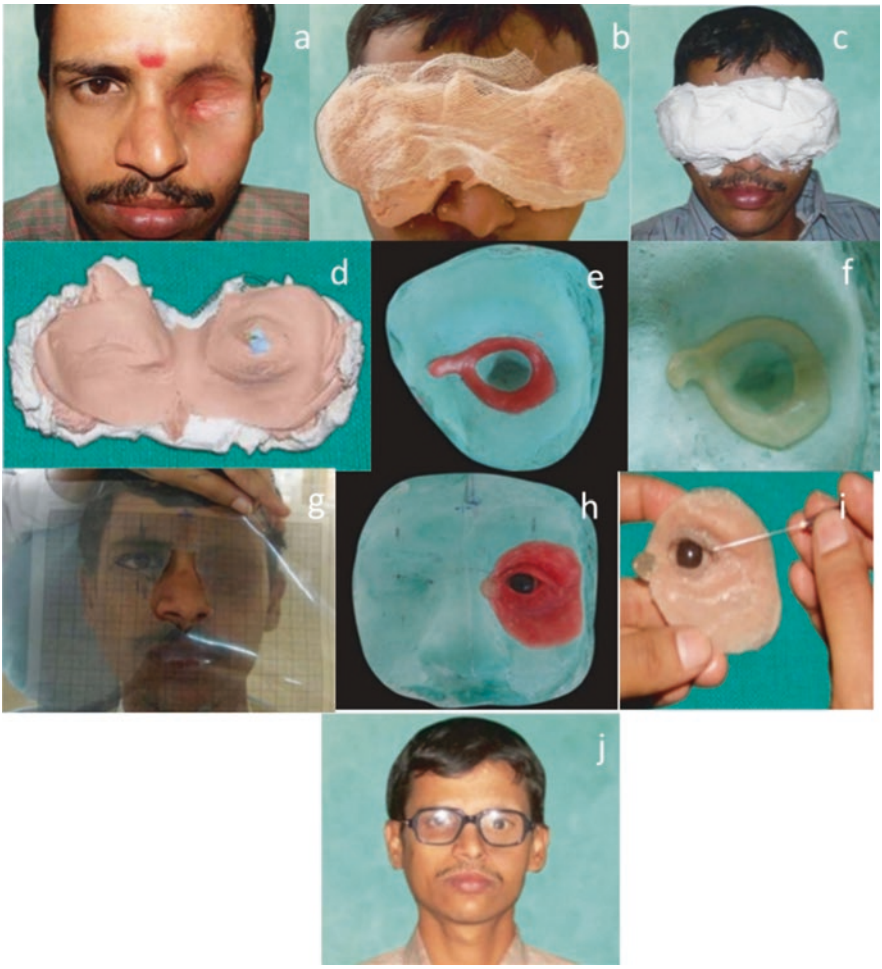

Fig. 6 Rehabilitation of exenteration defect by orbital prosthesis. (**a**) Pretreatment photograph. (**b**) Direct impression with alginate. (**c**) Reinforcement of alginate by dental plaster. (**d**) Impression after retrieval. (**e**) Wax pattern for the fabrication of acrylic shim. (**f**) Heat polymerizing clear acrylic shim on the master cast. (**g**) Grid in place. (**h**) Sculpted wax pattern. (**i**) Stitching of natural hair to the silicone orbital prosthesis. (**j**) Post-treatment photograph with silicone artificial eye

was obtained. The wax sculpted prosthesis with the duplicated cast was flasked and dewaxed. Room temperature vulcanizing (RTV) medical-graded silicone material (Molloplast) was mixed according to the manufacturer's instructions. Pigment stains were blended into the base color of silicon for intrinsic staining at the time of mix to gain the approximate skin shade of the patient. After a close shade match with the patient, medical-graded silicone was packed into the mold and was left to cure at room temperature. Following polymerization, the prosthesis was deflasked, retrieved, and finished. Natural hair was stitched over the eyebrow area and upper, lower eyelids of the silicone prosthesis using 23 gauge syringe needle (Fig. 6i). The eyeglass frame was selected and tried on the patient. With both the eyeglass frame

and prosthesis placed in situ, the glass frame was attached to the acrylic shim with the help of cyanoacrylate resin adhesive. The attachment was reinforced with clear autopolymerizing acrylic resin (Fig. 6).

5.5 *CASE 5: Implant-Retained Nasal Prosthesis for a Patient Following Partial Rhinectomy [29]*

A 58-year-old male patient diagnosed with basal cell carcinoma of the nasal vestibule who had undergone partial rhinectomy, reported with iatrogenic absence of the entire cartilage of the nose, ala, and part of the nasal septum due to the surgery (Fig. 7a). As a bank employee who interacts with customers, the patient was deeply concerned about his esthetics and was seeking prosthetic rehabilitation soon after

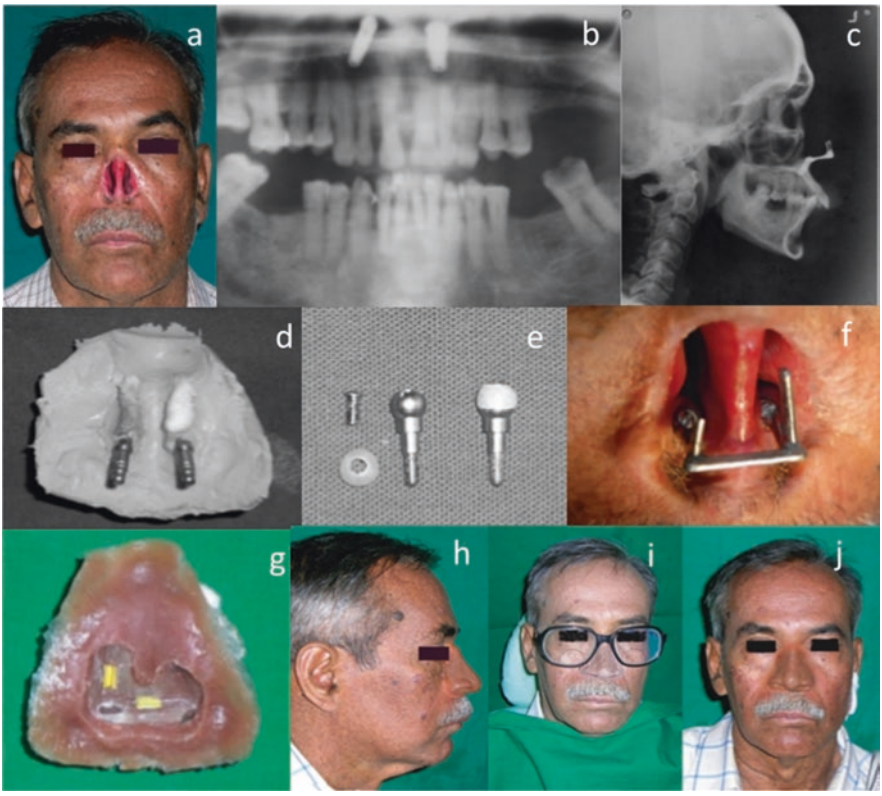

Fig. 7 Implant-retained nasal prosthesis. (**a**) Nasal defect after partial rhinectomy. (**b**) Orthopantomograph following implant surgery. (**c**) Lateral cephalograph. (**d**) Polysiloxane impression with lab analogs. (**e**) Resin copings fabricated on ball abutments. (**f**) Try-in of cast titanium framework. (**g**) Tissue side of the prosthesis showing acrylic resin substructure with clips. (**h**) Lateral profile of the patient subsequent to prosthesis placement. (**i**, **j**) Comparison of acrylic resin prosthesis and silicone prosthesis

surgery. Since an immediate definitive prosthesis was not feasible, the patient was temporarily rehabilitated with an acrylic resin nasal prosthesis attached to an eyeglass frame (Fig. 7i). During the subsequent follow-up appointment, it was noted that retention and marginal fit of the temporary prosthesis was lost due to post-surgical marginal tissue changes. At this stage, the option of the implant-retained silicone prosthesis was given. The temporary nasal prosthesis and a clear acrylic resin surgical template with properly angulated pilot holes were used as a guide for the implant placement. Under local anesthesia, a full thickness mucoperiosteal flap was elevated, exposing the anterior border of the nose and the nares. Two implants of 3.75-mm diameter and 10-mm length were placed into the anterior maxilla through the nasal fossa on either side of the nasal septum (Fig. 7b, c). The mucoperiosteal flaps were then repositioned and closed with 4-0 VICRYL sutures. 6 months later, a small mucoperiosteal flap was raised, debulking of the soft tissue was performed, and the healing abutments were placed. Three weeks later, the soft tissue edema had subsided, and a peri-implant mucosal seal was observed. The nasal defect was packed with moist gauze to prevent the flow of the impression material and implant components falling into the nasal cavity. Healing abutments were removed, and impression posts were connected to the implants. An impression was made using medium-body vinylpolysiloxane impression material. The impression posts were unthreaded and connected to the laboratory analogs (Fig. 7d). The master cast was then made with dental stone. Pattern resin copings were fabricated on both the ball abutments. Screw channels were made to place the screw that will retain the copings onto the ball abutments (Fig. 7e). Rigid castable bars were attached to the resin copings using inlay wax. The framework included two vertically oriented elements overlying the defect on both sides of the nasal septum and one horizontal bar connecting the implants and resin copings. The casting was done in a semiautomatic two-chambered titanium-casting machine under argon gas pressure. The titanium bar was positioned on the master cast and threaded to the ball abutments. The nasal prosthesis was sculpted in wax on the master cast. Care was taken to avoid any interference to the bar. The morphology and the anatomic contours of the nose were developed according to the patient's own description of his presurgical appearance and also the references given by the patient's immediate circle of relatives. The wax pattern of the prosthesis was hollowed to make space for the acrylic resin substructure, which housed the retentive elements. The bar and the acrylic resin substructure were designed to fit within the confines of the final nasal prosthesis. The ball abutments, along with the titanium framework, were threaded onto the implants (Fig. 7f) and trial placement of the wax pattern of the prosthesis was done. At the time of trial, the fit of the bar, size, contours, and marginal adaptation of the wax pattern of the prosthesis were evaluated and found satisfactory. The titanium framework was repositioned on the master cast, and the borders of the wax pattern were sealed. A dental stone mold was produced in a conventional manner. Mold releasing agent was sprayed after the wax elimination to facilitate the removal of the silicone prosthesis. Primer was applied on the acrylic resin substructure after cleaning with acetone, for mechanical retention of the silicone elastomer. Silicone was packed in layers into the mold, developed with intrinsic color to match the patient's skin tone, and allowed to cure at room temperature. The acrylic resin housing had bonded well

to the silicone. Nostrils were cut open in the acrylic resin for air exchange (Fig. 7g). The silicone nasal prosthesis was retrieved and finished. Initial trial was done on the patient to check the color match of the prosthesis. Extrinsic colors were used to match the small-pigmented dots present on the skin (Fig. 7h, j).

5.6 *CASE 6: Rehabilitation of a Missing Ear with an Implant-Retained Auricular Prosthesis [30]*

A 47-year-old male patient reported with facial disfigurement along with the loss of the right ear after severe burn injury to the face (Fig. 8a). The patient was extremely concerned about his facial disfigurement and requested for an economic solution for replacing the missing ear. A thorough evaluation of the affected area, medical history, and physician's consent was taken. External examination revealed scarring of tissue with gross discoloration and complete loss of hearing from the right ear. A dermatologic evaluation was conducted which revealed that the patient had scarred tissue, decreased blood supply to the area, increased contracture formation, and reduced epithelialization and collagen formation. A radiographic evaluation showed suitable bone quality, adequate thickness of the temporal bone, and density of the mastoid air cells to receive implants. Three-dimensional lateral cephalography was recorded of the affected and normal side along with soft tissue reconstruction. A stereolithographic model was obtained of the patient's temporal bone and temporomandibular joint (Fig. 8b). Sites for the placement of implants were located and

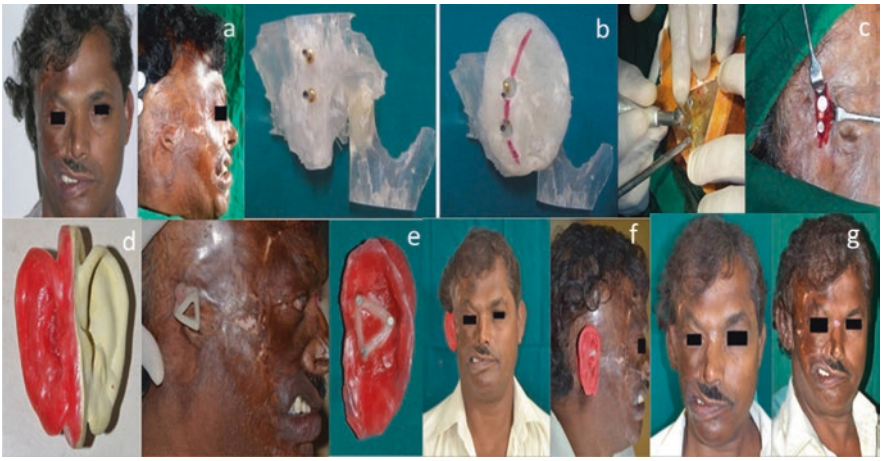

Fig. 8 Implant-retained auricular prosthesis. (**a**) Preoperative frontal and profile view of the patient. (**b**) Surgical stent fabricated on the stereolithographic model of temporal bone. (**c**) Intraoperative photograph of implant placement. (**d**) Wax up of mirror image of contralateral ear. (**e**) Acrylic shim trial on patient's face. (**f**) Trial of waxed up ear on patient's face—frontal and profile view. (**g**) Final prosthesis—frontal and profile view

marked and used as a guide to fabricate a surgical stent for use during surgery. A single stage implant placement surgery was carried out. The surgical site was isolated, and the surgical stent was fastened in place with surgical tape and used as a guide. The surgical procedure was conducted as a routine under local anesthesia. Two (3.75 mm × 10 mm) implants were placed in the region of the missing right auricle, in the mastoid process of the temporal bone of the patient (Fig. 8c). The higher placed implant showed adequate stability and osseointegration 4 months postoperatively while the lower placed implant showed repeated signs of infection and was subsequently submerged and left as a sleeping implant. The opposing left ear was normal and healthy, and was used as a guide for the fabrication of the wax pattern for the missing auricle. To make an impression of the healthy ear, an unused casting ring of adequate dimensions was used to hold the irreversible hydrocolloid impression material. The surrounding hair was coated with petroleum jelly and the ear canal was blocked with cotton. The alginate was first coated into the folds of the ear in a thin consistency, followed by application in bulk. The impression was further stabilized using the impression plaster. The impression was beaded and boxed and poured in dental stone. Using this mold of the left ear, a wax pattern of the right ear was carved out as a mirror image of the opposite side using modeling wax (Fig. 8d). The implant abutment was blocked out with carding wax. The surrounding tissue was coated with petroleum jelly. Light body consistency of polyvinyl siloxane elastomeric impression material was applied to the implant and surrounding tissues, followed by a base of putty consistency polyvinyl siloxane elastomeric material. Impression compound was further layered above to give rigidity to the impression. The impression was boxed and poured in die stone. The retrieved cast was used as a template to fabricate a shim of clear autopolymerizing acrylic resin. A triangular-shaped acrylic shim was fabricated which was attached to an acrylic cap to be cemented on the implant abutment. Samarium cobalt magnets of 4-mm diameter were embedded into the three angles of the acrylic triangle using an autopolymerizing acrylic resin (Fig. 8e). Another acrylic triangle of similar dimensions as the original was fabricated to support the magnets of the opposing poles to be embedded into the final prosthesis. It was ensured that the magnets were of differing polarities such that the two triangular shims fit together in only one orientation. Care was taken to ensure proper incorporation of the magnets with the autopolymerizing resin to avoid abrasion during the final polishing. The sculpted wax model of the missing right ear was tried on the patient's face, and its size, orientation, and position were confirmed to ensure symmetry with the opposing side (Fig. 8f). The acrylic shim with cap was cemented in position onto the implant abutment using glass ionomer cement in luting consistency. Excess was removed allowing space for cleansibility around the implant. The opposing acrylic shim was embedded into the sculpted auricular model, and the position was finalized chairside. After satisfactory positioning, the acrylic shim was sealed into the wax pattern, and the entire framework was flasked and invested using a combination of dental stone and die stone forming a three-piece mold. After wax elimination, the die stone component was separated out of the flask to aid in layered packing of the maxillofacial silicone. Gold Primer was applied to the acrylic to assist bonding with the silicone. Color matching was done using intrinsic colors to blend with the patient's skin tone and

the medical-grade silicone was packed into the mold and left to cure for 1 h at 100 °C. The prosthesis was retrieved and finished, and an initial trial was performed. Extrinsic tinting was performed to further blend with the patient's skin tone. The excess silicone was cut out. The lightweight of the prosthesis ensured easy support by the magnets (Fig. 8g).

5.7 CASE 7: Rehabilitation of Orbital Defect with Silicone Orbital Prosthesis Retained By Dental Implants [31]

A 27-year-old male complained of facial asymmetry and poor looks due to loss of the right eye. A history of retinoblastoma, followed by exenteration of the orbit was recorded. The surgical intervention had been carried out when the patient was 5 months old, and thereby the growth was retarded. The facial asymmetry was apparent as an ophthalmic defect included the right orbit and extended laterally along the outer canthus of the eye, towards the temporal region as well along the malar eminence towards the zygomatic arch. The patient underwent a CT scan on basis of which a stereolithographic model was fabricated. A mock surgery (Fig. 9a) on the stereolithography model revealed optimal bone thickness along the inferolateral orbital rim composed of zygomatic bone while the lateral aspect of superolateral rim composed of frontal bone showed moderately optimal bone in terms of thickness and density. A surgical stent was fabricated as per the mock preparation. Two intra-oral dental implants were placed depending on the availability of the bone at the defect site under short general anesthesia. A 3.75 mm × 10 mm implant was placed in inferolateral region and 3.75 mm × 8 mm implant was placed in superolateral region (Fig. 9b). A healing period of 4 months was given following which the extra-oral radiographs—PA Water's view and lateral cephalogram (Fig. 9c) were made. The defect impression was made with implant components in place (Fig. 9d). A metal framework was cast to attach it to the implant abutment with the magnetic keepers embedded in it (Fig. 9e). The metal framework was threaded onto implant in the patient's defect. The wax orbital prosthesis had the corresponding magnets embedded in it (Fig. 9f). Wax trial was taken (Fig. 9g). Intrinsic coloring was done to blend the silicone with the adjacent skin color. Finally, the silicone orbital prosthesis was placed in-situ (Fig. 9h).

6 Role of Nanobiomaterials in Maxillofacial Prosthesis

Maxillofacial rehabilitation by implantation of biocompatible prostheses helps restore the esthetics and functions (such as speaking, eating, and chewing) in patients affected by trauma, congenital defects, or disease-related deformities. Having a proper rehabilitation of the craniofacial region goes a long way in boosting the confidence, social acceptance, and psychological well-being of the individual.

Fig. 9 Implant-retained magnetic support-based orbital prosthesis. (**a**) Mock surgery on stereolithography model. (**b**) Implant placement. (**c**) Lateral cephalograph and PA Water's view. (**d**) Defect impression with implant components in place. (**e**) Metal framework with implant abutments and magnetic keepers. (**f**) Wax orbital prosthesis with corresponding magnets. (**g**) Wax trial. (**h**) Silicone orbital prosthesis in situ

Hence, a key role is played by the structure, properties, and physiological responses of the prosthetics used for reconstructive surgeries.

The upsurge in the field of nanotechnology and tissue engineering has played a major role in medical intervention for adequately fixing cases of maxillofacial reconstruction. By applying nanobiomaterials and/or inducing surface modifications on the prostheses, the challenge is to improve upon the integration, retention, and long-term functionality of the implanted prostheses. In this section, we will elaborate on the application of nanobiomaterials to maxillofacial prostheses in terms of their unique properties, physiological responses within the host, and cellular signaling, all leading to early integration and adequate retention of the implant.

Some key aspects to the application of maxillofacial prostheses that determine the ultimate fate of such implants include:

1. **Physiological and cellular changes inside the host upon implantation**: Immediately upon implantation of the prosthesis inside the host tissues, a cascade of events is initiated at the implantation site. Blood is usually the first biological fluid that interacts with the biomaterial surface and enables the adsorption of several biologically active molecules (fibronectin) and serum proteins from the *in vivo* milieu on the material surface. This initial wetting of the material surface, also known as flash spread, is one of the most critical determinants of the performance of the biomaterials. Protein adsorption is accompanied by platelet activation resulting in the formation of clot. This coagulum at the implant surface facilitates further deposition of proteins, releases inflammatory molecules instigating a series of signaling molecules that exert influence on the migration of monocytes, neutrophils (both involved in inflammation), and mesenchymal cells (cells that can differentiate into osteoblasts) towards the implant surface. Following the aggregation of inflammatory mediators, growth factors, and differentiation factors, the process of angiogenesis and tissue regeneration is initiated. For instance, mineralized materials (ceramics) and metals commonly carry a negative charge on their surface under physiological conditions, selectively allowing positively charged biomolecules to adsorb on the surface [32].
2. **Surface modification of materials**: Various surface modifications like Grit-blasting, acid etching, and sandblasting are promising techniques used to improve the surface interactions of materials with biological moieties. The predominant reason being increase in the surface area, generation of micropores resulting in a roughened or textured surface as compared to the smoothened, machined surfaces. This in turn has a direct impact on the cell attachment and proliferation, which results in increased implant stability. Coating with nanobiomaterials is another promising strategy for improving osteoconductivity. For instance, plasma-sprayed hydroxyapatite (HA) coating is a clinically proven method for increasing the osteoconductivity and promoting early osseointegration in bone implants. In the process, HA particles are blasted on the implant surface at very high temperature range to enhance bone-to-implant contact. However, the irregular HA coating on the implant surface results in nonuniform thickness leading to unpredictable degradation profile *in vivo*. In addition, nano-crystalline deposition of calcium phosphate and fluoride to titanium surfaces has also been with varying success rates.

7 Materials Proposed

The conventional materials proposed for maxillofacial applications face some severe setbacks in terms of biocompatibility, early integration, tear strength, and mechanical properties. Under an ideal scenario, the hunt is on for materials possessing “similar” if not the “same” features to the missing facial tissue to adequately reconstruct a patient’s intrinsic esthetic features of mastication, speech resonance, and facial gesture. Nanoparticles have increasingly been exploited in biomedical

applications due to their small size, large interface area, interaction with biological tissues, and strong interfacial interaction with the organic polymer. Hollow cores of nanobiomaterials are often loaded as delivery vehicles with drugs for targeted therapy. Some clinically popular materials and their respective modifications with nanobiomaterials are summarized below:

1. **Silicon elastomers for maxillofacial prostheses**: A documented usage is to develop an improved maxillofacial prosthetic material with optimum mechanical properties. In this context, SiO_2 is often mixed with silicone elastomers (3% by weight) for maxillofacial applications [33] and boosts the mechanical properties of the resultant composite as compared to 3% wt. of nano-oxides of Ti, Zn, or Ce (non-surface treated) [34]. Nano-TiO_2 powder was applied as a nanofiller. The effect of 0.25 wt% titanium oxide in maxillofacial elastomers, VST50F RTV and Cosmesil M511 HTV showed 1.17-fold and 1.1-fold increase in tear strength of resultant composites [35]. While HTV possessess excellent thermal, color, and chemical stability, prosthetics due to opacity and lesser elastic strength are certain limiting factors. RTV, on the other hand, generates by-products, excessive curing time, easy degradation by hydrolysis, and low tear strength have a negative impact on the long-term retention of the prostheses [36]. Another similar study illustrated that the increase in the mechanical properties of the organic polymer was gradual as the filler concentration increases. Increasing concentration of the nanofiller will apparently result in filler to filler binding, hence taking up small voids in the polymer thereby making it more rigid towards indentation and penetration [37]. Natural nanobiomaterials synthesized from pomegranate peels (0.2% by weight) and dates Ajwa (0.3% by weight) have also been found to significantly improve the mechanical properties of silicone rubber [38].
2. **Titanium implants for osseointegration**: Titanium implants have constituted an enormous market share over the last many decades in the reconstruction and rehabilitation of bone deformities of the craniofacial region. It is known that early osseointegration is imperative for congruent bone formation and proper integration of implant in the defect site. Osseointegration relies upon surface chemistry and surface topography of the material. Nano-sized particle coating with materials, mostly of ceramic composition, helped such metal implants attain bone-like surface chemistry [39, 40]. Not only in terms of similar composition, but the nano-textured implant surface with roughened morphology coming from the irregular micropores enabled enhanced protein and cellular interactions at the molecular level (increased expression of osteocalcin and collagen type I) [41] between the material and host tissue, ultimately forming strong bonding between the two. In addition, marked reduction in TRAP and TNF-α activity showed a reduced bone turnover rate around the HA-coated implant. A striking contrast was the work of Svanborg et al. who failed to observe any marked differences in the extent of bone formation in HA nano-coated titanium screws over uncoated ones. However, such discrepancies could be attributed to several variables in study parameters such as differences in the implant design, method of evaluation, and surgical technique demonstrated [42].

3. **Antimicrobial coatings, dressings, and local carriers**: Surface colonization of biomaterials post implantation *in vivo* could induce an inflammatory reaction and generate an increased risk for mucositis and peri-implantitis [43]. If the bacteria adhere to the implant surface, biofilm formation initiates immediately, leading to the formation of an extremely resistant biofilm within a few hours. Hence, in a way, the fate of the biomaterial is decided at the time of implantation itself. Application of local antibiotic carriers/coatings such as antibiotic-loaded polymethyl methacrylate (PMMA), poly-L-lactic acid (PLLA) matrix with gentamicin sulfate, bone grafts, has an initial outburst (nearly 80%) of the antibiotic within the first 2 days [44]. More stable coatings, such as silver nano-coatings, form reactive oxygen species, mechanisms that potentially inhibit the growth of prokaryotic cells. A retrospective case-control study reported the results of silver-coated tumor prostheses in 85 patients showed that there was a significant reduction in the overall postoperative infection rate from 22.4% to 11.8% in favor of the silver-coated implant group, with a mean reduction of approximately 48% in infection rate post operations [45].

Irrespective of a wide range of options available for treatment and regeneration of disfigured maxillofacial cases, there is immense room for improvement. Some of these include the fabrication protocol of prostheses, time, effort, cost plus retention, and matching the esthetic complexity. These limitations make access to global patient's community almost denied; only a small number of these patients can get access to this sophisticated device, those who can afford the high cost of the prosthesis, whereas people at the other poor global regions such as Africa and India cannot easily obtain a good prosthesis.

8 Advanced Approaches for Maxillofacial Rehabilitation

Despite advances in surgical techniques, a patient undergoing severely debilitating head and neck surgery more than often requires a maxillofacial prosthesis, fabricated to the utmost precision to carry out unhindered day-to-day functioning. Silicone is one of the most preferred elastomer materials for their fabrication owing to its chemical inertness, strength, durability, and ease of manipulation. Despite its commendable properties, it is often seen to deteriorate over a period of functional use, generally 6 months, on grounds of its color stability, thus requiring refabrication. To counter this drawback, nanoparticles have been added to silicone and have shown to improve not only its biological, mechanical, electrical, and magnetic properties, but also enhance the optical properties. A variety of nano-oxides have been tried with to evaluate the best possible outcome. Akash et al., under *in-vitro* conditions, assessed the effect of titanium oxide (TiO_2) with that of zinc oxide (ZnO) in comparison to no additional incorporation as a control sample. Incorporation of these nano-sized oxides provided with intrinsic coloring ability with least amount of color changes seen with nano-sized ZnO [46]. Kiat-amnuay et al. investigated the

effect of oil pigments in varying concentrations with opacifiers on color stability of maxillofacial elastomer which was then spectrometrically evaluated before and after artificial aging. 5%, 10%, and 15% were the different concentrations of the opacifiers used [47]. A total of five opacifiers were tested namely; neutral kaolin powder, calcined kaolin powder, Artkin white, dry pigment Ti white, and Ti white artists' oil color. These were used alone or in combination with cadmium-barium red deep, yellow ochre, burnt sienna, or a mixture of these. Dry Ti pigment showed the most color stable results. In one of the initial attempts, Haug et al. tested the effect of different environmental conditions on the elastomer prosthesis fabricated with and without coloring agent [48]. It was noticed that the silicone material underwent changes and was not as stable as previously thought by the pioneers whether a coloring agent was added or not. However, addition of coloring agent helped protect the prosthesis from varying weather conditions. Inorganic coloring agents such as dry earth pigments, kaolin, artist's oil, and liquid cosmetic were found to provide better and stable color results compared to inorganic agents like rayon fiber flocking. Polyzois et al. also evaluated the effect of weathering on three different non-pigmented silicone elastomers. They concluded after a period of 1-year study evaluation that significant color changes were seen in all three materials [49]. However, Elastosil M3500 and Ideal materials were more stable than Silskin 2000 and did not show significant variation between them. There is a necessity to experiment and investigate various combinations of nanomaterials to enhance and stabilize the desired color of the prosthesis. Also, nanomaterials can be used to enhance the stability of acrylic metallic junctions.

With the advent of 3D printing and additive manufacturing in the fields of medicine and surgery, the idea of closely mimicking facial features down to nano-scale level seems believable. In a recent study by Zardawi et al. [50], color matched 3D printed soft tissue facial prostheses produced by Z-Corp-Z510 and infiltrated with Sil-25 maxillofacial silicone polymers were generated utilizing starch-based biocompatible materials. With slightly compromised mechanical properties (replacement period *in vivo* ranging from 6 to 12 months), the technology applied enabled construction of several copies of the prostheses in a shorter time frame and at a lower cost than handmade silicone polymer prostheses. Another advantage of applying rapid prototyping is that producing the required thickness of the missing part that rendering a lightweight prosthesis, which is mostly valued by the patients showed a significant improvement over the existing fabrication protocols.

References

1. Sybil D. Anatomic challenges in surgical reconstruction and functional rehabilitation of maxillofacial skeleton. Int J Recent Sci Res. 2018;9(2):23899–903.
2. Booth PW, Schendel SA, Hausamen JE. Maxillofacial surgery, vol. 2. 2nd ed. Philadelphia, PA: Elsevier; 2007. p. 83–92.
3. Guerrero-Santos J, Altamirano JT. The use of lingual flaps in repair of fistulas of the hard palate. Plast Reconstr Surg. 1996;38:123–8.

4. Tiwari R. Masseter muscle crossover flap in primary closure of oral-pharyngeal defects. J Laryngol Otol. 1987;101:172–8.
5. Egyedi P. Utilization of the buccal fat pad for the closure of oro-antral and oro-nasal communications. J Maxillofac Surg. 1977;5:241–4.
6. Cohen IK, Edgerton MT. Transbuccal flaps for the reconstruction of the floor of mouth. Plast Reconstr Surg. 1971;48:8–10.
7. Lentz J. Ankylose osseuse de la mâchoire inférieure, résection du col condyle avec interposition du muscle temporal entre les surfaces de résection. Congrés Franc de Chir 1895;113.
8. McGregor IA. The temporal flap in intra-oral cancer. Br J Plast Surg. 1963;16:318–23.
9. McGregor IA, Jackson IT. The extended role of the deltopectoral flap. Br J Plast Surg. 1970;23:173–9.
10. Jiano J. Paralizie faciale dupa extriparea unei tumori a parotidee trata prin operatia dlui gomoue. Bull Mem Soc Clin Bucharest 1908:22.
11. Conley J. Use of composite flaps containing bone for major repairs in the head and neck. Plast Reconstr Surg. 1972;49:522–6.
12. Ariyan S. The pectoralis major myocutaneous flap: a versatile flap for reconstruction in the head and neck. Plast Reconstr Surg. 1979;63:73–81.
13. Futrell JW, Johns ME, Edgerton MT, et al. Platysma myocutaneous flap for intraoral reconstruction. Am J Surg. 1978;136:504–7.
14. Quillen CG, Shearing JG, Georgade NG. Use of Latissmusdorsimyocutanoeus island flap for reconstruction in the head and neck area: case report. Plast Reconstr Surg. 1978;62:113–7.
15. Martin D, Pascal JF, Baudet J, Mondie JM, Farhat JB, Athoum A, et al. The submental island flap: a new donor site: anatomy and clinical applications as a free or pedicled flap. Plast Reconstr Surg. 1993;92:867–73.
16. Wang HS, Shen JW, Ma D, Wang JD, Tian AL. The infrahyoidmyocutaneous flap for reconstruction after resection of head and neck cancer. Cancer. 1986;57:663–8.
17. Taylor GI. Reconstruction of mandible with free composite iliac bone grafts. Ann Plast Surg. 1982;9:361–8.
18. Ueba Y, Fujikawa S. Nine years follow up of a free vascularized fibular graft in neuro fibromatosis: a case report and literature review. Int J Orthop Trauma Surg. 1983;26:595–600.
19. O'Brien BM, Morrison WA. Reconstructive microsurgery, vol. 76. Edinburgh: Churchill Livingstone; 1987. p. 97–101.
20. Soutar DS, Scheker LR, Tanner NSB, McGregor IA. The radial forearm flap: a versatile method for intraoral reconstruction. Br J Plast Surg. 1983;36:1–8.
21. dos Santos LF. The vascular anatomy and dissection of the free scapular flap. Plast Reconstr Surg. 1984;73:599–605.
22. McCraw JB, Furlow LT. The dorsalis pedis arterialized flap. Plast Reconstr Surg. 1975;55:177–85.
23. Forrest C, Boyd JB, Manktelow RT, Zuker R, Bowen V. The free vascularized iliac crest tissue transfer: donor site complications associated with 82 cases. Br J Plast Surg. 1992;45:89–93.
24. Han Y, Kiat-amnuay S, Powers JM, Zhao Y. Effect of Nano-oxide concentration on the mechanical properties of a maxillofacial silicone elastomer. J Prosthet Dent. 2008;100:465–73.
25. Guttal SS, Patil NP, Nadiger RK, Hasti A. Nasal prosthesis for a patient with mammalian bite injury. Case report. J Indian Prosthodont Soc. 2007;7:43–5.
26. Guttal SS, Patil NP, Shetye AD. Case report: Prosthetic rehabilitation of a midfacial defect resulting from lethal midline granuloma—a clinical report. J Oral Rehabil. 2006;33:863–7.
27. Guttal SS, Patil NP, Nadiger RK, Rachana KB, Dharnendra, Basutkar N. Use of acrylic resin base as an aid in retaining silicone orbital prosthesis. J Indian Prosthodont Soc. 2008;8:112–5.
28. Avinash CKA, Nadiger R, Guttal SS, Lekha K. Orbital prosthesis: a novel treatment approach. Int J Prosthodont Restor Dent. 2012;2(1):19–23.
29. Guttal SS, Patil NP, Thakur S, Kumar SMV, Kulkarni S. Implant-retained nasal prosthesis for a patient following partial rhinectomy: a clinical report. J Prosthodont. 2009;18:353–8.

30. Guttal SS, Shanbhag S, Kulkarni SS, Thakur SL. Rehabilitation of a missing ear with an implant retained auricular prosthesis. J Indian Prosthodont Soc. 2015;15:70–5.
31. Guttal SS, Desai J, Kudva A, Patil BR. Rehabilitation of orbital defect with silicone orbital prosthesis retained by dental implants. Indian J Ophthalmol. 2016;64:93–5.
32. Melek LN. Tissue engineering in oral and maxillofacial reconstruction. Tanta Dent J. 2015;12(3):211–23.
33. Zayed SM, Alshimy AM, Fahmy AE. Effect of surface treated silicon dioxide nanoparticles on some mechanical properties of maxillofacial silicone elastomer. Int J Biomater. 2014;2014:750398, 7 p.
34. Van Schooneveld MM, Vucic E, Koole R, et al. Improved biocompatibility and pharmacokinetics of silica nanoparticles by means of a lipid coating: a multimodality investigation. Nano Lett. 2008;8(8):2517–25.
35. Shakir DA, Abdul-Ameer FM. Effect of nano-titanium oxide addition on some mechanical properties of silicone elastomers for maxillofacial prostheses. J Taibah Univ Med Sci. 2018;13(3):281–90.
36. Mitra A, Choudhary S, Garg H, et al. Maxillofacial prosthetic materials-an inclination towards silicones. J Clin Diagn Res. 2014;8(12):ZE08–13.
37. Alsmael MA, Moudhaffer M, Ali M, et al. The effect of nano titanium silicate addition on some properties of maxillofacial silicone material. J Res Med Dent Sci. 2018;6:127–32.
38. Salih SI, Oleiwi JK, Ali HM. Modification of silicone rubber by added PMMA and natural nanoparticle used for maxillofacial prosthesis applications. ARPN J Eng Appl Sci. 2019;14(4):781–91.
39. Yazdani J, Ahmadian E, Sharifi S, et al. A short view on nanohydroxyapatite as coating of dental implants. Biomed Pharmacother. 2018;105:553–7.
40. García C, Ceré S, Durán A. Bioactive coatings deposited on titanium alloys. J Non-Cryst Solids. 2006;352(32–35):3488–95.
41. Breding K, Jimbo R, Hayashi M, et al. The effect of hydroxyapatite nanocrystals on osseointegration of titanium implants: An in vivo rabbit study. Int J Dent. 2014;2014:171305.
42. Svanborg LM, Hoffman M, Andersson M, et al. The effect of hydroxyapatite nanocrystals on early bone formation surrounding dental implants. Int J Oral Maxillofac Surg. 2011;40(3):308–15.
43. Carinci F, Lauritano D, Bignozzi CA, et al. A new strategy against peri-implantitis: antibacterial internal coating. Int J Mol Sci. 2019;20(16):3897.
44. Romanò CL, Tsuchiya H, Morelli I, et al. Antibacterial coating of implants: are we missing something? Bone Joint Res. 2019;8(5):199–206.
45. Wafa H, Grimer RJ, Reddy K, et al. Retrospective evaluation of the incidence of early periprosthetic infection with silver-treated endoprostheses in high-risk patients: case-control study. Bone Joint J. 2015;97-B(2):252–7.
46. Akash RN, Guttal SS. Effect of incorporation of nano-oxides on color stability of maxillofacial silicone elastomer subjected to outdoor weathering. J Prosthodont. 2015;24:569–75.
47. Kiat-Amnuay S, Mekayarajjananonth T, Powers JM, Chambers MS, Lemon JC. Interactions of pigments and opacifiers on color stability of MDX4–4210/type A maxillofacial elastomers subjected to artificial aging. J Prosthet Dent. 2006;95:249–57.
48. Haug SP, Andres CJ, Moore BK. Color stability and colorant effect on maxillofacial elastomers. Part III: weathering effect on color. J Prosthet Dent. 1999;81:431–8.
49. Polyzois GL. Color stability of facial silicone prosthetic polymers after outdoor weathering. J Prosthet Dent. 1999;82:447–50.
50. Zardawi FM, Xiao K. Optimization of maxillofacial prosthesis. In: Prosthesis. London: IntechOpen; 2019. https://doi.org/10.5772/intechopen.85034.

Potential Applications of Graphene-Based Nanomaterials in Biomedical, Dental, and Implant Applications

Dinesh Rokaya, Viritpon Srimaneepong, Pasutha Thunyakitpisal, Jiaqian Qin, Vinicius Rosa, and Janak Sapkota

Abstract Graphene-based materials have gained extensive attention in the field of research seeking novel materials for biomedicine, dentistry, and implantology due to their unique physicochemical properties, high strength, thermal stability, electrical conductivity, chemical purity, large surface area, and the possibility of functionalization. Graphene-based nanomaterial can be used for various applications, such as antimicrobial agent, biocompatible coatings and anticorrosion, drug delivery, and therapy. This chapter summarizes the basic properties of graphene and the latest progress based on current knowledge. The comprehensive review of graphene-based materials and their possible applications focusing on dentistry and dental implantology is described.

D. Rokaya
Research Unit of Herbal Medicine, Faculty of Dentistry, Chulalongkorn University, Bangkok, Thailand

V. Srimaneepong (✉)
Department of Prosthodontics, Faculty of Dentistry, Chulalongkorn University, Bangkok, Thailand
e-mail: viritpon.s@chula.ac.th

P. Thunyakitpisal
Research Unit of Herbal Medicine, Faculty of Dentistry, Chulalongkorn University, Bangkok, Thailand

Department of Anatomy, Faculty of Dentistry, Chulalongkorn University, Bangkok, Thailand

J. Qin
Metallurgy and Materials Science Research Institute, Chulalongkorn University, Bangkok, Thailand

V. Rosa
Oral Sciences, Faculty of Dentistry, National University of Singapore, Singapore, Singapore

J. Sapkota
Institute of Polymer Processin, Department of Polymer Engineering and Science, Montan Universitaet Leoben, Leoben, Austria

R. S. Chaughule, R. Dashaputra (eds.), *Advances in Dental Implantology using Nanomaterials and Allied Technology Applications*,
https://doi.org/10.1007/978-3-030-52207-0_4

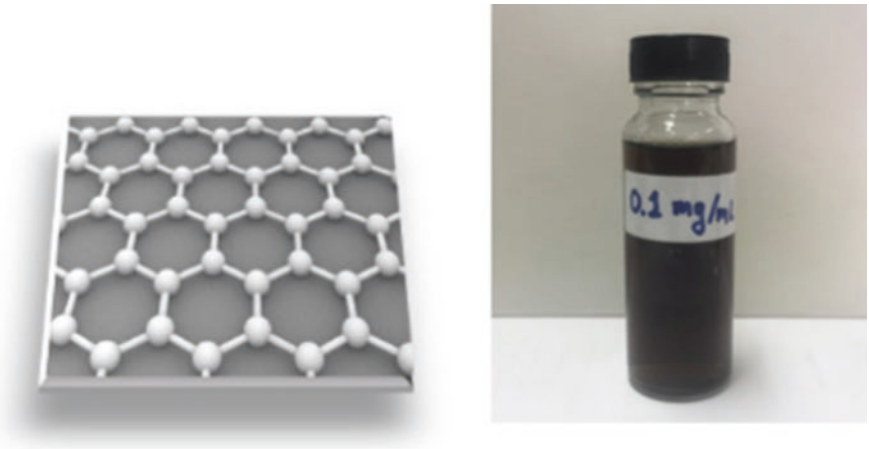

Fig. 1 Graphene structure and graphene in deionized water solution

Keywords Graphene · Dental implant · Coatings · Bone regeneration

1 Introduction

Graphene, discovered in 2004 [1], is a thin sheet of sp^2 bonded carbon atoms [2, 3] as shown in Fig. 1. Graphene consists of carbon atoms and can be in the form of pure graphene (pristine graphene), graphene oxide (GO) containing –C–O–O–H, –C–O–C–, or –C–O–H, and reduced GO (rGO). Graphene has remarkable properties of high surface area, high mechanical strength, stiffness, elasticity, high electrical, thermal conductivity, good biocompatibility, and ease of functionalization compared to other materials, such as collagen and hydrogel [4–8]. Hence, it is attracted to various fields including dentistry and implantology [3, 9–11]. A nomenclature for 2D carbons has been mentioned which gives a description of their subject materials and allowed to move forward with a deeper understanding of graphene-based materials [12].

2 Production of Graphene

Graphene can be prepared from various methods according to the need and applications. The common methods for the production are mentioned below [3, 4, 13]:

(a) Exfoliation of graphite prepared mechanically
(b) Epitaxial growth (SIC)
(c) Liquid phase exfoliation (LPE)

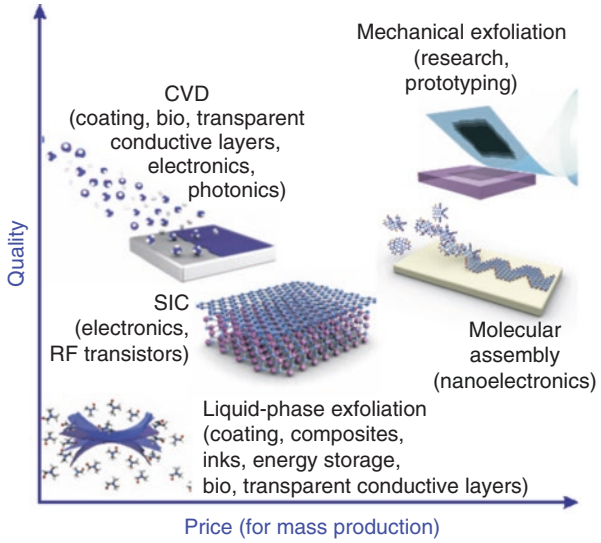

Fig. 2 Various production methods of graphene [4]

(d) Chemical vapor deposition (CVD)
(e) Molecular assembly (MA)

From the above techniques, various grades of graphene are produced in various amounts by varying defects and substrates (Fig. 2).

Mechanical exfoliation is the simplest of the preparation methods. In this technique, a piece of graphite undergoes repeated tape exfoliation and is then transferred to a substrate [14, 15]. This method still makes the highest quality crystals but is only useful for lab-scale experiments and prototyping as it is not possible to scale-up the process and used only for very small sample areas [16].

Epitaxial growth of graphite on silicon carbide has a long history [16]. The epitaxial graphene can be grown on SiC using a high-temperature sublimation growth process (1300–1800 °C) in an ultrahigh vacuum or inert atmosphere [17]. The number of graphene layers, stacking of layers, and coupling to the substrate varies with crystal face orientation and growth conditions [18]. The produced graphene nanostructures are thus with atomically smooth edges. The graphene produced consists of certain structural and manufacturing defects.

Molecular self-assembly is a technique to induce a modulation on graphene for improving the electronic properties [19, 20]. For this purpose, metal phthalocyanines (MPc) are excellent candidates [21]. They consist of a coordinated metal ion surrounded by an organic macrocycle, and charge transfer between graphene and MPc has been reported. Commonly, MPc form a square lattice on epitaxial graphene on iridium 111 [Ir(111)] [22] and a Kagome lattice on epitaxial graphene on ruthenium 0001 [Ru(0001)] [23]. For this technique, molecular ordering is likely to be crucial for achieving potential shapes [19]. In addition, this process is sensitive to the interaction between the graphene and the substrate on which it is grown [24].

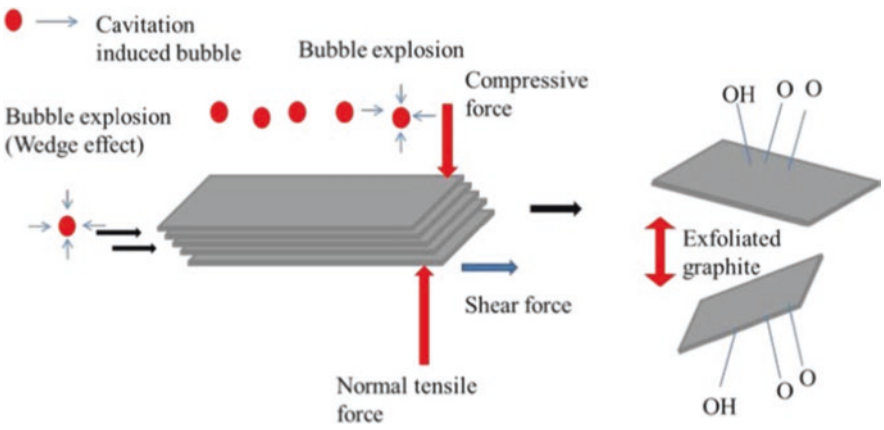

Fig. 3 Liquid-phase exfoliation (LPE) of graphite using sonication [33]

Liquid phase exfoliation (LPE) is a straightforward procedure with high potential for the mass production of graphene and is the main method for mass production [25, 26]. Common techniques of LPE have been reported, such as sonication [27], jet cavitation [28], high-shear mixing [26], and microfluidization [29]. Sonication is an effective exfoliation method and has the potential to produce monolayer or few-layer graphene at relatively high concentrations [27, 30]. This process involves three steps, viz., the preparation of dispersion of graphite in a specific solvent, the exfoliation of dispersion via sonication, and the purification of graphene [27]. Sonication results in the growth and collapse of the microbubbles in liquids which causes cavitation-induced pressure pulsations and shock waves, which will produce normal and shear forces on graphite [31]. Various factors affecting the exfoliation are the power of sonication (cavitation), the liquid medium for dispersion of graphene nanosheets, the rate of centrifugation, and shear forces [31–33]. The liquid provides an environment for stable dispersions of graphene during sonication. The mechanism of exfoliation of graphite using sonication is shown in Fig. 3 [33]. Jet cavitation helps to produce graphene sheets from exfoliation of graphite crystals in aqueous solution, and this method is a facile, low-cost, time-saving, and laborsaving route potentially for mass production of graphene [28]. High-shear mixing of graphite in suitable stabilizing liquids results in large-scale exfoliation to give dispersions of graphene nanosheets and the graphene produced can be applied in conductive coatings [26]. Production of graphene by microfluidization can be possible by the exfoliation of graphite in aqueous solutions under high-shear rate [~10^8 s^{-1}] turbulent flow conditions, and this is a simple and scalable production route for conductive inks for large-area printing in flexible electronics [29].

Chemical vapor deposition (CVD) is a scalable strategy for large-scale production of graphene with a controllable number of layers and crystallinity [34]. Figure 4 shows the adopted transfer process [35]. At first, graphene thin film is grown on Ni foil using CVD, and then it is transferred to a glass slide. This procedure is expensive and time-consuming, and often results in contamination of metal ions, wrin-

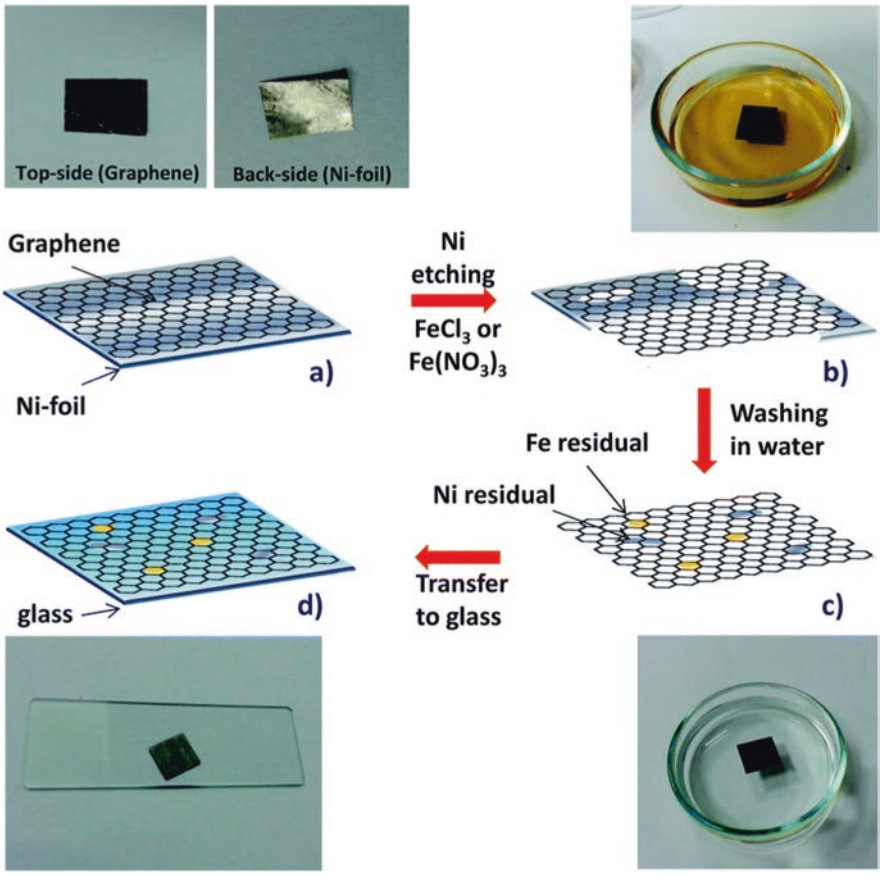

Fig. 4 Graphene transfer process: (**a**) production of graphene thin film on Ni by CVD, (**b**) etching of Ni using iron chloride ($FeCl_3$) or iron nitrate ($Fe(NO_3)_3$) solution and allowed dissolution completely, (**c**) washing in water, and (**d**) transfer of graphene to a clean glass slide [35]

kling, and defects or breakage of graphene during transferring steps [35, 36]. Hence, an effective method would be growing graphene directly on selected semiconductor and dielectric substrates. The challenge is the direct growth of graphene using CVD both on insulators and on semiconductors as they have low catalytic activity for carbon [37].

Graphene can be grown on nonmetallic substrates like SiO_2, h-BN, or quartz using low-temperature plasma-enhanced CVD (PECVD) and this allows direct deposition of high-quality graphene (Fig. 5) [37, 38]. Graphene may be directly produced on dielectrics like ZrO_2, SiO_2, HfO_2, h-BN, Al_2O_3, Si_3N_4, quartz, MgO, $SrTiO_3$, TiO_2, etc., and semiconductors like SiC, Si, Ge, and GaN using a low-temperature PECVD technique [34]. The high temperature causes the dissociation of carbon atoms from methane that reacts with the metal substrate allowing the formation of the typical honeycomb carbon structure on its surface. Thereafter, the

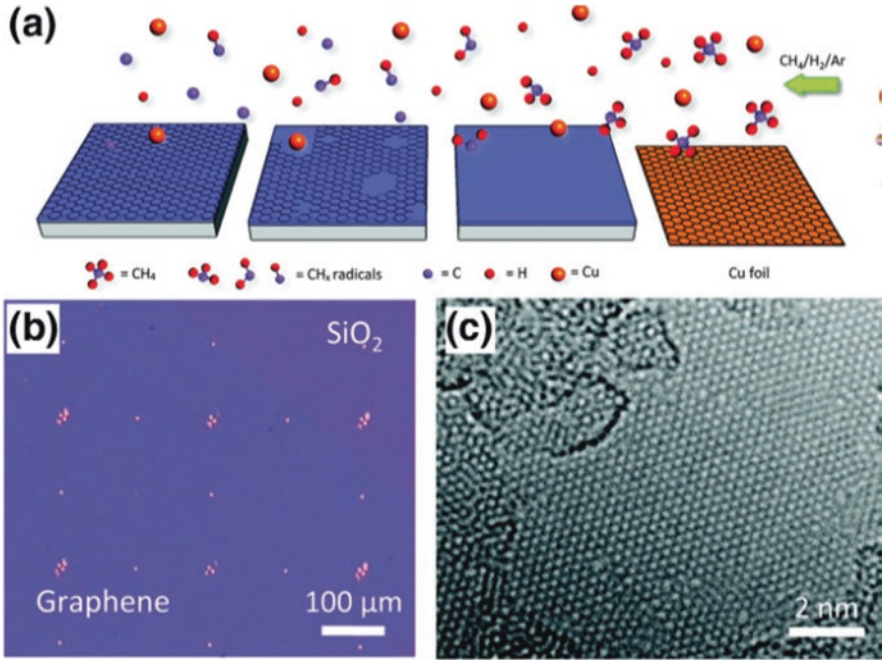

Fig. 5 Growing graphene directly on SiO_2 substrate using a metal catalyst: (**a**) process of graphene growth, (**b**) optical image of the graphene, and (**c**) structure of graphene lattice [38]

graphene films are transferred onto target substrates via different techniques [39, 40].

Chemical vapor deposition growth of graphene can result in 3D structure [34] as shown in Fig. 6 [41, 42] which can have high specific surface area, low density, and fast electron transport. They are great for energy-related applications, engineering, and nanotechnology including biomedical science.

3 Properties and Characterization of Graphene

Graphene has good mechanical properties, such as high electron mobility (15,000 $cm^2\ V^{-1}\ s^{-1}$) [43], large surface area (2630 $m^2\ g^{-1}$) [44], high thermal conductivity (5000 $W\ m^{-1}\ K^{-1}$) [45], good electrical conductivity (250,000 $cm^2\ V^{-1}\ s^{-1}$) [15], high modulus of elasticity (~1 TPa) [46], high stiffness and high strength (42 $N\ s^{-1}$) [46], unique friction and wear properties [4, 7] making it attractive for use in vast applications. Large surface, porous structure, and capability to make nanocomposite properties have biomedical applications in drug delivery and regenerative medicine. High strength, low friction, and good wear properties are used in coatings and nanocomposites. Good electrical conductivity is used in semiconductors,

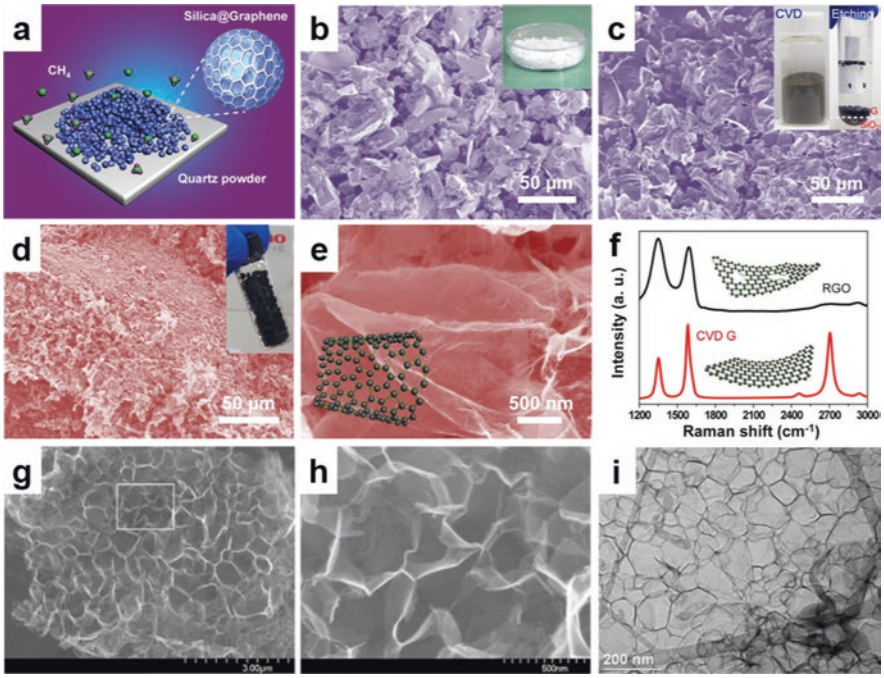

Fig. 6 Chemical vapor deposition (CVD)-grown 3D graphene on quartz powder: (**a**) graphene flakes grown from CVD, (**b**) scanning electron microscopy (SEM) images of quartz powder before CVD growth of graphene, (**c**) SEM images of quartz powder after CVD growth of graphene with pictures of samples before and during chemical etching, (**d**, **e**) SEM images of graphene after separation from quartz with picture of purified graphene powder, (**f**) Raman spectra of graphene and RGO [41], (**g**) low magnification field emission scanning electron microscopy FESEM image of honeycomb-structured graphene, (**h**) enlarged FESEM image, and (**i**) transmission electron microscopy (TEM) image of graphene showing honeycomb structure [42]

biosensors, and supercapacitors. The details in each application are discussed in later sections.

The surface structure of graphene can be studied from scanning electron microscope (SEM), transmission electron microscopy (TEM), energy dispersive spectroscopy (EDS), surface profilometer, Raman spectroscopy, X-ray diffraction (XRD), atomic force microscopy (AFM), and X-ray photoelectron spectroscopy (XPS) [47–51]. Some important characterization of GO is shown in Fig. 7. In SEM, the surface morphology generally shows little rough structure as shown in Fig. 7a [50, 51]. The EDS spectra help to indicate the presence of various elements. Raman spectra of graphene, GO, and rGO show D band at approx. 1320 cm^{-1} and G band 1570 cm^{-1} as shown in Fig. 7b [52]. D bands signify the breathing mode of κ-point phonons with A_{1g} symmetry, and the G band shows the tangential stretching mode of the E_{2g} phonon of the carbon sp^2 atoms. The ratio of D band and G band (I_D/I_G) is approx. 0.84–0.97 [47].

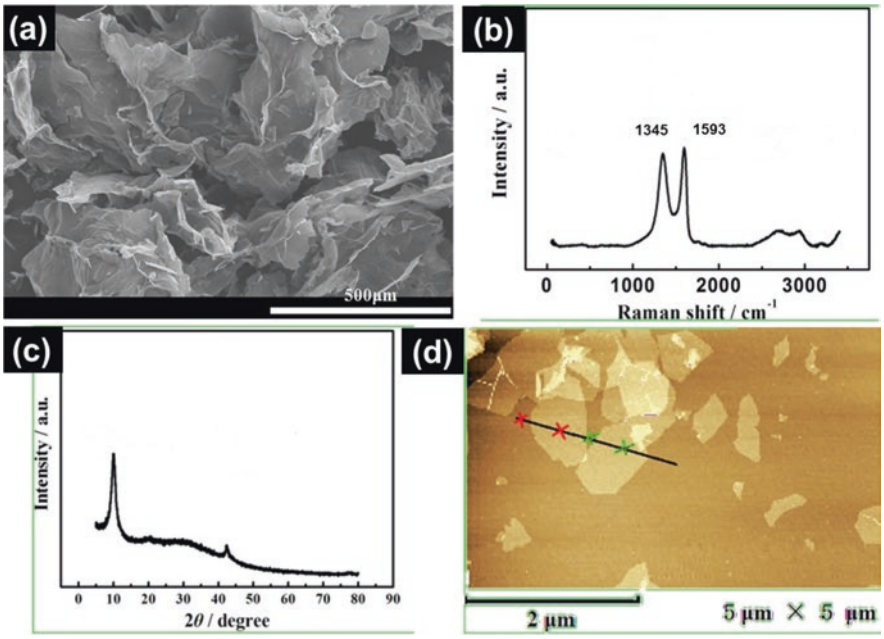

Fig. 7 Characterization of GO sheet: (**a**) Scanning electron microscopy (SEM) of GO fabricated via the modified Hummers method showing crumbling [50], (**b**) Raman spectra, (**c**) X-ray diffraction (XRD) pattern, and (**d**) atomic force microscopy (AFM) [51]

X-ray diffraction (XRD) is used to calculate the crystallinity and interplanar spacing of the graphene-based materials as shown in Fig. 7c. The measurement is performed in contact mode, and the height, deflection, and 3D images are captured at the micron and nanoscale. AFM also shows the surface morphology and allows observing the molecular and atomic level features as shown in Fig. 7d. R_a can also be determined via the surface profilometer and AFM. XPS helps to study the elemental and chemical analysis of graphene. The XPS spectra also help to show the elements present in the graphene and investigate the binding energy between C–C and C–O–C and elements [53].

4 Classification of Graphene-Based Materials

Graphene is a very versatile material that can have great variability in terms of chemical structure, production methods modification, number of layers, forms, and production methods which are briefly summarized in Table 1.

Table 1 Classification of graphene-based materials

Classification of graphene-based materials	
Based on	Graphene derivatives
A. Chemical structure	(a) Pure graphene (pG) (b) Graphene oxide (GO) (c) Reduced graphene oxide (rGO)
B. Production methods	(a) CVD processed graphene (CVD-G) (b) Mechanically exfoliated graphene (ME-G) (c) Solution-processed graphene (S-PG) (d) Epitaxial growth graphene (SiC-G) (e) Molecular assembly graphene (MA-G)
C. Number of layers	(a) Mono/single layer (b) Bilayer (c) Multilayer
D. Physical form [4, 34]	(a) Sheets (b) Flakes (c) Foam (d) Shell (e) Powder (f) Planar
E. Chemical doping	(a) n-doping on graphene: e.g., Nitrogen doping (N-G) and ammonia doping (NH_3-G) (b) p-doping on graphene: e.g., Phenylboronic acid doping ($C_6H_7BO_2$-G), diborane doping (B_2H6-G), oxygen doping (O_2-G), and fluoroalkylsilane (FAS-G)
F. Hybrid materials/ nanocomposites	(a) With metals: e.g., G-Ag, GO-Ag, GO-Cu, and rGO-Cu (b) With nonmetals: e.g., G-Epoxy and G-HA

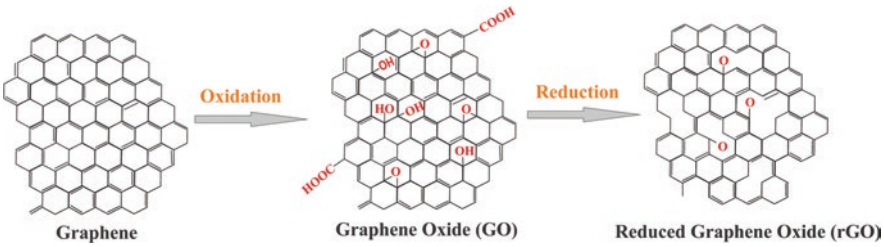

Fig. 8 Production of GO and rGO from graphene [54]

4.1 Chemical Modification

The structure and production of the GO and rGO are shown in Fig. 8 [54]. Generally, GO is yielded by oxidative treatment of graphite by Hummers [55] and modified Hummers method [56]. The rGO is produced from GO by chemical, thermal, or electrochemical reduction. GO and rGO have the advantages of ease of production and the capability to render its functionalities and have wide applications than pris-

Table 2 Some important properties of graphene [3, 58]

Properties	Graphene	GO	rGO
Electrical resistivity	10^{-6} Ω cm	NA	NA
Thermal conductivity	5000 W m^{-1} K^{-1}	2000 W m^{-1} K^{-1}	0.14–0.87 W m^{-1} K^{-1}
Optical transmission	97.7%	<50%	60–90%
Coefficient of thermal expansion	-6×10^{-4} K^{-1}	NA	NA
Electrical conductivity	10^{4} S cm^{-1}	10^{-1} S cm^{-1}	200–35,000 S cm^{-1}
Elastic modulus	1 TPa	0.22 TPa	NA
Tensile strength	130 GPa	120 GPa	NA
Poisson's ratio	0.18	–	–

Table 3 Important properties shown by graphene produced by various methods [4]

Method	Crystallite size (μm)	Sample size (mm)	Charge mobility (cm^2 V^{-1} s^{-1})
CVD processed (CVD-G)	>1000	~1000	10,000
Mechanically exfoliated graphene (ME-G)	>1000	>1	$>2 \times 10^5$ and 10^6
Solution-processed graphene (S-PG)	~100	Infinite as a layer of graphene flakes	100 (for a layer of overlapping graphene flakes)
Epitaxial growth (SiC-G)	50	100	10,000
Molecular assembly (MA-GO)	<50	>1	NA

tine graphene [57]. Some important properties of graphene GO and rGO are given in Table 2.

4.2 Production Methods

Graphene can be classified into five categories according to the production, i.e., CVD processed (CVD-G), mechanically exfoliated graphene (ME-G), solution-processed graphene (S-PG), epitaxial growth (SiC-G), and molecular assembly (MA-G). Their characteristics may vary accordingly as shown in Table 3.

4.3 Number of Layers

Graphene film may contain monolayer, bilayer, or multilayer. Single-layer graphene has a thickness of 0.35 ± 0.01 nm [59]. For multilayer graphene, it is generally accepted to be <10 layers as shown in Fig. 9a, b [6]. Various techniques to study graphene film thickness include Raman scattering, optical contrast, and scanning probe microscopy [60].

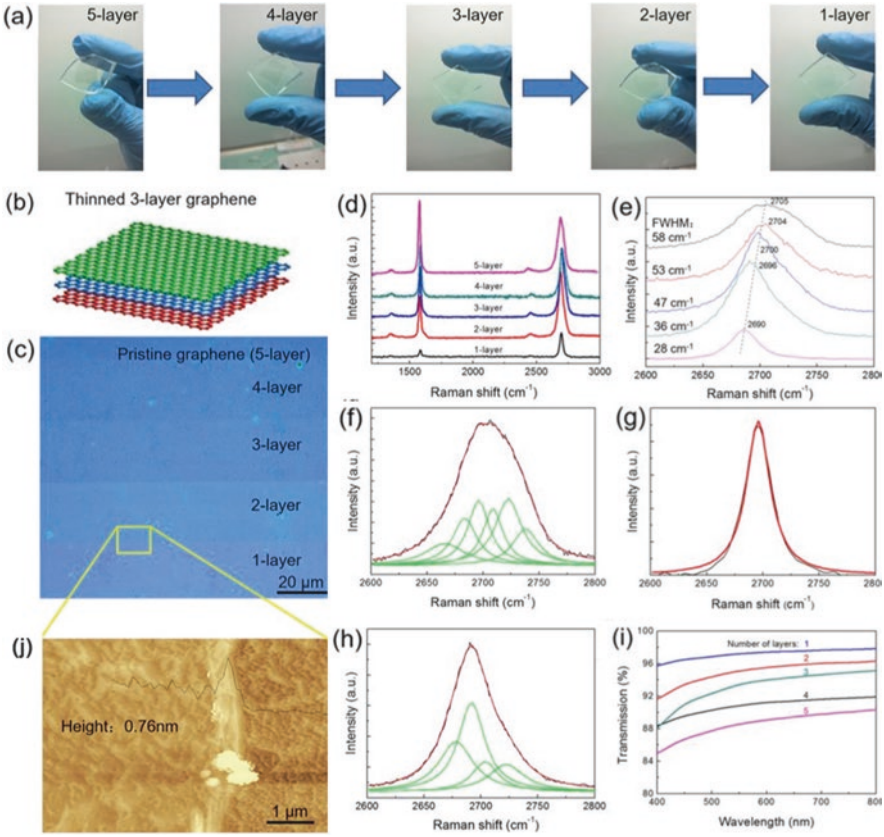

Fig. 9 Graphene layers: (**a**) photographs of various layers of graphene, (**b**) schematic diagram of graphene layers, (**c**) graphene obtained by laser thinning (optical image), (**d**) Raman spectra of various graphene layers, (**e**) 2D peak and full width at height maximum, (**f**–**h**) splitting of 2D peak by Lorentzian fitting: (**f**) 5-layer, (**g**) monolayer, (**h**) bilayer graphene, (**i**) transmittance spectra, and (**j**) atomic fluoroscope microscopy (AFM) image of graphene 1–2 layers [61]

4.4 Physical Forms

Graphene sheet is single layer to multilayer as shown in Figs. 1 and 9b. Graphene 3D structures can be produced in various forms (flakes, foams, shells, and hierarchical structures) [34]. The images of 3D graphene flakes are shown in Fig. 6a. Graphene, GO, or rGO flakes help to produce composite materials. Planar graphene (2D) can be also produced for lower to high performance devices [4]. The 2D graphene layers having pore size of submillimeter can be built into 3D porous graphene forms [62]. The 3D foam has large surface area, lightweight, good thermal and electronic conductivity, provides pathways for ionic transport, high strength, and stiffness properties.

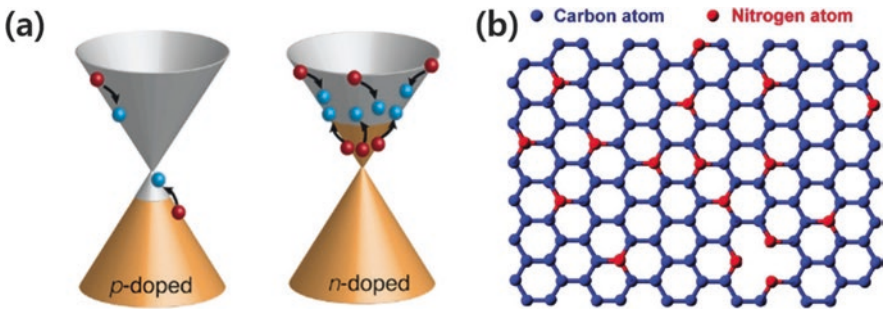

Fig. 10 Doping on graphene: (**a**) types of doping (p- and n-type) [71] and (**b**) doping by hetero-atom replacement into the graphene lattice [72]

Graphene can be reinforced in various composites (e.g., epoxy and polyketone) and metal composites (e.g., Cu, Al, and Ag) [9, 63–66]. Graphene is a conducting material which is atomically thin and flat and can be used for manufacture of energy storage devices [67]. The graphene can be applied in the thin electronic devices of various capacities as the electrodes can be made from 1–2 layer graphene or multilayer rGO.

4.5 Chemical Doping on Graphene

Although graphene has outstanding properties for possible applications in engineering and biomedicine due to sp^2 carbon atoms, it can be further modified to improve its electronic properties, i.e., doping [68–70]. Fermi level production typically occurs in graphene known as n- or p-type doping (Fig. 10a) [71]. Two methods bonding for doping occurs: substitution of carbon atoms or incorporation of dopants by physical or chemical bond (Fig. 10b) [72].

Doping of nitrogen (N) with graphene is usually n-type doping that occurs by the opening of a bandgap by replacing a carbon atom in the graphene lattice which is used for the application in biosensing [69, 73].

4.6 Graphene-Based Nanocomposites

Development of nanocomposites has a long history. Polymer nanocomposites have shown superiority due to the addition of fillers (glass or carbon fibers) [74]. Various graphene-based nanocomposites can be produced with metals (Ag, Zn, Au, Mg, and Ni), nonmetals, and polymers for various applications, including biomedical applications [9, 65, 73, 75]. Important properties of graphene nanocomposites include improved surface properties [3, 64], mechanical properties [64], protective coatings, anticorrosion coatings [76, 77], friction reduction [64], antibacterial applications

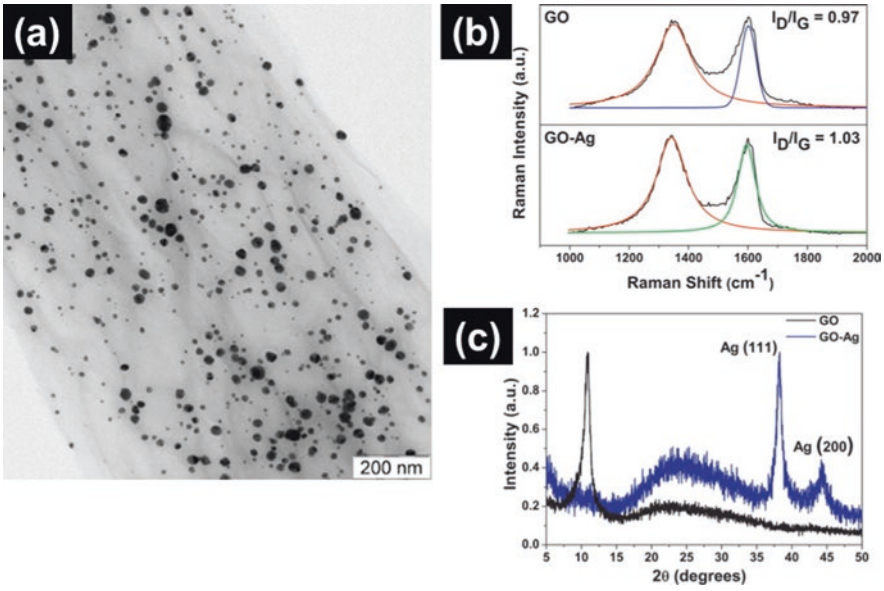

Fig. 11 Characterization of nanocomposite formed from GO sheets decorated with Ag (GO-Ag). (**a**) Transmission electron microscopy (TEM) image, (**b**) Raman spectra, and (**c**) X-ray diffraction (XRD) [47]

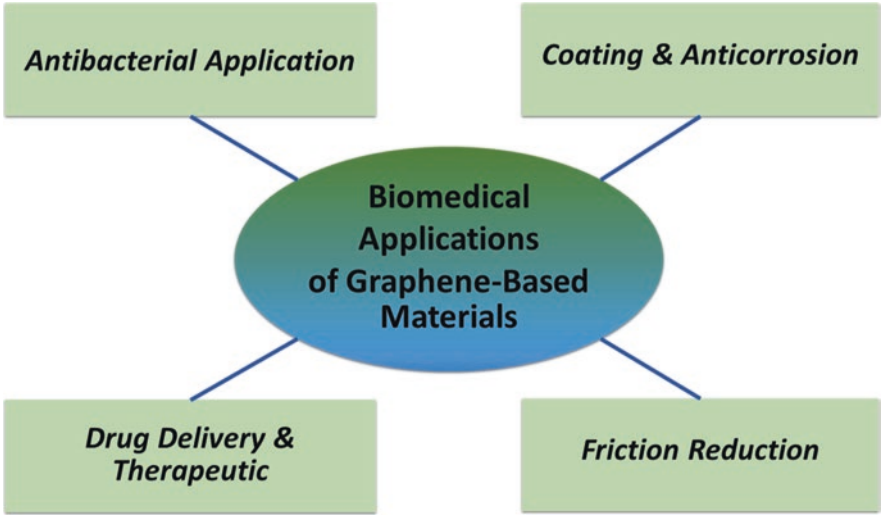

Fig. 12 Various applications of graphene-based materials

[78], biocompatibility [76, 77, 79], etc. The silver nanoparticles (AgNPs) can be decorated on GO to produce GO/Ag nanocomposite (Fig. 11) [47, 79]. The nanocomposite can be used as a coating and an antimicrobial agent [47]. The I_D/I_G ratio of GO/Ag nanocomposite may be slightly increased due to an increase in the disorder of the GO/Ag matrix [47, 80]. The details of other graphene nanocomposites for various applications are discussed in the later parts.

5 Graphene for Dental and Implant Applications

Graphene has useful potentially promising properties for biological applications. In addition, the use of graphene materials in fabricating nanocomposites with different polymers has been explored [3, 9]. The biomedical applications of graphene-based materials include various applications, such as antibacterial, coating material and anticorrosion, friction reduction, drug delivery, and therapeutics (Fig. 12) [76]. Graphene is also considered as an alternative candidate for implant coatings as it is chemically inert and highly durable.

5.1 Antibacterial Application

Bacteria and fungi survive in nature by forming biofilms (self-produced polymer matrix consisting of polysaccharide, protein, and extracellular DNA) on surfaces of teeth, prostheses, or implant-anchored restorations [81]. The biofilm formation on dental implants can result in a serious infection leading to its failure.

An implant is a prosthetic device placed in the human body for various purposes, and in dentistry, it is widely used for replacing teeth or aids in the retention of the dental prosthesis [82]. There is always a challenge to produce implant having good osseointegration inhibiting the bacterial colonization to prevent infection, simultaneously [83–85]. Despite long-term survival rates of dental implants, the complications and peri-implant diseases (peri-implant mucositis and peri-implantitis) are common and, in severe cases, it results in the loss of the implants and their prostheses [86, 87]. Peri-implant mucositis is the inflammation limited to the peri-implant mucosa in the absence of continuing marginal loss following initial bone remodeling. It is reversible through an early intervention and removal of etiology. Peri-implantitis is a pathologic condition characterized by inflammation of soft tissue with further loss of supporting bone exceeding the bone remodeling around the implant, thereby leading to its loss. The peri-implantitis and bone resorption generally start from the implant neck due to the complex environment in this region. The bacterial colonization of implant surfaces is a major cause of peri-implantitis and its failure.

Many materials are known for antimicrobial properties, such as gold nanoparticles (AuNPs), AgNPs, nanodiamond (ND), and graphene-based nanomaterials [88]. Although AgNPs show the antibacterial characteristics, practical applications of

AgNPs are often hampered by their aggregation and subsequent loss of antibacterial activity [88, 89]. In addition, concerns about the cytotoxicity of AgNPs towards human cells have been noticed [90]. Hence, the concentration of AgNPs should be minimal to avoid complications. Therefore, AgNPs can be decorated on GO to produce GO-Ag nanocomposite for increasing antimicrobial activity [47, 53]. AuNPs have been used more on microbial identification rather than antimicrobial applications [91, 92]. In addition, NDs are highly stable in corrosive media, which limits their decomposition or transformation to materials with potential toxicity and decreased activity [88]. Hence, graphene-based materials are biocompatible having strong antimicrobial properties to prevent bacterial colonization [78, 83, 93]. Agarwalla et al. [93] studied the surface and wettability characteristics of graphene coating on titanium (Ti) and their microbial biofilm interaction for *Streptococcus mutans*, *Enterococcus faecalis*, *Pseudomonas aeruginosa*, and *Candida albicans*. Graphene was deposited on Ti (Control) via a liquid-free technique and transferred once, repeated twice and five times. They found that repeated twice showed high quality and coverage, and decreased biofilm formation for all species. For the graphene transfer process, wet transfer onto substrates employs hazardous chemicals limiting the clinical applications. A dry transfer technique based on a hot-pressing method allows to coat Ti substrates with high-quality graphene and coverage area >90% with a single transfer [83]. The increased hydrophobicity of graphene films was correlated with the decreased biofilm formation for various species. All these findings show that the graphene coatings produced by dry transfer technique on Ti implants is a promising strategy to prevent biofilm formation on implants.

Graphene coatings enhance cell adhesion and osteogenic differentiation. Gu et al. [94] modified the surface of Ti implants and studied the antibacterial and osteoinductive effects of single-layer graphene sheets. CVD-grown single-layer graphene sheets were transferred to Ti disks, followed by a thermal treatment of 2 h at 160 °C to enhance the adhesion strength of graphene. Graphene coatings of Ti enhanced cell adhesion and osteogenic differentiation showed antibacterial activity to Ti substrate which was not affected by the thermal treatment. Similarly, another study found that the graphene layer promoted the osteogenesis differentiation of mesenchymal stem cells and surface bioactivity [95]. Hence, graphene can be used as a bioactive layer to improve the surface properties of NiTi-based dental and orthopedic implants.

GO can be functionalized to increase antimicrobial activity. Silver nanoparticles (AgNPs) can be decorated on GO to produce GO/Ag nanocomposite for increasing antimicrobial applications (Fig. 11) [47, 53]. The nanocomposite showed excellent antibacterial activity against *Escherichia coli* (*E. coli*) and *Staphylococcus aureus* (*S. aureus*) [53]. Zhao et al. [58] fabricated gelatin-functionalized GO (GOGel) surface coatings on nitinol substrates. The antimicrobial property and biocompatibility were studied. The GOGel showed the best cell adhesion, proliferation, and differentiation of mouse osteoblastic cell performance. In addition, they found that *E. coli* was inhibited on GOGel and GO. The bacterial cell membrane failed their integrity and showed the low live/dead ratio of *E. coli* after incubation on GOGel and GO in fluorescent images. Hence, the GO-based coatings have both antimicrobial activity and biocompatibility.

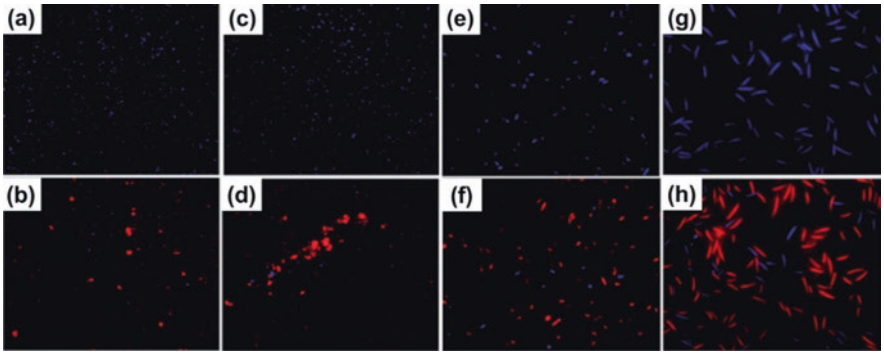

Fig. 13 Cell viability on microscopy images: (**a**) *X. campestris* pv. *undulosa*, (**c**) *P. syringae*, (**e**) *F. oxysporum*, and (**g**) *F. graminearum* after staining with propidium iodide (PI) and fluorescence stain (FS), and (**b**, **d**, **f**, and **h**) fluorescence microscope images of cells after exposure to GO (500 μg mL^{-1}). Fluorescence assay shows the antimicrobial activity of GO as the % of bacteria or spores stained with PI (red color) or % of loss of viability [96]

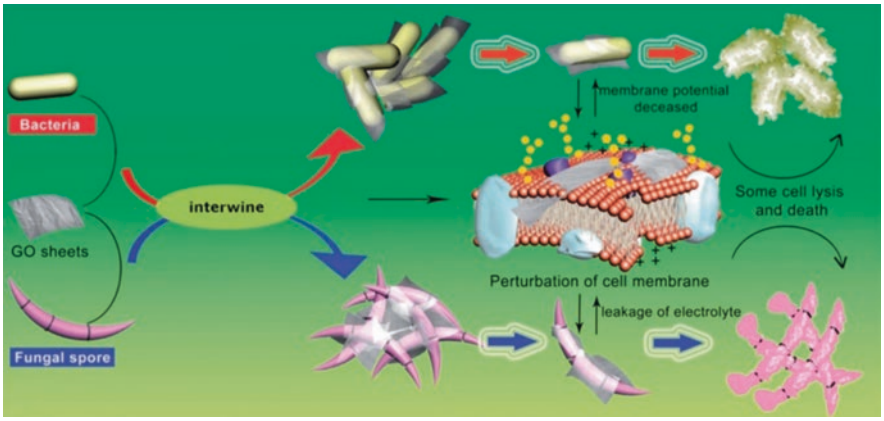

Fig. 14 Diagram showing the mechanism of antibacterial activity of GO against bacterial pathogens and fungal spores [96]

Chen et al. [96] conducted a study on the interaction between GO and four phytopathogens. They studied the antimicrobial activity of GO against two bacterial pathogens, *Xanthomonas campestris* pv. *undulosa* (*X. campestris* pv. *undulosa*) and *pseudomonas* (*P. syringae*), and two fungal pathogens, *Fusarium oxysporum* (*F. oxysporum*) and *Fusarium graminearum* (*F. graminearum*) (Fig. 13). They reported that 90% of the bacteria were killed and 80% macroconidia germination was suppressed along with cell lysis by the GO.

In addition, Chen et al. [96] proposed a mechanism where GO connects the multiresistant bacterial and fungal spores with GO sheets decreasing the potential of bacterial membrane causing cell lysis and the electrolytes leakage of fungal spores (Fig. 14).

5.2 *Coating and Anticorrosion*

Metallic biomaterials are widely used in joint replacements, dental implants, orthopedic fixations, stents, orthodontic, and endodontic applications [97]. Coating on metal alloys becomes sometimes an important aspect to prevent the release of metal ions such as Ni, Ti, and Ag [97, 98]. Although various polymer composite coatings have been tried on metal alloy especially NiTi, there has always been difficult to make successful coatings [99–111]. The drawbacks of polymers coating include roughness, porosity, nonuniformity, and toxicity of the components [112]. The polymer coating on metal may become rough or detach from the metal surface after long-term use. Although graphene is only one atom thick, it is extremely inert and impermeable to gasses (oxygen) and liquids (water) [4]. The use of graphene as a coating and preventing corrosion has been widely studied and found that it can be used as a corrosion barrier film because it is chemically inert, atomically stable, and highly durable [77, 113–116]. In addition, it can be grown directly on from simple to complex metal surfaces. Graphene coating protects metal (Mg, Zn, Ni, Al, etc.) surfaces from corrosive environments [113, 115, 117]. Singh et al. [118] found that graphene composite coating reduced the corrosion of Cu. The promising potential

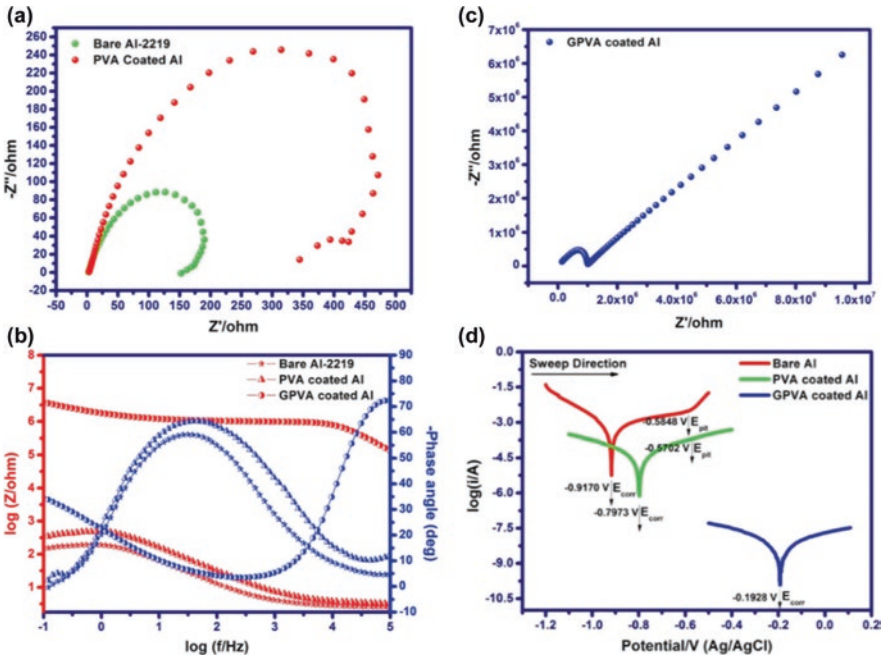

Fig. 15 Graphene-blended polyvinyl (GPVA) nanocomposite coating for corrosion protection: (**a**) Nyquist plot for bare aluminum-2219 alloy (Al-2219) and polyvinyl-coated (PVA-coated) Al-2219, (**b**) Nyquist plot for GPVA-coated Al-2219, (**c**) Bode plot obtained from the impedance analysis, and (**d**) Tafel plot of bare Al, polyvinyl alcohol (PVA)-coated Al, and GPVA-coated Al

observed from anticorrosion effects of graphene suggested that it can be used in orthodontics (archwires), endodontics (files and reamers), and prosthodontics (metal prostheses) [75, 77, 113].

Hikku et al. [119] tested the corrosion of graphene/polyvinyl nanocomposite coating for aluminum-2219 alloy (Al-2219). They found that GPVA-coated Al-2219 showed good corrosion property compared to others (corrosion rate for Al-2219 was 45.25 mm $year^{-1}$, for polyvinyl alcohol (PVA)-coated Al-2219 was 2.576 mm $year^{-1}$) and graphene-blended polyvinyl alcohol (GPVA)-coated Al-2219 alloy showed 3.853×10^{-4} mm $year^{-1}$ in 3.5% NaCl solution as shown from Nyquist plot, a Bode plot, and Tafel plot (Fig. 15). In conclusion, based on these findings, it shows that graphene has a promising anticorrosion potential.

Graphene as a coating material has the potential to improve implant surface properties and corrosion reduction [120–122]. Podila et al. [120] grew graphene on Copper *via* CVD and then transferred onto nitinol implant substrates and studied the effect of graphene coatings on cell adhesion and morphology. They found that the graphene coating on nitinol substrates improved the biological response (cell adhesion, smooth muscle actin expression, and protein adsorption) compared to uncoated nitinol. Thus, graphene-coated nitinol is a viable candidate for a stent material. In addition, surface modification of Ti can enhance the osseointegration of implants. Suo et al. [121] developed homogeneous and crack-free GO/chitosan/hydroxyapatite (GO/CS/HA) composite coating by electrophoretic deposition on Ti substrates. Their results showed that the wettability and bonding strength of the coating were enhanced compared with HA, GO/HA, and CS/HA coatings. Furthermore, the coating greatly increased the cell-material interactions in vitro and enhanced osseointegration in vivo. Hence, the GO/CS/HA-Ti could be a potential alternative in implant dentistry.

Mg is a promising safe biodegradable implant material, but its corrosion speed and hydrogen gas production need to be controlled for biomedical applications. Catt et al. [117] developed a conducting polymer 3,4-ethylenedioxythiophene (PEDOT) and GO composite coating as a corrosion control layer using electropolymerization. They found that the PEDOT/GO coating significantly reduced the rate of corrosion as evidenced by lower Mg ion concentration and pH of the corrosion media. In addition, the coating decreased the evolved hydrogen. PEDOT/GO corrosion protection was attributed to three factors: an initial passive layer preventing solution ingress, buildup of negative charges in the film, and formation of corrosion protective Mg phosphate layer through redox coupling with Mg corrosion. In addition, the coating showed no toxicity to cultured neurons showing the biocompatibility of the coated implants in vitro. These results suggest that PEDOT/GO coating is an effective treatment for controlling corrosion of Mg-based medical implants.

GO coating is also a promising material for regenerative dentistry. Zhou et al. [116] evaluated the bioactivity of human periodontal ligament stem cells (PDLSCs) on GO-coated Ti (GO-Ti) substrate in vitro as compared to sodium titanate (Na-Ti) substrate. They found that with GO-Ti substrate, PDLSCs exhibited significantly higher proliferation rate, alkaline phosphatase (ALP) activity, and upregulated gene expression level of osteogenesis-related markers of collagen type I, ALP, bone sialoprotein (BSP), runt-related transcription factor 2 (Runx2), and osteocalcin (OCN) compared to Na-Ti substrate. Moreover, GO promoted the protein expression of

BSP, Runx2, and OCN. These findings suggest that the combination of GO and PDLSCs provides a promising construct for regenerative dentistry.

5.3 Friction Reduction

There is a role of friction in dentistry and implant dentistry. Friction is a part of the resistance to movement as a bracket slide along an archwire [123]. A considerable amount of force is lost during friction in orthodontic teeth movement [123, 124]. Hence friction reduction becomes often an important part to accelerate the teeth movement in orthodontics.

Various biomaterials have been studied for friction reduction in biomedicine, such as polymers, hydrogel, chitosan derivatives, silicone, protein lubrication, and ZnO NPs [125–127]. But the results show that the friction reduction property is not as expected and coating is not stable, and further research is needed to develop stable coating with good lubricating properties.

The lubrication and friction reduction properties of graphene film coatings have been studied widely and show that they have promising friction reduction properties [49, 128, 129]. One study shows that GO in water improved the lubrication with a friction coefficient of 0.05. Similar results were found by other studies that used graphene coatings [49, 129]. Hence, graphene can help to reduce the friction of various metal-based prostheses [128]. GO/AgNPs coatings can be used as a coating material to reduce friction. Rokaya et al. [64] developed GO/AgNPs coatings on medical-grade NiTi alloy using electrophoretic deposition and studied the mechanical and tribological properties. The coating thickness ranged from 0.46 to 1.34 μm. The friction coefficients of the coated NiTi alloy were significantly lower compared with that of the uncoated NiTi alloy. From these studies, it shows that thin film of graphene-based coatings having favorable hardness and Young's modulus helps in friction reduction.

The role of friction in implant dentistry is a clear understanding of the factors influencing secure preload necessary to prevent screw loosening. Bulaqi et al. [130] studied the effect of coefficient of friction and tightening speed on screw tightening. They found that the coefficient of friction is the most influential factor on efficiency. Increasing the tightening speed lowered the response rate to the frictional resistance, thus diminishing the coefficient of friction and slightly increasing the preload. Increasing the tightening speed has the same result as reducing the coefficient of friction. Hence, GO coatings can be used for the reduction of coefficient of friction.

5.4 Drug Delivery and Therapeutics

Biomaterials have been used as controlled release reservoirs for drug delivery [131]. Therapeutics drug delivery to bones to treat skeletal diseases or prevent postsurgical infections is challenging due to complex and solid bone structure that limits blood

supply and diffusion of therapeutics administered by systemic routes to reach effective concentration. Various materials are used for the drug delivery: polymers in the form of tablets, implants, microspheres, nanoparticles, drug-eluting stents, and polymeric scaffolds to achieve the goal of controlled drug delivery [132], and nanoscale drug delivery systems include nanoparticles, nanocapsules, nanotubes, nanogels, and dendrimers [131]. But the key issue faced by most of the above drug delivery systems are low efficacy and therapeutic profile [133]. Other limitations include suboptimal bioavailability, limited effective targeting, and potential cytotoxicity [131]. Drug delivery systems should be synthesized with controlled composition, shape, size, and morphology and their surface properties should be manipulated to increase solubility, immunocompatibility, and cellular uptake. Hence, graphene-based materials have favorable properties for advanced drug delivery systems and therapeutics as the planar structure of graphene has an excellent capacity to immobilize metals, drugs, biomolecules, probes, and cells [134, 135]. Graphenes have a large surface area and can be easily functionalized which provides opportunities for drug delivery [4, 136]. They can bind to drug molecules and thus form as carriers of small molecules to the desired spot [4, 137]. In addition, it can pass through the membrane barrier as it is lipophilic. In addition, GO-based gene delivery can be achieved through conjugating hybrid gene carrier polyethylenimine (PEI) to GO which improves binding of DNA and condensation and makes efficient transfection (Fig. 16) [138].

Ti and their alloys are employed as mainstream implant materials in dentistry and orthopedics. Recently, Ti drug-releasing implants, with emphasis on nanoengineered Ti nanotubes structures, are developed for solving key problems to improve implants osseointegration, overcome inflammation and infection together with providing localized drug delivery for bone diseases [139]. Graphene may be integrated with Ti nanotubes to bones that can address many disorders and postsurgical condi-

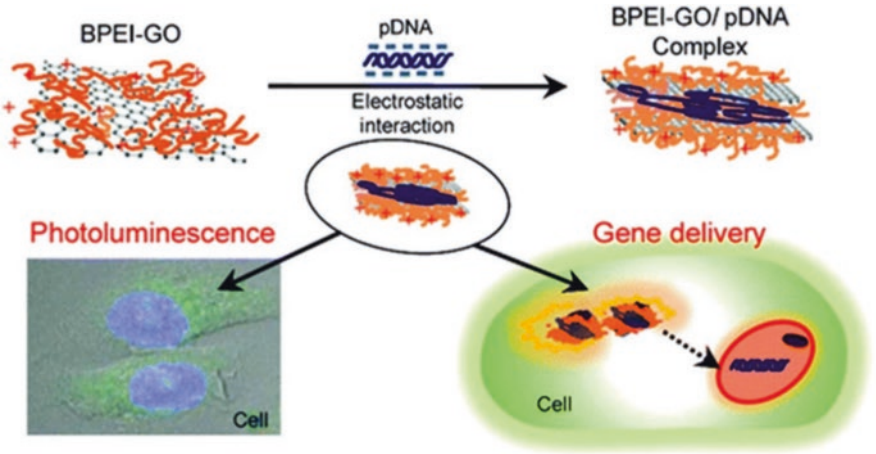

Fig. 16 Diagram showing the plasmid DNA delivery into cells using polyethyl-enimine modified GO (PEI–GO) [138]

tions, such as inflammation, implants rejection, and infection. Hence, graphene-based implant is useful in the treatment of various diseases including peri-implantitis using local drug delivery and gene therapy.

GO can be functionalized covalently with chitosan for successful drug delivery and gene therapy. Bao et al. [140] used chitosan with GO (CS–GO) as a nanocarrier to transport a water-insoluble drug and a plasmid DNA (pDNA) into human cancer cell lines efficiently. But further investigations are needed before clinical use. Moreover, GONPs have the potential to exert inhibitory effects on tumor cells [141–143]. GO with amine groups (GO–NH_2) leads to increased reactivity of the NPs. Krasteva et al. [144] evaluated GO–NH_2 as new molecules for the therapy of colorectal cancer. They found that GO–NH_2 can result in cytotoxicity effect on cancer cell through the induction of reactive oxygen causing DNA damage and apoptosis.

GO is also an efficient carrier for the delivery of therapeutic proteins [135]. La et al. [135] coated Ti substrates with GO using layer-by-layer assembly of positively charged GO sheets (GO-NH_3^+) and negatively charged GO sheets (GO-COO^-). Later, a therapeutic protein (bone morphogenetic protein-2, BMP-2) was loaded on the GO-coated Ti substrate with the coating layer of GO-COO^- (Ti/GO^-). The GO coating on Ti substrate enabled the loading of large doses and the sustained release of BMP-2 with preservation of the structure and bioactivity of the drug. The extent of in vitro osteogenic differentiation of human bone marrow-derived mesenchymal stem cells was higher when they are cultured on Ti/GO-carrying BMP-2 than when they are cultured on Ti with BMP-2. Eight weeks after implantation in mouse models of calvarial defects, the Ti/GO-/BMP-2 implants showed more new bone formation compared with Ti, Ti/GO-, or Ti/BMP-2 implants. Hence, GO is an effective carrier for the controlled delivery of therapeutic proteins, such as BMP-2, which promotes osteointegration of orthopedic or dental Ti implants.

Graphene-based materials are also useful in the treatment of cancer. The conventional cancer therapy/chemotherapy has sometimes failed to treat cancer because of lack of targeting capacity, its side effects, or its toxicity. The major challenge is the lack of efficient gene delivery vectors or vehicles and small biomolecules are digested easily in the body [145]. Graphene-based materials (especially GO and rGO) are also promising candidates for cancer therapy [37, 136, 146, 147]. Due to their unique physicochemical and optical properties including the extremely large surface area, modifiable active groups, and strong photothermal effect, they can act either as tunable carriers or as active agents for advanced chemotherapeutics delivery and cancer therapy [136]. In addition, the pH-dependence of GO emission provides the sensing of acidic extracellular environments of cancer cells, therefore killing the cancer cells [146]. Similarly, gene therapy has become successful in the treatment of genetic disorders and cancer as gene therapy has advantages of high potency with low off-target toxicity, and can treat tumor recurrence and drug resistance [11, 133, 148–152]. Figure 17 shows the gene therapy with the use of transgenes that can produce proteins or convert a compound into a drug after introducing into tumor cells. Therefore, combing photothermal therapy, targeted drug delivery, and chemotherapy would have great potentials for efficient cancer therapy. Graphene

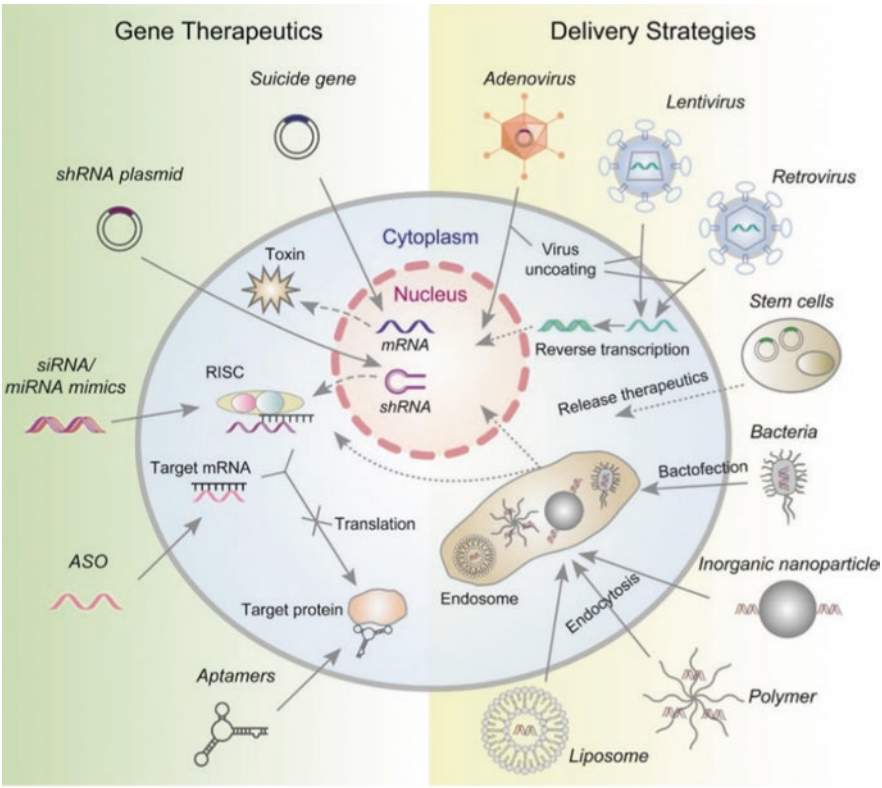

Fig. 17 Diagram showing the gene therapy and delivery strategy. Left side shows the gene therapies using a suicide gene, short hairpin RNA (shRNA), and antisense oligonucleotide (ASO). Right side shows the delivery strategies using viral vectors (adenovirus, lentivirus, retrovirus, and stem cells) and nonviral-based delivery vectors (nanoparticles, polymers, and liposomes) [148]

and its derivatives have been also been found to activate immune cells (IL-6, IL-8, and IL-10) [153, 154]. This immunomodulation can be useful in a developing new vaccine, drug delivery, and biosensors.

6 Conclusion

Graphene-based materials are promising materials in biomedicine, dental, and implant applications. Although the applications of graphene show several challenges, many attempts have been tried and have shown promising results regarding biofunctionalization and applications. Through the multidisciplinary approach among biomedicine, dentistry, chemistry, and engineering, it may assist the deeper understanding of graphene-based materials bioapplications efficiently.

References

1. Novoselov KS, Geim AK, Morozov SV, Jiang D, Zhang Y, Dubonos SV, et al. Electric field effect in atomically thin carbon films. Science. 2004;306:666–9.
2. Katsnelson MI. Graphene: carbon in two dimensions. Mater Today. 2007;10:20–7.
3. Kuill T, Bhadra S, Yao D, Kim NH, Bose S, Lee JH. Recent advances in graphene based polymer composites. Prog Polym Sci. 2010;35:1350–75.
4. Novoselov KS, Fal'ko VI, Colombo L, Gellert PR, Schwab MG, Kim K. A roadmap for graphene. Nature. 2012;490:192–200.
5. Si Y, Samulski ET. Synthesis of water soluble graphene. Nano Lett. 2008;8:1679–82.
6. Geim AK, Novoselov KS. The rise of graphene. Nat Mater. 2007;6:183–91.
7. Dubey N, Bentini R, Islam I, Cao T, Castro Neto AH, Rosa V. Graphene: a versatile carbon-based material for bone tissue engineering. Stem Cells Int. 2015;2015:804213.
8. Rosa V, Zhang Z, Grande RH, Nor JE. Dental pulp tissue engineering in full-length human root canals. J Dent Res. 2013;92:970–5.
9. Stankovich S, Dikin DA, Dommett GHB, Kohlhaas KM, Zimney EJ, Stach EA, et al. Graphene-based composite materials. Nature. 2006;442:282–6.
10. Mao HY, Laurent S, Chen W, Akhavan O, Imani M, Ashkarran AA, et al. Graphene: promises, facts, opportunities, and challenges in nanomedicine. Chem Rev. 2013;113:3407–24.
11. Shen H, Zhang L, Liu M, Zhang Z. Biomedical applications of graphene. Theranostics. 2012;2:283–94.
12. Bianco A, Cheng H-M, Enoki T, Gogotsi Y, Hurt RH, Koratkar N, et al. All in the graphene family—a recommended nomenclature for two-dimensional carbon materials. Carbon. 2013;65:1–6.
13. Al-Sherbini A-S, Bakr M, Ghoneim I, Saad M. Exfoliation of graphene sheets via high energy wet milling of graphite in 2-ethylhexanol and kerosene. J Adv Res. 2017;8:209–15.
14. Geim AK. Nobel Lecture: random walk to graphene. Rev Mod Phys. 2011;83:851–62.
15. Papageorgiou DG, Kinloch IA, Young RJ. Mechanical properties of graphene and graphene-based nanocomposites. Prog Mater Sci. 2017;90:75–127.
16. Guy OJ, Walker K-AD. Chapter 4—Graphene functionalization for biosensor applications. In: Saddow SE, editor. Silicon carbide biotechnology. 2nd ed. Amsterdam: Elsevier; 2016. p. 85–141.
17. Michon A, Vézian S, Ouerghi A, Zielinski M, Chassagne T, Portail M. Direct growth of few-layer graphene on 6H-SiC and 3C-SiC/Si via propane chemical vapor deposition. Appl Phys Lett. 2010;97:171909.
18. de Heer WA, Berger C. Epitaxial graphene. J Phys D Appl Phys. 2012;45:150301.
19. Järvinen P, Hämäläinen SK, Banerjee K, Häkkinen P, Ijäs M, Harju A, et al. Molecular self-assembly on graphene on SiO2 and h-BN substrates. Nano Lett. 2013;13:3199–204.
20. Wang QH, Hersam MC. Room-temperature molecular-resolution characterization of self-assembled organic monolayers on epitaxial graphene. Nat Chem. 2009;1:206–11.
21. Wang X, Xu J-B, Xie W, Du J. Quantitative analysis of graphene doping by organic molecular charge transfer. J Phys Chem C. 2011;115:7596–602.
22. Hämäläinen SK, Stepanova M, Drost R, Liljeroth P, Lahtinen J, Sainio J. Self-assembly of cobalt-phthalocyanine molecules on epitaxial graphene on Ir(111). J Phys Chem C. 2012;116:20433–7.
23. Mao J, Zhang H, Jiang Y, Pan Y, Gao M, Xiao W, et al. Tunability of supramolecular kagome lattices of magnetic phthalocyanines using graphene-based Moiré patterns as templates. J Am Chem Soc. 2009;131:14136–7.
24. MacLeod JM, Rosei F. Molecular self-assembly on graphene. Small. 2014;10:1038–49.
25. Xu Y, Cao H, Xue Y, Li B, Cai W. Liquid-phase exfoliation of graphene: an overview on exfoliation media, techniques, and challenges. Nanomaterials (Basel, Switzerland). 2018;8:942.
26. Paton KR, Varrla E, Backes C, Smith RJ, Khan U, O'Neill A, et al. Scalable production of large quantities of defect-free few-layer graphene by shear exfoliation in liquids. Nat Mater. 2014;13:624–30.

27. Ciesielski A, Samori P. Graphene via sonication assisted liquid-phase exfoliation. Chem Soc Rev. 2014;43:381–98.
28. Shen Z, Li J, Yi M, Zhang X, Ma S. Preparation of graphene by jet cavitation. Nanotechnology. 2011;22:365306.
29. Karagiannidis PG, Hodge SA, Lombardi L, Tomarchio F, Decorde N, Milana S, et al. Microfluidization of graphite and formulation of graphene-based conductive inks. ACS Nano. 2017;11:2742–55.
30. Lotya M, King PJ, Khan U, De S, Coleman JN. High-concentration, surfactant-stabilized graphene dispersions. ACS Nano. 2010;4:3155–62.
31. Han JT, Jang JI, Kim H, Hwang JY, Yoo HK, Woo JS, et al. Extremely efficient liquid exfoliation and dispersion of layered materials by unusual acoustic cavitation. Sci Rep. 2014;4:5133.
32. Pavlova AS, Obraztsova EA, Belkin AV, Monat C, Rojo-Romeo P, Obraztsova ED. Liquid-phase exfoliation of flaky graphite. J Nanophoton. 2016;10:012525.
33. Lin Z, Karthik PS, Hada M, Nishikawa T, Hayashi Y. Simple technique of exfoliation and dispersion of multilayer graphene from natural graphite by ozone-assisted sonication. Nanomaterials (Basel). 2017;7:125.
34. Chen K, Shi L, Zhang Y, Liu Z. Scalable chemical-vapour-deposition growth of three-dimensional graphene materials towards energy-related applications. Chem Soc Rev. 2018;47:3018–36.
35. Ambrosi A, Pumera M. The CVD graphene transfer procedure introduces metallic impurities which alter the graphene electrochemical properties. Nanoscale. 2014;6:472–6.
36. Khan A, Islam SM, Ahmed S, Kumar RR, Habib MR, Huang K, et al. Direct CVD growth of graphene on technologically important dielectric and semiconducting substrates. Adv Sci (Weinh). 2018;5:1800050.
37. Wang H, Yu G. Direct CVD graphene growth on semiconductors and dielectrics for transfer-free device fabrication. Adv Mater. 2016;28:4956–75.
38. Teng PY, Lu CC, Akiyama-Hasegawa K, Lin YC, Yeh CH, Suenaga K, et al. Remote catalyzation for direct formation of graphene layers on oxides. Nano Lett. 2012;12:1379–84.
39. Morin JLP, Dubey N, Decroix FED, Luong-Van EK, Castro Neto AH, Rosa V. Graphene transfer to 3-dimensional surfaces: a vacuum-assisted dry transfer method. 2D Materials. 2017;4:025060.
40. Rodriguez CLC, Kessler F, Dubey N, Rosa V, Fechine GJM. CVD graphene transfer procedure to the surface of stainless steel for stem cell proliferation. Surf Coat Technol. 2017;311:10–8.
41. Chen K, Chai Z, Li C, Shi L, Liu M, Xie Q, et al. Catalyst-free growth of three-dimensional graphene flakes and graphene/g-C3N4 composite for hydrocarbon oxidation. ACS Nano. 2016;10:3665–73.
42. Wang H, Sun K, Tao F, Stacchiola DJ, Hu YH. 3D honeycomb-like structured graphene and its high efficiency as a counter-electrode catalyst for dye-sensitized solar cells. Angew Chem Int Ed Engl. 2013;52:9210–4.
43. Novoselov KS, Geim AK, Morozov SV, Jiang D, Katsnelson MI, Grigorieva IV, et al. Two-dimensional gas of massless Dirac fermions in graphene. Nature. 2005;438:197–200.
44. Zhu Y, Murali S, Cai W, Li X, Suk JW, Potts JR, et al. Graphene and graphene oxide: synthesis, properties, and applications. Adv Mater. 2010;22:3906–24.
45. Balandin AA, Ghosh S, Bao W, Calizo I, Teweldebrhan D, Miao F, et al. Superior thermal conductivity of single-layer graphene. Nano Lett. 2008;8:902–7.
46. Lee C, Wei X, Kysar JW, Hone J. Measurement of the elastic properties and intrinsic strength of monolayer graphene. Science. 2008;321:385–8.
47. de Faria AF, Martinez DST, Meira SMM, de Moraes ACM, Brandelli A, Filho AGS, et al. Anti-adhesion and antibacterial activity of silver nanoparticles supported on graphene oxide sheets. Colloids Surf B Biointerfaces. 2014;113:115–24.
48. Graf D, Molitor F, Ensslin K, Stampfer C, Jungen A, Hierold C, et al. Spatially resolved Raman Spectroscopy of single- and few-layer graphene. Nano Lett. 2007;7:238–42.

49. Lin J, Wang L, Chen G. Modification of graphene platelets and their tribological properties as a lubricant additive. Tribol Lett. 2011;41:209–15.
50. Park JH, Park JM. Electrophoretic deposition of graphene oxide on mild carbon steel for anti-corrosion application. Surf Coat Technol. 2014;254:167–74.
51. Hao J, Ji L, Wu K, Yang N. Electrochemistry of ZnO@reduced graphene oxides. Carbon. 2018;130:480–6.
52. Chen J, Zheng X, Wang H, Zheng W. Graphene oxide-Ag nanocomposite: in situ photochemical synthesis and application as a surface-enhanced Raman scattering substrate. Thin Solid Films. 2011;520:179–85.
53. Shao W, Liu X, Min H, Dong G, Feng Q, Zuo S. Preparation, characterization, and antibacterial activity of silver nanoparticle-decorated graphene oxide nanocomposite. ACS Appl Mater Interfaces. 2015;7:6966–73.
54. Priyadarsini S, Mohanty S, Mukherjee S, Basu S, Mishra M. Graphene and graphene oxide as nanomaterials for medicine and biology application. J Nanostruct Chem. 2018;8:123–37.
55. Hummers WS Jr, Offeman RE. Preparation of graphitic oxide. J Am Chem Soc. 1958;80:1339.
56. Kovtyukhova NI, Ollivier PJ, Martin BR, Mallouk TE, Chizhik SA, Buzaneva EV, et al. Layer-by-layer assembly of ultrathin composite films from micron-sized graphite oxide sheets and polycations. Chem Mater. 1999;11:771–8.
57. Sang Tran T, Dutta NK, Roy Choudhury N. Graphene-based inks for printing of planar micro-supercapacitors: a review. Materials (Basel). 2019;12:978.
58. Zhao C, Pandit S, Fu Y, Mijakovic I, Jesorka A, Liu J. Graphene oxide based coatings on nitinol for biomedical implant applications: effectively promote mammalian cell growth but kill bacteria. RSC Adv. 2016;6:38124–34.
59. Gupta A, Chen G, Joshi P, Tadigadapa S, Eklund PC. Raman Scattering from high-frequency phonons in supported n-graphene layer films. Nano Lett. 2006;6:2667–73.
60. Shearer CJ, Slattery AD, Stapleton AJ, Shapter JG, Gibson CT. Accurate thickness measurement of graphene. Nanotechnology. 2016;27:125704.
61. Lin Z, Ye X, Han J, Chen Q, Fan P, Zhang H, et al. Precise control of the number of layers of graphene by picosecond laser thinning. Sci Rep. 2015;5:11662.
62. Lu L, De Hosson JTM, Peia Y. Three-dimensional micron-porous graphene foams for lightweight current collectors of lithium-sulfur batteries. Carbon. 2019;144:713–23.
63. Wang L, Yang Z, Cui Y, Wei B, Xu S, Sheng J, et al. Graphene-copper composite with micro-layered grains and ultrahigh strength. Sci Rep. 2017;7:41896.
64. Rokaya D, Srimaneepong V, Qin J, Siraleartmukul K, Siriwongrungson V. Graphene oxide/silver nanoparticles coating produced by electrophoretic deposition improved the mechanical and tribological properties of NiTi alloy for biomedical applications. J Nanosci Nanotechnol. 2018;18:1–7.
65. Rokaya D, Srimaneepong V, Sapkota J, Qin J, Siraleartmukul K, Siriwongrungson V. Polymeric materials and films in dentistry: An overview. J Adv Res. 2018;14:25–34.
66. Ramanathan T, Abdala AA, Stankovich S, Dikin DA, Herrera-Alonso M, Piner RD, et al. Functionalized graphene sheets for polymer nanocomposites. Nat Nanotechnol. 2008;3:327–31.
67. Yoo JJ, Balakrishnan K, Huang J, Meunier V, Sumpter BG, Srivastava A, et al. Ultrathin planar graphene supercapacitors. Nano Lett. 2011;11:1423–7.
68. Banerjee AN. Graphene and its derivatives as biomedical materials: future prospects and challenges. Interface Focus. 2018;8:20170056.
69. Usachov D, Vilkov O, Gruneis A, Haberer D, Fedorov A, Adamchuk VK, et al. Nitrogen-doped graphene: efficient growth, structure, and electronic properties. Nano Lett. 2011;11:5401–7.
70. Hoik L, Keewook P, Ick SK. A review of doping modulation in graphene. Synth Met. 2018;244:36–47.
71. Johannsen JC, Ulstrup S, Crepaldi A, Cilento F, Zacchigna M, Miwa JA, et al. Tunable carrier multiplication and cooling in graphene. Nano Lett. 2015;15:326–31.

72. Wei D, Liu Y, Wang Y, Zhang H, Huang L, Yu G. Synthesis of N-doped graphene by chemical vapor deposition and its electrical properties. Nano Lett. 2009;9:1752–8.
73. Zhang C, Fu L, Liu N, Liu M, Wang Y, Liu Z. Synthesis of nitrogen-doped graphene using embedded carbon and nitrogen sources. Adv Mater. 2011;23:1020–4.
74. Potts JR, Dreyer DR, Bielawski CW, Ruoff RS. Graphene-based polymer nanocomposites. Polymer. 2011;52:5–25.
75. Yang Y, Asiri AM, Tang Z, Du D, Lin Y. Graphene based materials for biomedical applications. Mater Today. 2013;16:365–73.
76. Tong Y, Bohm S, Song M. Graphene based materials and their composites as coatings. Aust J Nanomed Nanotechnol. 2013;1:1003.
77. Kirkland NT, Schiller T, Medhekar N, Birbilis N. Exploring graphene as a corrosion protection barrier. Corros Sci. 2012;56:1–4.
78. Nam JA, Nahain A-A, Kim SM, In I, Park SY. Successful stabilization of functionalized hybrid graphene for high-performance antimicrobial activity. Acta Biomater. 2013;9:7996–8003.
79. Rokaya D, Srimaneepong V, Qin J, Thunyakitpisal P, Siraleartmukul K. Surface adhesion properties and cytotoxicity of graphene oxide coatings and graphene oxide/silver nanocomposite coatings on biomedical NiTi alloy. Sci Adv Mater. 2019;11:1474–87.
80. Hui KS, Hui KN, Dinh DA, Tsang CH, Cho YR, Zhou W, et al. Green synthesis of dimension-controlled Silver nanoparticle-graphene oxide with in situ ultrasonication. Acta Mater. 2014;64:326–32.
81. Høiby N, Ciofu O, Johansen HK, Song Z-J, Moser C, Jensen PØ, et al. The clinical impact of bacterial biofilms. Int J Oral Sci. 2011;3:55–65.
82. Amornvit P, Rokaya D, Bajracharya S, Keawcharoen K, University M, Supavanich W. Management of obstructive sleep apnea with implant retained mandibular advancement device. World J Dent. 2014;5:184–9.
83. Dubey N, Ellepola K, Decroix FED, Morin JLP, Castro Neto AH, Seneviratne CJ, et al. Graphene onto medical grade titanium: an atom-thick multimodal coating that promotes osteoblast maturation and inhibits biofilm formation from distinct species. Nanotoxicology. 2018;12:274–89.
84. Raphel J, Holodniy M, Goodman SB, Heilshorn SC. Multifunctional coatings to simultaneously promote osseointegration and prevent infection of orthopaedic implants. Biomaterials. 2016;84:301–14.
85. Gallo J, Holinka M, Moucha CS. Antibacterial surface treatment for orthopaedic implants. Int J Mol Sci. 2014;15:13849–80.
86. Smeets R, Henningsen A, Jung O, Heiland M, Hammächer C, Stein JM. Definition, etiology, prevention and treatment of peri-implantitis—a review. Head Face Med. 2014;10:1–13.
87. Monje A, Insua A, Wang H-L. Understanding peri-implantitis as a plaque-associated and site-specific entity: on the local predisposing factors. J Clin Med. 2019;8:279.
88. Szunerits S, Boukherroub R. Antibacterial activity of graphene-based materials. J Mater Chem B. 2016;4:6892–912.
89. Wong KKY, Liu X. Silver nanoparticles—the real "silver bullet" in clinical medicine? MedChemComm. 2010;1:125–31.
90. Kong H, Jang J. Antibacterial properties of novel poly(methyl methacrylate) nanofiber containing silver nanoparticles. Langmuir. 2008;24:2051–6.
91. Huang CC, Chen CT, Shiang YC, Lin ZH, Chang HT. Synthesis of fluorescent carbohydrate-protected Au nanodots for detection of Concanavalin A and Escherichia coli. Anal Chem. 2009;81:875–82.
92. Senapati T, Senapati D, Singh AK, Fan Z, Kanchanapally R, Ray PC. Highly selective SERS probe for Hg(ii) detection using tryptophan-protected popcorn shaped gold nanoparticles. Chem Commun. 2011;47:10326–8.
93. Agarwalla SV, Ellepola K, Costa M, Fechine GJM, Morin JLP, Castro Neto AH, et al. Hydrophobicity of graphene as a driving force for inhibiting biofilm formation of pathogenic bacteria and fungi. Dent Mater. 2019;35:403–13.

94. Gu M, Lv L, Du F, Niu T, Chen T, Xia D, et al. Effects of thermal treatment on the adhesion strength and osteoinductive activity of single-layer graphene sheets on titanium substrates. Sci Rep. 2018;8:8141.
95. Li J, Wang G, Geng H, Zhu H, Zhang M, Di Z, et al. CVD growth of graphene on NiTi alloy for enhanced biological activity. ACS Appl Mater Interfaces. 2015;7:19876–81.
96. Chen J, Peng H, Wang X, Shao F, Yuan Z, Han H. Graphene oxide exhibits broad-spectrum antimicrobial activity against bacterial phytopathogens and fungal conidia by intertwining and membrane perturbation. Nanoscale. 2014;6:1879–89.
97. Prasad K, Bazaka O, Chua M, Rochford M, Fedrick L, Spoor J, et al. Metallic biomaterials: current challenges and opportunities. Materials (Basel, Switzerland). 2017;10:884.
98. McMahon RE, Ma J, Verkhoturov SV, Munoz-Pinto D, Karaman I, Rubitschek F, et al. A comparative study of the cytotoxicity and corrosion resistance of nickel-titanium and titanium-niobium shape memory alloys. Acta Biomater. 2012;8:2863–70.
99. Goryczka T, Szaraniec B. Characterization of polylactide layer deposited on Ni-Ti shape memory alloy. J Mater Eng Perform. 2014;23:2682–6.
100. Li P, Li L, Wang W, Jin W, Liu X, Yeung KWK, et al. Enhanced corrosion resistance and hemocompatibility of biomedical NiTi alloy by atmospheric-pressure plasma polymerized fluorine-rich coating. Appl Surf Sci. 2014;297:109–15.
101. Li P, Wu G, Xu R, Wang W, Wu S, Yeung KWK, et al. In vitro corrosion inhibition on biomedical shape memory alloy by plasma-polymerized allylamine film. Mater Lett. 2012;89:51–4.
102. Mazumder MM, Mehta JL, Mazumder NNA, Trigwell S, Sharma R, et al. Encased stent for rapid endothelialization for preventing restenosis. In: Publication PA, editor. Patent pending, A61F 2/06 Edition. United States; 2004. p. 1–27.
103. Schellhammer F, Walter M, Berlis A, Bloss H-G, Wellens E, Schumacher M. Polyethylene terephthalate and polyurethane coatings for endovascular stents: preliminary results in canine experimental arteriovenous fistulas. Radiology. 1999;211:169–75.
104. Villermaux F, Tabrizian M, Yahia LH, Czeremuszkin G, Piron DL. Corrosion resistance improvement of NiTi osteosynthesis staples by plasma polymerized tetrafluoroethylene coating. Biomed Mater Eng. 1996;6:241–54.
105. Tepe G, Schmehl J, Wendel HP, Schaffner S, Heller S, Gianotti M, et al. Reduced thrombogenicity of nitinol stents—in vitro evaluation of different surface modifications and coatings. Biomaterials. 2006;27:643–50.
106. Anjum SS, Rao J, Nicholls JR. Polymer (PTFE) and shape memory alloy (NiTi) intercalated nano-biocomposites. Mater Sci Eng. 2012;40:1–7.
107. De Jesús C, Cruz GJ, Olayo MG, Gómez LM, López-Gracia OG, García-Rosales G, Ramírez-Santiago A, Ríos LC. Coatings by plasmas of pyrrole on nitinol and stainless steel substrates. Superficies y Vacío. 2012;25:157–60.
108. Yang M-R, Wu SK. DC plasma-polymerized hexamethyldisilazane coatings of an equiatomic TiNi shape memory alloy. Surf Coat Technol. 2000;127:274–81.
109. Bhattacharyya A, Dervishi E, Berry B, Viswanathan T, Bourdo S, Kim H, et al. Energy efficient graphite–polyurethane electrically conductive coatings for thermally actuated smart materials. Smart Mater Struct. 2006;15:1–9.
110. Bravo LA, de Cabanes AG, Manero JM, Ruperez ER, Gil JF. NiTi superelastic orthodontic archwires with polyamide coating. J Mater Sci Mater Med. 2014;25:555–60.
111. Carroll WM, Rochev Y, Clarke B, Burke M, Bradley DJ, Plumley DL. Influence of Nitinol wire surface preparation procedures, on cell surface interactions and polymer coating adherence. In: Materials & processes for medical devices conference. Anaheim, CA: ASM International; 2003. p. 63–8.
112. Raza MA, Rehman ZU, Ghauri FA, Ahmad A, Ahmad R, Raffi M. Corrosion study of electrophoretically deposited graphene oxide coatings on copper metal. Thin Solid Films. 2016;620:150–9.
113. Nayak PK, Hsu C-J, Wang S-C, Sung JC, Huang J-L. Graphene coated Ni films: a protective coating. Thin Solid Films. 2013;529:312–6.

114. Catta K, Lia H, Cuia XT. Poly (3,4-ethylenedioxythiophene) graphene oxide composite coatings for controlling magnesium implant corrosion. Acta Biomater. 2016;15:530–40.
115. Asgar H, Deen KM, Rahman ZU, Shah UH, Raza MA, Haider W. Functionalized graphene oxide coating on Ti6Al4V alloy for improved biocompatibility and corrosion resistance. Mater Sci Eng C Mater Biol Appl. 2019;94:920–8.
116. Zhou Q, Yang P, Li X, Liu H, Ge S. Bioactivity of periodontal ligament stem cells on sodium titanate coated with graphene oxide. Sci Rep. 2016;6:19343.
117. Catt K, Li H, Cui XT. Poly (3,4-ethylenedioxythiophene) graphene oxide composite coatings for controlling magnesium implant corrosion. Acta Biomater. 2017;48:530–40.
118. Singh BP, Nayak S, Nanda KK, Jena BK, Bhattacharjee S, Besra L. The production of a corrosion resistant graphene reinforced composite coating on copper by electrophoretic deposition. Carbon. 2013;61:47–56.
119. Hikku GS, Jeyasubramanian K, Venugopal A, Ghosh R. Corrosion resistance behaviour of graphene/polyvinyl alcohol nanocomposite coating for aluminium-2219 alloy. J Alloys Compd. 2017;716:259–69.
120. Podila R, Moore T, Alexis F, Rao A. Graphene coatings for biomedical implants. J Vis Exp. 2013;73:e50276.
121. Suo L, Jiang N, Wang Y, Wang P, Chen J, Pei X, et al. The enhancement of osseointegration using a graphene oxide/chitosan/hydroxyapatite composite coating on titanium fabricated by electrophoretic deposition. J Biomed Mater Res B Appl Biomater. 2019;107:635–45.
122. Li K, Wang C, Yan J, Zhang Q, Dang B, Wang Z, et al. Evaluation of the osteogenesis and osseointegration of titanium alloys coated with graphene: an in vivo study. Sci Rep. 2018;8:1843.
123. Prashant PS, Nandan H, Gopalakrishnan M. Friction in orthodontics. J Pharm Bioallied Sci. 2015;7:S334–8.
124. Kumar S, Singh S, Hamsa PRR, Ahmed S, Prasanthma, Bhatnagar A, et al. Evaluation of friction in orthodontics using various brackets and archwire combinations-an in vitro study. J Clin Diagn Res. 2014;8:ZC33–6.
125. Bhushan B, Kwak KJ, Gupta S, Lee SC. Nanoscale adhesion, friction and wear studies of biomolecules on silane polymer-coated silica and alumina-based surfaces. J R Soc Interface. 2009;6:719–33.
126. Liao YS, Benya PD, McKellop HA. Effect of protein lubrication on the wear properties of materials for prosthetic joints. J Biomed Mater Res. 1999;48:465–73.
127. Behroozian A, Kachoei M, Khatamian M, Divband B. The effect of ZnO nanoparticle coating on the frictional resistance between orthodontic wires and ceramic brackets. J Dent Res Dent Clin Dent Prospects. 2016;10:106–11.
128. Kinoshita H, Nishina Y, Alias AA, Fujii M. Tribological properties of monolayer graphene oxide sheets as water-based lubricant additives. Carbon. 2014;66:720–3.
129. Berman D, Erdemir A, Sumant A. Few layer graphene to reduce wear and friction on sliding steel surfaces. Carbon. 2013;54:454–9.
130. Bulaqi HA, Mousavi Mashhadi M, Geramipanah F, Safari H, Paknejad M. Effect of the coefficient of friction and tightening speed on the preload induced at the dental implant complex with the finite element method. J Prosthet Dent. 2015;113:405–11.
131. Goldberg M, Langer R, Jia X. Nanostructured materials for applications in drug delivery and tissue engineering. J Biomater Sci Polym Ed. 2007;18:241–68.
132. Song R, Murphy M, Li C, Ting K, Soo C, Zheng Z. Current development of biodegradable polymeric materials for biomedical applications. Drug Des Dev Ther. 2018;12:3117–45.
133. Liu J, Cui L, Losic D. Graphene and graphene oxide as new nanocarriers for drug delivery applications. Acta Biomater. 2013;9:9243–57.
134. Wang Y, Li Z, Wang J, Li J, Lin Y. Graphene and graphene oxide: biofunctionalization and applications in biotechnology. Trends Biotechnol. 2011;29:205–12.
135. La WG, Park S, Yoon HH, Jeong GJ, Lee TJ, Bhang SH, et al. Delivery of a therapeutic protein for bone regeneration from a substrate coated with graphene oxide. Small. 2013;9:4051–60.

136. Liu J, Dong J, Zhang T, Peng Q. Graphene-based nanomaterials and their potentials in advanced drug delivery and cancer therapy. J Control Release. 2018;286:64–73.
137. Yang X, Niu G, Cao X, Wen Y, Xiang R, Duan H, et al. The preparation of functionalized graphene oxide for targeted intracellular delivery of siRNA. J Mater Chem. 2012;22:6649–54.
138. Kim H, Namgung R, Singha K, Oh I-K, Kim WJ. Graphene oxide–polyethylenimine nanoconstruct as a gene delivery vector and bioimaging tool. Bioconjug Chem. 2011;22:2558–67.
139. Maher S, Mazinani A, Barati MR, Losic D. Engineered titanium implants for localized drug delivery: recent advances and perspectives of Titania nanotubes arrays. Expert Opin Drug Deliv. 2018;15:1021–37.
140. Bao H, Pan Y, Ping Y, Sahoo NG, Wu T, Li L, et al. Chitosan-functionalized graphene oxide as a nanocarrier for drug and gene delivery. Small. 2011;7:1569–78.
141. Mendonca MC, Soares ES, de Jesus MB, Ceragioli HJ, Batista AG, Nyul-Toth A, et al. PEGylation of reduced graphene oxide induces toxicity in cells of the blood-brain barrier: an in vitro and in vivo study. Mol Pharm. 2016;13:3913–24.
142. Yi L, Zhang Y, Shi X, Du X, Wang X, Yu A, et al. Recent progress of functionalised graphene oxide in cancer therapy. J Drug Target. 2019;27:125–44.
143. Wang S-B, Ma Y-Y, Chen X-Y, Zhao Y-Y, Mou X-Z. Ceramide-graphene oxide nanoparticles enhance cytotoxicity and decrease HCC xenograft development: a novel approach for targeted cancer therapy. Front Pharmacol. 2019;10:69.
144. Krasteva N, Keremidarska-Markova M, Hristova-Panusheva K, Andreeva T, Speranza G, Wang D, et al. Aminated graphene oxide as a potential new therapy for colorectal cancer. Oxidative Med Cell Longev. 2019;2019:3738980.
145. El-Aneed A. An overview of current delivery systems in cancer gene therapy. J Control Release. 2004;94:1–14.
146. Campbell E, Hasan MT, Pho C, Callaghan K, Akkaraju GR, Naumov AV. Graphene oxide as a multifunctional platform for intracellular delivery, imaging, and cancer sensing. Sci Rep. 2019;9:416.
147. Wang K, Kievit FM, Jeon M, Silber JR, Ellenbogen RG, Zhang M. Nanoparticle-mediated target delivery of TRAIL as gene therapy for glioblastoma. Adv Healthc Mater. 2015;4:2719–26.
148. Wang K, Kievit FM, Zhang M. Nanoparticles for cancer gene therapy: recent advances, challenges, and strategies. Pharmacol Res. 2016;114:56–66.
149. Feng L, Wu L, Qu X. New horizons for diagnostics and therapeutic applications of graphene and graphene oxide. Adv Mater. 2013;25:168–86.
150. Goncalves G, Vila M, Portoles MT, Vallet-Regi M, Gracio J, Marques PA. Nano-graphene oxide: a potential multifunctional platform for cancer therapy. Adv Healthc Mater. 2013;2:1072–90.
151. Yang K, Feng L, Shi X, Liu Z. Nano-graphene in biomedicine: theranostic applications. Chem Soc Rev. 2013;42:530–47.
152. Feng L, Liu Z. Graphene in biomedicine: opportunities and challenges. Nanomedicine (Lond). 2011;6:317–24.
153. Srimaneepong V, Rokaya D, Thunyakitpisal P, Qin J, Saengkiettiyut K. Corrosion resistance of graphene oxide/silver coatings on Ni–Ti alloy and expression of IL-6 and IL-8 in human oral fibroblasts. Sci Rep. 2020;10:3247.
154. Lategan K, Alghadi H, Bayati M, de Cortalezzi MF, Pool E. Effects of graphene oxide nanoparticles on the immune system biomarkers produced by RAW 264.7 and human whole blood cell cultures. Nanomaterials (Basel). 2018;8:125.

Implant Materials and Surfaces to Minimizing Biofilm Formation and Peri-implantitis

Morena Petrini, Milena Radunovic, Serena Pilato, Antonio Scarano, Adriano Piattelli, and Simonetta D'Ercole

Abstract The objective of research in implantology is to provide materials and surfaces that could accelerate the healing and osteogenesis, minimize the failures, and provide long-term success.

The production of treated surfaces with additive or subtractive techniques have permitted to increase the bone–implant contact, to accelerate the loading protocols and decrease the early failures; some authors have hypothesized that the increased wettability of these novel surfaces could also increase the bacterial adhesion and the risk of peri-implantitis; however, there are many parameters that influence the biofilm formation.

One of these is represented by the average roughness, Ra, but also other factors, like free energy, chemistry, and titanium purity, have a great role in the establishment of the microbiota.

In this chapter, we will discuss the novel materials and surfaces that could decrease early failure and improve long-term success in implantology.

Keywords Wettability · Roughness · Texture · Titanium · Zirconia · Peek · Biofilm

M. Petrini · A. Scarano · S. D'Ercole (✉)
Department of Medical, Oral and Biotechnological Science, University G. d'Annunzio of Chieti, Chieti, Italy

M. Radunovic
Department of Microbiology and Immunology, School of Dental Medicine, University of Belgrade, Belgrade, Serbia

S. Pilato
Department of Pharmacy, University G. d'Annunzio of Chieti, Chieti, Italy

A. Piattelli
Department of Medical, Oral and Biotechnological Science, University G. d'Annunzio of Chieti, Chieti, Italy

Biomaterials Engineering, Universidad Catolica de San Antonio de Murcia, Murcia, Spain

Fondazione Villa Serena per la Ricerca, Città S. Angelo, Italy

R. S. Chaughule, R. Dashaputra (eds.), *Advances in Dental Implantology using Nanomaterials and Allied Technology Applications*,
https://doi.org/10.1007/978-3-030-52207-0_5

1 Introduction

Recent advancements in all implantology fields, in techniques, biomaterials, and implant micro and macro design, have permitted to simplify the surgical procedure, to accelerate the treatment time and to adopt immediate loading protocol with lower insertion torque values, compared to the past [1, 2]. However, although the concept of implant survival is different from those of successful criteria, implant failure is still a significant concern for implantology [3].

Early implant failures have been associated to endogenous host factors that could affect the bone healing, like the bone quality and quantity, the presence of systemic or metabolic diseases, and smoke, but also to exogenous factors like implant features, the surgical technique, and implant site infections [1, 4]. Late failures are a consequence of bone resorption promoted by an inflammation mediated by bacterial or prosthetic factors.

In particular, Albrektsson et al. have defined the marginal bone loss around dental implants as "immune-osteolytic reactions," because the delicate balance between the osteoblast and the osteoclast results in bone resorption as a consequence of systemic and local factors and habits of the patient [5].

- Systemic factors: comprehend the genetic and systemic disease.
- Local factors: comprehend cement or impression material debris in the peri-implant sulcus, bacterial contamination of the implant components, and technical issues such as loose screws, mobile components, or fractured materials.
- Habits of the patients: like smoking.

As recently stated by the 2017 World Workshop on the Classification of Periodontal and Peri-Implant Diseases and Conditions, peri-implant health is characterized by the absence of erythema, bleeding on probing, swelling, and suppuration. Peri-implant health can exist around implants with reduced bone support and it was not possible to define a range of probing depths compatible with health [6].

The peri-implant disease comprehends two different pathologies: mucositis, characterized by a prevalence of 43% (95% CI: 32–54) and peri-implantitis that is present in the 23% (95% CI: 14–30) of cases as recently reported by a review [7]. The first is characterized by a reversible inflammatory process similar to gingivitis that occurs in the peri-implant soft tissues and that not necessarily transform in peri-implantitis [8]. In histological studies of mucositis, the inflammatory infiltrate did not extend the "apical" of the junctional/pocket epithelium into the supracrestal connective tissue zone [6].

Peri-implantitis is an inflammatory disease that causes the destruction of the bone around dental implants (Fig. 1). In this photograph it is possible to appreciate the clinical signs of peri-implantitis: inflammation of the peri-implant tissues, bleeding and/or presence of suppuration at gentle probing and the increase of pocking deep. The prevalence of peri-implantitis ranges between 15% and 20% after 10 years [9]. Figure 2 represents radiological signs of peri-implantitis on the fixture. The intraoral radiography permits to appreciate the clinical signs of peri-implantitis;

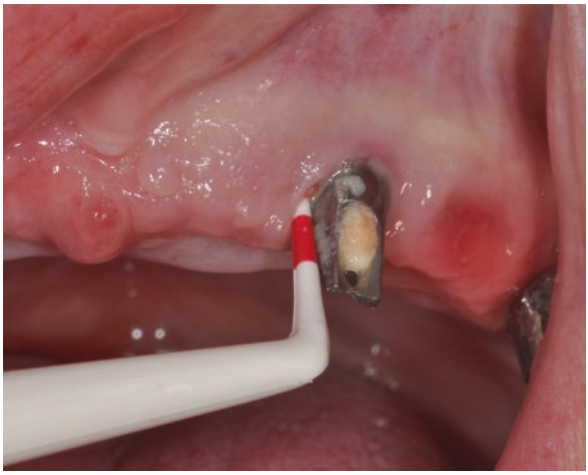

Fig. 1 Clinical signs of peri-implantitis

on the left there is a healthy fixture and on the right an implant is affected by peri-implantitis. The area that surrounds the bone defect has been highlighted in red.

Criteria for diagnosis of peri-implantitis comprehends bleeding (BOP) and/or suppuration on probing, increasing pocket depth, and signs of increasing crestal bone loss [8]. However, the use of BOP as a diagnostic tool is not appropriate for peri-implantitis since up to 90% of implants with stable bone conditions bleed on probing [5].

Although these symptoms are very similar to those of periodontitis, recent literature has shown that they are characterized by a different onset and progression. They are both originated by the contemporary presence of bacteria and excessive host response [10]. However, contrary to periodontitis, there is no consensus about what species of bacteria could lead to dysbiosis causing the pathology. Peri-implantitis is characterized predominantly by nonculturable gram-negative species compared with periodontitis [11].

In particular, a recent article by Lafaurie et al. has shown the microbiological differences between periodontitis and peri-implantitis [11]. The microbiological surveys have shown that both diseases are characterized by the presence of *Porphyromonas gingivalis*, however, periodontitis is characterized by a higher presence of some species, like *Prevotella intermedia*, *Campylobacter rectus*, and *Tannerella forsythia* [11]; on the contrary, a greater presence of enteric rods, *Pseudomonas aeruginosa*, *Staphylococcus aureus*, and *Candida albicans* was recovered more frequently and at higher levels in periimplantitis.

Other differences between periodontitis and peri-implantitis are connected to the absence of periodontal ligaments around implants, so the peri-implantitis affecting directly the bone can be considered an osteitis. In particular, Albrektsson has defined this disease as “immune-osteolytic reactions” [5].

A histological study on dogs, published by Carcuac et al., has shown that samples from peri-implantitis sites were characterized by higher size, were more close

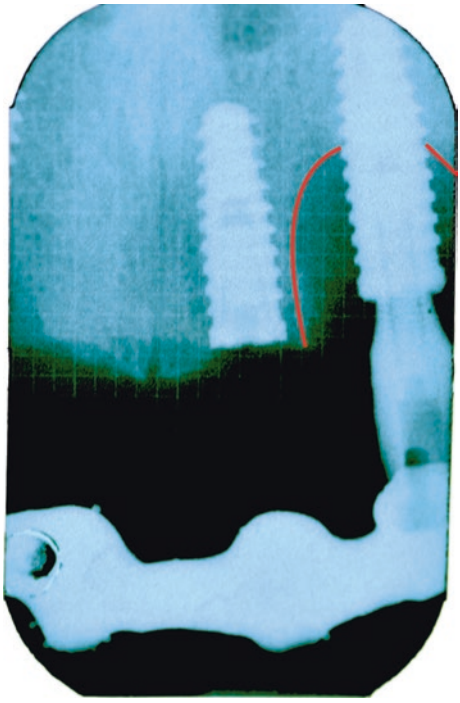

Fig. 2 Radiological signs of peri-implantitis on the fixture on the right side; the area of bone defect has been highlighted in red

to the crestal bone, and contained larger proportions of neutrophil granulocytes and osteoclasts [12]. They also highlighted that the amount of bone loss that occurred during the period following the ligature removal was significantly larger at implants with modified surface than at machined implants and natural teeth [12]. Moreover, in periodontitis lesions, the bone was not directly involved by the inflammation but surrounded by a non-infiltrated connective and the same bacterial biofilm was separated from the connective tissue by a pocket epithelium.

In a later study on humans, the same author has shown that periodontitis lesions were surrounded on one side of the pocket by epithelium and on the other side by a portion of non-infiltrate connective tissue [13]. On the contrary, peri-implantitis lesions were characterized by a greater infiltrated connective tissue, twice larger; it extended more apically in the pocket epithelium and it was not surrounded by a not infiltered connective. Peri-implantitis sites were characterized by a higher vascular density, but the vascular diameter was larger on periodontitis sites. The density of inflammatory cells, like CD68-(macrophages), was greater on peri-implantitis sites, and in particular, Myeloperoxidase MPO-positive cells (neutrophil granulocytes) and CD138-positive cells (plasma cells) occurred in three to six times larger numbers than their counterparts in periodontitis lesions [13].

The study of the aetiological factors and modalities of prevention of peri-implantitis is fundamental: there is not a specific bacterial complex that initiates the disease, on the contrary, emerging importance is gaining the interaction between titanium surface and peri-implant microbiota [14].

Potential mechanisms of peri-implant bone loss include [9]:

- The microbial biofilm
- Cement excess
- Implant malposition
- Metal ion/particle release

Additional trigger mechanisms for peri-implant bone loss comprehend [5]:

- Susceptible host
- Prosthetic factors
- Surgical factors
- Biomechanical factors

2 Titanium

The material normally used for the realization of endosteal dental implants is commercially titanium pure (cpTi); it is more rarely associated with other elements such as vanadium (V), aluminum (Al), molybdenum (Mo), niobium (Nb), and zirconium (Zr) that they often generate better mechanical properties, but have a different response in terms of biocompatibility compared to the pure form [15].

It is important to highlight that at about 883 °C pure titanium transforms from the allotropic "α-form" with a closed packed hexagonal crystal structure, to the "β" with a body-centered cubic structure. However, the presence of such elements in the alloy tends to stabilize the α form, like Al, O, and N, and others tend to stabilize the β, like V, Mo, Nb, Fe, and Cr [16]. The ratio of the two allotropic forms in the titanium alloys influences the mechanical properties of strength, ductility, modulus of elasticity, cycle fatigue, and fracture toughness.

Titanium is in the fourth period of the table of elements, that is, the transition metals, in the group 4B; it is characterized by a low atomic and ionic volume and a high melting and boiling points. It is a light, hard material with a low density, 40% less than steel, but with equal resistance; it weighs 60% more than aluminum but with double the resistance.

The main characteristics of titanium are:

- The excellent biocompatibility
- Low density
- The great electrochemical stability
- High mechanical resistance
- Sufficient rigidity and tenacity

All these features make the titanium the ideal material for the production of fixtures.

The American Society for Testing and Materials (ASTM) classified commercially pure titanium (cpTi) in grades from 1 to 4, based on the content of oxygen (increasing from 0.18 to 0.40) and iron (increasing from 0.20 to 0.50): this increase is accompanied by the improvement of the mechanical characteristics. Grade V

refers to the titanium alloys Ti-6Al-4V [17]. Titanium (Ti) and its alloys in contact with air or water form a titanium dioxide (TiO_2) layer, characterized by biocompatibility, high resistance to corrosion and to the fluids excreted or secreted from the human body, minimizing the metallic ion release [18–20]. Thanks to these characteristics they are widely used for biomedical applications or dental implants production; however chemically and/or physically superficial treatments are able to trigger specific molecular events at the cell-material interface, influencing the speed, strength, and degree of osseointegration [21, 22].

Titanium shows more than one state of oxidation, so from titanium originate titanium monoxide (TiO), titanium dioxide (TiO_2), and titanium trioxide (Ti_2O_3). The crystal lattices in which titanium oxide exists, anatase, rutile, and brookite influence the iatrogenicity; anatase is better in attracting calcium and phosphate ions from the physiological environment to form an appetite coating. However, rutile is characterized by both basic and acidic hydroxyl groups on the surface and by surface energy, so the mixture of rutile and anatase could help to improve the osteogenic activity of titanium [23].

When titanium fixtures are inside the bone structure, the stoichiometric relationship between Ti/O is in relation to the distance that occurs with the external environment, richer in oxygen. Furthermore, within the bone structure, the layer of titanium oxide undergoes gradual maturation, increasing its thickness from 7 nm up to 200 nm, meanwhile its composition changes, for the establishment of a balance with the tissues surrounding and the formation of precipitates. Steinemann reports constant stability of the dioxide of titanium between pH 3 and 12 in a special solution [24].

The Ti6Al4V alloy is characterized by higher tensile strength and toughness, which is similar to Cr/Co alloys. It is largely used in orthopedic surgery where high and repeated stresses occur.

There are no significant advantages of using this alloy in dentistry: the presence of Al and V are particularly implicated in toxic phenomena and aluminum seems to negatively affect the expression of osteocalcin and the mineralization of the extracellular matrix. Moreover, in vivo and in vitro studies have shown that the release of particles from this alloy increases the release of inflammation-inducing mediators such as prostaglandin E2, interleukin-1, interleukin-6, and tumor necrosis factor [17].

2.1 Superficial Characterization of Titanium

The superficial characterization of titanium is fundamental both for increasing the initial bone–implant contact (BIC) and for the interaction with host and bacterial cells. The first implants used in the history were characterized by a machined smooth surface with a 30–40% of BIC (Fig. 3). Superficial treatments have permitted to increase this value to 60–70% [15]. Regardless of the material, the initial interaction between the cells and the implant surface is fundamental for achieving

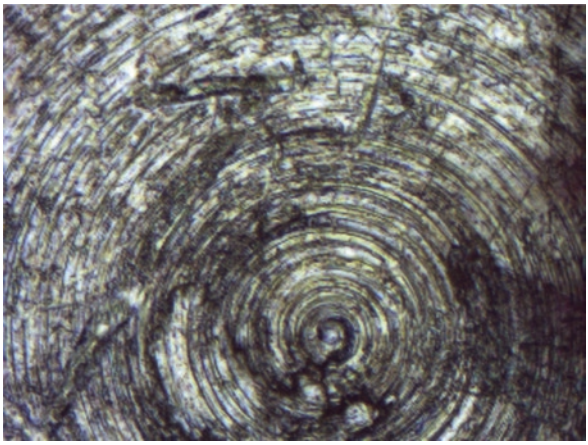

Fig. 3 A machined titanium observed at 10× magnification through an optical camera associated to a Bruker Atomic Force Microscopy (AFM). The machined surfaces are not totally smooth, but are characterized by a superficial topography, that is the resultant of the manufacturing procedures

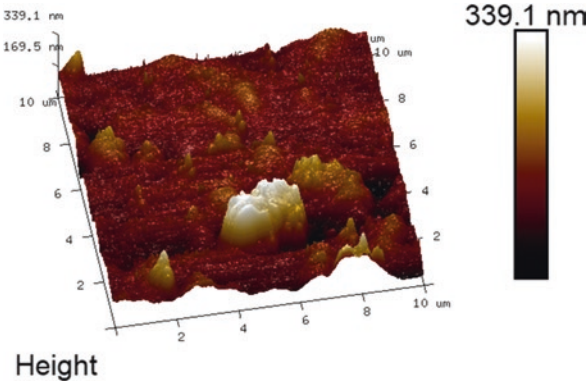

Fig. 4 3D image of a Machined surface obtained from AFM observation (scan size 10 μm × 10 μm)

osseointegration. Figure 4 observes the nano-roughness that characterizes the surface of machined titanium using 3D image. Also in a macroscopical observation, it is possible to see that this surface, which is traditionally considered as smooth, is characterized by the presence of concentric lines that are the results of manufacturing procedures (Fig. 5). It is possible to observe the increase of roughness, the darker color, the opacity of the discs, and the absence of the concentrical lines that characterize the machined discs (Fig. 6). The increase of roughness, the opacity of the discs, and the absence of the concentrical lines that characterize the machined discs can be observed as shown in Fig. 7.

According to Albrektsson and Wennerberg, the surface roughness can be classified into four categories, or roughness [25]:

- Smooth surfaces (average roughness value Sa <0.5 μ)
- Surfaces with minimum roughness (Sa 0.5–1 μ)
- Moderate roughness surfaces (Sa 1–2 μ)
- Rough surfaces (Sa >2 μ)

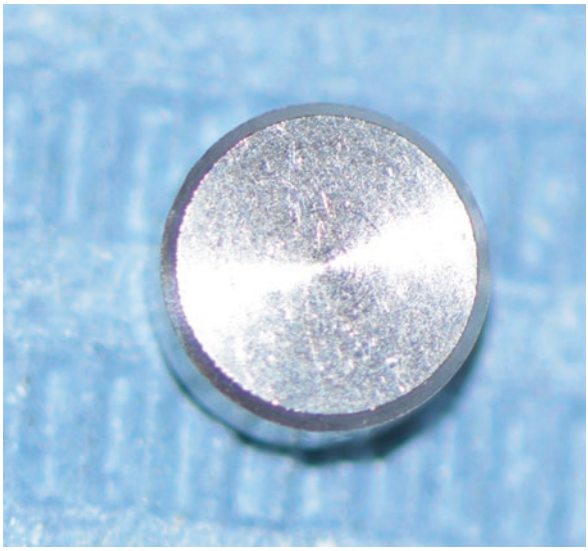

Fig. 5 Macroscopical aspect of a titanium machined disc

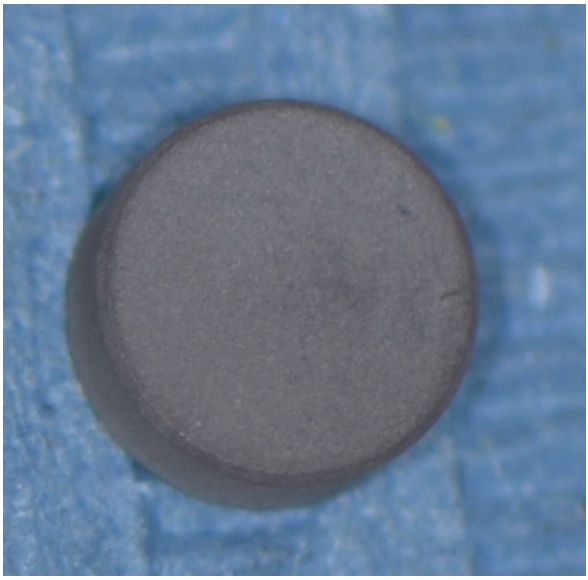

Fig. 6 Macroscopical aspect of a double etched surface

Superficial roughness can be obtained with subtractive or additive techniques. The more numerous subtractivetechniques are:

- Sandblasting, that is the bombardment of the surface of titanium by granules of variable diameter, of 60–90 μm, consisting of oxides such as trioxide of aluminum (Al_2O_3), titanium dioxide (TiO_2), zirconium dioxide (ZrO_2), and silicon carbide (SiC).

Fig. 7 Microscopical aspect of an acidified and sanded titanium

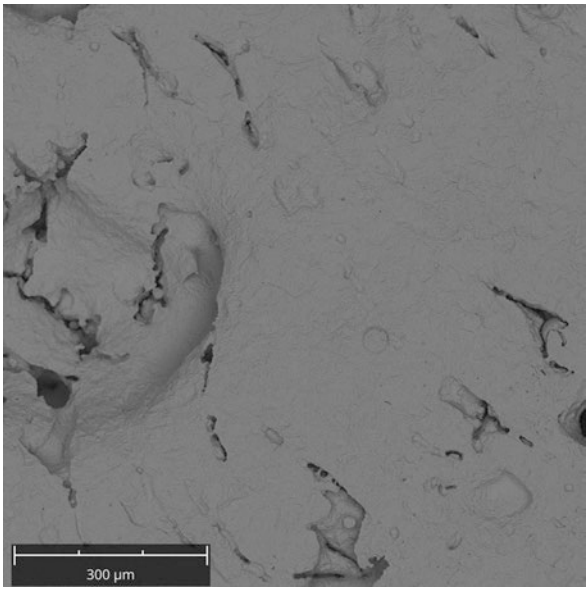

Fig. 8 SEM observation at low magnification of a laser sintered titanium modified with organic acids

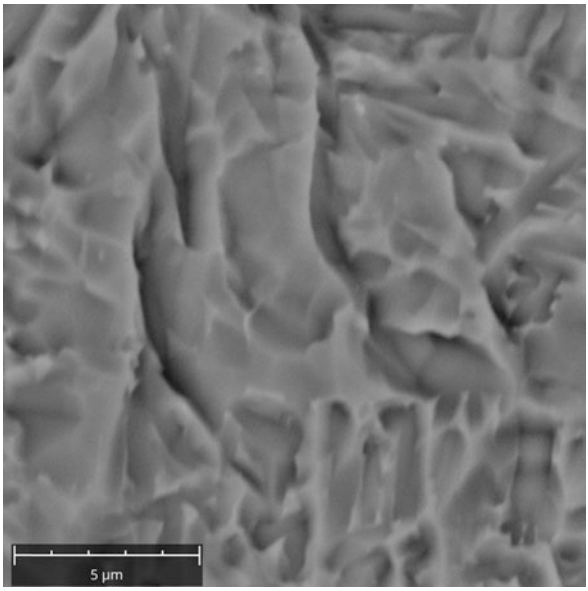

Fig. 9 SEM observation at low magnification of a laser sintered titanium modified with organic acids

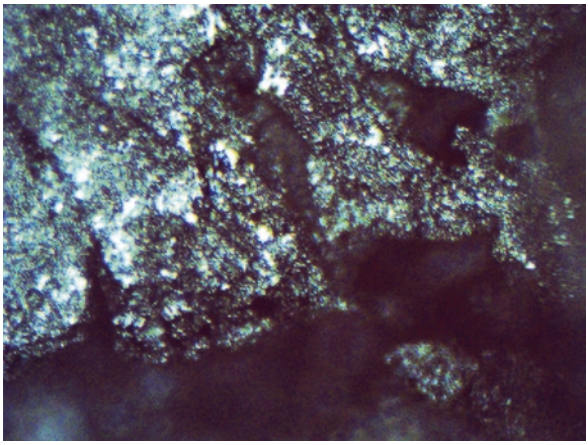

Fig. 10 A laser sintered titanium modified with organic acids observed at 10× magnification through an optical camera associated to a Bruker Atomic Force Microscopy (AFM)

- Acid etching, by using sulfuric acid, hydrochloric acid, hydrofluoric acid, etc. (Figs. 8, 9, 10, and 11). The ripples that are present in Fig. 9 are better represented in Fig. 11. The laser-sintered titanium modified by acid treatment is characterized by the presence of elongated reliefs of different measure, height, and orientation.
- Combination of sandblasting and etching.
- Oxidation in a galvanic bath.
- Spark erosion.
- Laser sintered titanium.

The additive techniques employ the use of a plasma flow which deposits titanium powder (plasma) on the system spray, hydroxyapatite powder, or titanium microspheres. However, it has been shown that the nanotopographic features, like depth, width, (an)isotropy, and spacing (ridge-groove ratio), interact with cells via membrane alteration and seem to be effective only if comprised between 70 nm and 5 μm [22, 26]. Moreover, nanoscale characterizations permit to increase the surface area, to improve the available sites for protein adsorption and cell interaction and consequently the bone-to-implant contact [21, 27]. For these reasons, the nano-roughness (1–100 nm) is becoming more popular than micro- (1–10 μm) and macro- (10 μm–1 mm) features [21].

Many methods have been described to modify the titanium oxide layer, like chemical (acid and alkaline) and electrochemical treatments (anodic oxidation), plasma spray deposition, sol-gel formation, ion implantation, and thermal oxidation [28–30]. It is important to highlight that the increase in surface roughness does not always promote an increase in the wettability. It depends both on the chemistry and

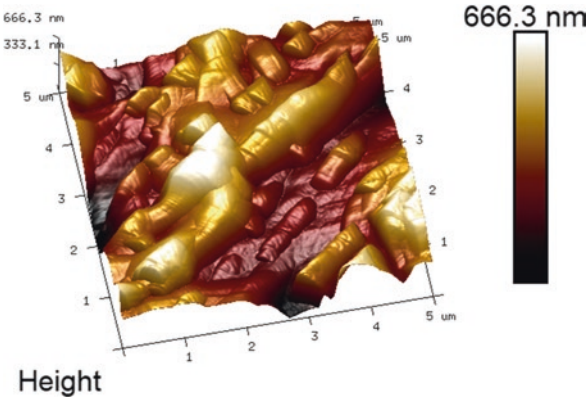

Fig. 11 AFM image of tridimensional topography of a laser sintered titanium disc modified with organic acids

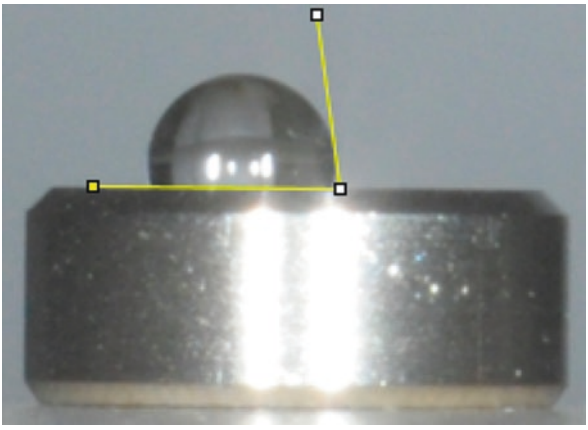

Fig. 12 Water contact angle of a titanium smooth surface

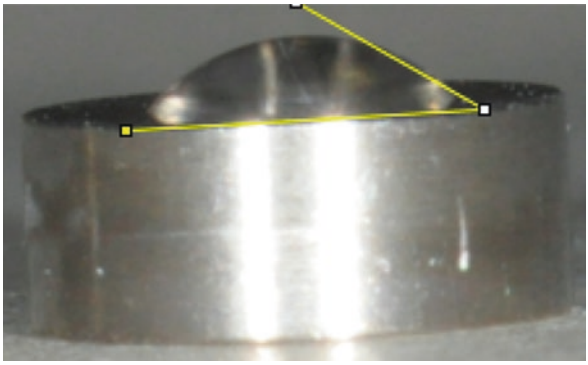

Fig. 13 Water contact angle of the same machined surface treated with acids

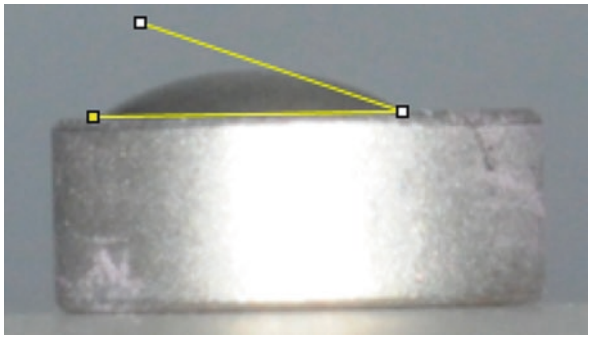

Fig. 14 Water contact angle after treatment with acids and sanded

on the roughness of the surface [31]. Indeed, in solid materials, the wettability and the surface free energy have parameters very similar.

The wettability can be measured through the static sessile method that permits to evaluate the water contact angle [32]. The wettability of a titanium surface is fundamental because it can influence the initial protein adhesion to the surface, the interaction of the tissues with the pre-conditioned surface, the bacterial and biofilm formation and consequently the in vivo osteointegration and long-term success [33]. Traditionally, if a surface is characterized by water contact angles lower than 90° [34], it is considered as hydrophilic; however, Vogler considered the cut-off at 65° [35] (Fig. 12). Figure 13 represents water contact angle of the same machined surface treated with acids. The effect of acidification and increasing the roughness of a hydrophilic surface contributes to increase its wettability. As shown by the theory of contact angle hysteresis, the increase of roughness has the ability to promote an increase of the water contact angles in hydrophobic materials and a decrease of the same parameter on hydrophilic ones [36]. Figure 14 represents water contact angle after treatment with acids and sanded. The effect of sandblasting increases the roughness of a hydrophilic surface and contributes to further increase its wettability. The wetted area is inversely proportional to the contact angle as seen in Fig. 15.

Fig. 15 Wetted area of three different titanium surfaces

The water contact angle is important also because the lower is the angle the greater is the wetting area, so during in vivo procedures, the blood will wet easer the implant surface [31]. However, there is still controversy in the literature about the ideal water contact angle of dental implants [32].

2.2 Microbiological Interaction with Surfaces Characterized by Different Roughness Wettability and Texture

The clinical performance, the plaque accumulation, the bacterial colonization, and the long-term success of dental implants are influenced by many fixture-related factors, like:

- Materials [37]
- Macro-geometry
- Type of connection between the fixture and abutment [38, 39]
- Implant profile
- Surface
  - Superficial micro-architecture [40–42]
  - Chemistry, wettability, and free energy [33]
  - Texture [43]

It is known that increased free energy and roughness values are associated to increased plaque retention and maturation; however, the role of these single parameters is not fully understood [44]. Bacterial colonization of the dental implants begins directly after exposure to the oral environment. The microbiota can be identified 30 min after implant installation and within 2 weeks, with an established community similar to that found around natural teeth in the same mouth [45]. The superficial parameters that mainly influence bacterial adhesion are roughness, wettability, and texture [43]. The wettability of material is also fundamental: it has been shown that hydrophilic surfaces increase the cellular and bacterial adhesion;

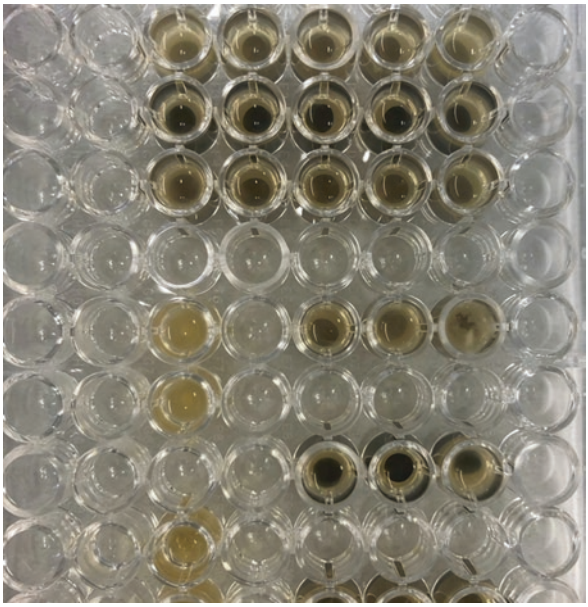

Fig. 16 Microbiological analysis on titanium discs

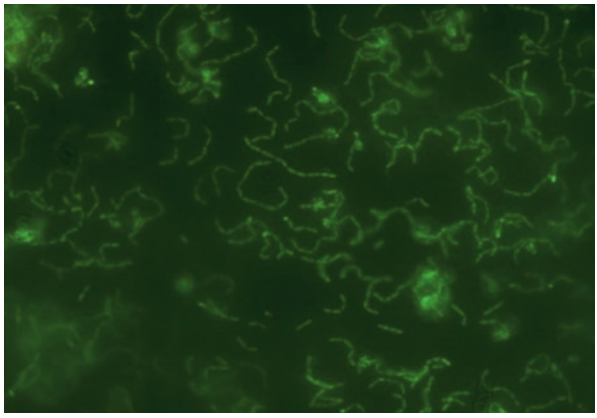

Fig. 17 Live dead images of *S. oralis* on titanium machined discs at 48 h (green live cells, red dead cells)

however, there are still conflicting hypotheses about the interaction between hydrophobic surfaces and bacteria.

It has been hypothesized that hydrophilic bacteria could prefer and adhere to hydrophobic surfaces and vice versa [43]. Moreover, it has been shown that in hydrophilic surfaces, an increase in the surface roughness (Ra) is related to a decrease in the water contact angle while for hydrophobic surfaces, an increase in the Ra is associated to an increase in the contact angle, because of the interposition of air bubbles between the surface and the water [46, 47]. Figure 16 shows microbiological analysis on titanium discs. It is possible to observe different types of

titanium discs immersed in a mixture of saliva and *S. oralis*. This type of experimentation permits to monitor the different effects of titanium treatment on bacteria.

The relationship between surface roughness and biofilm formation has been largely studied but there is not a total consensus about this topic. Bollen et al. have found a threshold surface roughness of 0.2 μm, under which, a further decrease of roughness values did not further influence the quantity of bacterial adhesion [48].

Many authors have found a positive correlation between surface roughness and the adhering bacteria [49–51]. However, there is not a total consensus in the literature and some authors concluded that only Ra parameter is inadequate to describe the interaction with bacteria [52].

Coelho et al. concluded that although implants with increased surface roughness were the ideal solution in case of low bone density, they could increase the microbial adhesion, as in the case of surface colonization [53]. Moreover, an in vitro study analyzed the early biofilm colonization up to 16.5 h on titanium surfaces with different surface roughness and concluded that there were no significant differences among different groups for what concerning the bacterial colonization [42]. Also Pita et al. have shown that biofilm formation was not affected by superficial roughness [40]. Other studies concluded that roughness increases the bacterial adhesion only in the first minutes, but then, with the biofilm formation these differences decrease and are nullified starting after the 15th h [54]. For the evaluation of cell viability, the biofilm on disc surfaces can be examined with a LIVE/DEAD Viability Kit (Fig. 17). This technique stains viable cells with a green fluorescent signal, and propidium iodide stains cells with impaired membrane activity red. Then, the images are observed at fluorescent microscopy. In this image, it is possible to observe many cocci joined together to form many chains.

A recent study of Wassmann et al. concluded that both surface roughness and wettability may influence the adhesion properties of bacteria on biomaterials; and that in this context, the predominant factor is dependent on the bacterial species [43]. Indeed, they found that wettability was the predominant factor for *S. epidermidis* and surface texture for *S. sanguinis*. In particular, *S. epidermidis* was characterized by a higher adhesion on hydrophobic surfaces, contrarily to *S. sanguinis* that was not affected by wettability but was increased proportionally to the surface roughness [43].

The nano-texture of the titanium is also fundamental for this reason. Wassmann et al. suggested that the only parameter of Ra analyzed through profilometer was not enough and that the use of AFM could permit to evaluate the nano-roughness of the materials [43]. A recent study analyzed the anti-inflammatory and antibacterial effects of titanium surfaces coated with three different shapes of nanostructured ceria nano-CeO_2 (nanorod, nanocube, and nano-octahedron) [55]. The anti-inflammatory effects measured as decreased ROS production were shown in all surfaces; however, results showed that nanorod CeO_2-modified Ti had more bacteria attachment of *Streptococcus sanguinis* in the early stages and exerted lower anti-inflammatory effect than the other two groups [55].

2.3 The Release of Titanium Particles and their Role in Peri-Implant Inflammation

Emerging evidence suggests also a possible role of metallic particles that are released during drilling sequences and implant insertion and function, on modulating the inflammatory response of the host and in the interaction with oral biofilm [14]. During implant insertion, indeed, the superficial oxide layer could be affected by many factors, both mechanical, like frictions, and chemical, like an acidic environment [56]. Moreover, the continuum exposition of the titanium oxide layer to saliva, bacteria, and chemicals can potentially dissolve it and corrosion cycles can be initiated, with the release of titanium particles in the surrounding tissues [56]. These factors could be exacerbated during the functional loading, in which particle release could increase for both action of chemical corrosion, friction and treatment for cleaning, disinfecting and debridement of the implants and abutments.

Titanium toxicity could manifest in several forms like hypersensitivity to titanium and allergic reactions, bone loss due to inflammation reactions due to implant corrosion, and yellow nail syndrome [9, 57]. Rarer are phenomena of titanium allergy, it was estimated to be about 0.6%; they could manifest both immediately after the implant insertion and after many years: in these cases the implant removal permit to eliminate symptoms manifested as stomatitis or eczema [58, 59]. A possible mechanism that could lead to the onset of an inflammatory response is that TiO_2 nanoparticles (TiO_2-NP) could adsorb CXCL8 (and IFN-γ), which leads to the disruption of neutrophil chemotaxis and modifies local inflammatory mediator concentration [17]. The release of titanium particles seems influenced by many factors, and in recent years a new field in research is developing, the tribocorrosion [17, 60]. This term was obtained by the union of three words:

- Tribology: analyzed the influence exerted by friction, wear, and presence of lubrication
- Corrosion: analyze the behavior of the material versus different environmental factors
- Biochemistry: analyze the interactions between cells and protein

Titanium corrosion is increased at lower pH and is further enhanced in the presence of fluorine ions; on the contrary, it seems less influenced by organic acids [61]. However, the release of titanium particles is also influenced by the presence of inflammation or the formation of microbial biofilm that affects the surrounding pH [17]. Moreover, other factors could influence in vivo the corrosion of titanium and its alloys: the contemporary presence of H_2O_2 and albumin have a synergic effect for what concerning the promotion of Ti6Al4V corrosion [62]. The release of titanium particles during surgery could be influenced also by other factors, like the superficial treatment of titanium and the friction with bone during the fixture insertion [63]. A comparative study of Martini et al. showed that particle release was higher in titanium plasma-spray-coated titanium screws (TPS-Ti) and fluorohydroxyapatite-coated titanium screws (FHA-Ti) [63]. Recent literature suggested that the release

of titanium particles in peri-implant tissues could be involved in the etiology of mucositis and peri-implantitis [64]. Olmedo et al. have found significantly higher levels of particles inside and outside the epithelial cells and macrophages from the exfoliative cytological test in peri-implantitis sites than controls [65].

At last but not the least, it has been shown that the presence of bacterial lipopolysaccharide (LPS) seems to have a crucial role in promoting Ti release from fixtures surfaces at the mildly acidic and neutral pH levels, and Ti particles could lead to inflammation and the peri-implant environment [66]. On the contrary, the contemporary presence of LPS and an acidic pH (pH = 2) significantly inhibited Ti release. Also, the material used for abutment production seems to influence the titanium wear and the release of particles: different studies have shown increased titanium wear with the abutment in zirconia after loading cycles, but there is not a marked evidence about this topic [67, 68].

3 Zirconia

Zirconia is a crystalline zirconium dioxide that can be stabilized with calcium oxide (CaO), magnesium oxide (MgO), cesium oxide (CeO_2), and yttrium oxide (Y_2O_3). This material is largely employed in dentistry, not only for the production of dental prosthesis but also for the fixtures, thanks to its properties of high flexural strength, corrosion resistance, biocompatibility, osseointegration, low plaque surface adhesion, absence of mucosal discoloration, and esthetics [69]. Zirconia used in dentistry is mainly stabilized by 3% yttrium oxide thanks to its high resistance to solicitations. It has mechanical properties similar to stainless steel. The tensile strength ranges from 900 to 1200 MPa and its compressive strength is around 2000 MPa. For this reason, this material could also be used for the production of drills. Recent studies have shown that zirconia drills are more resistant to wear if subjected to a repeated number of cycles of decontaminants or sterilization processes. SEM observations and EDX analysis have shown that zirconia drills, contrarily to steel ones, after different cycles of decontaminants were not affected by significant changes, respect new drills [70]. On the contrary, stainless steel drills were affected by different treatments [71]. ZrO_2 is not cytotoxic and is unable to generate changes in the cellular genome. Furthermore, zirconium oxide creates less inflammatory reactions at tissue level than to other materials such as titanium.

Another advantage of zirconia is the esthetic color that is more similar to dental hard tissues and for this reason, contrarily to titanium, it prevents bluish discoloration of peri-implant soft tissues and may be beneficial if soft tissue recession occurs in the long term [69]. Zirconia implants are mainly produced as one-piece components, in order to avoid technical problems connected to the fracture of some components [72]. Currently, the percentage of success of zirconia fixtures after 1 year is about 96%. One issue concerning the use of zirconia is aging: in presence of water or vapor, in presence of compressive stresses and microcracking, it is slowly transformed from the tetragonal phase into the monoclinic phase leads to slow

development of roughness, thus producing a progressive deterioration of the material [73]. This process may be influenced by various aspects of the production process, such as the macroscopic shape and the superficial characteristics of an implant, but this has not yet been fully elucidated.

Another technical problem is fracture that seems to be influenced by the implant production method. In one piece, no-prepared, zirconia implants, fracture lines were mainly horizontal, on the contrary, in implants modified by grinding, the fracture lines were vertically parallel to the long axis and the fracture strength was decreased from 2084 N when not prepared to 804 N when prepared [74].

3.1 Comparative Studies of Zirconia Versus Titanium

For what concerning the clinical performance of zirconia implants, different in vitro and in vivo studies have analyzed the BIC and removal torque of zirconia vs. titanium fixtures with similar values of osteointegration [75, 76]. BIC ranged between 26–71% on zirconia and 24–84% in titanium implants. Removal torque was comprised between 12–98 N cm in zirconia and 42–74 N cm for titanium.

As for titanium, the superficial roughness in zirconia is able to influence the interaction with host cells and, in particular, the expression of adhesion molecules like integrins alpha5 and beta1 [72]. The surface topography appeared to play a major role in the success of zirconia implants. It has been shown that the initial attachment of osteoblast-like cells was significantly higher on specimens with a mean roughness of 1.04 μm than those with lower values [77].

For what concerning the microbiological behavior, the polished zirconia exhibited lower surface free energy, wettability, and a lower percentage of bacterial adhesion compared with polished titanium surfaces [78]. These results have been obtained also by other studies [37] and, in particular, Rimondini et al. have found in vivo, lower level of both total bacteria and presence of potential putative pathogens such as rods on zirconia specimens, versus titanium ones [79]. A recent study compared the inflammatory reaction after experimental plaque accumulation on titanium and zirconia implants versus natural tooth: titanium implants, seem to display a higher inflammation and higher IL-1β values [80]. On the contrary, natural teeth presented an increase in IL-6 and TNF-α than other groups.

For what concerning the inflammatory reaction around tissues, a comparative study analyzed different biopsies around titanium and zirconia healing caps: results have shown higher inflammatory infiltrate, micro-vessel density, expression of vascular endothelial growth factor and expression of nitric oxide synthase around the first type of samples [81]. Comparing the level of metallic particles around titanium and zirconia implants, it has been found that zirconia particles were present only in peri-implantar tissues of patients with zirconia implants. On the contrary, titanium particles were found both in those with titanium and zirconia fixtures: these elements could be a consequence not only of corrosion, but also of wear due to friction during implant insertion and prophylaxis treatments, and we have not to forged that

titanium dioxide is contained also in many products that are used in daylife, like toothpaste [82]. Other studies compared the expression of the inflammatory biomarkers around zirconia and titanium implants: interleukin-1RA, interleukin-8, granulocyte colony-stimulating factor, and macrophage inflammatory protein-1beta.

Results suggest that there were no significant differences among the two materials, on the contrary a greater role is due to the different host responses [72]. Another study compared the inflammatory expression around natural teeth and zirconia: the latter were characterized by higher levels of inflammatory cytokines [83]. The bacterial interaction between bacteria and zirconia have been studied and compared with titanium. Wassmann et al. have shown that in zirconia samples, independent of hydrophobic or hydrophilic, the *S. sanguinis* adhesion was higher than the titanium samples [43]. In particular, they found not a significant role for what concerning the superficial wettability and roughness for zirconia groups, contrarily to what described for titanium. Contrarily, the same authors have found no differences between titanium and zirconia for what concerning *S. epidermidis*. The authors explained these differences with the nano-roughness that was not measured by a profilometer, but that was measured through the use of atomic force microscopy on zirconia samples.

4 PEEK

Polyetheretherketone, PEEK, has potential use in implantology and dentistry because it is characterized by mechanical properties that can be modulated by means of the addition of other elements, like carbon fibers, and in this way, it is

Fig. 18 A typical example of PEEK disc

possible to reach values similar to human bone. It is a thermoplastic polyaromatic semi-crystalline polymer with a temperature fusion of about 340 °C [84]. A typical example of PEEK disc is shown in Fig. 18. It is a very esthetic material, thanks to the ivory color which makes it very similar to the teeth, unlike the gray titanium.

PEEK's Young's (elastic) modulus (3–4 GPa) is similar to human medullary bone and dentine, contrarily to those of titanium that is higher [85], but by the addition of carbonium fibers to PEEK, it is possible to reach an elastic modulus of 18 GPa, which is similar to the cortical bone that is 15 GPa [84, 86]. Other advantages of PEEK are the excellent chemical resistance, the wear resistance, the biocompatibility, the natural radiolucency and magnetic resonance imaging (MRI) compatibility, the esthetics, because its color is similar to the tooth, and the possibility to be manufactured by means of 3D printers [87–89]. Figure 19 represents to evaluate PEEK wetting properties by using the sessile method. This technique consists of placing a microliter drop of physiological solution on the surface and then measuring the water contact angle. Figure 20 shows the evaluation of wetted surface area. Greater is the wetted area, greater is the hydrophilicity of the surface. In this case, we can appreciate a greater wettability with respect to the machined titanium shown in the center of Fig. 15, but lower with respect to the other two surfaces. Figure 21 shows the measurement of the water contact angle on a PEEK disc. In this

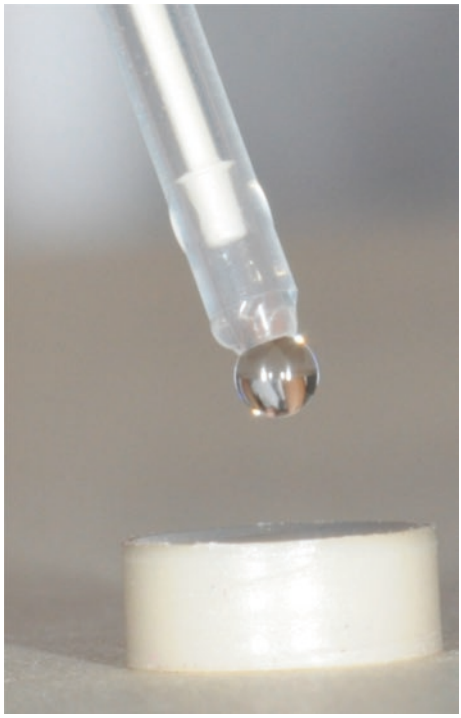

Fig. 19 Evaluation of PEEK wetting properties by using the sessile method

Fig. 20 Evaluation of wetted surface area on a peek sample

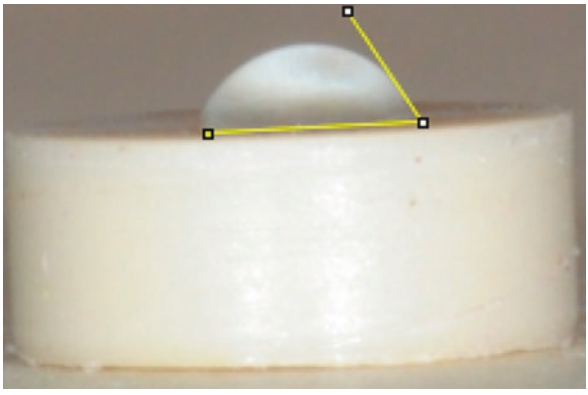

Fig. 21 Measurement of the water contact angle on a PEEK disc

case, we can appreciate a greater wettability with respect to the machined titanium shown in the center of Fig. 12, but lower with respect to the other two surfaces (Figs. 13 and 14).

The wettability of PEEK is influenced by the fabrication process, like the injection molding or machining processes, and, as for titanium, smooth surfaces exhibit less osteoinductivity compared to more topographically complex ones [90].

However, it has been shown that the superficial characterization of dental implants with macro- and micro-porous structures can influence both the apposition

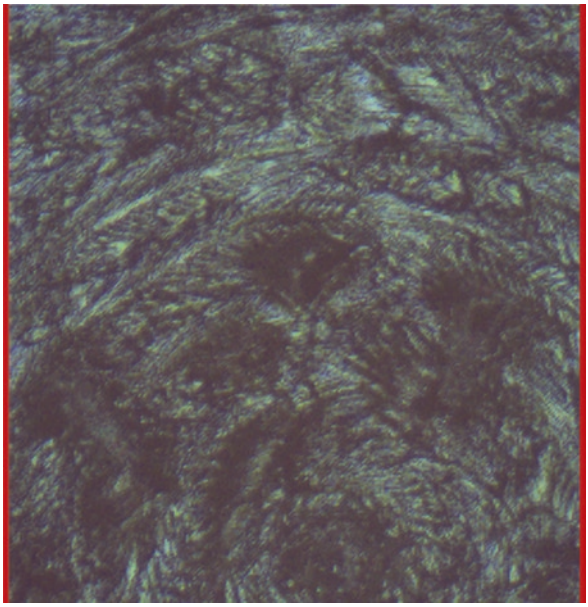

Fig. 22 PEEK disc observed at 10× magnification through an optical camera associated to a Bruker Atomic Force Microscopy (AFM)

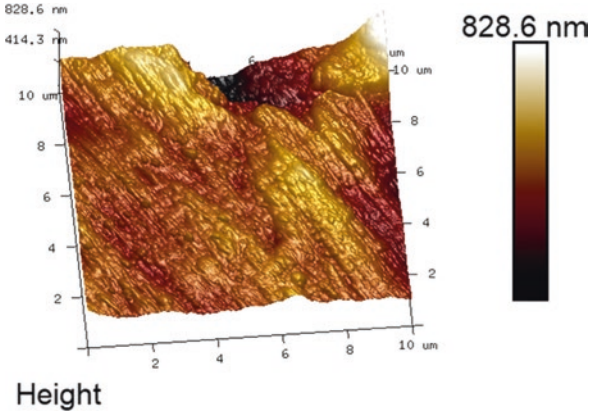

Fig. 23 3D reconstruction of AFM images of PEEK machined surface obtained from atomic force microscopy observation

of bone during neo-osteogenesis and the removal torque, while the macrostructure has more influence on the angiogenesis [1, 91, 92]. Figures 22 and 23 are the AFM images of PEEK disc and PEEK machined surface respectively.

The interaction of bacteria with PEEK surface has been analyzed in few studies and results are controversial: some authors reported a lower antibacterial activity with respect to titanium [93] and others recorded lower level of bacterial biomass on PEEK samples [94]; however, other authors suggest that a higher role is exerted by superficial treatment with respect to the material [95]. Barkamo et al. have recently shown results about biofilm formation of different bacteria on PEEK and titanium

surfaces: data were analyzed after 72 and 120 h [96]. They concluded that no significant differences were found between smooth PEEK, machined cp-Ti, and Ti6Al4V but that blasted PEEK was characterized by a higher biofilm formation. However, a recent study showed the antibacterial and anti-adhesive properties of PEEK discs at 24 and 48 h against an oral pioneer such as *S. oralis*, if compared with machined and double etched titanium [97]. Other studies should analyze the effects of this material on oral microbiota; however, current literature suggests that for the onset of peri-implantar inflammation, there are many variables that could interfere with tissues and it is not possible to consider only one variable alone: the material, its integration in the tissues, macro- and micro-architecture of the devices, the oral microbiota, the immune variation of the patient, and the presence of contaminants.

The use of PEEK comprehends also the production of implant abutments: a comparative study evaluated the biofilm formation on different materials [94]. PEEK abutments showed less superficial free energy and roughness, and also the lowest amount of adherent viable biomass was identified on these surfaces with respect to zirconia and titanium after 20 h. However, these differences decreased and were nullified after 40 h [94].

5 Conclusions

Recent advancements have shown that bacterial adhesion is influenced by many parameters [98], like:

- Materials of the fixture
- Surface roughness
- Free energy and wettability
- Peri-implantar chemistry

Actually, we do not have yet the ideal material and surface, but we have a great opportunity to choose among many varieties in order to find a better option for our clinical conditions.

Acknowledgments Authors would like to express their sincere thanks to Prof. Domenico Tripodi and Dr. Domenico Fulco for purchasing us the photographs of water contact angles, and to Prof. Luigina Cellini and the Microbiological Unit of the University of Chieti for the live dead observations.

References

1. Del Giudice R, Piattelli A, Grande N, Cataneo E, Crispino A, Petrini M. Implant insertion torque value in immediate loading: a retrospective study. Med Oral Patol Oral Cir Bucal. 2019;24:e398–403. https://doi.org/10.4317/medoral.22845.

2. Iezzi G, Piattelli A, Scarano A, Degidi M, Shibli JA, Mangano C, et al. Histological evaluation of early and immediately loaded implants retrieved from human jaws. In: Atlas of immediate dental implant loading. Cham: Springer International Publishing; 2019. p. 29–47. https://doi.org/10.1007/978-3-030-05546-2_3.
3. Karthik K, Sivakumar, Sivaraj, Thangaswamy V. Evaluation of implant success: a review of past and present concepts. J Pharm Bioallied Sci. 2013;5:S117–9. https://doi.org/10.4103/0975-7406.113310.
4. Giro G, Tovar N, Marin C, Bonfante EA, Jimbo R, Suzuki M, et al. The effect of simplifying dental implant drilling sequence on osseointegration: an experimental study in dogs. Int J Biomater. 2013;2013:1. https://doi.org/10.1155/2013/230310.
5. Albrektsson T, Canullo L, Cochran D, De Bruyn H. "Peri-implantitis": a complication of a foreign body or a man-made "disease". Facts and fiction. Clin Implant Dent Relat Res. 2016;18:840. https://doi.org/10.1111/cid.12427.
6. Berglundh T, Armitage G, Araujo MG, Avila-Ortiz G, Blanco J, Camargo PM, et al. Peri-implant diseases and conditions: consensus report of workgroup 4 of the 2017 World Workshop on the Classification of Periodontal and Peri-Implant Diseases and Conditions. J Clin Periodontol. 2018;45:S286. https://doi.org/10.1111/jcpe.12957.
7. Derks J, Tomasi C. Peri-implant health and disease. A systematic review of current epidemiology. J Clin Periodontol. 2015;42:S158. https://doi.org/10.1111/jcpe.12334.
8. Lang NP, Berglundh T, Working Group 4 of Seventh European Workshop on Periodontology. Periimplant diseases: where are we now?—consensus of the Seventh European Workshop on Periodontology. J Clin Periodontol. 2011;38(Suppl 11):178–81. https://doi.org/10.1111/j.1600-051X.2010.01674.x.
9. Fretwurst T, Nelson K, Tarnow DP, Wang HL, Giannobile WV. Is metal particle release associated with peri-implant bone destruction? An emerging concept. J Dent Res. 2018;97:259. https://doi.org/10.1177/0022034517740560.
10. Heitz-Mayfield LJA, Lang NP. Comparative biology of chronic and aggressive periodontitis vs. peri-implantitis. Periodontology 2000. 2010;53:167–81. https://doi.org/10.1111/j.1600-0757.2010.00348.x.
11. Lafaurie GI, Sabogal MA, Castillo DM, Rincón MV, Gómez LA, Lesmes YA, et al. Microbiome and microbial biofilm profiles of peri-implantitis: a systematic review. J Periodontol. 2017;88:1066–89. https://doi.org/10.1902/jop.2017.170123.
12. Carcuac O, Abrahamsson I, Albouy J-P, Linder E, Larsson L, Berglundh T. Experimental periodontitis and peri-implantitis in dogs. Clin Oral Implants Res. 2013;24:363–71. https://doi.org/10.1111/clr.12067.
13. Carcuac O, Berglundh T. Composition of human peri-implantitis and periodontitis lesions. J Dent Res. 2014;93:1083–8. https://doi.org/10.1177/0022034514551754.
14. Daubert DM, Weinstein BF. Biofilm as a risk factor in implant treatment. Periodontology 2000. 2019;81:29–40. https://doi.org/10.1111/prd.12280.
15. Spoto G. et al. Materiali e Tecnologie Odontostomatologiche 3 Edizione (Ed. Ariesdue 2019, Como, Milano), ISBN:978-88-98789-16-0
16. Geetha M, Singh AK, Asokamani R, Gogia AK. Ti based biomaterials, the ultimate choice for orthopaedic implants—a review. Prog Mater Sci. 2009;54:397–425. https://doi.org/10.1016/J.PMATSCI.2008.06.004.
17. Tae Kim K, Young Eo M, Thi Hoang Nguyen T, Min Kim S. General review of titanium toxicity. Int J Implant Dent. 2019;5:10. https://doi.org/10.1186/s40729-019-0162-x.
18. Lausmaa J, Kasemo B, Mattsson H. Surface spectroscopic characterization of titanium implant materials. Appl Surf Sci. 1990;44:133–46. https://doi.org/10.1016/0169-4332(90)90100-E.
19. Roy P, Berger S, Schmuki P. TiO2 nanotubes: synthesis and applications. Angew Chem Int Ed. 2011;50:2904–39. https://doi.org/10.1002/anie.201001374.
20. Tengvall P, Lundström I. Physico-chemical considerations of titanium as a biomaterial. Clin Mater. 1992;9:115–34. https://doi.org/10.1016/0267-6605(92)90056-Y.

21. Kulkarni M, Patil-Sen Y, Junkar I, Kulkarni CV, Lorenzetti M, Iglič A. Wettability studies of topologically distinct titanium surfaces. Colloids Surf B Biointerfaces. 2015;129:47–53. https://doi.org/10.1016/j.colsurfb.2015.03.024.
22. Ventre M, Causa F, Netti PA. Determinants of cell-material crosstalk at the interface: towards engineering of cell instructive materials. J R Soc Interface. 2012;9:2017–32. https://doi.org/10.1098/rsif.2012.0308.
23. Wang G, Li J, Lv K, Zhang W, Ding X, Yang G, et al. Surface thermal oxidation on titanium implants to enhance osteogenic activity and in vivo osseointegration. Sci Rep. 2016;6:31769. https://doi.org/10.1038/srep31769.
24. Steinemann SG. Titanium—the material of choice? Periodontology 2000. 1998;17:7. https://doi.org/10.1111/j.1600-0757.1998.tb00119.x.
25. Albrektsson T, Wennerberg A. Oral implant surfaces: part 1—review focusing on topographic and chemical properties of different surfaces and in vivo responses to them. Int J Prosthodont. 2004;17:536–43.
26. Lamers E, van Horssen R, te Riet J, van Delft FCMJM, Luttge R, Walboomers XF, et al. The influence of nanoscale topographical cues on initial osteoblast morphology and migration. Eur Cells Mater. 2010;20:329–43. https://doi.org/10.22203/eCM.v020a27.
27. Simchi A, Tamjid E, Pishbin F, Eng M, Boccaccini AR. Recent progress in inorganic and composite coatings with bactericidal capability for orthopaedic applications. Nanomed Nanotechnol Biol Med. 2011;7:22–39. https://doi.org/10.1016/j.nano.2010.10.005.
28. Huang H, Lan P-H, Zhang Y-Q, Li X-K, Zhang X, Yuan C-F, et al. Surface characterization and in vivo performance of plasma-sprayed hydroxyapatite-coated porous Ti6Al4V implants generated by electron beam melting. Surf Coat Technol. 2015;283:80–8. https://doi.org/10.1016/J.SURFCOAT.2015.10.047.
29. Kulkarni M, Mazare A, Gongadze E, Perutkova Š, Kralj-Iglič V, Milošev I, et al. Titanium nanostructures for biomedical applications. Nanotechnology. 2015;26:062002. https://doi.org/10.1088/0957-4484/26/6/062002.
30. Tan AW, Ismail R, Chua KH, Ahmad R, Akbar SA, Pingguan-Murphy B. Osteogenic potential of in situ TiO2 nanowire surfaces formed by thermal oxidation of titanium alloy substrate. Appl Surf Sci. 2014;320:161–70. https://doi.org/10.1016/J.APSUSC.2014.08.160.
31. Marmur A. A guide to the equilibrium contact angles maze. In: Contact angle, wettability and adhesion, vol. 6. Boca Raton, FL: CRC Press; 2010. https://doi.org/10.1163/ej.9789004169326.i-400.5.
32. Strnad G, Chirila N, Petrovan C, Russu O. Contact angle measurement on medical implant titanium based biomaterials. Procedia Technol. 2016;22:946. https://doi.org/10.1016/j.protcy.2016.01.094.
33. Gittens RA, Scheideler L, Rupp F, Hyzy SL, Geis-Gerstorfer J, Schwartz Z, et al. A review on the wettability of dental implant surfaces II: biological and clinical aspects. Acta Biomater. 2014;10:2907. https://doi.org/10.1016/j.actbio.2014.03.032.
34. Rupp F, Gittens RA, Scheideler L, Marmur A, Boyan BD, Schwartz Z, et al. A review on the wettability of dental implant surfaces I: theoretical and experimental aspects. Acta Biomater. 2014;10:2894. https://doi.org/10.1016/j.actbio.2014.02.040.
35. Vogler EA. Structure and reactivity of water at biomaterial surfaces. Adv Colloid Interf Sci. 1998;74:69. https://doi.org/10.1016/S0001-8686(97)00040-7.
36. Chau TT, Bruckard WJ, Koh PTL, Nguyen AV. A review of factors that affect contact angle and implications for flotation practice. Adv Colloid Interf Sci. 2009; 150:106–115
37. Scarano A, Piattelli M, Caputi S, Favero GA, Piattelli A. Bacterial adhesion on commercially pure titanium and zirconium oxide disks: an in vivo human study. J Periodontol. 2004;75:292. https://doi.org/10.1902/jop.2004.75.2.292.
38. Assenza B, Tripodi D, Scarano A, Perrotti V, Piattelli A, Iezzi G, et al. Bacterial leakage in implants with different implant–abutment connections: an in vitro study. J Periodontol. 2012;83:491. https://doi.org/10.1902/jop.2011.110320.

39. D'Ercole S, Tripodi D, Ravera L, Perrotti V, Piattelli A, Iezzi G. Bacterial leakage in Morse cone internal connection implants using different torque values: an in vitro study. Implant Dent. 2014;23:175. https://doi.org/10.1097/ID.0000000000000044.
40. Pita PPC, Rodrigues JA, Ota-Tsuzuki C, Miato TF, Zenobio EG, Giro G, et al. Oral streptococci biofilm formation on different implant surface topographies. Biomed Res Int. 2015;2015:159625. https://doi.org/10.1155/2015/159625.
41. Quirynen M, Bollen CML, Schotte A, Marechal M, van Steenberghe D, van der Mei HC, et al. An in vivo study of the influence of the surface roughness of implants on the microbiology of supra- and subgingival plaque. J Dent Res. 1993;72:1304. https://doi.org/10.1177/00220345930720090801.
42. Schmidlin PR, Müller P, Attin T, Wieland M, Hofer D, Guggenheim B. Polyspecies biofilm formation on implant surfaces with different surface characteristics. J Appl Oral Sci. 2013;21:48–55. https://doi.org/10.1590/1678-7757201302312.
43. Wassmann T, Kreis S, Behr M, Buergers R. The influence of surface texture and wettability on initial bacterial adhesion on titanium and zirconium oxide dental implants. Int J Implant Dent. 2017;3:32. https://doi.org/10.1186/s40729-017-0093-3.
44. Berger JC, Driscoll CF, Romberg E, Luo Q, Thompson G. Surface roughness of denture base acrylic resins after processing and after polishing. J Prosthodont. 2006;15:180. https://doi.org/10.1111/j.1532-849X.2006.00098.x.
45. Fürst MM, Salvi GE, Lang NP, Persson GR. Bacterial colonization immediately after installation on oral titanium implants. Clin Oral Implants Res. 2007;18:501. https://doi.org/10.1111/j.1600-0501.2007.01381.x.
46. Di Giulio M, Traini T, Sinjari B, Nostro A, Caputi S, Cellini L. Porphyromonas gingivalis biofilm formation in different titanium surfaces, an *in vitro* study. Clin Oral Implants Res. 2016;27:918–25. https://doi.org/10.1111/clr.12659.
47. Riveiro A, Maçon ALB, del Val J, Comesaña R, Pou J. Laser surface texturing of polymers for biomedical applications. Front Phys. 2018;6:16. https://doi.org/10.3389/fphy.2018.00016.
48. Bollen CM, Lambrechts P, Quirynen M. Comparison of surface roughness of oral hard materials to the threshold surface roughness for bacterial plaque retention: a review of the literature. Dent Mater. 1997;13:258–69. https://doi.org/10.1016/s0109-5641(97)80038-3.
49. Lima EMCX, Koo H, Vacca Smith AM, Rosalen PL, Del Bel Cury AA. Adsorption of salivary and serum proteins, and bacterial adherence on titanium and zirconia ceramic surfaces. Clin Oral Implants Res. 2008;19:780. https://doi.org/10.1111/j.1600-0501.2008.01524.x.
50. Leonhardt Å, Dahlén G. Effect of titanium on selected oral bacterial species in vitro. Eur J Oral Sci. 1995;103:382. https://doi.org/10.1111/j.1600-0722.1995.tb01861.x.
51. Bundy KJ, Butler MF, Hochman RF. An investigation of the bacteriostatic properties of pure metals. J Biomed Mater Res. 1980;14:653. https://doi.org/10.1002/jbm.820140511.
52. Bürgers R, Gerlach T, Hahnel S, Schwarz F, Handel G, Gosau M. In vivo and in vitro biofilm formation on two different titanium implant surfaces. Clin Oral Implants Res. 2010;21:156–64. https://doi.org/10.1111/j.1600-0501.2009.01815.x.
53. Coelho PG, Granjeiro JM, Romanos GE, Suzuki M, Silva NRF, Cardaropoli G, et al. Basic research methods and current trends of dental implant surfaces. J Biomed Mater Res B Appl Biomater. 2009;88B:579. https://doi.org/10.1002/jbm.b.31264.
54. Fröjd V, Chávez de Paz L, Andersson M, Wennerberg A, Davies JR, Svensäter G. In situ analysis of multispecies biofilm formation on customized titanium surfaces. Mol Oral Microbiol. 2011;26:241. https://doi.org/10.1111/j.2041-1014.2011.00610.x.
55. Li X, Qi M, Sun X, Weir MD, Tay FR, Oates TW, et al. Surface treatments on titanium implants via nanostructured ceria for antibacterial and anti-inflammatory capabilities. Acta Biomater. 2019;94:627–43. https://doi.org/10.1016/j.actbio.2019.06.023.
56. Delgado-Ruiz R, Romanos G. Potential causes of titanium particle and ion release in implant dentistry: a systematic review. Int J Mol Sci. 2018;19:3585. https://doi.org/10.3390/ijms19113585.

57. Chaturvedi T. Allergy related to dental implant and its clinical significance. Clin Cosmet Investig Dent. 2013;5:57–61. https://doi.org/10.2147/CCIDE.S35170.
58. Lim HP, Lee KM, Koh Y-I, Park SW. Allergic contact stomatitis caused by a titanium nitride-coated implant abutment: a clinical report. J Prosthet Dent. 2012;108:209–13. https://doi.org/10.1016/S0022-3913(12)60163-2.
59. Sicilia A, Cuesta S, Coma G, Arregui I, Guisasola C, Ruiz E, et al. Titanium allergy in dental implant patients: a clinical study on 1500 consecutive patients. Clin Oral Implants Res. 2008;19:823. https://doi.org/10.1111/j.1600-0501.2008.01544.x.
60. Souza JCM, Henriques M, Teughels W, Ponthiaux P, Celis JP, Rocha LA. Wear and corrosion interactions on titanium in Oral environment: literature review. J Bio Tribo Corrosion. 2015;1:13. https://doi.org/10.1007/s40735-015-0013-0.
61. Schiff N, Grosgogeat B, Lissac M, Dalard F. Influence of fluoride content and pH on the corrosion resistance of titanium and its alloys. Biomaterials. 2002;23:1995. https://doi.org/10.1016/S0142-9612(01)00328-3.
62. Yu F, Addison O, Davenport AJ. A synergistic effect of albumin and H2O2 accelerates corrosion of Ti6Al4V. Acta Biomater. 2015;26:355. https://doi.org/10.1016/j.actbio.2015.07.046.
63. Martini D, Fini M, Franchi M, De Pasquale V, Bacchelli B, Gamberini M, et al. Detachment of titanium and fluorohydroxyapatite particles in unloaded endosseous implants. Biomaterials. 2003;24:1309–16. https://doi.org/10.1016/S0142-9612(02)00508-2.
64. Olmedo DG, Paparella ML, Brandizzi D, Cabrini RL. Reactive lesions of peri-implant mucosa associated with titanium dental implants: a report of 2 cases. Int J Oral Maxillofac Surg. 2010;39:503–7. https://doi.org/10.1016/j.ijom.2009.11.007.
65. Olmedo DG, Nalli G, Verdú S, Paparella ML, Cabrini RL. Exfoliative cytology and titanium dental implants: a pilot study. J Periodontol. 2013;84:78–83. https://doi.org/10.1902/jop.2012.110757.
66. Yu F, Addison O, Baker SJ, Davenport AJ. Lipopolysaccharide inhibits or accelerates biomedical titanium corrosion depending on environmental acidity. Int J Oral Sci. 2015;7:179–86. https://doi.org/10.1038/ijos.2014.76.
67. Stimmelmayr M, Edelhoff D, Güth JF, Erdelt K, Happe A, Beuer F. Wear at the titanium-titanium and the titanium-zirconia implant-abutment interface: a comparative in vitro study. Dent Mater. 2012;28:1215. https://doi.org/10.1016/j.dental.2012.08.008.
68. Sikora CL, Alfaro MF, Yuan JCC, Barao VA, Sukotjo C, Mathew MT. Wear and corrosion interactions at the titanium/zirconia interface: dental implant application. J Prosthodont. 2018;27:842–52. https://doi.org/10.1111/jopr.12769.
69. Thomas A, Sridhar S, Aghyarian S, Watkins-Curry P, Chan JY, Pozzi A, et al. Corrosion behavior of zirconia in acidulated phosphate fluoride. J Appl Oral Sci. 2016;24:52. https://doi.org/10.1590/1678-775720150435.
70. Scarano A, Petrini M, Mastrangelo F, Noumbissi S, Lorusso F. The Effects of liquid disinfection and heat sterilization processes on implant drill roughness: Energy Dispersion X-ray Microanalysis and Infrared Thermography. J Clin Med. 2020;9:1019; https://doi.org/10.3390/jcm9041019.
71. Scarano A, Noumbissi S, Gupta S, Inchingolo F, Stilla P, Lorusso F. Scanning electron microscopy analysis and energy dispersion X-ray microanalysis to evaluate the effects of decontamination chemicals and heat sterilization on implant surgical drills: zirconia vs steel. Appl Sci. 2019;9:2837. https://doi.org/10.3390/app9142837.
72. Cionca N, Hashim D, Mombelli A. Zirconia dental implants: where are we now, and where are we heading? Periodontology 2000. 2017;73:241. https://doi.org/10.1111/prd.12180.
73. Lughi V, Sergo V. Low temperature degradation-aging-of zirconia: a critical review of the relevant aspects in dentistry. Dent Mater. 2010;26:807. https://doi.org/10.1016/j.dental.2010.04.006.
74. Kohal RJ, Wolkewitz M, Tsakona A. The effects of cyclic loading and preparation on the fracture strength of zirconium-dioxide implants: an in vitro investigation. Clin Oral Implants Res. 2011;22:808. https://doi.org/10.1111/j.1600-0501.2010.02067.x.

75. Kohal RJ, Weng D, Bächle M, Strub JR. Loaded custom-made zirconia and titanium implants show similar osseointegration: an animal experiment. J Periodontol. 2004;75:1262. https://doi.org/10.1902/jop.2004.75.9.1262.
76. Sennerby L, Dasmah A, Larsson B, Iverhed M. Bone tissue responses to surface-modified zirconia implants: a Histomorphometric and removal torque study in the rabbit. Clin Implant Dent Relat Res. 2005;7:s13. https://doi.org/10.1111/j.1708-8208.2005.tb00070.x.
77. Yamashita D, Machigashira M, Miyamoto M, Takeuchi H, Noguchi K, Izumi Y, et al. Effect of surface roughness on initial responses of osteoblast-like cells on two types of zirconia. Dent Mater J. 2009;28:461. https://doi.org/10.4012/dmj.28.461.
78. Al-Radha ASD, Dymock D, Younes C, O'Sullivan D. Surface properties of titanium and zirconia dental implant materials and their effect on bacterial adhesion. J Dent. 2012;40:146. https://doi.org/10.1016/j.jdent.2011.12.006.
79. Rimondini L, Cerroni L, Carrassi A, Torricelli P. Bacterial colonization of zirconia ceramic surfaces: an in vitro and in vivo study. Int J Oral Maxillofac Implants. 2002;17:793–8.
80. Clever K, Schlegel KA, Kniha H, Conrads G, Rink L, Modabber A, et al. Experimental peri-implant mucositis around titanium and zirconia implants in comparison to a natural tooth: part 1—host-derived immunological parameters. Int J Oral Maxillofac Surg. 2019;48:554. https://doi.org/10.1016/j.ijom.2018.10.018.
81. Degidi M, Artese L, Scarano A, Perrotti V, Gehrke P, Piattelli A. Inflammatory infiltrate, microvessel density, nitric oxide synthase expression, vascular endothelial growth factor expression, and proliferative activity in peri-implant soft tissues around titanium and zirconium oxide healing caps. J Periodontol. 2006;77:73. https://doi.org/10.1902/jop.2006.77.1.73.
82. Cionca N, Hashim D, Meyer J, Michalet S, Mombelli A. Inductively coupled plasma mass spectrometry detects zirconium and titanium elements in peri-implant mucosa. J Dent Res. 2016;995–1002
83. Cionca N, Hashim D, Cancela J, Giannopoulou C, Mombelli A. Pro-inflammatory cytokines at zirconia implants and teeth. A cross-sectional assessment. Clin Oral Investig. 2016;20:2285. https://doi.org/10.1007/s00784-016-1729-z.
84. Najeeb S, Zafar MS, Khurshid Z, Siddiqui F. Applications of polyetheretherketone (PEEK) in oral implantology and prosthodontics. J Prosthodont Res. 2016;60:12–9. https://doi.org/10.1016/j.jpor.2015.10.001.
85. Skinner H. Composite technology for total hip arthroplasty. Clin Orthop Relat Res. 1988;235:224–36.
86. Xin H, Shepherd DET, Dearn KD. Strength of poly-ether-ether-ketone: effects of sterilisation and thermal ageing. Polym Test. 2013;32:1001–5. https://doi.org/10.1016/J.POLYMERTESTING.2013.05.012.
87. Walsh WR, Pelletier MH, Bertollo N, Christou C, Tan C. Does PEEK/HA enhance bone formation compared with PEEK in a sheep cervical fusion model? Clin Orthop Relat Res. 2016;474:2364–72. https://doi.org/10.1007/s11999-016-4994-x.
88. Feng X, Yu H, Liu H, Yu X, Feng Z, Bai S, et al. Three-dimensionally-printed polyether-ether-ketone implant with a cross-linked structure and acid-etched microporous surface promotes integration with soft tissue. Int J Mol Sci. 2019;20:3811. https://doi.org/10.3390/ijms20153811.
89. Almasi D, Iqbal N, Sadeghi M, Sudin I, Abdul Kadir MR, Kamarul T. Preparation methods for improving PEEK's bioactivity for orthopedic and dental application: a review. Int J Biomater. 2016;2016:1. https://doi.org/10.1155/2016/8202653.
90. Torstrick FB, Lin ASP, Potter D, Safranski DL, Sulchek TA, Gall K, et al. Porous PEEK improves the bone-implant interface compared to plasma-sprayed titanium coating on PEEK. Biomaterials. 2018;185:106–16. https://doi.org/10.1016/J.BIOMATERIALS.2018.09.009.
91. Cordioli G, Majzoub Z, Piattelli A, Scarano A. Removal torque and histomorphometric investigation of 4 different titanium surfaces: an experimental study in the rabbit tibia. Int J Oral Maxillofac Implants. 2000;15:668–74.

92. Scarano A, Degidi M, Perrotti V, Degidi D, Piattelli A, Iezzi G. Experimental evaluation in rabbits of the effects of thread concavities in bone formation with different titanium implant surfaces. Clin Implant Dent Relat Res. 2014;16:572–81. https://doi.org/10.1111/cid.12033.
93. Webster TJ, Patel AA, Rahaman MN, Sonny BB. Anti-infective and osteointegration properties of silicon nitride, poly(ether ether ketone), and titanium implants. Acta Biomater. 2012;8:4447. https://doi.org/10.1016/j.actbio.2012.07.038.
94. Hahnel S, Wieser A, Lang R, Rosentritt M. Biofilm formation on the surface of modern implant abutment materials. Clin Oral Implants Res. 2015;26:1297. https://doi.org/10.1111/clr.12454.
95. Rochford ETJ, Jaekel DJ, Hickok NJ, Richards RG, Moriarty TF, Poulsson AHC. Bacterial interactions with polyaryletheretherketone. In: PEEK biomaterials handbook. Amsterdam: Elsevier; 2012. https://doi.org/10.1016/B978-1-4377-4463-7.10008-9.
96. Barkarmo S, Longhorn D, Leer K, Johansson CB, Stenport V, Franco-Tabares S, et al. Biofilm formation on polyetheretherketone and titanium surfaces. Clin Exp Dent Res. 2019;5:427–37. https://doi.org/10.1002/cre2.205.
97. D'Ercole S, Cellini L, Pilato S, Di Lodovico S, Iezzi G, Piattelli A, Petrini M. Material characterization and *Streptococcus oralis* adhesion on Polyetheretherketone (PEEK) and titanium surfaces used in implantology. J Mater Sci: Mater Med. 2020;31:84. https://doi.org/10.1007/s10856-020-06408-3
98. Han A, Tsoi JKH, Rodrigues FP, Leprince JG, Palin WM. Bacterial adhesion mechanisms on dental implant surfaces and the influencing factors. Int J Adhes Adhes. 2016;69:58. https://doi.org/10.1016/j.ijadhadh.2016.03.022.

Biomaterials for Bone Grafting and Craniofacial Bone Regeneration

Lohitha Kalluri and Yuanyuan Duan

Abstract Reconstruction of craniofacial defects poses a challenging task for craniofacial surgeons. Reconstruction of the underlying craniofacial bone is crucial for successful outcome of these defects. Bone grafting is the standard technique employed for bone reconstruction. However, with the advent of novel biomaterials as bone substitutes for grafting procedures, attractive alternatives have unlocked for surgeons. Since a few decades, the field of craniofacial bone regeneration has expanded enormously with the advent of novel biomaterials and innovative concepts such as bioprinting and drug delivery. At present, several natural and synthetic bone graft materials are available as bone substitutes. In this chapter, the authors will focus on the various biomaterials that are currently used as bone substitutes in craniofacial bone regeneration along with an update of the active research among each class of biomaterials going on in this area. Also, the authors will brief-in the recent concepts for craniofacial bone regeneration.

Keywords Bioceramics · Bone grafts · Biometals · Biopolymers · Bioprinting · Craniofacial bone regeneration

1 Introduction

1.1 Brief Introduction of Craniofacial Bone Regeneration

Craniofacial bone defects are the defects associated with bones of skull and face. Congenital birth defects (1/700 live births) such as cleft lip, cleft palate, craniosynostosis, and hemifacial microstomia are the most common causes of craniofacial defects in children. Acute trauma such as vehicle accidents, falls, sports injuries and physical assaults, cancer surgeries, and inflammation are the most frequent causes

L. Kalluri · Y. Duan (✉)
Department of Biomedical Materials Science, University of Mississippi Medical Center, Jackson, MS, USA
e-mail: kalluri@umc.edu

R. S. Chaughule, R. Dashaputra (eds.), *Advances in Dental Implantology using Nanomaterials and Allied Technology Applications*,
https://doi.org/10.1007/978-3-030-52207-0_6

for craniofacial defects in adults. Reconstruction of the craniofacial defects is challenging as craniofacial tissue construct itself is complex, comprising bone, cartilage, neurovascular tissues, and soft tissues [1]. Accurate reconstruction of craniofacial bone is crucial in these defects to provide support and structural stability for adjacent soft tissues, thereby improving the appearance of associated facial structures. These bony defects could vary from small periodontal defects to complex segmental defects. Especially, in case of large craniofacial defects, soft tissue reconstruction is relatively easier with sufficient underlying bone structure [2].

Unlike skeletal bones, craniofacial bones are flat bones with some peculiar features, but they do have similar bone repair mechanism and metabolic turnover rate as the skeletal bone [3]. There are few major differences between craniofacial and skeletal bones such as their embryonic origin, homeostatic mechanisms, and bone shapes. Craniofacial bones originate from cranial neural crest, unlike the skeletal bones which originate from somites and lateral plate mesoderm [4]. Several authors [5, 6] stated that the bone grafts harvested from craniofacial region had better survival and longer volumetric maintenance compared to skeletal bone grafts, demonstrating different homeostatic mechanisms. Several growth factors, receptors, and associated signaling cascades play distinct roles in the formation of craniofacial and skeletal bones [7]. Also, unlike long bones, craniofacial bones exhibit extremely complex 3D shapes, impeding the precise fit of long bone grafts into these defect regions.

2 Biomaterials Used for Craniofacial Bone Grafts

Biomaterials play a vital role in biomedical applications for restoring the structural and functional integrity of damaged tissues. Biomaterials can either replace or regenerate a damaged tissue [8]. Ideally, the biomaterials to be used as craniofacial grafts should have the following requisites as described underneath [9]:

- They should be biocompatible.
- They should either be osteoinductive, osteoconductive, and/or osteopromotive in nature.
- They should be dimensionally stable under stress.
- They should be biodegradable after their intended response at the implanted site.
- They should be easily moldable in order to conform to the craniofacial defect.
- They should be easily sterilizable.
- They should be stable and promote long-term integration of implants.

The biomaterials used as grafts could either be natural or synthetic and are categorized as follows:

1. **Natural biomaterials**
   (a) Autografts
   (b) Allografts

(c) Xenografts
(d) Natural degradable biopolymers

2. **Synthetic biomaterials**

(a) **Biometals**

- Biodegradable
- Nonbiodegradable

(b) **Biopolymers**

- Biodegradable
- Nonbiodegradable

(c) **Bioceramics**

- Bioinert ceramics
- Bioactive ceramics
- Bioresorbable ceramics

3. Biocomposites and their hybrids
Advancements in biomaterials for craniofacial regeneration

(a) Biomaterials for controlled delivery of drugs, growth factors, and stem cells.
(b) Additive manufacturing and bioprinting.

2.1 Natural Biomaterials

Natural biomaterials are the biomaterials that can be obtained naturally from organisms. For craniofacial bone regeneration, natural biomaterials comprise bone grafts such as autografts, allografts, and xenografts.

Ideally, the bone graft material should possess the following properties as [10]:

1. Osteogenesis: The formation of new bone by osteoblasts derived from the graft material itself.
2. Osteoinduction: The ability of a material to induce the formation of osteoblasts from the surrounding tissue at the graft host site, resulting in bone growth.
3. Osteoconduction: The ability of a material to support the growth of bone over a surface.
4. Structural integrity: Structural strength of the grafted material in compressive strength, and resistance to torsion and shear.
5. Osteointegrative ability: The capability of the graft to integrate and bond to the host bone.

2.1.1 Autografts

Autografts, autologous, or autogenous bone grafts are the bone grafts that are harvested from one site and implanted into another site within the same individual. They may either be cancellous, cortical (non-vascularized or vascularized), or corticocancellous grafts. For craniofacial reconstruction, possible sources of autologous bone grafts could be calvarium, chin, retromolar pad area of mandible, iliac crest, tibial plateau, rib, etc. [11]. The main disadvantage of autografts is the morbidity of donor site, and other possible advantages and disadvantages are outlined in Table 1.

2.1.2 Allografts

Allografts are the graft tissues that are obtained from genetically nonidentical members of the same species. These are potential alternatives to autografts in craniofacial reconstruction. Bone allografts are unique in that the cellular component is typically removed to minimize their rejection. In addition, they are thoroughly treated to eliminate any possibility of disease transmission. Allograft is available as cortical, cancellous, or corticocancellous graft in the form of powder, chips, wedges, pegs, dowels, or struts. It can also be customized to desired shapes [12]. Allografts are commercially available as Freeze-Dried Bone Allograft (FDBA), Demineralized Freeze-Dried Bone Allograft (DFDBA), and Demineralized Bone Matrix (DBM) in various bone banks accredited from American Association of Tissue Banks [13].

DBM is mainly used for defects and is available commercially in various forms as moldable pastes, putty, strips, gel, granules, and freeze-dried powder. This DBM is often mixed with harvested autograft, bone marrow, or other allografts to increase autograft volume and augment bone healing. The advantages and disadvantages of allografts are outlined in Table 1.

Table 1 Advantages and disadvantages of three types of commonly used natural bone grafts [18]

Bone graft	Advantages	Disadvantages
Autografts	Optimal osteogenic, osteoinductive, and osteoconductive properties; gold standard for bone grafting; no risk of immunogenicity and disease transmission	Pain and morbidity in the donor site, limited quantity and availability, need for additional surgery, hematoma, infection, the need for general sedation or anesthesia, longer operative time, and blood loss
Allografts	Osteoinductive and osteoconductive properties, no donor site morbidity, possible with local anesthesia, high availability, easy handling	Lack of osteogenic properties, potential antigenic response and disease transmission, variable osteoinductivity, limited supply, loss of biologic and mechanical properties due to its processing, nonavailability worldwide due to religious and financial concerns and increased cost
Xenografts	Osteoinductive and osteoconductive properties, low cost, high availability	Lack of osteogenic properties, the risk of immunogenicity and transmission of infectious and zoonotic diseases, poor outcome

2.1.3 Xenografts

Xenografts or heterologous grafts are another alternative to autografts and are harvested from nonhuman species, i.e., animals. They possess osteoconductive and osteoinductive properties, but lack osteogenic properties. The advantages and disadvantages of xenografts are outlined in Table 1.

A deproteinized bovine bone graft, commercially known as "Bio-Oss," is the most common bone substitute used in dentistry for guided bone regeneration [14]. Apart from Bio-Oss, another commonly used xenograft in dentistry is "Gen-Os." Gen-Os is a corticocancellous heterologous bone graft harvested either from porcine (Porcine Gen-OS) or equine (Equine Gen-OS) [15].

Also, porous pure hydroxyapatite (commercially available as "Interpore" and "Pro-osteon") derived from marine coral is used as a bone substitute in dentistry for orthognathic surgeries, alveolar ridge augmentation, and periodontal bone defects [16, 17].

2.1.4 Natural Degradable Polymers

The use of natural degradable polymers as potential bone substitutes can be attributed to their close resemblance of native extracellular matrix. These polymers can be categorized either into proteins (collagen, gelatin, fibrinogen, elastin, keratin, silk), polysaccharides (glycosaminoglycans, cellulose, amylose, dextran, chitin), or polynucleotides (DNA, RNA) based on their chemical composition [19]. These polymers are mainly used as bone tissue scaffolds and are highly osteoinductive due to their similarity to extracellular matrix. They can be fabricated from decellularized bone tissue obtained either from autologous, allogenic, or xenograft [20]. These natural polymers are highly biocompatible and undergo extensive hydration to form hydrogels under physiological conditions. However, these hydrogels lack adequate mechanical strength, rendering them impossible to use in bone regeneration systems in vivo. Thus, hybrid scaffold systems are developed, wherein these hydrogels are loaded onto ceramic scaffolds to improve mechanical stability [21].

2.2 Synthetic Biomaterials

Synthetic biomaterials range from biometals to biocomposite materials and could either be biodegradable or nondegradable. These advantages of synthetic grafts are their wide availability, uniform quality, reduced morbidity, and sterility. However, in vivo performance of synthetic bone grafts is inferior to autografts due to the lack of inherent osteogenic and osteoinductive potential.

2.2.1 Biometals

Biometals are used in craniofacial bone reconstruction in various forms as bone reconstruction plates, screws, implants, and scaffolds for tissue engineering. They could either be degradable or nondegradable and are selected based on application.

2.2.1.1 Biodegradable Metals

These are defined as the metals that are expected to corrode gradually in vivo, with an appropriate host response elicited by released corrosion products, then dissolve completely upon fulfilling the mission to assist tissue healing with no implant residues [22]. Also, from the materials science point of view, Zheng et al. [22] classified biodegradable metals into three categories as "Pure metals," "Biodegradable alloys," and "Biodegradable metal matrix composites." At present, a lot of research is directed at this particular class of biometals in order to design an ideal material to be used as temporary implants and scaffolds so that it could obviate the need for revision surgeries and promoting a safe and effective bone repair.

Currently, magnesium (Mg) and its alloys are gaining wide popularity as biodegradable temporary implant material in craniofaial applications due to its excellent biocompatibility and better matching of mechanical properties such as the density, elastic modulus, and yield strength with that of bone. However, the major drawback of Mg is its high rate of corrosion in physiological environment. Various metals, such as calcium, zinc, tin, and zirconium, have been alloyed with magnesium in order to control their degradation rate. However, additional research is still required in this area [23].

Apart from Mg, a lot of research is also focussed on developing other biodegradable metal alloys such as iron-based and zinc-based alloys. Unlike Mg, these alloys do have low rate of corrosion in physiological environment. These alloys are gaining wide attention from researchers and are still at an experimental stage [22].

2.2.1.2 Nondegradable Metals (Titanium and its alloy)

Titanium (Ti) is the material of choice for fabrication of bone plates, screws, craniofacial and dental implants, tissue engineering scaffolds, meshes for guided bone regeneration, etc., owing to its biocompatibility, corrosion resistance, and superior mechanical properties. However, the potential drawbacks of these alloys are their high elastic modulus relative to the bone, cost, and low wear resistance [8, 24]. Mismatch between the elastic modulus of titanium (110 GPa) and bone (10–30 GPa) results in "stress-shielding effect." Hence, lot of research is directed to minimize the elastic modulus mismatch between titanium and bone.

Titanium and its alloys exist in three forms as α-form, β-form, and (α + β)-form. Elastic moduli of α- and (α + β)-type titanium alloys such as Ti and Ti–6Al–4V ELI are higher than those of β-type titanium alloys. Thus, β-titanium alloys are more

favorable for the development of titanium alloys in biomedical applications [25]. Currently, β-titanium alloy systems, Ti–Nb–Ta–Zr system, known as Gum metal (Ti–29Nb–13Ta–4.6Zr) and a Ti–35Nb–7Zr–5Ta system, known as TiOsteum® are gaining attention in biomedical field owing to their low elastic modulus and better osseointegration properties [8, 25].

Apart from β-titanium alloy systems, Takizawa et al. introduced titanium fiber plate with Young's modulus similar to bone to prevent the stress-shielding effect commonly observed with traditional titanium plates. Also, porous structure suitable for cell adhesion could be formed from titanium fibers to be used as a bone repair scaffold [26].

Additionally, novel porous titanium structure is also advantageous to reduce elastic modulus mismatch between implant and bone tissue. Ti-based biomaterials with customized porosity are crucial for cell adhesion, viability, differentiation, and growth, aiding as scaffolds for bone tissue engineering. They facilitate bone-ingrowth and achieve long-term biological fixation [27].

Also, Titanium mesh, commercially available as "BoneShields, Ti-Micromesh, Tocksystem," is widely used as synthetic nonresorbable plate in Guided Bone Regeneration (GBR) to cover large bony defects [28].

Furthermore, surface morphology of the titanium implant is modified either using additive or subtractive techniques such as plasma spraying, anodization, laser peening, and grit blasting to improve wettability, cell-implant adhesion and attachment, cell proliferation, and osseointegration [8].

Tantalum Alloy

Tantalum has been introduced as an ideal bone graft material due to its cytocompatibility and osteoinductive nature. Porous tantalum bears a similar porous structure and mechanical properties to natural bone, facilitating bone ingrowth, "osteocorporation," and revascularization [27].

Tantalum-based trabecular structured biomaterial is developed by means of trabecular metal technology [29] (Trabecular Metal™ Material, Zimmer Biomet TMT, Parsippany, NJ, USA). Recently, Zimmer Inc. developed a dental implant with porous tantalum components in midsection (commercially available as "Trabecular Metal™ Dental Implant") to treat immunocompromised patients and for placement in immediate loading implant cases [30].

Stainless Steel

316L is the medical-grade stainless steel (SS) used for biomedical applications. 316LSS is widely used as internal fixation devices, such as screws, bone plates, pins, and wires, to treat craniofacial bone fracture. However, in future, biodegradable metals and polymers might replace 316LSS as internal fixation devices. The main limitations of this alloy are the adverse effect of metal ions and fretting debris due to wear and corrosion in body fluids as well as the stress-shielding effect on bone due to higher elastic modulus. Nickel and chromium present in the 316LSS are the potential

allergens. So, medical-grade high-nitrogen nickel-free austenitic stainless steel (commercially available as Biodur 108, Panacea P558, P2000, and BIOSSN4) is developed, wherein the nickel is replaced by nitrogen for austenitic structure stability and it improves the mechanical properties of steel significantly [31].

Niobium and Zirconium Alloys

Zirconium (Zr) belongs to the same group as Ti and possess lower magnetic susceptibility than Ti. It is due to this property, Zr is emerging as a potential alternative to Ti, which when implanted in patient distorts MRI scans. Niobium is added to Zr to enhance its wear and corrosion resistance in body fluids. Nb–2Zr alloy exhibited excellent corrosion resistance, fatigue strength, and crack propagation in simulated bodyfluids [32].

2.2.2 Synthetic Biopolymers

These biopolymers are highly crystalline thermoplastics and could either be homopolymer, copolymer, or heteropolymers. Polymers can be broadly classified as degradable or nondegradable on the basis of the reactivity of their chemical backbone. Natural biopolymers were discussed under natural bone substitutes and synthetic biodegradable and nondegradable polymers will be described in this section.

2.2.2.1 Degradable

This synthetic class of biomaterials is widely used in bone tissue engineering as scaffolds and as temporary bone implants owing to their strength and biodegradability, wherein they undergo hydrolysis in response to local environmental factors like pH, enzymes, temperature changes, etc., yielding carbon dioxide and water as the metabolic by-products. Also, the rate of biodegradation and strength of the scaffold could easily be customized by varying certain variables such as the type of polymer used, porosity, and fabrication techniques. However, Scaffolds composed of synthetic polymers are osteoconductive, allowing ingrowth of bony tissue, but are not osteoinductive in their native form [8].

Saturated aliphatic polyesters, such as Poly(glycolic acid) (PGA), Poly(lactic acid) (PLA), PLGA copolymers, and Poly(ε-caprolactone) (PCL) are the widely used synthetic polymers for tissue engineering purposes. PCL is also used as a temporary implant due to its slow rate of biodegradation (2–4 years). Biodegradable polyurethane, commercially available as "Degrapol® (Abmedica)" is currently being used to develop a highly porous scaffold for tissue engineering applications [21].

Also, these polymers are used as resorbable membranes in Guided Bone Regeneration (GBR) procedures. These synthetic barrier membranes are usually made of either PLA or PGA and several commercial formulations of these polymers are tabulated in Table 2 [28].

2.2.2.2 Nondegradable

Poly(ethylene)(PE)(HDPE,UHMWPE), Poly(propylene) (PP), Poly(tetrafluoroethylene) (PTFE), Poly(methylmethacrylate) (PMMA), Polyether ether ketone (PEEK), etc., are the nondegradable polymers used in biomedical applications. For craniofacial applications, PTFE, PMMA, and PEEK are widely used. PTFE and e-PTFE were appealing first-generation biomaterials for use in GBR. Recently, Ti-reinforced e-PTFEs were developed to enhance mechanical properties of e-PTFE and are used to augment large bony defects. These PTFE membranes are marketed under the trade names Cytoflex, TefGen-FD, Gore-Tex, and Cytoplast™ Ti [28].

PMMA is widely used as a bone substitute material in skull reconstruction procedures and also as a drug carrier for embedding bioactive substances to promote bone healing. It is supplied in the form of a powder and liquid (Cranioplastic™) which when mixed forms a paste that can be shaped intraoperatively to fit the defect precisely. However, its use has been limited due to its potential risks, such as the release of toxic unreacted methylacrylate monomers, lack of osteoconductive or osteoinductive properties, and exothermic setting reaction [33].

Apart from PMMA, several other polymers such as PEEK (poly-ether-ether ketone), polypropylene polyester knitwear, and PEKK (poly-ether-ketone ketone) are used as cranial implants due to similar properties to the surrounding bone, especially with regard to young's modulus [34].

2.2.3 Bioceramics

"Bioceramics" is a term applied to ceramics with biological functionality. These can be classified as bioinert (alumina and zirconia), bioresorbable (tricalcium phosphate), or bioactive (hydroxyapatite, bioactive glasses, and glass-ceramics) based on their chemical surface reactivity.

Table 2 Commercially available resorbable synthetic barrier membranes [28]

Trade name	Material	Resorption period (months)
Guidor® (Sunstar)	PLA (Polylactic Acid)	1.5–2
Resorb X® (KLS Martin)	PDLLA (Poly-DL-Lactic Acid)	1.5–2
Cytoflex Resorb® (Unicare Biomedical)	PLGA (Poly-Lactic-Glycolic Acid)	4
Resolute® (Gore®)	PGA-TMC (Polyglycolic Acid Trimethylene Carbonate)	4–6
Epi-Guide® (Curasan, Inc.)	PDLLA (Poly-DL-Lactic Acid)	6–12
Atrisorb® (Tolmar)	P(DL)LA–NMP (Poly-DL-Lactic Acid dissolved in N-methyl-2-pyrrolidone (NMP))	9–12
Inion™ GTR (Inion)	PLDLGA-TMC (Poly-LD-Lactic-Glycolic Acid Trimethylene Carbonate)	12–24
Vivosorb® (Polyganics)	PDLLCL (Poly-DL-Caprolactone)	16

2.2.3.1 Bioinert Ceramics

High purity alumina and zirconia are the bioinert ceramics used in medical applications. They do not play a significant role in craniofacial applications but are widely used in dentistry as dental prosthesis and implants. Currently, tetragonal zirconia polycrystal, particularly 3 mol% yttrium oxide (yttria)-stabilized zirconia, is emerging as an alternative to traditional titanium dental implants owing to its promising mechanical properties, good biocompatibility, white opaque hue, and low plaque affinity. However, failure rates of zirconia implant systems tested so far were generally higher compared with titanium implants [35]. To date, zirconia implants are manufactured largely as single-piece system. Nonetheless, few two-piece zirconia implants (NobelPearl™, ZERAMEX® XT, and Straumann® PURE Ceramic two-piece Implant) are evolving. Further research and clinical investigations based on the longevity and success of these evolving two-piece zirconia implants are necessitated.

2.2.3.2 Bioactive Ceramics

Bioactive ceramics are defined as "bioceramics that bond directly with bone without having fibrillar connective tissue between them." These include hydroxyapatite, bioactive glass. and bioactive glass-ceramics.

Bioactive Glass and Glass-Ceramics

These are amorphous silica-based biomaterials. When implanted in vivo, these glasses react with physiological fluids and forms a crystallized hydroxycarbonate apatite (HCA) layer at the glass/bone interface. This HCA layer mimics inorganic bone component and forms a strong bond with bone without intervening fibrous tissue. The rate of activity and physiological response depends on chemical composition of the glass (ratio of the network former, SiO_2 to network modifier, Cao + Na_2O + K_2O) and the specific surface area (morphology of scaffold, porosity, etc.). 45S5 (Na_2O-CaO-P_2O_5-SiO_2) is the first bioactive glass formulation, consisting of 45% silica. Despite its high bioactivity in physiological fluids, their applications were limited as filler or coating on polymer-based scaffolds and are not used in load-bearing situations or large bony defects due to their low fracture toughness values and poor mechanical strength [36]. These formulations are marketed as GlassBone® (Noraker), BonAlive® (BonAlive Biomaterials Ltda), Vitoss® (Stryker), and Perioglass® (NovaBone) [37].

Subsequently, scientists focussed on improving the mechanical properties of the bioactive glass matrix, which led to the development of apatite/wollastonite (A/W), Ceravital and Bioverit glass-ceramics. A/W glass-ceramics demonstrate increased fracture toughness values than bioactive glasses due to the assembly of apatite phases reinforced by ß-wollastonite ($CaSiO_3$) and can be used in load-bearing applications [38].

Hydroxyapatite

Synthetic hydroxyapatite (S-HA) is a stable calcium phosphate-based bioceramic and closely mimics natural calcium apatite ($Ca_{10}(PO4)_6(OH)_2$) mineral present in human bone. As a bone graft material, it is biocompatible, osteoconductive, bioactive, has a high affinity for proteins and growth factors, and has high wear resistance. It can be prepared either as dense sintered blocks or as macroporous forms. Dense S-HA is nonbiodegradable and is not osteoinductive. But, Porous S-HA, commercially available as "Osbone®Dental" has osteoinductive potential and has low degradation rate in body fluids. This biomaterial is stiff and strong but brittle, limiting its use to nonweight-bearing regions like maxillofacial applications limited to use in situations where there is no physical loading of the apatite as in maxillofacial applications [39].

2.2.3.3 Bioresorbable Ceramics

Tricalcium phosphate ($Ca_3(PO4)_2$) (TCP) is a bioresorbable calcium phosphate-based bioceramic with a Ca/P ratio of 1:5. It exists either in α phase or β phase. α-TCP degrades faster than β-TCP. The degradation rate of β-TCP is 3–12 times higher than that of HA. β-TCP is highly compatible and is the widely used synthetic graft material for bone reconstruction purposes in orthopedic and maxillofacial surgery. However, its use is limited as filler and coatings on implant surfaces or scaffolds due to insufficient biomechanical strength and mechanical properties. Some of the commercially available TCP products are Ceros®, ChronOS®, Cerasorb M®, Vitoss®, IngeniOs™, Macrobone, etc.

Consequently, bioactive β-TCP is combined with mechanically stable HA, to develop a composite material "Biphasic calciumphosphate (BCP)." BCP (marketed under the trade names "Osteosynt®, Triosite®, MBCP®, Hatric®, OptiMX®") is available in block form or granular form and demonstrates superior osteoinductive effect than S-HA alone [39].

Furthermore, BCP is doped with metal ions such as Mn^{2+}, Fe^{3+}, Co^{2+}, Ni^{2+}, Cu^{2+}, and Zn^{2+} to simulate the mineral constituent of bone and it enhances the osteoinductive capability of the biomaterial [40].

2.3 Biocomposites and Their Hybrids

A biocomposite is a material composed of two or more distinct constituent materials (one usually being naturally derived), which are combined to yield a new material with improved performance over individual constituent materials. These biocomposites can overcome the limitations of single bone substitute materials. These are formed by optimizing the combination or by surface modification and have the ability to stimulate specific reactions in the bone defect area at the molecular level [41].

A biocomposite can be constructed by either of the following procedures as follows:

1. Incorporating bioceramic particles or fibers as a dispersed phase into the polymer matrix.
2. Coating polymer, metal, or ceramic with a thin layer of bioceramic.
   Most commonly used biocomposites as bone substitutes are xenohybrids, which are a combination of xenografts and synthetic bone graft substitutes. "PepGen P-15" is a commercially available xenohybrid composed of an organic bovine mineral with a synthetic biomimetic of the 15 AA sequence of Type-1 collagen [42].

3 Advancements in Biomaterials for Craniofacial Regeneration

3.1 Biomaterials for Controlled Delivery

3.1.1 Drug-Loaded Biomaterials

Drugs such as antibiotics, statins (simvastatin), and anti-inflammatory drugs can be enclosed within biodegradable synthetic polymer scaffolds, such as PLA, PGA, PLGA, and PCL, or natural hydrogels, such as fibrin, collagen, gelatin, chitosan, and alginate. The rate of drug delivery in natural hydrogels can be controlled by means of physical or chemical cross-linking. Additionally, with the advancement of nanotechnology, nanoparticle delivery systems, which can penetrate through the capillaries into cells are developed as carriers for therapeutic agents. These biomaterials help in local delivery of drugs at tissue site. These drug-loaded biomaterials are commercially available as Simplex®P, Osteoset-T®, Collatamp®, Septocoll®, Septopal®, Herafill® beads, and Stimulan® [43].

3.1.2 Growth Factor Delivery

Various growth factors such as TGF-β, FGF, VEGF, PDGF, IGFs, and BMPs play a significant role in craniofacial growth and development. At present, various delivery vehicles based on natural or synthetic polymers, ceramics, and their composites have been devised in the form of sponges, nanofibrous membranes, micro/nanoparticles, and hydrogels, to either chemically or physically entrap GFs into or onto the substrate. Few commercial products based on rhBMP-loaded carrier are approved by FDA for clinical use. These include Infuse® (an absorbable collagen sponge loaded with rhBMP-2 growth factor), OP-1® Putty (a bovine-derived collagen infiltrated with rhBMP-7), and GEM 21S® (rhPDGF incorporated into a β-TCP porous carrier) [37].

3.1.3 Stem Cell Delivery

Stem cell delivery using hydrogels and tissue engineering scaffolds is another promising application of these biomaterials. Mesenchymal stem cells (MSCs) incorporated tissue engineering scaffolds produce promising results in bone defect repair. These scaffolds function as native extracellular matrix and aid in the attachment and growth of encapsulated cells, thereby preventing anoikis. Also, these biomaterials protect stem cells against host immune attack and can trigger major cellular processes necessary for bone regeneration. Currently, all the commercial bone grafts incorporating MSCs were based on DBM and these include Allostem®, Map3™, Osteocel Plus®, and Trinity Evolution Matrix™ [37].

3.1.4 Bioprinting and Additive Manufacturing

The advent of rapid prototyping technology has revolutionized the field of craniofacial bone reconstruction. The terms 3D printing and 3D bioprinting are used interchangeably in the field of rapid prototyping. However, "3D printing" is the term used to describe the fabrication of inert or bioactive scaffold materials without the presence of living cells, whereas, 3D bioprinting refers to printing of cells and scaffolds together (cell-laden biomaterials) or dense aggregates of cells free from scaffold [37]. Currently, 3D bioprinting is advancing further to 4D bioprinting by incorporating a fourth dimension "dynamic stimulus-responsive environment" [44].

3D printing has been used largely in craniofacial reconstruction to fabricate custom cranial implants using various biomaterials such as titanium and PEEK. Recently, FDA has approved a custom 3D printed titanium craniofacial implant manufactured by BioArchitects [45].

Additive manufacturing modalities like extrusion printing, inkjet printing, or laser printing can be used for bioprinting. The main advantage of this 3D printing is customization, precision, and ease of fabrication. Using 3D printing, internal and external 3D architecture of scaffold systems can be easily customized as per the specific requirements.

Currently, "OsteoFlux" (3D printed CaP osteoinductive material sold by Vivos Dental AG), is the commercially available pre-3D printed scaffold system for craniofacial regeneration [37].

4 Conclusion

For the past few decades, the field of craniofacial reconstruction has witnessed an immense advancement with the advent of novel biomaterials, concepts, and technologies. But, so far, neither of these available bone grafts, except for freshly harvested autografts, have osteogenic or truly osseoinductive properties. Hence, an

ongoing quest for perfect bone substitute material to replace autografts still persists. However, the amalgamation of additive technology with tissue engineering might unlock new potential and possibilities in craniofacial regeneration techniques in near future.

References

1. Petrovic V, Zivkovic P, Petrovic D, Stefanovic V. Craniofacial bone tissue engineering. Oral Surg Oral Med Oral Pathol Oral Radiol. 2012;114(3):e1–9.
2. Genden EM. Reconstruction of the mandible and the maxilla: the evolution of surgical technique. Arch Facial Plast Surg. 2010;12(2):87–90.
3. Leucht P, Kim J-B, Amasha R, James AW, Girod S, Helms JA. Embryonic origin and Hox status determine progenitor cell fate during adult bone regeneration. Development. 2008;135(17):2845–54.
4. Karaplis AC. Chapter 3—Embryonic development of bone and regulation of intramembranous and endochondral bone formation. In: Bilezikian JP, Raisz LG, Martin TJBT, editors. Principles of bone biology. 3rd ed. San Diego, CA: Academic Press; 2008. p. 53–84.
5. Peer LA. Fate of autogenous human bone grafts. Br J Plast Surg. 1951;3(4):233–43.
6. Sullivan WG, Szwajkun PR. Revascularization of cranial versus iliac crest bone grafts in the rat. Plast Reconstr Surg. 1991;87(6):1105–9.
7. Abzhanov A, Rodda SJ, McMahon AP, Tabin CJ. Regulation of skeletogenic differentiation in cranial dermal bone. Development. 2007;134(17):3133–44.
8. Ratner BD, Hoffman A, Schoen FJ, Lemons JE. Biomaterials science: an introduction to materials in medicine. 3rd ed. Kidlington, Oxford: Academic/Elsevier; 2012. p. 1–1555.
9. Kolk A, Handschel J, Drescher W, Rothamel D, Kloss F, Blessmann M, et al. Current trends and future perspectives of bone substitute materials—from space holders to innovative biomaterials. J Craniomaxillofac Surg. 2012;40(8):706–18.
10. Bhatt RA, Rozental TD. Bone graft substitutes. Hand Clin. 2012;28(4):457–68.
11. Jakoi AM, Iorio JA, Cahill PJ. Autologous bone graft harvesting: a review of grafts and surgical techniques. Musculoskelet Surg. 2015;99(3):171–8.
12. Griffin KS, Davis KM, McKinley TO, Anglen JO, Chu TMG, Boerckel JD, et al. Evolution of bone grafting: bone grafts and tissue engineering strategies for vascularized bone regeneration. In: Clinical reviews in bone and mineral metabolism, vol. 13. Totowa, NJ: Humana Press Inc.; 2015. p. 232–44.
13. Statement of the American Association of Tissue Banks. 2009. Available from: https://www.aatb.org/.
14. Schlegel AK, Donath K. BIO-OSS—a resorbable bone substitute? J Long-Term Eff Med Implants. 1998;8(3–4):201–9.
15. Rombouts C, Jeanneau C, Camilleri J, Laurent P, About I. Characterization and angiogenic potential of xenogeneic bone grafting materials: role of periodontal ligament cells. Dent Mater J. 2016;35(6):900–7.
16. White E, Shors EC. Biomaterial aspects of Interpore-200 porous hydroxyapatite. Dent Clin N Am. 1986;30(1):49–67.
17. Shors EC. Coralline bone graft substitutes. Orthop Clin North Am. 1999;30(4):599–613.
18. Oryan A, Alidadi S, Moshiri A, Maffulli N. Bone regenerative medicine: classic options, novel strategies, and future directions. J Orthop Surg Res. 2014;9:1–27.
19. Ghassemi T, Shahroodi A, Ebrahimzadeh MH, Mousavian A, Movaffagh J, Moradi A. Current concepts in scaffolding for bone tissue engineering. Arch Bone Joint Surg. 2018;6(2):90–9.

20. Pei M, Li JT, Shoukry M, Zhang Y. A review of decellularized stem cell matrix: a novel cell expansion system for cartilage tissue engineering. Eur Cell Mater. 2011;22:333–43.
21. Song R, Murphy M, Li C, Ting K, Soo C, Zheng Z. Current development of biodegradable polymeric materials for biomedical applications. In: Drug design, development and therapy, vol. 12. Albany, NY: Dove Medical Press Ltd.; 2018. p. 3117–45.
22. Zheng YF, Gu XN, Witte F. Biodegradable metals. Mater Sci Eng R Rep. 2014;77:1–34.
23. Kamrani S, Fleck C. Biodegradable magnesium alloys as temporary orthopaedic implants: a review. Biometals. 2019;32(2):185–93.
24. Sidambe AT. Biocompatibility of advanced manufactured titanium implants—a review. Materials. 2014;7(12):8168–88.
25. Niinomi M, Nakai M. Titanium-based biomaterials for preventing stress shielding between implant devices and bone. Int J Biomater. 2011;2011:836587.
26. Takizawa T, Nakayama N, Haniu H, Aoki K, Okamoto M, Nomura H, et al. Titanium fiber plates for bone tissue repair. Adv Mater. 2018;30(4):1703608.
27. Li Y, Yang C, Zhao H, Qu S, Li X, Li Y. New developments of Ti-based alloys for biomedical applications. Materials. 2014;7(3):1709–800.
28. Rodriguez IA, Selders GS, Fetz AE, Gehrmann CJ, Stein SH, et al. Barrier membranes for dental applications: a review and sweet advancement in membrane developments. Mouth Teeth. 2018;2(1):1–9.
29. Cohen R. A porous tantalum trabecular metal: basic science. Am J Orthop (Belle Mead NJ). 2002;31(4):216–7.
30. Clinical evidence reveals unique biological response to Trabecular Metal dental implant. Available from: https://us.dental-tribune.com/news/clinical-evidence-reveals-unique-biological-response-to-trabecular-metal-dental-implant/.
31. Yang K, Ren Y. Nickel-free austenitic stainless steels for medical applications. Sci Technol Adv Mater. 2010;11(1):14105.
32. Zhou FY, Qiu KJ, Bian D, Zheng YF, Lin JP. A Comparative in vitro Study on Biomedical Zr–2.5X (X = Nb, Sn) Alloys. J Mater Sci Technol. 2014;30(4):299–306.
33. Zhang Q, Wu W, Qian C, Xiao W, Zhu H, Guo J, et al. Advanced biomaterials for repairing and reconstruction of mandibular defects. Mater Sci Eng C. 2019;103:109858.
34. Bonda DJ, Manjila S, Selman WR, Dean D. The Recent Revolution in the Design and Manufacture of Cranial Implants: Modern Advancements and Future Directions. Neurosurgery. 2015;77(5):814–824. https://doi.org/10.1227/NEU.0000000000000899.
35. Cionca N, Hashim D, Mombelli A. Zirconia dental implants: where are we now, and where are we heading? Periodontology 2000. 2017;73(1):241–58.
36. Wang W, Yeung KWK. Bone grafts and biomaterials substitutes for bone defect repair: a review. Bioactive Mater. 2017;2(4):224–47.
37. Thrivikraman G, Athirasala A, Twohig C, Boda SK, Bertassoni LE. Biomaterials for craniofacial bone regeneration. Dent Clin N Am. 2017;61:835–56.
38. Duminis T, Shahid S, Hill RG. Apatite glass-ceramics: a review. Front Mater. 2017;3:59.
39. Owen GR, Dard M, Larjava H. Hydroxyapatite/beta-tricalcium phosphate biphasic ceramics as regenerative material for the repair of complex bone defects. J Biomed Mater Res B. 2018;106:2493–512.
40. Bouler JM, Pilet P, Gauthier O, Verron E. Biphasic calcium phosphate ceramics for bone reconstruction: a review of biological response. Acta Biomater. 2017;53:1–12.
41. Dorozhkin SV. Biocomposites and hybrid biomaterials based on calcium orthophosphates. Biomatter. 2011;1(1):3–56.
42. Butz F, Bächle M, Ofer M, Marquardt K, Kohal RJ. Sinus augmentation with bovine hydroxyapatite/synthetic peptide in a sodium hyaluronate carrier (PepGen P-15 Putty): a clinical investigation of different healing times. Int J Oral Maxillofac Implants. 2011;26(6):1317–23.

43. Dorati R, DeTrizio A, Modena T, Conti B, Benazzo F, Gastaldi G, et al. Biodegradable scaffolds for bone regeneration combined with drug-delivery systems in osteomyelitis therapy. In: Pharmaceuticals, vol. 10. Basel: MDPI AG; 2017.
44. Yang GH, Yeo M, Koo YW, Kim GH. 4D bioprinting: technological advances in biofabrication. In: Macromolecular bioscience, vol. 19. Weinheim: Wiley-VCH Verlag; 2019.
45. BioArchitects receives FDA approval for 3D printed titanium cranial plate. Available from: https://additivemanufacturingtoday.com/bioarchitects-receives-fda-approval-for-3d-printed-titanium-cranial-plate.

Nanobiomaterials: Stem Cell Interaction and Role in Tissue Engineering

Swati Midha, Anjali Chauhan, Deborah Sybil, and R. S. Neelakandan

Abstract The aim of regenerative medicine is to achieve structural and functional rehabilitation of the damaged tissues and organs affected by trauma, age-related, congenital, or disease incurred injuries. In view of the recent findings, the field of nanotechnology has evolved as a promising candidate for providing advanced nano-functional biomaterials with customizable morphologies, properties, and functions that can recapitulate the exact in vivo microenvironment down to the extracellular matrix level that can promote cellular adhesion, proliferation, differentiation, and morphogenesis in a controlled spatiotemporal manner. In this chapter, we intend to summarize the role of nanobiomaterials in the field of tissue engineering and regenerative medicine by elaborating on their properties, biological interaction with stem cells, and applications in musculoskeletal research, particularly in bone and cartilage.

Keywords Scaffolds · Nanotechnology · Tissue regeneration · Stem cells · Nanobiomaterials

1 Introduction

The foremost principle of tissue reconstruction is to replace "like with like." The "gold standard" graft material for lost tissue has been autogenous tissue: skin grafts for burns, muscle grafts for bulk loss, bone for skeletal reconstruction, etc. Autogenous grafting provides the best results but has disadvantages of donor site

S. Midha · A. Chauhan (✉)
Special Centre for Nanoscience, Jawaharlal Nehru University, New Delhi, India

D. Sybil
Faculty of Dentistry, Jamia Millia Islamia, New Delhi, India

R. S. Neelakandan
Meenakshi Ammal Dental College and Research Centre, Chennai, India

R. S. Chaughule, R. Dashaputra (eds.), *Advances in Dental Implantology using Nanomaterials and Allied Technology Applications*,
https://doi.org/10.1007/978-3-030-52207-0_7

morbidity, limited availability, additional surgical time, and post-operative temporary mobility impairment [1]. Allogeneic grafting overcomes the shortcomings associated with autogenous grafts. Allografts are considered to be biocompatible, exhibit good post-operative response, without donor site morbidity [2]. These have the advantage of shorter surgery time, abundant bone supply, and elimination of donor site morbidity but there are risks of infection transmission, immune reaction, and insufficient literature support. Alloplastic grafts and xenografts are limited in use and their clinical success is not adequately supported by literature. These drawbacks have led to the search for better alternatives. Alternatives to autologous graft should satisfy three criteria assured by autogenous grafting: cell laden grafts, production of biological moieties stimulating tissue formation, and stimulation of endogenous tissue-forming cells to migrate into the defect. Unfortunately, none of the currently available grafting alternatives intrinsically satisfy all the above criteria. One of the most promising techniques currently being developed for tissue regeneration is tissue engineering using autogenous cell transplantation. Tissue engineering aims to regenerate damaged and/or lost tissues by integrated use of biomaterials, optimal source of cells along with biological factors, providing new tools for regenerative therapy [3].

2 Tissue Engineering

Two major kinds of cells can be used: undifferentiated mesenchymal stem cells (UMSC) and differentiated precursor cells. Literature suggests that UMSC enhance tissue formation as compared to their differentiated counterparts. So far, bone marrow stem cells have shown undebatable potential in bone regeneration. Their unique properties, such as stemness, multilineage differentiation under different stimuli, and relative cell harvesting density, make them a popular source for cell-based approaches [4]. The various tissue sources of stem cells are listed in Table 1.

Table 1 Various cell sources and scaffolds currently used in tissue engineering

Sources of cells	Scaffolds			
	Natural	Mineral based	Synthetic	Hybrid
Bone marrow Adipose tissue Periosteum Umbilical cord Cancellous bone Dental pulp	Collagen Hyaluronic acid Chitin Chitosan Alginate Agarose Silk	Calcium phosphate Ceramics	Polyglycolic acid Polylactic acid Polydioxanone Polycaprolactone Pluronics (polypropylene + polyethylene)	Polymer with noncrystalline apatite coating

Scaffolds used in tissue engineering must fulfill certain standards like ease of fabrication, ease of cell penetration, proliferation and distribution, ability to vascularize once implanted, ability to maintain mature cell phenotype, appropriate biodegradation, and their ability to get completely replaced by neo-tissue. An ideal scaffold material is the one that resorbs at the same time as the new tissue formation occurs. In cases where resorption occurs too fast, the graft site contracts before new tissue is formed, whereas, if the resorption is too slow, delay in the process of neo-tissue formation occurs [5]. Various scaffolds used in tissue engineering are listed in Table 1.

The role of growth factors in tissue engineered grafts is to provide signals and induct progenitor cells at the defect site. Platelet-rich blood substances which are autologous have shown to provide various growth factors, like platelet-derived growth factor (PDGF), vascular endothelial growth factor (VEGF), transforming growth factor (TGF), insulin-like growth factor (IGF), epithelial growth factor (EGF), and recombinant human basic fibroblast growth factor. Table 2 lists the various growth factors used in bone tissue engineering.

A wide variety of natural and synthetic polymers have been utilized for formation of various human tissues. Among all the available materials, collagen and PGA have been widely tested for most of the tissues regenerated in humans. Natural, synthetic, and electroconductive polymers were used in vivo for neural tissue regeneration but human studies are yet to be conducted. Only collagen among natural polymers has been used in clinical human studies [6]. Autologous scaffolds have the advantage of biocompatibility and minimal tissue reaction but lack structural and mechanical durability. Table 3 enlists the scaffolds utilized in regeneration of various tissues for human application.

3 Nanobiomaterials

As already discussed, tissue engineering (TE) is primarily the study of engineering new tissues and organs in order to replace or regenerate the lost or diseased parts. The three basic components that drive the TE process are cells, scaffolds, and biological milieu. The scaffolds serve as three-dimensional (3D) substrates that facilitate the attachment, growth, proliferation, migration, and differentiation of progenitor cells into desirable lineages. The growth factors or the biological milieu introduced into the scaffolds or the culture media direct the transition of cells

Table 2 Growth factors used in bone tissue engineering

Osteoinductive	Osteoconductive	Osteogenic
Demineralized lyophilized bone Bone morphogenetic protein 2,4,7,9	Lyophilized bone Ceramics Bioglass Coral-derived Polylactic (PLA) and polyglycolic acid (PGA)	Mesenchymal stem cells Marrow Platelet-rich plasma Gene therapy Fibroblast growth factors Platelet-derived growth factors

Table 3 Tissue specific scaffolds

Tissue	Scaffolds utilized
Cardiac tissue	Polyglycolic acid (PGA), poly-L-lactic acid (PLLA), poly (lactic-co-glycolic acid (PLGA), polyurethane [7]
Liver tissue	Alginate beads encapsulating inducible pluripotent stem cells encapsulated with human hepatic stellate cells, synthetic polymers (polylactide-co-glycolide, polyethylene glycol (PEG), and polycaprolactone), and naturally derived hydrogels (alginates, celluloses, polyethylene) [8]
Skin	Human dermal fibroblasts, foreskin-derived keratinocytes, keratinocyte stem cells, hair follicle stem cells, angiogenic endothelial progenitor cells, bone marrow-derived mesenchymal stem cells, and adipose tissue-derived mesenchymal stem cells [9]
Cartilage	Hydrogel scaffold, solid scaffolds (collagen sponge, decellularized cartilage, small intestinal mucosa), PGA, PEG, hyaluronic acid, chitosan, cellulose [10, 11]
Bone	Hydroxyapatite, PLGA, calcium phosphate, PLA, gelatine, chitosan, collagen, PLLA, hydrogels [12]
Pancreatic tissue	Collagen, gelatin, fibrin, agarose, alginate, silk, PLA, PGA, PLGA copolymers, polycaprolactone [13]
Vascular tissue	Polyethylene terephthalate (PTFE), PGA, polycaprolactone, PLLA, decellularized xenogenic tissue [6]
Neural tissue	Natural polymers: Collagen, alginate, chitosan, silk, elastin, hyaluronic acid, keratin Synthetic polymers: PLA, PGA, PGLA, PEG, poly(2-hydroxyethylmethacrylate) Electrically conductive polymers: Polypyrrole in combination with other biodegradable synthetic polymers, polyaniline, poly(3,4-ethylenedioxythiopene) (PEDOT), indium phosphide nanowire scaffold Carbon-based nanomaterials: Graphene, carbon nanotubes [14]

towards mature and functional tissue and organs that are capable of implantation in the body to perform the necessary functions. Despite extensive research over the past several decades, developing clinically conformant and functionally stable TE products is still a huge challenge. Mimicking the natural properties of the biological extracellular matrix (ECM) in terms of structure and function requires nano-level precision in the design and fabrication of TE scaffolds. Nanotechnology has the potential to solve this problem by engineering customized nanoparticles and their integration with TE systems.

So far, nanoparticles have found numerous applications in the biomedical field, including bioimaging, drug delivery, vaccine adjuvants, biosensors, photothermal ablation of cells, and gene delivery, with TE being the most recent one. With this wide applicability, nanomaterials have proven therapeutic potential for the treatment of diabetes, magnetic hyperthermia for cancer therapy, inflammation, infection, and so on. The nano-dimensional structure of nanomaterials renders them with unique physico-chemical characteristics, making them promising candidates for a wide range of such applications. The first and foremost is the biomimetic property of nanoparticles with the native nanoscale ECM components of tissues, making them promising candidates for TE applications. The small size and corresponding large surface area to volume ratio, comparable to the small biomolecules, offers

another significant advantage to nanoparticles in TE. This makes them easily diffusible across membranes and barriers in the body and uptake by cells. They are also tunable in terms of shape, size, and composition to suit the target application. Additionally, limitations of biomolecule reagents such as low solubility, high expenses, and short half-life (of growth factors, drugs, etc.) have further provoked investigations around the use of nanoparticles as most suitable candidates for drug delivery applications.

Taking advantage of their similarity to natural ECM components, scientists are extensively exploring the integration of nanoparticles to TE scaffolds. Several studies have reportedly conjugated nanoparticles of different compositions either inside the scaffolds as a part of the synthesis process or coated them onto the surface of the scaffolds in order to improve their mechanical and/or biological responses. Among these, the antimicrobial role of silver, conduction of gold nanoparticles, fluorescence of quantum dots, and electromechanical properties of carbon nanotubes (CNTs) and graphene oxides are most popular. In addition, several nanoparticles when integrated within the 3D scaffolds lead to guided cellular responses by regulating the shape and morphology of cultured cells, provide mechano-transductional cues, facilitate improved interaction with the biological fluids, and lead to guided differentiation of cell laden constructs into functional 3D tissues. The physical and chemical properties of NPs based on metal oxides, such as the shape, hydrodynamic size, surface roughness, and zeta potential, dictate their interaction with biological systems.

Here we give an overview of the different nanoparticles used for a range of TE applications. Their applications are mainly an outcome of the specific intrinsic properties of each of the nanomaterials that tends to dictate their unique functions.

3.1 Desirable Properties of Nanoparticles

Along with nanoparticles, other products of nanotechnology that have profound applications in TE for modulating cell behavior include nanofibers and nanopatterns. Other uses include, but are not limited to, their therapeutic potential and contrasting agent property, incorporation in novel biomaterials (either in bulk material or as surface coating) with precise spatiotemporal control, and controlled release as bioactive agents for drug delivery, especially directing growth factors to regulate stem cell fate, regulating mechano-transductional behavior of scaffolds to direct stem cell fate and morphogenesis, and encompassing superior mechanical strength to the scaffolds for TE applications, along with enhancing biocompatibility. Some of the applications are discussed below.

(a) *Improving cellular responses*: Nanoparticles, both inorganic and living systems (like viruses), fall under this category. Gold nanoparticles (AuNPs) of two different dimensions (4 and 40 nm) were compared in terms of the differentiation rate of human bone marrow stem cells (hBM-MSCs) [15]. The smaller sized AuNPs promoted adipogenic lineage in seeded hBM-MSCs, while suppressing osteogenic differentiation which is attributed to ROS production in AuNPs,

albeit only in smaller size. TiO_2 nanotubes with slightly higher dimensions (70 nm) were found to be ideal for osteogenic induction of hASCs exploiting epigenetic mechanisms for stem cell modulation. The process was mediated by increased methylation in the promoter regions of two osteo-specific genes, OCN and RUNX2 [16], along with inhibition of demethylase retinoblastoma binding protein 2. TiO_2 nanotubes (15–30 nm) and associated modifications (TiO_2–NH_2, TiO_2–COOH, and TiO_2–PEG) [17] promote high cell adhesion by increased production of focal adhesion kinase (FAK), which in turn increases osteogenic differentiation of seeded BM-MSCs [18], hASCs [16], and AD-MSCs [19]. Many plants and phage-based viral nanoparticles like unmodified TMV nanoparticles can trigger osteogenic commitment in stem cells, drawback being their lesser affinity towards mammalian cells [20]. TMV nanoparticles coupled with azide-derivatized Arg-Gly-Asp-(RGD) sequence with tyrosine residues decorated on the scaffold increased cell adhesion on material surface. With added advantage of economic viability, inability to infect mammalian cells, tunable geometry and chemistry, and uniform sizes, plant viral nanoparticles have seen an upsurge in biomedical applications.

(b) *Improving mechanical properties*: Scaffolds either in the form of nanoparticle-embedded polymers (hydrogels, electrospun fibers) or nanoparticle reinforcements or surface coatings have been implemented in TE. Surface modification of a 3D porous poly(lactic acid) (PLA) scaffold was carried out using hydroxyapatite nanoparticles (nHA) by ultrasonication to fabricate nHA-modified PLA/HA scaffold. Strong interfacial adhesion occurring between the nHA and the PLA matrix resulted in ~3 times higher compressive modulus and compressive strength and hydrophilicity in the PLA/HA scaffolds than PLA scaffolds alone, resulting in improved cytocompatibility of cultured mouse embryonic osteoblasts cells (MC3T3-E1) [21]. In another study, nHA loaded bio-nanocomposites were developed with various weight fractions of copper oxide nanoparticles (CuONPs), coated with gelatin-coated ibuprofen [22]. The mechanical properties including fracture toughness (0.65–0.80 MPa $m^{1/2}$), compressive strength (1.25–0.90 MPa), and electrical conductivity (2–3 eV) of nHA-CuO composites corresponded to the weight fractions of the CuO NPs added.

(c) *Imparting Antimicrobial behavior*: Nanoparticles present a suitable alternative to antimicrobial agents, especially oxides of silver (Ag), copper (Cu), and titanium (Ti). Apart from antimicrobial activity, their applications further extend towards the food industry, water purification, and textile [23]. In terms of antimicrobial properties, AgNPs are a safe choice with unprecedented literature available [24]. The NPs, typically ranging from 1 to 10 nm, get attached to the cell membrane compromising the permeability and respiratory functions, followed by penetration inside the bacteria and introducing damage by releasing silver ions. The dimensions of the Ag NPs are critical determinants in the target population, i.e., gram-positive or gram-negative bacteria [25]. Katas et al. [26] proposed a simple, cost-effective, and environment-friendly method of producing spherical AuNPs in the range of 49–82 nm with effective antibacterial properties biosynthesized from *Lignosus rhinocerotis sclerotial* extract (LRE) and

chitosan [27]. However, in-depth research is needed in the area in light of recent findings that have raised concerns about their possible toxicity in humans, demanding more background search on nanotoxicology.

(d) *Electrical conductivity*: Incorporation of nanoparticles that impart electrical conductivity to scaffolds can be highly beneficial to cardiac tissues such as in the treatment of myocardial infarction. Soft hydrogels such as fibrous decellularized matrices incorporated with AuNPs exhibited improved morphology of cardiac cells, striation behavior, and increased expression of electrical coupling proteins [28]. Bone scaffolds have been formulated with electrical conductivity to accelerate the behavior of MSCs towards osteogenic lineage.

(e) *Gene delivery*: Therapeutic usage of nucleic acids or oligonucleotides for disease treatment is restricted due to their low cell transfection efficiency, poor permeability of the plasma membrane, and relatively rapid degradation in vivo, hence requiring non-viral strategies. Conjugating magnetic nanoparticles with gene vectors enhanced the process of gene transfer under the influence of a magnetic field [29]. For instance, peptide-conjugated iron oxide (Fe_3O_4) nanoparticles reportedly exhibited improved efficiency of cellular uptake in lung cancer cells after activation, under the effect of an alternate magnetic field [30]. A recent application of nanoparticles in gene delivery is the use of cell-penetrating peptides (CPPs, ~30 amino acids long) as non-viral vectors. CPPs form stable complexes with oligonucleotides, can carry multiple peptides, facilitate delivery of gene therapeutic agents, and are able to translocate via cellular plasma membranes. Fe_3O_4 NPs (6.4 nm in dimensions) were able to form stable complex with CPPs and showed superior transfection efficiency (>5 fold) than commercial vector called Lipofectamine™2000 [31].

(f) *Constructing 3D tissues*: Taking cues from the nanoscale dimensions of tissue ECM, nanotechnology has profound applications across TE field. Recent literature has reported manipulation and control over cellular functions such as cell adhesion, migration, and morphogenesis using nanoscale materials. Several nanomaterials have been fabricated into 3D structures and used as TE constructs for skin, bone, cartilage, and muscles. Additionally, MNPs due to their exceptional properties and dimensions (up to 300 nm) have been found to support thermal fluctuations in biological microenvironments. Magnetic labeling of cells using MNPs renders precise control over cell functions and movements by application of an external magnetic field for guided organ regeneration, a process often referred to as magnetic force-based tissue engineering. Table 4 shows various types of nanomaterials and their potential applications in TE.

3.2 Application of Nanomaterials in TE

It is well known that the need for tissue regeneration and organ transplantation is increasing due to limited donor availability. In order to compensate for this need, organ-assisted medical devices that mimic the functions of organs have been

Table 4 Nanobiomaterials and their potential applications in TE

Nanomaterials	Applications	References
Gold nanorods	Chemical and biological sensing resolution	[36]
Gold nanowires	Alginate scaffold for cardiac patches	[37]
Silver nanoparticles	Wound healing, enhanced antibacterial activity	[38]
Carbon nanotubes (CNT)	Coating over bone scaffolds for improved mechanical strength	[39]
CNT	Neural tissue regeneration to promote growth, cell differentiation, cell attachment, long-term survival	[40, 41]
Alumina and titania nanopowder	Bone regeneration for enhanced osteoblast adhesion	[42]
Nanocrystalline hydroxyapatite (HA) in PLLA	Osteoblast growth and mineralization	[43]

explored. Nanomaterial-based fabricated systems is one of the potential candidates that mimics the indigenous tissue constituents that can effectively help in replicating in vitro 3D models as well as successful biomedical devices for in vivo testing applications.

3.2.1 Bone TE

At the level of micrometer scale, bone has an inner spongy architecture possessing high porosity with an outer layer of lamellar bone comprising compact cylindrical osteons. At the nanometer scale, bone has ordered and aligned pattern of collagen fibrils and hydroxyapatite. In the musculoskeletal system, various tissues, which fall under the category of soft and hard tissues, are connected to one another [32]. Therefore, the structure and physico-chemical properties of a scaffold are crucial to consider when fabricating a substitute for composite tissues, like osteochondral grafts. Conventional approaches for the fabrication of porous composites includes freeze-drying and freeze-gelation methods. The technique has been used to develop porous chitosan-gelatin composites, in previous studies. Both methods have demonstrated remarkable biocompatibility, in terms of the attachment, long-term viability, and differentiation of several cell types, such as nucleus pulposus cells of the human intervertebral disk [33].

3.2.2 Cartilage TE

Cartilage, at the ultrastructural level, comprises a dense ECM network of elastin fibers, collagen type II, and proteoglycans. Typically, cartilage is avascularized, porous, non-homogeneous, and viscoelastic tissue with embedded chondrocytes [34]. Synthesis methods have been employed for the generation of materials for cartilage tissue engineering, such as rapid prototyping, micromachining, electros-

pinning, photolithography, fiber bonding, electrostatic spray deposition, plasma deposition, and molecular self-assembly, with varying degrees of success [35].

3.3 Nanomaterials and Stem Cell Interaction

Stem cells are pluripotent cells having an inherent capacity of self-renewal and differentiation into multiple cell lineages [44]. Depending upon the source, stem cells are primarily classified into three categories: embryonic stem cells (ESCs), adult stem cells (ASCs), and induced pluripotent stem cells (iPSCs). ESCs, harvested from the inner mass of the blastocyst, possess unlimited potential of self-renewal and hence ideal for regenerative medicine [45]. ASCs have self-renewal capacity, but limited differentiation potential, and are found throughout the body post-development [46]. However, use of ESCs is associated with ethical problems. Another type of stem cells called iPSCs were produced by inducing programming in somatic cells. iPSCs can be generated using different transcription factors and growth factors [47]. In the present day, nanomaterials are extensively used in the induction of cellular programming. However, generating iPSCs are associated with many challenges, which include but are not limited to controlled self-renewal capacity, rapid proliferation, and precisely regulated differentiation.

Over the past few decades, a series of multifunctional nanomaterials have been developed and investigated for stem cell-based therapy applications. However, most studies have focused on the fabrication of novel nanomaterials for therapy and imaging [48, 49], but the underlying mechanism of interaction between nanomaterials and stem cells is not well understood. Due to smaller size and bioactive characteristics, nanomaterials have the potential to affect the stem cell functions in the absence of inductive agents [46]. For instance, aqueous suspension of nanoparticles (silicate nanoparticles, CNTs, and AuNPs) has been reported to promote the differentiation of mesenchymal stem cells (MSCs) towards osteogenic lineage [50, 51]. Table 5 illustrates the nanomaterial-mediated stem cell differentiation. Different nanomaterials trigger different signaling pathways for differentiation of stem cells. Hence, it is very crucial to investigate the underlying mechanisms involved in the interaction between the stem cells and nanomaterials, specifically the differentiation capability of the cells influenced by nanomaterials.

Cell membrane plays a pivotal role in the interaction of nanoparticles. Nanoparticles can easily cross the cell membranes through diffusion/receptor-mediated endocytosis and be distributed in the cytoplasm, endosomes, or lysosomes, thus affecting certain signaling pathways responsible for induction or inhibition of cellular differentiation [64]. Receptor-mediated endocytosis includes clathrin-mediated, caveolin-mediated endocytosis and micropinocytosis, and clathrin and caveolin independent endocytosis [65, 66]. Internalization of nanoparticles and their possible mode of mechanism of differentiation are significantly affected by the physico-chemical properties of nanoparticles, such as size, shape, hydrophobicity, composition, and surface chemistry of nanoparticles [46].

Table 5 Nanobiomaterial-based stem cell differentiation

Category	Nanomaterials used	Cell type used	Differentiation specification (Osteogenic differentiation: OD, adipogenic: AD, chondrogenic: CD, neurogenic: ND)	References
Polymeric	PLGA-BSA	MSCs	OD preferred AD was impaired	[51]
Ceramic	HAP NPs (20 nm)	MSCs, ADSCs	OD	[49]
Ceramic	Nanosilicates	MSCs	OD	[52]
Carbon	SWCNTs	MSCs	OD, AD, CD	[53]
Carbon	SWCNTs	MSCs	ND	[54]
Carbon	MWCNTs	PC12	AD preferred Inhibited OD	[55]
Carbon	rGO nanosheets	MSCs	OD	[56]
Metal/ metal oxide	Citrate-AuNPs	Human fetal neural stem cells (hfNSCs)	OD preferred Inhibited AD	[57]
Metal/ metal oxide	Chitosan-AuNPs	MSCs	OD	[58]
Metal/ metal oxide	BSA-AuNPs	MSCs	OD	[59]
Metal/ metal oxide	BSA coated gold nanorods (70 nm)	MSCs	OD	[59]
Metal/ metal oxide	PEG-AuNPs (40 nm)	MSCs	OD	[60]
Metal/ metal oxide	PEG-AuNPs (4 nm)	MSCs	AD preferred OD inhibited	[60]
Metal/ metal oxide	AgNPs	Urine-derived stem cells	OD	[61]
Metal/ metal oxide	TiO2-NPs	MSCs	ND	[62]
Metal/ metal oxide	CeO_2 NPs (40, 60 nm)	Osteoblasts	Accelerated adipogenic trans-differentiation	[63]

Abbreviations: *SWCNTs* single-walled carbon nanotubes, *MWCNTs* multi-walled carbon nanotubes, *rGO* reduced graphene oxide, *BSA* bovine serum albumin

Nanoparticles in the size range of 20–70 nm are considered optimal for stem cell differentiation due to the size-dependent cellular uptake [60, 67]. Higher amount of cellular uptake has occurred in 30–50 nm size range, while nanoparticles in the range of 50–200 nm have minor effect on cellular uptake [60]. Cellular uptake is also affected by the shape of the nanoparticles [67]. Nanospheres are internalized by the cells at a much higher rate as compared to nanorods or quasi-ellipsoid of similar size [68, 69]. The rate of NP uptake by MSCs decreases as the aspect ratio increases (polar axis: equatorial axis). Furthermore, cellular uptake is also affected by the charge and functional groups present on the surface of nanoparticles. Positively charged nanoparticles showed higher rate of internalization and higher cytotoxicity. Besides these factors, hydrophobicity and the mechanical properties of nanoparti-

cles could also affect the stem cell behavior [70]. The less stiffer and more hydrophobic nanoparticles have higher cellular uptake. The hydrophobic surface of the nanoparticle plays a critical role in modulating their interaction with the cellular microenvironment, including proteins, lipid membranes, and intracellular uptake rate. Research has shown that hydrophobic nanoparticles, synthesized from poly(*n*-butyl methacrylate) (PBMA), poly(hexyl methacrylate) (PHMA), and poly(lauryl methacrylate) (PLMA), have higher rate of cellular uptake as compared to the hydrophilic nanoparticles of poly(methyl methacrylate) (PMMA), poly(propyl methacrylate) (PPMA), and poly(stearyl methacrylate) (PSMA) nature [70]. However, the underlying mechanism responsible for the enhanced cellular uptake by such less stiff nanoparticles is still unclear. One possible explanation could be that the softer nanoparticles deform easily to enable cellular interactions; however, exact mechanism remains unclear.

In recent years, studies have discussed about the effect of nanomaterials on the differentiation capacity of stem cells [46]. Indeed, nanomaterials have been characterized as a new set of differentiation activators which operate via several pathways, with oxidative stress being one of them [71]. Reactive oxygen species (ROS) is a common by-product of nanomaterial exposure to cells. Recent studies have shown that ROS significantly influenced the cell differentiation process. Research by Su et al. showed that ROS-mediated p38/MAPK-dependent pathway played a key role in the differentiation of vascular smooth muscle cells [72]. In contrast, another study by Mody et al. demonstrated the differentiation of bone pre-osteoblast cells (MC3T3-E1) was inhibited by ROS [73]. These studies suggest that the modulation in the levels of ROS generation are general regulators for stem cell differentiation mechanism, nevertheless, lineage-specific differentiation needs to be further explored. For instance, high ROS level will propel the cell into adipogenesis lineage while impede osteogenesis of stem cells [59].

Mechanical stress is another factor that can play an important role in modulating the differentiation potential of stem cells. The mechanical properties of the cell and cytoskeleton may change due to intracellular accumulation of nanomaterials [74]. Higher mechanical properties have previously been related to increased osteogenic differentiation while inhibiting adipogenic differentiation in progenitor cells [75]. The accumulated intracellular nanomaterials will influence the assembly of cytoskeletons and increase the Young's modulus of stem cells, thereby enhancing the osteogenic differentiation [59].

Nanomaterials interact with cell membrane receptors and are internalized by the cells through receptor-mediated endocytosis. This is followed by packing of these nanomaterials into vesicles and their transportion inside the cells. This is a dynamic process as the nanomaterials are in constant motion inside the cells and interact with the intracellular microenvironment. Nanomaterials interact with various biomolecules that may trigger intracellular signaling pathways to induce the specific differentiation of stem cells [76]. Additionally, protein adsorption on the surface of nanomaterials and cytotoxic behavior induced by the concentration, shape, and size of nanomaterials may play a significant role in influencing the final fate of the stem cells. Extensive research is required to recapitulate conditions similar to in vivo

microenvironment using nanomaterials for promoting stem cell-specific differentiation to cater to individual tissues or organs.

4 Conclusion

Taken together, the field of nanotechnology has provided a better modality of fabricating biomimetic constructs with more satisfactory reconstruction of patient tissues and organs, both esthetically and in terms of functional rehabilitation. The stem cells of the host tissue or autologous cells incorporated along with the constructs presumably help in a more rapid and effective regeneration process by enhanced cell-matrix interactions. However there is enormous scope for further progress in tissue engineering and regenerative medicine on the design and manufacturing of traditional biomaterials to deliver more patient-specific and patient-friendly approaches. The boost in nanotechnology should ensure precisely engineered nanoarchitectures more closely replicating the structural, physico-mechanical, and biological aspects of human tissues. In parallel, ongoing research is focussed towards investigating ex vivo methods to design nano surfaces that can more efficiently promote biocompatibility for cell and tissue integration. The conjugation of AuNPs for enhanced cellular adhesion and electrical conductivity in cardiac tissues, protein conjugated Fe_3O_4 nanoparticles to increase cellular uptake or addition of nHA to polymers to increase the mechanical properties of orthopedic implants will help in guided tissue responses by activating signaling cascades that direct cellular interactions in situ, are some specific examples highlighting the role of nanomaterials. In addition to this, bringing together teams of biomedical scientists, engineers, clinicians, and focussed patient groups is extremely critical for efficient development of biomedical materials to push them closer towards commercialization.

Acknowledgment Swati Midha is supported by Department of Science and Technology (DST) Inspire Faculty Grant (DST/INSPIRE/04/2017/000645).

References

1. Ochs MW. Alveolar cleft bone grafting (part II): secondary bone grafting. J Oral Maxillofac Surg. 1996;54:83–8.
2. Aghaloo TL, Moy PK. Which hard tissue augmentation techniques are the most successful in furnishing bony support for implant placement? Int J Oral Maxillofac Implants. 2007;22(Suppl):49–70.
3. Strietzel FP. Tissue-engineered bone for lateral alveolar ridge augmentation: a case report. Int J Oral Maxillofac Implants. 2006;21:131–5.
4. Lieberman JR, Daluiski A, Einhorn TA. The role of growth factors in the repair of bone. Biology and clinical applications. J Bone Joint Surg Am. 2002;84-A:1032–44.
5. Pradel W, Tausche E, Gollogly J, Lauer G. Spontaneous tooth eruption after alveolar cleft osteoplasty using tissue-engineered bone: a case report. Oral Surg Oral Med Oral Pathol Oral Radiol Endod. 2008;105:440–4.

6. Song HHG, Rumma RT, Ozaki CK, Edelman ER, Chen CS. Vascular tissue engineering: progress, challenges, and clinical promise. Cell Stem Cell. 2018;22(3):340–54.
7. Rodrigues ICP, Kaasi A, Filho RM, Jardini AL, Gabriel LP. Cardiac tissue engineering: current state-of-the-art materials, cells and tissue formation. Einstein (Sao Paulo). 2018;16(3):eRB4538.
8. Mazza G, Al-Akkad W, Rombouts K, Pinzani M. Liver tissue engineering: from implantable tissue to whole organ engineering. Hepatol Commun. 2018;2(2):131–41.
9. Vig K, Chaudhari A, Tripathi S, Dixit S, Sahu R, Pillai S, Dennis VA, Singh SR. Advances in skin regeneration using tissue engineering. Int J Mol Sci. 2017;18(4):789.
10. Liu Y, Zhou G, Cao Y. Recent progress in cartilage tissue engineering—our experience and future directions. Engineering. 2017;3(1):28–35.
11. Vinatier C, Guicheux J. Cartilage tissue engineering: from biomaterials and stem cells to osteoarthritis treatments. Ann Phys Rehabil Med. 2016;59(3):139–44.
12. Amini AR, Laurencin CT, Nukavarapu SP. Bone tissue engineering: recent advances and challenges. Crit Rev Biomed Eng. 2012;40(5):363–408.
13. Kumar N, Joisher H, Ganguly A. Polymeric scaffolds for pancreatic tissue engineering: a review. Rev Diabet Stud. 2017;14(4):334–53.
14. Boni R, Ali A, Shavandi A, Clarkson AN. Current and novel polymeric biomaterials for neural tissue engineering. J Biomed Sci. 2018;25(1):90.
15. Dayem AA, Choi HY, Yang GM, Kim K, Saha SK, Kim JH, et al. The potential of nanoparticles in stem cell differentiation and further therapeutic applications. Biotechnol J. 2016;11:1550–60.
16. Lv L, Liu Y, Zhang P, Zhang X, Liu J, Chen T, et al. The nanoscale geometry of TiO2 nanotubes influences the osteogenic differentiation of human adipose-derived stem cells by modulating H3K4 trimethylation. Biomaterials. 2015;39:193–205.
17. Shrestha S, Mao Z, Fedutik Y, Gao C. Influence of titanium dioxide nanorods with different surface chemistry on the differentiation of rat bone marrow mesenchymal stem cells. J Mater Chem B. 2016;4:6955–66.
18. Vercellino M, Ceccarelli G, Cristofaro F, Balli M, Bertoglio F, Bruni G, et al. Nanostructured TiO2 surfaces promote human bone marrow mesenchymal stem cells differentiation to osteoblasts. Nanomaterials. 2016;6:124.
19. Pozio A, Palmieri A, Girardi A, Cura F, Carinci F. Titanium nanotubes stimulate osteoblast differentiation of stem cells from pulp and adipose tissue. Dent Res J (Isfahan). 2012;9:S169.
20. Raja IS, Kim C, Song S-J, Shin YC, Kang MS, Hyon S-H, et al. Virus-incorporated biomimetic nanocomposites for tissue regeneration. Nanomaterials. 2019;9:1014.
21. Si J, Lin J, Su C, Yu S, Cui Z, Wang Q, et al. Ultrasonication-induced modification of hydroxyapatite nanoparticles onto a 3D porous poly (lactic acid) scaffold with improved mechanical properties and biocompatibility. Macromol Mater Eng. 2019;304:1900081.
22. Sahmani S, Shahali M, Nejad MG, Khandan A, Aghdam M, Saber-Samandari S. Effect of copper oxide nanoparticles on electrical conductivity and cell viability of calcium phosphate scaffolds with improved mechanical strength for bone tissue engineering. Eur Phys J Plus. 2019;134:7.
23. Vega-Jiménez AL, Vázquez-Olmos AR, Acosta-Gío E, Álvarez-Pérez MA. In vitro antimicrobial activity evaluation of metal oxide nanoparticles. In: Nanoemulsions-properties, fabrications and applications. London: IntechOpen; 2019.
24. Morones JR, Elechiguerra JL, Camacho A, Holt K, Kouri JB, Ramírez JT, et al. The bactericidal effect of silver nanoparticles. Nanotechnology. 2005;16:2346.
25. Pandey A, Midha S, Sharma RK, Maurya R, Nigam VK, Ghosh S, et al. Antioxidant and antibacterial hydroxyapatite-based biocomposite for orthopedic applications. Mater Sci Eng C. 2018;88:13–24.
26. Gurunathan S, Han JW, Kwon D-N, Kim J-H. Enhanced antibacterial and anti-biofilm activities of silver nanoparticles against Gram-negative and Gram-positive bacteria. Nanoscale Res Lett. 2014;9:373.

27. Katas H, Lim CS, Azlan AYHN, Buang F, Busra MFM. Antibacterial activity of biosynthesized gold nanoparticles using biomolecules from Lignosus rhinocerotis and chitosan. Saudi Pharm J. 2019;27:283–92.
28. Shevach M, Fleischer S, Shapira A, Dvir T. Gold nanoparticle-decellularized matrix hybrids for cardiac tissue engineering. Nano Lett. 2014;14:5792–6.
29. Plank C, Anton M, Rudolph C, Rosenecker J, Krötz F. Enhancing and targeting nucleic acid delivery by magnetic force. Expert Opin Biol Ther. 2003;3:745–58.
30. Hauser AK, Anderson KW, Hilt JZ. Peptide conjugated magnetic nanoparticles for magnetically mediated energy delivery to lung cancer cells. Nanomedicine. 2016;11:1769–85.
31. Dowaidar M, Abdelhamid HN, Hällbrink M, Freimann K, Kurrikoff K, Zou X, et al. Magnetic nanoparticle assisted self-assembly of cell penetrating peptides-oligonucleotides complexes for gene delivery. Sci Rep. 2017;7:9159.
32. Limongi T, Tirinato L, Pagliari F, Giugni A, Allione M, Perozziello G, et al. Fabrication and applications of micro/nanostructured devices for tissue engineering. Nano-Micro Lett. 2016;9:1.
33. Karimi Z, Ghorbani M, Hashemibeni B, Bahramian H. Evaluation of the proliferation and viability rates of nucleus pulposus cells of human intervertebral disk in fabricated chitosan-gelatin scaffolds by freeze drying and freeze gelation methods. Adv Biomed Res. 2015;4:251.
34. Camarero-Espinosa S, Rothen-Rutishauser B, Foster EJ, Weder C. Articular cartilage: from formation to tissue engineering. Biomater Sci. 2016;4:734–67.
35. Santo VE, Gomes ME, Mano JF, Reis RL. From nano-to macro-scale: nanotechnology approaches for spatially controlled delivery of bioactive factors for bone and cartilage engineering. Nanomedicine. 2012;7:1045–66.
36. Lee K-S, El-Sayed MA. Gold and silver nanoparticles in sensing and imaging: sensitivity of plasmon response to size, shape, and metal composition. J Phys Chem B. 2006;110:19220–5.
37. Dvir T, Timko BP, Brigham MD, Naik SR, Karajanagi SS, Levy O, et al. Nanowired three-dimensional cardiac patches. Nat Nanotechnol. 2011;6:720–5.
38. Rujitanaroj P-O, Pimpha N, Supaphol P. Wound-dressing materials with antibacterial activity from electrospun gelatin fiber mats containing silver nanoparticles. Polymer. 2008;49:4723–32.
39. Yu MF, Files BS, Arepalli S, Ruoff RS. Tensile loading of ropes of single wall carbon nanotubes and their mechanical properties. Phys Rev Lett. 2000;84:5552–5.
40. Mattson MP, Haddon RC, Rao AM. Molecular functionalization of carbon nanotubes and use as substrates for neuronal growth. J Mol Neurosci. 2000;14:175–82.
41. Hu H, Ni Y, Montana V, Haddon RC, Parpura V. Chemically functionalized carbon nanotubes as substrates for neuronal growth. Nano Lett. 2004;4:507–11.
42. Webster TJ, Siegel RW, Bizios R. Osteoblast adhesion on nanophase ceramics. Biomaterials. 1999;20:1221–7.
43. Kim SS, Park MS, Gwak SJ, Choi CY, Kim BS. Accelerated bonelike apatite growth on porous polymer/ceramic composite scaffolds in vitro. Tissue Eng. 2006;12:2997–3006.
44. Watt FM, Driskell RR. The therapeutic potential of stem cells. Philos Trans R Soc Lond B Biol Sci. 2010;365:155–63.
45. Tesar PJ, Chenoweth JG, Brook FA, Davies TJ, Evans EP, Mack DL, et al. New cell lines from mouse epiblast share defining features with human embryonic stem cells. Nature. 2007;448:196–9.
46. Kerativitayanan P, Carrow JK, Gaharwar AK. Nanomaterials for engineering stem cell responses. Adv Healthcare Mater. 2015;4:1600–27.
47. Sapsford KE, Algar WR, Berti L, Gemmill KB, Casey BJ, Oh E, et al. Functionalizing nanoparticles with biological molecules: developing chemistries that facilitate nanotechnology. Chem Rev. 2013;113:1904–2074.
48. Rosi NL, Mirkin CA. Nanostructures in biodiagnostics. Chem Rev. 2005;105:1547–62.
49. Gaharwar AK, Mihaila SM, Swami A, Patel A, Sant S, Reis RL, et al. Bioactive silicate nanoplatelets for osteogenic differentiation of human mesenchymal stem cells. Adv Mater. 2013;25:3329–36.

50. Namgung S, Baik KY, Park J, Hong S. Controlling the growth and differentiation of human mesenchymal stem cells by the arrangement of individual carbon nanotubes. ACS Nano. 2011;5:7383–90.
51. Baglioni P, Carretti E, Chelazzi D. Nanomaterials in art conservation. Nat Nanotechnol. 2015;10:287–90.
52. Kim KJ, Joe YA, Kim MK, Lee SJ, Ryu YH, Cho DW, et al. Silica nanoparticles increase human adipose tissue-derived stem cell proliferation through ERK1/2 activation. Int J Nanomed. 2015;10:2261–72.
53. Tay CY, Gu H, Leong WS, Yu H, Li HQ, Heng BC, et al. Cellular behavior of human mesenchymal stem cells cultured on single-walled carbon nanotube film. Carbon. 2010;48:1095–104.
54. Meng L, Chen R, Jiang A, Wang L, Wang P, Li CZ, et al. Short multiwall carbon nanotubes promote neuronal differentiation of PC12 cells via up-regulation of the neurotrophin signaling pathway. Small. 2013;9:1786–98.
55. Akhavan O, Ghaderi E, Akhavan A. Size-dependent genotoxicity of graphene nanoplatelets in human stem cells. Biomaterials. 2012;33:8017–25.
56. Akhavan O, Ghaderi E, Emamy H, Akhavan F. Genotoxicity of graphene nanoribbons in human mesenchymal stem cells. Carbon. 2013;54:419–31.
57. Choi SY, Song MS, Ryu PD, Lam ATN, Joo S-W, Lee SY. Gold nanoparticles promote osteogenic differentiation in human adipose-derived mesenchymal stem cells through the Wnt/β--catenin signaling pathway. Int J Nanomed. 2015;10:4383.
58. Ko WK, Heo DN, Moon HJ, Lee SJ, Bae MS, Lee JB, et al. The effect of gold nanoparticle size on osteogenic differentiation of adipose-derived stem cells. J Colloid Interface Sci. 2015;438:68–76.
59. Li J, Chen Y, Yang Y, Kawazoe N, Chen G. Sub-10 nm gold nanoparticles promote adipogenesis and inhibit osteogenesis of mesenchymal stem cells. J Mater Chem B. 2017;5:1353–62.
60. Li JJ, Kawazoe N, Chen G. Gold nanoparticles with different charge and moiety induce differential cell response on mesenchymal stem cell osteogenesis. Biomaterials. 2015;54:226–36.
61. Pauksch L, Rohnke M, Schnettler R, Lips KS. Silver nanoparticles do not alter human osteoclastogenesis but induce cellular uptake. Toxicol Rep. 2014;1:900–8.
62. Hou Y, Cai K, Li J, Chen X, Lai M, Hu Y, et al. Effects of titanium nanoparticles on adhesion, migration, proliferation, and differentiation of mesenchymal stem cells. Int J Nanomed. 2013;8:3619.
63. Rocca A, Mattoli V, Mazzolai B, Ciofani G. Cerium oxide nanoparticles inhibit adipogenesis in rat mesenchymal stem cells: potential therapeutic implications. Pharm Res. 2014;31:2952–62.
64. Zhao F, Zhao Y, Liu Y, Chang X, Chen C, Zhao Y. Cellular uptake, intracellular trafficking, and cytotoxicity of nanomaterials. Small. 2011;7:1322–37.
65. Deng J, Zheng H, Zheng X, Yao M, Li Z, Gao C. Gold nanoparticles with surface-anchored chiral poly(acryloyl-L(D)-valine) induce differential response on mesenchymal stem cell osteogenesis. Nano Res. 2016;9:3683–94.
66. Deng J, Yu D, Gao C. Biological identity of nanomaterials: opportunities and challenges. Sci China Chem. 2013;56:1533–41.
67. Li J, Li JEJ, Zhang J, Wang X, Kawazoe N, Chen G. Gold nanoparticle size and shape influence on osteogenesis of mesenchymal stem cells. Nanoscale. 2016;8:7992–8007.
68. Rivera-Gil P, Jimenez de Aberasturi D, Wulf V, Pelaz B, del Pino P, Zhao Y, et al. The challenge to relate the physicochemical properties of colloidal nanoparticles to their cytotoxicity. Acc Chem Res. 2013;46:743–9.
69. Florez L, Herrmann C, Cramer JM, Hauser CP, Koynov K, Landfester K, et al. How shape influences uptake: interactions of anisotropic polymer nanoparticles and human mesenchymal stem cells. Small. 2012;8:2222–30.
70. Lorenz S, Hauser CP, Autenrieth B, Weiss CK, Landfester K, Mailander V. The softer and more hydrophobic the better: influence of the side chain of polymethacrylate nanoparticles for cellular uptake. Macromol Biosci. 2010;10:1034–42.
71. Tsimbouri PM. Adult stem cell responses to nanostimuli. J Funct Biomater. 2015;6:598–622.

72. Su B, Mitra S, Gregg H, Flavahan S, Chotani MA, Clark KR, et al. Redox regulation of vascular smooth muscle cell differentiation. Circ Res. 2001;89:39–46.
73. Mody N, Parhami F, Sarafian TA, Demer LL. Oxidative stress modulates osteoblastic differentiation of vascular and bone cells. Free Radic Biol Med. 2001;31:509–19.
74. Ciofani G, Ricotti L, Canale C, D'Alessandro D, Berrettini S, Mazzolai B, et al. Effects of barium titanate nanoparticles on proliferation and differentiation of rat mesenchymal stem cells. Colloids Surf B Biointerfaces. 2013;102:312–20.
75. Wang X, Hu X, Dulinska-Molak I, Kawazoe N, Yang Y, Chen G. Discriminating the independent influence of cell adhesion and spreading area on stem cell fate determination using micropatterned surfaces. Sci Rep. 2016;6:28708.
76. Li J, Li X, Zhang J, Kawazoe N, Chen G. Induction of chondrogenic differentiation of human mesenchymal stem cells by biomimetic gold nanoparticles with tunable RGD density. Adv Healthcare Mater. 2017;6:1700317.

Polyurethane Foam as a Model to Study Primary Implant Stability: A Series of In Vitro Studies

Margherita Tumedei, Luca Comuzzi, Morena Petrini, Adriano Piattelli, and Giovanna Iezzi

Abstract Primary stability of dental implants is defined as the absence of movement of an implant after surgical insertion. Primary stability is influenced by bone density, bone quality, surgical technique, and implant body geometry. A direct relationship seemed to exist between implant primary stability and bone density. So far, several nondestructive methods have been suggested to evaluate implant stability, such as insertion torque measurement (IT) and resonance frequency analysis (RFA). IT measures the compression induced by implant placement into the surgical site and it determines the primary implant stability, which is considered the most important factor for successful implant treatment. The ISQ values, obtained through the RFA, reflect the micromobility of the implant, which is in turn determined by factors such as bone density, surgical technique, implant design, and healing time. Polyurethane foam has been proposed for in vitro tests to simulate the consistency and the density of the bone. These rigid blocks have been produced as an alternative test medium to human cancellous bone. This material displays mechanical properties in the range of human cancellous bone as described by the ASTM (American Society Testing Materials) F-1839-08 2012 standard. Its features make it an ideal material for comparative testing of different implant materials. The physical features of polyurethane are homogenous throughout their volume, so as to obtain a good standardization of the procedures with the exclusion, then, of factors inherent to anatomical and structural differences of bone. Polyurethane blocks of different densities have been used, e.g., to evaluate the primary stability of different types of implants (cylindrical vs. conical implants), different lengths (short implants vs. standard length implants), and different diameters (narrow, regular, and wide implants).

M. Tumedei (✉) · M. Petrini · A. Piattelli · G. Iezzi
Department of Medical, Oral and Biotechnological Sciences, University of Chieti-Pescara, Chieti, Italy

L. Comuzzi
Private Practice, Conegliano, TV, Italy

R. S. Chaughule, R. Dashaputra (eds.), *Advances in Dental Implantology using Nanomaterials and Allied Technology Applications*,
https://doi.org/10.1007/978-3-030-52207-0_8

Keywords Bone density · Implant stability quotient · Insertion torque · Polyurethane foam blocks · Pull-out torque · Resonance frequency analysis

1 Introduction

Primary dental implant stability (PS) is the absence of implant micromotion immediately after placement, and it has been reported to play a relevant role in osseointegration [1–3]. PS is closely related to the bone quality and quantity, to the implant macrodesign, to the implant length and implant diameter, to the surgery, and to the implant fitting into the site [1–5]. There is also a correlation between bone density and the amount of the bone-to-implant contact (BIC) [1], and between BIC and PS [2]. There are several different techniques to measure bone: Insertion Torque (IT), Removal Torque (RT), and Resonance Frequency Analysis (RFA); this latter technique produces a value called the Implant Stability Quotient (ISQ) [6]. Polyurethane foam has been used, since a few years, as a standard material for instrument testing according to the American Society for Testing and Materials (ASTM F-1839-08) [7]. Polyurethane foam has been extensively used as an alternative material to animal and human cadaver bone for biomechanical tests evaluating, e.g., dental implants, because it shows consistent mechanical characteristics, has features quite similar to bone tissue, is very reliable, easy to use, and does not require a special handling [6, 8, 9]. Moreover, it has constant mechanical characteristics, and it can be used for comparative testing of different types of implants. The structure of polyurethane is homogenous, and with this material it is possible to standardize the study procedures, eliminating the anatomical and structural differences present in animal or human cadaver bone [2, 3]. Different types of solid rigid polyurethane 120 mm × 170 mm × 31 mm foam blocks (SawBones H, Pacific Research Laboratories Inc., Vashon, Washington) with homogeneous densities are present in the market. The densities of polyurethane foam that we have used vary from 10 PCF (pounds per cubic foot) to 20 and 30 PCF. To all these blocks, a 1 mm thin layer of 30 PCF can be added, to simulate cortical bone (Fig. 1).

Fig. 1 Polyurethane blocks in different densities. 10 PCF, similar to D3 bone quality; 20 PCF, corresponding to D2 bone; and 30–40 PCF density, similar to D1 bone

Bone density during insertion of the implants plays a determinant role in the primary stability of dental implants [5, 6], and it could be, then, necessary to try to understand, in a deeper way, the correlations between bone density and primary implant stability so to be able to plan an implant treatment in a proper way [6]. To get mineralized tissues at the interface with the implants there is an absolute need to obtain a primary implant stability, i.e., the initial biomechanical engagement and interlocking between bone and implant must be strong enough to not allow any relative micromovements between these two structures immediately after implant insertion [2–4, 8]. Poor bone density has a negative influence on primary stability [2, 8, 9]. Higher bone quality, on the other hand, has been found to be closely correlated with a higher primary implant stability [1, 3]. The main factors influencing primary stability are, then, the percentage of bone-to-implant contact (BIC) and the compressive stresses at the implant-bone interface [2]. Higher stability values were described in denser bone compared to softer bone [3]. Primary stability is, moreover, related, besides bone quantity and bone quality, to implant macrogeometry and macrodesign (length and diameter) and to the surgery used to prepare the implant insertion sites [1]. A low primary stability has been correlated with a higher risk of implant failure and loss, while, on the contrary, better conditions for the formation of mineralized tissues at the bone–implant interface are realized when there is a high primary stability [1]. Moreover, it must also be stressed that a high level of primary stability is associated, in a positive way, also with secondary implant stability [1]. It is, then, extremely important to be able to assess, in an accurate way, the primary stability of the implants [1]. We have already said that so far, several noninvasive methods have been suggested to evaluate implant stability, such as insertion torque measurement (IT) and resonance frequency analysis (RFA). IT measures the compression produced by the implant during its insertion into the site [9] and is closely correlated to the primary implant stability. RFA is used to follow the progression of implant osseointegration over time.

In the last year, we have performed several in vitro studies, using polyurethane foam, to make an evaluation of the primary implant stability using implants of different lengths, different diameters, and different macrodesigns.

In the following sections, we will report the most relevant features and conclusions of the most important and interesting studies performed.

2 Short (SI) vs. Standard Length (SL) Cone Morse Connection Implants

Short implants (SI) (with a length of less than 8 mm) have been used especially in atrophic alveolar ridges of the posterior jaws [10–12] (Fig. 2).

With SI there is no need of maxillary sinus augmentation procedures, zygomatic implants, guided bone regeneration procedures, onlay grafts, inlay grafts, distraction osteogenesis, and lateralization of the inferior alveolar nerve with no increased morbidity, higher costs, and higher risks of complications [13–18].

Fig. 2 Implant site preparation by the universal test machine. Implants were inserted following a suggested drill protocol. The final insertion torque of the implants into the polyurethane blocks was evaluated

Systematic reviews followed by meta-analyses have shown a similar survival of short and standard length implants, no differences in marginal bone loss (MBL), lower biological complications in SI, good primary stability in SI, but higher mechanical complications in SI [13–18] (Fig. 3).

In the past few years, implants with a reduced length (4, 5, and 6 mm) (Ultrashort or Extrashort Implants) have been used [11, 19] (Fig. 4).

There are also implants with a still reduced length (2.5/3.5 mm) (NanoShort Implants) [20]. SI with a Cone Morse connection and a conical shape (Test Implants: Test Implant A—diameter 5.5 mm and length 6 mm) (Test Implant B—diameter 5.5 mm and length 5 mm) were used for the present in vitro investigation (Fig. 5).

Implants (4 mm diameter and 10 mm length) with a Cone Morse connection and a conical shape were used as Control Implant A and as Control Implants B (Fig. 6).

The conclusions of the present in vitro study, using polyurethane foam sheets, were:

- Implants with a conical shape presented a high stability even in blocks with a low density (10 PCF).
- No differences were found between 5 and 6 mm long implants.
- Very good values of insertion torque and pull-out tests were found in Short Implants in both polyurethane densities.
- The ISQ values of both Short Implants were very high, with a very good clinical sensation of high stability of the implants.
- SL presented slightly lower values of insertion torque and pull-out torque.
- SL presented very high ISQ values.

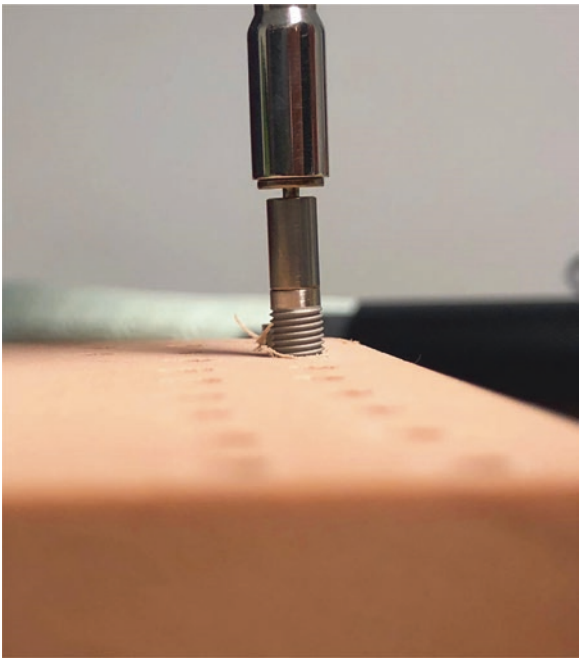

Fig. 3 Polyurethane foam block after drilling protocol. The block densities of polyurethane samples used in the present figure was 10 PCF, similar to D3 bone quality

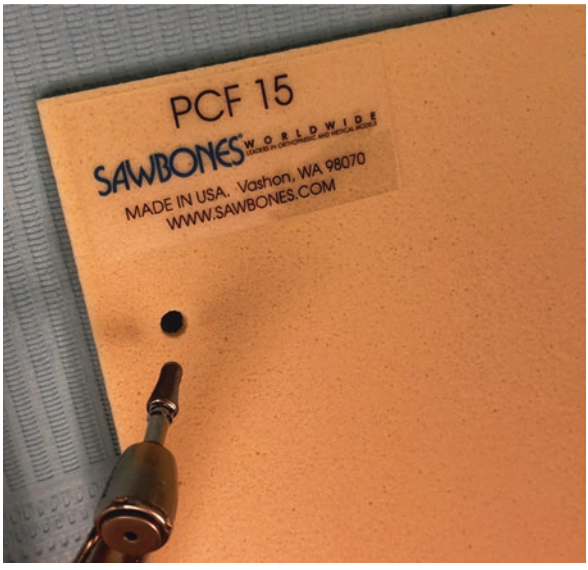

Fig. 4 Details of site preparation of the polyurethane blocks after the drillings protocols

Fig. 5 Implant insertion performed following the protocol of the manufacturer

Fig. 6 Implant insertion. The insertion torque (IT, N cm) peaks indicated the force of the maximum clockwise movement of the dental fixture positioned into the material

Fig. 7 Implants positioned into polyurethane foam blocks in 20 PCF corresponding to D2 bone density

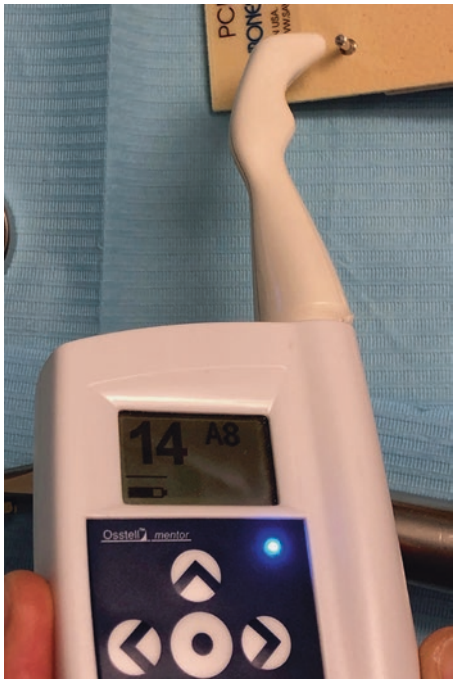

Fig. 8 After the fixture positioning, the primary stability was evaluated using Resonance Frequency Analysis (RFA) values expressed in the implant stability quotient (ISQ) by a hand-screwed Smart-Pegs type 7 for test implants (Osstell Mentor Device, Integration Diagnostic AB, Savadelen, Sweden)

In conclusion, when comparing SI and SL, SI had a similar if not better performance in low-quality polyurethane foam blocks (10–20 PCF), corresponding to D3 and D4 bone (Fig. 7).

2.1 Primary Stability of Dental Implants in Low-Density (10 and 20 PCF) Polyurethane Foam Blocks: Conical vs. Cylindrical Implants

The implant macrodesign, conical or cylindrical, has been reported to play a key role in the implant performance and stability. Implants (4 mm diameter and 10 mm legth) with a Cone Morse connection and a conical shape were used as Test Implants. A cylindrical screw-shaped implant was used as Control Implant: 13 mm length, diameter of the platform 4.1 mm, and body diameter 3.75 (Fig. 8).

In Test implants, the insertion torque was quite low in the 10 PCF blocks (16–28 N cm). Better results were found in the 20 PCF blocks, with a very good stability of the implants. The pull-out values for Test Implants were slightly lower than the insertion torque values. High ISQ values were found in Test Implants (57–80 N cm). Control implants, on the other hand, presented very low insertion torque values (6–12 N cm) in both polyurethane densities (10 and 20 PCF). Also the pull-out values were very low (5–10 N cm). Furthermore, the ISQ values were in the very low range (10–37).

The conclusions of the present study were as follows: implants with a conical shape performed much better, in low-density polyurethane foam blocks, than implants with a cylindrical shape. Cylindrical implants, for the shape and pitch of their threads, are, probably, not indicated in low-quality bone density, such as in the posterior areas of the jaws.

3 Insertion Torque (IT), Pull-Out Torque Values, and Resonance Frequency Analysis (RFA) in NanoShort (2.5/3.5 mm Length) Implants

A marked reduction in the implant length of implants has been reported in recent years, with the use of Extrashort and Ultrashort implants (5–6 mm length) [10–12, 19]. These implants seemed to be able to osseointegrate and to be functionally loaded [19]. Also NanoShort implants with a still reduced implant length (2.5/3.5 mm length) are available in the market. Systematic reviews followed by meta-analyses reported that Short Implants (SI) could be a suitable alternative when compared to more invasive procedures used to treat atrophy of the posterior jaws [10, 12–19] (Fig. 9).

NanoShort implants presented a good primary stability in 20 and 30 PCF densities. They can, then, be used in the posterior regions of the mandible, where the bone quality is good and is similar to 30 PCF polyurethane. Values of PCF 10–20, on the contrary, are comparable to D3 bone type. The present study showed that NanoShort Implants could reach a good stabilization (Fig. 10).

In the case of the NanoShort Implants used in the present study, probably a conical shape would have been better than a cylindrical design, and also a different pitch

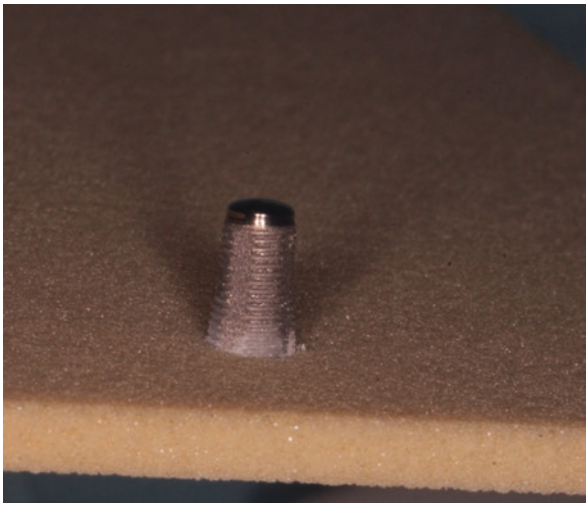

Fig. 9 Primary stability measured using RFA values. The RFA evaluation was performed following two different orientations separated by a 90° angle, and the mean ISQ peaks were calculated

Fig. 10 Implant stability quotient (ISQ) measurement device. The ISQ values ranged from 0 to 100 (measured by a frequency in the range 3500–85,000 Hz), and was classified into Low (less than 60 ISQ), Medium (in the range 60–70 ISQ), and High stability rate (more than 70 ISQ)

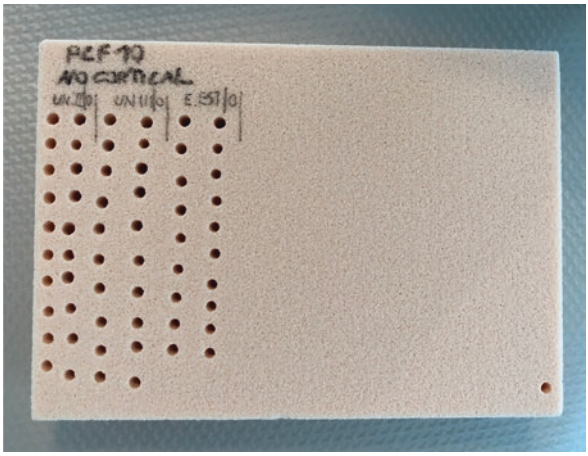

Fig. 11 Detail of the implant preparation quotient

of the threads could have helped to engage better the material. Falco et al. [5] have demonstrated that larger implant threads with a greater pitch could contact more bone trabeculae and better compact the bone debris in a peri-implant location.

In conclusion, NanoShort Implants, evaluated in the present study, showed a good primary stability and could, probably, be used in posterior jaws atrophy, instead of a more complicated vertical ridge augmentation (Fig. 11).

4 Effects of a Self-condenser Dental Implant on Insertion and Pull-Out Torque Values

The dental implant self-condensing design used in this in vitro study showed a high level of stability in all experimental conditions, and could represent a useful tool for a one-stage surgical approach in the presence of limited residual native bone in alternative to a delayed approach (Fig. 12).

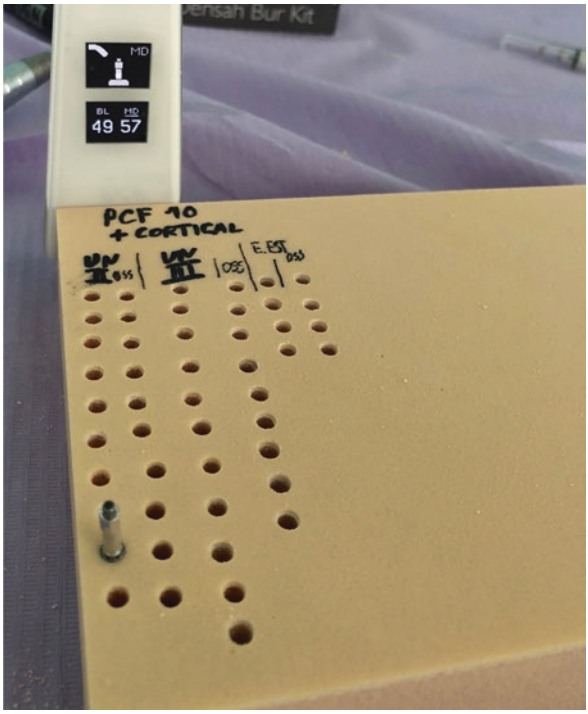

Fig. 12 Details of the back view of the positioned implant

5 Discussion and Conclusions

The primary stability of the implant, the bone tissue quantity and quality, the implant macro- and microdesign, and the surface characteristics are all necessary factors for the successful osseointegration of implants. Achieving and maintaining adequate implant stability are key prerequisites for the long-term outcome of osseointegrated implants. Primary stability is mechanical stability in the bone tissue after dental implant placement with an absence of mobility of the implant. Primary stability derives from the mechanical engagement of the device with the cortical bone. This interface is determined by the surgical technique and by the size of the implant (length and diameter, design and macrotopography). Bone density has been reported to be a critical factor for implant primary stability. It has been classified into four different categories, based on the perception of the subjective operator during osteotomy perforation (D1 is the hardest and D4 the softest). Different geometries of the implant shape threads have been proposed to improve the primary stability in different densities of bone [21, 22]. Obtaining primary stability, after placement of dental implants in the posterior maxilla, represents a critical factor due to the poor bone density of this anatomical region, especially for an immediate functional loading protocol [23–26]. Maximum torque of the implant placement provided the rotational stability of the implant.

In conclusion:

- The use of artificial bone substitutes is useful to eliminate the interspecies bone qualities.
- High values of insertion torque, resonance frequency analysis, and removal torque indicated good stability of the implants.
- Implants placed in dense bone presented a higher primary stability.
- The thickness of the cortical layer increased the resonance frequency analysis values.
- Tapered implants presented an increased primary stability.
- Short implants performed in an equal, if not better fashion, than standard implants.
- There is a positive association between primary stability and bone density.

References

1. Möhlhenrich SC, Heussen N, Elvers D, Steiner T, Hölzle F, Modabber A. Compensating for poor primary implant stability in different bone densities by varying implant geometry: a laboratory study. Int J Oral Maxillofac Surg. 2015;44:1514–20.
2. Gehrke SA, Guirado JLC, Bettach R, Fabbro MD, Martínez CP, Shibli JA. Evaluation of the insertion torque, implant stability quotient and drilled hole quality for different drill design: an in vitro investigation. Clin Oral Implants Res. 2018;29:656–62.
3. Romanos GE, Bastardi DJ, Moore R, Kakar A, Herin Y, Delgado-Ruiz RA. In vitro effect of drilling speed on the primary stability of narrow diameter implants with varying thread designs placed in different qualities of simulated bone. Materials (Basel). 2019;12:E1350.
4. Yamaguchi Y, Shiota M, FuJii M, Sekiya M, Ozeki M. Development and application of a direct method to observe the implant/bone interface using simulated bone. Springerplus. 2016;5:494.
5. Falco A, Berardini M, Trisi P. Correlation between implant geometry, implant surface, insertion torque, and primary stability: in vitro biomechanical analysis. Int J Oral Maxillofac Implants. 2018;33:824–30.
6. Di Stefano DA, Arosio P, Gastaldi G, Gherlone E. The insertion torque-depth curve integral as a measure of implant primary stability: an in vitro study on polyurethane foam blocks. J Prosthet Dent. 2018;120:706–14.
7. ASTM F-1839-08: Standard specification for rigid polyurethane foam for use as a standard material for testing orthopaedic devices and instruments, vol. 1. West Conshohocken, PA: ASTM International; 2012.
8. Tsolaki IN, Najafi B, Tonsekar PP, Drew HJ, Sullivan AJ, Petrov SD. Comparison of osteotome and conventional drilling techniques for primary implant stability: an in vitro study. J Oral Implantol. 2016;42:321–5.
9. Oliveira G, Borelli Barros Filho LA, Borrelli Barros LA, Pereira Queiroz T, Marcantonio E. In vitro evaluation of the primary stability of short and conventional implants. J Oral Implantol. 2016;42:458–63.
10. Deporter D, Ogiso B, Sohn DS, Ruljanich K, Pharaoh M. Ultrashort sintered porous-surfaced dental implants used to replace poster teeth. J Periodontol. 2008;79:1280–6.
11. Lombardo L, Pighi J, Marincola M, Corrocher G, Simancas-Pallares M, Nocini PF. Cumulative success rate of short and ultrashort implants supporting single crowns in the posterior maxilla: a 3-year retrospective study. Int J Dent. 2017;2017:8434281.
12. Markose J, Eshwar S, Srinivas S, Jain V. Clinical outcome of ultrashort sloping shoulder implant design: a survival analysis. Clin Impl Dent Relat Res. 2018;20:646–52.

13. Lemos CA, Ferro-Alves ML, Okamoto R, Mendonca MR, Pellizzer EP. Short dental implants versus standard dental implants placed in the posterior jaws: a systematic review and meta-analysis. J Dent. 2016;47:8–17.
14. Fan T, Li Y, Deng WW, Wu T, Zhang W. Short implants (5 to 8 mm) versus longer implants (>8 mm) with sinus lifting in atrophic posterior maxilla: a meta-analysis of RCT. Clin Implant Dent Relat Res. 2017;19:207–15.
15. Cruz RS, Lemos CAA, Batista VES, Oliveira HFFE, Gomes JML, Pellizzer EP, Verri FR. Short implants versus longer implants with maxillary sinus lift. A systematic review and meta-analysis. Braz Oral Res. 2018;32:e86.
16. Nielsen HB, Schou S, Isidor F, Christiansen A-E, Starch-Jensen T. Short implants (<8 mm) compared to standard implants (>8 mm) in conjunction with maxillary sinus floor augmentation: a systematic review and meta-analysis. Int J Oral Maxillofac Surg. 2019;48:239–49.
17. Tolentino DA, Rosa De Souza P, Binhame Albini Martini M, Reis Azevedo-Alanis L. Do short implants have similar survival rates compared to standard implants in posterior single crown? a systematic review and meta-analysis. Clin Implant Dent Relat Res. 2018;20:890–901.
18. De N, Dias FJ, Pecorari VGA, Martins CB, Del Fabbro M, Casati MZ. Short implants versus bone augmentation in combination with standard length implants in posterior atrophic mandibles: systematic review and meta-analysis with the Bayesian approach. Int J Oral Maxillofac Surg. 2019;48:90–6.
19. Urdaneta RA, Daher S, Leary J, Emanuel KM, Chuang SK. The survival of ultrashort locking-taper implants. Int J Oral Maxillofac Implants. 2012;27:644–54.
20. Piattelli A, Balice P, Scarano A, Perrotti V. Chapter 5: Threaded implants in the posterior maxilla. In: Deporter D, editor. Short and ultrashort implants. Berlin: Quintessence Publishing; 2018. p. 59–74.
21. Elias CN, Rocha FA, Nascimento AL, Coelho PG. Influence of implant shape, surface morphology, surgical technique and bone quality on the primary stability of dental implants. J Mech Behav Biomed Mater. 2012;16:169–80.
22. Lima de Andrade C, Carvalho MA, Bordin D, da Silva WJ, Del Bel Cury AA, Sotto-Maior BS. Biomechanical behavior of the dental implant macrodesign. Int J Oral Maxillofac Implants. 2017;32:264–70.
23. Möhlhenrich SC, Kniha K, Heussen N, Hölzle F, Modabber A. Effects on primary stability of three different techniques for implant site preparation in synthetic bone models of different densities. Br J Oral Maxillofac Surg. 2016;54:980–6.
24. Marquezan M, Osório A, Sant'Anna E, Souza MM, Maia L. Does bone mineral density influence the primary stability of dental implants? A systematic review. Clin Oral Implants Res. 2012;23:767–74.
25. González-Serrano J, Ortega-Aranegui R, López-Quiles J. In vitro comparison of primary stability of two implant designs in D3 bone. Med Oral Patol Oral Cir Bucal. 2017;22:e473–7.
26. Herekar M, Sethi M, Ahmad T, Fernandes AS, Patil V, Kulkarni H. A correlation between bone (B), insertion torque (IT), and implant stability (S): BITS score. J Prosthet Dent. 2014;112:805–10.

Peri-implantitis: A Serious Problem of Dental Implantology

Alicja Porenczuk and Bartłomiej Górski

Abstract Since decades, dental implantology has become a vital and ubiquitous rehabilitation treatment method, providing edentulous or semi-edentulous patients with an artificial dentition.

Along with the popularity of dental implants, the problems with their maintenance in the oral cavity have gradually evolved, leading to confusion over classification, recognition, treatment, and prevention of diseases correlated with them. In 2017, the World Workshop on the Classification of Periodontal and Peri-implant Diseases and Conditions developed a new classification of periodontal diseases, in which peri-implant health problems were separately outlined. The experts came to an agreement that placement of dental implants has led to the occurrence of new clinical problems related to them. Peri-implant diseases, such as peri-implant mucositis and peri-implantitis, correspond to periodontal states, gingivitis and periodontitis, and, likewise, are considered serious and chronic diseases jeopardizing the undertaken rehabilitation treatment. Peri-implantitis, which is defined as a pathologic condition of all tissues supporting dental implant, can lead to its loss, if not recognized and treated on time. In this chapter, the etiology of peri-implant health problems was assessed. Moreover, risk factors influencing the state of periodontal tissues supporting dental implants were distinguished, facilitating recognition of patients at risk and establishement of possible treatment methods.

This chapter aims to bring closer prevalence and risk factors of peri-implantitis. Prevention and treatment methods are distinguished in this paper.

Keywords Dental implants · Oral rehabilitation · Peri-implant health · Peri-implantitis · Peri-implant mucositis · Risk factors

A. Porenczuk (✉)
Restorative Dentistry Department, Medical University of Warsaw, Warsaw, Poland
e-mail: alicja.mackiewicz@wum.edu.pl

B. Górski
Department of the Periodontology and Oral Diseases, Medical University of Warsaw, Warsaw, Poland

R. S. Chaughule, R. Dashaputra (eds.), *Advances in Dental Implantology using Nanomaterials and Allied Technology Applications*,
https://doi.org/10.1007/978-3-030-52207-0_9

1 Introduction

The history of restoring missing dentition with dental implants reaches as far as 600 AD, when the ancient Mayas used pieces of shells as a replacement for lost mandibular teeth [1]. Since then, humankind has tried many means to gain an alternative dentition, such as transferring and implanting teeth from one patient to another (Dr. J. Hunter, 1700), or inserting artificial objects, such as gold implant tube into fresh extraction site (Dr. J. Maggiolo, 1809), a 24-gauge hollow latticed cylinder of iridio-platinum soldered with 24-karat gold (Dr. E.J. Greenfield, 1913) or orthopedic screw fixtures made of chromium-cobalt alloy (Dr. A. Strock and Dr. M. Strock, 1930) [1]. But it was not until 1978 when Dr. P. Brånemark presented a two-stage threaded titanium root-form dental implant that started the era of a continuous progress in the field of dental implantology [1]. Nowadays, dental implants bring out new possibilities in the reconstruction of the lost dentition. With a high range of success, reaching up to 100% [2], rising accessibility and affordability, implantation is regarded as the most reliable treatment method for partially and/or completely edentulous patients. Along with the progress in technical aspects of implants such as their surfaces, shapes, and coatings, dental surgeons have gained new possibilities and experience in treating even the most extreme cases. For example, even in an esthetically difficult region of the incisive canal, where the bone loss is quickly visible after extraction and/or when the patient stays edentulous for a long period of time due to extraction and/or dental trauma, the success rate can now reach as high as 84.6–100% [2]. In a clinical study aimed to assess the success rate of dental screws placed in an unfavourable conditions, Lee and colleagues [3] observed implants with low primary stability at various follow-ups (min. 34 days/max. 9.28 years). They proved that the clinical success depended on both the patient qualification to either “simple” or “advanced” surgery group and on a protected, unloaded healing. Based on that, their long-term treatment success rate reached 95% [3]. A wide meta-analysis comparing the success rate in groups of smokers and nonsmokers showed that the nonsmokers kept their implants in a significantly higher rate than the smokers [4]. In case of implants supporting full-arch rehabilitation, Papaspyridakos and colleagues [5] reported a cumulative success rate of 98.7% after more than 5 years from definite prosthesis insertion. All of these studies advocate the idea that rehabilitation using dental implants could be very effective, regarding patient’s qualification for the procedure.

When the first dental implants were placed, clinicians worried mostly about their osteointegration with the alveolar bone, as reaching good osteointegration was the most important treatment goal at that time. However, along with broadening of the clinical indications for implant placement and making it less dependent on the financial aspect, a new challenge was defined—peri-implantitis.

1.1 Definition and Classification

Proceedings of the first European Workshop on Periodontology in 1994 defined peri-implantitis as an inflammatory reaction with loss of supporting bone around a functioning implant [6]. This broad definition provided no guideline on the criteria for recognition and treatment of this disease. The 2017 World Workshop introduced a new classification of the peri-implant health problems, which distinguished peri-implant health, peri-implant mucositis, peri-implantitis, and peri-implant soft and hard tissue deficiencies [7]. The term peri-implant health refers to all states that exist around dental implants with normal or reduced bone support. Peri-mucositis is defined as an inflammation of the mucous membrane surrounding dental implant, with or without visible plaque. In addition, it may precede peri-implantitis [8, 9]. Its characteristics covers inflammation of the gum (redness, swelling, pain when touched), bleeding on probing (BoP) with or without suppuration from the periodontal pocket, and no visible bone loss around dental implant on function seen on a radiograph. Peri-implantitis stands for a condition in which the inflammation around dental implant spreads on a wider area, covering both the mucous membrane and the bone support. Clinical and radiological symptoms of peri-implantitis cover inflammation of the gum (redness, swelling, pain when touched), bleeding on probing (BoP) with or without suppuration from the periodontal pocket, a visible, progressive loss of the bone support around dental implant on function seen on a radiograph. If not treated, it may progress in a nonlinear and accelerating pattern [10]. Hard and soft tissue implant deficiencies recognize the fluctuations of the dimensions of the alveolar process/ridge caused by various factors such as tooth's extraction, former periodontal diseases, medications, systemic diseases, trauma, endodontic infections, root fractures, thin buccal bone plate, tooth's malposition in the dental arch leading to an occlusal overload, pneumatization of the maxillary sinus, and pressure from dental prostheses [7].

1.2 Incidence and Prevalence of Peri-implantitis

Incidence, which stands for a frequency of cases of a disease with which it occurs in a period of time, defines how many new cases of peri-implantitis are there in a population (e.g., during month/year/longer period of time). Such longitudinal prospective studies are hard to perform [11]. On the other hand, prevalence shows how many cases are there in a specific population in a period of time (e.g., patients of one study, patients of one dental clinic), and it may be obtained from clinical studies performed by clinicians from academia or private clinics. Both rates are essential for a practitioner to estimate the range of the problem he or she may face in their own practice. However easy as it may seem, the numbers vary due to inconsistency of peri-implantitis' identification resulting from lack of its clear definition before the year 2017. Therefore, both the incidence and prevalence of peri-implantitis are

still hard to be estimated. Several factors influencing proper calculation of its rate among patients may be outlined, such as differences in sampling procedures (inadequate sample size, counting only patients, counting only implants, counting both patients and implants, patients from private clinics/public schools), studies made on various implant systems, inadequate observation time (mostly less than 5 years), rating only radiographs (often without clinical examination), rating only BoP (without radiological examination), differences in BoP examination criteria (defining peri-implantitis using ambiguous pathological pocket depths (PD), using different instrumentation (standard periodontological probe, calibrated periodontological probe, standard dental probe, other), using nonstandardized probing force), and differences in estimated bone loss (often counted in millimeters (mm), defining progressive bone loss (often not defined in mm)) [11, 12]. Chosen studies from 2015 to 2019 (Table 1) show how many differences may be seen in evaluation of peri-implant health problems, especially the observation time, methods of patients' examination at follow-ups, lack of manufacturer names and/or types of placed dental implants, various numbers of implants (which in most cases exceed the number of treated patients), and taking or not taking the individual risk factors into account.

With all these differences, the prevalence of peri-implantitis is high, varying between 1–47% [11], 10–40% [12], 4.6% on the implant level and 12.7% on the patient level [14] or even 34% on the patient level and 21% on the implant level [18]. The meta-analyses of the subject estimated the peri-implantitis prevalence rate up to 9.25% (estimated weighted mean implant-based prevalence; 95% confidence interval (CI): 7.57–10.93%), 19.83% (estimated weighted mean patient-based prevalence; 95% CI: 15.38–24.27%) [19], and 22% (without recognition of implant/patient base; 95% CI: 14–30%) [11]. It should be emphasized that the examination methods as well as the amount of the lost alveolar bone in most cases were individually determined by the operator. Moreover, most reports concluded that multiple factors, such as inconsistent definitions, reporting methods, study sample, and diagnostic criteria, prevented them from gaining objective, nonbiased epidemiologic results. For example, Dudek and colleagues [17] introduced their own classification scale to assess the prevalence of peri-implantitis, which they observed in only 9.8% of all implants, regardless of their type. Regardless of the chaos in the literature, from a clinical point of view, peri-implantitis must be treated as a serious threat in implantology and the findings in this area of dentistry taken into consideration upon patient's qualification for the surgery.

2 Bacteria Species in Peri-implantitis

Like periodontal diseases, peri-implantitis is caused by bacteria biofilm colonizing the implant area. The bacterial colonization of the crevice around dental implant and the biofilm's development has been a subject of many studies, which tried to explain how the bacteria survived on an artificial subject and gradually damaged it. The search for the bacteria responsible for the onset and progression of peri-implantitis

Table 1 Prevalence and variety of used diagnostic criteria of peri-implantitis in chosen papers

Investigator (year of publication)	Time of observation	Number of patients (sex)/ number of implants	Type of implant (number of patients/ implants)	Healing	Implant loading	Methods and treatment	Results
De Martinis Terra (2019) [13]	1 yr.	6 (nd)/6	nd	nd	nd	Peri-implantitis criteria: BoP and bone loss >2 mm compared to bone level at baseline clinical and RTG evaluations at three time points: implant placement, final prosthetic delivery, yearly follow-ups All patients received fixed cement-retained (methacrylate cement) implant restorations	All patients were diagnosed with peri-implantitis Nonsurgical treatment: prosthetic crown removal, scaling, rinsing with a mixture of saline solution and antibiotics (2 × 250 mg metronidazole capsules and 2 × 300 mg tetracycline capsules in 5 mL saline solution), chlorhexidine gel 1% mixed with metronidazole and tetracycline placed in the implant screw hole before the abutment repositioning, crown's re-fixation with a resorbable cement
Francetti (2019) [14]	Mean 8 yrs. (1–13.7 yrs.)	77 (45 females, 32 males)/384	Brånemark System Mk IV TiUnite (nd/nd) Nobel Speedy Groovy (nd/nd)	nd	Immediate (within 48 hrs. from surgery)	Peri-implantitis criteria: BoP and/or suppuration, concomitant bone resorption of 2 mm or more when compared to the baseline and follow-up RTG	After 5 yrs., prevalence of peri-implantitis was 4.6% on the implant level and 12.7% on the patient level Smoking/previous history of periodontitis not regarded as risk factors

(continued)

Table 1 (continued)

Rodrigo (2018) [15]	Mean 9.0 yrs. (5–13 yrs.)	275 (151 females, 124 males)/474	nd	nd	nd	Clinical evaluation: standardized periodontal probe (SEPA probe, with marks at 3.5 and 5.5 mm), presence of clinical signs of inflammation, plaque (four sites/implant), probing depths (mm; four sites/implant), BoP (four sites/implant), suppuration, presence of keratinized tissue >1 mm, accessibility to interproximal hygiene, RTG Peri-implantitis criteria: healthy implants—no BoP, RTG bone levels <2 or <3 mm Peri-implantitis—BoP, RTG bone level ≥2 or ≥3 mm	Peri-implantitis prevalence 20% at implant level, 24% at patient level Significant associations for peri-implantitis: gender, peri-implant supportive therapy, implant location, implant diameter and surface, type of prosthesis, adequate access to interproximal hygiene Access to interproximal hygiene was adequate in 95%

Papaspyridakos (2018) [5]	Mean 7.5 yrs. (2.7–13 yrs.)	52 (21 females, 31 males)/457	Nobel Biocare (100%)	nd	Delayed	Peri-implantitis criteria: BoP and/or suppuration, RTG bone loss > 2 mm	Total number of implants diagnosed with peri-implantitis = 46 13 implants (2.8%)—advanced bone loss reaching half of their length, present BoP and/or suppuration 33 implants (7.2%)—average bone loss of 2.9 mm High PI seen as a significant risk factor for crestal bone loss
Goh (2017) [16]	Mean 5.9 yrs. (0.2–19.1 yrs.; group with periodontitis) mean 5.7 yrs. (0.2–19.1 yrs.; group with current peri-implantitis)	Overall study group: 444 (219 females, 225 males)/1485 Group with periodontitis: 370 (183 females, 187 males)/1189 Group with current peri-implantitis: 318 (156 females, 162 males)/1004	nd	nd	nd	Peri-implantitis criteria: Implant bone loss of 3 threads on RTG (equivalent to 2.4–2.5 mm); pocket depth on probing > 5 mm with BoP	Prevalence of peri-implantitis calculated at the patient and implant levels ranged 6.7–19.7% Patients with periodontitis without periodontal support treatment showed higher chances of having peri-implantitis Implants supporting fixed dental prostheses and with subjective discomfort were associated with a higher prevalence of peri-implantitis than single implants

(continued)

Table 1 (continued)

Dudek (2015) [17]	4 yrs.	200 (84 females, 116 males)/610	Ankylos (67/220) Implant Direct (94/286) Adin Implants (39/104)	Closed	Immediate	Peri-implantitis criteria: Own classification 0°—PD up to 3 mm, no BoP, no discomfort on probing/in palpal study, no bone loss, RTG correct I°—PD >3 mm, BoP, no discomfort on probing/in palpal study, bone loss up to 3 mm (scaling, ozone therapy, CHX, home hygiene protocol) II°—PD >3 mm, BoP, discomfort on probing/in palpal study, bone loss >3 mm (regenerative surgery or explantation with additional bone augmentation) III°—PD >3 mm, BoP, suppuration and discomfort on probing/palpal study, bone loss >3 mm with clinically visible implant exposure (regenerative surgery or explantation with additional bone augmentation) Bacteriological tests	PI in 9.8% (60) of implants (in 5.39% during first 12 weeks; in 4.41% up to 2 yrs.) Comparable percentage share of peri-implantitis prevalence in all implant types Cultivated bacteria species (*Aggregatibacter actinomycetemcomitans*, *Treponema denticola*, *Porphyromonas gingivalis*)

Abbreviations: *yr.* year, *yrs.* years, *nd* no data, *BoP* bleeding on probing, *mm* millimeter, *mg* milligram, *mL* milliliter, *RTG* radiograph, *PI* plaque index, *PD* pathologic pocket depth

is still biased, as until recently there has been no widely accepted definition of this disease. The reliability of the conducted research is related to their methodology: sequencing techniques (conventional PCR, quantitative PCR, metagenomic techniques, DNA hybridization), culture methods, pairing/nonpairing study design (peri-implantitis vs periodontitis, peri-implantitis vs 'healthy' implant), risk factors (confounding factors yes/no), clinical evaluation (pocket depth yes/no, BoP yes/no), and previous history of periodontitis [20]. Taking all these factors into consideration, it was finally concluded that the species responsible for periodontal diseases are also present in the inflamed sulci around dental implants. Peri-implantitis has also been connected with an opportunistic microbiome and commensal-depleted pathogens [21]. The microbiome of peri-implantitis is quite heterogenous, though. A native study by Dudek and colleagues [17] determined the bacteria species present in the pathological pockets around dental implants using a standard PET test. The study confirmed the presence of *Aggregatibacter actinomycetemcomitans*, *Treponema denticola,* and *Porphyromonas gingivalis*, which are also found in periodontal diseases [17]. Contrarily, Lafaurie and colleagues [20] compared the frequency of bacteria related to periodontitis to those in peri-implantitis, and what they found out was that the red complex bacteria (*Porphyromonas gingivalis*, *Treponema denticola*, and *Tannerella forsythia*) were found more often in peri-implantitis in only 38% of studies. Moreover, only 42.8% of the papers confirmed the presence of the orange complex bacteria (*Prevotella intermedia*, *Prevotella nigrescens*, *Fusobacterium nucleatum*, and *Peptostreptococcus micros*) [20]. Contrarily to periodontitis, non-cultivable microorganisms, such as asaccharolytic anaerobic gram-positive rods (AAGPRs, e.g., *Eubacterium nodatum*, *Eubacterium brachy*, *Eubacterium saphenus*, *Filifactor alocis*, *Slackia exigua*, *Parascardovia denticolens*), anaerobic gram-negative rods (OGNRs, e.g., *Leptotrichia hofstadii*, *Kingella dentrificans*, and *Treponema lecithinolyticum*), and opportunistic pathogens like *Staphylococcus aureus* were more likely to develop in peri-implantitis [20]. Quite recently, Soriano-Lerma and colleagues [22] revealed that the infection associated with peri-implantitis stems from common oral bacteria, or from environmental bacteria. They divided patients into three groups with different microbiome and described three strata. Stratum 1 was associated with the presence of *Ralstonia* and *Sphingomonas*. Both taxa are nonoral, gram-negative genera that may be found in environment (e.g., water supplies). They are also causative agents of nosocomial infections. In stratum 2 microbiota from purple and yellow complexes were found (*Streptococcus*, *Veillonella*, *Neisseria*, *Rothia*), all of which represent gram-positive facultative species, so-called early colonizers. The most prevalent was stratum 3, which included gram-negative, anaerobic species such as *Fusobacterium*, *Prevotella*, *Porphyromonas*, *Treponema*, *Campylobacter,* and *Tannerella*. The abovementioned genera belong to orange and red complexes that represent middle and late colonizers. There also seems to be some variations in compositions of biofilms on normal, healthy implants and on those affected by peri-implantitis. For example, the red complex bacteria*Porphyromonas gingivalis* was present in 0–65% of cases of peri-implantitis and in 0–79% cases of "healthy" implants, while *Treponema forsythia* was present in 0–80.3% in peri-implantitis and in 0–80% in "healthy" implants.

Only *Prevotella intermedia* was cultivated from 22–66% of sites with diagnosed peri-implantitis, while 6.6–23% colonized "healthy" implants [20]. What seems to distinguish healthy implant sulcus from those with peri-implantitis are counts of OGNRs (10–65% in peri-implantitis against 6–13% in "healthy" implants) and *Staphylococcus aureus* at the level of 0–43.4% (peri-implantitis) and 0–19.1% ("healthy" implants) [20]. These inconsistencies in percentage share of bacteria species in periodontal and peri-implant diseases indicate that these two entities differ, thus should not be considered alike, with clear differences on behalf of the opportunistic bacteria in peri-implantitis. Furthermore, external factors such as smoking or the titanium composition of the implant might modulate the peri-implant microbiome and transform it into a more pathogenic entity [23, 24].

3 Risk Factors

Dental clinicians are aware of the existence of multiple pathologies, whose appearance in patients, apart from their well-known etiology, can be attributed to other, sometimes not so obvious, elements. For example, dental caries is normally attributed to a plaque formation on tooth's surfaces, leading to the acidic degradation of its hard tissues. However, the onset and progression of caries may be facilitated by other factors, such as overhanging restorations enabling the biofilm's formation, deep pits and fissures seen in children and young adolescents favoring plaque accumulation, patient's health problems changing the immunologic response to bacterial activity, and so on. In accordance with this, peri-implantitis is caused by a biofilm created on a dental implant's surface, the bacteria species of which induce inflammatory response leading to the damage of the adjacent tissues [9]. The research on peri-implantitis depicted additional elements, called the risk factors, which facilitate the onset and progression of this disease. There are different reactions of bone to the presence of implants, such as zero bone loss, stable remodeling, progressive bone loss, bone demineralization and remineralization, corticalization, and bone growth (Fig. 1) [25].

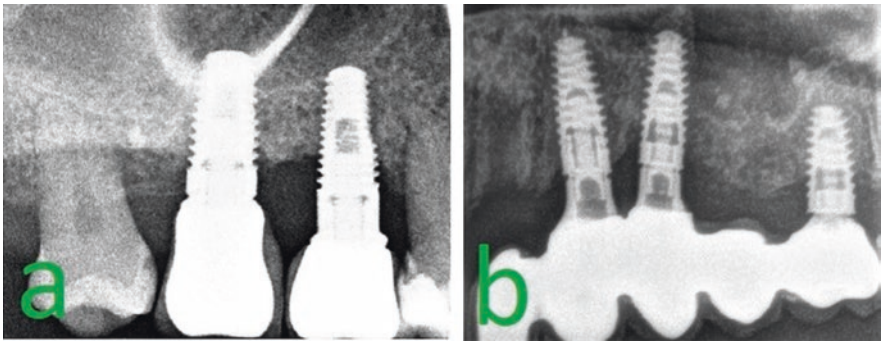

Fig. 1 Different patterns of bone destruction in peri-implantitis defects. Horizontal defects (**a**) do not have a regenerative potential, so resective treatment should be implemented. Defects with predominant vertical component (**b**) may be treated with a regenerative approach

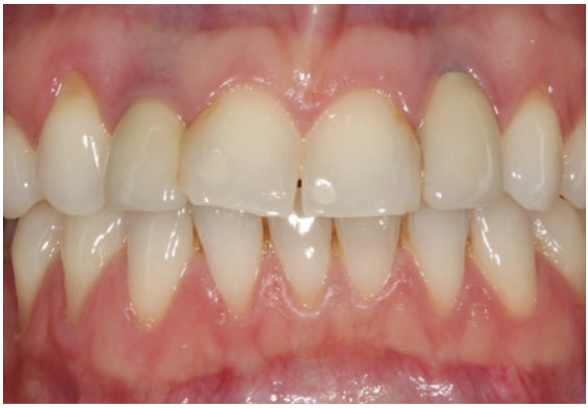

Fig. 2 The grayish appearances of soft tissues around the right implant and soft tissue recession around the left implant indicate crestal bone loss and undermine the esthetics of the restorations

The key point for a successful implant treatment seems to be crestal bone stability in the long run, while crestal bone loss is a phenomenon with multifaceted etiology (Fig. 2).

The authors of this chapter decided to picture the peri-implantitis' risk factors as a scheme (Fig. 3), followed by a short written description, which hopefully will give a clear feedback on this issue. We believe that patient's thorough clinical and radiographic examination, medical interview and treatment provided by trained specialists in oral surgery, prosthodontics and periodontics would limit the occurrence of the factors dependent on the human mistakes, providing long, functional years of the implanted screws.

3.1 Factors Related to Patient

3.1.1 Previous History of Periodontitis

It seems that patients suffering from chronic periodontitis are prone to develop peri-implantitis as well, as a confirmed history of periodontitis may increase the risk of future peri-implantitis even 3.63 times (Fig. 4) [18, 26–32].

Acute forms of periodontal disease are associated with higher rates of implant loss, even in patients who received a supportive periodontal treatment [15, 33]. Rodrigo and colleagues [15] conducted a 16-years observation study on this aspect, the results of which indicated a relevantly lower rate of implant placement success in patients provided with an additional supportive periodontal treatment (79.22–100%), compared to "healthy" patients (91.67–100%).

Fig. 3 Risk factors of peri-implantitis

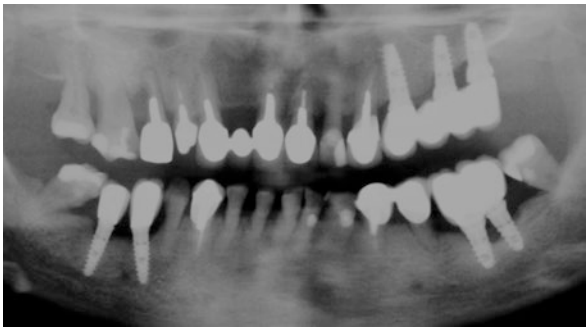

Fig. 4 Periodontitis predisposed this patient to a massive crestal bone loss around dental implants restoring missing teeth number 26, 27, 36, 45 and 46

3.1.2 Plaque Index and Oral Hygiene

Daily oral hygiene aims at removal of the bacterial biofilm forming on a natural or artificial dentition. Plaque control is one of the most important preventive aspects of dental caries, periodontal and peri-implant health problems, as bacteria and their products of metabolism activate inflammatory response in tissues surrounding both the natural dentition and the dental implants [28, 30–32]. It is also one of the few elements that can be self-modified by patients [28]. On the other hand, it is advocated that the dental plaque alone should not be regarded as the peri-implantitis' risk factor, as differences in gene expression between patients with peri-implantitis and those with periodontitis were found [34], and other elements than the plaque emerged to favor its occurrence [29, 30]. Nevertheless, patients with poor personal oral hygiene and/or those with poor or none professionally administered hygiene are said to develop peri-implantitis more easily [26]. Even an effective plaque removal from the implant's surface does not prevent peri-implantitis, as the inflammatory process may spread through interaction between the biofilms localized on the adjacent teeth or implants [28]. A good access to interproximal niches, ensured by a well-designed prosthesis guarantees an adequate plaque removal, diminishing the risk of the inflammation onset [15]. The patients should therefore be educated by their dentists or dental hygienists of how effectively and safely remove the bacterial plaque, as Van Velzen and colleagues [35] reported several cases where floss remnants left in the crevices around dental implants caused an inflammation, which healed spontaneously after their mechanical removal.

3.1.3 Full Mouth Bleeding Score

The peri-implant tissues are noncomparable to those surrounding a natural tooth, therefore differences in their responses to bacterial action may occur. In periodontitis, the percentage value of full-mouth bleeding on probing in clinical examination divides patients into three risk categories—green (0–15%) meaning low risk level, amber (15–20%) indicating moderate risk level, and red (20–100%) standing for high risk level [36]. In relation to the patients with dental implants, the clinically

stated BoP higher than 10% corresponds to an augmented level risk of peri-implantitis [31], while full mouth bleeding index higher than 25% is an indicator of an ongoing peri-implantitis at the patient level [37]. However, the probability of a clinically stated presence of BoP at a peri-implant site with a PD of 4 mm is estimated to be only 27% [38], while suppuration has been reported in only 10–20% of cases [39, 40]. Hence, both the BoP and suppuration are considered weak clinical factors in peri-implantitis' diagnosis. Moreover, de Araújo Nobre and colleagues [29] emphasized that personal oral hygiene prevents plaque accumulation and, consequently, diminishes BoP value, meaning that it may be a prominent factor only in patients with poor oral hygiene. Nevertheless, high BoP informs the clinician about the ongoing inflammation in the peri-implant tissues, and, as such, should be seen as a risk indicator [30–32].

3.1.4 Maintenance After Implant Placement

The recall regimen is a foundation for the prevention of both the periodontal and peri-implant diseases (Fig. 5) [41].

The patients with dental implants should call in for a check-up appointment every 5–6 months [26, 42]. Lack of regular check-ups along with supportive peri-implant treatment may increase progression of peri-implantitis in up to 40% of cases [27]. Contrary opinions undermine the need for every half a year recall, claiming that the percentage impact of this variable is only 5.89% [41]. In other words, patients' negligence in following check-ups with a dental surgeon may result in peri-implantitis development in approximately 6% of cases. Nevertheless, dentists should insist on their patients to follow a recall regimen in order to (1) provide education and motivation in a personal hygiene in the implant area, (2) provide professional hygiene, and (3) guarantee quick recognition and treatment of the unfolding disease.

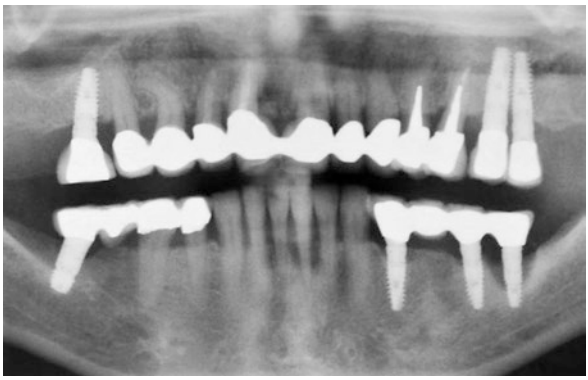

Fig. 5 General crestal bone loss around implants in patients without supportive peri-implant treatment

3.1.5 Patient Sociodemographic Information

Atieh and colleagues [27] did not regard the patient's sex as a risk factor, on contrary to Rodrigo and colleagues [15], who proved that male gender acted protectively. The patient's age is a risk factor worth recognition, as elderly patients (>60 years of age) are more prone to develop peri-implantitis [18].

3.1.6 Smoking

Smoking is one of the most important risk factors of peri-implantitis [27, 29, 43]. Statistically, smokers are at much higher risk of peri-implantitis than nonsmokers, especially those additionally affected with a history of periodontitis [44]. Tobacco downregulates the expression of bone matrix proteins through suppression of certain transcription factors for osteogenesis, or through activation of certain factors for osteoclastogenesis, which fastens the progression from peri-implant mucositis to peri-implantitis [45, 46].

3.1.7 Concurrent Health Conditions

Patient's systemic health problems such as diabetes mellitus, osteoporosis, cardiac problems, hypertension, and various viral diseases may enhance peri-implantitis occurrence [47, 48]. However, not all researchers approve that health conditions have a major impact on peri-implant diseases [27], so this aspect needs further evaluation.

3.2 Factors Related to Prosthesis

3.2.1 Type of Implant-Supported Prosthesis and Prosthesis Design

The implant screw itself, its design and surface characteristics, may promote problems in the implant site. However, a clinician must not forget that implant's function is restoration of the lost dentition, so it should be regarded as unity with a prosthetic device it supports (e.g., a single crown, multiple crowns in a fixed dental bridge, or any other type of multipoint denture). It is underlined that retentive components of poorly designed prosthesis bear more risk of inducing peri-implantitis, as they favor bacterial plaque accumulation around the implant and obstruct its removal by the patient (Fig. 6) [9, 27, 49, 50].

Serino and Ström [50] revealed that more than 90% of patients with implants could not perform adequate oral hygiene due to improper prosthesis design. Another example shows that bone-level single crowns with an emergence angle of over 30° and a convex profile can be strongly associated with peri-implantitis [51]. Type of

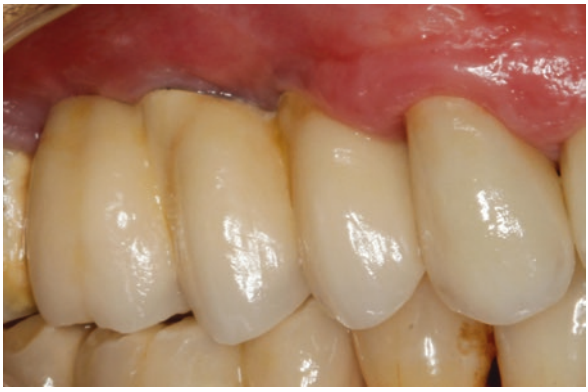

Fig. 6 The construction of prosthetic restoration makes home plaque control impossible

the construction material of the artificial dentition should also be taken into consideration, as restorations based on metal proved to be more risky [15, 28]. Fully edentulous patients, equipped with complete prostheses, especially hybrid ones (made of various materials), are at higher risk of peri-implantitis [15]. Other factors related to prosthesis design are lack of prosthetic fit or nonoptimal screw joint [28] and malpositioning on the abutment and/or the abutment's design [52]. Longer transmucosal abutments (>2 mm) [53] and internal connection (including platform switching [54] and Morse cone connections [55]) have been associated with good preservation of the peri-implant bone level, while type of the implant-abutment joint (external vs internal vs conical) [56], number of abutment connections/disconnections [52], or difficulty in removing excess cement [9, 13, 57] may increase the bone loss. The geometry of the titanium base has an impact on crestal bone stability [58]. Titanium base that is wide and has a short gingival height may lead to bone loss, especially in case of subcrestally placed implants. When designing the form of the emergence profile, the clinician should take into account the depth of the subcrestal implant position, since the height of the titanium base should be correlated with the depth of implant placement. Furthermore, the emergence profile angle of the restoration with respect to the implant should not be greater than 25°, otherwise crestal bone loss may occur [59, 60]. Among other prosthetic factors that should be considered, there are prosthetic materials (abutment materials, veneering materials) and type of retention (cement-retained restorations, screw-retained restorations). The other factors involve choosing prosthetic materials for abutments and crowns. The most biocompatible material is zirconia, followed by titanium and polished lithium disilicate ceramics. The least biocompatible for contact with peri-implant tissues is the veneering ceramics (feldspathic ceramics). Zirconia is the most biocompatible material due to low surface free energy and very limited bacterial adhesion [61, 62]. Compared to titanium, zirconia determines better adhesion for epithelial cells and stimulates more favorable responses of the soft tissues [63, 64]. Moreover, probing pocket depths (PD) were lower around zirconia abutments, when compared to titanium abutments [62]. Smoother surfaces support better adhesion of the epithelial cells and on the ultrapolished zirconia abutments a thin layer of epithelium lines the

fibroblasts, thus there is no direct contact between zirconia and fibroblasts from the connective tissue. It was found that the epithelial cells attach to the surface of titanium stronger than the fibroblasts, and this connection is more tough to the abutment surface than to the connective tissue [65, 66]. The epithelial cells attach more efficiently on smooth than on the rough titanium surfaces [67]. As epithelial adhesion to glazed ceramic is very poor, this material should not be used subgingivally [52]. On the other hand, highly polished lithium disilicate surface allows for stable fibroblasts adherence [68]. Taking all of these elements into consideration, the dentist's role is to design the future replacement in a way that ensures mastication adapted to patient's occlusion and enables non-problematic access to oral hygiene. Fulfilling these criteria requires years of specialistic training and experience in implantology, prosthodontics, and periodontology. Moreover, mutual understanding and communication between surgeon, prosthodontist, and technician secures the overall treatment's success.

3.2.2 Occlusal Overload and Remnants of the Cement

An occlusal overload, resulting from either patient's malocclusion or the prosthetic design, can be clinically seen in the patient's mouth as the presence of wear facets on the prosthesis. An excessive load on the implant increases the risk of peri-implantitis development around it [32, 69]. Remnants of an adhesive in the crevice around the implant have a catastrophic effect on the health of the surrounding tissues [9, 13, 32, 48, 69]. Residual cement was recognized as a risk factor for the development of peri-implant mucositis and peri-implantitis [70]. Linkevičius and colleagues [71] observed that peri-implantitis resolved in 85% of the cases, where the excess of the bonding agent was left in the pocket, especially in patients with history of periodontitis. Both in vitro and in vivo studies demonstrated that it is virtually impossible to remove all excess cement if the restorative margins are located subgingivally [72, 73]. The deeper the margin position, the more cement remnants were left. All residual cement was removed only when the margin position was visible. Moreover, standard abutments have inherent undercuts (the distance between the restoration emergence profile margin and the cementation line), which makes them inaccessible to thorough cleaning from the cement remnants [74]. Therefore, the adhesive cement has to be thoroughly removed while placing the prosthesis on the abutment. Apart from the adhesive remnants, its type also matters. For instance, methacrylates may surely induce inflammation of the implant surrounding tissues with subsequent development of peri-implantitis, while classic, chemically set cements, such as zinc oxide-eugenol (ZOE), are far less irritant [13]. When peri-implant tissue inflammation occurs, with suspicion of the adhesive as a base of the problem, the recommended treatment comprises prosthesis removal from the abutment, professional cleaning of the crevice, involving scaling and chemical disinfection with chlorhexidine (CHX) or other disinfectants, and re-bonding of the prosthesis with an antibacterial and resorbable cement, such as ZOE. If methacrylate cement is required, a reduction of its amount may also be

helpful [48]. Placement of the prosthesis on the abutment using resin-based cement ought to be proceeded with a rubber dam isolation, and, after its initial polymerization, the crevice has to be precisely cleaned with a dental floss or hand instruments before further setting. As there is no reliable technique of intraoral cementation to guarantee a complete cement removal, custom abutments with supragingival cementation margins and without undercuts should be used to avoid leaving cement remnants in the pocket. The alternative is to use cementless solutions (e.g., screw-retained restorations).

3.3 Factors Related to Surgery/Operator/Implant

Factors related to the implant and/or the surgery are the most controversial of all discussed. The reason for it is that as the literature findings are based on various study types, study design with/without clinical evaluation, various study groups (in terms of age, gender, patient characteristics), inclusions/exclusion criteria, whether the researchers have any clinical experience.

3.3.1 The Characteristics of the Implant Site

The presence of a keratinized gingivae is assumed to be a preventive factor of peri-implantitis in patients with deficient oral hygiene [9, 75]. The beneficial effect of its presence was underlined by Monje and colleagues [76], who concluded that a thin-tissue gingivae phenotype poses higher risk of peri-implantitis. A wide band of gingivae surrounding a natural tooth or its artificial substitute prevents the bacterial biofilm's access into the crevice, which would be otherwise facilitated by a movable, thin mucosa [77]. Moreover, a thick gum barrier diminishes pain during brushing and flossing, helping to keep good hygiene and, in effect, diminishing inflammatory process around the implant (Fig. 7) [78].

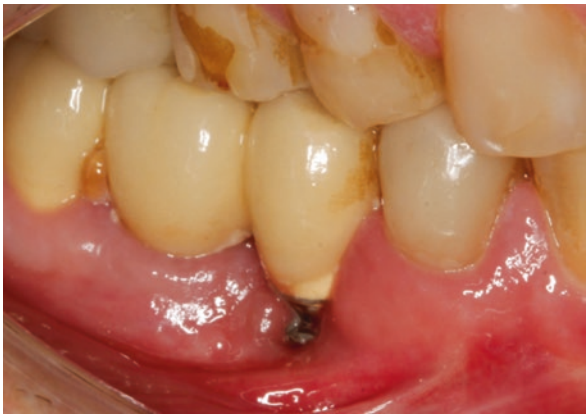

Fig. 7 Lack of keratinized tissues around implant causes crestal bone loss and impairs home plaque control

It is stated that the presence of ≥4 mm of keratinized mucosa around dental implant (2 mm buccally and 2 mm lingually) of an adequate horizontal thickness of 2 mm is crucial for the prevention of peri-implant diseases [75]. Another very important parameter is vertical soft tissue thickness. It was reported in dogs that sites with vertical tissue thickness of ≥4 mm had no bone loss after 2 months of healing period, whereas sites with a vertical thickness ≤2 mm underwent significant bone resorption [79]. It was explained that bone resorption occurred in order to allow an adequate soft tissue attachment to develop as a defensive biologic phenomenon to keep bacteria further away from bone. Quite recently Linkevičius and colleagues [80] placed 80 bone-level implants in 80 patients, half of whom had ≤2 mm of vertical soft tissue (group 1, thin tissue) and the other half had >2 mm of vertical soft tissue (group 2, thick tissue). At a 1-year follow-up, mean bone loss was 1.18 mm in group 1 and 0.22 mm in group 2. Based on the outcomes of the subsequent study that crestal bone loss could be reduced to 0.22 mm around platform-switched implants provided vertical soft tissue thickness >3 mm, it was concluded that 3 mm should be a threshold to differentiate between thin and thick tissues [81].

3.3.2 Implant Characteristics

A full osseointegration process combines two stages—primary stability resulting from a mechanical anchoring of the implant in bone, and secondary stability, which is obtained through bone's apposition and remodeling. The created link between the bone and the implant is called a functional ankylosis [82]. Albrektsson [83] distinguished six factors, which are essential to establish a proper connection:

1. Parameters of a dental implant's construction material (biocompatible, resistant to occlusal loads and corrosion).
2. Geometry of the screw (providing maximal contact between the bone and the screw).
3. Implant's surface characteristics.
4. Bone's biological status.
5. Surgical technique.
6. Implant loading conditions.

Modern implants differ in surface topographies (presence of macro/micro-roughness) and coatings, which ensure a quick osseointegration, minimizing future complications [9, 84, 85]. Examples of such surface modifications cover TiUnite by Nobel Biocare, which is a moderately rough, thickened titanium oxide layer with high crystallinity, or SLA introduced by Straumann in 1998 (a macro-rough, sand-blasted, and acid-etched surface for a better cell attachment). The aim of these sophisticated surface topographies is to provide full direct implant-bone contact that guarantees good osteointegration without the patient's compliance. However, some researchers favor the idea that both the implant surface type and the particles freed from it may promote a change from a stable immune system, which

is normally seen in a well-maintained osteointegration, to an active one leading to the implant's rejection [86]. For instance, patients equipped with TiUnite coated implants had greater implant pocket probing depths and radiographic bone loss, which could have been related to pits and grooves on the implant surface facilitating bacterial colonization and inflammation's onset [87]. It has also been advocated that implant surface modifications either have no impact on biological complications [27] or may severely complicate the peri-implantitis treatment [88, 89]. The factors linked to the implant's technological design are quite controversial. Some findings suggest that implant manufacturers, dimensions, location, antibiotics taken in tandem with the surgery, implant placement immediately after tooth extraction or in native bone, and the use of bone grafting materials should not be regarded as risk factors due to lack of supportive evidence [18]. However, the opposers claim that the narrower implant's diameter (≤3.5 mm) or its smoother surface, the higher risk of peri-implantitis [15]. All things considered, the presence or the absence of a polished implant neck and the type of implant-abutment connection are considered to be the most crucial implant design factors with reference to crestal bone stability. A polished implant neck was connected with the pathogenesis of crestal bone loss, as it did not osseointegrate, thus this type of implants should be placed above the bone crest in such a way that only the rough part is submerged in the bone [90, 91]. As all modern implants are two-piece designed, all of them have a microgap at the implant-abutment connection, which might be associated with bacterial contamination and micromovements of the abutment. The stability of the abovementioned connection and the reduction of micromovements are provided with a conical connection. Quite recently it was reported that the smaller the angle of the inclination, the more resistant to lateral movements the abutment will be [92]. Consequently, due to the microbial leakage at the implant-abutment interface, an inflammatory cell infiltration in the connective tissue next to the microgap may develop resulting in a a microgap-related bone loss [93]. The introduction of platform switching has shifted the bacterial leakage inwards and away from the bone towards the implant. . Vela-Nebot and colleagues [94] showed that a mean marginal bone loss for implant with platform switching was 0.76–0.77 mm after a 1-year follow-up, compared to 2.53–2.56 mm for implants with a regular connection. At least 0.4 mm of platform switching is necessary to be efficient for bone protection.

Table 2 Differences in temperatures of the osteotome drills and the bone depending on the rotation speed calculated at a drilling force of 30 N and drilling depth of 10 mm

Rotation speed (rpm)	Drilling depth (mm)	Time elapse between start of drilling and temperature measurement (s)	Temperature of the drill (°C)	Time elapse between start of drilling and temperature measurement (s)	Temperature of the bone (°C)
500	10	5	51.4 ± 3.8	7	42.7 ± 2.7
1200	10	5	68.5 ± 3.9	9	44.0 ± 1.9
2000	10	4	82.7 ± 5.7	9	50.6 ± 4.2

3.3.3 Technical Performance of the Surgery

Drilling in bone is an inevitable step in dental implant placement, as the space in bone has to be mechanically adjusted to the shape, diameter, and length of the artificial root. The hole in the bone is later replenished by a new bone created in the osteointegration process. The mechanical preparation of the implant socket requires using special drills called osteotomes, which are allowed for rotation by a machine called physio dispenser enabling operation with desired parameters of speed, torque, and sterile water/saline cooling. A rise of temperature and compression of the peri-implant bone are the consequences of this aspect of the procedure and may determine the future success of the treatment (compression-related bone loss). The cancellous bone's matrix is built of multiple trabeculae arranged along lines of stress providing bone's capacity to bear loads [95]. Therefore, the atraumatic surgical procedures minimizing the risk of bone loss should be implemented on a routine basis [9, 96]. The use of osteotome condenser drills may increase the primary stability and osseointegration [97], yet it may also disrupt the connectivity of the trabecular network, reducing its potential to transmit occlusal forces, thus the secondary stability is not obtained [95]. Moreover, using osteotomes applies high compressive force on the crestal bone, leading to its 22–50% more prominent decrease than during the conventional implantation [98], and to a 41% reduction in the amount of bone-to-implant contact [99]. Similar complications may be caused by high drilling torque, causing delayed healing [100, 101]. Drilling speed and the drill's diameter may also affect bone healing in the implant socket. In the trabecular bone, areas of osteocyte necrosis emerge when the drilling speed reaches 1500 rpm [97]. The larger the drill, the larger the area of damage (e.g., drill diameter 1.6 mm—distance of tissue necrosis 1040 μm; drill diameter 5 mm—distance of tissue necrosis 1400 μm), and less new bone created, which are associated with a higher drilling energy and rise of the temperature transmitted to the bone [97, 102, 103]. Thermal damage during drilling is inevitable, resulting in a local tissue necrosis when it lasts for more than 1 min at a temperature higher than 47 °C. A rise of temperature above this level

Table 3 Differences in temperature rise depending on the drill's diameter and rotation speed calculated at a force of 10 N and a drilling depth of 13 mm

Diameter of the drill (mm)	Rotation speed (rpm)	Temperature of the bone (°C)
3.0	800	37.3 ± 2.3
	1200	35.1 ± 2.2
	1600	34.2 ± 2.4
3.4	800	34.4 ± 2.0
	1200	34.1 ± 2.0
	1600	31.4 ± 0.4
3.8	800	38.5 ± 0.4
	1200	40.5 ± 1.3
	1600	35.6 ± 1.5

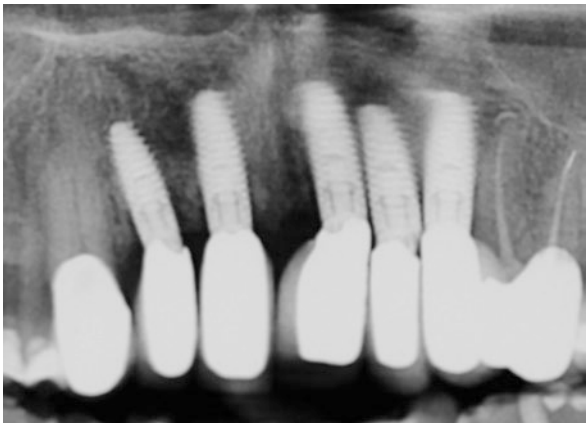

Fig. 8 The inappropriate implants position caused crestal bone loss 12 months after surgical treatment

impairs primary osseointegration, as the damaged osteocytes lack the ability for proper osseous remodeling [104–106]. The bone activity is arrested even after short exposure at 70 °C [107]. Bogovič and colleagues [108] used a thermal camera to picture the change in temperature during drilling, which showed that the highest temperatures were obtained upon drilling through the cortical bone and at the contact of the drill tip to the bone. A study utilizing an artificial bone model estimated the correlation between drilling speed and temperature changes in the implant socket on different drilling depths [104]. Repeatable patterns of temperature change at various drilling speeds (Table 2) were noticed.

The maximum rise of temperature was recorded at the depth of 10 mm, compared to 5 mm and 1 mm, without water cooling [104]. The study indicated that higher temperature and its faster increase were more eminent on the drill than in the bone, therefore following the manufacturer's speed recommendations ranging between 1000 to 1500 rpm with an adequate internal or external irrigation of the surgical site should substantially decrease the degree of the thermal damage. On the final note, it has to be reminded that blunt drills generate more heat than sharp ones, so their use should be avoided [109]. Another question arising is the sufficient amount of coolant to protect the surgical site from overheating. Sindel and colleagues [96] proved that the heat generated during drilling is not directly proportional to the coolant volume. In their study, the temperature of four drills of various diameter (2.8, 3.4, 3.8, 4.4 mm), rotating at 800 rpm and a torque of 55 N cm without any irrigation was statistically higher than when water cooling of 12 and 30 mL/min was administered. They also found no difference between 12 and 30 mL/min irrigation. Based on their report it was concluded that an external irrigation of 12 mL/min is sufficient in heat reduction during implant bed preparation, while excessive water cooling reduces the visibility of the surgical site [96]. Other studies speculated that the temperature rise was influenced by irrigation at a uniform speed of 90 mL/min during drilling, but not by a drill type [106]. Contrarily, a test on a bovine rib proved that the drill's diameter had the largest effect on the temperature rise (Table 3), while the drilling force and speed had a similar effect, with the

temperature decreasing almost equally with the increasing of both the force and the speed, due to their positive impact on the reduction of the drilling time [108].

In conclusion, recklessness and lack of experience in using the dedicated mechanical devices during implantation procedure may damage the bone's trabecular network, impair its ability to bear occlusal stress, and cause delay in a new bone formation around the implant [99].

3.3.4 Implant Position and Angulation

The position of the implanted screw and its angulation has its part in the peri-implantitis occurrence in patients (Fig. 8) [69].

More than 40% of the implants diagnosed with peri-implantitis presented with a too-buccal position [76]. The critical buccal bone thickness for preventing buccal-lingual bone resorption is estimated to be 1.5 mm [110]. An insufficient amount of crestal bone favors peri-implantitis development as a consequence of the implant's micro-rough surface contamination by the plaque-associated bacteria causing its chronic infection [110]. On the other hand, an apico-coronal implant position might dictate the long-term stability of the peri-implant tissues [9]. The depth of the implant placement is considered as risk factor when it measures ≥6 mm from the cement enamel junction of the adjacent tooth [111]. The implant location in the maxilla bears the risk of peri-implantitis [30], while in mandible is regarded safe [18], apart from the lower anterior region [15]. Generally speaking, implants with platform switching can be placed either at the bone level or subcrestally (up to 3 mm depending on implant design and local factors), while tissue-level implants need to be placed with its entire polished portion above the bone crest. Too deep placement of tissue-level implants will result in crestal bone loss. As mentioned previously, crestal bone stability requires previous development of soft tissue attachment that is determined by vertical thickness of gingiva. In vertically thick tissues, implant depth placement is decided upon the implant design. In order to increase the vertical dimension of soft tissues in case of thin phenotype, appropriate surgical approach should be chosen, that depends on anatomical limitations (e.g., subcrestal implant placement or soft tissue augmentation). All of these methods should protect the neck of the implant from exposure to peri-implant soft tissues in a process of crestal bone remodeling.

3.3.5 Bone Grafting and Antibiotics

There is no evidence to associate the use of a bone grafting material during surgery with peri-implantitis [27, 69], but some studies showed that grafts are less resistant to infection in comparison to the native bone [112]. Proceeding with an open flap technique during surgery is regarded as a risk factor, as it may be a cause of an interruption in periosteal blood supply from the elevated periosteum, which may further reduce the necessary blood supply to the cortical bone and impair its further

healing [113]. Insertion of the implant in the bone may disturb the blood flow inside it (a process called an avascular necrosis), promoting peri-implantitis development [114]. The administration of antibiotics at any time (pre/post-surgery) acts as a protective factor against peri-implantitis [18].

3.3.6 Number of Implants and Distance Between Them

The literature states that risk factors are the bone level counted in the implant's middle third and the implant's proximity to other teeth/implants [28]. The mesiodistal position could be a risk factor of peri-implantitis as it dictates space for performing oral hygiene and bacterial plaque removal. Also, if the distance between two adjacent dental implants or one implant with the adjoining teeth measures less than 3 mm, the process of bone remodeling may be impaired [115]. It is estimated that having more than two implants bears a higher risk of peri-implantitis [27].

4 Treatment

The treatment of peri-implantitis is still difficult and unreliable. It should be cause-related, as its etiology covers bacterial contamination and toxic activity of their by-products left on the implant surface. The therapy of all peri-implant diseases should be focused on minimization of the dental plaque deposition, while the prevention of peri-implantitis must cover prevention and treatment of its preceding form—peri-implant mucositis [116, 117]. The literature findings support the idea that lack of professionally administered supportive treatment of peri-implant mucositis can be attributed to a higher risk of peri-implantitis occurrence [116], therefore patient's motivation should be directed to an adequate plaque control. Effective teeth brushing, using mouth rinses, diminishing the influence of the patient-dependent risk factors, e.g., smoking, and balancing of the occlusion should be seen as prerequisites for a successful peri-implantitis treatment. The peri-implant mucositis responds well to the nonsurgical treatment, which is focused mainly on the patient's oral hygiene regimen. An efficient plaque removal ensures the effectiveness of peri-implant mucositis treatment methods [118, 119]. Colonization of the implant surfaces with bacterial biofilm occurs rapidly [120]. There are four types of bacteria adherence to the implant's surface [84]:

Type 1: random transport of bacteria to the surface
Type 2: initial, reversible adhesion
Type 3: strong adhesion to the surface by specific interactions
Type 4: surface colonization by multiple bacteria species, biofilm formation, and maturation

There are no widely accepted therapy standards of peri-implantitis treatment. The main goal is the plaque control in the implant area through debridement and

decontamination [117]; however, it has to be emphasized that peri-implantitis does not respond to nonsurgical methods as well as peri-implant mucositis [121–123]. The nonsurgical treatment methods of peri-implantitis cover:

1. Patient's education and motivation in keeping good oral hygiene
2. Decreasing role of patient-dependent risk factors
3. Ultrasonic cleaning
4. Sub-gingival closed flap debridement

The biofilm's removal from the implant's surface is a priority and the patient should be motivated to keep his hygiene at the level of type 2 of the bacterial adhesion (initial and reversible). Dudek and colleagues [17] treated peri-implant diseases according to their own classification scale (Table 1). In case of patients classified as stage I, the proposed treatment involved professional hygiene (scaling, ozone treatment, and decontamination with 0.12% CHX) and intensification of the home oral hygiene with additional mouth rinsing with 0.12% CHX. This treatment was effective in 66.6% of the stage I cases. Clinical studies on the effectiveness of a mechanical debridement alone using carbon/titanium fiber curettes, the Vector® system (Dürr Dental, Bietigheim-Bissigen, Germany), or ultrasonic devices showed that BoP was only slightly improved, while PD remained unchanged or even worsened [124, 125]. A photodynamic therapy (PDT), which stands for an application of photosensitive dyes into pathological pockets and their activation with light of a specific wavelength, results in the eradication of periodontal pathogens [126]. A toluidine blue O-mediated PDT proved to be effective in eradication of *Prevotella intermedia/nigrescens*, *Fusobacterium*, and beta-hemolytic *Streptococcus* [127]. In a clinical procedure, a photosensitive dye, e.g., chloride (HELBO® Blue Photosensitizer; Photodynamic Systems GmbH) is applied submucosally from the bottom to the top of the peri-implant pocket, is activated for 10 s using a hand-held diode laser (e.g., HELBO® TheraLite Laser, HELBO® 3D Pocket Probe; Photodynamic Systems GmbH) with a wavelength of 660 nm and a power density of 100 mW, and is left in situ for 3 min. Subsequently, the pocket should be irrigated with 3% hydrogen peroxide, according to the manufacturer's instructions. The procedure should be repeated after one week. Patient should be instructed to continue flossing the day

Table 4 The assumptions of the cumulative interceptive supportive therapy

Stadium	Clinical and radiological symptoms	Proposed treatment
A	PI (+); BoP (+); PD ≤3 mm; RTG (−)	Professional hygiene instructions and debridement
B	PI (+); BoP (+); PD 4–5 mm; RTG (−)	Professional hygiene instructions and debridement, administration of local antiseptics (e.g., CHX)
C	PI (+); BoP (+); PD >5 mm; RTG (bone loss ≤2 mm)	Professional hygiene instructions and debridement, microbiological tests, administration of antibiotics
D	PI (+); BoP (+); PD >5 mm; RTG (bone loss >2 mm)	Surgical treatment: resection and/or regeneration

Abbreviations: *PI* (+) presence of dental plaque, *BoP* bleeding on probing, *PD* pocket depth, *RTG* radiograph, *RTG* (−) no pathological changes on radiograph, *CHX* chlorhexidine

after treatment. In a 6-month observation study, Schär and colleagues [128] observed no statistically relevant differences between subjects treated with either PDT or local drug delivery in terms of BoP, PD, clinical attachment level (CAL), and mucosal inflammation. They suggested that an adjunctive PDT may be used as an alternative nonsurgical treatment. A review by an American Academy of Periodontology confirmed that PDT may provide similar clinical improvements in PD and CAL when compared with conventional periodontal therapy in both periodontal and peri-implant patients [129]. Moreover, a study conducted by Romeo and colleagues [130] showed a 70% reduction in the PI values and a 60% reduction in PD values, when PDT was used as an additional therapy to supportive nonsurgical treatment. Based on that, PDT should be considered an additional procedure in both nonsurgical and surgical treatment methods of peri-implantitis [130].

The nonsurgical treatment methods of peri-implantitis may be considered successful if they fulfill the short-term goal, which is the reduction of a supragingival dental plaque and therewith preparation of the corrective (surgical) phase, and a long-term goal, which is maintenance of the treatment success after the corrective phase [131]. The surgical phase should be implemented only when the oral hygiene regimen is achieved, validated by the PI <1 [131].

The surgical treatment methods of peri-implantitis cover:

1. Implant surface debridement
   (a) closed flap debridement

Table 5 The assumptions of the BMP scale

Stadium	Clinical symptoms	Radiological symptoms (bone loss)	Treatment and prognosis
1	BoP (−); PD 2–3 mm; tooth mobility (−)	Bone loss 10–25%	No treatment Good prognosis
2	BoP (+); PD 4–6 mm; tooth mobility stage 1	Bone loss 25–50% Bone loss configuration: A. Vertical <2–4 mm B. Horizontal < half length of the implant screw C. Combined	 GBR, osteoplasty APF, GBR, osteoplasty Bone augmentation, GBR Good prognosis
3	BoP (+); PD 6–8 mm; tooth mobility stage 2	Bone loss >50% Bone loss configuration: A. Vertical <2–4 mm B. Horizontal < half length of the implant screw C. Combined	 GBR, ABWG Bone augmentation, GBR Explantation Questionable prognosis
4	BoP (+); PD >8 mm; tooth mobility stage 3	Bone loss >50%	Explantation Bad prognosis

Abbreviations: *BoP* bleeding on probing, *PD* pocket depth, *GBR* guided bone regeneration, *APF* apical positioning of the flap, *ABWG* autogenous bone wedge grafting

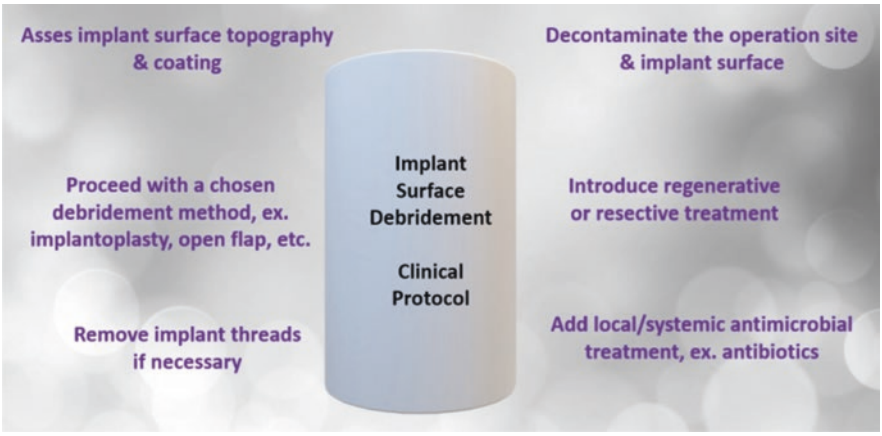

Fig. 9 Correlation of treatment methods supporting implant surface debridement

(b) open flap debridement alone or with an adjunctive resective therapy (e.g., apical positioning of the flap, osteoplasty)
(c) implantoplasty

2. Soft tissue grafting procedures

(a) enlargement of the width of the keratinized mucosa by means of an apically positioned flap/vestibuloplasty (alone or in combination with a free gingival graft)
(b) gain of soft tissue volume using a subepithelial connective tissue graft or soft tissue graft

3. Bone grafting

(a) using bone fillers/autografts
(b) guided bone regeneration
(c) replacement graft

4. Explantation

The variety of treatment methods exceeds the rate of this chapter, but the chosen therapy methods are discussed below. In 2004, Lang and colleagues [132] introduced a treatment protocol known as a cumulative interceptive supportive therapy (CIST) (Table 4), which relied on the clinical and radiological state of the tissues surrounding dental implant.

The range of the treatment methods was correlated to the stage of the disease, which resulted from both the clinical and radiological symptoms, such as presence of the dental plaque on four surfaces of the prosthesis placed on the implant, presence of BoP, evaluated PD counted in mm, and the presence of radiological signs of bone loss around the implant screw. According to this protocol, if a PD is $\leq$3 mm and there is no presence of PI and/or BoP, no medical intervention should be

Table 6 Examples of antimicrobial therapy in association with peri-implant nonsurgical/surgical treatment

Author (year of publication)	Treatment	Way of administration	Duration
Cha (2019) [136, 139]	Open flap debridement + minocycline ointment (10 mg of minocycline in 0.5 g of ointment applicator) + (Amoxicillin 500 mg + Ibuprofen 600 mg)	Minocycline local Amoxicillin and Ibuprofen systemic	During surgery + at check-ups after 1 month and 3 months 3 times for 3 days
Shibli (2019) [137]	Non-surgical treatment + debridement + (Amoxicillin 500 mg + Metronidazole 400 mg)	Systemic	Both 3× daily for 14 days
Dudek (2015) [17]	Clindamycin 1200 mg (24 h dosage)	Local	1200 mg daily for 10 days
Roos-Jansåker (2014) [138]	Surgical treatment (bone substitute with/without membrane + implant decontamination with 3% H_2O_2 + mouth rinse (0.1% CHX) + (Amoxicillin 375 mg + Metronidazole 400 mg) + (Ibuprofen 400 mg)	CHX local Amoxicillin, Metronidazole and Ibuprofen systemic	0.% CHX rinse daily for 5 weeks following surgery Amoxicillin: 375 mg 3× daily for 10 days following surgery Metronidazole: 400 mg 2× daily for 10 days following surgery Ibuprofen 400 mg once a day for 3 days
Serino and Turri (2011) [139]	Resective therapy + osteoplasty + implant decontamination with CHX + mouth rinse (0.12% CHX) + (Clindamycin 300 mg)	CHX local Clindamycin systemic	0.12% CHX rinse 2× daily for 1 min for 2 weeks following surgery Clindamycin: 300 mg 3× daily for 7 days before surgery
Mombelli et al.(2001) [140]	Non-surgical treatment + debridement + mouth rinse (0.2% CHX) + Tetracycline fibers	Local	0.2% CHX rinse daily for 2 weeks Tetracycline fibers left in pocket for 10 days, coated with cyanoacrylate adhesive for protection

implemented. The peri-implantitis lesions with more than 2 mm of bone loss require initial therapy followed by either resective or regenerative surgery [133]. It must be emphasized that this protocol justifies using surgical methods only at the worst stage of the disease, with PD >5 mm and bone loss >2 mm seen on the radiograph. Further limitations of this protocol are the lack of diversity of the treatment methods depending on the configuration of the bone loss and lack of the treatment's prognosis. Therefore, Passi and colleagues [134] introduced a new protocol, called bleeding, bone loss, mobility, probing depth, proposed treatment, and prognosis (BMP) scale, which completes the CIST scale (Table 5).

Implant surface's debridement alone is considered insufficient to promote regeneration of the bone and/or its re-osteointegration with the alveolar process. Therefore, surgical treatment methods may be supplemented by other methods, including decontamination and antimicrobial treatment (Fig. 9).

The methods of implant surface decontamination include air-powder abrasives, citric acid, and antimicrobial agents, such as CHX, 3% H_2O_2, and betadine. Geremias and colleagues [135] have evaluated three debridement methods (implantoplasty, open flap debridement alone and combined with an additional chemical decontamination using citric acid for two minutes) and came out with a conclusion that the growth of Streptococcus mutans was similarly arrested after implantoplasty and debridement following disinfection with citric acid. Both nonsurgical and surgical peri-implantitis treatment may be coupled with an antimicrobial therapy (Table 6).

Bacteria in peri-implantitis are sensitive to amoxicillin, penicillin G, combination of amoxicillin and metronidazole, and combination of amoxicillin and clavulanate [141]. The most common antibiotics used in peri-implantitis are metronidazole and amoxicillin (alone or combined), as their adjunctive action suppresses gram-negative bacteria development [137, 142], apart from the patients treated by an open flap debridement [143]. The oral administration of antibiotics cover the time before and after the surgery, while minocycline and tetracycline are mainly used as a local therapy, placed directly into the surgical area [136, 144]. Local and/or systemic administration of antimicrobial agents along with the nonsurgical peri-implantitis therapy was proven to be effective only if the bone loss is less than 2 mm [145]. Administration of the systemic antibiotics should also be preceded by bacterial susceptibility tests [133], and it has to be remembered that the repeated systemic application of antibiotics may increase the risk of reinfection resulting from their gained resistance to drugs [144].

The aim of the surgical treatment, such as open flap debridement, osteoplasty, and implantoplasty, is to dispose of the inflammatory granuloma around the implant screw when it is unveiled and can be mechanically cleaned under direct sight. Further procedures, such as regenerative therapies, depend on the clinical situation disclosed during reinspection of the implant screw. An implantoplasty is a surgical procedure which stands for a smoothening of the bacteria-contaminated implant's surface using a fine grid polishing diamond and a rubber polisher. In this procedure, the roughness of the implant surface is diminished, so the bacterial biofilm formation is disrupted. It is usually done with diamond coated or carborundum rotary burs; however, plastic curettes are also acceptable [146, 147]. An additional

Fig. 10 Classification of the bone defects around dental implants by Schwarz [150]

chemical disinfection of the cleaned surfaces and/or bone grafting is recommended. Using rotary burs with an additional cooling proved to be safe to the surrounding bone [135], yet the most important disadvantage of the procedure is the marginal recession leading to exposure of the abutment and further food impaction. The reduction in the bacterial load at sites with peri-implantitis by means of mechanical debridement alone may be difficult because of the design of the suprastructure and the topography of the implant surface [84, 87–89, 128, 137, 148, 149].

The bone grafting materials are used simultaneously with the surgical procedure to regenerate the lost bone. These combined methods proved to be effective, as a diminished BoP, improved PD, CAL, and radiographic bone view were shown in a long-term clinical trial [146]. Schwarz and colleagues divided the bone defects around dental implants into categories (Fig. 10) [150].

The most common defects in human are mixed, vertical, and horizontal defects. Taking only the intrabony defects, the most common are defects Ie (55.3%), while Ia are the most rare (5.4%) [150]. The best results of the bone regenerative therapy with bone grafts are expected in Ie defects, as they have the best biological potential and provide good stabilization for the bone grafts. The therapy protocol proposed by Dudek and colleagues [17] for the patients classified as stages II and III (Table 1) was mainly surgical and involved bone regeneration using pure titan granulate Tigran Natix® White and collagen membranes OsteoBiol® (Tecnoss® Dental s.r.l., Italy), or implant removal and bone augmentation. These methods were effective in 41.6% of class II cases and in 26.9% of class III cases, which indicates far less successful rate of the proposed regenerative treatment than expected. The outcomes of a retrospective analysis showed that the initial bone grafting procedures (lateral ridge augmentation using a particulated bone substitute and collagen membrane for maxillary sinus floor elevation) at the implant sites did not influence the effectiveness of a combined surgical therapy of peri-implantitis [147]. Based on that, some researchers concluded that there are no indications for an additional bone grafting or use of barrier membranes during the surgical peri-implantitis treatment [151]. The need for an independent grafting vs combined surgical methods should be

respected individually based on the clinical and radiological outcomes and the patient's wishes.

The coexisting defects of the mucosa around dental implant can be corrected using soft tissue plastic reconstruction therapies. Miller and colleagues have introduced a scale of the gingival recession defects in which four classes are recognized:

1. Class I—marginal tissue recession which does not extend to mucogingival junction, with no bone loss in the interdental area
2. Class II—marginal tissue recession which extends to or beyond the mucogingival junction, with no bone loss in the interdental area
3. Class III—marginal tissue recession which extends to or beyond the mucogingival junction, with bone loss in the interdental area. The presence of teeth malpositioning is detected, which interrupts with the necessary regenerative treatment

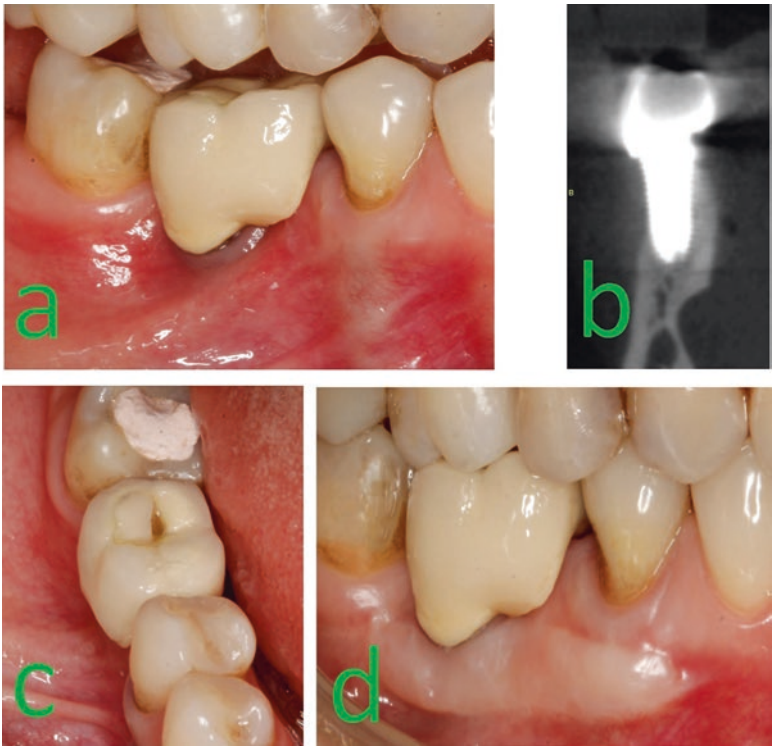

Fig. 11 An example of a reconstruction of the keratinized gingiva around dental implant using a free gingival graft from the palate. (**a**) Lack of keratinized gingiva and signs of soft tissue inflammation around the implant in the position 46. Probing pocket depth <4 mm. (**b**) Lack of buccal bone on the implant in CBCT scan. (**c**) The tissues around implant are mobile, there is visible muscle pull. (**d**) Clinical situation 6 months after reconstruction of keratinized gingiva with free gingival graft taken from the palate. The tissues become immobile. Probing pocket depth <3 mm and no signs of inflammation

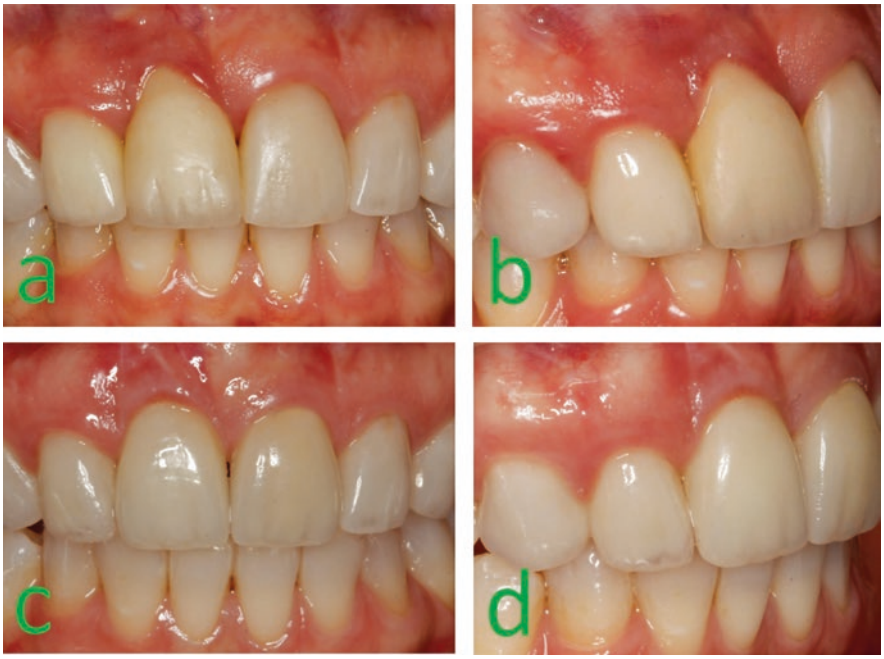

Fig. 12 Coverage of gum recession using a connective tissue graft from the palate in a tunnel technique. (**a**) Recession around the implant in the position of tooth 11—front view. (**b**) Recession around the implant in the position of tooth 11—lateral view. (**c**) Clinical situation 6 months after soft tissue augmentation with subepithelial connective tissue graft taken from the palate and tunnel technique—significant improvement and partial recession coverage. (**d**) Clinical situation 6 months after soft tissue augmentation—lateral view

4. Class IV—marginal tissue recession which extends to or beyond the mucogingival junction and a severe bone loss of the alveolar process is detected, with exposure of more than one proximal root surface [152]

The subepithelial connective tissue grafts are mainly taken from the palate and, according to research, are the best treatment options in Miller Class I and II gingival recession defects, as they provide reliable results, such as an increase in keratinized tissue width, CAL level, and esthetics [153]. Shah and colleagues [154] recommend a two-stage procedure in case of a thin mucosa profile with a minimal width or lack of peri-implant keratinized gingiva—a subepithelial connective tissue graft from the palate in combination with a coronally advanced flap in order to cover the dehiscence in the first instance, and secondly, after a healing period of 3 months, a vestibuloplasty in combination with a free gingival graft to create an adequate peri-implant cuff of a keratinized mucosa. As the proper width and horizontal thickness of the keratinized mucosa surrounding dental implant is crucial for the prevention of peri-implant diseases, the connective soft tissue grafts are highly appreciated, as they provide reliable and long-term results (Figs. 11 and 12).

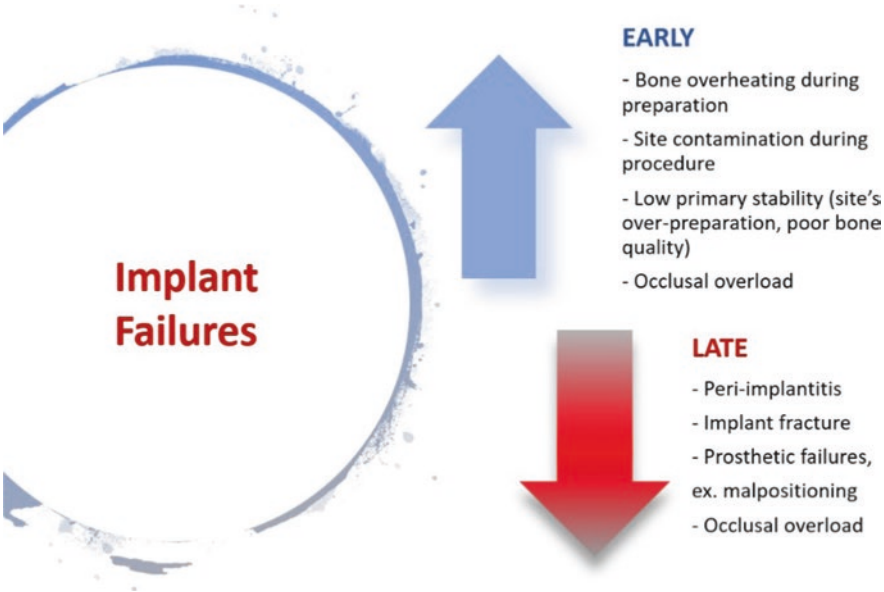

Fig. 13 Early and late causes of implant failure

Implant failures can be divided according to the time of their occurrence (Fig. 13) [155]. The early failures occur before the implants are functionally loaded. In such cases, the osteointegration process is not obtained, so the implants are mobile and can be easily removed. On the other hand, late failures are observed after loading, and are mainly due to biological or prosthetic reasons (Fig. 14) [155].

Implant's explanation should be regarded as the last treatment option. Unfortunately, peri-implantitis remains the main reason for late implant failure [156]. The indications for this procedure must be thoroughly examined, and the only absolute indication for it should be the implant's mobility due to the advanced bone resorption [157]. The implant type might also affect the decision of its removal, as threaded screws are far more easy to be removed, on contrary to circumferential plateau design implants, whose surface area is more sophisticated, making their removal more risky in terms of extensity of the procedure. The patient's opinion should be also taken into consideration, as explanation might be emotionally and financially stressful [157]. The indications in favor of explanation include patients before radiotherapy with an advanced peri-implantitis (if the implants are positioned in the area of radiation), bone loss of more than two-thirds of the implant length, and hollow-cylinder implants (if they are early recognized on the radiograph as unsuccessful) [156]. It must be remembered that the idea of strictly following the level of bone loss of two-thirds of the implant length may not be applicable to short and tapered implants (e.g., 8 mm implants) [158]. During the explanation procedure, the bony defects should be regenerated to prepare the alveolar process for the

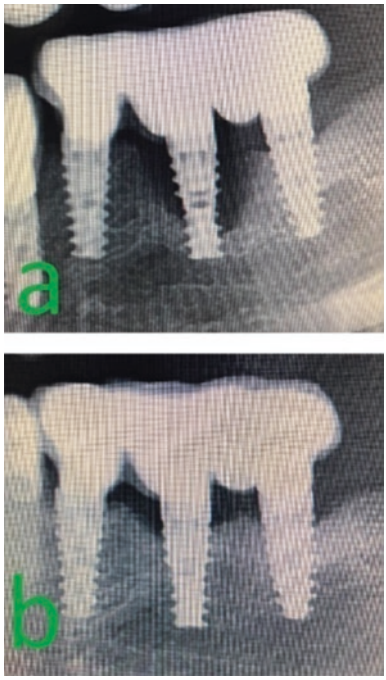

Fig. 14 Prosthetic mistakes may lead to an implant loss: (**a**) Crestal bone loss around all three implants due to prosthetic mistreatment. There are indications for the explanation of the middle implant and the removal of prosthetic restoration. However, the patient did not give his consent for the proposed treatment. (**b**) Radiological situation 12 months after surgical treatment (guided tissue regeneration with deproteinized bovine bone mineral and collagen membrane). Significant defect fill. Due to abovementioned factors, the long-term prognosis is poor. (Thanks to the courtesy of Dr. Kamila Kozak-Jastrzębska)

next implant placement. It is also acceptable for the successor implant to be larger to fit the space after the predecessor's removal, especially when an immediate replacement procedure is administered [159].

5 Conclusion

The high success rates of placing dental implants are mostly attributed to establishing a long-standing osseointegration of the screw. Along with the rising number of dental implants installed in patients, long-term complications may occur, involving bacterial contamination and loss of bone support. Peri-implant health problems, involving peri-implant mucositis and peri-implantitis, are complex diseases, which occurrence is modified by a specific bacteria flora infecting dental implants and multiple patient and nonpatient risk factors. The recognition and treatment of the

peri-implant health problems is difficult and the dentists' experience in this field is a must. The treatment methods cover both the nonsurgical and surgical aspects, and their coordination depends on the clinician. The main goal is to prevent dental implants from bacteria attack through professionally administered and home oral hygiene. Well designed and balanced occlusion of the prosthetic devices based on implants screws are vital in the prevention of peri-implant health problems, and their impact on the patient's oral health lies within the dentist's experience.

References

1. Abraham CM. A brief historical perspective on dental implants, their surface coatings and treatments. Open Dent J. 2014;8(Suppl. 1-M2):50–5.
2. de Mello JS, Faot F, Correa G, Chagas Júnior OL. Success rate and complications associated with dental implants in the incisive canal region: a systematic review. Int J Oral Maxillofac Surg. 2017;46(12):1584–91.
3. Lee KJ, Cha JK, Sanz-Martin I, Sanz M, Jung UW. A retrospective case series evaluating the outcome of implants with low primary stability. Clin Oral Implants Res. 2019;30(9):861–71.
4. Moraschini V, Barboza E. Success of dental implants in smokers and non-smokers: a systematic review and meta-analysis. Int J Oral Maxillofac Surg. 2016;45(2):205–15.
5. Papaspyridakos P, BarizanBordin T, Kim YJ, DeFuria C, Pagni SE, Chochlidakis K, Rolim Teixeira E, Weber HP. Implant survival rates and biologic complications with implant-supported fixed complete dental prostheses: a retrospective study with up to 12-year follow-up. Clin Oral Implants Res. 2018;29(8):881–93.
6. Albrektsson T, Isidor F. Consensus report of session IV. In: Lang NP, Karring T, editors. Proceedings of the 1st European workshop on periodontology. Chicago, IL: Quintessence; 1994. p. 365.
7. Caton JG, Armitage G, Berglundh T, Chapple ILC, Jepsen S, Kornman KS, Mealey BL, Papapanou PN, Sanz M, Tonetti MS. A new classification scheme for periodontal and peri-implant diseases and conditions—introduction and key changes from the 1999 classification. J Clin Periodontol. 2018;45(Suppl. 20):S1–8.
8. Fu JH, Wang HL. Can periimplantitis be treated? Dent Clin N Am. 2015;59(4):951–80.
9. Monje A, Insua A, Wang HL. Understanding peri-implantitis as a plaque-associated and site-specific entity: on the local predisposing factors. J Clin Med. 2019;8(2):279–97.
10. Schwarz F, Derks J, Monje A, Wang HL. Peri-implantitis. J Clin Periodontol. 2018;45(Suppl. 20):S246–66.
11. Derks J, Tomasi D. Peri-implant health and disease. A systematic review of current epidemiology. J Clin Periodontol. 2015;42(Suppl. 16):S158–71.
12. Charalampakis G, Jansåker E, Roos-Jansåker A-M. Definition and prevalence of peri-implantitis. Curr Oral Health Rep. 2014;1(4):239–50.
13. De Martinis TE, Berardini M, Trisi P. Nonsurgical management of peri-implant bone loss induced by residual cement: retrospective analysis of six cases. Int J Periodontics Restorative Dent. 2019;39(1):89–94.
14. Francetti L, Cavalli N, Taschieri S, Corbella S. Ten years follow-up retrospective study on implant survival and prevalence of peri-implantitis in implant-supported full-arch rehabilitation. Clin Oral Implants Res. 2019;30(3):252–60.
15. Rodrigo D, Sanz-Sánchez I, Figuero E, Llodrá JC, Bravo M, Caffesse RG, Vallcorba N, Guerrero A, Herrera D. Prevalence and risk indicators of peri-implant diseases in Spain. J Clin Periodontol. 2018;45(12):1510–20.

16. Goh MS, Hong EJ, Chang M. Prevalence and risk indicators of peri-implantitis in Korean patients with a history of periodontal disease: a cross-sectional study. J Periodontal Implant Sci. 2017;47(4):240–50.
17. Dudek D, Segiet O, Reichman-Warmusz E, Wałach K, Matusek M, Koleżyńska B, Sołtykiewicz K, Helewski K. The compare study of periimplantitis—4 years of clinical observation. Implant Dent. 2015;2:6–13.
18. KordbachehChangi K, Finkelstein J, Papapanou PN. Peri-implantitis prevalence, incidence rate and risk factors: a study of electronic health records at a U.S. dental school. Clin Oral Implants Res. 2019;30(4):306–14.
19. Lee CT, Huang YW, Zhu L, Weltman R. Prevalences of peri-implantitis and peri-implant mucositis: systematic review and meta-analysis. J Dent. 2017;62:1–12.
20. Lafaurie GI, Sabogal MA, Castillo DM, Ricón MV, Gómez LA, Lesmes YA, Chambrone L. Microbiome and microbial biofilm profiles of peri-implantitis: a systematic review. J Periodontol. 2017;88(10):1066–89.
21. Sanz-Martin I, Doolittle-Hall J, Teles RP, Patel M, Belibasalius GN, Hämmerle CHF, Jung RE, Teles FRF. Exploring the microbiome of healthy and diseased peri-implant sites using illumina sequencing. J Clin Periodontol. 2017;44:1274–84.
22. Soriano-Lerma A, Magán-Fernández A, Gijón J, Sánchez-Fernández E, Soriano M, Garcia-Salcedo JA, Mesa F. Short-term effects of hyaluronic acid on the subgingival microbiome in peri-implantitis. A randomized controlled clinical trial. J Periodontol. 2019; https://doi.org/10.1002/JPER.19-0184. [Epub ahead of print].
23. Schincaglia GP, Hong BY, Rosania A, Barasz J, Thompson A, Sobue T, Panagakos F, Burleson JA, Dongari-Bagtzoglou A, Diaz PI. Clinical, immune, and microbiome traits of gingivitis and peri-implant mucositis. J Dent Res. 2017;96:47–55.
24. Pimentel SP, Fontes M, Ribeiro FV, Corrêa MG, Nishii D, Cirano FR, Casati MZ, Casarin RCV. Smoking habit modulates peri-implant microbiome: a case-control study. J Periodontal Res. 2018;53:983–91.
25. Linkevičius T. Surgical factors for establishing crestal bone stability. In: Linkevičius T, editor. Zero bone loss concepts. Batavia: Quintessence Publishing Co., Inc.; 2019. p. 4–15.
26. Monje A, Aranda L, Diaz KT, Alarcón MA, Bagramian RA, Wang HT, Catena A. Impact of maintenance therapy for the prevention of peri-implant diseases: a systematic review and meta-analysis. J Dent Res. 2016;95(4):372–9.
27. Atieh MA, Pang JK, Lian K, Wong S, Tawse-Smith A, Ma S, Duncan WJ. Predicting peri-implant disease: chi-square automatic interaction detection (CHAID) decision tree analysis of risk indicators. J Periodontol. 2019;90(8):834–46.
28. de Araújo NM, Mano Azul A, Rocha E, Maló P, Salvado F. Attributable fractions, modifiable risk factors and risk stratification using a risk score for peri-implant pathology. J Prosthodont Res. 2017;61(1):43–53.
29. de Araújo Nobre M, Mano Azul A, Rocha E, Maló P. Risk factors of peri-implant pathology. Eur J Oral Sci. 2015;123(3):131–9.
30. Konstantinidis IK, Kotsakis GA, Gerdes S, Walter MH. Cross-sectional study on the prevalence and risk indicators of peri-implant diseases. Eur J Oral Implantol. 2018;8(1):75–88.
31. Gurgel BCV, Montenegro SCL, Dantas PMC, Pascoal ALB, Lima KC, Calderon PDS. Frequency of peri-implant diseases and associated factors. Clin Oral Implants Res. 2017;28(10):1211–7.
32. Dalago HR, Schuldt Filho G, Rodrigues MA, Renvert S, Bianchini MA. Risk indicators for peri-implantitis. A cross-sectional study with 916 implants. Clin Oral Implants Res. 2017;28(2):144–50.
33. Veitz-Keenan A, Keenan JR. Implant outcomes poorer in patients with history of periodontal disease. Evid Based Dent. 2017;18(1):5.
34. Becker ST, Beck-Broichsitter BE, Graetz C, Dörfer CE, Wiltfang J, Häsler R. Peri-implantitis versus periodontitis: functional differences indicated by transcriptome profiling. Clin Implant Dent Relat Res. 2014;16(3):401–11.

35. Van Velzen FJ, Lang NP, Schulten EA, Ten Bruggenkate CM. Dental floss as a possible risk for the development of peri-implant disease: an observational study of 10 cases. Clin Oral Implants Res. 2016;27(5):618–21.
36. Rotundo R, Prato GPP. A new computerized method for evaluating risk profiles of periodontal patients. PERIO. 2007;4(2):139–49.
37. Vignoletti F, Di Domenico DL, Di Martino M, Montero E, de Sanctis M. Prevalence and risk indicators of peri-implantitis in a sample of university-based dental patients in Italy: a cross-sectional study. J Clin Periodontol. 2019;46(5):597–605.
38. Farina R, Filippi M, Brazzioli J, Tomasi C, Trombelli L. Bleeding on probing around dental implants: a retrospective study of associated factors. J Clin Periodontol. 2017;44(1):115–22.
39. Ramanauskaite A, Becker K, Schwarz F. Clinical characteristics of peri-implant mucositis and peri-implantitis. Clin Oral Implants Res. 2018;29(6):551–6.
40. Monje A, Caballé-Serrano J, Nart J, Peñarrocha D, Wang HL, Rakic M. Diagnostic accuracy of clinical parameters to monitor peri-implant conditions: a matched case-control study. J Periodontol. 2018;89:407–17.
41. de Araújo Nobre M, Salvado F, Nogueira P, Rocha E, Ilg P, Maló P. A peri-implant disease risk score for patients with dental implants: validation and the influence of the interval between maintenance appointments. J Clin Med. 2019;8(2):252–64.
42. Howe MS. Implant maintenance treatment and peri-implant health. Evid Based Dent. 2017;18(1):8–10.
43. Sgolastra F, Petrucci A, Severino M, Gatto R, Monaco A. Smoking and the risk of peri-implantitis. A systematic review and meta-analysis. Clin Oral Implants Res. 2015;26(4):e62–7.
44. Stacci C, Berton F, Perinetti G, Frassetto A, Lombardi T, Khoury A, Andolsek F, Di Lenarda R. Risk factors for peri-implantitis: effect of history of periodontal disease and smoking habits. A systematic review and meta-analysis. J Oral Maxillofac Res. 2016;3(7):e3.
45. Monje A, Asa'ad F, Larsson L, Giannobile W, Wang HL. Editorial epigenetics: a missing link between periodontitis and peri-implantitis? Int J Periodontics Restorative Dent. 2018;38(4):476–7.
46. Razzouk S, Sarkis R. Smoking and diabetes. Epigenetics involvement in osseointegration. N Y State Dent J. 2013;79(2):27–30.
47. Monje A, Catena A, Borgnakke WS. Association between diabetes mellitus/hyperglycaemia and peri-implant diseases: systematic review and meta-analysis. J Clin Periodontol. 2017;44(6):636–48.
48. Cho-Yan Lee J, Mattheos N, Nixon KC, Ivanovski S. Residual periodontal pockets are a risk indicator for peri-implantitis in patients treated for periodontitis. Clin Oral Implants Res. 2012;23(3):325–33.
49. Berglundh T, Armitage G, Araújo MG, Avila-Ortiz G, Blanco J, Camargo PM, Chen S, Cochran D, Derks J, Figuero E, Hämmerle CHF, Heitz-Mayfield LJA, Huynh-Ba G, Iacono V, Koo KT, Lambert F, McCauley L, Quirynen M, Renvert S, Salvi GE, Schwarz F, Tarnow D, Tomasi C, Wang HL, Zitzmann N. Peri-implant diseases and conditions: consensus report of workgroup 4 of the 2017 World Workshop on the Classification of Periodontal and Peri-Implant Diseases and Conditions. J Periodontol. 2018;89(Suppl. 1):S313–8.
50. Serino G, Ström C. Peri-implantitis in partially edentulous patients: association with inadequate plaque control. Clin Oral Implants Res. 2009;20(2):169–74.
51. Katafuchi M, Weinstein BF, Leroux BG, Chen YW, Daubert DM. Restoration contour is a risk indicator for peri-implantitis: a cross-sectional radiographic analysis. J Clin Periodontol. 2018;45(2):225–32.
52. Abrahamsson I, Berglundh T, Lindhe J. The mucosal barrier following abutment dis/reconnection. An experimental study in dogs. J Clin Periodontol. 1997;24(8):568–72.
53. Galindo-Moreno P, León-Cano A, Ortega-Oller I, Monje A, Suárez F, O'Valle F, Spinato S, Catena A. Prosthetic abutment height is a key factor in peri-implant marginal bone loss. J Dent Res. 2014;93(Suppl. 7):S80–5.

54. Galindo-Moreno P, León-Cano A, Monje A, Ortega-Oller I, O'Valle F, Catena A. Abutment height influences the effect of platform switching on peri-implant marginal bone loss. Clin Oral Implants Res. 2015;27(2):167–73.
55. Degidi M, Daprile G, Piattelli A. Marginal bone loss around implants with platform-switched Morse-cone connection: a radiographic cross-sectional study. Clin Oral Implants Res. 2017;28(9):1108–12.
56. Galindo-Moreno P, Fernández-Jiménez A, O'Valle F, Monje A, Silvestre FJ, Juodzbalys G, Sánchez-Fernández E, Catena A. Influence of the crown-implant connection on the preservation of peri-implant bone: a retrospective multifactorial analysis. Int J Oral Maxillofac Implants. 2015;30(2):384–90.
57. Wilson TG Jr. The positive relationship between excess cement and peri-implant disease: a prospective clinical endoscopic study. J Periodontol. 2009;80(9):1388–92.
58. Nóvoa L, Batalla P, Caneiro L, Pico A, Liñares A, Blanco J. Influence of abutment height on maintenance of peri-implant crestal bone at bone-level implants: a 3-year follow-up study. Int J Periodontics Restorative Dent. 2017;37:721–7.
59. López-López PJ, Mareque-Bueno J, Boquete-Castro A, Aguilar-Salvatierra Raya A, Martinez-González JM, Calvo-Guirado JL. The effects of healing abutments of different size and anatomic shape placed immediately in extraction sockets on peri-implant hard and soft tissues. A pilot study in foxhound dogs. Clin Oral Implants Res. 2016;27:90–6.
60. Souza AB, Alshihri A, Kämmerer PW, Araújo MG, Gallucci GO. Histological and micro-CT analysis of peri-implant soft and hard tissue healing on implants with different healing abutments configurations. Clin Oral Implants Res. 2018;29:1007–15.
61. Scarano A, Piattelli M, Caputi S, Favero GA, Piattelli A. Bacterial adhesion on commercially pure titanium and zirconium oxide disks: an *in vivo* human study. J Periodontol. 2004;75:292–6.
62. van Brakel R, Cune MS, van Winkelhoff AJ, de Putter C, Verhoeven JW, van der Reijden W. Early bacterial colonization and soft tissue health around zirconia and titanium abutments: an *in vivo* study in man. Clin Oral Implants Res. 2011;22:571–7.
63. Nothdurft FP, Fontana D, Ruppenthal S, May A, Aktas C, Mehraein Y, Lipp P, Kaestner L. Differential behaviour of fibroblasts and epithelial cells on structured implant abutment materials: a comparison of materials and surface topographies. Clin Implant Dent Relat Res. 2015;17:1237–49.
64. Linkevičius T, Vaitelis J. The effect of zirconia or titanium as abutment material on soft peri-implant tissues: a systematic review and meta-analysis. Clin Oral Implants Res. 2015;26(Suppl. 11):139–47.
65. Kawahara H, Kawahara D, Hashimoto K, Takashima Y, Ong JL. Morphologic studies on the biologic seal of titanium dental implants. Report I. *In vitro* study on the epithelialization mechanism around the dental implant. Int J Oral Maxillofac Implants. 1998;13:457–64.
66. Kawahara H, Kawahara D, Mimura Y, Takashima Y, Ong JL. Morphologic studies on the biologic seal of titanium dental implants. Report II. *In vivo* study on the defending mechanism of epithelial adhesions/attachment against invasive factors. Int J Oral Maxillofac Implants. 1998;13:465–73.
67. Baharloo B, Textor M, Brunette DM. Substratum roughness alters the growth, area, and focal adhesions of epithelial cells, and their proximity to titanium surfaces. J Biomed Mater Res A. 2005;74:12–22.
68. Mehl C, Kern M, Zimmermann A, Harder S, Huth S, Selhuber-Unkel C. Impact of cleaning procedures on adhesion of living cells to three abutment materials. In J Oral Maxillofac Implants. 2017;32:976–84.
69. Canullo L, Peñarrocha-Oltra D, Covani U, Botticelli D, Serino G, Penarrocha M. Clinical and microbiological findings in patients with peri-implantitis: a cross-sectional study. Clin Oral Implants Res. 2016;27(3):376–82.
70. Peri-implant mucositis and peri-implantitis: a current understanding of their diagnoses and clinical implications. J Periodontol. 2013;84:436–43.

71. Linkevičius T, Puisys A, Vindasiute E, Linkeviciene L, Apse P. Does residual cement around implant-supported restorations cause peri-implant disease? A retrospective case analysis. Clin Oral Implants Res. 2013;24(11):1179–84.
72. Sailer I, Mühlemann S, Zwahlen M, Hämmerle CH, Schmeider D. Cemented and screw-retained implant reconstructions: a systematic review of the survival and complication rates. Clin Oral Implants Res. 2012;23(Suppl. 6):163–201.
73. Linkevičius T, Vindašiūte E, Puišys A, Pečiulienė V. The influence of margin location on the amount of undetected cement excess after delivery of cement-retained implant restorations. Clin Oral Implants Res. 2011;22:1379–84.
74. Vindašiūtė E, Puišys A, Maslova N, Linkevičienė L, Pečiulienė V, Linkevičius T. Clinical factors influencing removal of the cement excess in implant-supported restorations. Clin Implant Dent Relat Res. 2015;17:771–8.
75. Monje A, Blasi G. Significance of keratinized mucosa/gingiva on peri-implant and adjacent periodontal conditions in erratic maintenance compliers. J Periodontol. 2019;90(5):445–53.
76. Monje A, Galindo-Moreno P, Tözüm TF, Suárez-López del Amo F, Wang HL. Into the paradigm of local factors as contributors for peri-implant disease: short communication. Int J Oral Maxillofac Implants. 2016;31(2):288–92.
77. Lang NP, Löe H. The relationship between the width of keratinized gingiva and gingival health. J Periodontol. 1972;43(10):623–7.
78. Zigdon H, Machtei EE. The dimensions of keratinized mucosa around implants affect clinical and immunological parameters. Clin Oral Implants Res. 2008;19(4):387–92.
79. Small PN, Tarnow DP. Gingival recession around implants: a 1-year longitudinal prospective study. Int J Oral Maxillofac Implants. 2000;15:527–32.
80. Linkevičius T, Puišys A, Steigmann M, Vindašiūtė E, Linkevičienė L. Influence of vertical soft tissue thickness on crestal bone changes around implants with platform switching: a comparative clinical study. Clin Implant Dent Relat Res. 2015;17:1228–36.
81. Puišys A, Vindašiūte E, Linkevičius T. The use of acellular dermal matrix membrane for vertical soft tissue augmentation during submerged implant placement. A case series. Clin Oral Implants Res. 2015;26:465–70.
82. Schroeder A, van der Zypen E, Stich H, Sutter F. The reactions of bone, connective tissue, and epithelium to endosteal implants with titanium-sprayed surfaces. J Maxillofac Surg. 1981;9(1):15–25.
83. Albrektsson T, Brånemark PI, Hansson HA, Lindström J. Osseointegrated titanium implants. Requirements for ensuring a long-lasting, direct bone anchorage in man. Acta Orthop Scand. 1981;52(2):155–70.
84. Teughels W, Van Assche N, Sliepen I, Quirynen M. Effect of material characteristics and/or surface topography on biofilm development. Clin Oral Implants Res. 2006;17(Suppl. 2):68–81.
85. Galindo-Moreno P, León-Cano A, Ortega-Oller I, Monje A, O'Valle F, Catena A. Marginal bone loss as success criterion in implant dentistry: beyond 2 mm. Clin Oral Implants Res. 2015;26(4):e28–34.
86. Apaza-Bedoya K, Tarce M, Benfatti CAM, Henriques B, Mathew MT, Teughels W, Souza JCM. Synergistic interactions between corrosion and wear at titanium-based dental implant connections: a scoping review. J Periodontal Res. 2017;52(6):946–54.
87. Fickl S, Kebschull M, Calvo-Guirado JL, Hürzeler M, Zuhr O. Experimental peri-implantitis around different types of implants—a clinical and radiographic study in dogs. Clin Implant Dent Relat Res. 2015;17(Suppl. 2):e661–9.
88. Carcuac O, Derks J, Charalampakis G, Abrahamsson I, Wennström J, Berglundh T. Adjunctive systemic and local antimicrobial therapy in the surgical treatment of peri-implantitis: a randomized controlled clinical trial. J Dent Res. 2016;95(1):50–7.
89. Carcuac O, Derks J, Abrahamsson I, Wennström JL, Petzold M, Berglundh T. Surgical treatment of peri-implantitis: 3-year results from a randomized controlled clinical trial. J Clin Periodontol. 2017;44(12):1294–303.

90. Jung YC, Han CH, Lee KW. A 1-year radiographic evaluation of marginal bone around dental implants. Int J Oral Maxillofac Implants. 1996;11:811–8.
91. Peñarrocha-Diago MA, Flichy-Fernández AJ, Alonso-González R, Peñarrocha-Oltra D, Balaguer-Martinez K, Peñarrocha-Diago M. Influence of implant neck design and implant-abutment connection type on peri-implant health. Radiological study. Clin Oral Implants Res. 2013;24:1192–200.
92. Zipprich H, Miatke S, Hmaidouch R, Lauer HC. A new experimental design for bacterial microleakage investigation at the implant-abutment interface: an *in vitro* study. Int J Oral Maxillofac Implants. 2016;31:37–44.
93. Abrahamsson I, Berglundh T, Linder E, Lang NP, Lindhe J. Early bone formation adjacent to rough and turned endosseous implant surfaces. An experimental study in the dog. Clin Oral Implants Res. 2004;15:381–92.
94. Vela-Nebot X, Rodriguez-Ciurana X, Rodado-Alonso C, Segalá-Torres M. Benefits of an implant platform modification technique to reduce crestal bone resorption. Implant Dent. 2006;15:313–20.
95. Wang L, Wu Y, Perez K, Hyman S, Brunski JB, Tulu U, Bao C, Salmon B, Helms JA. Effects of condensation on peri-implant bone density and remodeling. J Dent Res. 2017;96(4):413–20.
96. Sindel A, Dereci Ö, Hatipoğlu M, Altay MA, Özalp Ö, Öztürk A. The effects of irrigation volume to the heat generation during implant surgery. Med Oral Patol Oral Cir Bucal. 2017;22(4):e506–11.
97. Aghvami M, Brunski JB, Serdar Tulu U, Chen CH, Helms JA. A thermal and biological analysis of bone drilling. J Biomech Eng. 2018;140(10):1010101–8.
98. Anitua E, Murias-Freijo A, Alkhraisat MH. Implant site under-preparation to compensate the remodeling of an autologous bone block graft. J Craniofac Surg. 2015;26(5):e374–7.
99. Büchter A, Kleinheinz J, Wiesmann HP, Jayaranan M, Joos U, Meyer U. Interface reaction at dental implants inserted in condensed bone. Clin Oral Implants Res. 2005;16(5):509–17.
100. Insua A, Monje A, Wang HL, Miron RJ, Wang H. Basis of bone metabolism around dental implants during osseointegration and peri-implant bone loss. J Biomed Mater Res. 2017;105(7):2075–89.
101. Cha JY, Pereira MD, Smith AA, Houschyar KS, Yin X, Mouraret S, Brunski JB, Helms JA. Multiscale analyses of the bone-implant interface. J Dent Res. 2015;94(3):482–90.
102. Monje A, Chan HL, Galindo-Moreno P, Elnayef B, Suárez-López del Amo F, Wang F, Wang HL. Alveolar bone architecture: a systematic review and meta-analysis. J Periodontol. 2015;86(11):1231–48.
103. Jimbo R, Janal MN, Marin C, Giro G, Tovar N, Coelho PG. The effect of implant diameter on osseointegration utilizing simplified drilling protocols. Clin Oral Implants Res. 2014;25(11):1295–300.
104. Mishra SK, Chowdhary R. Heat generated by dental implant drills during osteotomy-a review: heat generated by dental implant drills. J Indian Prosthodont Soc. 2014;14(2):131–43.
105. Pallan FG. Histological changes in bone after insertion of skeletal fixation pins. J Oral Surg Anesth Hosp Dent Serv. 1960;18:400–8.
106. Koo KT, Kim MH, Kim HY, Wikesjö UM, Yang JH, Yeo IS. Effects of implant drill wear, irrigation, and drill materials on heat generation in osteotomy sites. J Oral Implantol. 2015;41(2):e19–23.
107. Lundskog J. Heat and bone tissue. An experimental investigation of the thermal properties of bone and threshold levels for thermal injury. Scand J Plast Reconstr Surg. 1972;9:1–80.
108. Bogovič V, Svete A, Bajsić I. Effects of a drill diameter on the temperature rise in a bone during implant site preparation under clinical condition. Proc Inst Mech Eng H. 2016;230(10):907–17.
109. Scarano A, Carinci F, Quaranta A, Di Iorio D, Assenza B, Piattelli A. Effects of bur wear during implant site preparation: an *in vitro* study. Int J Immunopathol Pharmacol. 2007;20(1 Suppl. 1):23–6.

110. Monje A, Insua A, Monje F, Muñoz F, Salvi GE, Buser D, Chappuis V. Diagnostic accuracy of the implant stability quotient in monitoring progressive peri-implant bone loss: an experimental study in dogs. Clin Oral Implants Res. 2018;29(10):1016–24.
111. Kumar PS, Dabdoub SM, Hegde R, Ranganathan N, Mariotti A. Site-level risk predictors of peri-implantitis: a retrospective analysis. J Clin Periodontol. 2018;45(5):597–604.
112. Salvi GE, Monje A, Tomasi C. Long-term biological complications of dental implants placed either in pristine or in augmented sites: a systematic review and meta-analysis. Clin Oral Implants Res. 2018;29(Suppl. 16):294–310.
113. Roush JK, Howard PE, Wilson JW. Normal blood supply to the canine mandible and mandibular teeth. Am J Vet Res. 1989;50(6):904–7.
114. Roux S, Orcel P. Bone loss. Factors that regulate osteoclast differentiation: an update. Arthritis Res. 2000;2(6):451–6.
115. Tarnow DP, Magner AW, Fletcher P. The effect of the distance from the contact point to the crest of bone on the presence or absence of the interproximal dental papilla. J Periodontol. 1992;63(12):995–6.
116. Jepsen S, Berglundh T, Genco R, Aass AM, Demirel K, Derks J, Figuero E, Giovannoli JL, Goldstein M, Lambert F, Ortiz-Vigon A, Polyzois I, Salvi GE, Schwarz F, Serino G, Tomasi C, Zitzmann NU. Primary prevention of peri-implantitis: managing peri-implant mucositis. J Clin Periodontol. 2015;42(Suppl. 16):S152–7.
117. Górski B, Ryncarz W, Górska R. Peri-implantitis—well-known problem in a new light. Orthodont Forum. 2017;13(4):301–14.
118. Valderrama P, Wilson TG Jr. Detoxification of implant surfaces affected by peri-implant disease: an overview of surgical methods. Int J Dent. 2013;2013:740680.
119. Schwarz F, Becker K, Renvert S. Efficacy of air polishing for the non-surgical treatment of peri-implant diseases: a systemic review. J Clin Periodontol. 2015;42:951–9.
120. Fürst MM, Salvi GE, Lang NP, Persson GR. Bacterial colonization immediately after installation on oral titanium implants. Clin Oral Implants Res. 2007;18:501–8.
121. Romanos GE, Weitz D. Therapy of peri-implant diseases. Where is the evidence? J Evid Based Dent Pract. 2012;12(3):204–8.
122. John G, Becker J, Schmucker A, Schwarz F. Non-surgical treatment of peri-implant mucositis and peri-implantitis at two-piece zirconium implants: a clinical follow-up observation after up to 3 years. J Clin Periodontol. 2017;44(7):756–61.
123. Ramos UD, Suaid FA, Wikesjö UME, Susin C, Taba M Jr, Novaes AB Jr. Comparison between two antimicrobial protocols with or without guided bone regeneration in the treatment of peri-implantitis. A histomorphometric study in dogs. Clin Oral Implants Res. 2017;28(11):1388–95.
124. Renvert S, Samuelsson E, Lindahl C, Persson GR. Mechanical non-surgical treatment of peri-implantitis: a double-blind randomized longitudinal clinical study. I: clinical results. J Clin Periodontol. 2009;36:604–9.
125. Karring ES, Stavropoulos A, Ellegaard B, Karring T. Treatment of peri-implantitis by the Vector system. Clin Oral Implants Res. 2005;16:288–93.
126. Konopka K, Gośliński T. Photodynamic therapy in dentistry. J Dent Res. 2007;86:694–707.
127. Shibli JA, Martins MC, Theodoro LH, Lotufo RF, Garcia VG, Marcantonio EJ. Lethal photosensitization in microbiological treatment of ligature-induced peri-implantitis: a preliminary study in dogs. J Oral Sci. 2003;45:17–23.
128. Schär D, Ramseier CA, Eick S, Arweiler NB, Sculean A, Salvi GE. Anti-infective therapy of peri-implantitis with adjunctive local drug delivery or photodynamic therapy: six-month outcomes of a prospective randomized clinical trial. Clin Oral Implants Res. 2013;24:104–10.
129. Chambrone L, Wang HL, Romanos GE. Antimicrobial photodynamic therapy for the treatment of periodontitis and peri-implantitis: an American Academy of Periodontology best evidence review. J Periodontol. 2018;89(7):783–803.

130. Romeo U, Nardi GM, Libotte F, Sabatini S, Palaia G, Grassi FR. The antimicrobial photodynamic therapy in the treatment of peri-implantitis. Int J Dent. 2016;2016:7692387. https://doi.org/10.1155/2016/7692387.
131. Schwarz F, Aoki A, Takasaki A, Sager M, Sculean A, Becker J. Therapy. In: Schwarz F, Becker J, editors. Peri-implant infection: etiology, diagnosis and treatment. London: Quintessence Publishing Co. Ltd.; 2007. p. 130–1.
132. Lang NP, Berglundh T, Heitz-Mayfield LJ, Pjetursson BE, Salvi GE, Sanz M. Consensus statements and recommended clinical procedures regarding implant survival and complications. Int J Maxillofac Implants. 2004;19(Suppl):150–4.
133. Heitz-Mayfield L, Lang NP. Antimicrobial treatment of peri-implantitis. Int J Oral Maxillofac Implants. 2004;19(Suppl):128–39.
134. Pasi D, Singh M, Dutta SR, et al. Newer proposed classification of peri-implant defects: a critical update. J Oral Biol Craniofac Res. 2017;7:58–61.
135. Geremias TG, Montero JFD, de Souza MR, Filho GS, de Margalhães Jr EB, Bianchini MA. Biofilm analysis of retrieved dental implants after different peri-implantitis treatment. Case Rep Dent. 2017;2017:e1–5.
136. Cha JK, Lee JS, Kim CS. Surgical therapy of peri-implantitis with local minocycline: a 6-month randomized controlled clinical trial. J Dent Res. 2019;98(3):288–95.
137. Shibli JA, Ferrari DS, Siroma RS, de Figueiredo LC, de Faveri M, Feres M. Microbiological and clinical effects of adjunctive systemic metronidazole and amoxicillin in the non-surgical treatment of peri-implantitis: 1 year follow-up. Braz Oral Res. 2019;33(Suppl. 1):e080.
138. Roos-Jansåker A-M, Lindahl C, Persson GR, Renvert S. Long-term stability of surgicalbone regenerative procedures ofperi-implantitis lesions in aprospective case–control studyover 3 years. J Clin Periodontol. 2011;38:590–597.
139. Serino G, Turri A. Outcome of surgical treatment ofperi-implantitis: results from a 2-yearprospective clinical study in humans. Clin Oral Impl Res. 2011;22:1214–20.
140. Mombelli A, Feloutzis A, Brägger U, Lang NP. Treatment of peri-implantitis by local delivery of tetracycline. Clin Oral Impl Res. 2001;12:287–294.
141. Leonhardt A, Renvert S, Dahlen G. Microbial findings at failing implants. Clin Oral Implants Res. 1999;10:339–45.
142. Sbordone L, Barone A, Ramaglia L, Ciaglia RN, Iacono VJ. Antimicrobial susceptibility of periodontopathic bacteria associated with failing implants. J Periodontol. 1995;66:69–74.
143. Meffert RM. How to treat ailing and failing implants. Implant Dent. 1992;1:25–33.
144. Hsu YT, Mason SA, Wang HL. Biological implant complications and their management. J Int Acad Periodontol. 2014;1:9–18.
145. Schwarz F, John G, Mainusch S, Sahm N, Becker J. Combined surgical therapy of peri-implantitis evaluating two methods of surface debridement and decontamination. A two-year clinical follow up report. J Clin Periodontol. 2012;39(8):789–97.
146. Ramanauskaite A, Becker K, Juodzbalys G, Swarz F. Clinical outcomes following surgical treatment of peri-implantitis at grafted and non-grafted implant sites: a retrospective analysis. Int J Implant Dent. 2018;4:27.
147. Sharon E, Shapira L, Wilensky A, Abu-hatoum R, Smidt A. Efficiency and thermal changes during implantoplasty in relation to bur type. Clin Implant Dent Relat Res. 2011;15(2):292–6.
148. Esposito M, Klinge B, Meyle J, Mombelli A, Rompen E, van Steenberghe D, Van Dyke T, Wang HL, van Winkelhoff AJ. Working group on the treatment options for the maintenance of marginal bone around endosseous oral implants, Stockholm, Sweden, 8 and 9 September 2011. Consensus statements. Eur J Oral Implant. 2012;5:105–6.
149. Almaguer-Flores A, Olivares-Navarette R, Wieland M, Ximenéz-Fyvie LA, Schwartz Z, Boyan BD. Influence of topography and hydrophilicity on initial oral biofilm formation on microstructured titanium surfaces *in vitro*. Clin Oral Implants Res. 2012;23(3):301–7.
150. Schwarz F, Herten M, Sager M, Bieling K, Sculean A, Becker J. Comparison of naturally occurring and ligature-induced peri-implantitis bone defects in humans and dogs. Clin Oral Implants Res. 2007;18:161–70.

151. Ayangco L, Sheridan PJ. Development and treatment of retrograde peri-implantitis involving a site with a history of failed endodontics and apicoectomy procedures: a series of reports. Int J Oral Maxillofac Implants. 2001;16(3):412–7.
152. Jain S, Kaur H, Aggarwal R. Classification systems of gingival recession: an update. Indian J Dent Sci. 2017;9(1):52–9.
153. Akram Z, Khawaja NA, Rashid H, Vohra F. Sub-epithelial connective tissue graft and enamel matrix derivative in the management of a localized gingival recession defect: a case report. Saudi J Dent Res. 2016; https://doi.org/10.1016/j.sjdr.2015.11.001.
154. Shah R, Shah H, Shetty O, Mistry G. A novel approach to treat peri-implantitis with the help of PRF. Pan African Med J. 2017;27:256–66.
155. Solderer A, Al-Jazrawi A, Sahrmann P, Jung R, Attin T, Schmidlin PR. Removal of failed dental implants revisited: questions and answers. Clin Exp Dent Res. 2019;5:712–24.
156. Anitua E, Piñas L, Begoña L, Alkhraisat MH. Prognosis of dental implants immediately placed in sockets affected by peri-implantitis: a retrospective pilot study. Int J Periodontics Restorative Dent. 2017;37:713–9.
157. Schwarz F, Aoki A, Takasaki A, Sager M, Sculean A, Becker J. Therapy. In: Schwarz F, Becker J, editors. Peri-implant infection: etiology, diagnosis and treatment. London: Quintessence Publishing Co. Ltd.; 2007. p. 154.
158. Wang WCW, Lagoudis M, Yeh CW, Paranhos KS. Management of peri-implantitis—a contemporary synopsis. Singap Dent J. 2017;38:8–16.
159. Chrcanovic BR, Kisch J, Albrektsson T, Wannerberg A. Survival of dental implants placed in sites of previously failed implants. Clin Oral Implants Res. 2017;28:1348–53.

Lasers in Implant Dentistry

Sanjay Miglani and Swadheena Patro

Abstract Both the terms Lasers and Dental Implantology have revolutionized the concept of dentistry and are considered as a proven treatment option. Dental implants and lasers are practised worldwide. Lasers have established their various applications in dentistry and they have a potential role in dental implantology too. The simultaneous expansions of lasers and dental implantology together have a predictable outcome. Both hard and soft tissue lasers have their use in dental implantology ranging from pre-surgical preparation and through various stages of implant placement.

The mechanism of lasers working is through stimulated emission. On targeting the biological tissue, they get reflected, absorbed, or scattered in surrounding tissues, thereby reducing the bacterial contamination absorbed by the implants and surrounding tissues or may also have an effect of rising in tissue temperature where the laser is reflected back by the implant. The most commonly used lasers are solid-state lasers, Nd:YAG, Nd:YAP, Er:YAG, Er, Cr:YSGG, semiconductor diode lasers and gas lasers like CO_2 lasers. These lasers have exhibited excellent coagulative properties.

In comparison to traditional methods, lasers are gentle, less invasive and less painful. Their characteristics are important as per the different reaction they produce on the implant surface. Thus, thorough knowledge and understanding is needed for the mechanism of laser action in implantology.

This chapter would highlight at a glance the various types of lasers and its various applications at different stages of dental implantology.

Keywords Lasers · Dental implantology · Laser wavelengths · Peri-implantitis

S. Miglani (✉)
Department of Conservative Dentistry and Endodontics, Faculty of Dentistry, Jamia Millia Islamia, New Delhi, India

S. Patro
Department of Conservative Dentistry and Endodontics, Kalinga Institute of Dental Sciences, Bhubaneswar, Odisha, India

R. S. Chaughule, R. Dashaputra (eds.), *Advances in Dental Implantology using Nanomaterials and Allied Technology Applications*,
https://doi.org/10.1007/978-3-030-52207-0_10

1 Introduction

Dental implantology has revolutionized the concept of dentistry and is considered as a proven treatment option [1]. The rigorous evolution in implant engineering and design over the decade has resulted in a success rate of 95% and above [2, 3]. Thus, making implant is a viable treatment plan for missing teeth [4, 5].

Lasers have established itself in the medical and dental field in 1960 by Maiman [6, 7, 8]. Drs. William and Terry Myers modified an ophthalmic laser (Nd:YAG) to dental laser in 1989 [9]. They are broadly classified as hard and soft tissue lasers based on their interaction with the tissues.

Lasers mainly work through stimulated emission. Lasers interact with biological tissues by either getting transferred to surrounding tissues or reflected, scattered, or absorbed [10]. There is an escalation of the use of lasers since 10–12 years. With the advent of soft tissue lasers of various wavelengths applicable to implant dentistry at various stages of the treatment phases, lasers are more cost effective, portable and reliable. Romanos et al. explored the uses of lasers in implantology and concluded its potential benefit in implant dentistry [1]. The advantages of lasers include haemostasis, decreased swelling, improved visibility, minimal damage to the surrounding tissues, decreased infection due to photosterilization effect and less post-operative pain [11, 12]. Dental implants and lasers are practised worldwide. The simultaneous expansions of laser and dental implantology together have a favourable outcome.

This chapter outlines role of dental lasers in various stages of implant dentistry, and thereby improving the pre-surgical, surgical, and post-surgical and prosthetic phases of implant dentistry [13]. Lasers help in dealing with complications specifically from placement of implant to prosthetic delivery. The various wavelengths of lasers exhibit various characteristics that enhance the clinical approach and overall experience of patient. The clinician must have an elaborate knowledge, understanding of the potential benefits and use of each individual laser that the particular is indicated to achieve the desired outcome of a given procedure corresponding to their wavelengths [13]. Both hard and soft tissue lasers like Er:YAG, Er:Cr:YSGG, Diode 10.6 μm and 9.3 CO_2 lasers have a role in implant dentistry.

2 Fundamentals of Lasers

A profound science and technology of today's world called laser-light amplification by stimulated emission of radiation has its own share of history, originating in the era of Albert Einstein (1916) [14] who gave the conceptual building blocks of laser; a cornerstone development in the history of lasers was Theodore Maiman building the first laser on May 16, 1960, at Hughes Research Laboratories. This chapter will give an insight into the science behind laser technology.

2.1 Light

It is a form of electromagnetic energy that travels in waves at a constant velocity. Photon is the basic unit of this radiant energy. Light shows properties of both particles and waves; therefore the waves of photons project two fundamental properties: (1) wavelength and (2) amplitude [13].

2.2 Wavelength

As mentioned earlier, a wave has a trough (lowest point) and a crest (highest point); the horizontal distance between two consecutive troughs or crests is known as wavelength denoted by (λ) and is measured in metres (m). Waves, rising and falling about the zero axis, a certain number of times per second, is described as oscillations. The number of oscillations per unit time is called frequency, which is measured in hertz (Hz). Hertz is also defined as the number of pulses per second of emitted laser energy [13]. The higher the frequency, the shorter is the wavelength; therefore wavelength and frequency are inversely proportional.

Ordinary light, i.e. the white light, is generally diffused and not a focused beam. However, the laser light beam is monochromatic (i.e. single colour), coherent (i.e. the frequency and amplitude of all the waves are alike) and directional (i.e. the beam of light is very less divergent). These features not only distinguish laser from ordinary white light, but also helps in accomplishing the treatment objectives of the lasers [13]. The beams emitted from laser instruments are collimated, i.e. all the waves produced are parallel to each other, over a long distance; however once the beam enters any optical fibre tips of any delivery system, it diverges at the tip. Spatial coherence is a major factor that enables lasers to carry out surgical procedures in medical field.

2.3 Amplitude

A wave has a trough and a crest; hence the vertical height of the wave from the zero axis to its peak as it moves around a fixed axis is called amplitude. Amplitude is associated with the brightness and the intensity of a wave. The larger the amplitude, the greater would be the amount of potential work that could be performed. The S.I. unit of energy is Joules.

2.4 Amplification

It is a process of intensifying the amplitude of a wave; this part of the process occurs inside the laser. The centre of the laser is called the laser cavity and there are three components that make up the laser cavity.

- Active medium: This constitutes chemical elements. Lasers are named after the material of active medium; for example, gas lasers, wherein there is a presence of a canister of carbon dioxide gas, CO_2. In a CO_2 laser or solid-state crystal lasers erbium doped YAG (Er:YAG) lasers are used in dentistry where the host material is yttrium aluminium garnet (YAG) and doped with erbium, or semiconductor which comprises a diode (positive-negative, i.e. p-n junction of an electronic circuit), for example, Gallium Arsenide (GaAs).
- Pumping mechanism: It surrounds the active medium. It is a source of energy that pumps energy into the active medium. The energy from the pumping mechanism should be sufficient in quantity and duration so that the occupation of higher energy level exceeds that of lower level; this is called population inversion which allows amplification.
- Optical resonators: These are the two mirrors placed parallel to each other in the laser cavity, one at each end of the optical cavity, or they can be two polished surfaces at each end in case of a semiconductor diode laser. They reflect the waves back and forth and help to collimate, amplify the developing beam. The other mechanical components included are focusing lenses, cooling systems and controlling mechanisms [13].

2.5 Stimulated Emission

Stimulated emission is the process by which laser beams are produced inside the laser cavity. In the year 1916 Albert Einstein proposed this theory. Using Bohr's model, Einstein further postulated that when an additional quantum of energy is absorbed by an already energized atom, it results in release of two quanta. Thus, the production of laser beam relies on the concept that, energy is radiated as identical photons, travelling as coherent wave. These photons in turn energize more atoms resulting in amplification of light energy [15, 16, 17].

2.6 Radiation

The electromagnetic spectrum is broadly divided into two divisions: ionizing radiation and non-ionizing radiation, with gamma rays, X-rays and ultraviolet light falling under ionizing radiation category, while all the wavelengths fall under non-ionizing radiation.

Most common laser devices used in dentistry have emission wavelengths of approximately 500 nanometre (nm) to 10,600 nm, which places them in the non-ionizing section of the spectrum called thermal radiation [18].

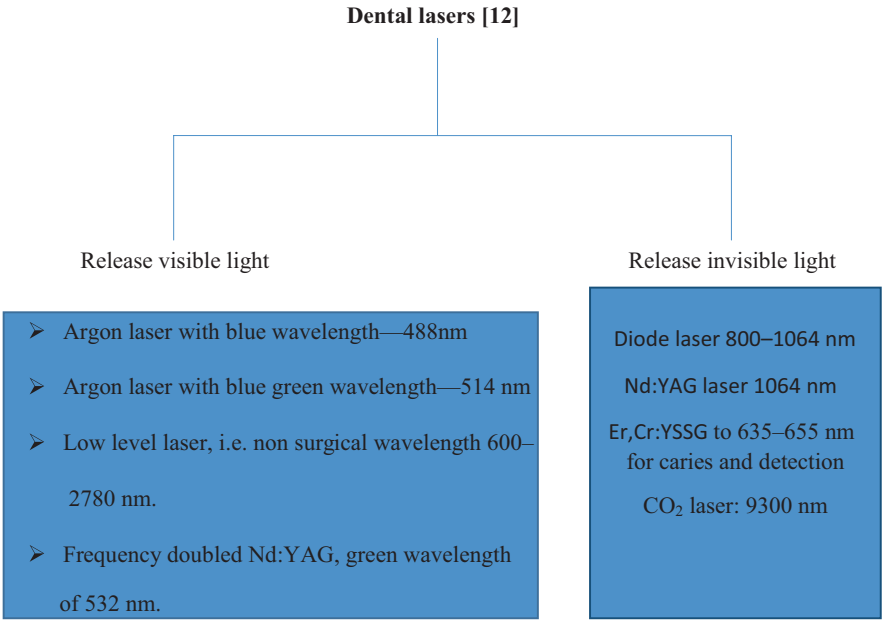

2.7 *Laser Delivery Systems*

Laser energy should be delivered to the surgical site by a method that is ergonomic and precise [19]. Optical fibre, hollow wave guide and articulated arm are the three modalities for the same [14].

Nd:YAG lasers and KTP diode have flexible and small fibre optic systems with bare glass fibres that project laser energy to target tissues. Erbium and CO_2 lasers are constructed articulating arm or semiflexible hollow waveguides. Some of these systems employ sapphire tips while others employ non-contacting tips for contact with target tissues. All dental lasers falling under invisible light spectrum like CO_2, diode, Nd:YAG and erbium are provided with a separate aiming beam which is delivered coaxially along the waveguide, which in turn directs the operator to the exact location on the target tissue.

2.8 Spot Size

Active beam is focused by lenses, at the point where the amount of energy is the greatest with hollow waveguide or articulated arm delivery system. For incisions and excisions in a surgery, this focal point is necessary. The focal point for contact delivery systems is near the tip of the fibre which has the greatest energy. With non-contacting delivery systems like CO_2 the focal point may range from 1 to 12 mm from the tissue surface. If the handpiece is moved away from the focal point, it may cause the beam to be defocused, resulting in more divergence and in turn delivers less energy to the surgical site.

2.9 Emission Modes

Dental lasers use two modalities such as "constant on and "pulsed off and on". These are dependent on function of time to emit light energy [19].

Pulsed lasers are further categorized into gated and free running modes for delivering energy to target tissues. These are:

1. Continuous wave mode: Beam is emitted at only one power mode till the operator depresses the foot switch.
2. Gate pulse mode: Characterized by periodic alteration of laser energy. This mode is achieved by opening and closing of a mechanical shutter in front of a beam path. All surgical devices that operate in continuous wave mode have this gate pulse feature.
3. Free running pulse mode: Also referred to as free pulsed mode. The emission is unique in those large peak energies of laser that are emitted usually for microseconds followed by a relatively long time when the laser is off.

3 Laser Wavelengths

3.1 Diode Laser

Diode laser comes in varying wavelengths manufactured and available in 810, 940 and 1064 nm more commonly [13]. They are supplied through a fibre contact mode and energy is targeted or delivered to soft tissues [1], thus making it more suitable for soft tissue procedures [20], mainly tissue containing melanin and haemoglobin. It works on the principle of conditioning or carbonization [21, 22]. The heat range is between 500 and 800 °C. Through vaporization it cuts the tissue when contacted with the heated tip. The 980 nm is more absorbed in water in comparison to 810 nm wavelength, thus making it safer and potentially more suitable for implants [13].

Lasers mainly work on the principle, i.e. more the absorption lesser will be the collateral thermal heat directed towards the implant [13]. Studies have shown, even at higher power setting 980 nm diode lasers are safer to use near titanium surface of the implant [23]. Studies show that 810 nm diode exhibits a high rise in temperature at the implant surface [24]. According to Romanos et al. [25] lasers of 810 nm can damage the implant surface.

When compared to Nd:YAG lasers the depth of the penetration is less, thus making it more convenient for the operator of better control of the laser and collateral thermal damage. Frequent cleaning of the fibre tip is needed as the debris collects on its tip [26]. Disadvantages include low cutting speed and gated pulse delivery mode, leading to rise in temperature in the tissue. Thus, the operator must be aware of the power density, especially when working close to implant surface [24].

To summarize, a 980 nm diode laser can be safely used for implant procedure, keeping its limitations such as the cutting depth, speed and efficiency. The advantages are its small size and relatively low cost [13].

3.2 Nd:YAG Laser

These lasers share common properties as of diode. They are fibre optic contact, free running pulse beam of energy of 1064 nm. They have a higher depth penetration in comparison to diode, are more readily absorbable in haemoglobin/melanin tissue and are poorly absorbed in water. They have excellent coagulative and haemostatic properties but due to their high penetration depth they may have potential to damage both soft and hard tissues as well as implant surface too [23].

The Nd:YAG laser has a potential indication in periodontal therapy and has marked a positive effect in treating pockets [27]. However, studies done by Block et al. [28] show that laser has the potential to dissolve the surface of plasma-coated titanium implants. Craters and cracks are also seen on titanium surface [13]. Similar studies done by Romanos et al. [29] and Schwarz et al. [30] have contraindicated the use of free running pulse Nd:YAG laser for treatment of titanium implant surface as the high peak power and moderate reflection rate can cause the melting of metal surface. Walsh [27] and Chu et al. [31] contraindicated the use of laser near the implant. However in an in vitro study Gonçalves et al. [32] reported that the use of Nd:YAG laser in non-contact mode with a long pulse duration caused no damage to the titanium surface. Till date, no studies have shown the safety of this laser in implant dentistry. To summarize, Nd:YAG laser is useful to use in any implant procedure or peri-implant surgery. Its use will continue in periodontal therapy successfully [23].

3.3 Carbon Dioxide (CO_2) Laser

The CO_2laser works at a wavelength of 10,600 nm. It is delivered in gated pulse or continuous mode, in non-contact mode by mirrored handpiece. It is also available in extremely short pulse of high peak power labelled "super-pulsed" and ultra-speed "ultra pulsed" mode. In comparison to other lasers, CO_2laser is readily absorbed in collagen, water and hydroxyapatite. From a very long time, because of their efficacy and speed in cutting soft tissues, it has been used in surgical procedures [33]. It exhibits strong haemostatic and bactericidal in nature with minimum wound contraction thus minimizing scarring [13]. Studies have shown that CO_2 lesser is effective against *Porphyromonas gingivalis* [34]. They provide disinfection and reduction in bacteria without much significant change on implant surface [14]. CO_2laser has minimal depth penetration, thereby causing less lateral thermal damage [23, 35]. The depth of penetration is usually in the range of 0.2–0.5 nm in soft tissue [14].

Earlier, the devices produced high carbonization due to high energy density created but with the newer devices the energy density ranges from 180 to 300 mJ/cm^2 with a speed of 400–800 μs, improving its working speed and efficiency and less carbonization and tissue charring. The technology has further advanced, with even shorter pulses with high peak power. Thus, CO_2laser can effectively cut deeper producing less carbonization when speed is increased and pulse width is decreased. The energy density is now in the range of 50–300 mJ/cm^2 with a speed of 30–80 μs [14]. This has increased the potential of CO_2 laser in treating periodontal pockets and incision 4–5 nm depth efficiently and speedily.

The energy is mostly absorbed in water (not pigments making) and is a safer option to use in implant dentistry [36, 37]. It is effectively and safely used in treating peri-implantitis and mucositis [13, 14] as the energy does not penetrate into implant surface; its effect is confined to bacteria's intracellular water. It exhibits excellent haemostatic properties, better visualization reducing procedure time and limiting post-operative complication [38].

The laser forms a thick carbon layer of approximately 0.1 mm when comes in contact with the bone; the water molecules gets dehydrated forming a layer, thus making it safe to use, as the surface layer absorbs energy and bone damage is clinically insignificant [39]. However CO_2laser can be used to re-establish bleeding for healing if needed. CO_2 laser is the most promising and versatile soft tissue laser for implant dentistry. A recent 9300 nm wavelength is delivered through an articulating arm. To date, not many studies have described the use of this laser wavelength in treating peri-implantitis and thus should be used with care and caution in this clinical application.

3.4 Erbium Laser

Er:YAG includes wavelength of 2940 nm and Er:G:YSGG has a wavelength of 2780 nm. It delivers in free running pulse mode. The energy is delivered both in contact and non-contact mode. It is delivered by mirror handpiece and articulated arm, waveguide or trunk fibre and handpiece with a quartz or sapphire fibre tip. The delivery system has a water spray to prevent heat buildup and rehydration of target tissue for better absorption.

Erbium lasers are highly absorbed in water and hydroxyapatite. Initially when it came into use, these lasers were applied for only hard tissue procedure. They are good in ablating tooth structures and bone. Microexplosion is created in the hydroxyapatite during the ablation process without carbonization or charring with minimal heat produced. It can ablate soft tissues too, especially more effective in vascularized tissue keeping its limitation. It is least effective in achieving haemostasis of all the lasers. As erbium laser's primary target is water; thus it can be applied for treating peri-implantitis and mucositis safely [40, 41]. They exhibit excellent bactericidal properties as the energy emitted ruptures the bacterial cell membrane when absorbed into intracellular water. To conclude, Er laser has more application in hard tissues than in soft tissues when compared to other soft tissue lasers as it is poor in achieving haemostasis.

4 Laser Application in Clinical Practice

4.1 Pre-operative Frenectomy and Tissue Ablation

At times soft tissue alterations are required before the placement of implant. Frenectomy is done to release the tension of the tissue around the implant site with high muscular attachment close to surgical site. Restoration of muscles aims to achieve less post-operative pain and swelling and thus contributing to success of implant surgery. Laser plays an advantage tool for both patient and clinician. It helps restoring tissues without causing much bleeding, swelling and post-operative pain [14].

4.2 Preparation of Surgical Site

It is the first step before implant placement. Prevention of contamination and sterilization of the surgical site is one of the key important steps of implant surgery. Antimicrobial rinse such as chlorhexidine is used before the initiation of surgery [42, 43]. These methods are partially effective, as oral cavity is a harbour to bacteria

and practically not possible to prevent contamination of the site with saliva during the procedure, to rinse repeatedly at every step.

Lasers can be used for sterilization of the site, as they are bactericidal, by exposing them for a few seconds. It is instantaneous and is profoundly effective [1, 37]. The contact lasers like diode or erbium could be used by touching every square mm of the surface, which needs a slow deliberated application technique. Larger the osteotomy site, longer is the sterilization procedure. A large diameter of fibre optic cable (800–1000 μm) of contact laser can be used for the sterilization procedure.

4.3 Decontamination and Implant Placement

CO_2 laser has an edge over contact laser as it is a non-contact type. It is easier to increase the spot size of the tissue by placing a wide aperture handpiece on the CO_2 laser to apply the laser beam out of focus, thus increasing spot size. Sterilization is achieved in few seconds of large osteotomy site. During the surgery procedure wherever necessary, laser energy can be used to sterilize the surgical site as and when required.

In cases where immediate implants are loaded following sterilization of the site is deemed necessary. The gross amount of soft tissues is removed with spoon curette followed with laser to remove any tissue tags. The laser is used to decontaminate the surface of the extraction socket. Before raising the flap the decontamination of soft tissue of surgical site can be done by erbium lasers and bony surface at lower power setting with a water coolant spray [44] as these lasers are less effective in achieving haemostasis as compared to other lasers. They leave the bone bleeding that helps in healing of the socket. CO_2 lasers can be used at lowest power densities to remove the soft tissue tags and decontaminate the bony surface. It has an excellent haemostatic property; thus the effect of haemostasis must be overcome by healing process.

4.4 Osteotomy

The preparation of the osteotomy must consider various lasers, suitable for cutting through both hard and soft tissues.

4.4.1 Soft Tissues

Cutting through soft tissues, clinician decides the various pattern of entry. In certain cases of minimal entry, punch procedure is followed. Here 1–2 or 3–4 mm of soft tissue is removed depending on location and biotype [13]. A CO_2/Erbium laser is preferred over a diode or Nd:YAG as it works in seconds over minutes (as it takes less time in comparison to diode or Nd:YAG). Achieving haemostasis with erbium

is difficult. However lasers are much more convenient and less time taking than conventional techniques. As the size of the entry site increases, it leads to complexity of flap design. Cutting speed and haemostasis becomes difficult as it gets deeper through multiple layer of keratinized (attached) and mucosal (not attached). CO_2 laser is best suitable as it provides excellent haemostasis, unobstructed vision, high cutting efficiency through all tissue biotypes and thickness [39].

Laser advantages: Through lasers we achieve a sterile cut, chances of being less infected. With laser incision the post-operative complications are reduced. These are swelling and inflammation as it seals all the blood vessels and lymphatic channels [45, 46]. Due to reduced swelling, sutures are less likely to pull through or undone. Antibiotics and analgesics are infrequently required. These advantages are beneficially in both major and minor surgical procedures.

4.4.2 Haemostasis

Excellent application of laser is haemostasis. Patient must be under anticoagulants; history must be received and updated. INR (international normalized ratio) must be ordered. Studies state that if INR is less than 4.0, anticoagulant regimen can be altered before initiating dental surgery [47, 48]. The final decision rests on the physician.

Use of lasers leads to increased tissue healing and decreased post-operative swelling. As compared to scalpel wounds laser provides (1) less tissue damage, (2) less traumatized wound and (3) precision in the depth of tissue damage [36].

4.4.3 Hard Tissue

Erbium lasers are the most preferred to ablate the hard tissue. It is less damaging as compared to conventional technique, as it creates less friction since it is a non-contact laser. The temperature is minimal due to reduced friction. Erbium lasers have shown better results in bone healing and new bone formation than conventional bone drills [44, 49, 50]. Till date many studies have not validated the use of 9–3 μm CO_2 laser. However the entire osteotomy procedure cannot be done using this laser. Researchers are still working on to replace the bone drills with erbium drills for osteotomy.

4.4.4 Block Graft Procedure

CO_2 or erbium laser in low energy setting can be used as indelible marker to mark measurement on bone surface, thereby negating frictional and mechanical stress from a drill on bone. The receptor site can be marked and visualized and similarly the donor block can be delineated and marked prior to cutting. Once the required size is cut, the erbium laser is used to create a screw hole, thereby eliminating the

frictional and mechanical stress of the drill. Erbium laser can also be used to modify the block.

4.4.5 Lateral Window Sinus Lift

CO_2 or erbium laser can be used to create a marking on the bone surface without damaging its integrity [51]. Erbium lasers can be used to cut through the bone; however the erbium laser will also cut the soft tissue attached to the bone which is a potential problem [51]. Cutting with bur requires shell for window creation not damaging the Schneiderian membrane (nasal mucous membrane). The best tool so far is piezo surgical device for sinus lift, causing vibrations through the bone, not cutting the soft tissues [52].

4.4.6 Uncovering Implants

The implant is covered by soft tissues and newly formed bone up to 2–3 mm of thickness during the healing process. To access the implant body, both the soft and hard tissues are removed. Except for Nd:YAG laser all lasers can be used for removal of soft tissues. CO_2 lasers work best, and have excellent visualization and quick removal.

Erbium laser is safe and efficient to remove the bone of any thickness. A study was done comparing the use of Er:Cr:YSGG and diode laser in the second stage of implant surgery to uncover implants and was found that post-operative pain was less in diode and erbium laser but statistically not significant [53].

4.5 Mucositis and Peri-implantitis

One of the main complications in implant dentistry is infection developed at a later stage once the implant integrates with the bone. Mucositis is a soft tissue infection around the abutment crown implant complex, at the cervical third of the implant. Peri-implantitis is an infection around the body or apex of the implant leading to the loss of bone [54]. Resulting in inflammatory reaction, presence of anaerobic plaque associated with a biofilm leads to swelling and inflammation of soft tissue and bone loss around the implant. Many factors contribute,like quality of the tissue surrounding the implant, implant design, surface texture, alignment mechanical loading on the implant during occlusion and presence of bacteria. Clinically there may be inflammatory colour change in surrounding tissue, bone loss, bleeding, suppuration and fistula formation. In extreme cases implant may have to be removed.

Figures 1, 2, 3, 4, 5, 6, 7 and 8 explain step-by-step procedure done for the treatment of peri-implantitis. Firstly, all the diagnostic aids are put in place. In Fig. 1, an intraoral periapical radiograph is taken for the targeted area, indicating bone loss

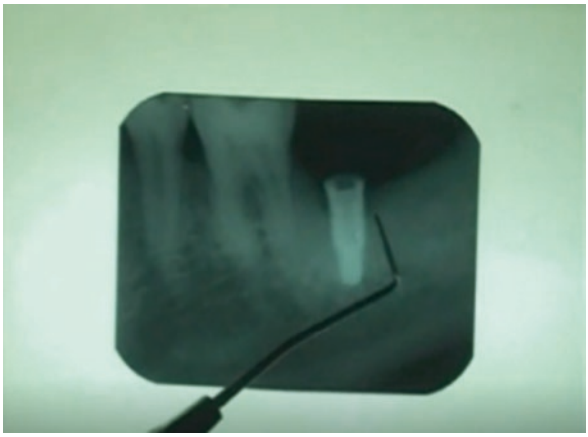

Fig. 1 Bone loss seen around the implant. (Case photos courtesy, Dr. Sanjay Jain)

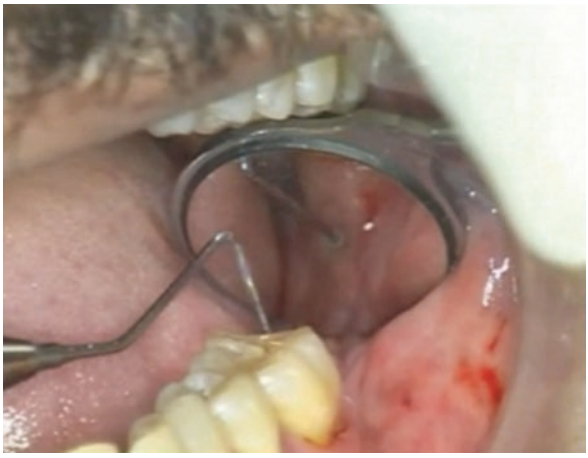

Fig. 2 Williams periodontal probe confirming the bone loss clinically. (Case photos courtesy, Dr. Sanjay Jain)

around the implant. In Fig. 2, Williams periodontal probe is used to check clinically the probing depth, confirming the bone loss. Figures 3 and 4 show the incision and the subsequent flap reflection done. Figure 5 shows the granulation tissue removed after the debridement of the targeted area. Figure 6 shows sterilization done using laser and the implant is disinfected using tetracycline solution. Figures 7 and 8 show the stripping of laser fibre done before the activation of laser which is a diode laser of 980 nm applicable at 1 W pulse mode.

4.5.1 Conventional Therapy

Surgical debridement along with antibiotic coverage is done. Topical tetracycline, chlorhexidine, citric acid and plastic instruments are used as therapeutic tools [52, 55]. Bone grafting is done for regeneration of peri-implant hard tissue. Studies

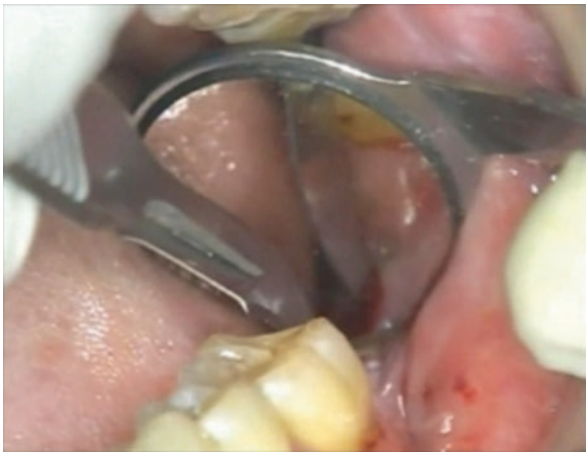

Fig. 3 Incision. (Case photos courtesy, Dr. Sanjay Jain)

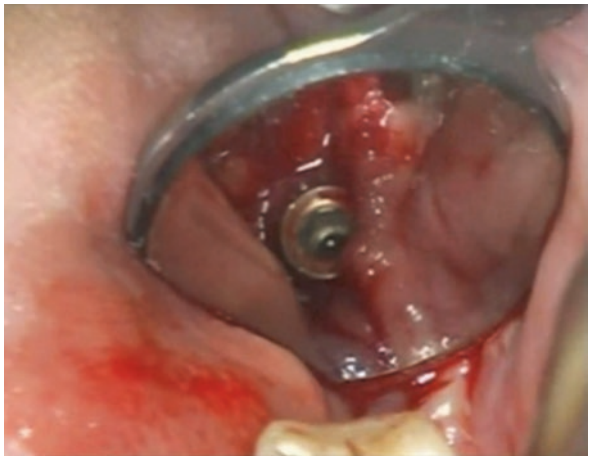

Fig. 4 After flap reflection. (Case photos courtesy, Dr. Sanjay Jain)

reveal that success rates are low. A 42% of failure rate is seen with conventional therapy for treating peri-implantitis [56].

4.5.2 Laser-Assisted Therapy

Erbium and CO_2 lasers are used for treating peri-implantitis and mucositis and provide a new dimension for treating peri-implantitis and mucositis.

4.5.2.1 Erbium Laser

The following steps are done.

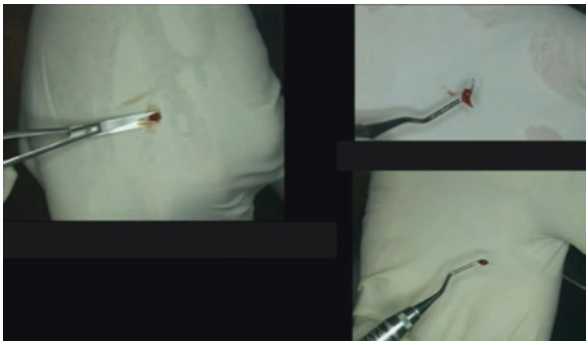

Fig. 5 Granulation tissue during debridement. (Case photos courtesy, Dr. Sanjay Jain)

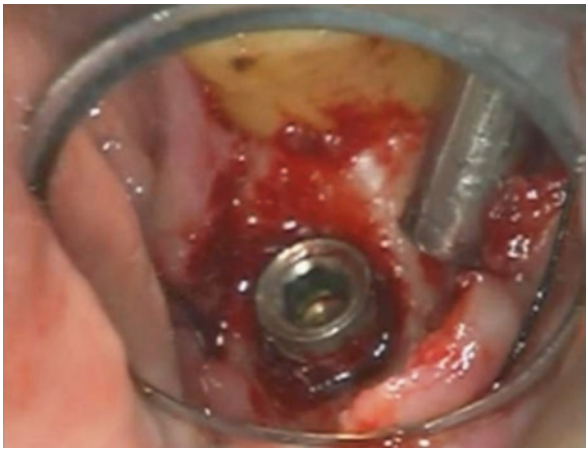

Fig. 6 After laser sterilization and implant disinfection done with freshly prepared tetracycline solution. (Case photos courtesy, Dr. Sanjay Jain)

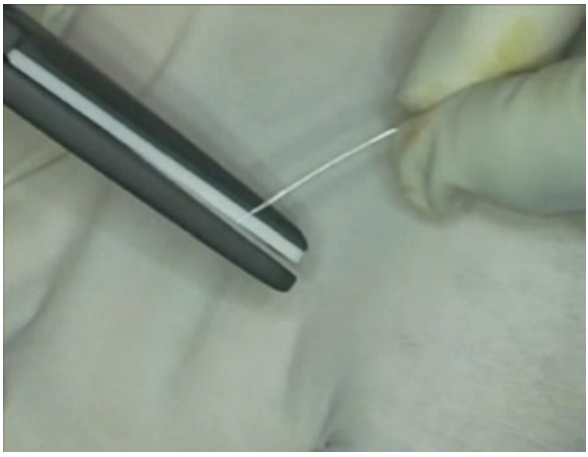

Fig. 7 Stripping of laser fibre prior to activation of laser. (Case photos courtesy, Dr. Sanjay Jain)

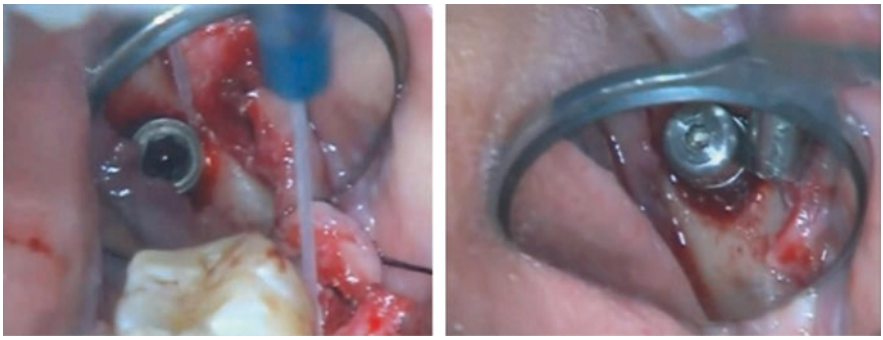

Fig. 8 Application of diode laser 980 nm at 1 W pulse mode. (Case photos courtesy, Dr. Sanjay Jain)

1. With an appropriate laser incision [57], implant is accessed.
2. After exposing the implant and surrounding bone, the laser energy is used to vaporize the infected tissue.
3. Decontamination of implant surface and bony crypt are done using laser.
4. A thin layer of bone layer is ablated, necrotic bone is removed and the area is decontaminated.

Decontamination and debridement are done using a single instrument. If needed, bone grafting can be done. Thus, healing is seen due to decreased inflammation and post-operative pain [1, 13].

4.5.2.2 CO_2 Laser

If CO_2laser is used, the following steps can be undertaken.

1. An incision is done, exposing the implant, bone and diseased soft tissue.
2. Tissue is ablated, implant and bony surface are decontaminated but CO_2 laser forms a carbonization of bone; thus before grafting scrapping of carbonization layer is done mechanically with a curette and bleeding is re-established. An increased success rate is seen due to a more sterile environment being created.
3. A diode laser can also be used for removal of granulation tissue and decontamination of implant surface.

4.5.3 Non-surgical Therapy

Lasers can be used for treating crestal mucositis with bone loss. Deppe and Horch [58] used CO_2 lasers to sterilize the exposed implant surface to rehabilitate ailing implant and have shown better results than the conventional areas.

4.5.3.1 Erbium Lasers

Schwarz et al. conducted a study using Er:YAG laser [59] to treat peri-implantitis of moderate to advanced lesion of 20 patients, at least having one implant. Er:YAG laser versus mechanical debridement with plastic curette and antiseptic therapy with chlorhexidine digluconate (0.2%) was used to treat on patients. The gingival recession, probing depth, bleeding on probing, plaque index, and clinical attachments were evaluated at 3- and 6-month period. Er:YAG lasers show better results.

4.5.3.2 CO_2 Laser

The studies done by Romonas [23] referred that an approximately 3 W power setting CO_2laser can decontaminate peri-implantitis affected restoration. He started a thorough decontamination of implant site which can be done when CO_2 laser is reflected off the implant surface, vaporizing the bacteria in deep bony lesion leading to a better healing and osseointegration. Deppe et al. [36] have shown decontamination by CO_2laser of ailing implants that lead to peri-implant bone growth in beagle dogs.

The laser energy delivered around the implant by placing CO_2 tip into the sulcus, procedure can be repeated 3–4 times every 7–10 days, coinciding with the time taken for the formation of sub-gingival biofilm [60]. Substantial reduction in bacterial count is seen, diseased soft tissue is vaporized. The results have shown the formation of bone up to 1–4 mm where there was a 6 mm of bone loss. Study conducted by Alagl et al. [61] has shown that erbium laser (Er:Cr:YSGG) is less effective in reducing bacterial contamination like *Acinetobacter baumannii* and *Pseudomonas aeruginosa* on implant surface.

New technologies like laser therapy and photodynamic therapy have shown to be potent in healing peri-implantitis [62, 63]. Researchers have been constantly trying to review and authenticate the use of lasers in treating peri-implantitis and osseointegration; the current data on various agents used for decontamination have concluded that there is no existing decontamination approach and failed to show influence of any current particular decontamination protocol on surgical therapy [64, 65]. Further clinical investigation needs to be done to check and determine the superiority of any existing decontamination protocol [66].

5 Future of Laser in Implant Dentistry

The practice of laser technology in dentistry and its application have expanded implant dentistry. Use of lasers seems to be a promising tool for increased and improved results. The application of laser like Erbium laser in osteotomy has a more potential outcome than conventional technique of drills. With erbium laser depth is controlled, less friction than drills which leads to overheating of the bone [67], less

traumatic, sterile as they cut, reduce the risk of post-operative infection and a better outcome [44].

Studies done by El-Montaser et al. [68] have shown better healing of implant site with erbium laser than bur. Better in growth of new bone is formed around titanium metal implants and osseointegration. Studies have shown the use of low-level laser techniques resulted in better wound healing. Presence of collagen fibrils, increased cell reproduction and increased prostaglandin levels are seen [69]. Mikhail et al. did a study comparing the effect of non-laser and low-level laser therapy, on the osseointegration of immediately loaded implant and inferred a significant bone healing and speeding osseointegration process due to laser bio-stimulatory effect [70]. Studies on the bio-stimulatory effect of PRF augmented with diode laser as compared to PRF alone shows no satisfactory difference between the two in post-operative pain, implant stability and bone density [71].

6 Conclusions

Lasers play a very important role in implant dentistry. It has its potential role in secondary stage surgery, decontamination of failing implants and healing peri-implantitis and osseointegration. Concern does arise about the implant surface being melted due to overheating [72]. Lasers have a significant benefits and advantages to modern dentistry, in specific to implant dentistry. The soft and hard tissue lasers like diode, erbium and CO_2 provide a more relaxing experience to the patient and high quality of care. Each laser has its own advantages and limitations, unique effects on dental tissue. Thus, depending on the clinical goal, skill and experience of the practitioner, lasers can be a tool for implant dentistry.

This chapter emphasized most of the procedures if not all that can be accomplished and enhanced with the laser. It is imperative on the clinicians to embrace laser technology as a practice in their profession imparting clinical benefits and positive patient outcome.

References

1. Romanos GE, Gupta B, Yunker M, Romanos EB, Malmstrom H. Lasers use in dental implantology. Implant Den. 2013;22(3):282–8.
2. Marder MZ. Treatment planning for dental implants: a rationale for decision making. Part 1. Total edentulism. Dent Today. 2005;24(5):74–6, 78, 80–83.
3. Lindh T, Gunne J, Tillberg A, Molin M. A meta-analysis of implants in partial edentulism. Clin Oral Implants Res. 1998;9(2):80–90.
4. Jivraj S, Chee W. Rationale for dental implants [abstract]. Br Dent J. 2006;200:661–5.
5. American Academy of Implant Dentistry. Dental implants preferred option for aging bridges [news release]. May 2008. http://www.aaid-implant.org.

6. Goldman L, Hornby P, Meyer R, Goldman B. Impact of the laser on dental caries. Nature. 1964;203:417.
7. Walsh LJ. The current status of laser applications in dentistry. Aust Dent J. 2003;48:146–55.
8. Frentzen M, Koort HJ. Lasers in dentistry: new possibilities with advancing laser technology? Int Dent J. 1990;40:323–32.
9. Myers TD, Myers ED, Stone RM. First soft tissue study utilizing a pulsed Nd:YAG dental laser. Northwest Dent. 1989;68:14–7.
10. Romanos GE, Gupta B, Yunker M, Romanos EB, Malmstrom H. Lasers use in dental implantology. Implant Dent. 2013;22(3):282–8.
11. Francis L, Pillai SB. Lasers in implant dentistry. J Dent Implants. 2017;7(2):41.
12. Martin E. Lasers in dental implantology. Dent Clin N Am. 2004;48:999–1015, viii.
13. Convissar RA. Principles and Practice of Laser Dentistry-E-Book. Elsevier Health Sciences; 2015 Mar 6.
14. Coluzzi DJ, Parker SP, editors. Lasers in dentistry—current concepts. Springer; 2017 Sep 21.
15. Daniel McCarthy. The photonics dictionary. 43rd ed. Pittsfield, MA: Laurin Publishing; 1997.
16. Charles Coulston Gillispie. Dictionary of scientific biography. New York: Charles Scribner's Sons; 1971.
17. Bohr N. The theory of spectra and atomic constitution. 2nd ed. Cambridge, MA: Cambridge University Press; 1922.
18. Manni JG. Denatl applications of advanced lasers. Burlington, MA: JGM Associate; 2004.
19. Coluzzi DJ, Convissar RA. Atlas of laser application in dentistry. Hanover Park, IL: Quintessence; 2007.
20. Romanos G, Nentwig GH. Diode laser (980 nm) in oral and maxillofacial surgical procedures. J Clin Laser Med Surg. 1999;17(5):193–7.
21. Gregg R. Laser resource and reference guide. Dent Today. Mar 2006. http://www.dentistrytoday.com/technology/lasers/1366. Accessed Oct 2014.
22. Fasbinder D. Dental laser technology. Compend Contin Educ Dent. 2008;29(8):459.
23. Romanos G. Laser surgical tools in implant dentistry for the long term prognosis of oral implants. Int Congress Series. 2003;1248:111.
24. Yousif A, Zwinger S, Beer F, et al. Investigation on laser dental implant decontamination. J Laser Micro/Nanoeng. 2008;3(2):119–23.
25. Romanos G. Question 1: is there a role for lasers in the treatment of peri-implantitis? J Can Dent Assoc. 2005;71:117–8.
26. Coluzzi D. Fundamentals of dental lasers: science and instruments. Dent Clin N Am. 2004;48:751–70.
27. Cobb CM. Lasers in periodontics: a review of the literature. J Periodontol. 2006;77:545–64.
28. Block CM, Mayo JA, Evans GH. Effects of the Nd:YAG Dental laser on plasma-sprayed and hydroxyapatite-coated titanium dental implants: surface alteration and attempted sterilization. Int J Oral Maxillofac Implants. 1992;7:441–9.
29. Romanos GE, Everts H, Nentwig GH. Effects of diode and Nd: YAG laser irradiation on titanium discs: a scanning electron microscope examination. J Periodontol. 2000;71(5):810–5.
30. Schwarz F, Aoki A, Sculean A, Becker J. The impact of laser application on periodontal and peri-implant wound healing. Periodontology 2000. 2009;51(1):79–108.
31. Walsh LJ. The use of lasers in implantology: an overview. J Oral Implant. 1992;18(4):335.
32. Gonçalves F, Zanetti AL, Zanetti RV, Martelli FS, Avila-Campos MJ, Tomazinho LF, Granjeiro JM. Effectiveness of 980-mm diode and 1064-nm extra-long-pulse neodymium-doped yttrium aluminum garnet lasers in implant disinfection. Photomed Laser Surg. 2010;28(2):273–80.
33. Strauss R, Fallon S. Lasers in contemporary oral and maxillofacial surgery. Dent Clin N Am. 2004;48:861–8.
34. Deppe H, Greim H, Brill T, et al. Titanium deposition after peri implant care with carbon dioxide laser. Int J Oral Maxillofac Implants. 2002;17(5):707–14.
35. Aoki A, Mizutani K, Takasakim AA, et al. Current status of clinical laser applications in periodontal therapy. Gen Dent. 2008;56(7):674–84.

36. Deppe H, Horch H, Helmut G, et al. Peri-implant care with the CO2 laser: in vitro and in vivo results. Med Laser Appl. 2005;20:61–70.
37. Pang P. Lasers in Cosmetic Dentistry. Gen Dent. 2008;56(7):663–4.
38. Israel M. Use of the CO2 laser in soft tissue and periodontal surgery. Pract Periodontics Aesthet Dent. 1994;6:57–64.
39. Forrer M, Frenz M, Romano V, et al. Bone-ablation mechanism using CO2 lasers of different pulse duration and wavelength. Appl Phys B Lasers Opt. 1993;56(2):104–12.
40. Aoki A, Sasaki KM, Watanabe H, et al. Lasers in nonsurgical periodontal therapy. Periodontology 2000. 2004;36:59–97.
41. Kato T, Kusakari H, Hoshino E. Bactericidal efficacy of carbon dioxide laser against bacteria-contaminated titanium implant and subsequent cellular adhesion to irradiated area. Lasers Surg Med. 1998;23(5):299–309.
42. Fonseca R. Oral and maxillofacial surgery, vol. 6. Philadelphia, PA: WB Saunders; 2000.
43. Scortecci G, Misch C, Benner K. Implants and restorative dentistry. New York: Martin Dunitz; 2001.
44. Bornstein ES. The safety and effectiveness of dental Er:YAG lasers: a literature review with specific reference to bone. Dent Today. 2003;22(10):129–33.
45. Dederich D, Bushick R. Lasers in dentistry: separating science from hype. J Am Dent Assoc. 2004;135(2):204–12.
46. Locke M. Clinical applications of dental lasers. Gen Dent. 2009;57(1):47–59.
47. Wahl M. Myths of dental surgery in patients receiving anticoagulant therapy. J Am Dent Assoc. 2000;131(1):77–81.
48. Pototski M, Amenabar J. Dental management of patients receiving anticoagulant or antiplatelet treatment. J Oral Sci. 2007;49(4):253–8.
49. Matjaz L, Marincek M, Grad L. Dental laser drilling: achieving optimum ablation with the latest generation Fidelis laser systems. J Laser Health Acad. 2007;7(1):1–3.
50. Walsh JT Jr, Flotte TJ, Deutsch TF. Er:YAG laser ablation of tissue: effect of pulse duration and tissue type on thermal damage. Lasers Surg Med. 1989;9:314–26.
51. Rayan G, Pitha J, Edwards J, Everett R. Effects of CO2 laser beam on cortical bone. Lasers Surg Med. 1990;11(1):58–61.
52. Vercellotti T, De Paoli S, Nevins M. The piezoelectric bony window osteotomy and sinus membrane elevation: introduction of a new technique for simplification of the sinus augmentation procedure. Int J Periodontics Restorative Dent. 2001;21(6):561–7.
53. Tunc SK, Yayli NZ, Talmac AC, Feslihan E, Akbal D. Clinical comparison of the use of Er, Cr: YSGG and diode lasers in second stage implant surgery. Saudi Med J. 2019;40(5):490.
54. Chen S, Darby I. Dental implants: maintenance, care and treatment of peri-implant infection. Aust Dent J. 2003;48(4):212–20.
55. Santos V. Surgical anti-infective mechanical therapy for periimplantitis: a clinical report with a 12-month follow-up. Gen Dent. 2009;57(3):230–5.
56. Leonhardt A. Five-year clinical, microbiological, and radiological outcome following treatment of peri-implantitis in man. J Periodontol. 2003;74(10):1415–22.
57. Yung F. The use of an Er:YAG laser in periodontal surgery: clinical cases with long-term follow up. J Laser Dent. 2009;17(1):13–20.
58. Deppe H, Horch H. Laser applications in oral surgery and implant dentistry. Lasers Med Sci. 2007;22:217–21.
59. Schwarz F, Bieling K, Bonsmann M, et al. Nonsurgical treatment of moderate and advanced periimplantitis lesions: a controlled clinical study. Clin Oral Invest. 2006;10:279–88.
60. Quirynent M, Vogels R, Pauwels M, et al. Initial subgingival colonization of “pristine” pockets. J Dent Res. 2005;84(4):340–4.
61. Alagl AS, Madi M, Bedi S, Al Onaizan F, Al-Aql ZS. The effect of Er, Cr: YSGG and diode laser applications on dental implant surfaces contaminated with Acinetobacter Baumannii and Pseudomonas Aeruginosa. Materials. 2019;12(13):2073.

62. Romanos G, Ko HH, Froum S, et al. The use of CO2 laser in the treatment of peri-implantitis. Photomed Laser Surg. 2009;27:381–6.
63. Vohra F, Al-Rifaiy MQ, Lillywhite G, et al. Efficacy of mechanical debridement with adjunct antimicrobial photodynamic therapy for the management of periimplant diseases: a systematic review. Photochem Photobiol Sci. 2014;13:1160–8.
64. Schwarz F, Schmucker A, Becker J. Efficacy of alternative or adjunctive measures to conventional treatment of peri-implant mucositis and peri-implantitis: a systematic review and meta-analysis. Int J Implant Dent. 2015;1:22–55.
65. Meyle J. Mechanical, chemical and laser treatments of the implant surface in the presence of marginal bone loss around implants. Eur J Oral Implantol. 2012;5(Suppl):S71–81.
66. Koo KT, Khoury F, Keeve PL, Schwarz F, Ramanauskaite A, Sculean A, Romanos G. Implant surface decontamination by surgical treatment of periimplantitis: a literature review. Implant Dent. 2019;28(2):173–6.
67. Miloro M, Ghali GE, Larsen P, Waite P. Peterson's principles of oral and maxillofacial surgery, vol. 2. Hamilton, OH: BC Decker; 2004.
68. El-Montaser M, Devlin H, Dickinson M, et al. Osseointegration of titanium metal implants in erbium-YAG laser prepared bone. Implant Dent. 1999;8(1):79–85.
69. Sun G, Tunér J. Low-level laser therapy in dentistry. Dent Clin N Am. 2004;48:1061–76.
70. Mikhail FF, El-Din M, Ibrahim T, Zekry K, Nemat A, Nasry S. Effect of laser therapy on the osseointegration of immediately loaded dental implants in patients under vitamin C, Omega-3 and calcium therapy. Open Access Maced J Med Sci. 2018;6(8):1468.
71. Sleem SS, Zayet MK, El-Ghareeb TI, Saleh HA. Evaluation of the bio-stimulatory effect of platelet rich fibrin augmented by diode LASER compared to platelet rich fibrin alone on dental implant replacing posterior mandibular teeth. Randomised Clinical Trial: Split Mouth Study. Open Access Maced J Med Sci. 2019;7(5):869.
72. Romanos G. Current concepts in the use of lasers in periodontal and implant dentistry. J Indian Soc Periodontol. 2015;19(5):490.

Applications of CAD/CAM Technology in Dental Implant Planning and Implant Surgery

Kathleen Manuela D'Souza and Meena Ajay Aras

Abstract Proper diagnosis and appropriate treatment planning is paramount to achieve the best long-term prognosis in implant dentistry. Computer-aided implant surgery has dramatically improved the quality of surgical procedures used for dental implant bed preparation and implant placement. The term computer-aided implant surgery encompasses computer-guided implant surgery using static surgical guides and dynamic surgical procedures using navigation systems and computer-oriented surgery. In this chapter, we will be extensively discussing computer-guided implant surgery. The three-dimensional assessment of the restorative goal [using cone beam computerized tomography (CBCT), radiographic template and implant design programs] allows realistic planning and optimized positioning of implants using surgical guides. Three patient case reports are discussed which included the use of Implant planning software, namely, NobelClinician™ software and 3Shape Implant Studio® CAD software and stereolithographic surgical guides for predictable implant placement. Advances in dynamic implant surgery will also be discussed towards the end of the chapter.

Keywords CAD/CAM technology · Computer-aided implant surgery · 3D printed surgical guide · CBCT in implants · Dynamic implant surgery

1 Introduction

Osseointegration of dental implants is significantly dependent on a thorough presurgical planning, followed by a precise surgical and prosthodontic approach [1]. The past three decades have witnessed an increasing use of dental implants. Advancing technologies have facilitated the application of dental implants for the replacement of missing teeth. Although conventional dental implant placement

K. M. D'Souza (✉) · M. A. Aras
Department of Prosthodontics, Crown and Bridge, Goa Dental College and Hospital, Bambolim, Goa, India

R. S. Chaughule, R. Dashaputra (eds.), *Advances in Dental Implantology using Nanomaterials and Allied Technology Applications*,
https://doi.org/10.1007/978-3-030-52207-0_11

encompasses reflection of a muco-periosteal flap, an increased level of patient satisfaction has been reported with minimally invasive surgical procedures and implementation of computer-aided implant surgery [2–4].

Use of conventional imaging techniques with clinical examination is considered insufficient for diagnosis and treatment planning for minimally invasive surgeries [5]. Consequently, advances in diagnostic imaging tools using cone beam computerized tomography (CBCT), interactive implant planning software and evolution of computer-aided design/computer-aided manufacturing (CAD/CAM) technology has revolutionized pre-surgical treatment planning and has promoted computer-aided implant surgery (CAIS). Hence, CAIS has become the mainstay of most oral and craniofacial reconstructive efforts.

This chapter will sensitize the reader to computer-aided implant surgery and provide an overview of the currently available systems that support computer-aided implant surgery. It will also review and illustrate the application of computer-guided technology and surgical guides in dental implant surgery with the help of three clinical case reports.

2 Overview of Technology

Computer-aided implant surgery is "the capability of performing virtual surgery based on the use of medical/dental imaging files (DICOM, STL, vrml, obj, etc.) using computer software. The results are used to develop digitally manufactured surgical guides or navigation directions for robotic guidance for surgery" [6].

It involves the following surgical protocols: (a) static navigation: computer-guided implant surgery using static surgical guides and (b) dynamic navigation: a computer navigation-based implant surgery or a computer-oriented implant surgery. A constant research in this field aims at a restoratively driven, patient-centred surgical outcome.

Computer-guided static navigation allows a fully guided (FG) bone implant drilling sequence and implant placement using static surgical guides. Whereas, dynamic navigation allows real-time monitoring of the bone drilling and implant placement using three-dimensional (3D) software [7–9].

The various benefits and drawbacks of each type of system [7–9] are enumerated in Table 1.

3 Need for Computer-Based Implant Surgery

Traditionally, the non-limiting and partially limiting designs of surgical guides provided guidance in angulations and positioning of implant drills at the bone entry point. A lack of correlation between the planned restoration and the underlying alveolar bone anatomy was commonly encountered. Also, 2D interpretation of radiographic

Table 1 Advantages and disadvantages of different systems in computer-based surgical protocol

Computer-based surgical protocol	Advantages	Disadvantages
Computer-guided surgery with surgical guides	• Minimally invasive treatment • Provides simplicity in surgical protocol as compared to conventional implant surgery • Improves precision, accuracy and efficacy of surgery • Economical compared to dynamic implant surgery	• Need for special dental materials and accessibility to manufacturing units or dental laboratory for surgical guide fabrication • Need additional patients visits to fabricate the surgical guide • Guidance failures due to fractured or poor fitting guides • Expensive compared to conventional implant surgery
Computer-navigated surgery	• Minimally invasive treatment • Allows real-time feedback of osteotomy site preparation and implant placement • Eliminates need for additional patient visits and dental materials needed to fabricate scan prosthesis and/or surgical guide • Simpler and faster planning • Improves accuracy and safety of surgery • No implant manufacturer-dependent armamentarium required	• Need for extensive training and operator experience • Upfront investment in workflow adjustments • Purchasing and managing cost • Errors in drill-tip to CBCT image mapping can occur causing guidance and placement errors • Improvements in software design and tracking system is needed • Human studies on the application of this system are less
Computer-oriented surgery	• Minimally invasive treatment • Allows real-time decision making during surgery • Eliminates the need for guiding or navigation systems • Improves accuracy and promotes surgical flexibility	• Huge investments in acquiring equipment and managing cost • Need for extensive training and operator experience • Much research is needed to establish the workflow

information obtained from panoramic and/or periapical radiographs presented with significant limitations to approach a realistic surgical scenario. This demanded the application of computer-guided implant surgery in complex and compromised cases. The objective of computer-based surgery was to alleviate inadequacies of conventional two-dimensional (2D) imaging tools and traditional surgical guides.

Computer-guided implant surgery minimizes the errors in implant positioning compared to manual/conventional surgical guide implant placement [10]. Implant surgery with completely limiting design of surgical guide increases safety, predictability and efficacy of the treatment outcome in cases with excessive hard and soft tissue loss, sinus pneumatisation or atrophic alveolar ridges [11, 12].

In addition, computer-guided protocol promotes minimally invasive surgeries with possibility of immediate delivery of prosthesis. It offers gold standard treatment, with minimal patient visits and lesser post-operative morbidity, at affordable cost [12].

This system favours the production of customized prosthetic and surgical components needed for the treatment, such as surgical guides, provisional restorations,

customized healing abutments and final prostheses. It increases productivity and reduces laboratory production delays. In addition, computer-guided implant surgery offers predictability with temporary restoration of dental implants and needs less time in adaptation of temporary prosthesis in immediate loading protocols [12, 13]. Nevertheless, it promotes an integrated prosthetic and surgical workflow.

It has shown favourable results in terms of accuracy and implant survival rates [14]. Even though literature reports deviations between planned and clinical positions of implants placed using completely limiting design of surgical guides, lesser deviation values were obtained with full-guided implant surgery as compared to half-guided surgery (HG) (implant placed without the surgical guide after osteotomy) [15–17]. It was also noted that computer-guided surgical guides provided greater accuracy and were more consistent in their deviation from the planned locations than conventional surgical guides and free-handed (FH) implant surgery [18–21].

4 What Is Computer-Guided Surgery?

"Computer-guided implant surgery" is defined as the use of a static surgical guide that reproduces the virtual implant position directly from CT data and does not allow for intra-operative modification of the implant position [22]. It involves reverse planning and fabrication of a static surgical guide, which is used to assist in proper surgical placement and angulation of dental implants [23]. A restorative treatment plan is created prior to establishing the surgical protocol. This is achieved by fabricating radiographic scan prosthesis or using intra-oral optical impressions and virtual models. This is followed by a CBCT scan. These images are then imported into a software program on a personal computer, which allows virtual treatment planning. Virtual surgical planning encompasses pre-surgical manipulation of 3D images of an anatomic site for the purpose of measuring outcomes and to design devices, grafts, and techniques. A digital plan, thus, obtained is used to fabricate a surgical guide. These surgical guides, accompanied by implant specific drilling instrumentation, allow precise implant placement in planned positions.

Typically, the surgical guide consists of two parts: (a) the guide body (contact surface) which fits either on the patient's mucosa, bone or teeth and (b) the guiding cylinder (sleeve) placed within the surgical guide to guide the drills in the exact position and angulation [24].

4.1 Classification of Computer-generated Surgical Guides

Based on method of fabrication, three types of guides have been reported:

(a) 3D printed surgical guide based on acrylic radiographic scan prosthesis [24].
(b) 3D printed surgical guide based on intra-oral optical scans/laboratory scan of dental cast [25].

(c) Computer milled guides or mechanical templates—are fabricated by drilling the final position of the implants in the radiographic template using a computer-guided drilling machine. This is followed by setting titanium guide cylinders in the exact same position and angulation as previously planned [5, 8].

Based on guide support, four types of guides have been reported [7, 26]:

(a) Mucosa-supported: These guides are associated with flapless surgery. In completely edentulous patients, these guides are supported by the buccal and lingual mucosal flanges and the palatal mucosa. In addition, transmucosal fixation pins help in its stabilization during the surgery. Whereas, in partially edentulous patients with a long span of edentulous area, these guides are supported partly by mucosa and partly by teeth adjacent to the edentulous space.
(b) Bone-supported: This surgical guide is supported by the bone surface which requires reflection of a full-thickness flap. They are indicated in cases with bone deficiencies requiring bone augmentation procedures, cases with anatomical limitations or in cases with lack of keratinized mucosa.
(c) Tooth-supported: the guide is supported on the teeth adjacent to the edentulous space.
(d) Special supported, (mini) implant, pin-supported surgical guides: this surgical guide is attached to implants inserted before or during the actual implant surgery.

4.2 Step-By-Step Protocol Involved in Fabrication of 3D Printed Surgical Guides for Dental Implant Surgery

The following workflow is adopted to obtain a conventional computer-generated surgical guide (Fig. 1).

4.2.1 Fabrication of Scan Prosthesis

A scan prosthesis or radiographic template is a partial or complete acrylic removable prosthesis, incorporated with radiographic markers, that conveys the ideal prosthetic positioning of the teeth for the definitive prosthesis during the CBCT scan. It can be either fabricated de novo from a diagnostic wax up or by duplicating the patient's existing denture, if it is aesthetically and functionally acceptable. Some of the crucial factors to be considered during the fabrication of a radiographic template are as follows [27, 28]: (a) precise fit of the prosthesis to the underlying mucosa, (b) precise extension of flanges to provide stability to the prosthesis during scanning, (c) involves mock-up of the ideally positioned artificial teeth, based on the patient's functional, biomechanical and aesthetic requirements, (d) proper incorporation of fiducial (registration/radiographic) markers [29] and (e) fabrication of an

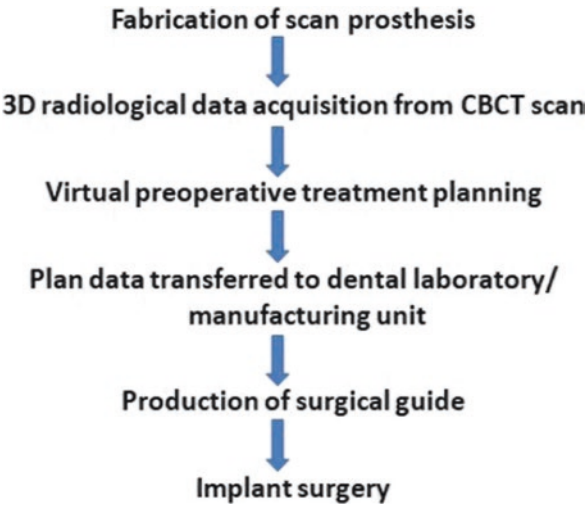

Fig. 1 Conventional workflow involved in computer-generated surgical guide and computer-guided implant surgery

interocclusal index (vinyl polysiloxane centric occlusion index) to stabilize the scan prosthesis during the CBCT scan [30]. These markers indicate the tooth or restoration outline by indicating the incisal edge position, bucco-lingual tooth position and denture base contour. They allow an accurate representation of the final restorative goal by ensuring adequate radiographic determination for implant placement. Moreover, these markers act as fiducial markers for registration. Literature reports the use of different radiographic markers, such as gutta-percha [31], metal tubes [32], ball bearings [33], lead foil [34], and barium sulphate in resin powder or radiopaque barium denture teeth [35]. When a radiographic template is used, a double scan procedure is carried out to help integrate the template within the craniofacial model. A scan of the edentulous site is carried out first, followed by a scan with the radiographic template and the interocclusal index fitted in the mouth. Both the scans are then aligned over each other using the radiographic markers as reference points. This dataset is then exported to an implant planning software, which allows a fusion of these files to provide an exact representation of the patient's bone architecture and the radiographic template in 3D space [36].

Nevertheless, creation of a virtual patient by superimposition and registration of digital intra-oral scans with CBCT data has helped to alleviate shortcomings in surface reproduction of teeth in a CBCT image [37–39]. Digital impressions or surface scans of dental models have been suggested to replace conventional fabrication of scan prosthesis in partially edentulous patients [40]. Although the marker-based method of digital registration is considered more accurate, newly developed surface registration algorithms have greatly increased accuracy [41, 42]. These registration algorithms allow the clinician or the laboratory to utilize readily available dental surface markers, such as cusp tips, denture borders and soft tissue profiles, to facilitate digital registration. The dentogingival model scanning is superimposed on

DICOM files using specific software to create a virtual model of the patient. This promotes optimization of the digital treatment workflow, simplifies communication between clinician and laboratory, reduces expensive laboratory work and dental appointments needed for the fabrication of the scan prosthesis and promotes efficient time-cost workflow since there is fast processing of surgical guide. Moreover, digital scans alleviate errors that may be caused by ill-fitting or inaccurately fabricated scan prosthesis [39, 42, 43]. However, one of the major limitations of this technique is that it is helpful only in partially edentulous patients. For completely edentulous patients, incorporating intra-oral scan images into the CBCT data would not be possible, since mutual landmarks on both digital images, such as part of the teeth, are required [37]. Another significant limitation is the influence of imaging artefacts in CBCT data on the registration accuracy. For the purpose of registration, areas on the tooth surface represented in the virtual stone cast and in the model produced from radiographic data are selected and these markings must be discernable in the respective images to be registered. However, scatter artefacts can obscure these markings. Also, radiopaque markers placed on the buccal or lingual aspect of restored teeth will not be visible on a CBCT scan. Composite resin markers in the vertical plane can be used to alleviate this problem [40, 44].

When a laboratory scanner is used, first the diagnostic cast is scanned to obtain a soft tissue representation and then a rescan of the manual wax-up and the interocclusal relationship of the upper and lower cast is carried out. The first scan facilitates the placement of the guide sleeve in the surgical guide and the second scan helps to create a virtual diagnostic waxing image. Alternatively, the mirror image of the contralateral teeth can also be used in the software to create a digital wax-up. The resulting files are then superimposed on the CBCT scan to facilitate the implant position planning in relation to the planned restoration [37].

Various intra-oral scanners are commercially available. Some popular ones include CEREC® Omnicam (Dentsply Sirona Global, NC, USA), Primescan® (Dentsply Sirona, Bensheim, Germany), 3Shape Trios® (3Shape A/S, Copenhagen, Denmark), Virtuo Vivo™ (Dental Wings Inc., Montreal, Canada) and iTero® (Align Technology, Inc., California, USA). Laboratory scanners for dental model scanning are also available, for example, 3Shape lab scanner (3Shape A/S, Copenhagen, Denmark), 7Series Model and Impression Scanner (Dental Wings Inc., Montreal, Canada) and Ceramill® Map 400+ Scanner (Amann Girrbach GmbH, Koblach, Austria).

The modified workflow for fabrication of computer-generated surgical guide using intra-oral scanners is presented in Fig. 2 [25].

4.2.2 CBCT Scanning Procedure

Dental CBCT offers a three-dimensional evaluation of the concerned oral and craniofacial region by generating images that precisely replicate the clinical situation on a computer. A CBCT scan along with a third-party software program allows the clinician to visualize and interpret the anatomical situation of the patient. It has

Fig. 2 Modified workflow involved in computer-generated surgical guide and computer-guided implant surgery

gained popularity over conventional CT scans since it provides radiographic images with minimal distortion and superimposition [45].

CBCT machines emit a cone-shaped X-ray beam which is detected on a flat panel detector (FDP) receptor, both of which are simultaneously rotating 180–360° around the patient's head. The captured 2D images of the maxillofacial region are converted to 3D volumetric data. This process is carried out on a computer using a modified Feldkamp algorithm to create DICOM (Digital Imaging and Communications in Medicine) files [46]. DICOM file is a standardized file format used for handling, storing, transmitting and communicating CBCT data. It is a set of axial images that are merged together to form the volume data of the anatomical structures. These files are exported to a third-party software that enables surgical planning, transfer of data to surgery via 3D printing of surgical guides/navigation systems and transfer of data for production of prosthetic solutions [47].

4.2.2.1 Indications

The following are the main indications for CBCT in implant placement: (1) evaluation of quality and quantity of residual bone, (2) three-dimensional assessment of implant site topography, (3) visualization of vital anatomic structures around implant site, (4) fabrication of surgical guides, (5) identification of any associated complexities and (6) patient education.

4.2.2.2 Advantages and Disadvantages of CBCT

The high spatial resolution, small size isotropic voxel and segmentation accuracy of reconstructed CBCT datasets allows production of a high-quality image. It involves relatively less radiation exposure, reduction in the size of irradiated area by collimation of the primary X-ray beam to the desired area, rapid scan time, compact size, easier handling and accessibility and is economical, as compared to the conventional CT.

Certain limitations associated with CBCT include (1) lack of distinct soft tissue contrast, (2) inability to estimate the bone density using Hounsfield units [48], (3) artefacts incorporation in the image due to patient motion, dense restorative materials or a combination of both and (4) need for adequate training to operate CBCT and diagnose datasets. However, recent research and development of software algorithms aim to alleviate these shortcomings: (1) software algorithms improving signal-to-noise ratio and thus, increasing contrast, (2) improvement in image quality allowing structural analysis of bone in contrast to the density-based analysis, (3) artefact suppression algorithms and increasing number of projections causing reduction in metal artefacts, e.g. Metal artefact reduction software (MARS) by Sirona [49].

4.2.2.3 Display Modes in CBCT

The CBCT machine produces multiple basis projection frames which are collectively known as the projection data. The projection data is primarily reconstructed by the CBCT software to produce axial slices, which are further processed to generate inter-relational images in three orthogonal planes (axial, coronal and sagittal views). In addition to these views, other display modes generated include multiplanar reformations (MPR) consisting of oblique planar reformation, curved planar reformation, serial trans-planar reformation and multiplanar volume reformation [47].

- Oblique planar reformation produces non-axial 2D planar images by cutting across a set of axial images at any angle. It is useful to evaluate particular structures, such as winding angles of mandibular canal.
- Curved planar reformation produces “simulated” distortion free panoramic images by aligning the long axis of the imaging plane with a specific anatomic structure. It is useful to trace the jaw during dental implant planning.
- Serial trans-planar reformation produces series of stacked cross-sectional images orthogonal to oblique or curved planar reformation with option of selecting the thickness and spacing. It is useful in assessment of specific morphologic features such as alveolar bone height and width for implant site assessment.
- Multiplanar volume reformation: produces an image that closely represents a specific volume of the patient by thickening the MPR slices:

- Ray sum or ray casting: this image can be generated by adding up adjacent voxels to the MPR slices. It is useful in generating virtual projections such as panoramic or cephalometric images identical to conventional radiographs without magnification and parallax distortion. However, this technique uses the entire volumetric data set and there can be superimposition of multiple structures [50].
- Volume rendering: this generates an image which allows visualization of volume by selectively displaying voxels within a data set to facilitate spatial orientation of the jaw and object placement control during planning. This involves direct volume rendering and indirect volume rendering. Direct volume rendering involves picking an arbitrary threshold of voxel values, below or above which all grey values are excluded. Most commonly used technique includes maximum intensity projection (MIP). MIP is useful for surgical follow-up and for visualization of soft tissue calcifications [46]. Indirect volume rendering (IVR) involves selection of the density of the voxels to be displayed within an entire data set (segmentation) resulting in a volumetric surface reconstruction with depth. It can either be a solid view (surface rendering) or a transparent view (volumetric rendering). IVR is useful for visualization and analysis of craniofacial conditions and determination of relationships of various anatomic features [46].

4.2.3 Virtual Planning and Transfer of Data to Production Unit

Simulation computer software is used to create a CAD model of the patient's jaw for the accurate transfer of the virtually planned implant position to the surgical site. The virtual model that is solely reconstructed from CBCT data does not display the teeth accurately enough for the manufacturing of a surgical guide. Thus, integration of a virtual model of the teeth (derived from a CBCT scan of the scan prosthesis or an intra-oral surface scan or extra-oral scan of a stone cast) with the radiographic model (derived from CBCT scan of the jaw) is required. The surface scan of the patient's oral cavity is exported to the software in the Standard tessellation language (STL) format. This procedure, which involves the integration of the DICOM data set (CBCT model) with the STL file (virtual model) by a process of alignment of the two data sets in one virtual coordinate and transformation of the three-dimensional images, is known as registration [44]. The registration process helps in the preoperative digital implant planning, surgical guide file creation based on the virtual model of the teeth and export of the created file to an external system for manufacturing.

The simulation software includes a realistic library of varied implant systems necessary for the virtual implant planning. It facilitates selection of a suitable implant fixture based on the anatomical situation, the planned prosthetic outcome and the specifications for each implant as delineated by the manufacturer. It permits import or export of DICOM data and STL files with third-party systems. The software also includes the tools needed to design and to enhance the surgical guide and

to design the planned prosthetics. Once the plan is formulated, the software automatically creates a surgical report in the PDF format on the implant plan (implant type, and specifications such as platform, length and width) and designed guide with all the necessary information needed for successful surgery. On approval of the plan, the software automatically creates a STL file that can be directly sent to a suitable 3D printer.

Several commercially available proprietary 3D interactive computer software programs are available, which include Simplant® (Materialise Dental, Leuven, Belgium), Nobel Clinician™ (Nobel Biocare, Zurich, Switzerland), CoDiagnostix® (Dental Wings Inc., Montreal, Canada), VIP 3® (BioHorizons, AL, USA), Planmeca Romexis® 3D (Planmeca Oy, Helsinki, Finland), 3Shape Implant studio® (3Shape medical A/S, Copenhagen, Denmark) and Blue Sky Plan® (BlueSkyBio, LLC, USA).

4.2.4 Fabrication of Surgical Guide

A completely limiting design of surgical guide further allows a predictable transfer of planned implant positions from computer to the patient. It helps to direct the surgical drills during the implant osteotomy and implant insertion. The process of building a three-dimensional object from a CAD model by successively adding material layer by layer is known as 3D printing or additive manufacturing process or rapid prototyping.

Resin 3D printing includes a vat polymerization technique in which a photosensitive resin is cured by a light source to produce solid layers. The resin is contained within a vat/tank and is cured against a build platform, which moves slowly away from the tank as the part is formed. Based on the light source used, there are three types of resin 3D printing technologies, namely, stereolithography (SLA), digital light processing (DLP) and liquid crystal display (LCD).

Stereolithography (SLA) is the most commonly used technology and it employs a vat of liquid ultraviolet (UV) curable photopolymer "resin" and a UV laser to build parts' layers one at a time. The laser beam is directed by mirror-like devices known as galvanometers. For each layer, the laser beam traces a cross section of the part pattern on the surface of the liquid resin. On polymerization of the surface layer, the mechanical table carrying the previously polymerized layer of the model moves down by 1 mm. Exposure to the UV laser light cures and solidifies the pattern traced on the resin and joins it to the layer below [6]. Only 80% of total polymerization is completed in the vat, whereas the remaining 20% needed to be achieved in a conventional UV light curing unit [28]. Based on the diameter and angle of the simulated implants, the SLA machine selectively polymerizes the resin around the planned implant position, forming a cylindrical guide. This cylindrical guide is then fitted with a metal sleeve to guide the implant drill [51]. Stereolithography uses a STL file which describes only the surface geometry of a 3D object without any representation of colour, texture or other common CAD model attributes. This file format is supported by all available 3D printers [24]. Thus, the stereolithographic-guided surgery system includes a stereolithographic surgical guide with implant

system-related mounts for fixture installation, additional guide sleeves for fixation screw installation, drill keys of different heights and depth-calibrated drills to prepare the osteotomies. Some systems use consecutive guides with different sleeves to allow increasing drill diameter during surgery, while some use a single guide with different adjustable drill handles. Sleeveless guide design is also available that helps reduce costs of the surgical guide, since it alleviates material costs for sleeves and additional work required to fasten them into the guide [26]. Various improvements have been reported in the presently available 3D printers, such as rising build platform, improvements in the material properties of the photopolymer resin used, improved optical system to prevent errors in focusing and inexpensive in-office desktop 3D printers [52].

Digital light projector (DLP) technology uses a high-intensity light source uniformly across the entire build surface for curing the photo-reactive polymers. The light is selectively directed using a digital micromirror device (DMD) consisting of multiple tiny mirrors. Liquid crystal display (LCD) is similar to DLP. It uses a high-resolution LCD screen with UV LED backlighting to cure photopolymers layer by layer. More accurate surgical guides are achieved by SLA and DLP as compared to LCD. However, DLP and LCD technology produce faster prints as compared to SLA and LCD technology is cheaper than its counter parts.

Various 3D printers are available commercially for the fabrication of computer-generated surgical guide, for example, Form 2 SLA (Formlabs Inc., MA, USA), SprintRay Pro® DLP (SprintRay CA, USA), Planmeca Creo™ C5 LCD (Planmeca Oy, Helsinki, Finland) and Zenith 3D® SLA (Dentis Global, Daegu, Korea).

4.3 Case Reports Illustrating Application of Computer-Guided Technology to Dental Implant Planning and Dental Implant Surgery

Patient 1 is treated with an "All-on-4®" (Nobel Biocare, Zurich, Switzerland) treatment concept using NobelActive (Nobel Biocare, Zurich, Switzerland), which involves CT-based computer-guided implant planning using NobelClinician™ software, conventional flap procedure and standardized All-on-4® guide (Nobel Biocare, Zurich, Switzerland). Patient 2 is treated with implant-supported overdenture prosthesis with DIOnavi. implants (DIO Implant, Busan, Korea), which involves CT-based computer-guided implant planning using 3Shape Implant studio® implant-planning software (3Shape medical A/S, Copenhagen, Denmark), flapless implant placement and stereolithographic surgical guide with guide sleeves (Form 2 3D printer, Formlabs Inc., MA, USA). Patient 3 is treated with an "All-on-4®" treatment concept using Osstem implants (Osstem Implant Co., Ltd., Seoul, Korea), which involves CT-based computer-guided implant planning using 3Shape Implant studio® implant-planning software (3Shape medical A/S, Copenhagen, Denmark),

flapless implant placement and stereolithographic surgical guide without guide sleeves (Zenith 3D® printer, Dentis Global, Daegu, Korea).

4.3.1 Patient 1 (*Courtesy of Department of Prosthodontics and Oral and Maxillofacial Surgery, Goa Dental College and Hospital*)

A 70-year-old female patient with severely mutilated dentition reported to the department for replacement of missing teeth. Patient reported that she lost most of her teeth due to caries and periodontal disease. After a complete diagnostic evaluation, complete extraction of teeth and the "All-on-4®" (Nobel Biocare, Zurich, Switzerland) treatment concept, with immediately loaded full arch restoration, was planned for both the jaws. The treatment protocol includes placement of two implants vertically in the anterior region with straight Multi-unit abutment and two implants at an angle of up to 45° in the posterior region with angled Multi-unit abutment. Here we will be discussing rehabilitation of the maxillary arch (Figs. 3, 4, 5, 6, 7, 8, 9 and 10).

4.3.2 Patient 2 (*Courtesy of Department of Prosthodontics and Oral and Maxillofacial Surgery, Goa Dental College and Hospital*)

A 65-year-old man presented with completely edentulous mandibular arch and a single implant with a locator attachment in the left mandibular canine region. Patient reported that all his mandibular teeth were extracted due to severe wearing pattern and gross breakdown of tooth structure. His lower jaw was restored with an implant-supported overdenture prosthesis using two implants, placed bilaterally in the canine region with locator attachments. However, failure of right mandibular implant was noted and patient requested rehabilitation of the lower arch. After a complete diagnostic evaluation, an implant-supported overdenture on ball attachments using four implants (DIOnavi.digital implant system, Busan, Korea) in 31, 32, 42, 43 region was planned (Figs. 11, 12, 13, 14, 15, 16, 17, 18, 19, 20, 21 and 22).

4.3.3 Patient 3 (*Courtesy of Department of Prosthodontics and Oral and Maxillofacial Surgery, Goa Dental College and Hospital*)

A 60-year-old female patient reported to the department for replacement of missing teeth in the maxillary arch. She reported that she lost her teeth due to caries and requested for a fixed option for replacement of missing teeth. After a complete diagnostic evaluation, "All-on-4®" (Nobel Biocare, Zurich, Switzerland) treatment concept using Osstem implants (Osstem Implant Co., Ltd., Seoul, Korea) and immediately loaded full arch restoration was planned for the maxillary arch (Figs. 23, 24, 25, 26, 27, 28, 29, 30 and 31).

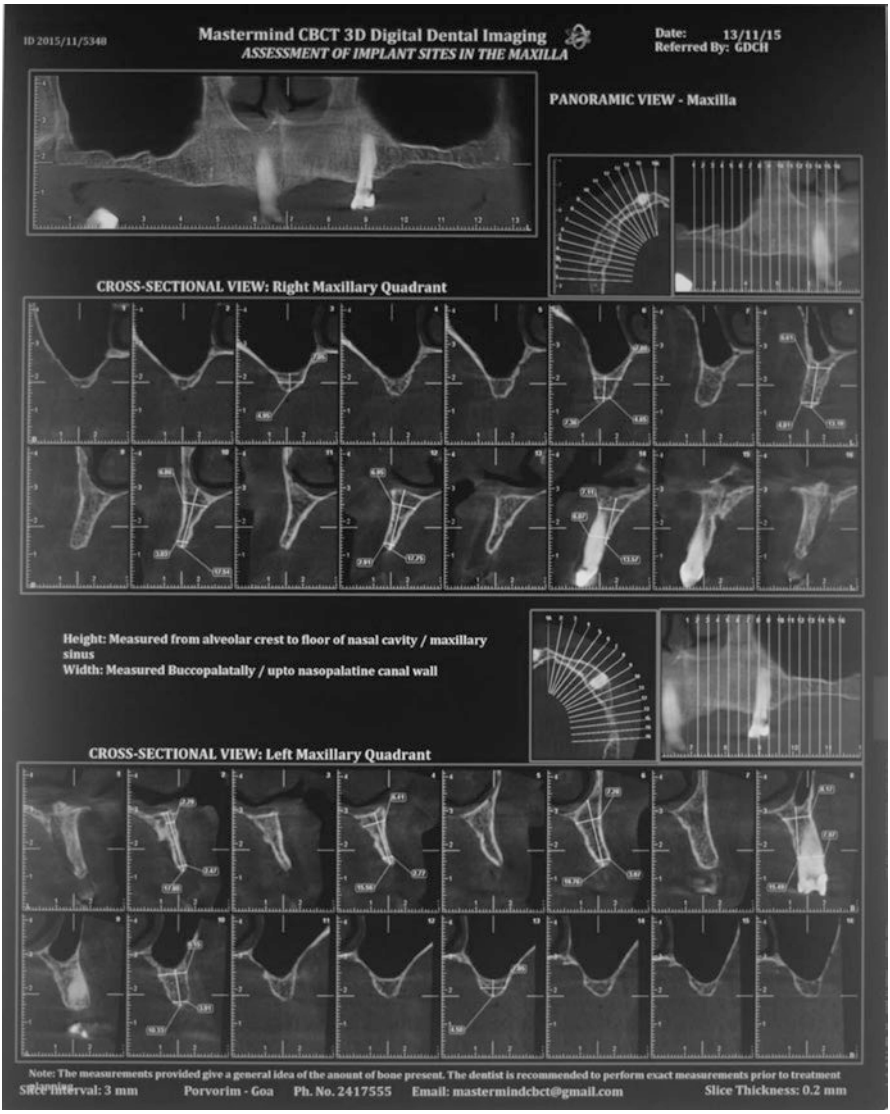

Fig. 3 Showing the CBCT (NewTom VGi, QR S.r.l, Verona, Italy) scan of the maxillary arch. Severe resorption in the posterior maxilla bilaterally with severely carious teeth, 11 and 24, seen on the scan. The scan shows cross-sectional view with 0.2 mm slice thickness and panoramic view of the maxilla

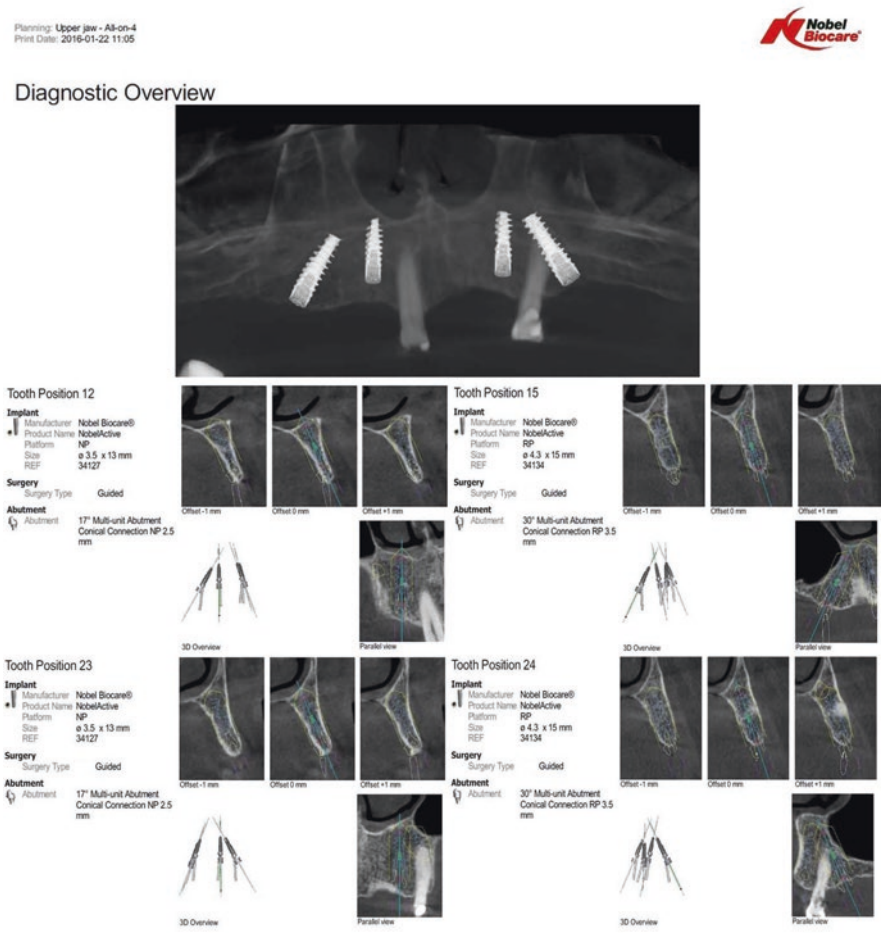

Fig. 4 Illustrates the diagnosis and treatment planning carried out in the implant planning software, NobelClinician™ (Nobel Biocare, Zurich, Switzerland). Four NobelActive (Nobel Biocare, Zurich, Switzerland) implants were planned in 12, 15, 23 and 24 region. 17° Multi-unit Abutment (Conical connection NP 2.5 mm) in the anterior implants (Ø3.5 × 13 mm) and 30° Multi-unit Abutment (Conical connection RP 3.5 mm) in posterior implants (Ø4.3 × 15 mm) were placed, respectively

5 What Is Computer-Navigated Surgery?

Computer-navigated implant surgery is designed to allow implant placement in real time by a computer using the virtual plan formulated based on patient's CBCT scan. This system requires a motion tracking technology (hand piece array, patient tracking array and light source), which tracks the position of the dental drill relative to the patient's position (bur tracking) using sensors, as seen in Fig. 32. This three-dimensional positional information is then correlated with the previously

Fig. 5 Illustrates the surgery overview indicating the necessary implant torque and prosthetic torque value needed for proper implant stability and successful surgery. For immediate function, the implants should withstand a final tightening torque between 35–45 N cm and the Multi-unit abutment tightened to 15 N cm

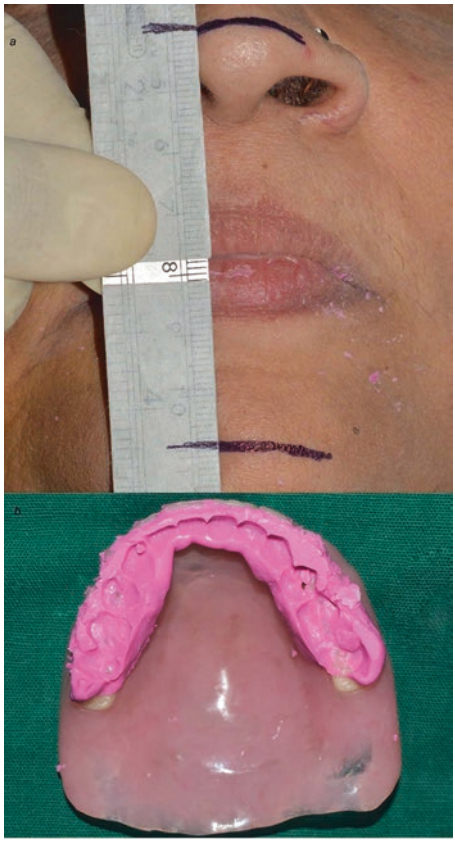

Fig. 6 Following complete arch extraction, an immediate acrylic complete denture was fabricated based on the patient's functional and aesthetic requirements. Prior to commencement of surgery, (**a**) the vertical dimension of occlusion was marked and measured, (**b**) the centric relation was recorded using bite registration material (Futar D, Kettenbach LP, CA, USA). This is done to maintain the patient's proper vertical dimension in the temporary screw-retained acrylic prosthesis, following bone reduction and implant placement

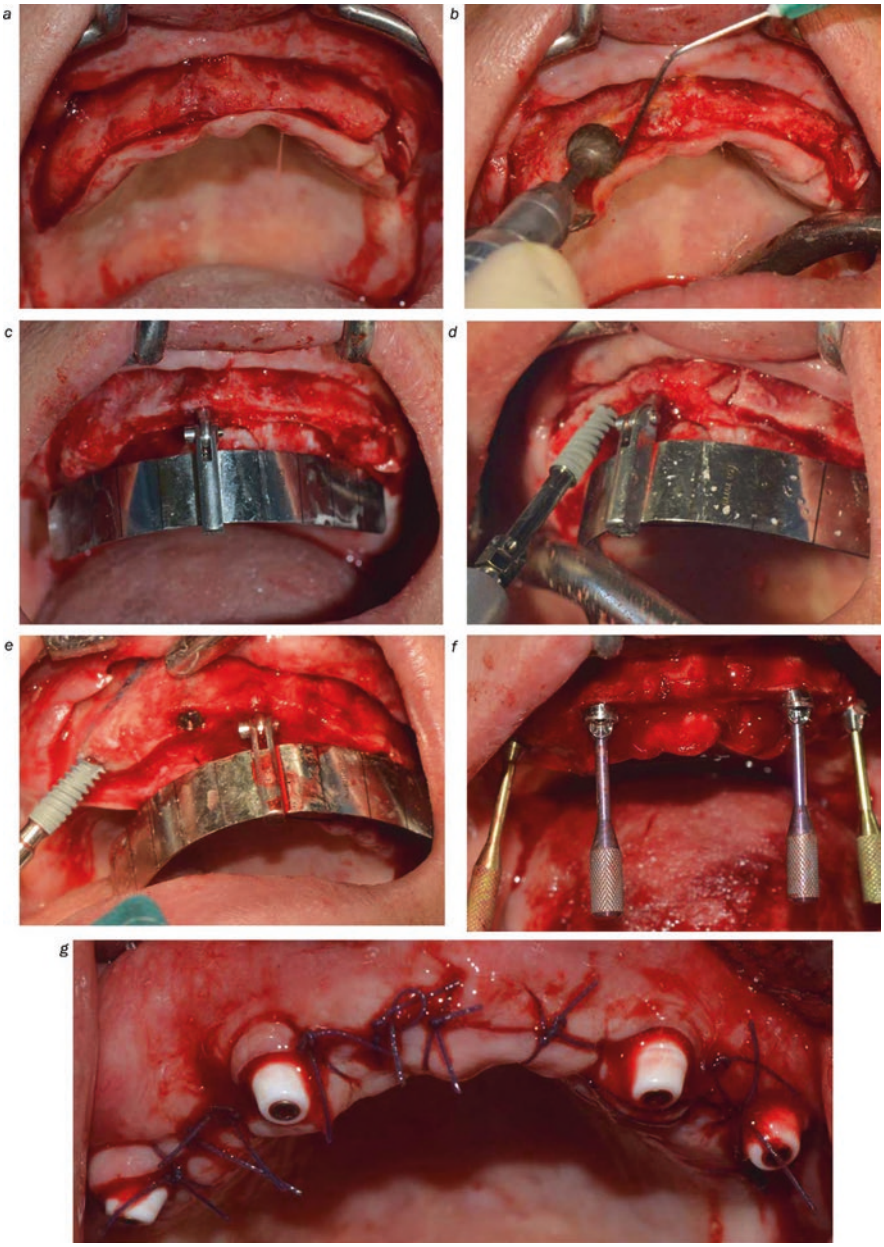

Fig. 7 Illustrates the surgical protocol followed, (**a**) a conventional flap elevation was performed from 16 to 26 region, (**b**) planned bone reduction was carried out based on the patient's smile line and the space required to accommodate the prosthesis, (**c**) All-on-4® guide was anchored into 8 mm long and 2 mm wide osteotomy in the midline of the maxilla, (**d**) implant bed preparation for anterior implant, followed by installation of NobelActive implant (Ø3.5 × 13 mm) using the all-on-4® guide was done, (**e**) implant bed preparation for posterior implant, followed by insertion

(continued)

Fig. 7 continued
of NobelActive implant (Ø4.3 × 15 mm) using the all-on-4® guide was done, (**f**) the anterior and posterior Multi-unit Abutments (17° and 30° respectively) were tightened using Unigrip Screwdriver Machine and Manual Torque Wrench Prosthetic. The angulations were verified using the pre-mounted holder which acts as a guide to allow for proper emergence of the prosthetic screw, (**g**) the Mutli-unit Abutment healing caps were placed on top of the Multi-unit Abutments prior to suturing. The position of the abutments was indexed on the denture by using heavy body impression material (Aquasil ultra heavy (Dentsply/Caulk, Konstanz, Germany) in the intaglio surface of the denture, to create space for the temporary coping Multi-unit cylinders

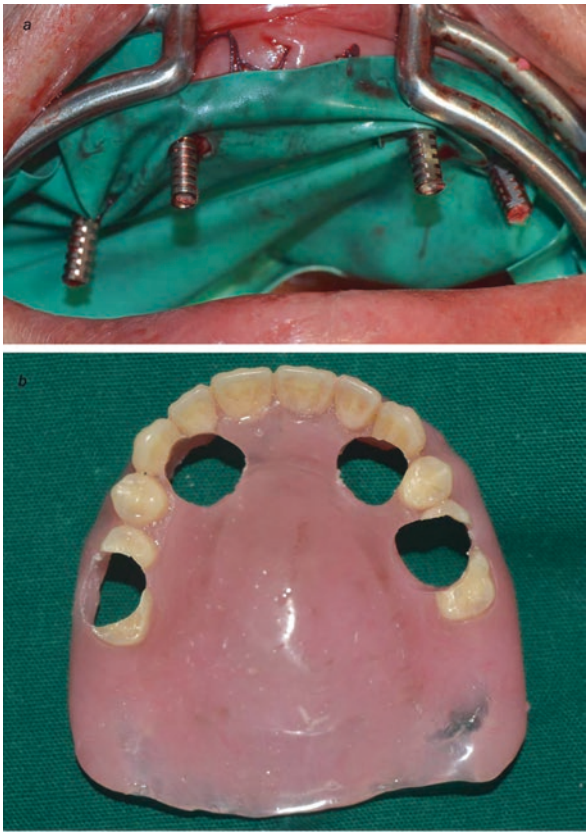

Fig. 8 Illustrates the denture conversion process, (**a**) a rubber dam was placed around the temporary coping Multi-unit cylinders to act as a barrier between the surgical and restorative material, (**b**) holes were prepared in the denture to accommodate the temporary coping Multi-unit cylinders. The denture was then placed over the cylinders intra-orally and auto-polymerizing acrylic resin was injected around the holes to facilitate the pick-up of the cylinders into the denture. Proper seating and alignment of the denture was verified using the pre-operative bite registration

determined virtual plan, to calculate the virtual position of the hand piece and implant drill. Thus, it improves surgical visualization and increases adaptability to intra-operative findings [8, 53].

The light source above the patient reaches the patient tracking array and the array on the hand piece. The light is reflected from the arrays to two high-definition cameras. The captured reflected light is transmitted to the system-specific navigation computer to create the dynamic real-time representation. If necessary, changes to the plan can be made intra-operatively to achieve accurate implant placement. This

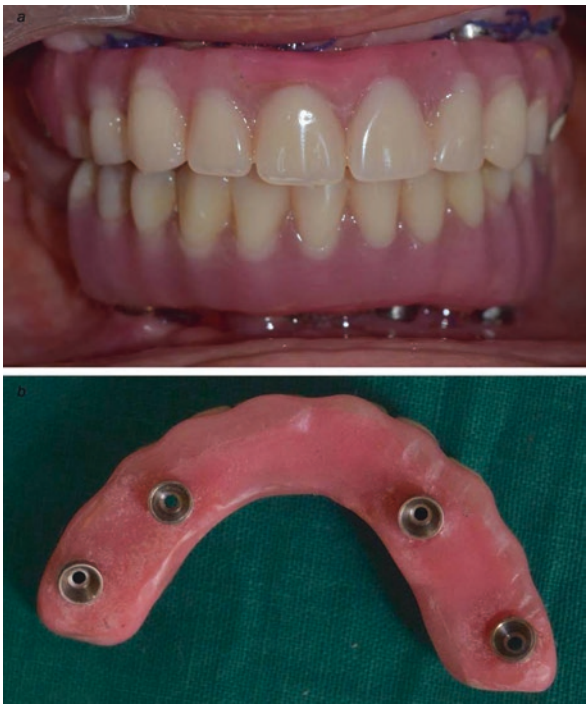

Fig. 9 Shows the fixed prosthesis. (**a**) Intra-oral frontal view of the provisional all-acrylic screw-retained prosthesis, (**b**) the immediate denture was converted to a fixed implant bridge

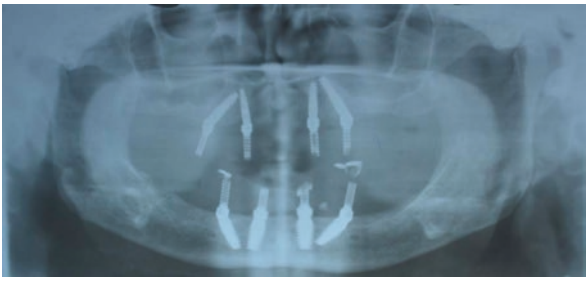

Fig. 10 Post-operative orthopantomogram showing application of "All-on-4®" treatment concept to maxillary and mandibular arches

system integrates dental implant surgical instruments, medical imaging technology (CBCT), optical positioning devices along with pre-operative planning software to perform precise dental implant surgeries [8, 53].

Navigation surgery is especially helpful in patients requiring dental implants in posterior maxillary/mandibular region where soft tissue in the vicinity of the planned implant site obstructs the view of the surgical field, or when short inter arch distance interferes with proper alignment of surgical drills with surgical guides [54].

Current dynamic navigation systems in implant dentistry include Image Guided Implant dentistry (IGI) (Image Navigation Ltd., New York, USA), X-Guide Dynamic 3D Navigation (X-Nav Technologies, Lansdale, USA), Navident

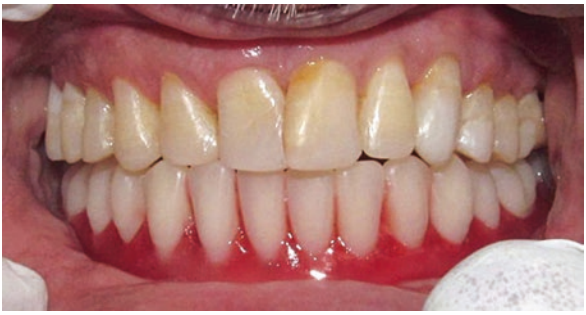

Fig. 11 Scan prosthesis was fabricated—mandibular complete trial denture with light-cured acrylic resin record base (Megatray®, Megadent, Radeberg, Germany) incorporating three composite resin radiographic markers (4 × 4 mm in size) in the incisor and first molar region

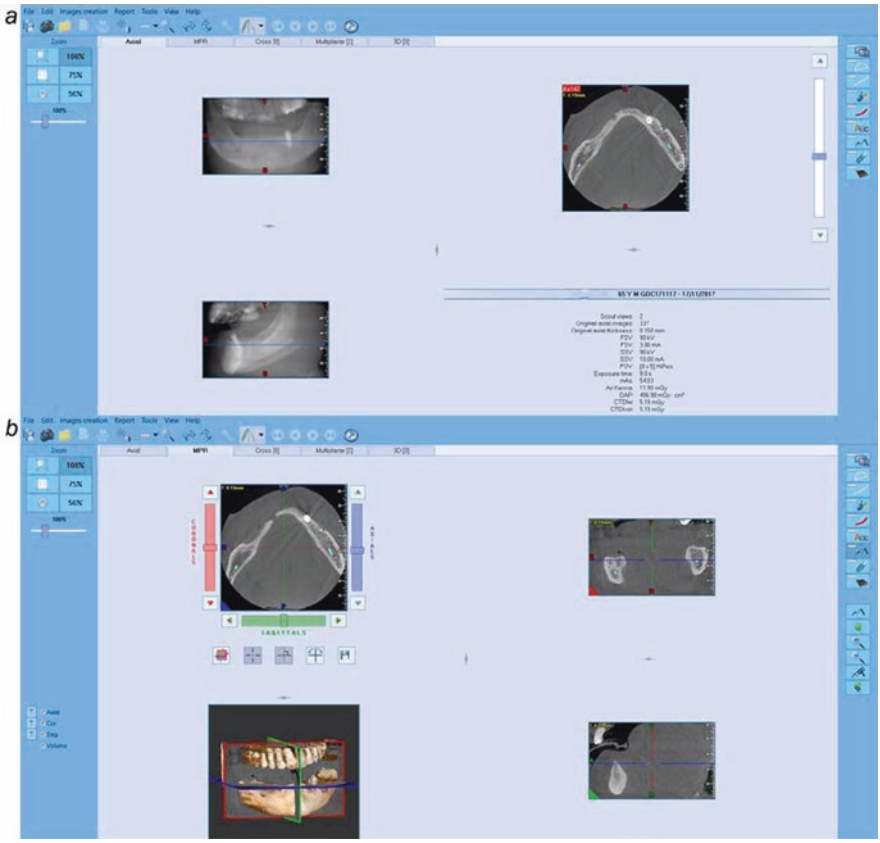

Fig. 12 A CBCT scan (NewTom VGi, QR S.r.l, Verona, Italy) was performed. The projection data was exported to NNT viewer (NewTom, QR S.r.l, Verona, Italy) for data analysis. This figure illustrates (**a**) basic orthogonal views (in the axial, sagittal and coronal plane). An endosseous implant is seen in the left mandibular canine region, (**b**) multiplanar reconstruction in the orthogonal plane

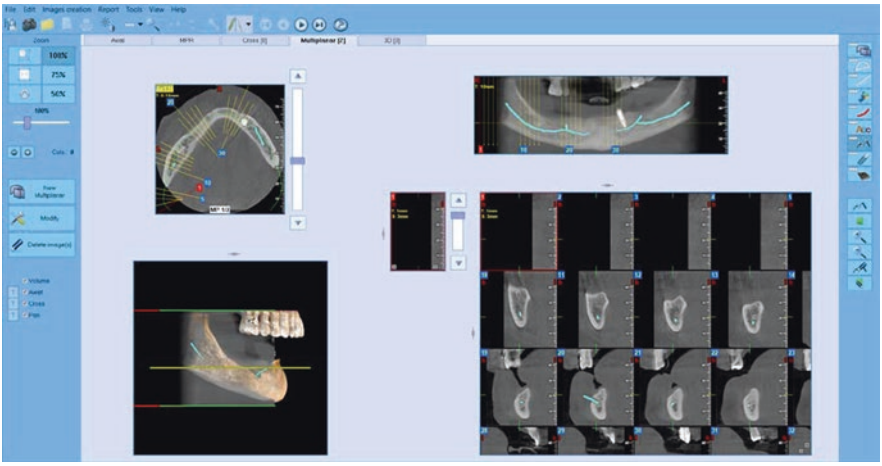

Fig. 13 This figure illustrates the multiplanar reconstruction in the oblique plane. It includes the panoramic curve, which identifies the dental arch position and allows the visualization of alveolar bone in cross sections by segmentation of bone along that curve in multi-slice windows. Inferior alveolar nerve canal tracing is also seen

(ClaroNav, Toronto, Canada) and Inliant (Inliant Dental Technologies, Vancouver, Canada).

6 What Is Computer-Oriented Surgery?

In this type of surgery, there is a simultaneous use of information from digital planning and data derived directly from the clinical reality at surgery to assist in the placement of dental implants. The objective is to provide a creative and flexible surgical environment that can adapt to diverse intra-oral scenarios as encountered during surgery. The surgeon gathers all the necessary information during the planning stage, which includes dental models, CBCT scan, panoramic radiograph, 3D virtual models with virtual implant placement and intra-oral photographs. This information is then relayed on a computer multi-screen along with the intra-operative intra-oral information gathered by the microscope camera during surgery, as seen in Fig. 33. This surgical protocol promotes interactive use of information to allow "documented real-time decision making". This system allows the use of surgical guides or navigation system during the initial drill phase of surgery to establish initial path of implant drill or the entire surgery can be carried out using the COIS method [53].

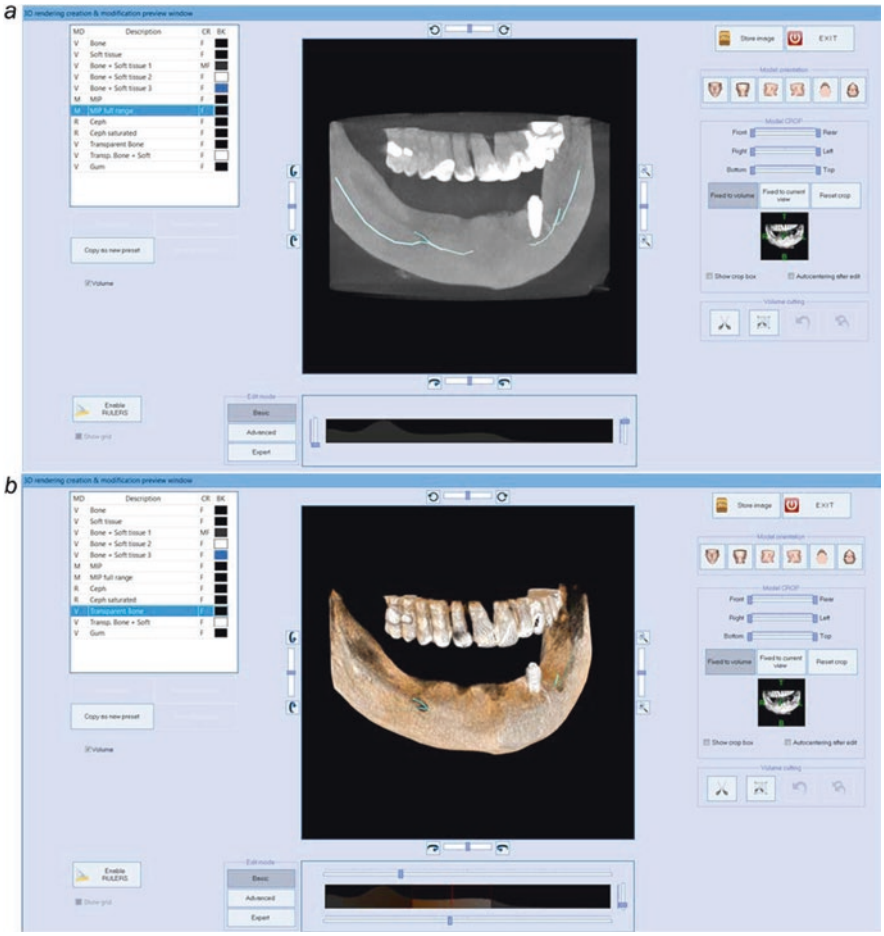

Fig. 14 3D volume rendering view allows visualization of large volumes of data generated by CBCT in three-dimensional space. This view shows the overall bone resorption pattern and relationship of crest of ridge to the inferior alveolar nerve canal. (**a**) Direct volume rendering showing the MIP mode, (**b**) indirect volume rendering showing the transparent view. Both views indicate a severe bone resorption pattern in the mandibular arch

7 Complications Associated with CT-Based Dental Implant Planning and Surgery

Literature reports various studies determining the accuracy of computer-guided technology for dental implant surgery, since safety and effectiveness of guided surgery are closely related to its accuracy. The accuracy of implant placement is often evaluated by the superimposed pre- and post-operative CBCT image and measurement of the deviations at the coronal or apical part of the implants along with mesiodistal and bucco-lingual discrepancies (distance error) and implant axis angle

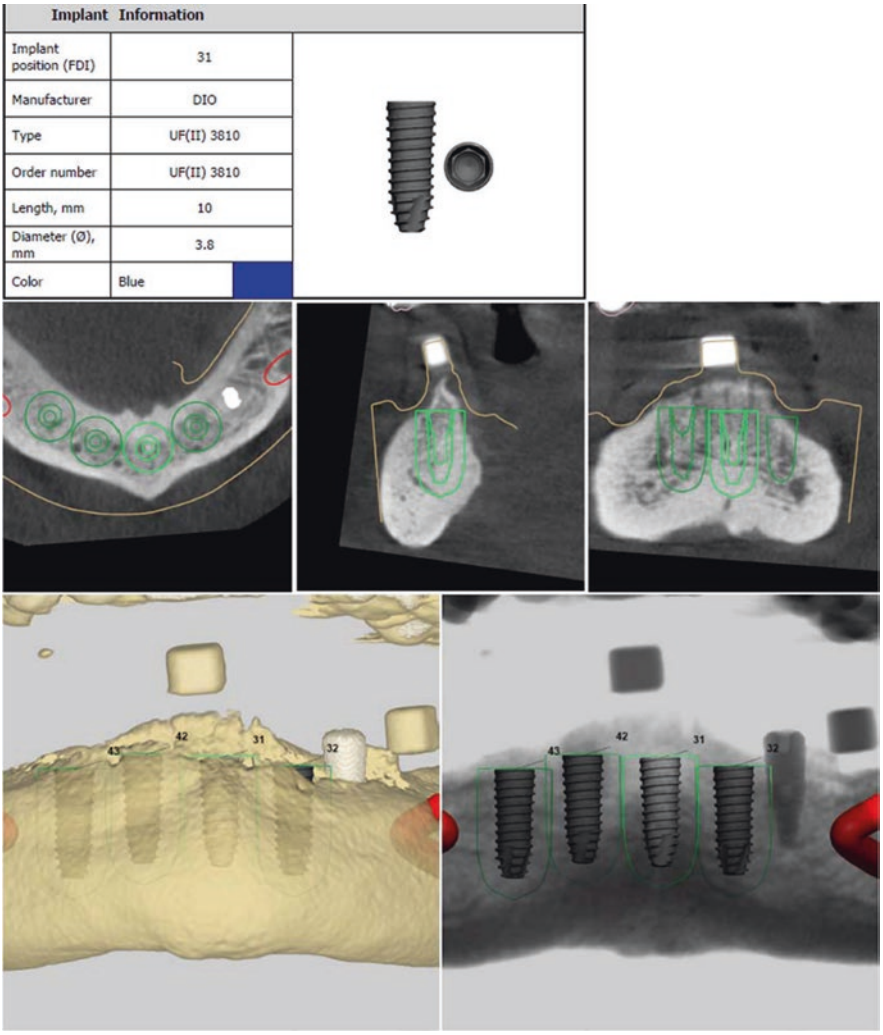

Fig. 15 Virtual implant planning of endosseous implant in 31 region (DIO Implant, Busan, Korea) in 3Shape Implant studio® implant planning software (3Shape medical A/S, Copenhagen, Denmark). Multi-slice windows illustrate the different cross sections, axial, panoramic and 3D volume rendering views of the scanned region

deviations (angular error). Also, vertical error (when placement is deeper or shallower than that in the plan) and horizontal error (when there is lateral displacement compared to the plan) are encountered in guided surgery [5, 15, 17–20, 51, 55–57].

The most common surgical and prosthetic complication encountered in computer-guided implant surgery is caused by the misfit between the installed implants and the prefabricated prosthesis. Deviations at the shoulder of the implants can hamper the correct fit of a prefabricated construction and require adaptation of fit or

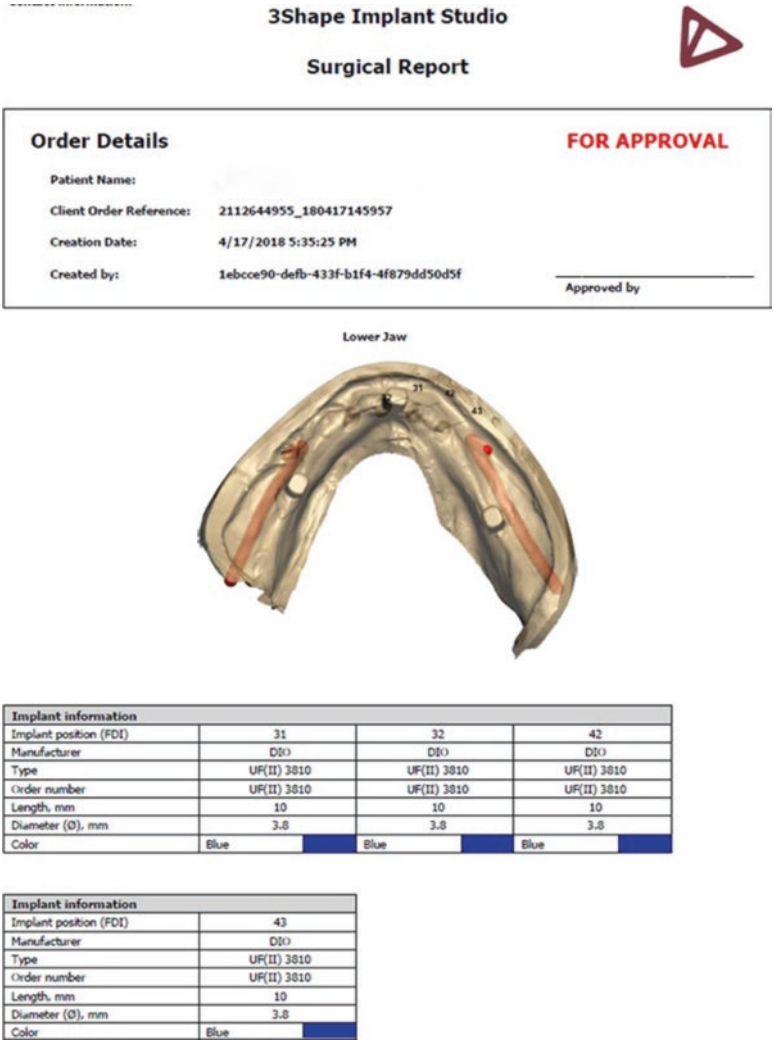

3Shape Implant Studio

Surgical Report

Order Details FOR APPROVAL

Patient Name:

Client Order Reference: 2112644955_180417145957

Creation Date: 4/17/2018 5:35:25 PM

Created by: 1ebcce90-defb-433f-b1f4-4f879dd50d5f

Approved by

Lower Jaw

Implant information			
Implant position (FDI)	31	32	42
Manufacturer	DIO	DIO	DIO
Type	UF(II) 3810	UF(II) 3810	UF(II) 3810
Order number	UF(II) 3810	UF(II) 3810	UF(II) 3810
Length, mm	10	10	10
Diameter (Ø), mm	3.8	3.8	3.8
Color	Blue	Blue	Blue

Implant information	
Implant position (FDI)	43
Manufacturer	DIO
Type	UF(II) 3810
Order number	UF(II) 3810
Length, mm	10
Diameter (Ø), mm	3.8
Color	Blue

Fig. 16 A surgical report in the pdf format generated for approval, which includes the digital dental model with the planned implant data for four UF(II)3810 implants (Ø3.8 × 10 mm, DIOnavi, DIO Implant, Busan, Korea) in 31, 32, 42, 43 region

occlusion. Deviations at the apex can impinge on the critical anatomical structures; thus, a minimum safety zone of at least 2 mm from adjacent vital structures is recommended [5].

Vertical error is commonly encountered than a horizontal error since superior border of alveolar bone is not distinctly demarcated in CT data during the implant plan, resulting in shallow placement of implants. Distance error is larger in the apex than coronal area, since angular displacement at the occlusal surface causes increased horizontal error at the apex [51].

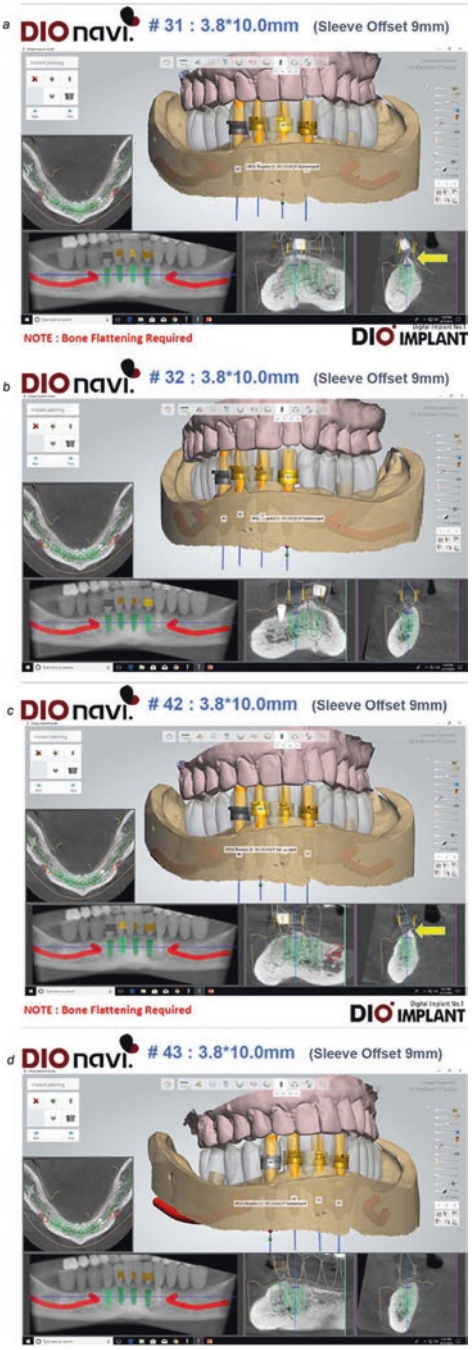

Fig. 17 The surgical report indicating the virtual surgical guide position and dimensions for printing. (**a**), (**b**), (**c**) and (**d**) provide information for each implant fixture separately, indicating the sleeve(s) position, the sleeve support diameter around the sleeve, the sleeve safety diameter and images of the virtual implant planning

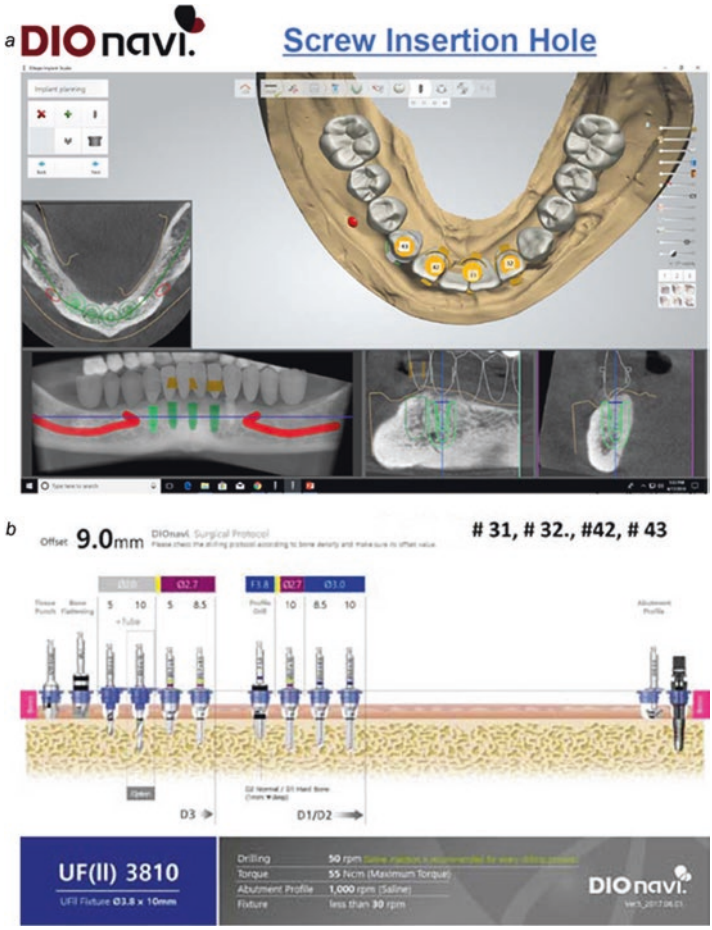

Fig. 18 Surgical report indicating (**a**) the screw insertion hole/s surface offset, which is a compensation value for dimensional errors of the printing material in the hole/s area (**b**) the selected surgical drill sequence

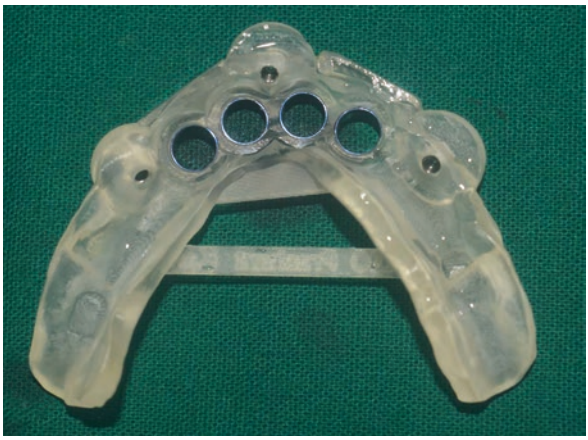

Fig. 19 Computer-generated stereolithographic surgical guide with guide sleeves to orient the drills

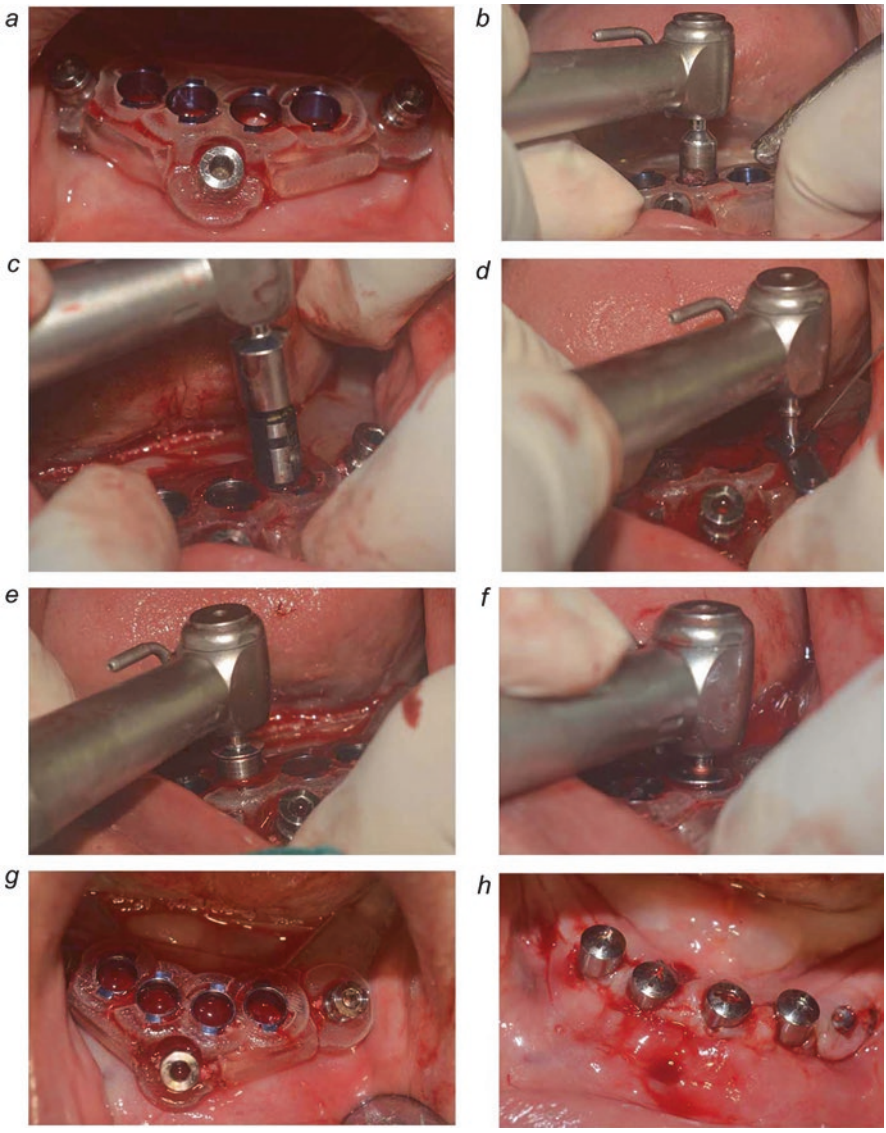

Fig. 20 Illustrates the flapless implant surgery procedure using 3D printed mucosa-supported surgical guide for a completely edentulous mandible with provision for four implant placement. (**a**) The guide was installed on the tissue with three fixation screws, one placed anteriorly and two placed in the posterior region, (**b**) tissue punch was used to remove a core of gingival tissue, (**c**) bone flattening drill was used to flatten uneven alveolar bone and remove gingival residue, (**d**) initial drill was used with the drill tube to form an osteotomy on the cortical bone. Drill tube helps to fix the initial drill with stability, (**e**) final drill was used to expand the drill hole until the final drilling, (**f**) abutment profile drill was used to form the emergency profile after removing the cortical bone when placing the abutment, (**g**) implant bed preparation was completed using guided-surgery drilling protocol, (**h**) healing abutments placed on the implants after removal of the surgical guide

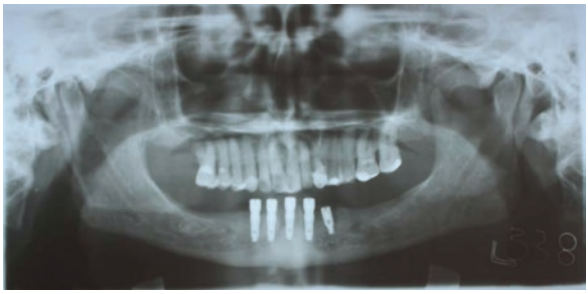

Fig. 21 Post-operative orthopantomogram showing guided implant placement in 43, 42, 31, 32 region

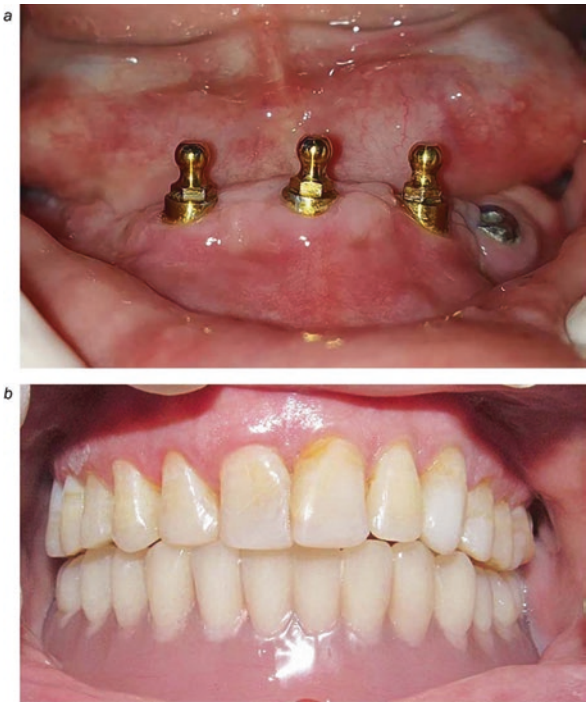

Fig. 22 Patient lost one implant in the 43 region due to poor bone quality during the post-surgical healing phase. (**a**) Shows three parallel implants with ball attachments in 31, 32 and 42 region. One submerged implant seen in 33 region, (**b**) shows an implant-supported overdenture

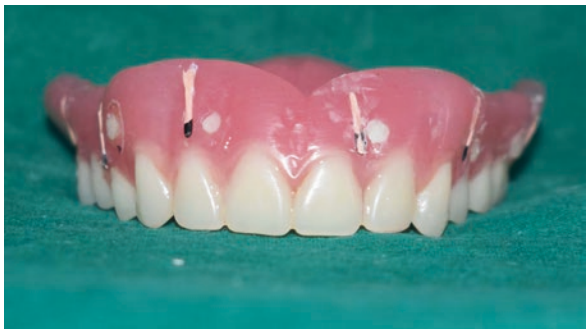

Fig. 23 Scan prosthesis—acrylic maxillary complete denture fabricated based on the patient's aesthetic and functional requirements with gutta-percha (fiducial) markers demarcating the favourable implant positions. This contains all the necessary information on the spatial positioning of the teeth and the fiducial marks for patient indexing, enabling virtual planning of the implants

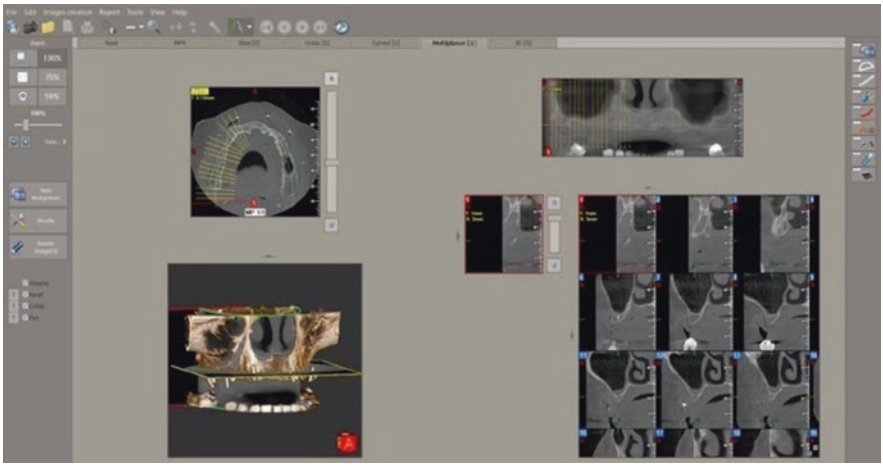

Fig. 24 A CBCT scan (ProMax® 3D Max, Planmeca OY, Helsinki, Finland) was performed. This figure illustrates the curved MPR of the maxilla along with the scan prosthesis. It includes the panoramic curve and allows the visualization of alveolar bone in cross sections by segmentation of bone along the panoramic curve in multi-slice windows. The radiographic analysis suggests severe bone resorption in the posterior maxilla

A meta-analysis assessing accuracy of implants placed with fully guided surgery compared to half-guided surgery suggested higher accuracy with fully guided surgery with mean coronal deviation of 1.00 mm in FG and 1.44 mm in HG, mean apical deviation of 1.91 mm in FG and 1.23 mm in HG, and mean angular deviation of 3.13° in FG and 4.30° in HG [15]. An in vivo study assessing the accuracy of a fully digitalized plan for generating a stereolithographic surgical guide yielded results comparable to conventional guided implant surgery. It indicated an angular pattern of deviation between the planned and achieved implant position, with mean coronal deviation of 1.05 mm, mean apical deviation of 1.63 mm and mean angle deviation of 3.85° [55]. A meta-analysis involving clinical and preclinical studies on computer-guided implant surgery with static guides revealed results similar to the aforementioned in vivo study with a mean coronal deviation of 1.12 mm, a mean apical deviation of 1.39 mm and 4° angle discrepancy. It also suggested that flapless surgery exhibited higher accuracy compared to muco-periosteal reflection. Mucosa- and tooth-supported guides exhibited better accuracy compared to bone-supported guides. Tooth-supported guides tended to be more accurate compared to mucosa- or mucosa- and pin-supported guides [17].

Studies assessing accuracy of dynamic navigation suggested the results obtained demonstrated accuracy which is equal [56] or better than the in vivo accuracy reported in the literature for static surgical guides, with mean coronal deviation of 0.71 mm, mean apical deviation of 1.00 mm and 2.26° of angle deviation [57]. Thus, it can be concluded that dynamic navigation is a reliable method for executing computer-aided implant surgery; however, it is directly influenced by the surgeon's experience level.

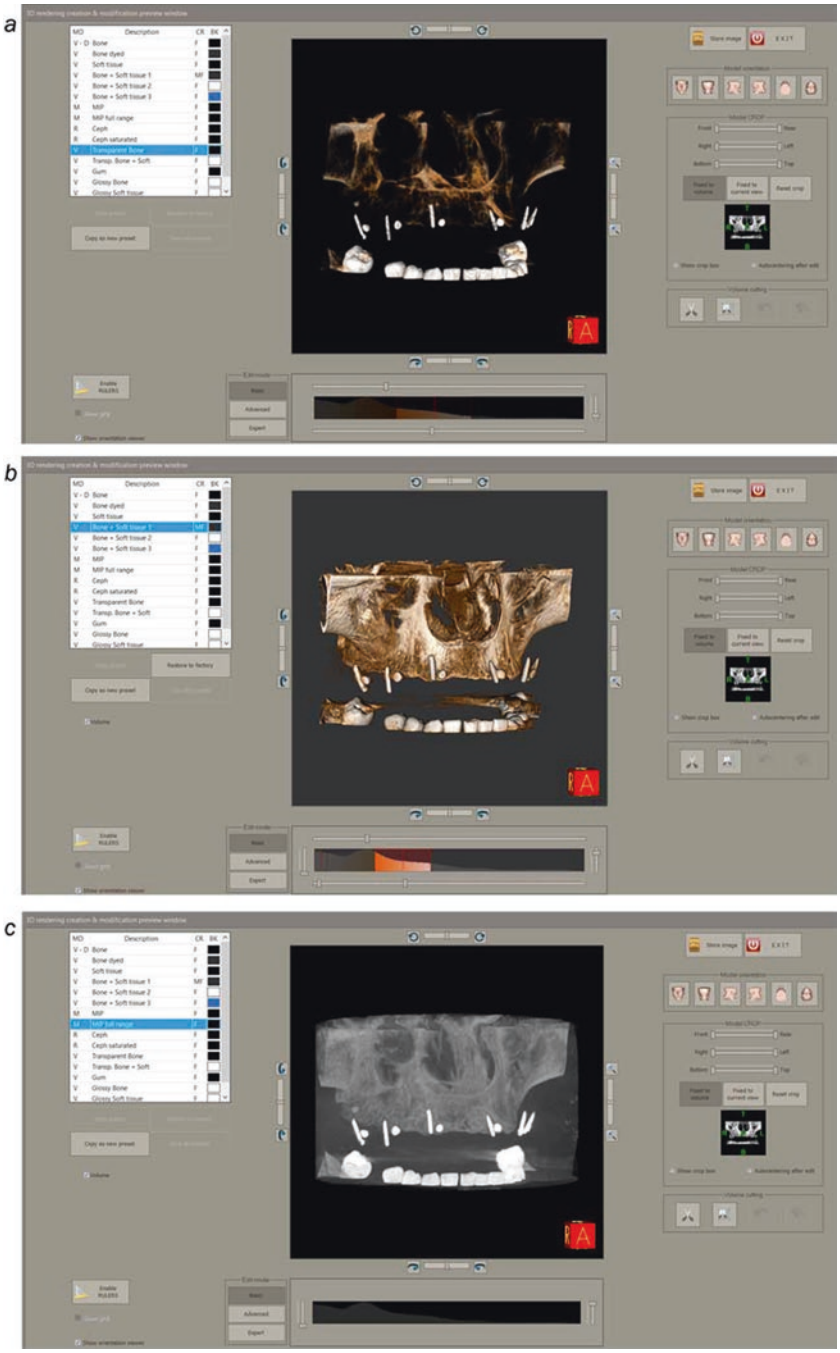

Fig. 25 Multiplanar volume rendering view. (**a**, **b**) Presents indirect volume rendering displaying transparent and solid view, respectively, (**c**) presents the MIP view. These views help to assess the overall anatomic configuration of the maxilla. It also helps to evaluate the bone architecture in relation to the radiographic markers

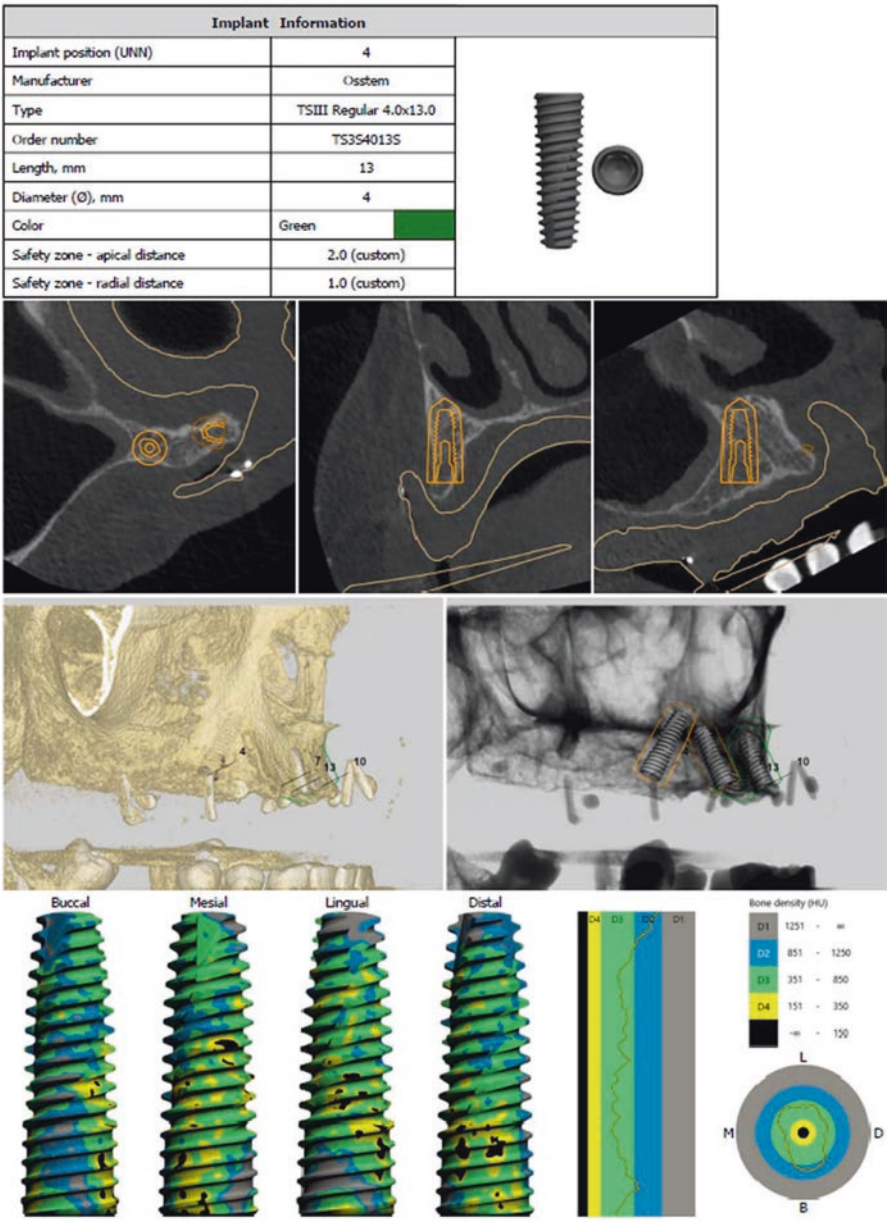

Fig. 26 Virtual implant planning of endosseous implant in 4 region (Osstem, Osstem Implant Co., Ltd., Seoul, Korea) in 3Shape Implant studio® implant planning software (3Shape medical A/S, Copenhagen, Denmark). Multi-slice windows illustrate implant planning using the MIP mode, solid 3D volume rendering, 3D bone density analysis around the implant and different cross-sectional views displaying virtual implant planning through the overlap of implant silhouette on the corresponding section of the bone

3Shape Implant Studio

Surgical Report

Order Details

FOR APPROVAL

Patient Name:

Client Order Reference: 1777231406_20181022_1215_42

Creation Date: 22-10-2018 12:37:45

Created by: Default operator - reports.ddfc@gmail.com (9be1604f-65ba-4e50-9066-a7e000f30b3e)

Approved by

Upper Jaw

Implant information			
Implant position (UNN)	4	7	10
Manufacturer	Osstem	Osstem	Osstem
Type	TSIII Regular 4.0x13.0	TSIII Mini 3.5x11.5	TSIII Mini 3.5x10.0
Order number	TS3S4013S	TS3M3S11S	TS3M3S10S
Length, mm	13	11.5	10
Diameter (Ø), mm	4	3.5	3.5
Color	Green	Yellow	Yellow

Implant information	
Implant position (UNN)	13
Manufacturer	Osstem
Type	TSIII Regular 4.0x13.0
Order number	TS3S4013S
Length, mm	13
Diameter (Ø), mm	4
Color	Green

Fig. 27 A surgical report in the pdf format generated for approval, which includes the digital dental model with the planned implant data for four TS III implants, two anterior implants (Ø3.5 × 10 mm and Ø3.5 × 11.5 mm, Osstem Implant Co., Ltd., Seoul, Korea) and two posterior implants (Ø4 × 13 mm, Osstem Implant Co., Ltd., Seoul, Korea) in 4, 7, 10 and 13 region

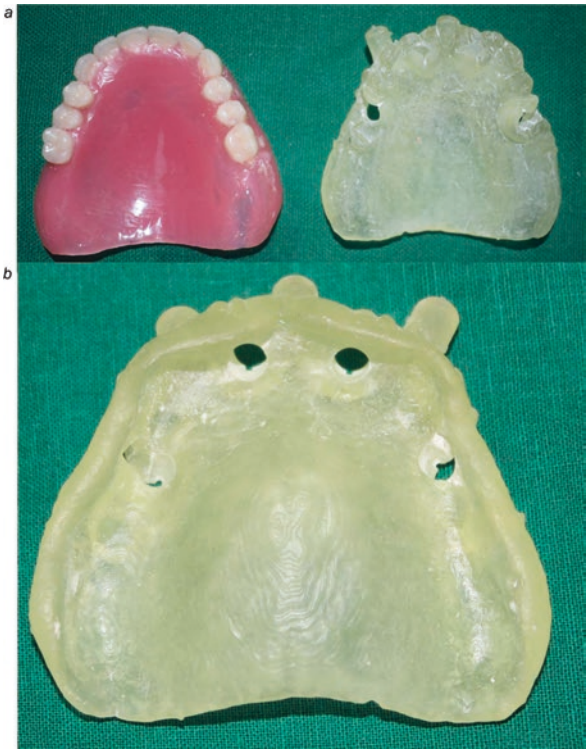

Fig. 28 Stereolithographic surgical guide. (**a**) Shows that the stereolithographic surgical guide is an exact replica of the scan prosthesis, (**b**) displays the intaglio surface of the computer-generated stereolithographic surgical guide

Complications can occur because of the following factors in static computer-guided implant surgery [58–60]:

1. Radiographic template error—Inaccurate planning can occur in case of non-ideal prosthetic wax-up, poor adaptation or orientation of the template during the scanning process.
2. Error during image acquisition and data processing, on average less than 0.5 mm. These errors include: (a) Scanning error-patient movement during the scan, extensive dental restoration artefact obscuring axial images, spatial resolution problems in CT, (b) Registration error—errors in data fusion due to limitations in CT resolution and metal scattering, improper placement of radiographic markers.
3. Planning error—improper virtual planning of implants on the software.
4. Error during manufacturing of the surgical guide, typically around 0.1–0.2 mm with stereolithography [44]—depends on the manufacturing process involved, improperly placed guide sleeves.
5. Mechanical error due to tolerance of surgical instruments (the bur-cylinder gap).
6. Error during surgical guide positioning—movement of the guide during the drilling, improper fixing of mucosa-supported guide using anchor pins.
7. Errors due to limited mouth opening.

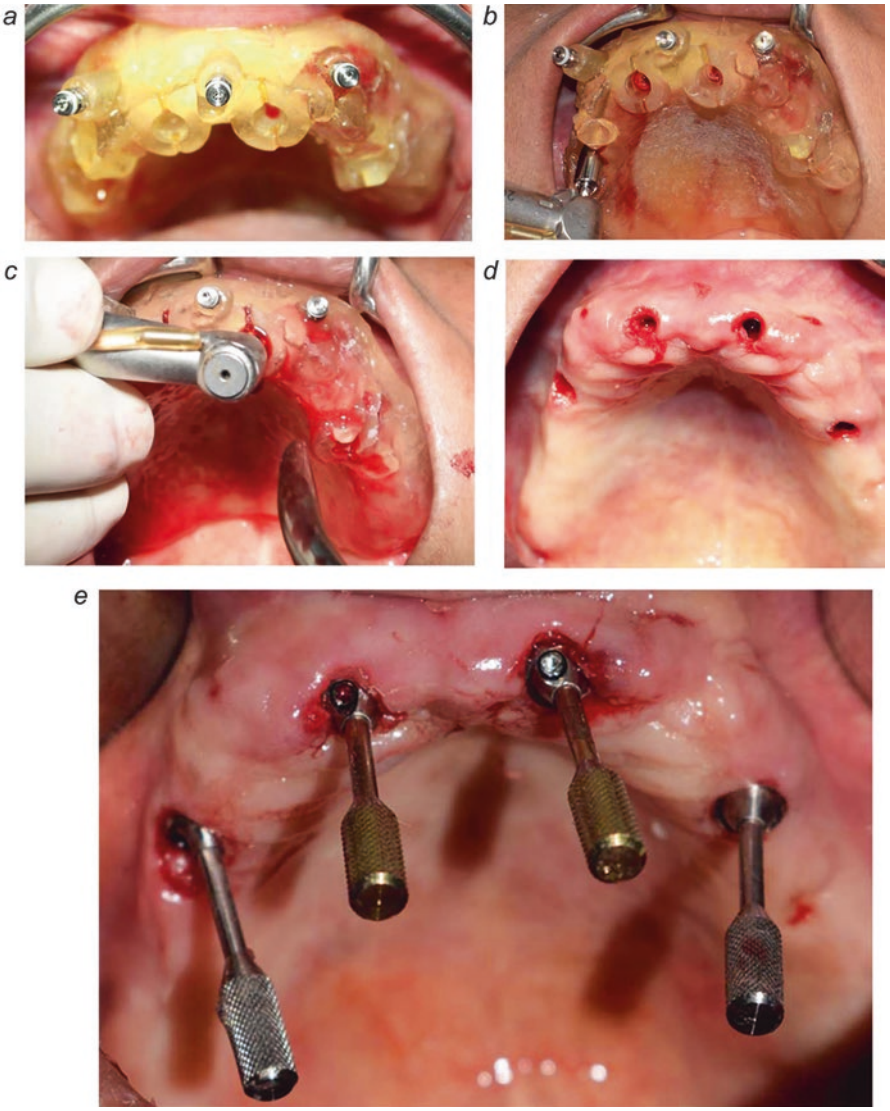

Fig. 29 Illustrates the flapless implant surgery procedure using 3D printed mucosa-supported surgical guide for a completely edentulous maxilla with provision for four implant placement. (**a**) The guide was installed on the tissue with three fixation screws placed anteriorly, (**b**) implant bed preparation and implant installed (Osstem Implant Co., Ltd., Seoul, Korea) in posterior region using guided-surgery drilling protocol, (**c**) implant bed preparation and implant installed (Osstem Implant Co., Ltd., Seoul, Korea) in anterior region using guided-surgery drilling protocol, (**d**) intra-operative placement of dental implants in 4, 7, 10 and 13 region, (**e**) the anterior and posterior Multi-unit Abutments were tightened using Unigrip Screwdriver Machine and Manual Torque Wrench Prosthetic

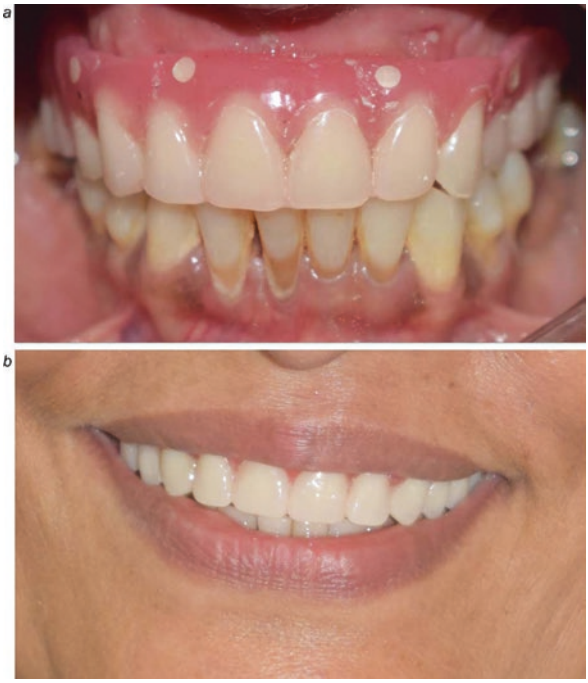

Fig. 30 Shows the fixed prosthesis. (**a**) Intra-oral frontal view of the provisional all-acrylic screw-retained prosthesis, (**b**) extra-oral frontal view of the provisional prosthesis

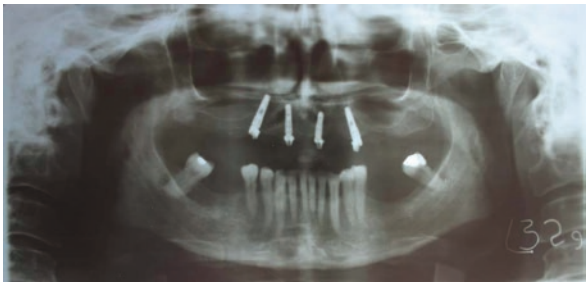

Fig. 31 Post-operative orthopantomogram showing application of "All-on-4®" treatment concept for maxillary arch

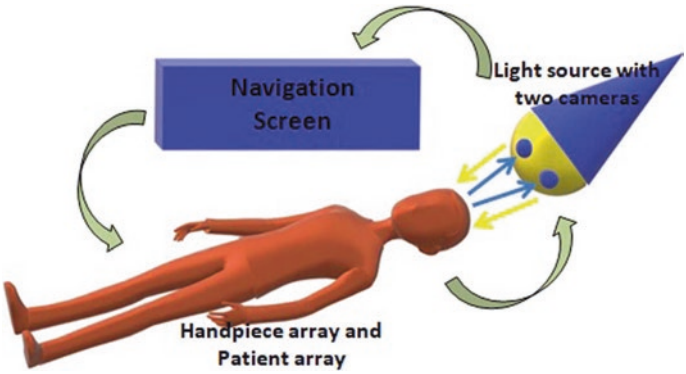

Fig. 32 Illustrates the protocol followed in computer-navigated implant surgery

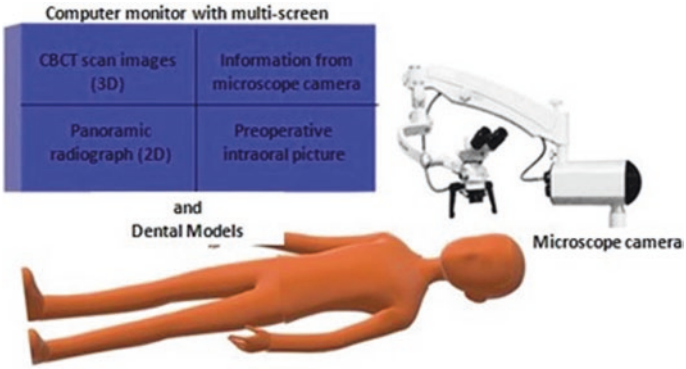

Fig. 33 Illustrates the protocol followed in computer-oriented implant surgery

8. Surgical guide fracture or drop out of metal sleeve.
9. Complication due to bone overheating.
10. Human error—setting the bur stop in an incorrect position.

These errors can result in early intra-operative or late prosthetic complications [5, 17, 26]:

The intra-operative complications include alteration of surgical plan and early implant loss due to limited primary implant stability, intra-operatively broken surgical guides, incomplete seating of prosthesis due to bony interference, incomplete placement of implant to the planned depth, implant dehiscence, and need for additional grafting procedures.

The prosthetic complications include prosthetic screw loosening, prosthetic misfit and prosthesis fracture.

8 Conclusion

Although errors in computer-guided implant surgery are in clinically acceptable range, for more accurate surgery, development of standardized methods to reduce the above-mentioned errors is necessary.

There is a need for further long-term clinical studies and randomized clinical trials to understand the factors influencing the accuracy, implant survival, bone loss and clinical complications associated with computer-aided implant surgery. Although advanced technology is applied, basic fundamentals such as proper case selection, patient preparation, surgical planning and execution are of paramount importance.

Acknowledgements I would like to acknowledge Dr. Vikas Dhupar (Prof. and Head, Department of Oral and Maxillofacial Surgery, Goa Dental College and Hospital), Dr. Prem Bhushan and Dr. Prithika Eswaramurthy for their contribution towards the case series.

References

1. Albrektsson T, Dahl E, Enbom L, et al. Osseointegrated oral implants. A Swedish multicenter study of 8139 consecutively inserted Nobelpharma implants. J Periodontol. 1988;59:287–96.
2. Drago C, del Castillo R, Peterson T. Immediate occlusal loading in edentulous jaws, CT-guided surgery and fixed provisional prosthesis: a maxillary arch clinical report. J Prosthodont. 2011;20:209–17.
3. Erkapers M, Ekstrand K, Baer RA, et al. Patient satisfaction following dental implant treatment with immediate loading in the edentulous atrophic maxilla. Int J Oral Maxillofac Implants. 2011;26:356–64.
4. Laleman I, Bernard L, Vercruyssen M, et al. Guided implant surgery in the edentulous maxilla: a systematic review. Int J Oral Maxillofac Implants. 2016;31:s103–17.
5. D'Haese J, Van De Velde T, Komiyama A. Accuracy and complications using computer-designed stereolithographic surgical guides for oral rehabilitation by means of dental implants: a review of the literature. Clin Implant Dent Relat Res. 2012;14:321–35.
6. Grant GT, Campbell SD, Masri RM, et al. American College of Prosthodontists Digital Dentistry Glossary Development Task Force. Glossary of digital dental terms: American College of Prosthodontists. J Prosthodont. 2016;25:S2–9.
7. Gargallo-Albiol J, Barootchi S, Salomó-Coll O, et al. Advantages and disadvantages of implant navigation surgery. A systematic review. Ann Anat. 2019;225:1–10.
8. Sicilia A, Rodriguez A, Cuesta I. Can I rely on software-guided surgery? In: Alfaro FH, editor. Controversial issues in implant dentistry. London: Quintessence Publishing; 2013. p. 107–23.
9. Zayed SM. Computer guided implant surgery: is it a holistic solution? EC Dent Sci. 2019;18:1302–12.
10. Tettamanti L, Andrisani C, Andreasi Bassi M. Immediate loading implants: review of the critical aspects. Oral Implantol (Rome). 2017;10:129–39.
11. Yepes JF, Al-Sabbagh M. Use of cone-beam computed tomography in early detection of implant failure. Dent Clin N Am. 2015;59:41–56.
12. Orentlicher G, Abboud M. Guided surgery for implant therapy. Dent Clin N Am. 2011;55:715–44.

13. Amorfini L, Migliorati M, Drago S, et al. Immediately loaded implants in rehabilitation of the maxilla: a two-year randomized clinical trial of guided surgery versus standard procedure. Clin Implant Dent Relat Res. 2017;19:280–95.
14. Komiyama A, Klinge B, Hultin M. Treatment outcome of immediately loaded implants installed in edentulous jaws following computer-assisted virtual treatment planning and flapless surgery. Clin Oral Implants Res. 2008;19:677–85.
15. Bover-Ramos F, Viña-Almunia J, Cervera-Ballester J, et al. Accuracy of implant placement with computer-guided surgery: a systematic review and meta-analysis comparing cadaver, clinical, and in vitro studies. Int J Oral Maxillofac Implants. 2018;33:101–15.
16. Brief J, Edinger D, Hassfeld S, et al. Accuracy of image guided implantology. Clin Oral Implants Res. 2005;16:495–501.
17. Tahmaseb A, Wismeijer D, Coucke W, et al. Computer technology applications in surgical implant dentistry: a systematic review. Int J Oral Maxillofac Implants. 2014;29:25–42.
18. Farley NE, Kennedy K, McGlumphy EA, et al. Split-mouth comparison of the accuracy of computer-generated and conventional surgical guides. Int J Oral Maxillofac Implants. 2013;28:563–72.
19. Younes F, Cosyn J, De Bruyckere T, et al. A randomized controlled study on the accuracy of free-handed, pilot-drill guided and fully guided implant surgery in partially edentulous patients. J Clin Periodontol. 2018;45:721–32.
20. Arisan V, Karabuda CZ, Mumcu E, et al. Implant positioning errors in freehand and computer-aided placement methods: a single-blind clinical comparative study. Int J Oral Maxillofac Implants. 2013;28:190–204.
21. Vercruyssen M, Cox C, Coucke W, et al. A randomized clinical trial comparing guided implant surgery (bone- or mucosa-supported) with mental navigation or the use of a pilot-drill template. J Clin Periodontol. 2014;41:717–23.
22. Hämmerle CH, Stone P, Jung RE, et al. Consensus statements and recommended clinical procedures regarding computer-assisted implant dentistry. Int J Oral Maxillofac Implants. 2009;24:126–31.
23. The glossary of prosthodontic terms: ninth edition. J Prosthet Dent. 2017;117:e1–105.
24. Ramasamy M, Giri RR, et al. Implant surgical guides: from the past to the present. J Pharm Bioallied Sci. 2013;5:S98–S102.
25. Flügge TV, Nelson K, Schmelzeisen R, et al. Three-dimensional plotting and printing of an implant drilling guide: simplifying guided implant surgery. J Oral Maxillofac Surg. 2013;71:1340–6.
26. D'Haese J, Ackhurst J, Wismeijer D, et al. Current state of the art of computer-guided implant surgery. Periodontology 2000. 2017;2017(73):121–33.
27. Ganz SD. Computer-aided design/computer-aided manufacturing applications using CT and cone beam CT scanning technology. Dent Clin N Am. 2008;52:777–808.
28. Lal K, White GS, Morea DN, et al. Use of stereolithographic templates for surgical and prosthodontic implant planning and placement. Part I. The concept. J Prosthodont. 2006;15:51–8.
29. Spinelli D, Ottria L, De Vico G, et al. Full rehabilitation with nobel clinician® and procera implant bridge®: case report. Oral Implantol (Rome). 2013;6:25–36.
30. Balshi SF, Wolfinger GJ, Balshi TJ. Surgical planning and prosthesis construction using computed tomography, CAD/CAM technology, and the internet for immediate loading of dental implants. J Esthet Restor Dent. 2006;18:312–25.
31. Pesun IJ, Gardner FM. Fabrication of a guide for radiographic evaluation and surgical placement of implants. J Prosthet Dent. 1995;73:548–52.
32. Takeshita F, Tokoshima T, Suetsugu T. A stent for presurgical evaluation of implant placement. J Prosthet Dent. 1997;77:36–8.
33. Tal H, Moses O. A comparison of panoramic radiography with computed tomography in the planning of implant surgery. Dentomaxillofac Radiol. 1991;20:40–2.
34. Kapadia Y, Jain V. Radiopacity of dental materials used for imaging guides in implant dentistry. EC Dent Sci. 2018;17:900–6.

35. Israelson H, Plemons JM, Watkins P, et al. Barium-coated surgical stents and computer assisted tomography in the preoperative assessment of dental implant patients. Int J Periodontics Restor Dent. 1992;12:52–61.
36. D'Souza KM, Aras MA. Applications of computer-aided design/computer-assisted manufacturing technology in dental implant planning. J Dent Implant. 2012;2:37–41.
37. Yilmaz B. Incorporating digital scans of diagnostic casts into computed tomography for virtual implant treatment planning. J Prosthet Dent. 2015;114:178–81.
38. Lee CY, Ganz SD, Wong N, et al. Use of cone beam computed tomography and a laser intraoral scanner in virtual dental implant surgery: part 1. Implant Dent. 2012;21:265–71.
39. Lanis A, Álvarez Del Canto O. The combination of digital surface scanners and cone beam computed tomography technology for guided implant surgery using 3Shape implant studio software: a case history report. Int J Prosthodont. 2015;28:169–78.
40. Hamilton A, Jamjoom F, Doliveux S, et al. Radiographic markers for merging virtual data sets. J Prosthet Dent. 2019;122:5–9.
41. Widmann G, Bale RJ. Accuracy in computer-aided implant surgery-a review. Int J Oral Maxillofac Implants. 2006;21:305–13.
42. Jamjoom FZ, Kim DG, McGlumphy EA, et al. Positional accuracy of a prosthetic treatment plan incorporated into a cone beam computed tomography scan using surface scan registration. J Prosthet Dent. 2018;120:367–74.
43. Mangano F, Gandolfi A, Luongo G, et al. Intraoral scanners in dentistry: a review of the current literature. BMC Oral Health. 2017;17:149.
44. Flügge T, Derksen W, Te Poel J, et al. Registration of cone beam computed tomography data and intraoral surface scans—a prerequisite for guided implant surgery with CAD/CAM drilling guides. Clin Oral Implants Res. 2017;28:1113–8.
45. Jacobs R, Salmon B, Codari M, et al. Cone beam computed tomography in implant dentistry: recommendations for clinical use. BMC Oral Health. 2018;18:88.
46. Venkatesh E, Elluru SV. Cone beam computed tomography: basics and applications in dentistry. J Istanb Univ Fac Dent. 2017;51:S102–21.
47. John GP, Joy TE, Mathew J, et al. Fundamentals of cone beam computed tomography for a prosthodontist. J Indian Prosthodont Soc. 2015;15:8–13.
48. Pauwels R, Jacobs R, Singer SR, et al. CBCT-based bone quality assessment: are Hounsfield units applicable? Dentomaxillofac Radiol. 2015;44:20140238.
49. Scarfe WC, Li Z, Aboelmaaty W, et al. Maxillofacial cone beam computed tomography: essence, elements and steps to interpretation. Aust Dent J. 2012;57:46–60.
50. Scarfe WC, Farman AG. What is cone-beam CT and how does it work? Dent Clin N Am. 2008;52:707–30.
51. Moon SY, Lee KR, Kim SG, et al. Clinical problems of computer-guided implant surgery. Maxillofac Plast Reconstr Surg. 2016;38:15.
52. Bencharit S, Staffen A, Yeung M, et al. In vivo tooth-supported implant surgical guides fabricated with desktop stereolithographic printers: fully guided surgery is more accurate than partially guided surgery. J Oral Maxillofac Surg. 2018;76:1431–9.
53. Block MS, Emery RW, Cullum DR, et al. Implant placement is more accurate using dynamic navigation. J Oral Maxillofac Surg. 2017;75:1377–86.
54. Sun TM, Lan TH, Pan CY, et al. Dental implant navigation system guide the surgery future. Kaohsiung J Med Sci. 2018;34:56–64.
55. Skjerven H, Riis UH, Herlofsson BB, et al. In vivo accuracy of implant placement using a full digital planning modality and stereolithographic guides. Int J Oral Maxillofac Implants. 2019;34:124–32.
56. Block MS, Emery RW, Lank K, et al. Implant placement accuracy using dynamic navigation. Int J Oral Maxillofac Implants. 2017;32:92–9.
57. Stefanelli LV, DeGroot BS, Lipton DI, et al. Accuracy of a dynamic dental implant navigation system in a private practice. Int J Oral Maxillofac Implants. 2019;34:205–13.

58. Block MS, Chandler C. Computed tomography-guided surgery: complications associated with scanning, processing, surgery, and prosthetics. J Oral Maxillofac Surg. 2009;67:13–22.
59. Valente F, Schiroli G, et al. Accuracy of computer-aided oral implant surgery: a clinical and radiographic study. Int J Oral Maxillofac Implants. 2009;24:234–42.
60. Schubert O, Schweiger J, Stimmelmayr M, et al. Digital implant planning and guided implant surgery—workflow and reliability. Br Dent J. 2019;226:101–8.

Modelling and Impressions in Implants

Rajesh Dashaputra, Irfan Kachwala, Adwait Aphale, and Snigdha Chitnis

Abstract Implantology has come a long way to be mainstay in routine dental rehabilitation. An extremely high level of accuracy is essential in successful surgical placement of implants and development of the prosthetic solutions which should work like or better than natural healthy teeth. An equally accurate replication of the clinical situations in a physical or virtual mode is required before and during the treatment for the planning or execution of the prosthetic phase by the laboratories. Impression making and modelling tools form a vital segment in the armamentarium of implantologists and these techniques need a high level of skill development.

Multiple components specific to any implant system are provided by the manufacturers for single, multiple, and full arch implant impressions. Similarly, there are a different set of tools for digital impressions with intraoral scanning methods by dentists (*in vivo*) or by model scanning (*in vitro*) by laboratory experts.

This chapter details all the techniques and critical steps essential in both modelling and impression making for accurate replications and success. Few case presentations for different scenarios too are added for better explanations.

Keywords Dental implants · Dental impression · Digital impressions · Prosthesis design · Workflow

1 Introduction

The success rates of dental implants and the predictability of osseointegration is a foregone conclusion with reported success rates ranging from 97% to 100% [1].

R. Dashaputra
Department of Dentistry, Bhabha Atomic Research Center Hospital, Mumbai, India

I. Kachwala
Diplomate American Board of Prosthodontics, Mumbai, India

A. Aphale
Dental Implants and Smile Rehabilitation Center, Kolhapur, India

Dental Implants and Smile Rehabilitation Center, Pune, India

S. Chitnis (✉)
Oral and Maxillofacial Surgeon, Pune, India

R. S. Chaughule, R. Dashaputra (eds.), *Advances in Dental Implantology using Nanomaterials and Allied Technology Applications*,
https://doi.org/10.1007/978-3-030-52207-0_12

However, the long-term success of a dental implant depends on the prosthesis. The key to the attainment of perfect prostheses depends on the passive fit between the connector of the selected prosthesis and the implant itself [2]. Thus, the technique selected for making the impression of the implant, which simulates the exact position of the implant on the working cast, forms a crucial step in the dental implant procedure and should be as precise as possible. An ideal implant impression is one that records the accurate three-dimensional (3D) spatial position of the implant, analog, or abutment with respect to the other structures in the oral cavity [3, 4]. This allows the fabrication of a passive and well-fitting prosthesis which ensures the longevity of the dental implant.

Impression techniques for dental implants may be conventional or digital. Conventional methods consist of the utilization of impression material and impression copings to transfer implant positions to a stone cast with implant analogs in the position of the original implant. The advent of technology has ushered in the era of digital impressions that use optical methods to obtain the positions of implants and transfer them to a virtual model [5]. Both the conventional and digital impressions facilitate recording and transferring of the impression to a working cast, either stone or virtual, for the fabrication of an implant-supported prosthesis. The accurate transfer of the implant position with respect to the neighboring implants or teeth is vital for the selection of the appropriate prosthesis design and ensuring a good fit of the fabricated implant-supported prosthesis. Thus, it ensures the long-term success of the implant without mechanical and biological complications [5]. This chapter attempts to acquaint the reader with the conventional impression techniques of dental implants before introducing the digital impression techniques and the workflows associated with it.

2 Conventional Impression Techniques

On the basis of components utilized and the techniques applied, conventional techniques are classified as follows:

- Direct impressions without impression copings
- Abutment level impressions with snap-on copings
- Implant level impressions

2.1 Direct Impressions Without Impression Copings

This method involves the insertion of the final abutment on the implant followed by modification of the abutment height, margins, and parallelism. An impression is then taken of the abutment using conventional methods of gingival retraction and the standard impression techniques used for fixed prosthodontics. Vinyl polysiloxane (addition silicone) is the recommended material for this technique. However,

this technique is not the method of choice as it attracts all the clinical and laboratory errors associated with conventional impressions such as a suboptimal recording of abutment margins, distortion while pouring the cast, etc. Impressions made with the use of impression copings have proven to be of greater accuracy [6].

2.2 *Abutment Level Impressions with Snap-on Copings*

Initially, the final abutment is inserted onto the dental implant (Fig. 1a) followed by placement of a snap-on impression cap on the abutment (Fig. 1b). The snap-on plastic cap is then picked up in the impression (Fig. 1c). The abutment is then connected with the implant analog (Fig. 1d) and carefully repositioned inside the impression with proper orientation (Fig. 1e). The concept is similar to the closed tray impression technique. Comparative analysis has shown no difference in the accuracy of abutment level impressions and closed tray implant level impressions [7].

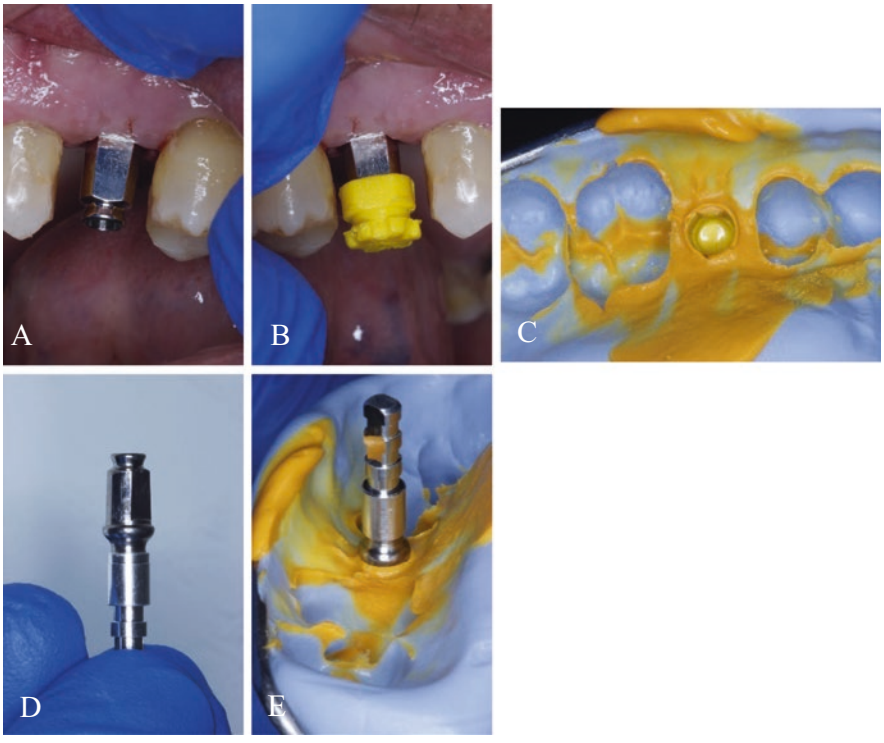

Fig. 1 Abutment level impression with final abutment in place (**a**), placement of a snap-on impression cap on the abutment (**b**), pick-up impression of the abutment cap (**c**), abutment connected with implant analog (**d**), and repositioned in the impression (**e**)

2.3 Implant Level Impressions

Implant level impressions record the 3D position of the implant in terms of its position in relation to adjacent teeth or implants. It also records the orientation of the implant in terms of the rotational position of the internal connection. Recording the shape and levels of the gingival tissue around the implant is another goal of the procedure. Polyether and vinyl polysiloxane are the materials of choice for this technique [8, 9]. The use of custom trays over stock trays for the impression procedure has been shown to be more accurate [10]. The reduced volume of material used in custom trays minimizes the volumetric shrinkage. Stock trays, when used, should be made of metal or rigid plastic [11, 12].

This method is preferred over direct impressions due to ease of use, reduced chairside time, and elimination of clinical and laboratory errors [6].

Implant level impressions can be accomplished by either the closed tray or the open tray impression techniques.

- Closed tray impression technique (Indirect/ transfer)
- Open tray impression technique (Direct/ Pick up)

2.3.1 Closed Tray Impression Technique

This technique consists of the utilization of an impression coping which is retained in the mouth when the set impression is removed. Hence, it is also termed as the indirect or transfer technique.

Before starting the procedure, the healing abutment or provisional restoration is removed (Fig. 2a). A closed tray or transfer impression coping is inserted onto the implant (Fig. 2b). Radiographs are taken for verification of fit and to ensure the fabrication of a passively fitting prosthesis (Fig. 2c). Tray adhesive is applied on the stock or custom tray. The low-viscosity impression material is injected around the impression copings, gingiva, and adjacent teeth. The tray is simultaneously loaded with high-viscosity impression material such as heavy body or putty in case of vinyl polysiloxane. In the case of a viscoelastic material like polyether, the same material is used in the syringe and in the tray. The tray is seated in the mouth and held steady till the material sets completely. The impression is then removed from the mouth and examined for errors (Fig. 2d). The impression coping is unscrewed and removed from the mouth followed by reinsertion of the healing abutment onto the implant. The impression coping is then connected with an implant analog and reinserted into the impression. Care is taken to ensure that the orientation grooves on the impression coping are aligned properly (Fig. 2e) and the coping itself is seated completely (Fig. 2f). Additionally, care is taken to ensure that there is no movement of the impression coping-implant analog assembly inside the impression. If any such disturbance is suspected, it is wise to repeat the impression. The impression is then disinfected and sent to the laboratory for pouring.

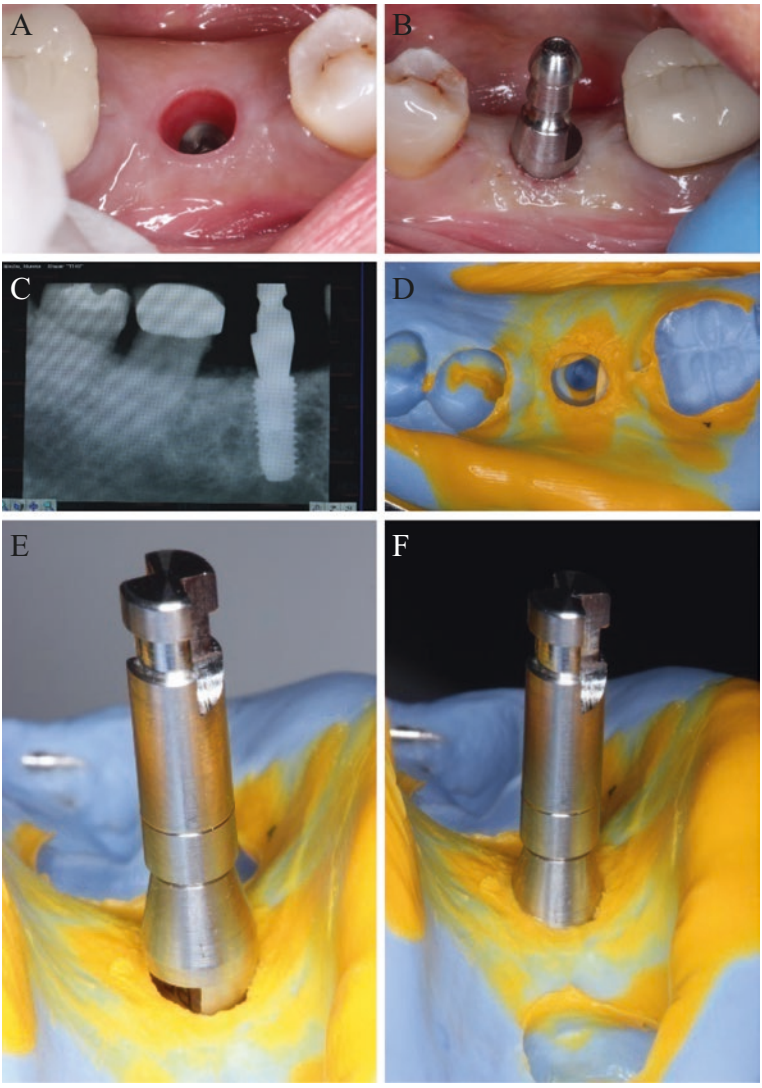

Fig. 2 Closed tray impression technique: removal of the healing abutment (**a**), transfer coping fitted onto the implant (**b**) and radiograph taken for the verification of the fit (**c**), the final impression (**d**), proper alignment of the orientation grooves of the impression coping (**e**), impression coping properly seated (**f**)

2.3.2 Open Tray Impression (With or Without Splinting of Impression Copings)

This technique consists of the utilization of an impression coping that is incorporated into the impression and is removed from the mouth along with the set impression. Hence, this technique is also known as the direct or pick-up impression.

Similar to the closed tray technique, the healing abutment or provisional restoration is removed before the procedure (Fig. 3a). The open tray impression coping is then inserted onto the implant (Fig. 3b). Radiographs are taken for verification of fit. A rigid plastic tray of appropriate size is selected. Special metal trays with removable windows in areas of the implants are also available. A custom tray is the ideal choice; however, it requires an additional visit and increased lab cost. A window is cut out in the tray after locating where the guide pin or screw of the impression coping needs to extrude from the tray. This window is then covered by wax to prevent the tray material from flowing out of the tray through the window (Fig. 3c). Tray adhesive is applied on the stock or custom tray. The low-viscosity impression material is injected around the impression copings (Fig. 3d), gingiva, and adjacent teeth. Loading of tray with a high-viscosity impression material such as heavy or medium body in case of vinyl polysiloxanes is carried out. In the case of a viscoelastic material like polyether, the same material is used in the syringe and tray. This is followed by careful positioning and seating of the tray in the mouth, until the guide screws of the impression copings extrude through the wax covering the window (Fig. 3e). The tray is held in place till the material has completely set.

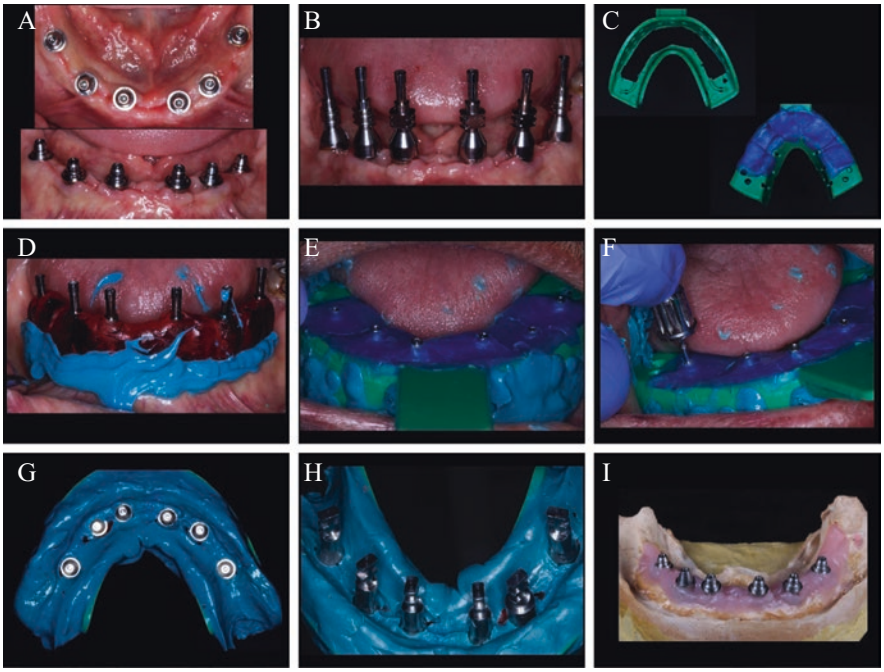

Fig. 3 Open tray impression technique: healing abutments removed before impression (**a**), pick-up impression copings inserted onto the implants (**b**), window covered by wax to prevent the tray material from flowing out (**c**), low-viscosity impression material injected around area to be recorded (**d**), proper seating of tray loaded with high-viscosity impression material (**e**), guide screws unscrewed (**f**) and impression copings picked up with the impression (**g**), implant analogs inserted onto the copings and the guide screws tightened (**h**), final poured cast (**i**)

Any wax or impression material from the head of the guide screw is removed and the guide screw is then completely unscrewed (Fig. 3f). The impression is then removed from the mouth. The impression coping is picked up in the impression (Fig. 3g), and the impression is inspected for any errors. Healing abutments are then reinserted onto the implant. An implant analog is inserted onto the impression coping (in the impression) and the guide screw tightened (Fig. 3h). The implant analog is held in place while tightening the screw to prevent rotation of the impression coping inside the impression. Care is taken to ensure that there is no movement of the impression coping-implant analog assembly inside the impression. If any disturbance is suspected, it is wise to repeat the impression. The impression is disinfected and sent to the laboratory for pouring (Fig. 3i).

Multiple studies and systematic reviews have demonstrated that open tray impression techniques are more accurate than closed tray impression techniques [8, 9, 13, 14].

A systematic review by Lee et al. [8] comparing the accuracy of open and closed tray impression techniques found no significant difference in both the techniques when making impressions for three or fewer implants. The open tray technique was recommended for situations involving four or more implants. Another systematic review by Papaspyridakos et al. [9] found open tray impressions to be more accurate for completely edentulous arches. No significant difference between the two techniques was found for partially edentulous arches.

2.4 Splinting of Implants

Another recommendation for increasing the accuracy of the impression in cases involving multiple implants is the splinting of the impression copings to one another or to the custom tray prior to impression making [8, 9, 15–17]. The open tray impression technique is used when the impression copings are splinted together.

Various materials and methods have been used for splinting the impression copings to each other [18, 19]. A few examples of the same are as follows:

- Splinting only with an auto-polymerizing acrylic resin (AAR)
- AAR and dental floss
- AAR with burs or stainless steel wire
- Light-cured composite resin with burs, stainless steel wire, or metallic sticks
- Impression plaster

The most commonly used AAR is Pattern Resin LS (GC America Inc., Illinois, USA) because of its desirable properties of low shrinkage (0.36% at 30 min, 0.37% at 24 h) and quick setting time [18]. The time line for splinting with AAR ranges anywhere from immediately prior to 24 h prior to the impression according to various authors [8]. It is recommended to section the AAR and re-splint the segments prior to impression [13]. This is done to compensate for the polymerization

shrinkage of the AAR, which affects the accuracy of the impression. Splinting can be accomplished intraorally on a model made from a previous unsplinted impression.

The technique for intraoral splinting with AAR and dental floss is as follows:

Open tray impression copings are inserted and tightened onto the implants as previously illustrated in Fig. 3b. Dental floss is wrapped in a criss-cross pattern between the impression copings and the loose ends secured (Fig. 4a). AAR (Pattern Resin) is then mixed to a thick consistency. The material has a working time of 2–3 min and reaches dough stage almost immediately. A roll of the AAR is adapted around the impression copings and dental floss making sure that there is enough thickness of material around the impression copings (Fig. 4b). Setting time of the material is 4 min. The material is pushed away from the gingival tissues with a spatula to avoid contact with monomer, prevent burns due the exothermic polymerization reaction, and make space for injection of light body impression material to record the tissues. The AAR can alternately be added completely by the brush technique through incremental additions. However, this is time consuming and the flow of the material is difficult to control.

The entire assembly of splinted impression copings is unscrewed and removed from the mouth. The impression copings are labelled for easy repositioning before sectioning. A diamond-coated disk with a straight micromotor hand piece is used to

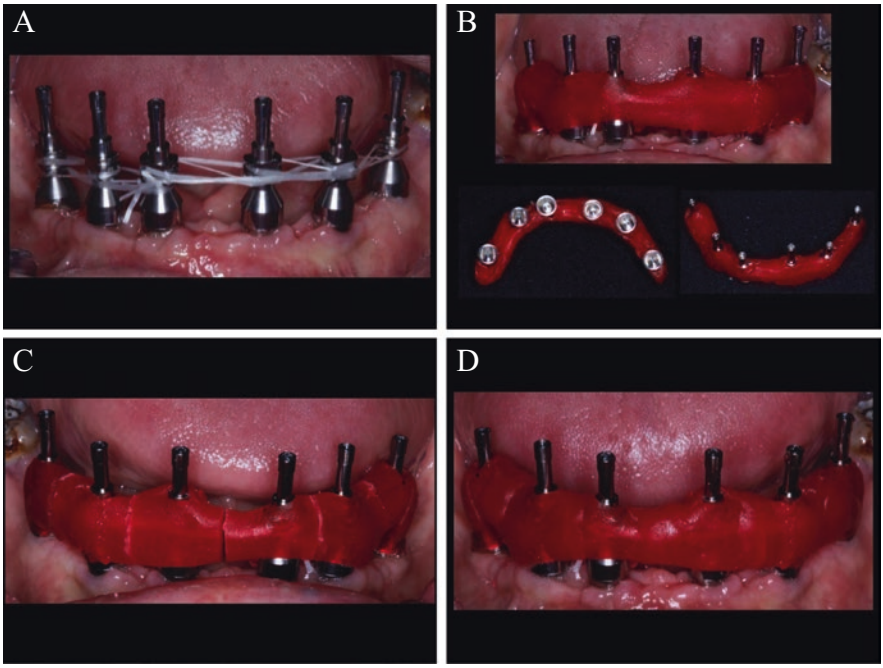

Fig. 4 Criss-cross pattern of dental floss between the impression copings (**a**), AAR adapted around the impression copings (**b**), impression copings reinserted into their original position after sectioning of the AAR splint (**c**), AAR segments rejoined with minimum amount of material (**d**)

section the connectors between the impression copings. Care is taken to ensure the cut is as thin as possible to reduce the volume of material used to re-splint and, hence, the shrinkage. The impression copings are reinserted into their original positions on the implants and tightened while making sure that there is minimal space but no contact between the AAR connector segments (Fig. 4c). The AAR segments are then rejoined with minimal amount of material using the brush technique (Fig. 4d). After setting, the AAR splint is then painted with tray adhesive. The open tray impression technique described previously is carried out to complete the procedure (Fig. 3c–h).

3 Digital Impression Techniques

The conventional techniques may incorporate many human errors such as tray design, errors in component fixing, impression making, and material flow at multiple levels if not followed meticulously. Additionally, the dimensional changes in impression materials, pouring techniques in the lab, and expansion of stone plaster are the major technical errors encountered in these techniques [20–22]. The discomfort to the patient due to additional components, required tolerance to mouth opening, and the taste and odor of silicone materials remains a disadvantage. It was due to these shortcomings that the intraoral scanning technologies came into existence [22].

3.1 Development of Dental CAD/CAM Systems

Dental computer-aided design (CAD) and computer-aided manufacture (CAM) systems have started to develop since the 1960s. Dr. Francois Duret developed the first CAD/CAM device for fabricating crowns based on digital impressions in 1971 [23–25]. Additionally, he developed the first CAD/CAM dental restoration in 1983 and the Sopha system in 1984 [23, 24]. Dr. Andersson developed the Procera system, which produced high-precision dental crowns and metal-free veneered restorations utilizing CAD/CAM in 1983 [26]. In 1987, Mörmann and Brandestini developed the CEREC system, which was the first dental system to combine digital scanning with the milling unit [25, 27].

The intraoral scanners have evolved towards more practicality and accuracy and have been made available chairside in the last two decades. Industrial grade machines for CNC or milling have catered to large institutional work outputs. Modern system allows the “scan to crown delivery” protocol with their integrated chairside system without outside lab intervention [28].

3.2 Intraoral Scanning Devices

The scanning or digitization technologies were introduced in the 1970s as indirect digitizations on models (extraoral digital impressions) utilizing extraoral scanners and direct digitizations (intraoral digital impressions) in the mouth and essentially came into existence along with development of CAD/ CAM. However, the direct digital impressions of abutments required considerable chair time and had limited accuracy. With the evolution of intraoral scanning, CAD/CAM systems are now clinically practical [29].

The last decade has witnessed the development of multiple devices for Intraoral Scanning (IOS) [29]. IOS comprises a system of medical optical camera device (hardware), a relevant computer Software Program (software), and a computer. The whole system is used to scan and capture the intraoral structures, save and process the input into a programmable file, and then design with soft tools to render output for manufacturing in the CAM lab. Alternatively, the hardware device may be used only to capture the image in the form of points cloud and meshwork [28] and render output in a universally used format called STL (Standard Tessellation Language) [29, 30], a computer code recognized by most CAD Software EXOCAD™.

The process of digitisation of oral structures can be done directly inside mouth with Intra oral scanning devices (**intraoral digitisation**) or by scanning the model derived from a physically made impression of the mouth (**extraoral digitisation**) as per earlier descriptions in earlier section.

1. **Intraoral digitization**: Intraoral scanning devices in the later decades revolutionized clinical workflows with their scanning and designing software with integrations for CAM. The complete digitized protocol increased accuracy and eliminated the need for conventional impressions and model pouring in labs [25, 29]. Earlier systems required the application of titanium dioxide or magnesium oxide powder or sprays to the glossy tooth surfaces in order to avoid reflection errors and to create a measurable surface. The powder layer applied to the tooth surface resulted in an additional thickness of 13–85 μm [31] which had to be adjusted in measurements. Also, the time taken and frequent need to re-powder areas washed by saliva made the process more uncomfortable for operator and the patient. Hence, modern optical intraoral scanning devices are powder free and more advanced [31].
2. **Extraoral digitization** involves two methods
   (a) **Contact digitization**: The capture is by means of a ruby ball and the 3D structure is measured. This method is distinguished by a high scanning accuracy, whereby the diameter of the ruby ball is set to the smallest grinder in the milling system so that all data collected by the system can be easily milled [26, 31]. One example is Procera Scanner. The drawbacks of this procedure are complicated mechanics, high expense, and its time-consuming procedure.
   (b) **Optical digitization**: This involves light systems in the form of point focus or line system which can scan the model or impression in detail forming mesh which is transferred to the designing system [30, 31] (Fig. 5a–c).

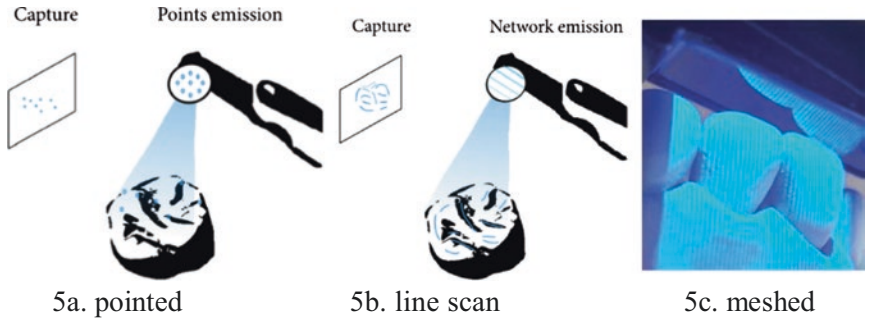

Fig. 5 (**a**, **b**) Light sources—pointed or meshed, (**c**) scanned model with line scan

The indirect methods involve options of three, four, or five axis scanning for accuracy required [25, 29, 32].

3.2.1 IOS Technology (Device Construction and Engineering)

The IOS system consists of a handheld camera device, relevant software, and the computer system. Goal of intraoral scanning is essentially to capture the intraoral 3D structures with precision and replicating the same geometry through the software for further processing [29, 30].

All these devices have a conventional light source in the form of LED or laser and a camera for capture of the tissues either in pictorial format (static images) or video recording (dynamic images) and then to generate scanned object POI (point of interest) in a points and triangulation cloud (meshwork) to rendering the shape in 3D form in the software with precision (Fig. 6) [28, 30, 31].

The images captured are at a very rapid rate as multiple images or in video formats to multiple sections finally joined in the software to create the 3D output for processing by combining these multiple captures.

Most of the systems developed today have the ability to render the output files in the universal industry format and are called open file systems. The output format is called STL which can be processed by all the milling systems. They may also use intrinsic proprietor formats for enhanced rendering, especially regarding to gingival and tooth color system, texture, translucency of dental tissues, and other parameters (e.g., Polygon File Format, PLY files) [25, 29, 30].

3.2.2 IOS Clinical Factors

The clinical protocols of the scan systems have a learning curve involved to render accurate reproduction of the captures. There are a lot of inaccuracies seen by failure of the operator to accurately identify and measure the POI [28–31].

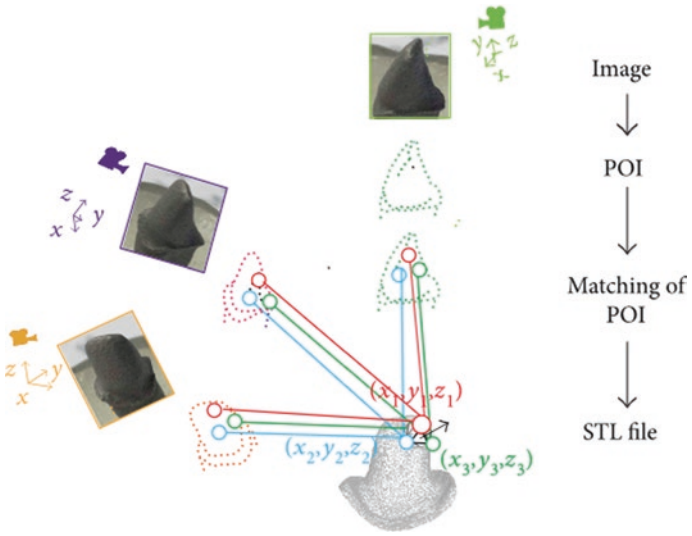

Fig. 6 Triangulation in scanning creating meshwork

3.2.2.1 Distance and Path of Scanning

Various devices have different diameter/size of the IOS component and different speeds of capture. Skills must be developed in scanning of the arch, minimizing repetition to avoid patient anxiety and discomfort. Both the direction of the path followed and distance of the scanner from object must be maintained as per the device manufacturer's guidelines [25, 30].

The usual path for scanning followed involves first rough scanning of the occlusal and occlusal to palatal arches going in a long "S-shaped" path in each quadrant. This is followed by a labial scan and then labial to palatal semicircular movements to get the interdental areas and contact embrasures. Many repeats may be required to detail the images where voids are depicted by the software [30]. Also the occlusion can also be recorded by scanning the teeth in occlusion. This will get transfer to the project file with virtual articulator features given in the software [30] (Fig. 7a–d).

3.2.2.2 Tracking with Software

Intraoral scanning is a dynamic process and watched live as the reproduction can be seen live in the capture software screen. It is useful to trace out the occlusal full quadrant with slight cross arch area and then repeat regions to gain more details as the software tracks every area depicting the correct areas and marking voids or error regions for repeat [30].

The errors arise when distance to object and scan path as well as speed and smoothness of movements is not respected. The scanning connection continuity in software gets lost and these areas have to be rescanned. The software can track new captures and correctly superimpose on the old data in accurate fashion without

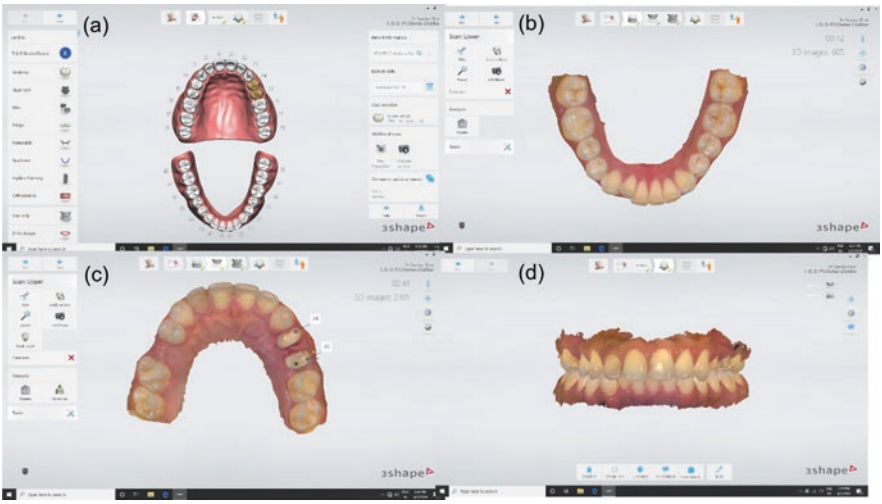

Fig. 7 **(a)** software interface; **(b)** lower jaw scan; **(c)** upper jaw scan; **(d)** both jaws scanned in occlusion. (Courtesy: Dentalarch Practice, Dr. Archana Dashaputra and Illusion Dental Lab, India)

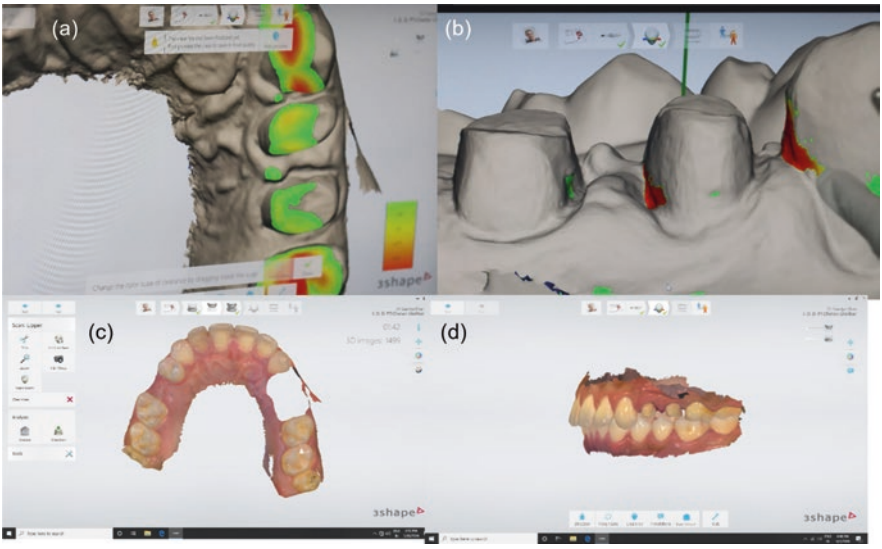

Fig. 8 **(a)** showing hot spots; **(b)** preparation errors; **(c)** old data cut from scan; **(d)** rescanning after tooth preparation. (Courtesy: Practice, Dr. Archana Dashaputra and Illusion Dental Lab, India)

distortions. This itself is a major boon of this technology, which in conventional methods requires a full retake of the impression. Also, in case there are errors found in preparation, it is shown in shaded pattern and the clearance pressure points in the occlusal relation are shown as hot spots. These can be corrected and superimposed on or replacing selected area by editing old scan (Fig. 8a–d).

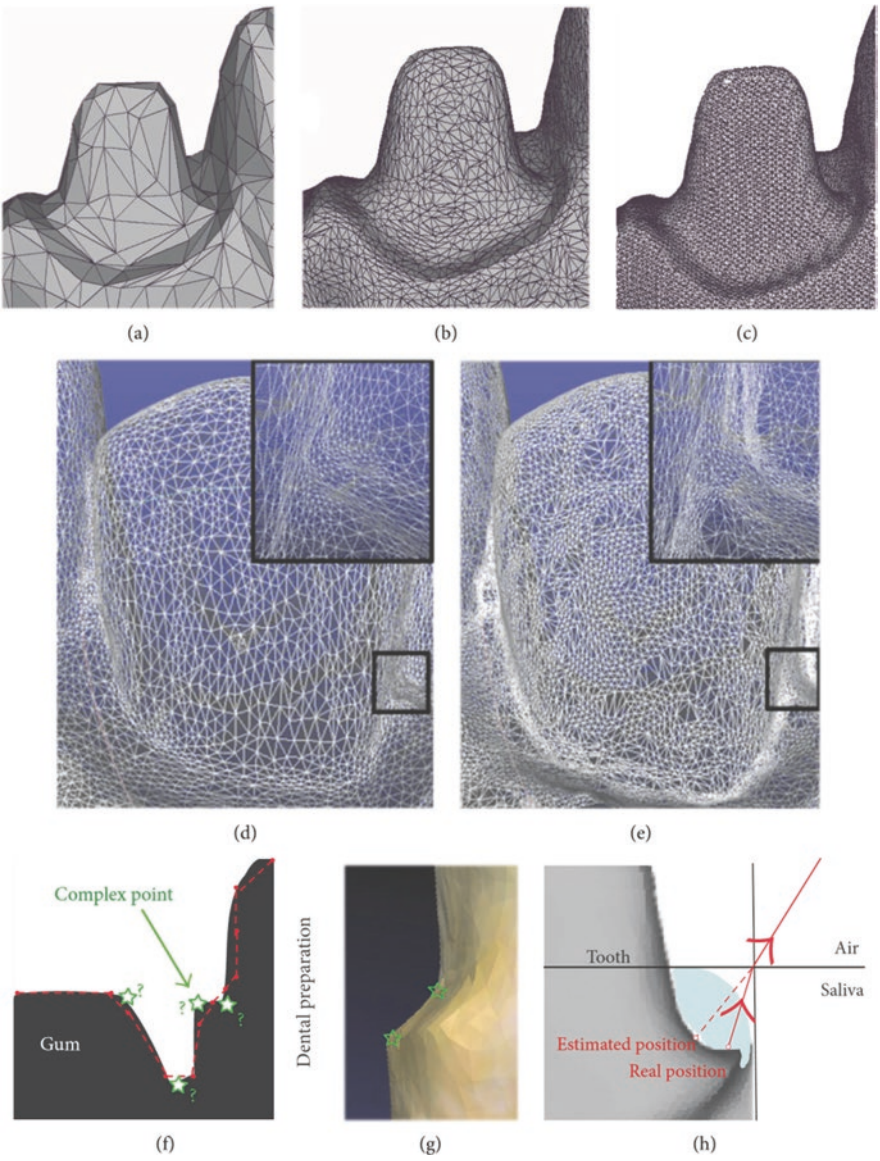

Fig. 9 The density of the meshwork defines accuracy. Small voids of air or saliva can create errors in scan. (**a–c**) Exhibits meshwork from scanned captures. (**d** and **e**) Exhibits increasing density with multiple recordings. (**f** and **g**) A more dense scan is required for complex curvatures. (**h**) Errors caused by voids

3.2.2.3 Image Accuracy and Mesh Quality

The quality of the rendered image depends on the quality of device engineering, the system guidelines and limitations, skill of the user and the software capabilities, and type of area or object scanned [28, 33].

The presence of air or saliva pockets and inaccessible subgingival areas need greater notice and correction with multiple repeats and scan corrections. The reconstruction process usually creates a meshwork from the scanned captures (Fig. 9a-c). The denseness of the mesh will differ as per options used, depth of scan, and multiple recordings done (Fig. 9d-e). All the areas need not be rendered by increasing the mesh density. Only areas where sharpness is required, as in margins of a preparation with extremely delicate curvatures, a detailed rendering with a very dense mesh quality is needed [30] (Fig. 9f-g).

Accuracy is the degree of veracity, that is, how well the measured value represents the "truth," whereas "precision" is the degree of reproducibility, that is, the repeatability of the measurement system [31]. Ideally, a measurement device is both accurate and precise, with the measurements close to and tightly clustered around the true value [31, 32].

Regardless of the digitizing mode applied, clinical parameters such as saliva, blood, and movements of the patient might affect the reproduction of teeth.

Ender et al. [34] have reported that the mean trueness of various IOS technologies is between 20 and 48 μm and the precision is between 4 and 16 μm, when the impression is partial and compared to conventional impression. The conclusion of these reports is that current IOS devices are clinically adapted for common practice, with at least similar accuracy to conventional impression making. However, in vivo full-arch impression is reported to be associated with a phenomenon of distortion, in particular for triangulation, confocal, or AWS technologies.

Most of the leading intraoral devices have optimum functionalities but vary in different functional parameters.

In vitro comparison of the accuracy of four intraoral scanners and three conventional impression methods for two neighboring implants suggest that optical impressions are superior to elastomeric impressions for placing two implants in one quadrant. Closed tray impression accuracy was significantly lower than that of open tray impressions for placing two implants in one quadrant [35].

The desirable features of a digital impression are as follows [36]:

- Ability to export any digital impression file to any software (open system)
- Ability to capture dental hard and soft tissue accurately over long spans
- Smaller size of intraoral wand that can reach all areas
- Fast acquisition time and ability to capture features in moist environment
- Ability to capture true color
- Portability
- Software should have face scanning ability
- Artificial intelligence incorporated in scanning protocol itself for implant component recognition

3.3 Clinical Applications

The goal of any dental implant procedure is to deliver perfectly fitting, functional teeth or prosthesis. With the recent developments in intraoral scanning techniques, software handling algorithms, and artificial intelligence incorporated in scanning, the predictability and precision of the fabricated implant prosthesis using a digital protocol is much more guaranteed [37].

The workflow: Similar to the conventional impression techniques for implants, the digital impressions are classified as follows:

1. Abutment level impression
2. Implant level impression

3.3.1 Abutment Level Impression

After the final abutment is placed onto the implant, the intraoral scanning progresses similar to the crown and bridge procedure. The challenge in implant abutment scanning is the reflective surface of abutment. The unprepped abutment is highly reflective and is difficult to capture precisely by the intraoral scanner.

Roughening the abutment with sandblasting or use of opaque powders such as occlusal markers is suggested in such cases. If the abutment has undergone preparation with diamond points or carbide burs prior to impression, it already has roughness and has lost its shine, making it conducive for the scanning. After the abutment has been prepared, a digital impression is taken following the standard practices of gingival retraction and after making sure that the margin of the abutment is visible and preferably equigingival (Figs. 10, 11 and 12).

The STL/OBJ/PLY file is then shared with the dental laboratory in the digital format. The respective file is then imported into the CAD software for designing the

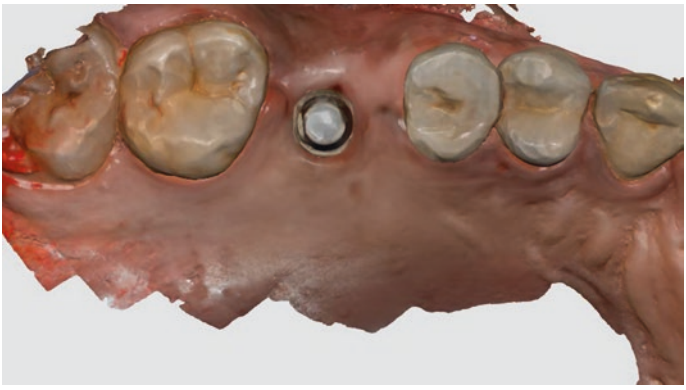

Fig. 10 Abutment in position with margin completely visible for scanner to scan it efficiently

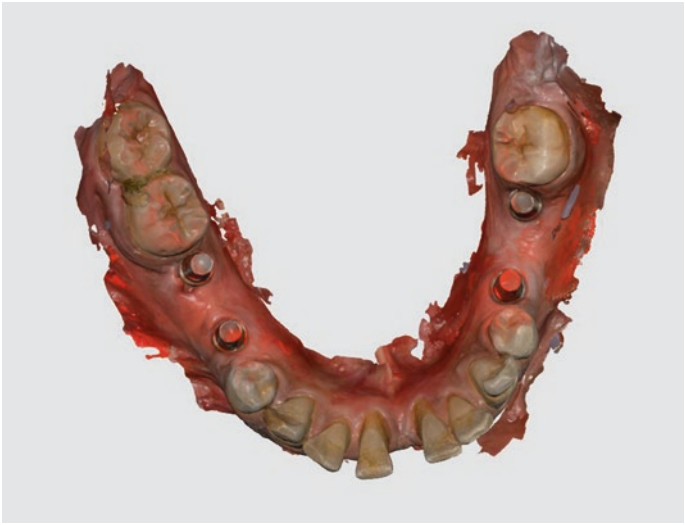

Fig. 11 Abutment scanning done with occlusal spray on abutment making it nonreflective and amenable for scanning

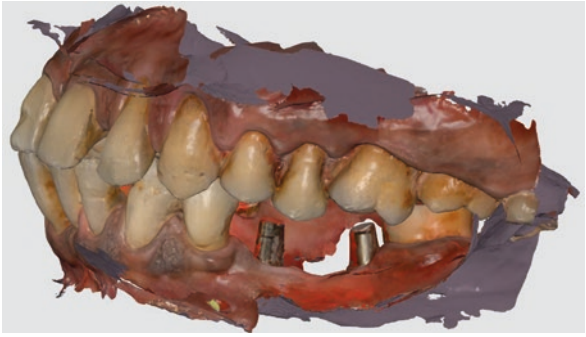

Fig. 12 Abutment prepped intraorally to remove possible undercuts. (View in Occlusion)

further prosthesis. The workflow for designing prosthesis for abutment level digital impression remains the same as that for the conventional crown and bridge prosthesis.

3.3.2 Implant Level Digital Impression

The fundamental function of registering an implant level digital impression is to accurately record the implant axis and position in bone in order to plan the prosthesis. This is done with the help of implant scan bodies. The correct engagement of the scan bodies with the implant reflects the angulation and position of the implant in bone. There are two types of scan bodies available:

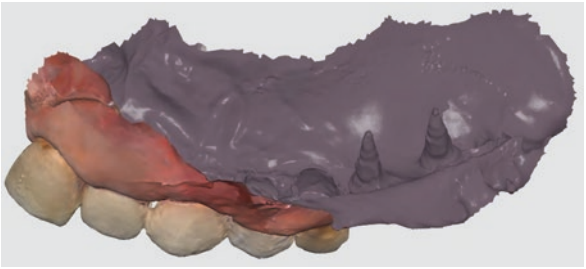

Fig. 13 Scan body captures the implant axis and position intraorally

(a) Intraoral scan bodies: Utilized for intraoral scanning by placing directly over the implant. Here, the whole sequence is followed digitally from capturing the digital impression to fabrication of the prosthesis with or without a printed resin model (Fig. 13).
(b) Extraoral scan bodies: Utilized extraorally in the dental laboratory. In this scenario, a conventional implant level or abutment level impression (in case of multiunit abutments) is registered. An extraoral scan body is then attached to the model in the dental laboratory and scanning is done using a lab scanner to facilitate the CAD process.

When performing complete-arch digital scans with more than two implants, clinicians should choose the intraoral scan body (ISB) and scan technique carefully, as these factors can significantly affect the accuracy of the scan when using the test scanner. Certain ISBs may be scanned faster than others [38].

Scanning technique is the technique of movement of the IOS wand over the teeth and implant area. Each company recommends its own protocol for scanning. Change in the path of scanning may result in the loss of the reference point and stitching of the resultant 3D image.

CAD process of implant level digital impression can be done in two ways depending on the prosthesis needed:

(a) Without model (No printing of resin model): This technique is indicated in single-implant or two-implant cases with a passive path of insertion and favorable angles of implants. Usually, single-implant cases with prosthesis which can be directly milled from CAD such as zirconia or E-max milled crowns can be executed without a model.
(b) With model: This technique is indicated in cases which need customized abutment fabrication, layered ceramic prosthesis, full-arch prosthesis, and in implants with severe angulation which need correction at abutment level.

Essentially, in any of above mentioned scenario capturing implant level digital impression with the help of implant scan body remains the same.

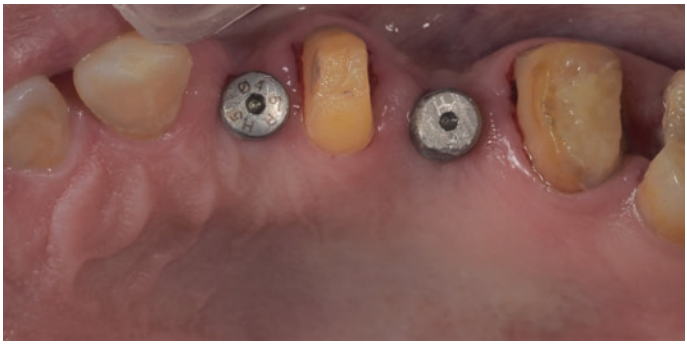

Fig. 14 Maxillary gingival formers in place

Fig. 15 Mandibular gingival formers in place

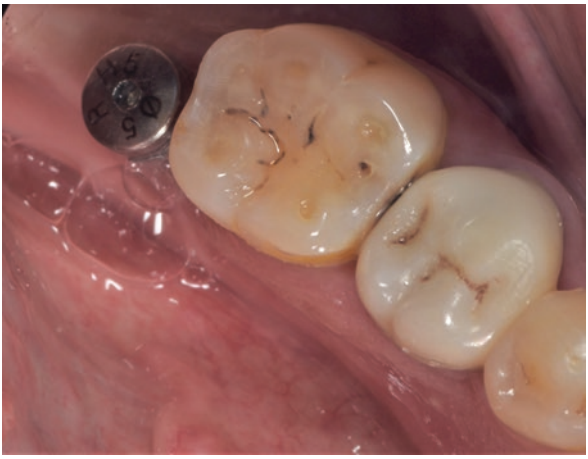

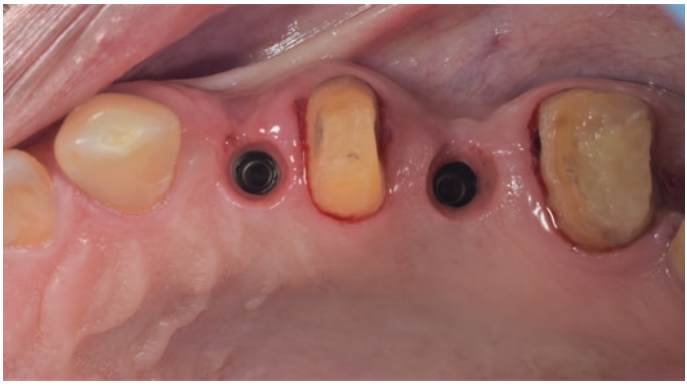

Fig. 16 Removal of maxillary gingival former with a healthy gingival profile prior to scanning

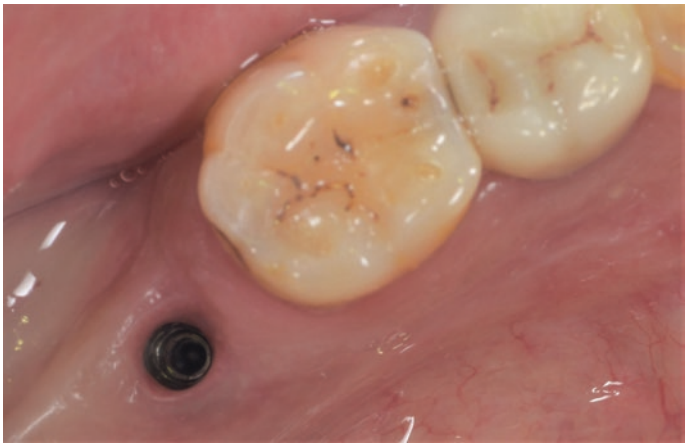

Fig. 17 Removal of mandibular gingival former with a healthy gingival profile prior to scanning

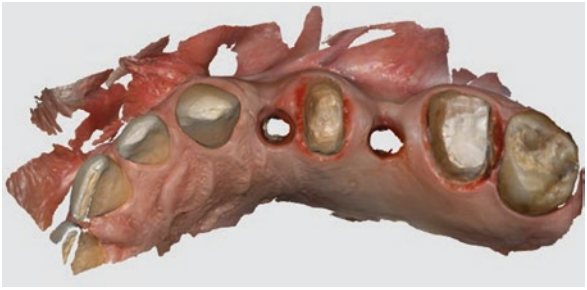

Fig. 18 Gingival profile scan along with the adjacent teeth for the maxillary arch

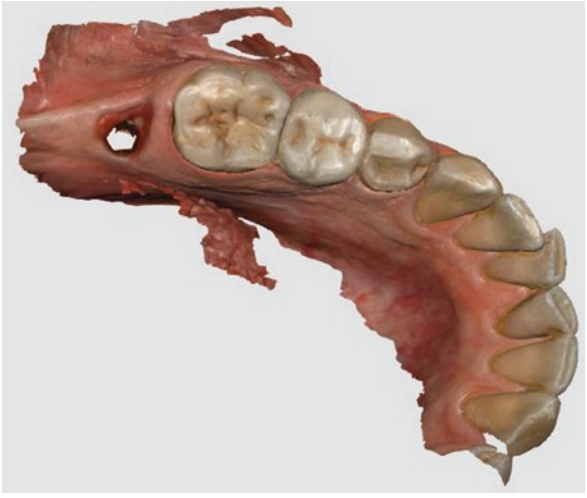

Fig. 19 Gingival profile scan for the mandibular arch

4 Workflow of Scanning with Scan Body and Fabrication of Prosthesis

4.1 Without Model

The patient and prosthesis details are filled in the scanning case sheet. The healing abutment or provisional restoration is removed before the procedure (Figs. 14, 15, 16 and 17). Scanning is then initiated with the scanning wand following the path of scanning as per the manufacturer's instructions. The gingival profile of the implant site is captured from all aspects along with the full or partial arch as per the case (Figs. 18 and 19). An appropriate intraoral scan body is screwed in the implant. The scan body is inserted in a way that the matching point faces either the buccal or lingual area. Scanning is started from the adjacent tooth with maximum scan depth and then the scanner tip is turned to the buccal area to scan the matching point followed by the lingual side. The artificial intelligence (AI) command for recognizing the scan body intraorally is fed into the software which will get transferred to lab along with file. If AI is not incorporated in the scanning software, the scan body has a specific code which needs to be provided to the lab. This information gets integrated during export of STL/OBJ/PLY file to laboratory and helps the laboratory to decode the scan body for CAD. The scan then progresses, and the scan body, opposing arch, and the occlusion are scanned according to the manufacturer's guidelines. The scan process is then completed; the final scan files are prepared and sent to the laboratory for fabrication of prosthesis (Figs. 20, 21, 22, and 23).

Fig. 20 Scanning of the intraoral scan body

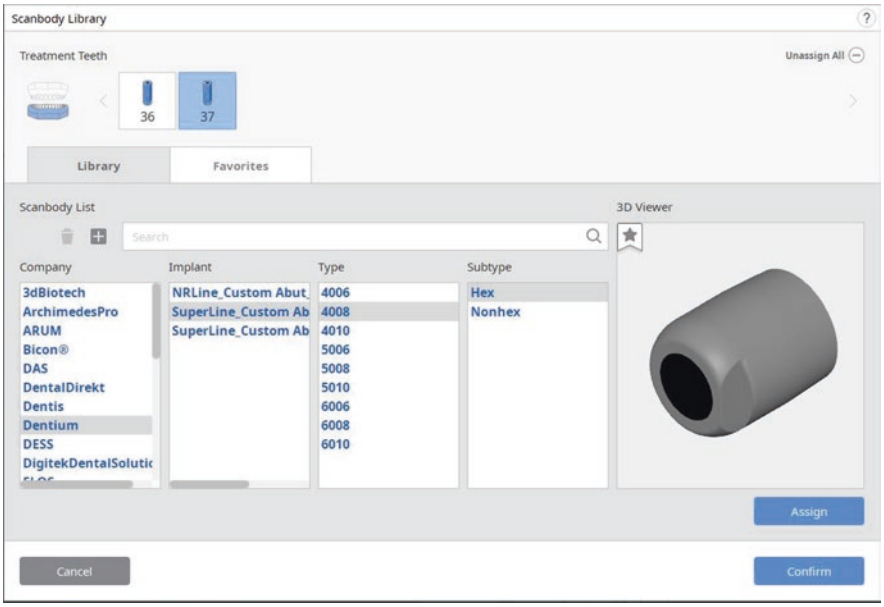

Fig. 21 The artificial intelligence in scanning software allows clinician to choose the scan body size and code which is specific to each implant company. Clinician has a choice to choose from the library incorporated in the IOS software. The same corresponding library should be present with the dental laboratory for decoding the same

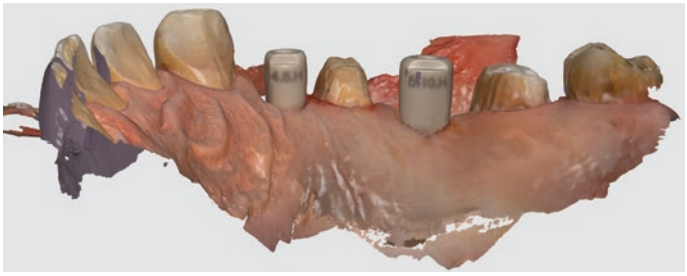

Fig. 22 The palatal scanning of the scan body

Selection of the abutment is done as per the instructions shared by the clinician (Fig. 24). A virtual wax build up is then done on to it which will be later converted to the fixed prosthesis. Gingival emergence can be easily calculated with the help of software. The tooth library present in the software is used to design the morphology of the final prosthesis (Figs. 25 and 26). It is customized as per the adjacent contact areas, emergence, and occlusion with antagonists. CAD is done and checked to

Fig. 23 Laboratory Interface

Fig. 24 Selection of the abutments

verify the occlusion as per the occlusal record received by scanner. Sometimes, virtual articulators are also utilized to simulate the jaw movements making it more predictable and reliable. After CAD is approved by the clinician and lab technician the same file is processed for CAM for prosthesis fabrication and the prosthesis is fabricated and cemented into the patient's mouth (Figs. 27, 28, 29, 30, 31, 32 and 33).

Fig. 25 Tooth library present in the software used to design the morphology of the final maxillary prosthesis

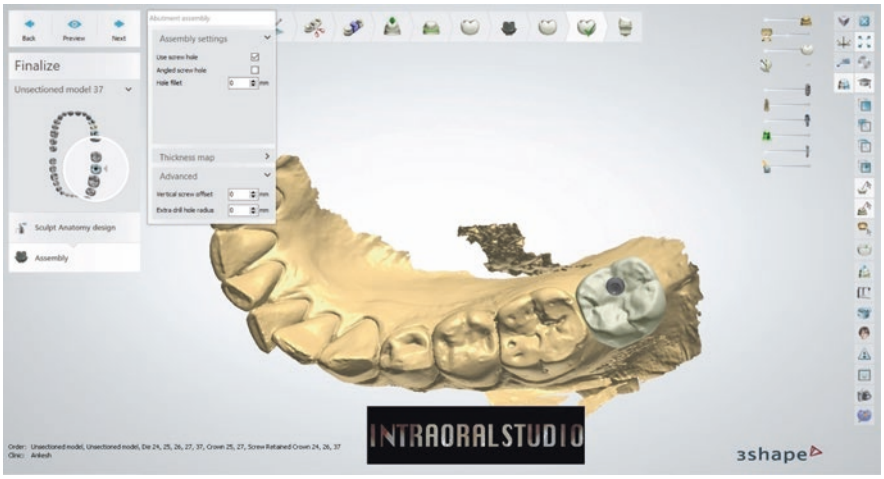

Fig. 26 Tooth library used to design morphology of the final mandibular prosthesis

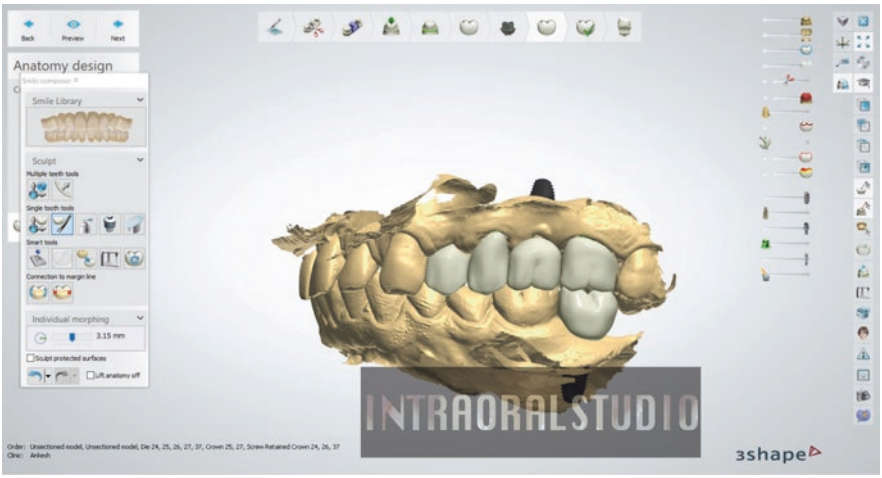

Fig. 27 Occlusion verified as per the occlusal record received by the scanner

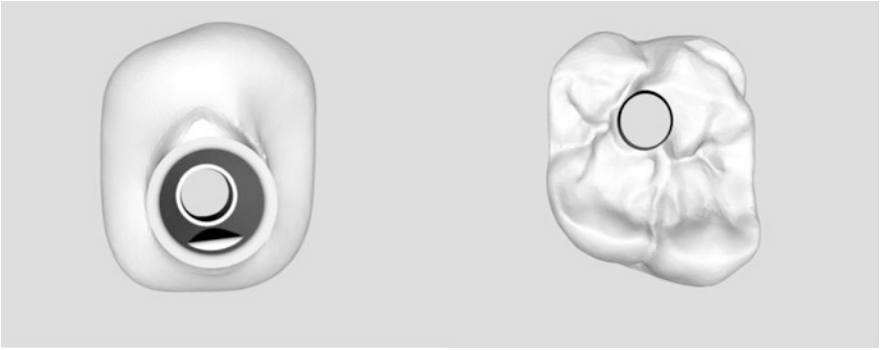

Fig. 28 Advantage of CAD: precise adaptation of the crown and the abutment margins

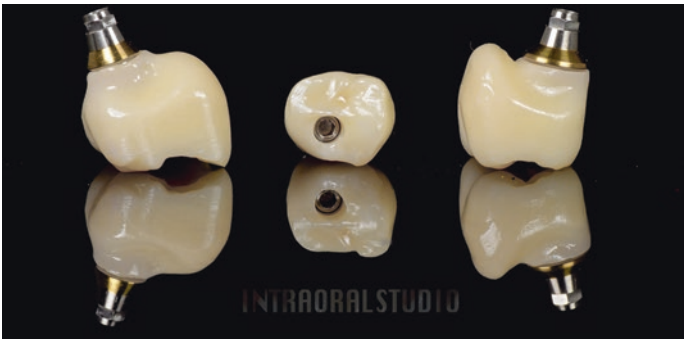

Fig. 29 Precise fit of the milled zirconia monolith crowns to abutment. The size of the implant is same as that of chosen during the CAD

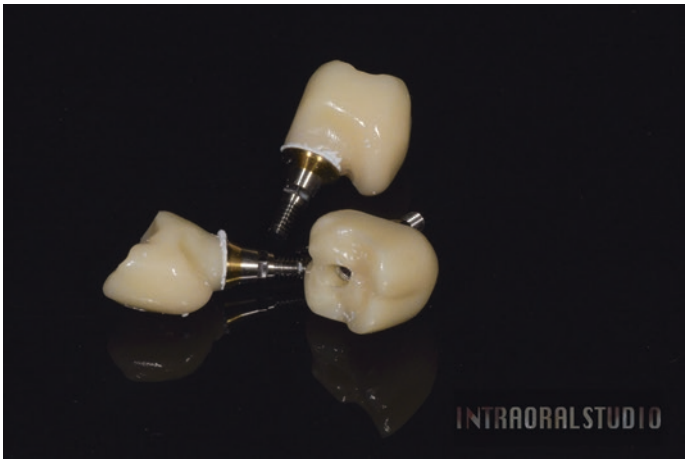

Fig. 30 Cementation of the crown to abutment extraorally in order to avoid inadvertent flow of excess cement in gingival sulcus

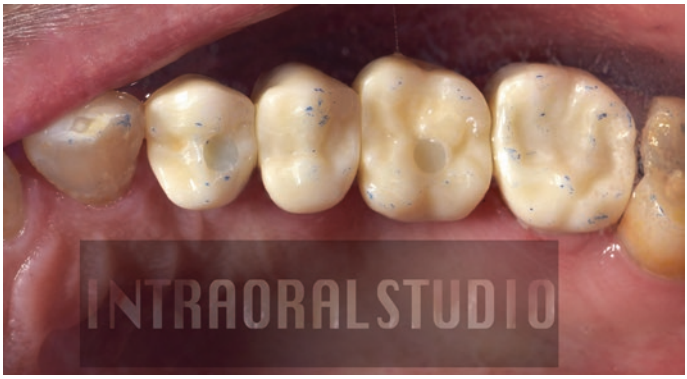

Fig. 31 Precise fit of the implant crowns and adjacent zirconia crown on natural abutments

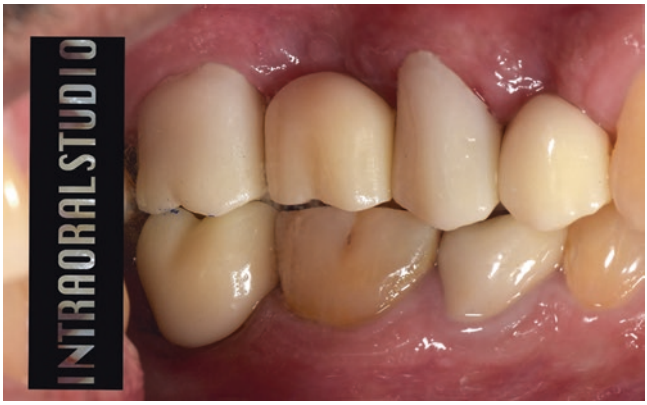

Fig. 32 In occlusion

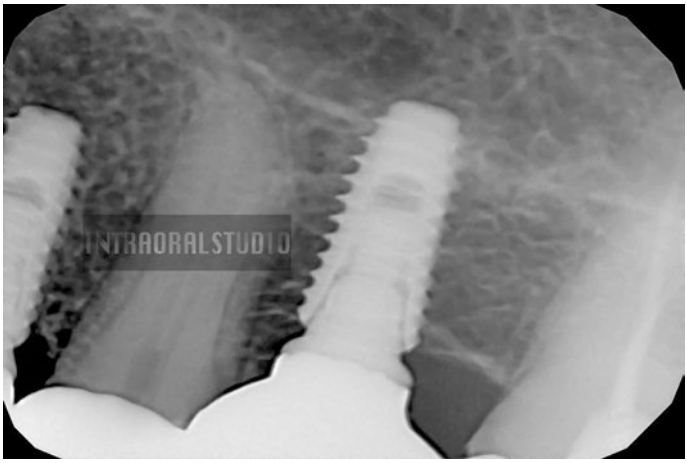

Fig. 33 RVG image showing the precise fit of the crown to abutment with no excess cement

4.2 With Model

The intraoral scanning procedure is followed similar to the one described in the previous case, whereas the laboratory procedure differs from the procedure described earlier. When the scan file is sent to the dental laboratory, it is opened in the respective CAD software and a model is designed for the implant prosthesis after decoding the scan bodies. When designing the model, the exact space for the incorporation of a physical lab analog needs to be created during the designing. Each implant company has separate STL files available in their library for the digital lab analog which is an exact replica of the physical form of the lab analog in the digital format. The upper and lower models are articulated as per the bite recorded in the occlusion scan. Some software allows use of virtual articulators for correcting mounting. After the customized abutments are ready, the rest of procedure remains the same as that of crown and bridge procedure, namely, coping, layering, and the final ceramic crowns. This procedure is especially indicated for multiple implants with an unfavorable path of insertion for the prosthesis. We have described a case to elicit this procedure (Figs. 34, 35, 36, 37, 38, 39, 40, 41, 42, 43, 44, 45, 46, 47, 48, 49, and 50).

5 Advantages, Complications, and Technical Challenges

Clinicians and technicians who are accustomed to be working with analog need to undergo learning curve to acquire knowledge of digital process.

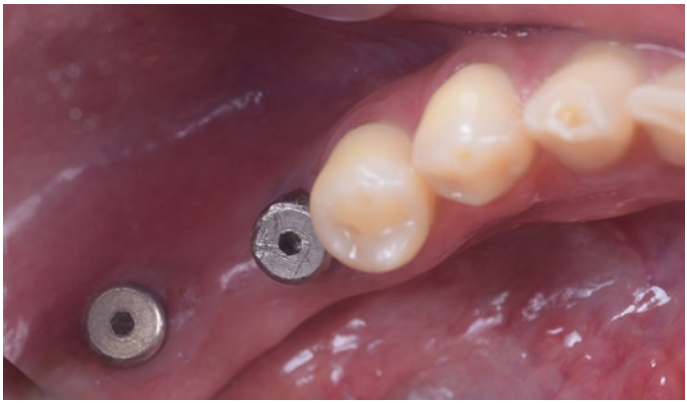

Fig. 34 Mandibular arch 36 and 37 implants placed with unfavorable path of insertion for the prosthesis

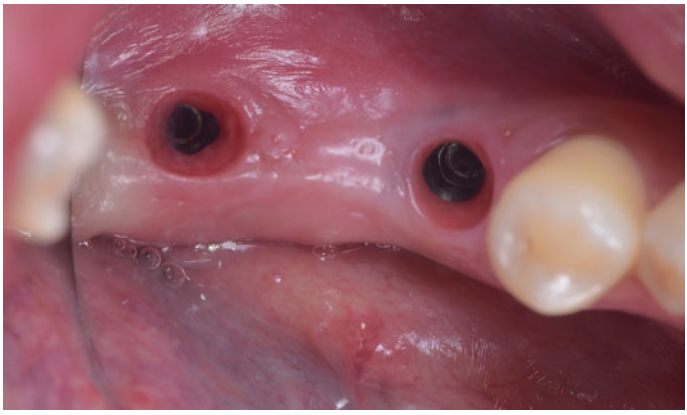

Fig. 35 Healed gingival profile ready to undergo intraoral scanning

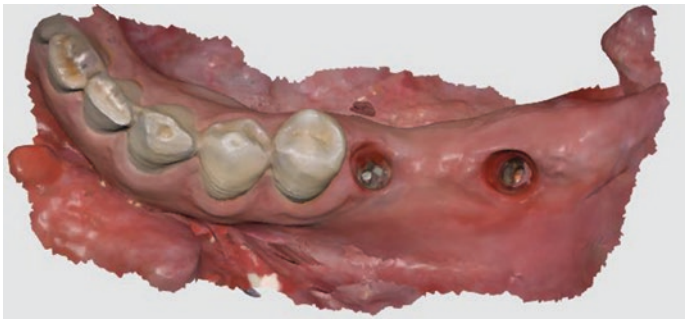

Fig. 36 Gingival profile scanning done along with adjacent teeth as per scanning protocol

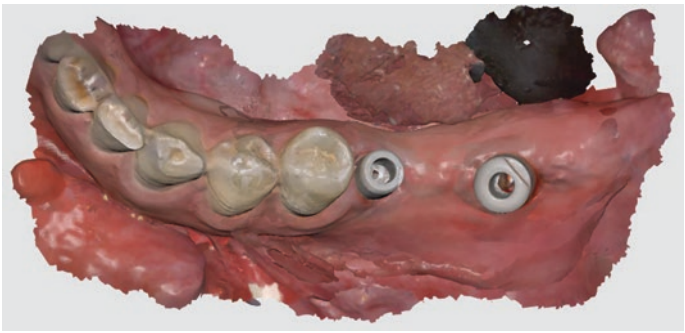

Fig. 37 Intraoral scan body scan; note the unfavorable path. The scan body scanning gives an overall idea about the implant position with respect to the adjacent implant, adjacent teeth, and opposing occlusion

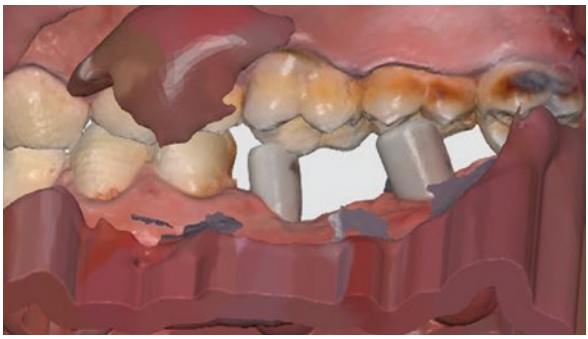

Fig. 38 Scanned bodies in occlusion

Fig. 39 The artificial intelligence in scanner feeds the info to the CAD software and make the task to decoding easy

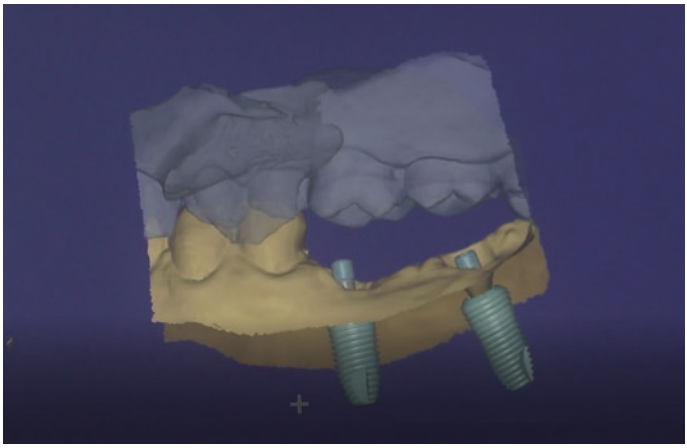

Fig. 40 After decoding the scan bodies' software gives the exact axis of the implant position in patient's mouth. Note the unfavorable angulations. The upper and lower models are articulated as per the bite recorded with occlusion scan. Some software allow the use of virtual articulators for correct mounting

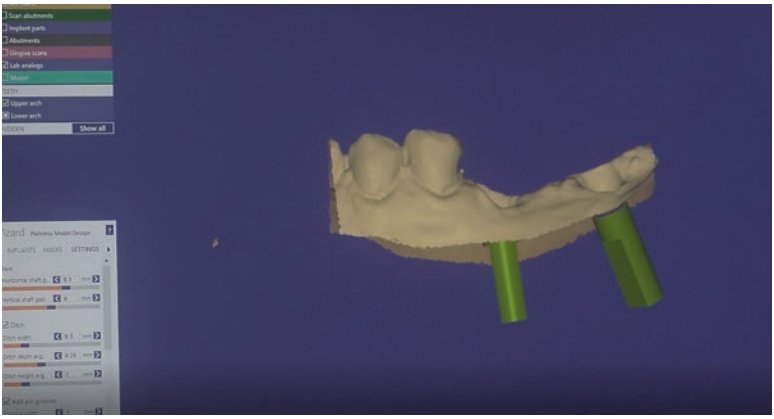

Fig. 41 Selection of the lab analog from the digital library present in the software

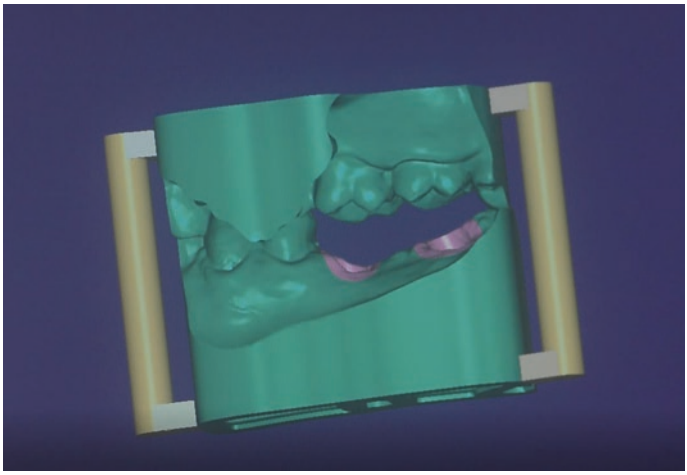

Fig. 42 Model ready to print

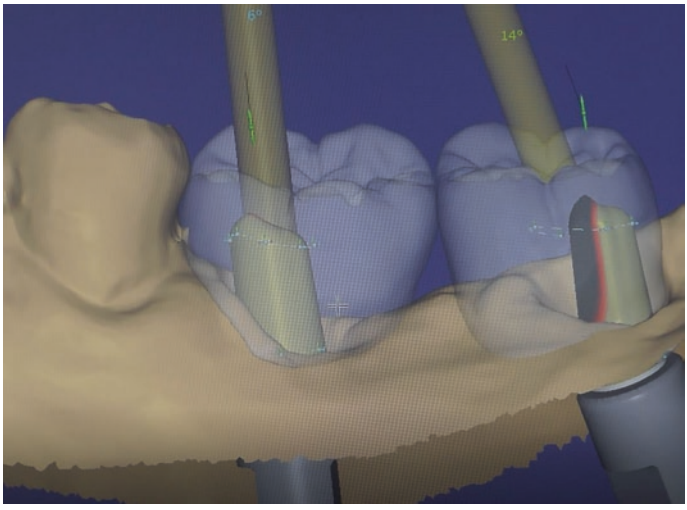

Fig. 43 Custom abutment designed to allow for a parallel path of insertion and a passive fit of the prosthesis

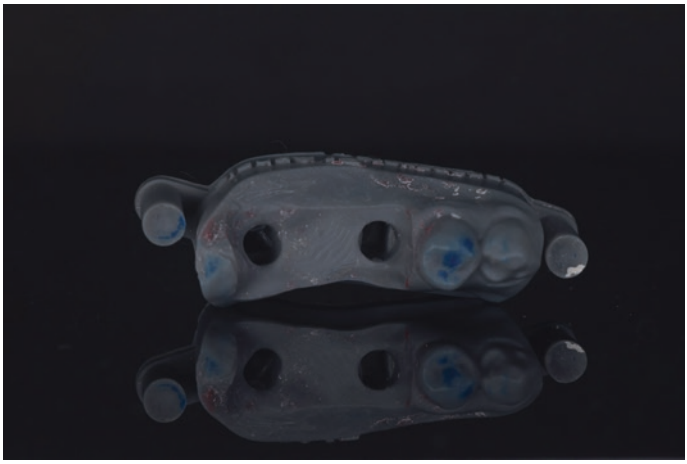

Fig. 44 Resin model with space for placing the lab analog

Fig. 45 Lab analog

Fig. 46 Custom milled abutment

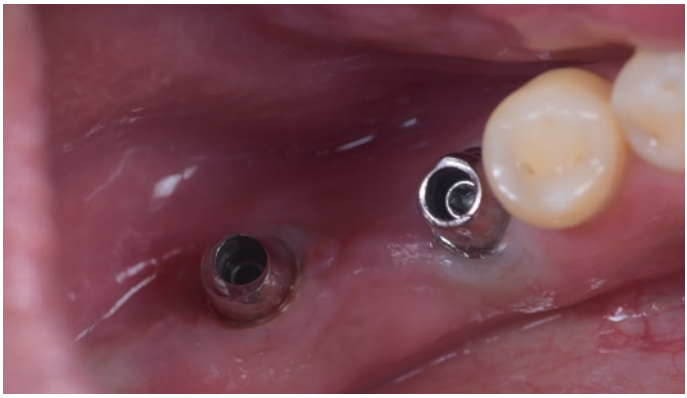

Fig. 47 Custom abutment trial for checking the fit with the implant. Any kind of misfit like hex mismatch, screw–hole mismatch, or connection mismatch warrants discarding the abutment and fabricating a new one

The advantages of digital impression technology in implant prosthodontics [39].

1. Precision over conventional impression technique
2. No change in the implant direction due to use of scan body and AI
3. Perfect capturing of the gingival profile
4. Elimination of the gag reflex
5. 3-D scope to study case and plan the prosthesis

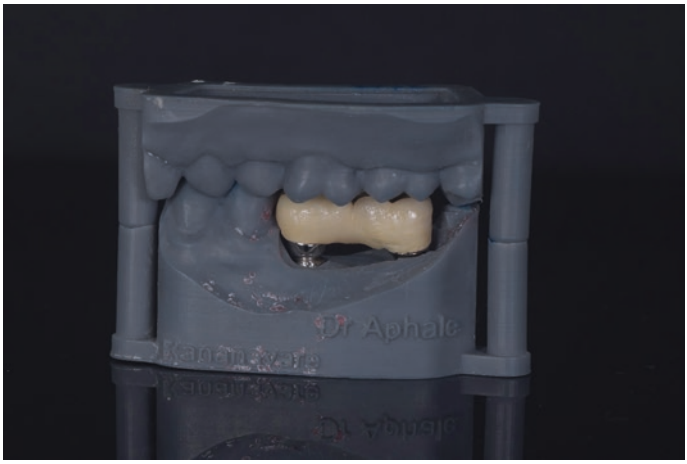

Fig. 48 Fit checked on model in all three dimensions and later sent for bisque trial and final cementation

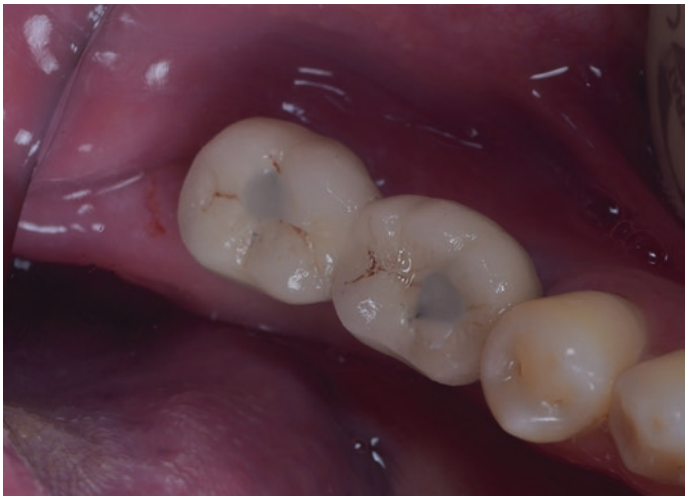

Fig. 49 Screw- and cement-retained prosthesis

6. Facial scan provides the relevant information of patient profile and its relation to dental prosthesis alignment
7. No flaws related with conventional impression making
8. STL model fabrication: less errors as compared to conventional model fabrication
9. Repeats of impression are not costly as compared to conventional

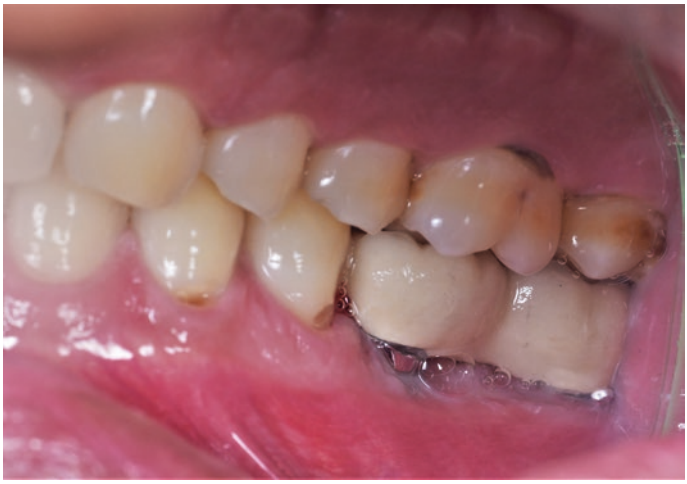

Fig. 50 Prosthesis in occlusion

10. Digital library of designs suggest better path of insertion for prosthesis to be passive

Disadvantage:

1. Initial investment is more as compared to conventional
2. Initial learning curves can be steep for some clinicians who are not so tech savvy
3. Cost of the final prosthesis is little high as compared to conventional

In general, complications can be classified into two categories:

(a) Scanning-related complications
(b) Software integration complications

5.1 Scanning-Related Complications

1. Intraoral scanning can get impeded by the size of the scanning tip itself limiting its proximity with intraoral scan body and acquiring correct information.
2. Deeply placed implants may not expose scan body sufficiently for correct reproduction in digital software. This problem is solved by using artificial intelligence in software by choosing body during scanning.
3. Poorly placed implants adjacent to teeth or adjacent to implant may prevent the use of scan body ad surface scanning as whole.
4. Manually modified scan bodies can never be matched digitally. Never modify any scan body manually.
5. Severely misaligned implants will not allow the use of digital workflow and a conventional impression and analog workflow will be necessary.

6. Careful repositioning of casts within desktop scanner is necessary to avoid errors in recording tissue height around implants which can lead to metal or marginal interface exposure.

5.2 Software Integration Complications

1. Merging complications
2. Not enough scanned data reference points on scan body or adjacent tooth
3. Changes in surfaces such as new restorations or presence of movable tissue being merged
4. If scan body selected by the operator and dental lab technician is not supported by software

6 Conclusion

The wise selection of proper technique and adopting suitable technology will make the dental implant prosthesis more accurate in future. Digital technology is already a part of modern medicine and dentistry in particular. The comfort for the patient, the dimensional accuracy of the reproduction of the oral tissues and prompt availability for processing the next steps of prostheses designing and manufacturing makes the technology extremely promising.

With numerous advantages, digital impressions are on path to become *rigueur de jour* in dental, especially implant, impression techniques.

References

1. Beschnidt SM, Cacaci C, Dedeoglu K, Hildebrand D, Hulla H, Iglhaut G, et al. Implant success and survival rates in daily dental practice: 5-year results of a non-interventional study using CAMLOG SCREW-LINE implants with or without platform-switching abutments. Int J Implant Dent. 2018;4:33. Published online 2 Nov 2018. https://doi.org/10.1186/s40729-018-0145-3.
2. Cabral LM, Guedes CG. Comparative analysis of 4 impression techniques for implants. Implant Dent. 2007;16(2):187–94.
3. Chee W, Jivraj S. Impression techniques for implant dentistry. Br Dent J. 2006;201(7):429–32.
4. Gayathridevi SK, Gowda H, Vaishali K. Suma, impression techniques in implants. J Dent Orofacial Res. 2016;12(02):11–9.
5. Flügge T, van der Meer WJ, Gonzalez BG, Vach K, Wismeijer D, Wang P. The accuracy of different dental impression techniques for implant-supported dental prostheses: a systematic review and meta-analysis. Clin Oral Implants Res. 2018;29(Suppl. 16):374–92.

6. Jahandideh Y, Moghaddam A, Pourkhalili H. Accuracy of implant abutment level impression with and without impression coping. J Contemp Dent Pract. 2018;19:1352–7. https://doi.org/10.5005/jp-journals-10024-2431.
7. Manchikalapudi G. Accuracy of abutment level impressions compared to implant level impressions—a systematic review. J Indian Prosthodont Soc. 2018;18(Suppl. 2):S78.
8. Lee H, So JS, Hochstedler JL, Ercoli C. The accuracy of implant impressions: a systematic review. J Prosthet Dent. 2008;100(4):285–91. https://doi.org/10.1016/S0022-3913(08)60208-5.
9. Papaspyridakos P, Chen CJ, Gallucci GO, Doukoudakis A, Weber HP, Chronopoulos V. Accuracy of implant impressions for partially and completely edentulous patients: a systematic review. Int J Oral Maxillofac Implants. 2014;29(4):836–45. https://doi.org/10.11607/jomi.3625.
10. Burns J, Palmer R, Howe L, Wilson R. Accuracy of open tray implant impressions: an in vitro comparison of stock versus custom trays. J Prosthet Dent. 2003;89(3):250–5. https://doi.org/10.1067/mpr.2003.38.
11. Carrotte P, Johnson A, Winstanley R. The influence of the impression tray on the accuracy of impressions for crown and bridge work—an investigation and review. Br Dent J. 1998;185:580–5. https://doi.org/10.1038/sj.bdj.4809870.
12. Del'acqua M, Avila E, Amaral Â, Pinelli L, Molo F. Comparison of the accuracy of plastic and metal stock trays for implant impressions. Int J Oral Maxillofac Implants. 2012;27:544–50.
13. Tafti AF, Hatami M, Razavi F, Ebadian B. Comparison of the accuracy of open-tray and snap-on impression techniques of implants with different angulations. Dent Res J. 2019;16:413. https://doi.org/10.4103/1735-3327.270785.
14. Izadi A, Heidari B, Roshanaei G, Allahbakhshi H, Fotovat F. Comparative study of dimensional accuracy in three dental implant impression techniques: open tray, closed tray with impression coping, and snap cap. J Contemp Dent Pract. 2008;19:974–81. https://doi.org/10.5005/jp-journals-10024-2368.
15. Vigolo P, Mutinelli S, Fonzi F, Stellini E. An in vitro evaluation of impression techniques for multiple internal- and external-connection implant prostheses. Int J Oral Maxillofac Implants. 2014;29:807–18. https://doi.org/10.11607/jomi.3460.
16. Assif D, Fenton A, Zarb G, Schmitt A. Comparative accuracy of implant impression procedures. Int J Periodontics Restorative Dent. 1992;12:112–21.
17. Al Quran FA, Rashdan BA, Zomar AA, Weiner S. Passive fit and accuracy of three dental implant impression techniques. Quintessence Int. 2012;43:119–25.
18. Lopes-Junior I, de Lima Lucas B, Gomide H, Gomes V. Impression techniques for multiple implants: a photoelastic analysis. Part I: comparison of three direct methods. J Oral Implantol. 2013;39:539–44. https://doi.org/10.1563/AAID-JOI-D-11-00040.
19. Junior I, Lucas B, Gomide H, Gomes V. Impression techniques for multiple implants: a photoelastic analysis. Part II: comparison of four acrylic resins. J Oral Implantol. 2011;39:545–9. https://doi.org/10.1563/AAID-JOI-D-11-00041.
20. Chen LC, Xu ZQ. Innovative 3D dental measurement for tooth model restoration. Key Eng Mater. 2005;295(12):145–50.
21. Hong-Seok P, Chintal S. Development of high speed and high accuracy 3D dental intra oral scanner. Procedia Eng. 2015;100:1174–81.
22. Ali AO. Accuracy of digital impressions achieved from five different digital impression systems. Dentistry. 2015;5:5.
23. Duret F. Toward a new symbolism in the fabrication of prosthetic design. Cah Prothese. 1985;13(50):65–71.
24. Duret F, Pélissier B. Différentes méthodes d'empreinte en CFAO dentaire. Médecine Buccale. Paris: EMC (Elsevier Masson SAS); 2010. p. 1–16.
25. Madhuri P, et al. Digitalization in dentistry: CAD/CAM—a review. Acta Sci Dent Sci. 2018;2(1):12–6.
26. Andersson M, Razzoog ME, Odén A, Hegenbarth EA, Lang BR. PROCERA: a new way to achieve an all-ceramic crown. Quintessence Int. 1998;29(5):285–96, 12 p.

27. Mormann WH. The evolution of CEREC system. J Am Dent Assoc. 2006;137(9 Suppl):7S–13S.
28. Rotar RN, Jivanescu A, Ille C, Podariu AC, Jumanca DE, Matichescu A-M, Balean O, Rusu LC. Trueness and precision of two intraoral scanners: a comparative in vitro study. Scanning. 2019. https://doi.org/10.1155/2019/1289570.
29. Takeuchi Y, Koizumi H, Furuchi M, Sato Y, Ohkubo C, Matsumura H. Use of digital impression systems with intraoral scanners for fabricating restorations and fixed dental prostheses. J Oral Sci. 2018;60(1):1–7.
30. Richert R, Goujat A, Venet L, Viguie G, Viennot S, Robinson P, Farges J-C, Fages M, Ducret M. Intraoral scanner technologies: a review to make a successful impression. J Healthcare Eng. 2017;2017:8427595, 9 p. https://doi.org/10.1155/2017/8427595.
31. Prajapati A, Prajapati A, Mody DR, Choudhary AB. Dentistry goes digital: a cad-cam way—a review article. IOSR J Dent Med Sci. 2014;13:53–9.
32. Sebastian Q, Heike R, Ralph G. Direct mechanical data acquisition of dental impressions for the manufacturing of CAD/CAM restorations. J Dent. 2007;35:903–8.
33. Menditto A, Patriarca M, Magnusson B. Understanding the meaning of accuracy, trueness and precision. Accred Qual Assur. 2007;12(1):45–7.
34. Ender A, Mehl A. Accuracy of complete-arch dental impressions: a new method of measuring trueness and precision. J Prosthet Dent. 2013;109(2):121–8.
35. Roig E, Roig E, Garza LC, Álvarez-Maldonado N, Maia P, Costa S, Roig M, Espona J. In vitro comparison of the accuracy of four intraoral scanners and three conventional impression methods for two neighboring implants. PLoS One. 2020;15:e0228266.
36. Galucci GO, Evans C, Tahmaseb A. ITI Treatment Guide. Digital Workflows in Implant Dentistry 2019;11:282.
37. Landwerlin O, Fages M, Subsol G. A challenge in dental computerised photogrammetry. Dental Tribune International; 2019. p. 30–40. https://hal-lirmm.ccsd.cnrs.fr/lirmm-02365224/document.
38. Mizumoto RM, Ryan M, Yilmaz B, McGlumphy EA, Seidt J, Johnston WM. Accuracy of different digital scanning techniques and scan bodies for complete-arch implant-supported prostheses. J Prosthet Dent. 2020;123(1):96–104.
39. Christensen GJ. Impressions are changing; deciding on conventional, digital or digital plus in-office milling. J Am Dent Assoc. 2009;140(10):1301–4.

3D Printing in Dentistry: Fundamentals, Workflows and Clinical Applications

Les Kalman

Abstract 3D printing, or additive manufacturing, has technologically exploded in the last few years. Improved accuracy, increased efficiency, lower cost, smaller units, and novel materials have significantly changed the fabrication landscape. Currently, additive manufacturing has been utilized industrially for the fabrication of motorcycle chassis by BMW and brake calipers by Bugatti. This exemplifies that the additive manufacturing workflow through a digital platform presents numerous desirable qualities. Moreover, the performance of additive manufactured high-performance vehicle components demonstrates that this fabrication process delivers functionality.

The health sciences have also seen a vast expansion of 3D printing. The development of unique materials and regulatory approvals has resulted in several patient-specific 3D printed structures restoring form and function.

Dentistry is currently experiencing a trend toward 3D printing. Implant dentistry was one of the first disciplines to experience 3D printed guides for predictable surgeries. A revolution in materials and technologies has resulted in further evolution, including the printing of prosthodontic frameworks, dentures, and implant components.

This chapter will explore the exciting advancement of 3D printing and its applications to industry and medicine, with an in-depth presentation of its application to dentistry. A glimpse into the past, a review of what is current, and a look into the future of 3D printing, will be presented.

The objectives of this chapter are for the reader to appreciate the fundamentals of 3D printing, understand the workflow and current materials, and identify clinical applications of 3D printing.

Keywords 3D printing · Additive manufacturing · Fabrication · Medical devices · Regulatory · Dental implants · Prosthodontics · Dental materials

L. Kalman (✉)
Department of Restorative Dentistry, Schulich School of Medicine and Dentistry, Western University, London, ON, Canada
e-mail: ljkalman@icloud.com

R. S. Chaughule, R. Dashaputra (eds.), *Advances in Dental Implantology using Nanomaterials and Allied Technology Applications*,
https://doi.org/10.1007/978-3-030-52207-0_13

1 Introduction

As a photographer, there's nothing more satisfying than enlarging one of your images as a print or canvas as a true representation of the image you have captured (Fig. 1). Having a print of an image that you have painstakingly composed, created, edited, processed, and printed is truly gratifying. Having your creativity, as something you can hold, display on a wall, or auction off to charity, brings that gratification to the next level. But the process is challenging, as a poor initial image will result in an even poorer enlargement, and that is disappointing. To be able to enlarge an image requires a proper camera body, with an appropriate sensor and related megapixels, and a superb lens. Assuming that ideal exposure criteria resulted in an ideal image (Fig. 1, UL), the next steps are arduous and critical. Images are transferred/exported from the camera into an appropriate image software program, for editing or post-processing (Fig. 1, UR). Once the image has been modified and perfected, it must be reviewed in great detail, to ensure clarity, sharpness, and balance (Fig. 1, LL). The print medium must be decided upon, such as canvas or photo paper, along with the desired enlargement size. The medium will have an impact on the final result and may be limited by technology. The product is then printed. The type of printer is essential to create or fabricate a product that is acceptable. A poor printer will result in a poor output. Once printed, the product is further processed, in the case of a cavass print it is stretched, mounted, and delivered (Fig. 1, LR).

Fig. 1 The workflow of a photograph to produce a tangible product. UL: Image acquisition with ideal settings to capture the moment. UR: Post-processing software modification of image. LL: Final image maximized for production. LR: Image printed on canvas medium, signed by the late MotoGP racer Nicky Hayden. The cavass was auctioned off to raise funds for Riders for Health

Inadequacies in any of the aforementioned steps will result in a poor and useless final product. This printing process is a cascade of events that are dependent upon each other for the production of an ideal result. It is interesting that a collection of millions of pixels arranged properly in two dimensions to produce a picture can have such an impact or leave an impression. The process of image acquisition, workflow and fabrication, is analogous to the 3D printing process.

2 Fundamentals

The scope of 3D printing is immense. The materials, processes, products, and applications are changing daily. This very brief overview is only meant to offer relevant background for those interested or involved in 3D printing in dentistry. The reader is encouraged to further their knowledge with recent journal publications, social media platforms, newsletters, exhibits, and conferences.

2.1 What Is 3D Printing?

3D printing refers to the production or fabrication of a three-dimensional object from a three-dimensional file (Fig. 2). 3D printing is a generic term, referring to a collection of different processes and different variables. The commonality is the use of a virtual Computer Aided Design (CAD) (Fig. 2, L) file to fabricate a tangible object [1] (Fig. 2, R).

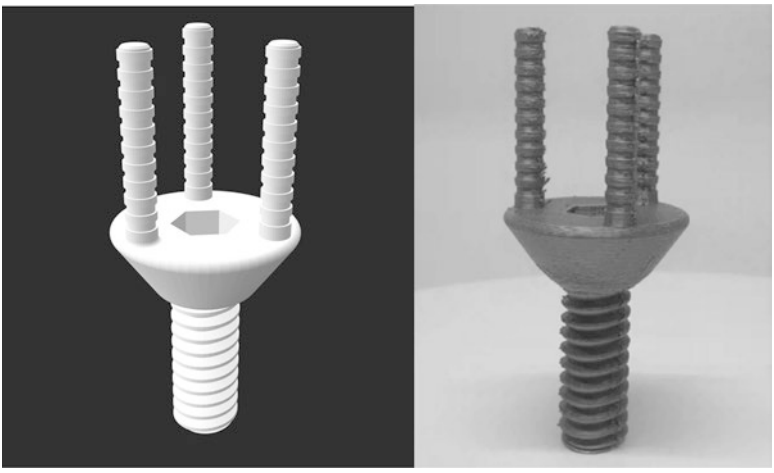

Fig. 2 CAD file (L) translated into an object (R) through 3D printing in plastic

3D printing tends to be synonymous with additive manufacturing, defining the fabrication process. With additive manufacturing, a product is created or built by adding material sequentially to create a specific object. This workflow requires material added in a very specific order to create the desired end result. Examples to illustrate this process include make-up application, Lego assembly and welding. This is the opposite of subtractive manufacturing, which by definition indicates the removal of material from a larger volume to fabricate the end product. Examples of this fabrication process include wood carving, milling, and die threading. Some fabrication workflows employ a combination of additive and subtractive manufacturing, called hybrid manufacturing.

3D printing has also been referred to as rapid prototyping, desktop manufacturing and on-demand printing. These terms give reference for the ability to fabricate a product fast, in-office and at any time, respectively. 3D printing may be commonly defined by the process of fabrication or the technology [2], which is based on the variability of materials and the production pathways. Some examples include [2]:

- FDM: Fused Deposit Modelling
- SLA: Stereolithography
- DLP: Digital Light Projector
- SLS: Selective Laser Sintering
- DMLS: Direct Metal Laser Sintering
- ALM: Additive layer Manufacturing
- SLM: Select Laser Melting
- EBM: Electron Beam Melting
- DOD: Drop on Demand
- Material Jetting
- Binder Jetting

Explaining all the technologies is beyond the scope of this chapter. The technologies relevant to dentistry will be explored. Aside from the various technologies, there are numerous materials available for 3D printing, including plastics, metals, and ceramics (see Sect. 3.2).

2.2 Brief History

Although 3D printing may seem like a new technology, it isn't. In 1981, Dr. Kodama applied to patent a rapid prototyping device, which was unsuccessful due to funding issues. Another unsuccessful patent was filed for rapid prototyping in 1984 by a French team. In the same year, Charles Hull applied to patent stereolithography, issued in 1986, and started his own company [3].

2.3 Why Use 3D Printing?

To understand why 3D printing should be used, it should be contrasted with other methods of production and fabrication. For instance, the conventional fabrication of a single prototype, device, component, or part can be very challenging. It may be fabricated by welding materials together or curing layers of plastic to create a desired form. Once fabricated, these forms require further shaping, sanding, polishing, and finishing. This is time consuming, expensive, frustrating, and the end result may not be satisfactory. Similarly, the mass production of a product through automation requires significant costs, time, and experience within an industrial setting. The production must be closely monitored to ensure accuracy and precision of parts. With the introduction of desktop 3D printers and a digital workflow, prototype fabrication can be greatly simplified. A prototype may be created and refined virtually, and then fabricated by 3D printing with many material options, design changes, and customization at a relatively inexpensive cost and through a relatively simple workflow. 3D manufacturing facilities can deliver mass production through an alternate workflow with high accuracy, precision, and efficiency, with easily adjusted modifications for customization at a reduced cost. Analogous to digital design in 3D printing, editing a document in a software program (Word) is so much more inviting than traditional typing.

3D printing should be utilized by individuals that are interested in [4]:

- Efficiency
- Convenience
- Cost-effectiveness
- Customization, for either mechanical parts or for patients
- Desirable physical properties
- Fabrication of complex geometries that may not be possible by other means
- A LEANer approach to manufacturing
- Less environmental impact

3D printing does have its disadvantages, which include limited information of mechanical properties and the required post-processing techniques to improve the surface finish.

2.4 Need to Know Information

The most common file for 3D printing is the STL [5]. It is an abbreviation for stereolithography [5]. The file only stores information on surface geometry. It is one of about 30 file formats associated with 3D printing. The STL file works with a “slicer” to transfer and translate the information to be printed (Fig. 3). 3D printer specifications are very critical and relevant to success. Resolution, or print quality, is critical in dentistry. Poor resolution, measured in microns, would result in inadequate prints (Fig. 4).

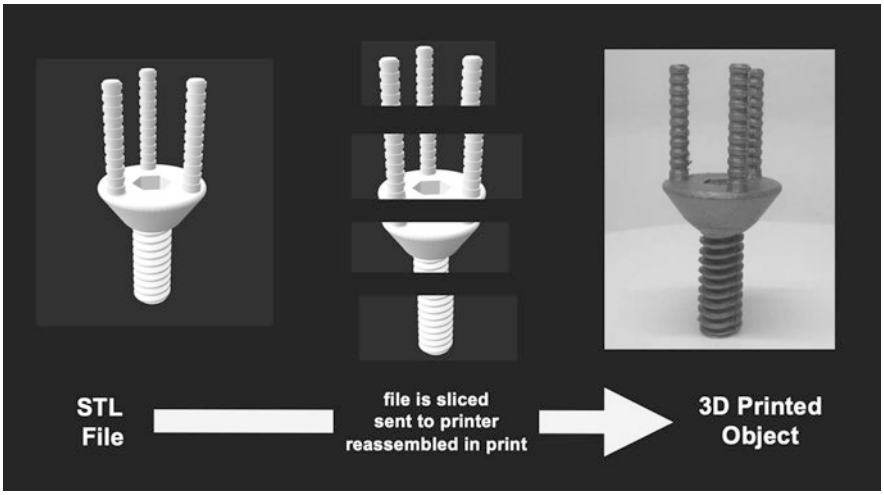

Fig. 3 Graphic representation of workflow from file to 3D print

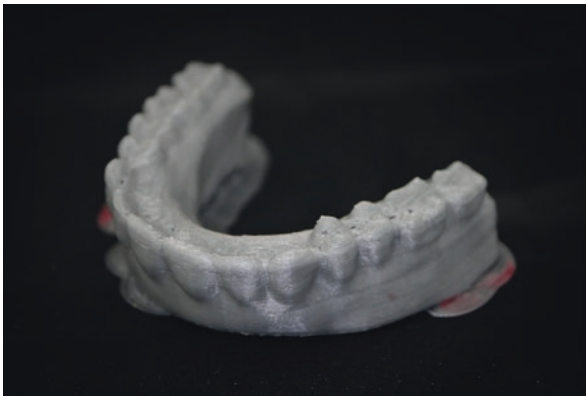

Fig. 4 Poor quality 3D printed maxillary arch due to low print resolution

3D printed structures require supports to hold the final printed product (Fig. 5). The supports need to be removed after a product is printed. The practice of removing supports and refining the fabricated product is called post-processing.

3 3D Printing in Dentistry

It has been stated that mother is the necessity of invention. From the author's perspective, 3D printing has had its initial introduction to dentistry through implantology. The prosthodontically driven surgical placement of dental implants requires the accurate placement of an endosseous implant [6]. If the surgical result is accurate (Fig. 6), then the restorative outcome will be compromised or worse, it will fail. It

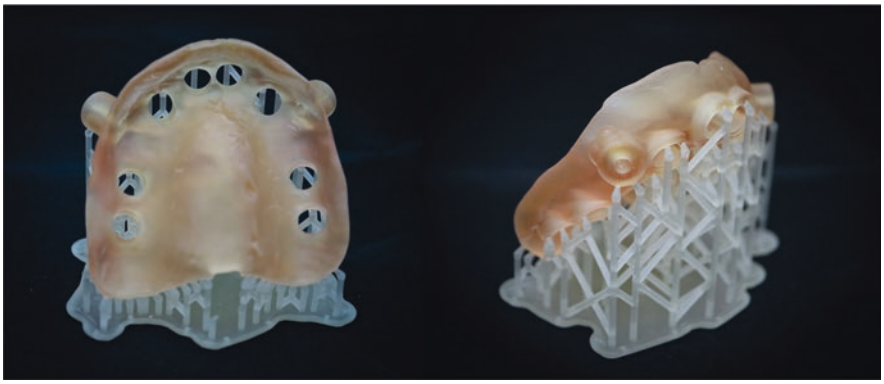

Fig. 5 3D printed surgical guide with supports

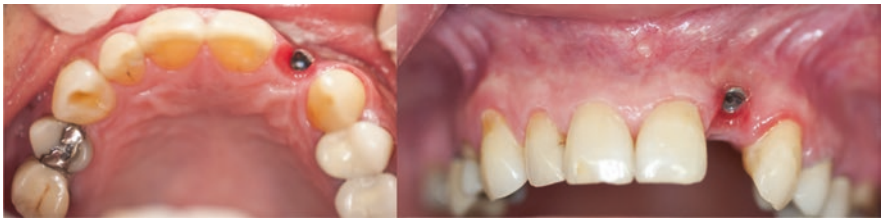

Fig. 6 Inaccurate placement of dental implants compromising the restorative outcome

seems that the fabrication of surgical guides for implantology introduced dentistry to 3D printing. Applications and workflows then advanced and expanded to include many other disciplines within dentistry.

3.1 Workflows

Dental records are an ethical and legal requirement of patient treatment [7]. Records are required to assist with diagnoses, facilitate treatment planning, aid patient presentation, and communicate with the laboratory [7]. The spectrum of records includes photographs, radiographs, CBCT, traditional impressions and models and virtual impressions and models. 3D printing is a form of dental records.

The starting point for 3D printing in dentistry is the generation of a digital file [8], which may be that of a patient's tooth, dentition, arch, impression, cast, or prosthesis. The digital or virtual patient image may be acquired from a computed tomography (CT), cone beam computed tomography (CBCT), or intra-oral hard or soft tissue scanning [8]. Files may be merged for increased information and improved planning. For instance, the CBCT may be merged with an intra-oral scan to provide information about osseous structures, and teeth and soft tissues, respectively. The

digital file of a patient's prosthesis can be generated by a variety of desktop scanners with the appropriate resolution.

Digital files may need to be digitally tweaked (Fig. 7) to ensure that they are suitable for 3D printing [9]. For instance, the digital file of a patient's maxilla may seem appropriate, but once the file is assessed in different planes, it is clear that only the outer surface has been digitized (Fig. 8). The digital file must be imported into a third-party software program to digitally "'box the impression" (Fig. 9). The digital file will then be of suitable form and volume for 3D printing [9]. Some digital impression programs many have this featured within their software not necessitating third-party software. If the digital file requires printing, as for a diagnostic model of a patient's dentition, then the file may be printed. If treatment planning is required, then the digital file must be imported into a dental planning software application. There are some dental software applications that enable digital impressions and planning into one. Digital planning in dentistry is beyond the scope of this chapter, but the understanding that several steps are required for the planning, and subsequent 3D printing, is important.

3.1.1 In-Office Printing

With advances in technology and a reduction in 3D printer size, in-office 3D printing has become attractive to many clinicians. The in-office workflow requires a printer, software, and printing material. Other requirements include physical space in the clinic, adequate time for the process, revenue to offset the time and costs and fortitude of the individual, as the learning curve for 3D printing may be steep for some.

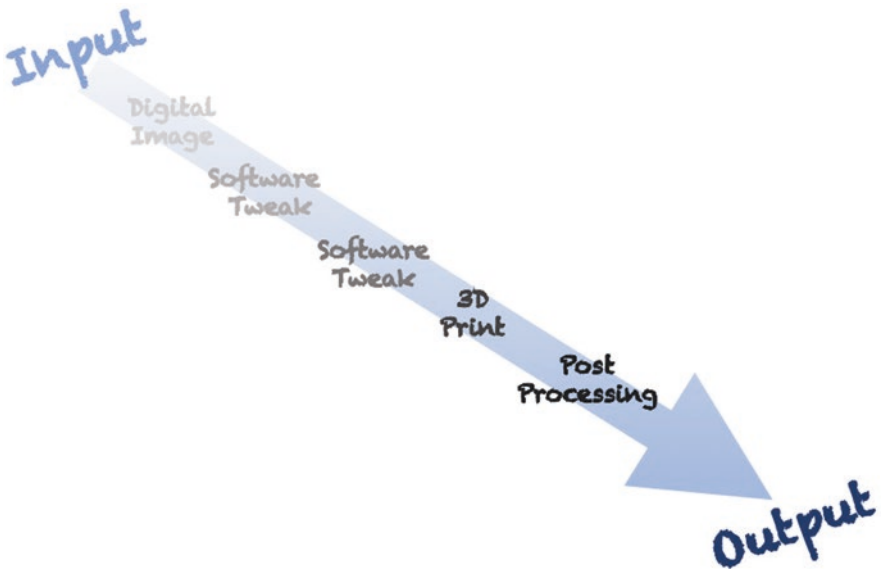

Fig. 7 Diagrammatic representation of the digital workflow associated with 3D printing

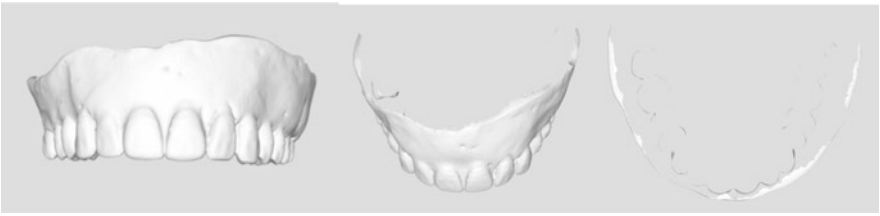

Fig. 8 Digital file (scan) of a hypothetical patient. Rotating the file indicates the lack of information required for an adequate 3D print

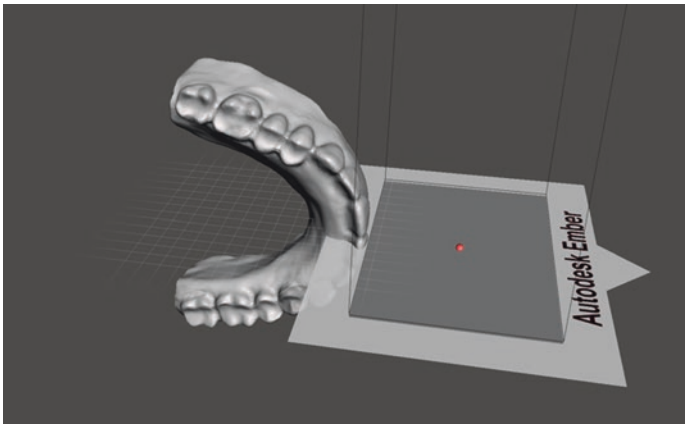

Fig. 9 Digital file imported and "boxed" in a third-party software program

Rather than reviewing specific printers, as 3D printing technology is expanding and improving rapidly, the intent of this section is to provide important technical features so that the clinician or technician may be able to formulate an informed decision based on their requirements and preferences.

Three common technologies in 3D printing in dentistry are stereolithography (SLA), digital light processing (DLP), and material jetting [10]. Each technology can deliver the required accuracy and precision for dental applications. Quality may vary from different systems.

SLA utilizes a vat of liquid resin that is selectively exposed to a laser beam across an area that is to be printed [10]. This technology offers high accuracy and a smooth surface finish with a wide variety of materials and large build volumes for dentistry. It is considered the most affordable approach for applicable dentistry printing but tends to be limited for smaller 3D printing projects.

DLP utilizes a similar chemical process but a projector, instead of a laser, is employed. This technology offers a simple workflow, high speed, and a wide range of materials but lacks the smooth surface finish and accuracy. This technology is more costly than SLA but offers a greater printing volume [10].

Material jetting delivers drops of liquid resin onto a build tray with an instant cure. Although this technology was common many years ago, it has started making a comeback, due to the (now) lower cost, high speed, and customization [11], especially multicolored layers. It will be interesting to see how far this technology will advance.

Several variables should be considered before deciding on a particular 3D printer [12], which includes:

- Convenience: ease of use (will training be provided and if so how ?)
- Reliability: how many hours can it run before issues develop and how will these be managed?
- Cost: both the capital investment of the printer, materials and running costs (servicing, upgrade) and the cost per 3D printed component
- Return on investment: the clinician should consider how the technology would benefit the practice and patients

Before selecting a printer, exercise proper due diligence. Attend trade shows, ask questions, schedule a demonstration, order sample parts, and communicate with colleagues regarding their experiences. The time commitment to the 3D printing workflow can be significant and the clinician should be well prepared for the investment.

3.1.2 Outsourcing

If in-office 3D printing does not seem appealing, then there is the alternative workflow of outsourcing. There are numerous lab-based workflows that will scan, design, print, and post-process your 3D printing requirements. Many have user-friendly online platforms for the simple and convenient transfer (uploading) of digital files with the appropriate selection of materials and applications. A team member will review the digital files and requisition and advise on the suitability. The 3D printed product is then fabricated and couriered to the individual. There are a range of products available, including diagnostic models, working models, appliances, guides, dentures, and provisionals.

Many 3D printing service providers may also assist with many other aspects of 3D printing related digital workflows. For example, CBCT scans may be evaluated and read; virtual treatment planning may be completed, followed by the 3D printing of appropriate guides. Dental labs may also be providing these types of workflows. The reader is encouraged to reach out to their laboratory and enquire on the services provided.

There are several other service providers available. Many non-dental generic 3D printing providers have online platforms for the 3D printing and delivery of digital files. The user may select the material and dimensions. The platform software processes the necessary conversion. These are ideal providers for patient education models and products.

There exist several service providers that specialize in materials. For instance, 3D printing in metal can be achieved by select service providers that utilize industrial grade metal 3D printers with an extremely specific technical workflow. Many possess a simple platform for product submission and the technicians will translate what your requirements may be and provide a completed finalized product.

It has been the experience of the author to utilize off-site service providers for patient and research-based 3D printing needs. The service providers possess specialized knowledge and experience to provide the appropriate 3D printed products.

3.2 Materials

Materials that can be 3D printed are being developed at an extremely rapid rate. A general classification of the most commonly used materials for 3D printing in dentistry [13] is presented below.

- Plastics
  - Acrylonitrile Butadiene Styrene (ABS)
  - Polylactic Acid (PLA)
  - Nylon
- Metals
  - Titanium alloy
  - Stainless steel
  - Chromium Cobalt
- Ceramics
- Carbon Fiber
- Biomaterials
  - Gelatin
  - Cellulose

Explaining the composition, properties, and applications are beyond the scope of this chapter. The author recommends that the reader follow a protocol for material section that includes:

- Understanding the application of the material (study model versus surgical stent)
- Ensuring that the material and application has been approved by the appropriate regulatory body
- Appreciating the properties of the material (available from suppliers and labs)
- Confirming that the material is compatible with the 3D printer (if in-office use)
- Selecting the proper material for 3D printing

3.3 Applications

Patient applications that utilize 3D printing for dentistry vary tremendously geographically, as related to regulatory approval. This section will be based on a general consensus of clinically acceptable, regulatory approved, clinical applications of 3D printing.

3.3.1 Models

Diagnostic models are an important component of patient records and may be required for pretreatment, diagnoses, treatment planning, and communication [14]. 3D printed diagnostic models (Fig. 10) would be the end result of a patient's digital impression, once the appropriate digital tweaking has occurred, to ensure that the file suitable for 3D printing. Proper printer resolution is required for practicality.

Working models are the records required for the delivery of specific patient treatment. 3D printed working models could be utilized for a multitude of treatments, including indirect restorative procedures (Fig. 11) (inlays, onlays, crowns) and prosthodontics (bridges, implant dentistry).

3.3.2 Removable Appliances

Removable appliance has seen a tremendous increase in the application of 3D printing, especially clear aligners [15]. Advances in software and the predictability of 3D printing, namely cost and convenience, have resulted in a surge in 3D printed clear aligners [15]. Occlusal splints (Fig. 12) have also gained 3D printing popularity, due to the workflow and the regulatory approval of materials. Mouth guards may also follow the same trend.

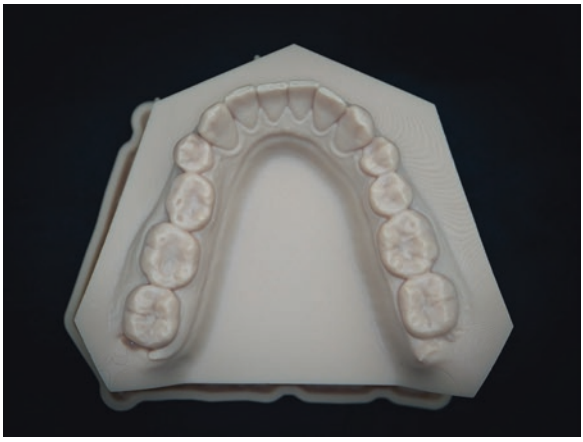

Fig. 10 3D printed diagnostic models

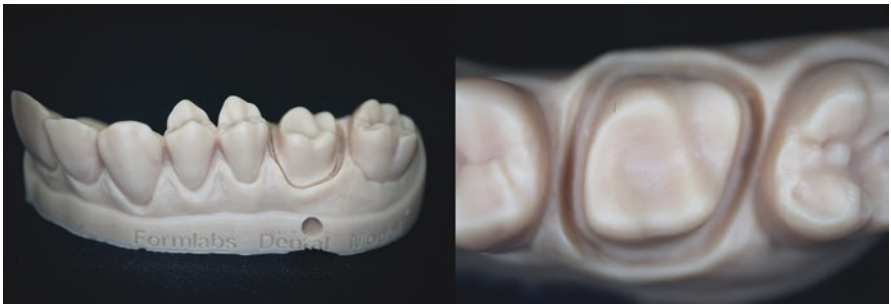

Fig. 11 3D printed working models: (L) segment and (R) tooth preparation

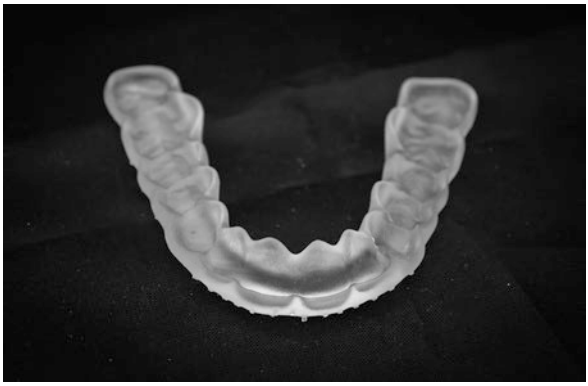

Fig. 12 3D printed maxillary occlusal appliance

3.3.3 Guides

There has been a significant surge in guided surgery in implant dentistry, due to advances in imaging and 3D planning software [16]. The guide assists the surgeon with the location of drilling, as is the case with endodontic guides (for endodontic access), bone reduction guides (for the predictable removal of bone pre-surgically), and implant guides (for the position of the osteotomy). The implant guide (Fig. 13) may also determine the position of implant placement [16]. Once patient imaging and treatment planning has occurred, 3D printing of the guide may be completed in a suitable material for the implant surgery (Fig. 14).

3.3.4 Dentures

The workflow for 3D printed dentures offers an accurate and efficient alternative pathway. It is the opinion of the author that 3D printing will have a significant impact on this prosthodontic workflow. Appropriately, a detailed case presented has been presented to outline the workflow.

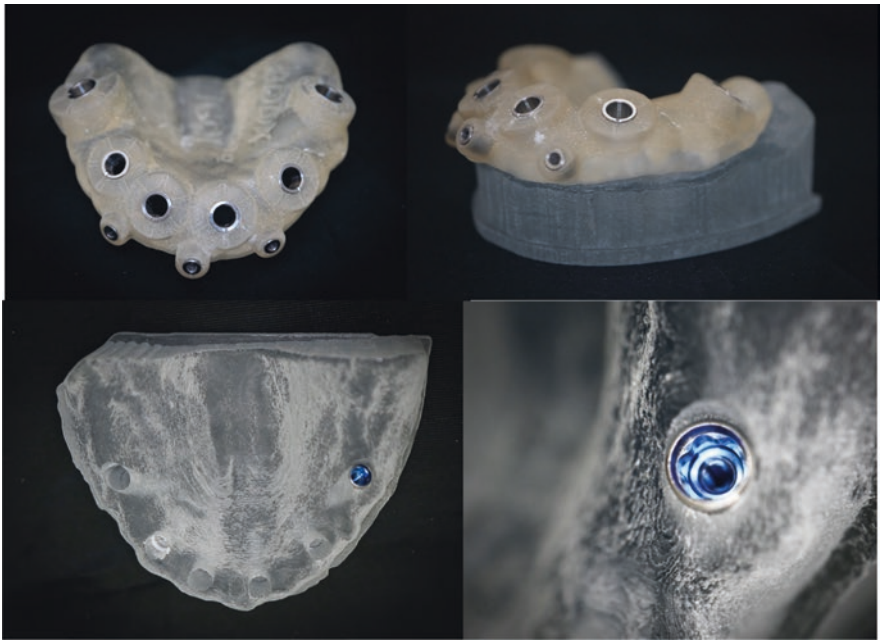

Fig. 13 3D printed implant surgical stent (UL) with printed edentulous maxilla (UR). Model with simulated osteotomies (LL) and simulated implant placement (LR)

Removable complete dentures are an important form of patient rehabilitation that increases the patient's oral health quality of life [17]. Complete dentures are typically rendered through several (5–6) clinical and laboratory appointments [18]. The clinical appointments can prove frustrating and time-consuming for both the clinician and patient. The laboratory component relies on flasking and processing, which may create problems through material distortion and possible technical errors. Dentca provides a novel hybrid workflow, utilizing modified patients records and 3D printed dentures [19]. This approach has been illustrated in the following clinical case.

3.3.4.1 Case Study

A 45-year-old male with a non-contributory medical history presented at an outreach clinic session (Fig. 15, L). His chief complaint(s) included pain and difficulty in chewing. A complete dental examination was completed with the appropriate radiographs (Fig. 15, R). Diagnoses included multiple caries and generalized severe periodontal disease. The patient also had poor oral hygiene with generalized heavy plaque and calculus. Treatment options were presented to the patient with an appropriate informed consent. The patient decided upon extraction of the remaining dentition with rehabilitation with complete dentures. 3D printed dentures were decided as the modality, to evaluate the process and expedite the delivery.

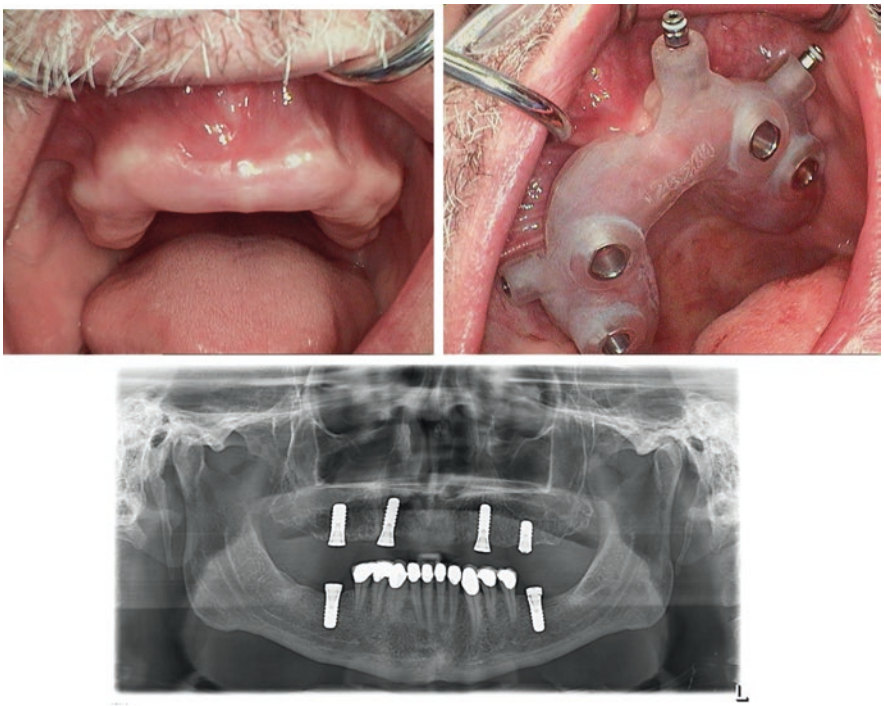

Fig. 14 3D printed surgical stent for the placement of 4 dental implants in an edentulous maxilla. (Photos courtesy of Dr. Mahn)

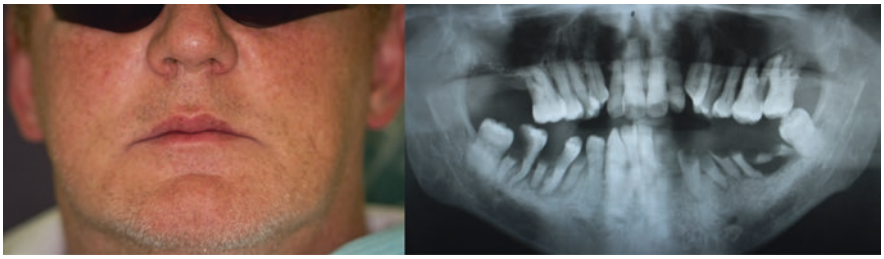

Fig. 15 Pretreatment photo (L) and panoramic radiograph (R)

3.3.4.2 Clinical Procedures

Oral Surgery

The maxillary and mandibular teeth were extracted, with an appropriate pre-prosthetic alveoplasty. Six months were provided to allow for resorption and healing. An examination was performed to confirm healing and denture suitability (Fig. 16).

Prosthodontics

After registering online with Dentca for the CAD/CAM dentures, the required clinical products were delivered. These products were proprietary and required for the clinical procedures.

Appointment 1

Selection of suitable tray size was initially determined. Medium size rays were selected for both arches (Fig. 17). Impressions were completed by first using Aquasil Ultra polyvinyl siloxane (PVS) heavy body (Dentsply). While the material sets, border moulding was performed through muscle activation. Once set, the impression was completely dried. A light body PVS material (Kerr) was then applied to the impression as a thin wash layer. The impression was reinserted to capture fine detail. Once set, the impression was assessed for quality.

Modification of the impression was required for the second step. The impression was sectioned with an #12 scalpel at the defined location. The tray was separated into two pieces (Fig. 18), and the anterior portion was utilized as an intra-oral device to establish vertical dimension and centric relation.

Once modified, a supplied pin was inserted into the tray portion. Both tray portions were then reinserted into the oral cavity. Vertical dimension was then assessed. Clinically, this was slightly difficult. The pin was completely down, yet the vertical dimension seemed excessive. The pin was modified with a hand piece bur and reinserted. An adequate vertical dimension was then determined.

Centric relation (CR) was then assessed. The tray portions and pin were reinserted intra-orally. The patient was guided into CR, and this was repeated. A hand piece bur was used to create a dimple on the upper tray portion, to register the pin position at CR. The depression provided a physical lock of the maxillo-mandibular relationship of CR. Quick Bite (Clinician's Choice) was also utilized to register the position of the tray portions intra-orally (Fig. 19). All materials were removed and disinfected appropriately.

Incisal length determination was performed utilizing a unique method. A lip ruler was supplied to measure from the incisive papillae to the upper lip line. The patient's measurement was 7 mm in length. Tooth selection was completed by

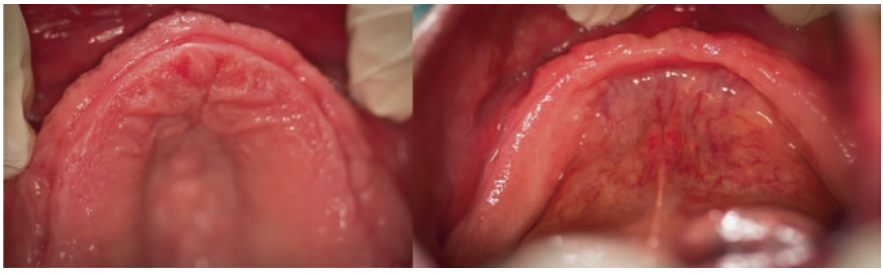

Fig. 16 Post-surgical healing of maxillary and mandibular ridges

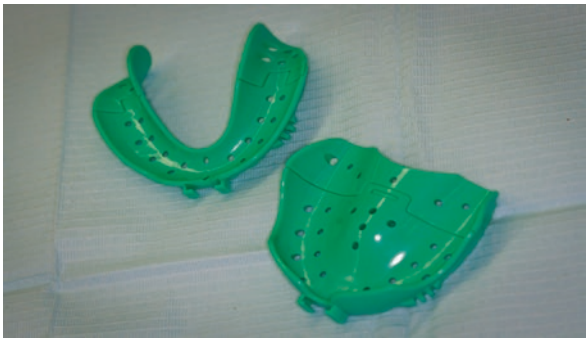

Fig. 17 Dentca impression trays

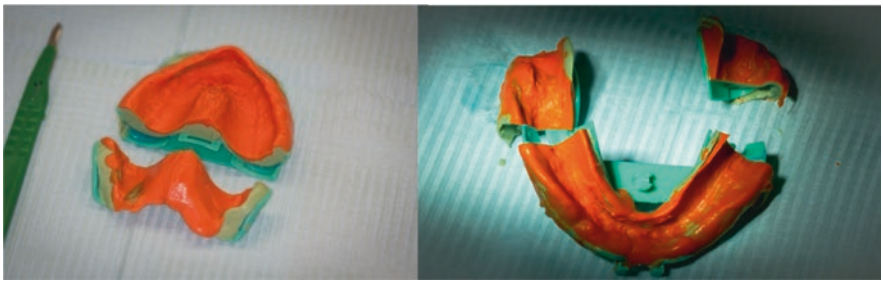

Fig. 18 Final maxillary and mandibular impressions sectioned

assessing the intercanine distance. Tooth shade was then determined as the final clinical requirement. Clinical information was then inputted online for processing.

Appointment 2: Try-In

For the try-in appointment, Dentca provides white 3D printed dentures (Fig. 20). The try-in requires the confirmation of all previous clinical data. Any change needed may be executed on the try-in dentures.

During the try-in appointment, clinical evaluation seemed outstanding, except for a slight anterior open bite with a mildly excessive vertical dimension. The posterior teeth of the try-in dentures were reduced to eliminate the open bite. The vertical dimension was re-assessed. Fit, retention, esthetics, and phonetics were assessed. The patient was satisfied with the try-in. After adjustments were completed, Quick Bite was used to register the new relationship (Fig. 21). The try-in dentures were couriered to the lab for final fabrication.

Appointment 3: Delivery

3D printed dentures were fabricated by (1) printing the bases (Fig. 22) and the denture teeth (Fig. 23) separately. The teeth were bonded to the bases (Fig. 24) and the dentures were post-processed for delivery (Figs. 25 and 26).

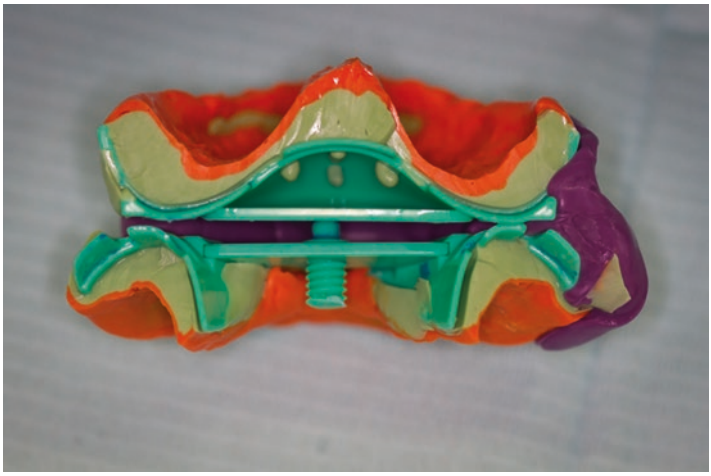

Fig. 19 Complete denture records with bite registration

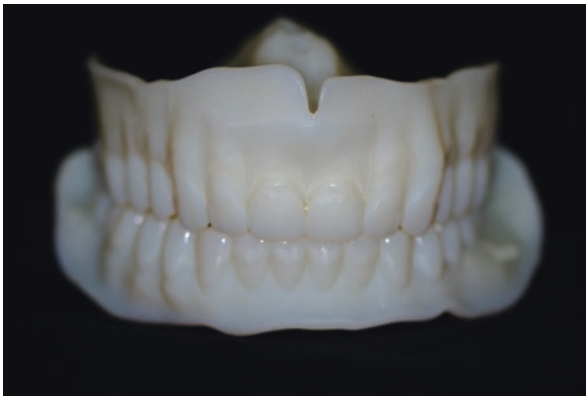

Fig. 20 3D printed denture try-in (analogous to compete try-in)

Complete 3D printed dentures were delivered for final try-in and delivery. Appearance and finish were of very high quality (Figs. 25 and 26). During denture delivery, assessment of fit, extension, retention, occlusion, function, esthetics, and phonetics were performed. Very minor occlusal adjustments were required. The patient was very satisfied with the result. Post-delivery instructions were given to the patient and post-delivery appointments were booked. Post-delivery appointments were unremarkable.

Discussion

The Dentca hybrid 3D printed denture approach seems to provide an efficient and accurate method for clinical procedures and denture fabrication of complete dentures. Although the method requires the clinician to work with a new procedural

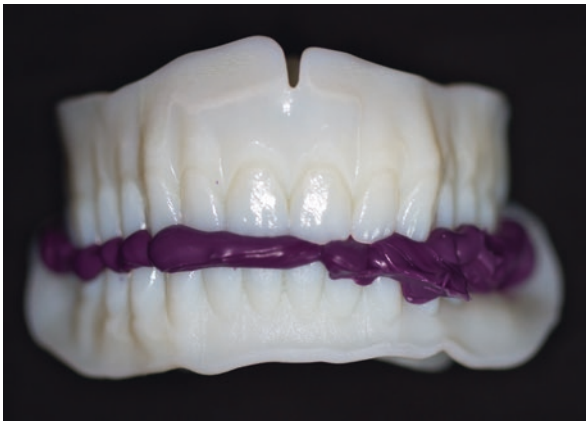

Fig. 21 Try-in dentures adjusted and a new bite registration

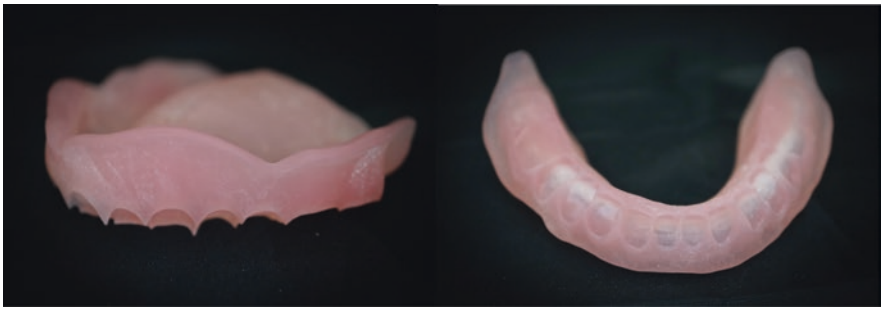

Fig. 22 3D printed completed denture bases

approach, the fundamentals and principles of removable prosthodontics remain the same. The dentures appeared to be of high quality. The fit, retention, function, occlusion, esthetics, and phonetics were clinically acceptable. The patient seemed to exhibit complete satisfaction with the delivered prosthesis, in both form and function.

Conclusions

Dentca's 3D printed dentures offer the clinician a hybrid alternative to the conventional method for complete denture delivery. The clinician must commit to learning new techniques with new equipment. However, the clinical outcome may be very rewarding.

In dentistry, the delivery of efficient yet uncompromised quality of care is crucial for both the patient and clinician. Dentca's 3D printed dentures offer a viable option for the efficient and accurate delivery of complete dentures. The timely rehabilitation of edentulous patients has particular value, both for the clinician and patient.

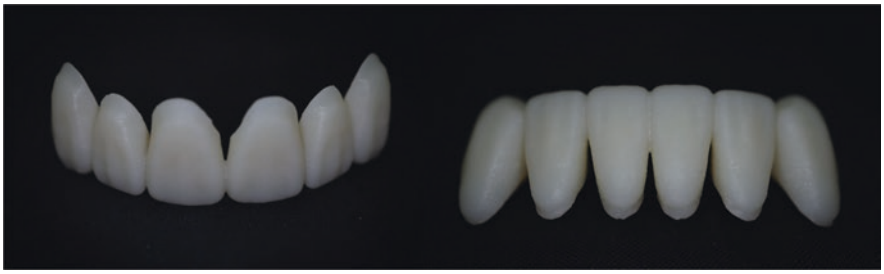

Fig. 23 3D printed denture teeth

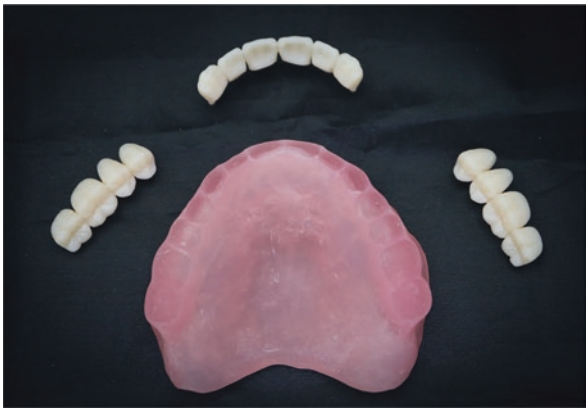

Fig. 24 Maxillary denture base with denture teeth

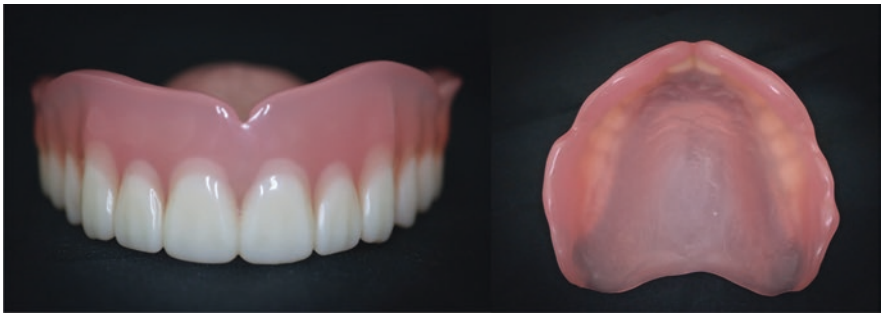

Fig. 25 3D printed post-processed maxillary complete denture

3D printed dentures may also be fabricated from several different workflows. Currently, a standard impression is required to compress the tissues. Digitally scanning of the impression or cast typically follows. There are various software platforms to digitally design the entire denture, including individual tooth position. 3D printing may follow several paths, from individual teeth, to arches. A standard accepted protocol has yet to be established.

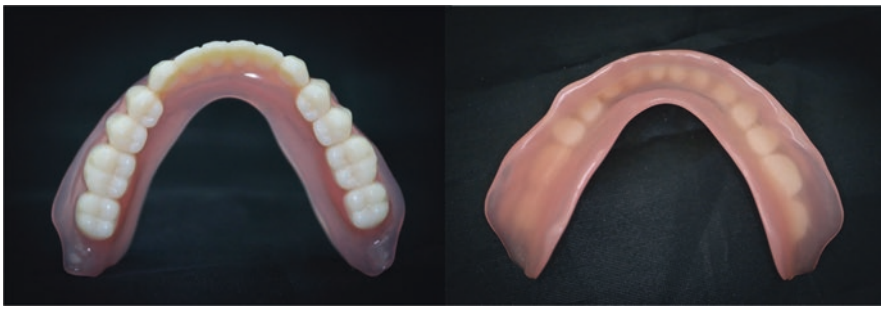

Fig. 26 3D printed post-processed mandibular complete denture

3.3.5 Provisionals

Based on a digital workflow, the 3D printing of provisionals seems to be an increasingly population procedure. Chairside luting of the provisionals with a variety of materials may provide an efficient and effective clinically acceptable restorative workflow [20]. The clinician must be aware of materials [21] that have been approved through their regulatory bodies.

3.3.6 Metal Prosthetic Frameworks

Casting and milling remain the industry standard for the fabrication of metal frameworks [22]. However, the metal prostheses may be manufactured through a digital workflow [22] and 3D printing in metal (Fig. 27). The metal is typically chromium-cobalt. The frameworks are 3D printed and undergo the appropriate post-processing. Esthetic materials can then be layered onto the metal (Fig. 28). 3D printing metal frameworks offer many benefits to clinicians, yet the regulatory approval and acceptance by the dental community has been limited.

4 Developments

Advances in technologies, materials, and applications are continually expanding the 3D printing space. Dentistry is slowly advancing, while medicine and industry continue to lead.

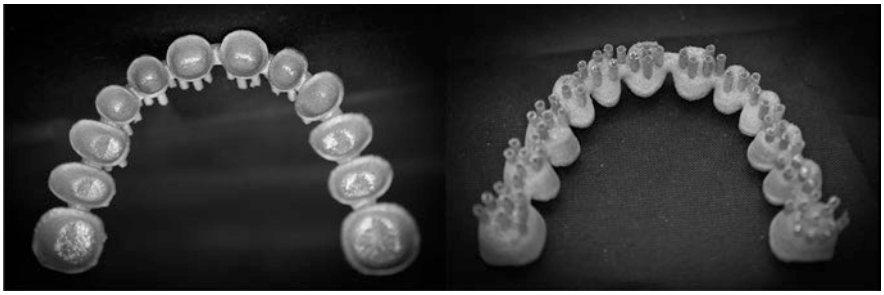

Fig. 27 3D printed metal full coverage crowns in chromium-cobalt without post-processing

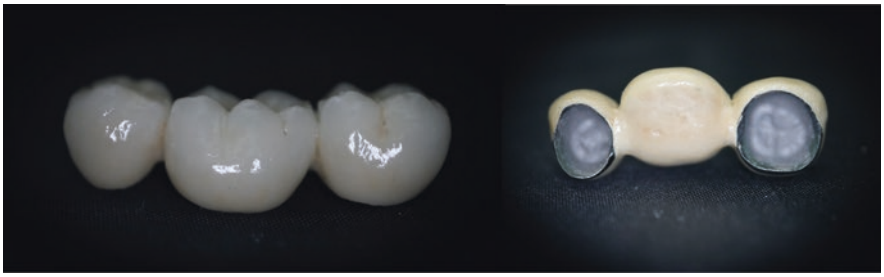

Fig. 28 3D printed metal three-unit bridge in chromium-cobalt with layered porcelain

4.1 Dental Research

As the conversion from casting and milling to 3D printing in metal commences, the applicability, utility, and physical performance of 3D printed components is crucial. Those questions provide an ample platform for research and innovation projects to asses and evaluate 3D printed products.

In implant dentistry, milling remains the platform for component fabrication. The subtractive manufacturing pathway has its disadvantages, and 3D printing in metal may be an alternative additive manufacturing platform.

The use of 3D printing in metal was utilized for a research investigation of an abutment. Specifically, a novel dental implant abutment (Fig. 29) was patented (U.S. Patent No.: 9, 642,686) for its design and technique. The abutment has been supported by publications to illustrate its advantages [23, 24]. The digital design of the abutment and the 3D printing in metal were performed at the ADEISS Centre [24] (London, Canada). The digital design was completed with Fusion 360 software (Autodesk, San Rafael, California, USA). The digital file was then 3D printed in dental grade titanium Ti64 (titanium 6-aluminum 4-vanadium) with an industrial Renishaw AM 400 Laser Melting System (Renishaw PLS, Gloucestershire, United Kingdom), which used Selective Laser Melting (SLM) technology. The process melts and fuses layers of metallic powders, with an average diameter 30–50 μm, with a 400 W laser [25], to 3D print the final component. The metal 3D process works by

Fig. 29 3D printed novel dental implant abutment in titanium alloy. Final hybrid manufacturing abutment (L) and proportion to Canadian nickel for scale (R)

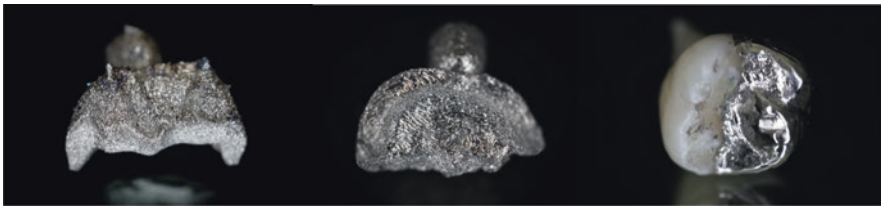

Fig. 30 3D printed chromium-cobalt onlay restoration. Occlusal surface (L), intaglio surface (C), and onlay cemented onto extracted tooth (R)

adding a single layer of the part's geometry, then the build plate becomes lowered, powder is then reintroduced, and another layer of metal is added until the 3D printing of the component is completed. The Renishaw printer uses a beam diameter of 70 μm and a build volume of 250 mm × 250 mm × 250 mm. Components may be 3D printed in titanium, cobalt-chrome, aluminum, stainless steel, and nickel [25].

Indirect prostheses (inlays, onlays, and crowns) are typically fabricated from esthetic materials (lithium disilicate, zirconia) [26]. Unfortunately, the cost of materials may be a barrier for a patient, especially marginalized populations, to consider the treatment option. An investigation (in progress) by the author is investigating 3D metal printed indirect restorations. The digital workflow has resulted in the successful 3D printing and the cementation of the prostheses (Fig. 30). An evaluation of the results will be published in the near future. 3D printing in metal will provide increased accessibility to treatment options by patients with limited resources for this treatment modality.

Dental research continues to push the advancement of 3D printing, including material advancements (printing ceramics), novel processes (bioprinting), and collaborative technologies (3D printing coupled with smart devices). In addition, 4D printing has started to gain momentum.

4.2 Industry

3D printing results in high accuracy and precision. It may be the only fabrication pathway available for research, based on complex geometries, or very unique structures [27]. Such is the case of the brake caliper for the Bugatti Chiron. Currently, 3D printing in metal is utilized for its fabrication [28]. The caliper is responsible for braking, that is, stopping the vehicle. The Chiron remains one of the fastest, most powerful super sport cars in the world [29]. That 3D metal printing is utilized for the fabrication of the caliper exemplifies the customization and reliability. In addition to complex geometries, the performance of 3D printed components has been exceptional. This may be inferred from the Chiron's caliper, as it is required to slow the world's fastest production car, or the many other applications of 3D printing in performance motorsports. BMW currently utilizes 3D printing in metal for the fabrication of their motorcycle frame [30].

3D printing also provides an alternative pathway for the mass production of components [31], such as a novel dental implant abutment (Fig. 31). Production would require a high degree of precision, ensuring that each component is identical to each other in quality. The application of 3D printing remains low, on a global scale [32], but increased research and data may support further applications.

4.3 Medicine

Medicine continues to utilize 3D orienting on many platforms. 3D printed patient models (Fig. 32) are employed for complex surgeries [33]. These models are typically composed of different colors and materials to provide a true to life representation of the patient. 3D printed models may require tens to hundreds of man-hours with highly specialized 3D printers. The models are essential for communication, both between the surgeon and the patient and the surgeon and the team, and are essential for the simulated procedure.

3D printing for patient-specific applications continues to expand [33]. Patients have received various 3D printed anatomical replacements, namely rib cages [34] and a bone implant in the finger [35]. As the regulatory process improves, patient applications will increase.

3D printing is largely associated with the fabrication of a structure. However, there are advances in 3D printed structures that perform functions. It has been estimated that a bioprinted pancreas will be transplanted within the next 5 years [36]. The opportunity for 3D printing to play a role in the patient-specific improvement of health and quality of life is exciting as it is hopeful.

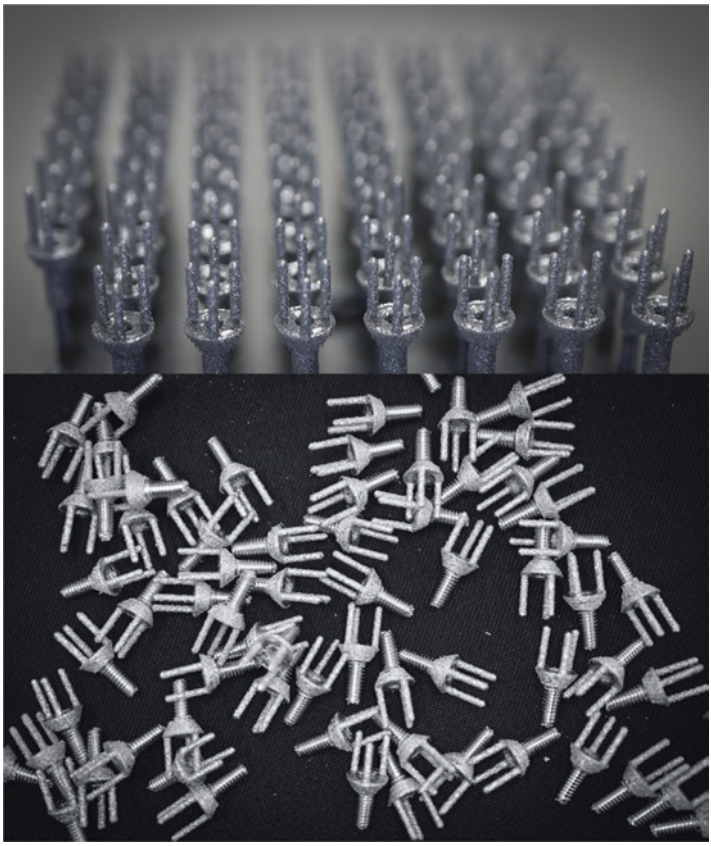

Fig. 31 3D printing in metal for the mass production of dental implant components. Pre-processed abutments directly from the build plate (top) and dental abutments after post-processing (bottom)

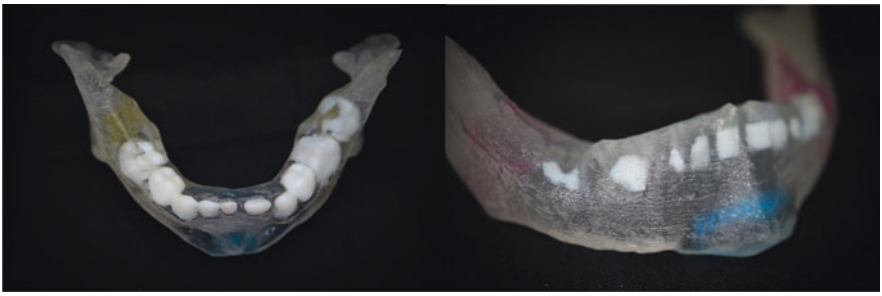

Fig. 32 Detailed patient-specific 3D printed model of a child's mandible

5 Conclusions

3D printing, and the associated digital workflow, will continue to evolve, advance, and have an impact on dentistry. Similar to the conversion of film cameras to digital cameras, 3D printing will continue to disrupt the dental industry. But with any technology, the clinician should weigh the pros and cons to make an informed decision whether or not to adopt the technology. 3D printing, and any other form of technology, is just another tool in the hypothetical toolbox of the clinician. The tool should provide a benefit in our quest to improve the oral health of our patients. The tool cannot take the place of fundamentals or principles. Moreover, the implementation of new technology should benefit the patient and/or the clinician without a compromise in quality of care.

References

1. Shahrubudin N, Lee TC, Ramlan R. An overview on 3D printing technology: technological, materials, and applications. Procedia Manuf. 2019;34:1286–96.
2. Szykiedans K, Credo W. Mechanical properties of FDM and SLA low-cost 3-D prints. Procedia Eng. 2016;136:257–62.
3. Gregurić L. History of 3D printing: when was 3D printing invented? Munich: All3DP. 2018.
4. Redwood B. The advantages of 3D printing. 3D Hubs. Available from: https://www.3dhubs.com/knowledge-base/advantages-3d-printing/.
5. Naftulin JS, Kimchi EY, Cash SS. Streamlines, inexpensive 3D printing of the brain and skull. PLoS One. 2015;10(8):e0136198.
6. Brugnami F, Caleffi C. Prosthetically driven implant placement. How to achieve the appropriate implant site development. Keio J Med. 2005;54(4):172–8.
7. Charangowda BK. Dental records: an overview. J Forensic Dent Sci. 2010;2(1):5–10.
8. Revilla-León M, Besné-Torre A, Sánchez-Rubio JL, Fábrega JJ, Özcan M. Digital tools and 3D printing technologies integrated into the workflow of restorative treatment: a clinical report. J Prosthet Dent. 2019;121(1):3–8.
9. Cascón WP, Revilla-León M. Digital workflow for the design and additively manufacture of a splinted framework and custom tray for the impression of multiple implants. J Prosthet Dent. 2018;120(6):805–11.
10. Groth CH, Kravitz ND, Jones PE, Graham JW, Redmond WR. Three-dimensional printing technology. J Clin Orthod. 2014;48(8):475–85.
11. Dilag J, Chen T, Li S, Bateman SA. Design and direct additive manufacturing of three-dimensional surface micro-structures using material jetting technologies. Addit Manuf. 2019;27:167–74.
12. D'Aveni RA. The 3D printing playbook. Harv Bus Rev. 2018;96(4):106–13.
13. Tappa K, Jammalamadaka U. Novel biomaterials used in medical 3D printing techniques. J Funct Biomater. 2018;9(1):17.
14. Devadiga A. What's the deal with dental records for practicing dentists? Importance in general and forensic dentistry. J Forensic Dent Sci. 2014;6(1):9–15.
15. Chen YJ, Chan LY, Yao CC. Clear aligner treatment with "in-office" virtual model set-up and 3D printing. J Dent Oral Care. 2017;3(1):21–5.
16. Colombo M, Mangano C, Mijiritsky E, Krebs M, Hauschild U, Fortin T. Clinical applications and effectiveness of guided implant surgery: a critical review based on randomized controlled trials. BMC Oral Health. 2017;17:150.

17. Ahmady E, Berger F, Dibadin M, Khojasteh SM, Tichenoff E. Comparing conventional complete dentures and implant-supported overdentures with respect to quality of life: a systematic review of the literature. Dissertation, University of Toronto, Faculty of Dentistry.
18. Zarb GA, Bolender CL, Boucher CO, Carlsson GE. Boucher's prosthodontic treatment for edentulous patients. St. Louis, MO: Mosby; 1990.
19. Dentca Inc. Dentca impression manual. Dentca. 2014. Available from: http://dentca.com/system/files/staticpage/Impression%20Manual%20DENTCA%20PDF_1.pdf. Cited 2 Jan 2020.
20. Mak A, Chio A. A full digital workflow with 3D-printed temporary restorations. GC Get Connected. 2018. Available from: https://getconnected-europe.gc.dental/media/articles/JSeHBXezsATaqYZwUMwreoRLWFE1uCnY4VFtvp4k.pdf?topic=documents&id=409. Cited 2 Jan 2020.
21. Molinero-Mourelle P, Canals S, Gómez-Polo M, Solá-Ruiz MF, Del Río Highsmith J, Viñuela AC. Polylactic acid as a material for three-dimensional printing of provisional restorations. Int J Prosthodont. 2018;31(4):349–50.
22. Abduo J, Lyons K, Bennamoun M. Trends in computer-aided manufacturing in prosthodontics: a review of the available streams. Int J Dent. 2014;2014:783948.
23. Kalman L, Estafanos L. Implant provisionals utilizing a novel abutment: assessing quality, efficiency and stability. Int J New Technol Sci Eng. 2017;4:37–47.
24. Kalman L. 3D printing of a novel dental implant abutment. J Dent Res Dent Clin Dent Prospects. 2018;12(4):299–303.
25. Renishaw. AM 400: flexible additive manufacturing for professional use in a wide range of metals. Available from: https://www.renishaw.com/en/am-400%2D%2D35456.
26. Stefano G, Thompson VP, Ferencz JL, Silva NR, Bonfante EA. A new classification system for all-ceramic and ceramic-like restorative materials. Int J Prosthodont. 2015;28(3):227–35.
27. cthornsberry. 3D printing advantages. 3SPACE. 2019. Available from: https://3space.com/blog/3d-printing-advantages/.
28. Jackson B. Bugatti prepares 3D printed brake caliper for series production. 3D Printing Industry. 2019. Available from: https://3dprintingindustry.com/news/watch-bugatti-prepares-3d-printed-brake-caliper-for-series-production-146163/.
29. Chang B. Bugatti's new $3.9 million hypecar broke a world record for going over 300 miles per hours—now it's for sale. Maxim. 2019. Available from: https://markets.businessinsider.com/news/stocks/bugatti-will-sell-worlds-fastest-car-hits-300-mph-2019-9-1028513987.
30. Alexandrea P. BMW incorporates 3D printed parts onto their new motorcycle. 3D Natives. 2018. Available from: https://www.3dnatives.com/en/bmw-3d-printing-motorcycle030520184/.
31. 3D Printing Progress. Volkswagen uses 3D printing for mass production. 2018. Available from: https://www.3dprintingprogress.com/articles/15362/volkswagen-uses-3d-printing-for-mass-production.
32. Market Watch. Global 3D printing market insights by size, share, future growth and forecast from 2018–2025. 2019. Available from: https://www.marketwatch.com/press-release/global-3d-printing-market-insights-by-size-share-future-growth-and-forecast-from-2018-2025-2019-10-17.
33. Shafiee A, Atala A. Printing technologies for medical applications. Trends Mol Med. 2016;22(3):254–65.
34. Commonwealth Scientific and Industrial Research Organisation (CSIRO). Cancer patient receives 3D printed rib cage. Available from: https://www.csiro.au/en/Research/MF/Areas/Metals/Lab22/Sternum-and-ribs.
35. Coffey L. St. Pete man receives first ever 3D printed finger bone. Tampa Bay Inno. 2019. Available from: https://www.americaninno.com/uncategorized/st-pete-man-receives-first-ever-3d-printed-finger-bone/.
36. Lee SJ, Lee JB, Park YW, Lee DY. 3D bioprinting for artificial pancreas organ. Adv Exp Med Biol. 2018;1064:355–74.

Maxillofacial Reconstruction: From Autogenous Bone Grafts to Bone Tissue Engineering

Fernando P. S. Guastaldi, Toru Takusagawa, Joseph P. McCain Jr, Joao L. G. C. Monteiro, and Maria J. Troulis

Abstract Maxillofacial reconstruction (using autogenous bone grafts, biomaterials, growth factors, distraction osteogenesis, dental implants, and bone tissue engineering) is complex and poses significant challenges to surgeons. The use of these techniques has profoundly improved patients' function, form, and quality of life. Several techniques are currently being used to treat bone defects of the jaws (ranging from minor to major defects), including autogenous bone grafting, guided bone regeneration, the use of growth factors with biomaterials, and distraction osteogenesis. Dental implants have become a routine treatment for the final and total rehabilitation of patients. Bioengineering of autologous bone is an exciting minimally invasive alternative to bone harvesting techniques to replace missing bone of any part of the skeleton. Advances in the field of bone tissue engineering over the past few decades offer promising new treatment alternatives using biocompatible scaffold materials, autologous mesenchymal stem cells, and growth factors. The purpose of this chapter is to provide a variety of different current evidence-based treatment options, as well as novel tissue engineering technologies for the reconstruction of minor and major jaw defects.

Keywords Maxillofacial reconstruction · Autogenous bone graft · Biomaterials · Growth factors · Distraction osteogenesis · Dental implants · Tissue engineering

F. P. S. Guastaldi (✉) · T. Takusagawa · J. P. McCain Jr · J. L. G. C. Monteiro
Skeletal Biology Research Center, Department of Oral and Maxillofacial Surgery, Massachusetts General Hospital, Harvard School of Dental Medicine, Boston, MA, USA
e-mail: fguastaldi@mgh.harvard.edu

M. J. Troulis
Walter C. Guralnick Distinguished Professor of Oral and Maxillofacial Surgery, Massachusetts eneral Hospital, Harvard School of Dental Medicine, Boston, MA, USA

R. S. Chaughule, R. Dashaputra (eds.), *Advances in Dental Implantology using Nanomaterials and Allied Technology Applications*,
https://doi.org/10.1007/978-3-030-52207-0_14

1 Introduction

Management of clinical cases in the field of maxillofacial reconstructive surgery is complex and poses significant challenges to surgeons. The use of techniques such as autogenous bone grafting, guided bone regeneration, growth factors, distraction osteogenesis (DO), dental implants, and bone tissue engineering (BTE) has profoundly improved patients' function, form, and quality of life. Maxillofacial defects can result from, but not limited to, congenital abnormalities, post-trauma, tumor resection, periodontal disease, severe ridge atrophy following tooth extraction, and infections [1–3].

The primary goal of reconstructive surgeries is to provide form and function. Autogenous bone, harvested from a variety of donor sites, is considered the gold standard. Donor site morbidity remains significant [4–6]. Resorption of grafted autogenous bone is a common and unwanted complication, and may compromise the long-term stability [3, 7].

Guided bone regeneration (GBR) [8, 9], the use of different growth factors such as platelet rich plasma (PRP), platelet rich fibrin (PRF), and bone morphogenetic protein (BMP) have shown promising preclinical and clinical results to promote and improve wound healing and bone regeneration [10–15]. Emerging technologies such as tissue engineering (TE) may represent a minimally invasive alternative to autogenous bone graft procedures. Tissue engineering would also provide patient-specific treatments [15–17]. The purpose of this chapter is to provide a variety of evidence-based treatment options, as well as novel TE technologies.

2 Maxillofacial Reconstruction

2.1 Autogenous Bone Grafts

Autogenous bone is still considered the "gold standard" [18]. Autogenous cortico-cancellous bone blocks from both membranous or endochondral origin can be harvested from jaws or distant sites. The choice of the donor site depends on aspects such as patient-specific conditions, donor site morbidity, and amount of bone required for reconstruction [3, 19–21]. In addition, the decision will also be driven by the size of the defect that needs to be reconstructed (i.e., alveolar regeneration versus reconstruction of major bone defects with bone discontinuity).

Intraoral autologous bone blocks can be safely harvested from the lateral zygomatic buttress, retromolar area, and the mandibular ramus [19, 20], and bone chips can be obtained using a bone scraper [22]. They are used for minor alveolar ridge reconstruction.

Severe alveolar ridge defects as well as bone discontinuity defects require larger bone quantity and, therefore, harvesting from distant sites. [iliac crest (anterior/posterior), calvaria, fibula, ribs, vascularized and non-vascularized]. However, this

treatment is more costly with more patient morbidity [4, 5, 23, 24]. Implant placement following grafting with autologous bone blocks usually is performed after a healing period of 3–5 months, which allows revascularization of the graft [19, 20]. Vascularized free grafts (for large bone defects) allow for immediate implants. Evidence from retrospective cohort studies demonstrates that implants placed in areas reconstructed with autogenous bone blocks have survival rates consistent with implants placed in native bone [19, 20, 25]. Despite the higher success rate of autogenous bone reconstruction, significant donor site morbidity is a major consideration [4, 5, 19, 20, 23, 25]. Graft resorption is also expected with grafts; therefore, many recommend overcorrection of defects to compensate this [26]. In some situations, in which there is insufficient implant coverage due to graft resorption or inadequate primary augmentation, secondary grafting may be required [19, 20].

2.2 Guided Bone Regeneration (GBR)

Guided bone regeneration (GBR) has been successfully reported for over 20 years and represents a safe and reliable option for alveolar regeneration for dental implant placement [22, 27, 28]. Guided bone regeneration (GBR) consists of preventing the migration of undesired cells to the site that is intended to be reconstructed by placing a barrier membrane in conjunction with particulate grafts biomaterials. This technique restricts the entry of soft tissue into the defect, avoids nonosteogenic cell migration, and allows accumulation of growth factors, ultimately providing stability to bone grafts [22, 28].

Membranes used in GBR should possess some desirable characteristics, such as biocompatibility, cell-occlusion properties, clinical manageability, and be able to maintain proper physical and mechanical properties [8]. Non-resorbable membranes are commonly referred as the "gold-standard" material for GBR, and some examples include those composed of polytetrafluorethylene (PTFE), and titanium-reinforced expanded PTFE [8]. These require a second surgical procedure for removal. Second generation of membranes that are resorbable such as poly(lactic acid) (PLA), poly(glycolic acid) (PGA), poly(ε-caprolactone) (PCL), inorganic compounds (i.e. calcium sulfate, calcium phosphate), and xenografic membrane (derived from bovine or porcine tissues) have been developed [8]. The GBR technique of choice depends on specific needs [22, 29].

Complications include soft tissue dehiscence, exposure of membranes, and infection [8, 30]. Exposure of resorbable membranes can occur and rapid degradation of the material may allow a spontaneous healing [8]. Major disadvantages of resorbable membranes include lack of rigidity (i.e., PLA, PGA, and PCL) and lack of plasticity (i.e., calcium sulfate, calcium phosphate) [8].

Enhancement of GBR outcomes by using growth factors such as BMP-2 and platelet-derived growth factor (PDGF) has been described. This can be obtained by soaking the membranes in a solution containing the growth factors, followed by lyophilization. Depending on additional reagents (i.e., heparin, cross-linkers), and

growth factors concentration, a faster release of factor usually occurs within the first day, followed by a phase characterized by a slower release. Blood-derived products, such as PRP or PRF membranes, have also been described as adjuncts to enhance the regenerated bone obtained by GBR [31]. Biological basis may be due to the availability of growth factors [32].

2.3 Bone Morphogenetic Proteins (BMPs)

Bone morphogenetic proteins were first described by Urist in 1965. BMPs are present in bone matrix, and there are about 30 proteins belonging to the human BMP family. Most of them constitute subfamilies in the transforming growth factor beta (TGF-β) superfamily [33].

It appears that BMP-2, BMP-6, and BMP-9 may be the most potent agents to induce osteoblast lineage-specific differentiation of MSCs [34]. BMP activates a signaling system called Smad. Smads are an important group of molecules that translocate and transmit signals from BMP-activated receptors into the cell nucleus [35, 36].

Despite the evidence showing the positive effects on bone formation, there are concerns regarding side effects of BMPs *in vivo*. Major side effects of BMP include edema, inflammation, and ectopic bone formation. Carcinogenic effects have been suggested [37].

Recombinant human bone morphogenetic protein-2 (rhBMP-2) is placed on an absorbable collagen sponge (ACS). It has been shown that this combination can induce and support bone formation [38–40]. Bone-forming cells migrate to the area of the rhBMP-2/ACS, and infiltrate into the ACS. Mesenchymal stem cells around the rhBMP-2/ACS also increase in number. Binding of rhBMP-2 to specific receptors on the surface of the MSC causes them to differentiate into bone-forming cells (osteoblasts). As the sponge degrades or dissolves trabecular bone and/or cartilage is formed, with angiogenesis occurring at the same time. The bone formation process develops from outer surface of the sponge towards the center until the entire area is replaced by trabecular bone [39].

A clinical study examined the efficacy of two doses of rhBMP-2/ACS in 80 in post-extraction sockets [41]. Recombinant BMP at concentrations of 0.75 and 1.5 mg/cc was comparted to controls. The results demonstrated that the 1.5 mg/cc rhBMP-2/ACS treated sites had about two times the amount of bone compared to the empty control group, preserving ridge height, and significantly increased width at 75%, 50%, and 25% of the extraction socket length. In addition, histological analysis showed no differences between the rhBMP-2-induced bone and native bone.

Bone morphogenetic proteins (i.e., rhBMP2) have been used for alveolar reconstruction, sinus augmentation, and tooth extraction socket healing [38–40]. However, despite several preclinical studies and clinical trials, a lack of consensus continues to exist concerning the clinical efficacy of rhBMP2 for larger defects in the maxillofacial region [42].

2.4 Platelet Rich Plasma (PRP) and Platelet Rich Fibrin (PRF)

Platelets contain high amounts of key growth factors [such as platelet-derived growth factor (PDGF), transforming growth factor β (TGF-β), vascular endothelial growth factor (VEGF), epidermal growth factor (EGF), insulin-like growth factor (IGF), and fibroblast growth factor (FGF)] which can stimulate cell proliferation, matrix remodeling, and angiogenesis and this stimulated its use in implantology [43, 44].

First-generation products such as PRP and plasma rich in growth factors (PRGF) are obtained by collecting peripheral blood and adding anticoagulants [45]. Second generation concentrates (such as PRF) were developed without the need of anticoagulants. The collected blood is immediately centrifuged to obtain a clot rich in platelets, fibrin, and leucocytes [43]. The presence of a fibrin network represents a potential innovation for regenerative purposes, since it acts as a scaffold for cell proliferation. Additionally, leucocytes release vascular endothelial growth factor (VEGF) and transforming growth factor (TGF), which improve chemotaxis and angiogenesis [45] that are fundamental for bone formation.

Platelet rich fibrin (PRF) was also suggested as sole graft material during simultaneous sinus floor elevation and implant placement [46]. The concomitant use of PRF and bone allografts significantly reduced bone resorption and accelerated bone healing during the initial stage of post-extraction alveolar healing [47]. However, a recent systematic review concluded that it remains unclear whether PRF can improve soft tissue healing [44]. Most commonly, PRP and PRF are used in conjunction or as adjuvant therapy for the treatment of alveolar defects.

2.5 Distraction Osteogenesis (DO)

Historically, distraction osteogenesis (DO) was initially performed using transcalcaneal metal pins as a method of correcting malformations caused by femoral fractures by Codivilla in 1905. It had not progressed until the revolutionary principles and devices proposed by Ilizarov in 1951. The principle is called the "Ilizarov effect" and involves stimulating tissue growth by applying tension to it [48, 49].

As a basic concept, undifferentiated mesenchymal cells in the bone fracture line are stimulated by pulling and elongating the young callus with an external force, which stimulates differentiation into osteogenic cells. In the maxillofacial region, Perrott et al. [50] applied it to produce widening of the mandible and soft tissue expansion in a syndromic patient and McCarthy [51] applied it to correct mandibular hypoplasia. In 1996, Chin and Toth used the technique for correction of traumatic bone defects. Distraction osteogenesis (DO) is considered an appropriate technique for correcting large soft and hard tissue defects [51, 52], eliminating the need of multiple bone grafts.

Distraction osteogenesis (DO) devices can be broadly divided into transcutaneous, implantable (bone borne), horizontal, and vertical. The current hurdle in DO is device size.

Treatment with DO devices consists in three parts. The first one (after implantation of the device) is commonly referred as the "latency period," ranges from 0 to 7 days, and no distraction force is applied to the tissues [53]. The second one, the rhythm of distraction in increments of 0.5–1 mm/day. After the desired bone distraction has being achieved, a fixation period in which the device is kept in place without activation is also recommended, and this varies between 8 and 12 weeks [54]. Efforts to reduce the latency period have been reported [55–58]. In addition, stable results in which no latency period was required before activation of the DO device have been demonstrated [59].

The greatest advantage of DO is that no bone harvesting is required, and soft tissue can be expanded and maintained with an adequate blood supply, since the periosteum of the distracted bone is maintained attached. Disadvantages of DO include patient discomfort to activate the device and inability to wear dentures [60]. Another problem is how to control the direction of the bone segment being distracted (transport disk) [61]. This can be done by slants and lingual ramps [59].

2.6 Bone Tissue Engineering (BTE)

Bioengineering of autologous bone is an exciting minimally invasive alternative to bone harvesting techniques [62–65]. Tissue engineering of bone requires the combination of three main elements: biocompatible scaffolds, growth factors, and osteoprogenitor stem cells [62–66]. This approach combined with recent advances in three-dimensional (3D) printing technologies may soon allow the generation of large, bioartificial bone grafts with custom, patient-specific architecture [62, 66, 67].

The use of scaffolds plays a key role in BTE [68]. Different methods for producing porous scaffolds have been used, including solvent-casting, particulate-leaching, electrospinning, gas foaming, and phase separation [64]. However, several drawbacks are associated with the use of organic solvents, long fabrication periods, labor-intensive process, poor repeatability, irregularly shaped pores, insufficient interconnectivity of pores, and thin structures [64]. Many of these issues have been addressed with rapid prototyping technologies such as 3D printing. For these reasons, 3D-printed scaffolds made with functional biomaterials and appropriate structures have been widely developed for dental tissue regeneration [64, 68–70].

Three-dimensional printed scaffolds can be produced using rapid prototyping (RP) techniques, using data from medical images such as magnetic resonance imaging (MRI) and computed tomography (CT) of patients [71–73]. Briefly, the process from image acquisition to obtention of the final scaffold is as follows: patient with a bone defect will undergo a CT scan [obtention of digital imaging and communication in medicine (DICOM) files]; DICOM files will be imported into a medical image processing software; CT images will be segmented, and 3D virtual models generated; selection of the 3D printing technique and the selection of the materials; obtention of the 3D-printed bone scaffold; post processing and sterilization [73].

Different synthetic polymers have been widely used to fabricate bone scaffolds such as polylactic acid (PLA), polyglycolic acid (PGA), copolymers of PLA and PGA [poly(DL-lactic-co-glycolic acid) (PLGA)], and polycaprolactone (PCL). Synthetic calcium phosphates' (CP) chemical similarity to the natural bone mineral content allows to apply it successfully as bone substitutes among a variety of other materials (ceramics, bioglasses, polymers, and their combinations) [74–76]. Furthermore, composite scaffolds such as those made with PCL and β-TCP combine advantages of polymers and ceramics and have been used successfully to repair mandibular defects *in vivo* [63, 67, 77, 78]; synthetic biomaterials are not affected by the immunologic reactions that can be problematic for natural scaffolds [76].

The osteoprogenitor cells can be bone marrow stem cells (BMSCs), adipose stem cells (ASCs), dental pulp stem cells (DPSCs), or other stem cells that can initiate osteoblastic differentiation [66, 67, 79, 80]. These stem cells will then be seeded within scaffolds. The stem cell growth can be regulated by direct stimuli (i.e., growth factors) or environmental control (i.e., bioreactors) [62, 66, 67, 79, 80].

For a clinically relevant application, autologous bioengineered constructs should display deep cell penetration and angiogenesis. Vascularization is the key challenge in TE of bone [66, 81, 82]. This early process of angiogenesis is critical to sustain the grafted cells' viability. To achieve early angiogenesis, the implanted construct must contain proangiogenic factors (such as vascular endothelial growth factor secreted by osteoblastic cells) that will induce new vessel formation from the surrounding connective tissue envelope [66, 81, 82]. In addition, the construct must physically allow for such vessels to reach the interior of the scaffold before extensive extracellular matrix deposition has occurred [67, 83].

New bioactive synthetic biomaterials, in combination with the establishment of rigorous protocols for the translation of mesenchymal stem cells therapies and the use of growth factors that can guide cellular and molecular pathways to improve the healing mechanisms that will assist the maxillofacial restoration. Mimicking the complex 3D architecture and functional dynamics of maxillofacial bone tissue is a challenging proposal that generates the need for a customized and on-demand tissue replacement strategy to make patient specificity that could not be achieved to date.

3 Final Considerations

Maxillofacial reconstruction and rehabilitation pose significant challenges for the surgeons [66, 84]. As the technology advances and with the development of new approaches, the ability to develop and create detailed bioactive tissues will become more sophisticated [80]. Tissue engineering is a well-established field of research in the preclinical setting and a highly active field to develop products and devices following all principles of regenerative medicine [64, 65, 81, 85]. Surgeons should be aware of these advances, should be able to select appropriate techniques and materials based on current scientific knowledge, and should have the necessary skills for the reconstruction of maxillofacial bone defects.

References

1. Checchi V, Gasparro R, Pistilli R, Canullo L, Felice P. Clinical classification of bone augmentation procedure failures in the atrophic anterior maxillae: esthetic consequences and treatment options. Biomed Res Int. 2019;2019:4386709.
2. Nguyen TTH, Eo MY, Kuk TS, Myoung H, Kim SM. Rehabilitation of atrophic jaw using iliac onlay bone graft combined with dental implants. Int J Implant Dent. 2019;5(1):11.
3. Sethi A, Kaus T, Cawood JI, Plaha H, Boscoe M, Sochor P. Onlay bone grafts from iliac crest: a retrospective analysis. Int J Oral Maxillofac Surg. 2020;49(2):264–71.
4. Dodson TB, Smith RA. Mandibular reconstruction with autogenous and alloplastic materials following resection of an odontogenic myxoma. Int J Oral Maxillofac Implants. 1987;2(4):227–9.
5. Dodson TB, Bays RA, Pfeffle RC, Barrow DL. Cranial bone graft to reconstruct the mandibular condyle in Macaca mulatta. J Oral Maxillofac Surg. 1997;55(3):260–7.
6. Nkenke E, Neukam FW. Autogenous bone harvesting and grafting in advanced jaw resorption: morbidity, resorption and implant survival. Eur J Oral Implantol. 2013;7:S203–17.
7. Hameed MH, Gul M, Ghafoor R, Khan FR. Vertical ridge gain with various bone augmentation techniques: a systematic review and meta-analysis. J Prosthodont. 2019;28(4):421–7.
8. Elgali I, Omar O, Dahlin C, Thomsen P. Guided bone regeneration: materials and biological mechanisms revisited. Eur J Oral Sci. 2017;125(5):315–37.
9. Yamada M, Egusa H. Current bone substitutes for implant dentistry. J Prosthodont Res. 2018;62(2):152–61.
10. Simonpieri A, Del Corso M, Vervelle A, Jimbo R, Inchingolo F, Sammartino G, Dohan Ehrenfest DM. Current knowledge and perspectives for the use of platelet-rich plasma (PRP) and platelet-rich fibrin (PRF) in oral and maxillofacial surgery part 2: bone graft, implant and reconstructive surgery. Curr Pharm Biotechnol. 2012;13(7):1231–56.
11. Wang J, Zheng Y, Zhao J, Liu T, Gao L, Gu Z, Wu G. Low-dose rhBMP2/7 heterodimer to reconstruct peri-implant bone defects: a micro-CT evaluation. J Clin Periodontol. 2012;39(1):98–105.
12. Potres Z, Deshpande S, Klöeppel H, Voss K, Klineberg I. Assisted wound healing and vertical bone regeneration with simultaneous implant placement: a histologic pilot study. Int J Oral Maxillofac Implants. 2016;31(1):45–54.
13. Fujioka-Kobayashi M, Sawada K, Kobayashi E, Schaller B, Zhang Y, Miron RJ. Osteogenic potential of rhBMP9 combined with a bovine-derived natural bone mineral scaffold compared to rhBMP2. Clin Oral Implants Res. 2017;28(4):381–7.
14. Gonzaga MG, Dos Santos Kotake BG, de Figueiredo FAT, Feldman S, Ervolino E, Dos Santos MCG, Issa JPM. Effectiveness of rhBMP-2 association to autogenous, allogeneic, and heterologous bone grafts. Microsc Res Tech. 2019;82(6):689–95.
15. Melville JC, Mañón VA, Blackburn C, Young S. Current methods of maxillofacial tissue engineering. Oral Maxillofac Surg Clin North Am. 2019;31(4):579–91.
16. Konopnicki S, Troulis MJ. Mandibular tissue engineering: past, present, future. J Oral Maxillofac Surg. 2015;73(12 Suppl):S136–46.
17. Aghaloo TL, Hadaya D. Basic principles of bioengineering and regeneration. Oral Maxillofac Surg Clin North Am. 2017;29(1):1–7.
18. Galindo-Moreno P, Ávila G, Fernández-Barbero JE, Mesa F, O'Valle-Ravassa F, Wang HL. Clinical and histologic comparison of two different composite grafts for sinus augmentation: a pilot clinical trial. Clin Oral Implants Res. 2008;19(8):755–9.
19. Sakkas A, Wilde F, Heufelder M, Winter K, Schramm A. Autogenous bone grafts in oral implantology—is it still a "gold standard"? A consecutive review of 279 patients with 456 clinical procedures. Int J Implant Dent. 2017;3(1):1–17.
20. Sakkas A, Schramm A, Winter K, Wilde F. Risk factors for post-operative complications after procedures for autologous bone augmentation from different donor sites. J Craniomaxillofac Surg. 2018;46(2):312–22.

21. Atef M, Osman AH, Hakam M. Autogenous interpositional block graft vs onlay graft for horizontal ridge augmentation in the mandible. Clin Implant Dent Relat Res. 2019;21(4):678–85.
22. Tolstunov L, Hamrick JFE, Broumand V, Shilo D, Rachmiel A. Bone augmentation techniques for horizontal and vertical alveolar ridge deficiency in oral implantology. Oral Maxillofac Surg Clin. 2019;31(2):163–91.
23. Ardekian L, Dodson TB. Complications associated with the placement of dental implants. Oral Maxillofac Surg Clin North Am. 2003;15(2):243–9.
24. Gjerde CG, Shanbhag S, Neppelberg E, Mustafa K, Gjengedal H. Patient experience following iliac crest-derived alveolar bone grafting and implant placement. Int J Implant Dent. 2020;6(1):4.
25. Chiapasco M, Tommasato G, Palombo D, Del Fabbro M. A retrospective 10-year mean follow-up of implants placed in ridges grafted using autogenous mandibular blocks covered with bovine bone mineral and collagen membrane. Clin Oral Implants Res. 2020;31:328–40.
26. Elnayef B, Porta C, Del Amo FSL, Mordini L, Gargallo-Albiol J, Hernández-Alfaro F. The fate of lateral ridge augmentation: a systematic review and meta-analysis. Int J Oral Maxillofac Implants. 2018;33(3):622–35.
27. Gaballah O, Abd-ElwahabRadi I. Limited evidence suggests guided bone regeneration with or without autogenous bone grafts are equivalently effective in horizontal bone gain. J Evid Based Dent Pract. 2019;19(4):101351.
28. Urban IA, Monje A. Guided bone regeneration in alveolar bone reconstruction. Oral Maxillofac Surg Clin. 2019;31(2):331–8.
29. Fontana F, Santoro F, Maiorana C, Iezzi G, Piattelli A, Simion M. Clinical and histologic evaluation of allogeneic bone matrix versus autogenous bone chips associated with titanium-reinforced e-PTFE membrane for vertical ridge augmentation: a prospective pilot study. Int J Oral Maxillofac Implants. 2008;23(6):2003–1012.
30. Soldatos NK, Stylianou P, Koidou VP, Angelov N, Yukna R, Romanos GE. Limitations and options using resorbable versus nonresorbable membranes for successful guided bone regeneration. Quintessence Int. 2017;48(2):131–47.
31. Del Corso M, Vervelle A, Simonpieri A, Jimbo R, Inchingolo F, Sammartino G, Dohan Ehrenfest DM. Current knowledge and perspectives for the use of platelet-rich plasma (PRP) and platelet-rich fibrin (PRF) in oral and maxillofacial surgery part 1: periodontal and dentoalveolar surgery. Curr Pharm Biotechnol. 2012;13(7):1207–30.
32. Kökdere NN, Baykul T, Findik Y. The use of platelet-rich fibrin (PRF) and PRF-mixed particulated autogenous bone graft in the treatment of bone defects. An experimental and histomorphometrical study. Dent Res J (Isfahan). 2015;12(5):418–24.
33. Patricia D, Gerard K. The family of bone morphogenetic proteins. Kidney Int. 2000;57(6):2207–14.
34. Cheng H, Jiang W, Phillips FM, Haydon RC, Peng Y, Zhou L, et al. Osteogenic activity of the fourteen types of human bone morphogenetic proteins (BMPs). J Bone Joint Surg A. 2003;85(8):1544–52.
35. Nishimura R, Hata K, Ikeda F, Matsubara T, Yamashita K, Ichida F, Yoneda T. The role of Smads in BMP signaling. Front Biosci. 2003;8:275–84.
36. Frédéric D, Luc S, Dominique H. Mechanisms of bone repair and regeneration. Trends Mol Med. 2009;15(9):417–29.
37. James AW, LaChaud G, Shen J, Asatrian G, Nguyen V, Zhang X, Ting K, Soo C. A review of the clinical side effects of bone morphogenetic protein-2. Tissue Eng B Rev. 2016;22(4):284–97.
38. Gothard D, Smith EL, Kanczler JM, Rashidi H, Qutachi O, Henstock J, Rotherham M, El Haj A, Shakesheff KM, Oreffo RO. Tissue engineered bone using select growth factors: a comprehensive review of animal studies and clinical translation studies in man. Eur Cell Mater. 2014;28:166–207; discussion 207–8.
39. Ben Amara H, Lee JW, Kim JJ, Kang YM, Kang EJ, Koo KT. Influence of rhBMP-2 on guided bone regeneration for placement and functional loading of dental implants: a radiographic and histologic study in dogs. Int J Oral Maxillofac Implants. 2017;32(6):265–76.

40. Li F, Yu F, Liao X, Wu C, Wang Y, Li C, Lou F, Li B, Yin B, Wang C, Ye L. Efficacy of recombinant human BMP2 and PDGF-BB in orofacial bone regeneration: a systematic review and meta-analysis. Sci Rep. 2019;9(1):8073.
41. Fiorellini JP, Howell TH, Cochran D, Malmquist J, Lilly LC, Spagnoli D, et al. Randomized study evaluating recombinant human bone morphogenetic protein-2 for extraction socket augmentation. J Periodontol. 2005;76(4):605–13.
42. Carreira AC, Lojudice FH, Halcsik E, Navarro RD, Sogayar MC, Granjeiro JM. Bone morphogenetic proteins: facts, challenges, and future perspectives. J Dent Res. 2014;93(4):335–45.
43. Ehrenfest DD, Rasmusson L, Albrektsson T. Classification of platelet concentrates: from pure platelet-rich plasma (P-PRP) to leucocyte-and platelet-rich fibrin (L-PRF). Trends Biotechnol. 2009;27(3):158–67.
44. Strauss FJ, Stähli A, Gruber R. The use of platelet-rich fibrin to enhance theoutcomes of implant therapy: a systematic review. Clin Oral Implants Res. 2018;29(Suppl 18):6–19.
45. Caruana A, Savina D, Macedo JP, Soares SC. From platelet-rich plasma to advanced platelet-rich fibrin: biological achievements and clinical advances in modern surgery. Eur J Dent. 2019;13(2):280–6.
46. Molemans B, Cortellini S, Jacobs R, Teughels W, Pinto N, Quirynen M. Simultaneous sinus floor elevation and implant placement using leukocyte-and platelet-rich fibrin as a sole graft material. Int J Oral Maxillofac Implants. 2019;34(5):1195–201.
47. Medikeri RS, Meharwade V, Wate PM, Lele SV. Effect of PRF and allograft use on immediate implants at extraction sockets with periapical infection—clinical and cone beam CT findings. Bull Tokyo Dent Coll. 2017;59(2):97–109.
48. Codivilla A. On the means of lengthening, in the lower limbs, the muscles and tissues which are shortened through deformity. Am J Onhop Surg. 1905;2(4):353–69.
49. Ilizarov G. The principles of the Ilizarov method. Bull Hospital Joint Dis Orthop. 1987;48(1):1–11.
50. Perrott DH, Berger R, Vargervik K, Kaban LB. Use of a skeletal distraction device to widen the mandible: a case report. J Oral Maxillofac Surg. 1993;51(4):435–9.
51. McCarthy JG. The role of distraction osteogenesis in the reconstruction of the mandible in unilateral craniofacial microsomia. Clin Plast Surg. 1994;21(4):625–31.
52. Chin M, Toth BA. Distraction osteogenesis in maxillofacial surgery using internal devices: review of five cases. J Oral Maxillofac Surg. 1996;54(1):45–53.
53. Moore C, Campbell PM, Dechow PC, Ellis ML, Buschang PH. Effects of latency on the quality and quantity of bone produced by dentoalveolar distraction osteogenesis. Am J Orthod Dentofac Orthop. 2011;140(4):470–8.
54. Rachmiel A, Shilo D, Aizenbud D, Emodi O. Vertical alveolar distraction osteogenesis of the atrophic posterior mandible before dental implant insertion. J Oral Maxillofac Surg. 2017;75(6):1164–75.
55. Troulis MJ, Padwa B, Kaban LB. Distraction osteogenesis: past, present, and future. Facial Plast Surg. 1998;14(3):205–16.
56. Glowacki J, Shusterman EM, Troulis M, Holmes R, Perrott D, Kaban LB. Distraction osteogenesis of the porcine mandible: histomorphometric evaluation of bone. Plast Reconstr Surg. 2004;113(2):566–73.
57. Peacock ZS, Tricomi BJ, Murphy BA, Magill JC, Kaban LB, Troulis MJ. Automated continuous distraction osteogenesis may allow faster distraction rates: a preliminary study. J Oral Maxillofac Surg. 2013;71(6):1073–84.
58. Onger ME, Bereket C, Sener I, Ozkan N, Senel E, Polat AV. Is it possible to change of the duration of consolidation period in the distraction osteogenesis with the repetition of extracorporeal shock waves? Med Oral Patol Oral Cir Bucal. 2017;22(2):e251–7.
59. Troulis M, Glowacki J, Perrott DH, Kaban LB. Effects of latency and rate on bone formation in a porcine mandibular distraction model. J Oral Maxillofac Surg. 2000;58(5):507–13.
60. Gunbay T, Koyuncu BÖ, Akay MC, Sipahi A, Tekin U. Results and complications of alveolar distraction osteogenesis to enhance vertical bone height. OOOE. 2008;105(5):7–13.

61. Mehra P, Figueroa R. Vector control in alveolar distraction osteogenesis. J Oral Maxillofac Surg. 2008;66(4):776–9.
62. Temple JP, Hutton DL, Hung BP, Huri PY, Cook CA, Kondragunta R, Jia X, Grayson WL. Engineering anatomically shaped vascularized bone grafts with hascs and 3d-printed pcl scaffolds. J Biomed Mater Res A. 2014;102(12):4317–25.
63. Tatara AM, Shah SR, Demian N, Ho T, Shum J, van den Beucken J, Jansen JA, Wong ME, Mikos AG. Reconstruction of large mandibular defects using autologous tissues generated from in vivo bioreactors. Acta Biomater. 2016;45:72–84.
64. Roseti L, Parisi V, Petretta M, Cavallo C, Desando G, Bartolotti I, Grigolo B. Scaffolds for bone tissue engineering: state of the art and new perspectives. Mater Sci Eng C Mater Biol Appl. 2017;78:1246–62.
65. Sparks DS, Saifzadeh S, Savi FM, Dlaska CE, Berner A, Henkel J, Reichert JC, Wullschleger M, Ren J, Cipitria A, McGovern JA, Steck R, Wagels M, Woodruff MA, Schuetz MA, Hutmacher DW. A preclinical large-animal model for the assessment of critical-size load-bearing bone defect reconstruction. Nat Protoc. 2020;15:877–924. [Epub ahead of print].
66. Bhumiratana S, Bernhard JC, Alfi DM, Yeager K, Eton RE, Bova J, Shah F, Gimble JM, Lopez MJ, Eisig SB, Vunjak-Novakovic G. Tissue-engineered autologous grafts for facial bone reconstruction. Sci Transl Med. 2016;8(343):343ra83.
67. Konopnicki S, Sharaf B, Resnick C, Patenaude A, Pogal-Sussman T, Hwang KG, Abukawa H, Troulis MJ. Tissue-engineered bone with 3-dimensionally printed beta-tricalcium phosphate and polycaprolactone scaffolds and early implantation: an in vivo pilot study in a porcine mandible model. J Oral Maxillofac Surg. 2015;73(5):1016.e1–1016.e11.
68. Shao H, Sun M, Zhang F, Liu A, He Y, Fu J, Yang X, Wang H, Gou Z. Custom repair of mandibular bone defects with 3d printed bioceramic scaffolds. J Dent Res. 2018;97(1):68–76.
69. Obregon F, Vaquette C, Ivanovski S, Hutmacher DW, Bertassoni LE. Three-dimensional bioprinting for regenerative dentistry and craniofacial tissue engineering. J Dent Res. 2015;94(9 Suppl):143S–52S.
70. Maroulakos M, Kamperos G, Tayebi L, Halazonetis D, Ren Y. Applications of 3d printing on craniofacial bone repair: a systematic review. J Dent. 2019;80:1–14.
71. Hollister SJ, Flanagan CL, Morrison RJ, Patel JJ, Wheeler MB, Edwards SP, Green GE. Integrating image-based design and 3D biomaterial printing to create patient specific devices within a design control framework for clinical translation. ACS Biomater Sci Eng. 2016;2(10):1827–36.
72. VanKoevering KK, Zopf DA, Hollister SJ. Tissue engineering and 3-dimensional modeling for facial reconstruction. Facial Plast Surg Clin North Am. 2019;27(1):151–61.
73. Wong ME, Kau CH, Melville JC, Patel T, Spagnoli DB. Bone reconstruction planning using computer technology for surgical management of severe maxillomandibular atrophy. Oral Maxillofac Surg Clin North Am. 2019;31(3):457–72.
74. Bohner M. Resorbable biomaterials as bone graft substitutes. Mater Today. 2010;13(1–2):24–30.
75. Dorozhkin SV. Calcium orthophosphates: occurrence, properties, biomineralization, pathological calcification and biomimetic applications. Biomatter. 2011;1(2):121–64.
76. Williams DF. Challenges with the development of biomaterials for sustainable tissue engineering. Front Bioeng Biotechnol. 2019;7:127.
77. Abukawa H, Zhang W, Young CS, Asrican R, Vacanti JP, Kaban LB, Troulis MJ, Yelick PC. Reconstructing mandibular defects using autologous tissue-engineered tooth and bone constructs. J Oral Maxillofac Surg. 2009;67(2):335–47.
78. Khojasteh A, Behnia H, Hosseini FS, Dehghan MM, Abbasnia P, Abbas FM. The effect of PCL-TCP scaffold loaded with mesenchymal stem cells on vertical bone augmentation in dog mandible: a preliminary report. J Biomed Mater Res B Appl Biomater. 2013;101(5):848–54.
79. Sandor GK, Numminen J, Wolff J, Thesleff T, Miettinen A, Tuovinen VJ, Mannerstrom B, Patrikoski M, Seppanen R, Miettinen S, et al. Adipose stem cells used to reconstruct 13 cases with cranio-maxillofacial hard-tissue defects. Stem Cells Transl Med. 2014;3(4):530–40.

80. Kawecki F, Clafshenkel WP, Fortin M, Auger FA, Fradette J. Biomimetic tissue-engineered bone substitutes for maxillofacial and craniofacial repair: the potential of cell sheet technologies. Adv Healthc Mater. 2018;7(6):e1700919.
81. Kasper FK, Melville J, Shum J, Wong M, Young S. Tissue engineered prevascularized bone and soft tissue flaps. Oral Maxillofac Surg Clin North Am. 2017;29(1):63–73.
82. Tian T, Zhang T, Lin Y, Cai X. Vascularization in craniofacial bone tissue engineering. J Dent Res. 2018;97(9):969–76.
83. Sharaf B, Faris CB, Abukawa H, Susarla SM, Vacanti JP, Kaban LB, Troulis MJ. Three-dimensionally printed polycaprolactone and β-tricalcium phosphate scaffolds for bone tissue engineering: an in vitro study. J Oral Maxillofac Surg. 2012;70(3):647–56.
84. Visscher DO, Farré-Guasch E, Helder MN, Gibbs S, Forouzanfar T, van Zuijlen PP, Wolff J. Advances in bioprinting technologies for craniofacial reconstruction. Trends Biotechnol. 2016;34(9):700–10.
85. Rai R, Raval R, Khandeparker RV, Chidrawar SK, Khan AA, Ganpat MS. Tissue engineering: step ahead in maxillofacial reconstruction. J Int Oral Health. 2015;7(9):138–42.

Use of Three-Dimensional Dental Impressions in Maxillofacial Surgeries

Irfan Mohammed

Abstract The construction process of 3D solid structures was first introduced by Charles Hull in the year 1983. His technique involved printing three-dimensional structures by using the technique of stereolithography. Today this technique has evolved a lot and took a very important place in modern dentistry. There exist many user-friendly 3D scanners which can be used in dental clinics. The prime objective of the 3D impression-taking process in oral surgeries is obtaining a high-quality copy of one or several implants. This requires structures, healthy adjacent and antagonist's teeth and other maxillofacial regions, establishing a proper interocclusal relationship and then converting this information into accurate replicas of the missing or abnormal implanted structures. This chapter addresses the technical aspects and applications of digital impressions in maxillofacial surgeries.

Keywords CAD/CAM · Bucco-maxillofacial surgeries · Maxillofacial pathology · Reconstruction · Orthognathic surgery · Maxillofacial prosthetics · 3D imaging technique

1 Introduction

Dental Imaging has advanced a lot since W.C. Roentgen has discovered X-rays in early 1896. Many landmark improvements have been in the dental imaging system over a century. It was until the 1990s when the development of digital radiography for dental use was commercialized by the Trophy company who released the RVGui system [1, 2]. Many other companies such as Kodak, Gendex, Schick, Planmeca, Sirona, and Dexis were also involved in design and technology pioneers of digital radiography which exist today in the dental imaging market.

The use of digital technology in dentistry in its various forms, maybe it is with radiography, crown preparation, or robotic surgeries, has been slow but steady and it seems to have been growing with a steep rise every year and have governed partly

I. Mohammed (✉)
School of Dentistry, Federal University of Pelotas, Pelotas, RS, Brazil

R. S. Chaughule, R. Dashaputra (eds.), *Advances in Dental Implantology using Nanomaterials and Allied Technology Applications*,
https://doi.org/10.1007/978-3-030-52207-0_15

by involvement of multidisciplinary professionals involved with dental innovations and technological research involved in this area. Clinical adoption of new technologies has not only saved our time in clinical practice but it has also increased the durability, perfection, and 100% esthetic accuracy in dental prosthesis made using digital dentistry [3].

There are many reasons to adopt digital radiography in daily clinical practice:

- It practically eliminates environmental burdens by removing toxic chemicals along with silver and iodide bromide.
- Accuracy in image processing is increased.
- Increased efficiency of patient treatment by decreasing image capture and visualization process.
- Reduced radiation dose to the patient and operator.
- Improved ability to involve the patient in the diagnosis and treatment planning process with co-diagnosis and patient education.
- Reduced image distortion and improved the final result in patient treatment.

Today computers interface with every facet of dentistry in clinical practice. In the early 1990s, computers were used only in dental clinical accounting and patient record maintenance, but today computers make part of almost all the dental treatments, starting from imaging to milling they are everywhere. These computers have not only increased efficiency and reliability in the financial side of clinical practices but they have also given durability to the dental prosthesis, hence advantage to both patient and dental practitioners [3]. Today one can have virtual patient for diagnosis at anywhere and anytime (Fig. 1), gone were those days where patient has to make various visits to the dental clinic to get his prosthesis done. Today with just two to three visits the dental protocols are ready and delivered to the patients. The digitization of three-dimensional imaging (Fig. 2) has improved communication among fellow and distance practitioners and has enhanced team-based approaches to

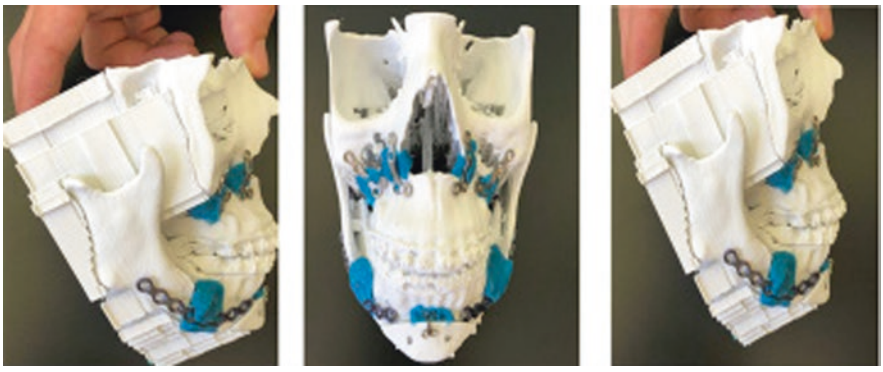

Fig. 1 Biomodel of class II orthognathic surgery for pre-bending plates. (*Image courtesy: Dr. Otacilio Chagas Junior & 3D technology laboratory of Prof. Fernanda Faot at FOUFPEL, UFPel, Brazil*)

Fig. 2 Intermediate splint Project on 3D image, (**a**) frontal view and (**b**, **c**) lateral views. (*Image courtesy: Prof. Dr. Otacilio Chagas Junior & 3D Technology Laboratory of Prof. Dr. Fernanda Faot at FOUFPEL, UFPel, Brazil*)

surgical planning, surgical simulations, and telesurgery that can be performed remotely using robotics.

Among all the benefits brought by three-dimensional dental technology, the role within oral and maxillofacial surgeries involving facial reconstructions is rapidly progressing with a promising future for the patient and dental surgeon. The efficacies of these new technologies were assessed and found to be far better than the conventional and traditional methods used in the past, the drawback was found only with the increased cost equipment installation, but which can be overcome with optimum surgical results, less treatment time, and minimum or no radiation exposure to the patient.

2 CAD/CAM Bucco-Maxillofacial Surgeries

In certain circumstances, facial prosthesis will be better than reconstructions with surgery, for example, in cases with high recurrence, patients undergoing radiation therapy, elderly patients that should undergo multiple reconstructive surgeries, and patients requiring a temporary prosthesis; sometimes the prosthesis is the only option for the suffering patient whose physical condition is not appropriate for reconstruction surgical procedure.

Types of CAD/CAM techniques in dentistry:

- Stereolithography
- Fused deposition modeling
- Selective laser sintering
- Laminated object manufacturing
- Multi-jet modeling inkjet technology
- Three-dimensional printing (3D printing)
- Solid ground curing

With the help of CAD/CAM technology, we can construct or fabricate customized tools to be used during the maxillofacial surgery in an efficient and accurate manner [4–6].

These surgical tools include various forms:

- Customized anatomical replicas.
- Cutting guides for osteotomy design.
- Implant placement guides.
- Anatomical replicas used in the preoperative bending of reconstruction plates.
- Customized bone appliances design.
- Fabrication of customized implants.

All surgical custom designs start with imaging process, where digital images are converted into a 3D format known as STL file format (Stereolithography file format) which is native to the stereolithography CAD software created by 3D Systems. STL has several backronyms such as "Standard Triangle Language" and "Standard Tessellation Language." STL files describe only the surface geometry of a three-dimensional object without any representation of color, texture, or other common CAD model attributes [7].

3 CAD/CAM Maxillofacial Pathology and Reconstruction

Preplanned osteotomies and segment positioning using CAD/CAM have made maxillofacial surgeries more efficient and with promising postoperative success (Fig. 3). The use of microvascular surgeries and advanced techniques in this field has become more widespread in maxillofacial pathology reconstruction with the

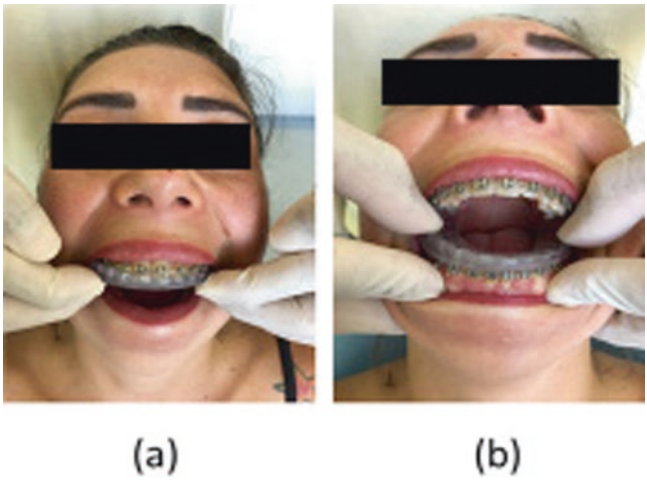

Fig. 3 (**a**) Pre- and (**b**) postoperative images of orthognathic surgery. (*Image courtesy: Prof. Dr. Otacilio Chagas Junior & 3D Technology Laboratory of Prof. Dr. Fernanda Faot at FOUFPEL, UFPel, Brazil*)

help of CAD/CAM [8], and has helped to recover large and complex buccofacial defects in a short intraoperative time.

3.1 The Principal Aim of Using CAD/CAM in Maxillofacial Pathology Reconstruction

The Principal Aim is the reduction of intraoperative time and ischemic time to the flap following ligation of the vascular pedicle, accurate superpositioning of the flap and anticipated reconstructed segment contouring [6].

Surgical steps/procedure are:

- First, planned resection virtual surgery is performed after uploading the imaging data.
- Margins are drawn which is followed by the interval of bone removal, and an image of the bone used for reconstruction is adjusted to the defect using virtual osteotomies.
- The collected data from the surgical plan is then used for the fabrication of cutting guides.
- The guides are designed with predetermined angled slots that allow the entry of surgical cutting blades for osteotomy of the boné.
- The guide's holes allow them to be secured to the bone during instrumentation.
- In instances where postoperative radiation is not anticipated, guides may also be used for the simultaneous placement of implants.

It is to be noted that before transection of the pedicle it can be performed the osteotomies, implant placement, and attachment of the reconstruction plate to the bone flap.

4 CAD/CAM Correction of Temporomandibular Joint Disorders

It was only possible with CAD/CAM technology the development of customized TMJ prostheses and it is evolving in reconstruction improvement day by day. Today long-term success in TMJ prostheses is seen due to minimal bony re-contouring process which is required to fit the unit in position. Also the reduction of operative time by decreasing the surgery table adjustments and special preparations for the surgery, all these advantages have reduced or completely eliminated multiple surgical procedures and the creation of complex anatomy in the surgery region (postoperatively) [6, 9]. The improved stability created by CAD/CAM can improve the long-time success and durability of the prosthesis.

5 CAD/CAM Orthognathic Surgery

Treatment planning, intraoperative process, and postsurgical analysis and evaluation have been highly influenced by three-dimensional imaging and CAD/CAM technologies which have greatly impacted the approach to orthognathic surgery (Fig. 4).

A considerable amount of data is collected during the presurgical evaluation. This includes the following:

- Clinical examination
- Dento-facial measurements
- Profile and intraoral photographs
- Dental impressions
- Bite registrations
- Cone-beam CT scan
- Virtual facebow

Following are the surgical data collection steps/procedures:

1. Acrylic resin jig with attached fiducial markers is used for the initial bite registration.
2. The bite jig is attached to a gyroscope and a virtual facebow is performed, which provides a numerical value for pitch.
3. The CT scan is performed with the bite jig in place. Using the data obtained from the gyroscope, the CT image can be reoriented to the patient's natural resting head position.
4. Next, the dental casts are sent for processing.
5. For better accuracy, digital imaging of the dentition is performed via a laser surface scan of the dental casts.

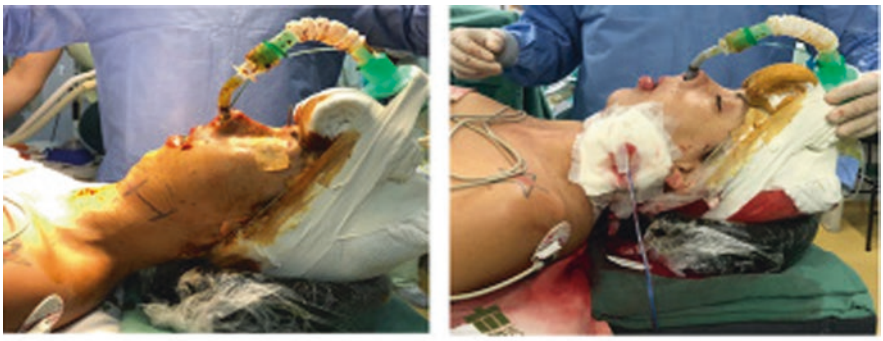

Fig. 4 Post 3D printing splint trial in the patient mouth, (**a**) superior splint and (**b**) inferior splint. (*Image courtesy: Prof. Dr. Otacilio Chagas Junior & 3D Technology Laboratory of Prof. Dr. Fernanda Faot at FOUFPEL, UFPel, Brazil*)

6. This data is then integrated with the CT scan. The DICOM files from the CT scan may be used for both 3D and 2D assessment.
7. Cephalometric analysis is performed using traditional landmarks in order to quantify the dental and skeletal relationships.

The three-dimensional analysis will help in identifying and quantifying facial asymmetries during the treatment plan. Cast surgery is performed after data collection and cephalometric analysis. This can be a time-consuming process and the accuracy of planning for complex movements can be challenging particularly for patients with asymmetries.

The real-time dental-skeletal relationship obtained by the 3D image assessment by performing various virtual surgical movements. In addition, this allows for the identification of various skeletal interferences that may arise, especially with mandibular setbacks. Repositioning of maxilla and mandible is done after confirmation of the surgical plan and with the help of CAD/CAM, the occlusal splints are fabricated. Finally, 3D imaging allows for an enhanced understanding of the postsurgical change during recall. Using stable skeletal landmarks in regions that were not changed by surgery, the pre- and postoperative CT images can be superimposed to demonstrate the final outcome.

6 CAD/CAM Esthetic Facial Surgery

Today CAD/CAM technology plays a very crucial role in custom facial implants fabrication. Many facial deficiencies and anomalies can be corrected by excellent facial contouring with custom implants made by CAD/CAM. Modified stock implants can fulfill the void of immediate implant procedures which requires little or no modifications prior to placement in the facial region in order to minimize contouring irregularities or surgical space fillings. Sometimes during this contouring or while surgery, implant correction procedures may prolong operative time and minor visible irregularities may persist after surgery.

Assessment of the operative region before the surgery using 3D CT scan imaging technology allows the surgeon to take better decision regarding the surgical approach and techniques used in correcting the hypoplastic regions. On the other hand, the CAD/CAM technology allows for the fabrication of a precision custom implant with increased predictable improvements of enhancement also which directly helps in better adaptation to the underlying skeletal structures giving an ideal anatomical contouring.

Gone those days where the patient required to take facial impressions and custom implants made without digital technologies which required lots of required patient compliance and most of the time impressions did not accurately capture the underlying skeletal structures making inaccurate impressions and quiet messy procedure.

There are a variety of ways to produce custom implants; most of them follow the same following methodology:

- Creation of a stereolithographic model and a modeling putty is provided.
- The área of interest is molded and adapted with modeling material.
- This is then sent to a manufacturer for the fabrication of the final implant.
- In this process, virtual planning is available as well which has the advantage of allowing for mirroring of the digital image which aids in the correction of facial asymmetries in unilateral defects.

7 CAD/CAM Maxillofacial Prosthetics

To esthetically correct the maxillofacial defects it is better served with a prosthetic implant approach along with microvascular surgery for excellent results in some cases. Retention is the prime problem in some of these cases. Various options are available to overcome these problems like including tissue adhesives, carriers such as eyeglasses, and osseointegrated implants and many more. Three-dimensional digital technologies have changed the treatment planning for the implant-associated maxillofacial prosthesis to a great extent. The accurate placement of intraoral and extraoral implants is only possible with advanced 3D digital impression technology; the no functionality created by improper spacing, depth, and angulation which was faced in the past is now overcome by the advantages of using 3D technology in dentistry. Apart from creating accurate implants, the three-dimensional imaging helps in the assessment of residual bone available and identification of the distances from vital anatomical structures [3, 5].

When it comes to interdisciplinary work the digitization of data images allows for enhanced collaborative communication among the surgery team members. The superimposition of soft tissue reformat with the help of 3D imaging over the skeletal structure helps us to overcome the problem of variability of over lying soft tissue thickness which otherwise poses another challenge to extraoral implant-retained prostheses.

Sometimes the trial pattern has marginal deficiencies while fabricating which needs to be adjusted; this is because some software cannot be used for superimposing or they do not superimpose accurately. The other way to overcome this problem is to take the digital data of a patient defect using photographs or scans, next superimpose the patient's data with data from the data bank. By doing this the margin and shape of the prosthesis can be adjusted according to the area of the defect. Hence the software selection is very important during the reconstruction process.

One of the areas that has developed most significantly has been the construction of metallic structures for prosthodontics. More recently, the additive technique of selective laser melting (SLM) was developed for construction of RPD infrastructure. SLM produces three-dimensional metal structures directly from a CAD model, with layers of powder materials which have been melted and layered over each

other using a laser. It allows for the creation of complex geometries with concave and thin zones at the base of the metal structure which are very difficult to achieve using subtractive methods [3, 4].

8 CAD/CAM Oral and Maxillofacial Surgery

Template guided approaches and surgical navigations obtained via CAD/CAM are part of digital surgeries in modern dentistry. Data obtained from the 3D imaging technique is used for navigation to provide directional and spatial assistance to surgeons during the surgery.

The use of CAD/CAM techniques in maxillofacial surgeries has several advantages over manual procedures such as clinicians have digital data that can be used repeatedly for the purpose of making a trial pattern or facial prosthesis. Trial pattern made with CAD/CAM technique can be adjusted for its thickness so that the final facial prosthesis can be made as light as possible while maintaining its shape and texture [10], apart from this it creates shorter fabrication time, requiring less excellent clinical skills but high software and technological knowledge.

It is very important to note that the image guidance is provided in real time and the imaging is obtained prior to surgical navigation. To overcome volumetric deformations associated with MRI data, CT scans are most commonly used which are precise images [10]. Image slices around 1 mm assure the accuracy of imaging techniques. The data obtained is then uploaded to the computer module. Anatomical landmarks are registered on the patient and interrelated with the same regions on the uploaded imaging.

The landmarks vary from the surface landmarks, screws placed and secured to bony prominences, or using landmarks attached to a mask secured to the patient. The landmark registration is performed using a stylus, which is recognized by a camera linked to the imaging display module. Each landmark is confirmed between the display image and the patient. The camera links to the registered stylus using either infrared, electromagnetic, or ultrasound data transfer [11].

During surgery, it is important to verify the previously registered landmarks. In some cases, the error may be introduced from any kind of surface tissue movement or following surgical manipulation. According to the literature, the accuracy of anatomical localization is near about 1 mm.

The main aim of this technology is to reduce morbidity and invasiveness and assist with image-guided localization of surgical landmarks. Access to the operation site is a common challenge of most surgeries, and also restricted visualization by anatomical structures and cosmetic demands. Deep orbital regions are sometimes difficult to reach and particularly challenging, in such cases the digital image guidance is helpful to avoid accidents with vital structures here such as the optic nerve. Normative values reference is used to determine safe dissection distances from the intraorbital rim to each structure situated nearby. These reference values become immaterial if there is extensive comminution of the rim which also complicates

proper reduction and subsequent esthetic outcome of traumatic bony defects. Verification of reduction is lost with the loss of bony landmarks. As a result, the accuracy in the projection of the involved bone is challenged and results in compromised facial esthetic.

Mirroring technique is used:

- To correct the unilateral facial defect the surgical navigation software can help restore facial symmetry through the use of mirroring.
- The image of the uninjured side is replicated, a mirror image is created and superimposed to the injured side.
- The malpositioned bone is then repositioned in its right anatomical position three-dimensionally until a desired projection is obtained and verified using the navigation module [12]. Fixation is then applied.

In some situations where the bilateral destruction is very vast that the mirroring techniques are not possible in such situations, the surgeon can go for the patient's siblings or children's facial impressions where the facial appearance and contours are more likely to match the reconstruction process.

9 CAD/CAM Robotic Maxillofacial Surgery

Minimally invasive surgery has evolved to include robotic or computer-assisted surgery. Robotic surgeries using smaller incisions and endoscopy technology have reduced manpower in the surgery hall; it has even benefited the postoperative patient care process by reducing blood loss, suture dimensions, decreased pain, and decreased use of analgesics postoperatively and all these have directly contributed to faster patient recovery.

The robotic surgeries have been around for many years but their use was limited to medical surgeries like cardiac, urological procedures and obstetrics, but in recent years it has been used in T1/T2 tumors treatment involving head and neck region. This technology is known as TORS (Transoral Robotic Surgery), which has eliminated the aggressive mandibulotomy procedures in many complex cases of oropharyngeal tumors and reduced surgical unnecessary mutilations of buccofacial region.

Following are the basic concepts of robotic surgeries:

- All the delicate and complex surgical movements are controlled by robotic arms distantly from a console.
- Direct instrument manipulation is eliminated completely.
- Most of the time the surgical procedure is performed from remote locations.
- Visualization is improved with high-end laparoscopic instruments and the delicate high precision robotic arm movements allow for more degree of surgical movements.

- Basic components involved include the surgeon's console, robotic arms with attached instruments, and a hi-definition camera, which transmits images to the console.
- Scaled-down micro-movements of the remote robotic arms are transmitted from the surgeon's finger movements from the console.

The initial setup of the Robotic unit may cost very high, but public funded units and government hospitals can install one of this surgical equipment which will decrease inpatient time and reduce other postoperative costs for government and patient, the drawbacks which involved also include the time and investment required to train the surgery staff and preoperative setup duration (Fig. 5).

10 The CAD/CAM Implant Manufacturing Procedure

There are two types of implant manufacturing procedures:

- Subtractive manufacturing
- Additive manufacturing
- Subtractive manufacturing: which cuts off a piece of material to form the final shape.
- Additive manufacturing: which builds up the material by stacking.

Subtractive manufacturing, the traditional machining technique, has the disadvantage in which it is difficult to make complicated shapes by computer numerical control (CNC) milling and there is a lot of material waste. Additive manufacturing, known as rapid prototyping or 3D printing, has the advantage of being very sophisticated, with less material waste, faster production times, and the ability to produce complex structures (Fig. 6)

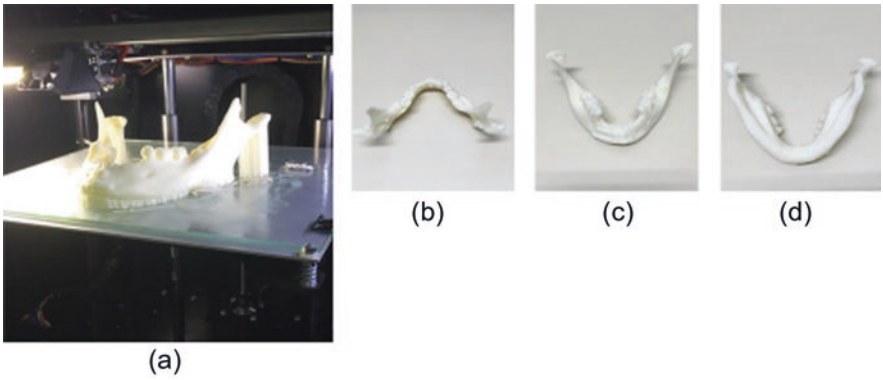

Fig. 5 Finalizing mandible printing at 3D printer set, printed mandible biomodel. (**a**) Mandible printing at 3D printer set, (**b**) Posterior view, (**c**) superior view, and (**d**) inferior view

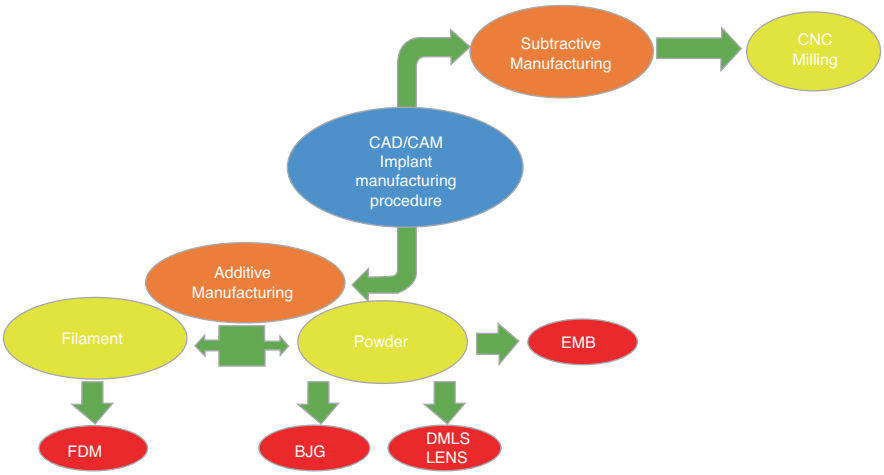

Fig. 6 Manufacturing process of CAD/CAM implants. (*Art by Dr. Mohammed Irfan*)

Types of additive manufacturing processes:

- Binder jetting (BJG)
- Direct metal laser sintering (DMLS)
- Electron beam melting (EBM)
- Laser engineered net shaping (LENS)
- Fused deposition modeling (FDM)

11 Conclusion

Technological developments are not intended to replace physical examinations or human to human health care assessment and service providing but to help as adjunct to investigation and care to provide, the outcome of the surgery exclusively depends on the surgeon's decision based on diagnosis and patient history gained by physical examination; hence physical examination along with the help of technology will continue to transform the health care industry.

The drawbacks of these modern technologies are their high costs and sophisticated digital tool and techniques expertise which keep us away from advantages of using these technologies in our day-to-day clinical practice, but some of our fellow professionals have used their creativity to breakthrough these difficulties. Gamarra et al. used a camera phone and free software to convert two-dimensional photographs into three dimensions to obtain digital data in the fabrication of facial prosthesis. This statement does not encourage to make use of free software to treat patients but it serves as the humanitarian use of scientific advancement removing the cost factor and making technology affordable to bring prosperity to the human

race; it is very important to remove the financial barriers which deprive human race from basic rights of health.

Always the patient should be given information about the treatment plan along with the limitations of the prosthesis. This is very important because of the patient's very high expectation of his new prosthesis. Many health research on the quality of life of patients with cancer in the head and neck areas show high levels of emotional stress, physical limitations, facial or body shape changes, and poor social relationships. Our face is a prime identity in society; hence we as buccofacial surgeons should make the treatment process as transparent as possible to our patients.

CAD/CAM technology has made surgeries much easier than before but we cannot lose sight of traditional methods such as imaging that may allow for a closed or limited access approach during surgery; there can be situations where the surgeon has to perform open approach as a result of equipment failure or complications during surgeries. These technologies have helped us treatment and evaluation predictions even before surgeries and made our understanding much refined regarding complex anatomical structures which are difficult to access in some situations. Today we have better understanding of anatomical limitations which are uniques to each patient apart from facilitating surgical procedures. The technology has also enhanced our learning by using these technologies as educational tools to our future buccofacial and dental surgeons.

Today the modern digital dentistry has made reconstruction intentions more quantized and applied more accurately offering more tailored end products with less intraoperative effort. Esthetic was never before much accurate than now and this was only possible by virtual surgical decisions before performing the surgery, predicting the soft tissue response to skeletal manipulation that has both functional and esthetic implications.

Digital workflows cannot be used for emergency situations due to their time-consuming process which can delay emergency post-traumatic surgery implants. It takes few days to weeks to construct the PSI in laboratory establishment outside the hospital or clinic; however, this can be overcome by 3D printers which are relatively inexpensive and modern researches have made them more accurate, making it possible to manufacture anatomical structures within the operating premisses reducing the time and risk of transport.

References

1. Mouyen F, Benz C, Sonnabend E, Lodter JP. Presentation and physical evaluation of RadioVisioGraphy. Oral Surg Oral Med Oral Pathol. 1989;68(2):238–42.
2. Benz C, Mouyen F. RadioVisioGraphie—system for film-free intraoral radiographs [Article in German]. Dtsch Zahnarztl Z. 1989;44(3):177–9.
3. Mendes TA, Marques D, Lopes LP, Caramês J. Total digital workflow in the fabrication of a partial removable dental prostheses: a case report. J SAGE Open Med Case Rep. 2019;7:1–5.
4. Koutsoukis T, Zinelis S, Eliades G, et al. Selective laser melting technique of Co-Cr dental alloys: a review of structure and properties and comparative analysis with other available techniques. J Prosthodont. 2015;24(4):303–12.

5. Yeung M, Abdulmajeed A, Carrico CK, Deeb GR, Bencharit S. Accuracy and precision of 3D-printed implant surgical guides with different implant systems: an in vitro study. J Prosthet Dent. 2020;123:821–8. https://doi.org/10.1016/j.prosdent.2019.05.027.
6. Takano M, Sugahara K, Koyachi M, Odaka K, Matsunaga S, Homma S, Abe S, Katakura A, Shibahara T. Maxillary reconstruction using tunneling flap technique with 3D custom-made titanium mesh plate and particulate cancellous bone and marrow graft: a case report. Maxillofac Plast Reconstr Surg. 2019;41(1):43.
7. Orentlicher G, Horowitz A, Abboud M. Computer-guided implant surgery: indications and guidelines for use. Compend Contin Educ Dent. 2012;33(10):720–32.
8. Zheng J, He H, Kuang W, Yuan W. Presurgical nasoalveolar molding with 3D printing for a patient with unilateral cleft lip, alveolus, and palate. Am J Orthod Dentofac Orthop. 2019;156(3):412–9.
9. Chen S, He Y, An JG, Zhang Y. Application of computer-aided virtual mandibular position in the simultaneous treatment of children with temporomandibular joint ankylosis and jaw deformity [Article was translated from Chinese]. Beijing Da Xue Xue Bao. 2019;51(5):954–8.
10. Wubulihasimu Z, Tuerhong M, Zhang Z, Li H, Kadir N, Xie M, Abulaiti M, Abulaiti A, Tulamaiti N, Maimaitiming B, Aili W, Ni Y. Clinical analysis and CT 3D-mediated precise internal fixation in maxillofacial fracture. Ear Nose Throat J. 2019; https://doi.org/10.1177/0145561319882114.
11. Kaduk WM, Podmelle F, Louis PJ. Surgical navigation in reconstruction. Oral Maxillofac Surg Clin North Am. 2013;25(2):313–33.
12. Bui TG, Bell RB, Dierks EJ. Technological advances in the treatment of facial trauma. Atlas Oral Maxillofac Surg Clin North Am. 2012;20(1):81–94.

Use of Zygomatic Implant on the Severe Atrophic Maxilla

Marcelo Melo Soares, Andrea Castilho, and Claudia Caminero Soares

Abstract Osseointegrated implants are the most effective tool for rehabilitation of total or partial edentulous patients; however, the presence of bone atrophy is an obstacle for the use of implants. On severely resorbed maxilla the limitations for the installation of conventional implants requires alveolar reconstructive procedures with the use of autogenous bone grafts harvested from iliac intraoral donor sites or autologous bone graft, increasing morbidity and cost of the treatment.

As an alternative to the use of large bone reconstruction, Brånemark in 1984 proposed that the zygoma bone can be used as anchorage for long implants supporting prosthetic rehabilitation. Actually, zygomatic implants are the most effective option to bone grafts on the rehabilitation of edentulous patients with severe resorbed maxilla.

Despite the high rate of success of zygomatic implants for edentulous patients, their indication on partial edentulous has been restricted to hemimaxillectomized patients. In this chapter we will discuss the importance of virtual planning to correctly disseminate the masticatory forces on these implants and the importance in technology as a fundamental factor of treatment success.

Keywords Zygomatic implants · Atrophic maxilla · Maxillary reconstruction · Bone graft · Dental implants · Oral rehabilitation · Atrophic maxilla

M. M. Soares (✉)
Osteogenesis Research Institute, São Paulo, Brazil

Oswaldo Cruz Hospital, São Paulo, Brazil

SENAC Trainee Program on Oral and Maxillofacial Surgery, São Paulo, Brazil

A. Castilho
SENAC Trainee Program on Oral and Maxillofacial Surgery, São Paulo, Brazil

C. C. Soares
Prosthodontics and Periodontist, Osteogenesis Research Institute, São Paulo, Brazil

R. S. Chaughule, R. Dashaputra (eds.), *Advances in Dental Implantology using Nanomaterials and Allied Technology Applications*,
https://doi.org/10.1007/978-3-030-52207-0_16

1 Introduction

Dental implants have revolutionized the rehabilitation of the masticatory function in edentulous patients, providing a predictable, functional, and esthetic alternative to conventional dentures. However, long-term edentulism, with severe bone loss and sinus pneumatization, leads to significant reduction in bone anchorage [1, 2]. Trauma, craniofacial deformities, or ablative surgery sequelae may reduce the amount of bone available, resulting in bone discontinuity and compromise the quality and quantity of the remaining soft tissue available for graft coverage [3–6]. The insufficient height and width of the alveolar ridge at the implant site in the severely atrophied maxilla constitutes a therapeutic challenge for surgeons, requiring advanced reconstructive alveolar surgery, increasing costs and morbidity [4, 7–9].

The original purpose of zygomatic implants (ZI) was the rehabilitation of patients with congenital deformities who underwent ablative surgery like maxillectomy tumor resection [10]. The severely atrophic maxilla shows less or no alveolar bone for implant anchorage, poor vascularization, and insufficient soft tissue for the coverage of grafts. The challenges faced by the surgeons in the rehabilitation of these patients are similar to those of maxillectomy patients [4, 9, 11]. Brånemark expanded the indications for zygomatic implants (ZI) and introduced ZI as an alternative system to overcome the problems associated with the rehabilitation of the atrophic maxilla [1, 10, 12].

Although the planning and execution of ZIs is more complex than that of conventional implants, the functional and esthetic results are very gratifying, with a success rate of 96–98% and a low rate of complications, making ZIs a reliable alternative for the rehabilitation of the complex severely atrophic maxilla [13–17].

2 Indications

The success of any bone graft is dependent on the quality of the soft tissue cover, graft stability, the osteogenic potential of the recipient bed, and the grafted material. A favorable flap placement and graft stabilization is achievable in the maxilla because it is fixed bone and has excellent vascularization. However local inflammatory factors such as chronic periodontitis, recurrent infections, traumatic surgeries, and previous graft failures may compromise flap mobility and dramatically reduce maxillary vascularization, compromising the success of reconstructive bone grafting procedures [5, 13, 15, 18]. The Schneider membrane is highly vascular and has high osteogenic potential, being one of the best graft receptor beds in the face, and one of the factors for the high success rate of sinus lift procedures. However factors such as age, systemic or sinus diseases, smoking, and others reduce this capacity of the sinus membrane, leading to extensive resorption of the sinus grafts [2, 9]. The primary indication for ZIs is cases where the prognosis of the grafts is poor or where contraindications to conventional reconstructive surgery exist [4, 14, 19].

ZIs may also be an alternative to grafting procedures by facilitating immediate loading, reducing the rehabilitation time, necessitating a less invasive surgery compared with autogenous bone graftings by eliminating the donor bed, reducing the

total cost of treatment as it can be performed in a single procedure, and eliminating bio-material or extraoral graft removal costs [6, 7, 14, 20, 21].

ZIs indicated in elderly patients not only for the poor prognosis of grafts in this age group but also due to the use of artificial gums as a tool to correct the high bone loss, resulting in a more acceptable prosthesis [6, 16, 17, 22]. The palatinized head position of the ZIs at the first protocols resulted in the adoption of ZIs as a last resort in patients with advanced atrophy of the maxilla. However, the high success rate and the polarization of the position of the implant head over the intrasinus insertion of the implant body according to the concept of prosthetic reverse planning [23, 24] have led more and more surgeons and patients to choose ZI modality over maxillary grafting for fixed prosthetic rehabilitation (Fig. 1).

2.1 Contraindications

ZIs are contraindicated in patients with chronic maxillary sinus diseases, malar bone defects or malformations, patients with irradiated head and neck (with doses over 70 Gy), patients on immunosuppressants, immunodeficient patients, and patients with psychiatric problems and uncontrolled diabetics.

The relative contraindications for ZIs are young patients, presence of oroantral communications, partial edentulism, pregnancy or lactation, and severe uncontrolled periodontal disease.

3 Biomechanics of Zygomatic Implants

Although ZIs have long screws, only one-third of the implant body is in contact with bone, so proper selection and placement of the implant is essential for successful

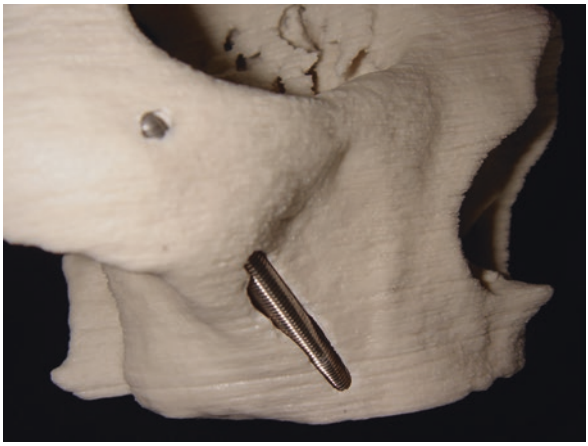

Fig. 1 ZIs are long implants that have a strong anchor in the zygoma, a dense bone of the face. Due to the high torque and proximity with alveolar bone, they can provide an excellent alternative to the rehabilitation of atrophic maxillae without the need of reconstructive surgeries, reducing time, morbidity, and cost of the treatment

rehabilitation [25]. The zygomatic bone is a pyramidal structure with a square base, with an average length of 14.1 ± 4.7 mm on the transverse axis of the zygoma body, allowing for an excellent area for insertion of implants and a high-quality dense bone. The jugal point which is the point of bone insertion of ZIs shows a wide and dense cortical bone on histologic analysis permitting an excellent anchorage point for the implants [26–28].

The surgical technique influences the bone-implant contact with the extramaxillary exhibiting higher bone-implant contact area compared with the intra sinus approach [29, 30]. Axial loads are favorable for conventional implants with limitations to the lateral and rotational (momentum) loads [26, 31]. ZI shows a unique load distribution, because it is an inclined implant and the occlusal stresses are not borne significantly by the alveolar crest. Mathematical models demonstrate that the vertical and axial loads are lesser in ZIs because the load is transmitted in several directions due to the three-dimensional angulation of the implants [26].

The occlusal load is distributed through the infrazygomatic crest and divided into the frontal and temporal processes of zygomatic bone, with a stress concentration along zygomatic-maxillary suture, similar to the stress load distribution in the edentulous jaw. Stress under lateral loads, is generated at the connection of fixture and abutment, showing possible marginal bone loss around the head of the implant and components failures. To prevent rotational loads the ZIs must be connected to conventional (or zygomatic) implants as anterior as possible and a contralateral zygomatic (or conventional) implant nullifying twist and reducing load under the fixture-abutment joint [25, 32].

3.1 Finite Element Analyses (FEA)

FEA shows that stresses due to occlusal forces are mainly withstood by zygomatic bone, being transferred through the infrazygomatic crest and divided into the frontal and temporal processes of zygomatic bone in two directions. Since Stress under the zygomatic-maxillary suture was also reported, it is reasonable to conclude that height stress also occurs *in vivo*. The stress in the implant model is generated at the center of the implants and into the joint of the fixture-abutment connection. Vertical and lateral loads are not favorable from a biomechanical perspective because though the angulation and three-dimensional space distribution of the zygomatic and conventional implants theoretically prevent rotational loads by load-stress dissipation in several directions, they cannot avoid fixture-abutment stress under lateral load [25, 31].

Despite the versatility and reproducibility of FEA for the evaluation of forces on biological models, the majority of FEA studies on ZIs use homogenous models. When pre-load stress is considered, the forces under the fixture-abutment connection are reduced, showing that more detailed models are needed for a better simulation as this is a critical point for force concentrations and failures [33].

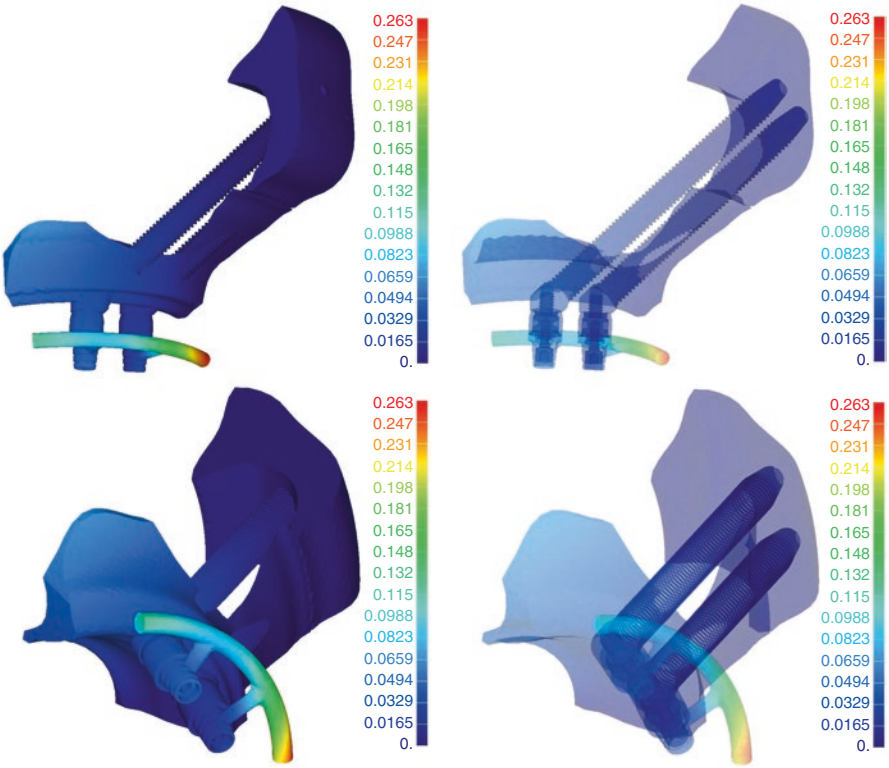

Fig. 2 The Von Missel scale shows the stress on the framework and distribution of load on the bar. This simulation demonstrates the importance or proper implant position and the use of metallic bars for abutment connection

FEA of the bridge (Fig. 2) shows that the magnitude of stress support is not increased by the presence of bone at the alveolar ridge, regardless of the direction of the load, being more than two times of occlusal forces, when no alveolar bone is present on the head of the implant. Thus, it shows that although the presence of alveolar bone anchorage is beneficial for force distribution, the crestal position of the head is more important for the bridge force dissipation than the palatal position [34] because stress is more gradually redistributed over the maxillary sinus and cranial structures by the extra-sinus approach [25].

In FEA studies anterior conventional implants reduce the stress generated on the body of the ZIs. ZI shows superior results in FEA when compared to all-on-4 techniques. There is no stress load in the alveolar processes of anterior implants when associated with ZIs. All-on-4 fixed dentures have no bone safety margin with significant reduction of stress values in posterior alveolar bone, but increase in stress on anterior alveolar bone. The stress value for ZIs is around 30% [11, 33, 35].

4 Surgical Technique

The technique of ZIs has evolved since it was introduced by Brånemark in 1998. Several modifications were introduced in order to improve implant head position, increase bone anchorage, reduce morbidity, or consider anatomical variations in the atrophic maxilla. We will describe the most significant modifications of the original technique.

4.1 The Zygoma Implant Set

The zygoma set is very similar to the conventional 4.1 mm implant set, with similar drill sequences, implant driver, cover screw and healing screw drivers, measurements of deeper gauge, zygoma retractor, lip commissure protector, assembler piece, adapter for drills, and a handpiece for manual implant insertion. Some implant sets also provide a very useful drill with lateral diamond cut surface for the opening of the antrostomy slot, resulting in a faster and safer procedure. All drills and instruments are adapted to the size and anatomy of zygoma.

The length of the drills and the angulation required to reach the zygoma have to be considered at the clinical evaluation, as the presence of mandibular teeth or prosthesis, mouth opening restrictions, etc. are the factors that may influence on the ease of the drilling process.

Although most sets are very basic, few sets offer an option of shorter and longer length of drills and options that can be useful for the adjustment of the implant position and variations according to jaw size. Based on this, some customization of the set may be helpful. Working with multiple sets will provide more than one standard drill size; the drills and deeper measurements gauge can offer more versatility on the first drilling and allows measurements on initial perforations.

Retractors are essential for proper surgical field visualization. The mouth opener used by orthodontists for appliance installation can provide an excellent general mouth view which can be improved by the utilization of a reverse Langenbeck retractor usually used for Le Fort I osteotomy, or a laster retractor, developed for the visualization of maxillary third molars. This will provide an excellent visualization of all the anatomic landmarks necessary for ZI installation (Fig. 3).

4.2 Classical Zygomatic Approach

The classical approach consists of a molar-to-molar palatal incision. A flap is reflected exposing the palatal and crestal bone. The detachment of the mucosal flap involves the exposure of the piriform rim with detachment of the nasal mucosa, the exposure of the anterior wall of the maxilla, the pterygoid buttress towards the

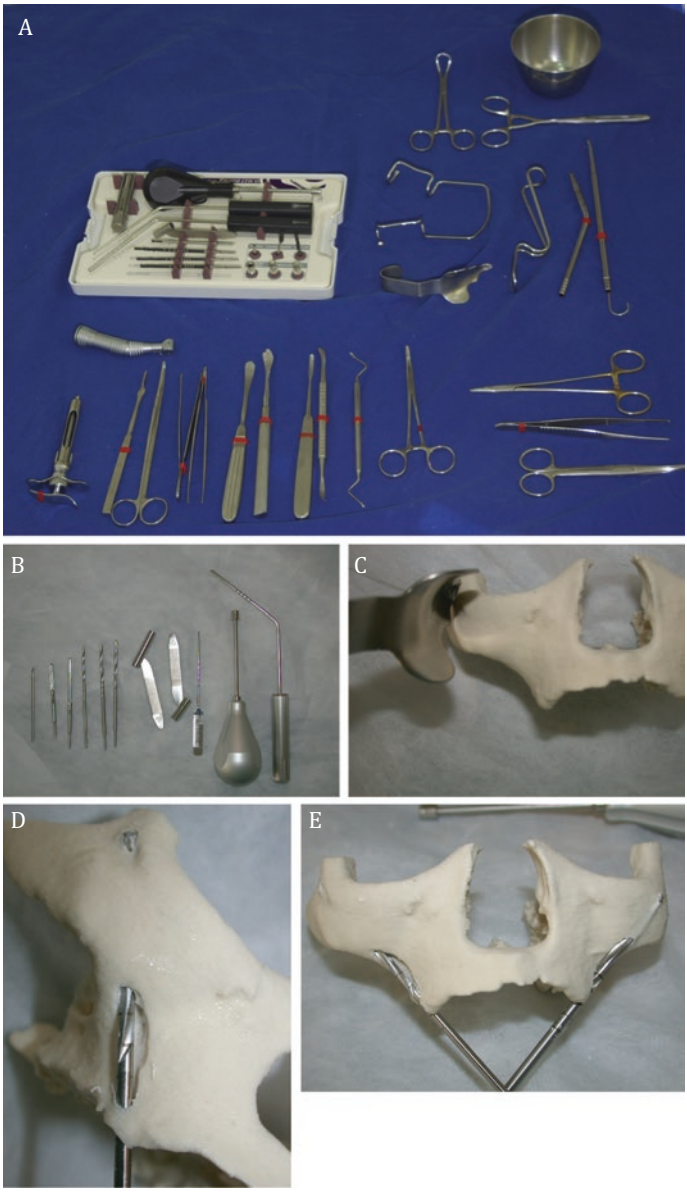

Fig. 3 Instruments for ZI surgery retractors, detachers for oral and sinus mucosa, set for irrigation and suture (**a**), components of the ZI set; drill sequence, lip retractors, measurements gauges, insert handpieces (**b**), Laster's retractor for visualization of zygoma base osteotomy point and implant top reference (**c**), perforation drill (2.8 mm) osteotomy at the base of zygoma showing entry point (**d**) and the symmetry between both sides (**e**)

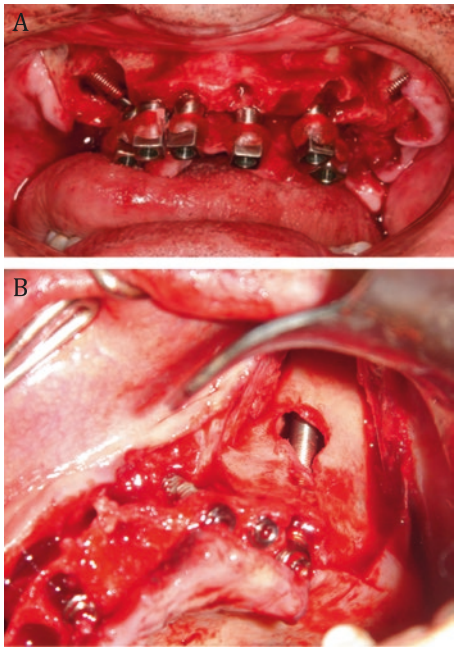

Fig. 4 Classical approach with the sinus membrane detachment and the intra sinusal path of ZI into the base of zygoma (**a**). Crestal incision and antrostomy reduction in order to preserve the alveolar ridge (**b**)

zygomatic bone, with the infraorbital nerve and the zygomatic body and arch into the zygomatic malar suture, providing a complete exposure of the anterior maxillary and zygomatic structures. Using a round bur a large window is opened in the anterior wall of the maxilla in order to access the sinus. The Schneiderian membrane is reflected creating an accessory cavity inside the maxillary sinus for implant drilling. The zygoma base is drilled while protecting the membrane and the implant body is inserted into the maxillary sinus [1, 7, 10] (Fig. 4).

4.3 Sinus Slot Approach

The sinus slot technique was proposed by Stella and Warner and consists of a molar-to-molar crestal incision with a bilateral posterior vertical releasing incision. The palatal mucosa is exposed just enough to expose the crest and bur position. The flap is reflected from the base of piriform rim up to the inferior aspect of the infraorbital nerve and zygomatic buttress and half of the body of zygoma.

A perforation through an alveolar bone in the direction of the zygoma body is made with a fissure or a Lindemann bur, on the position planned for the implants head after a depth gauge is placed on the hole. The path of the implant is simulated and the superior point is marked. A second bur is then used to prepare a small window (slot) connecting the alveolar ridge (or the implant head), through the sinus, with the base of zygoma. The slot produces a small antrostomy that allows the

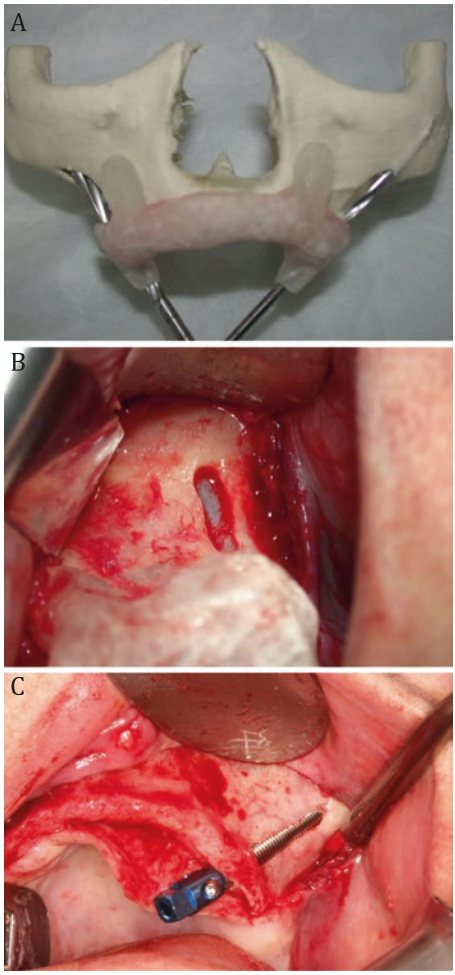

Fig. 5 (**a**) 3D stereolithographic model for surgical and prosthetic planning. Surgical guide was fabricated for determination of implant head position and as a path to avoid drilling angulation error. (**b**) Slot and membrane deflection for drill irrigation and implant insertion in the base of zygoma. (**c**) Implants installed according to the prosthetic planning

reflection of Schneiderian membrane, allowing safe drilling for the implant and proper irrigation on the top of the drill [23, 24] (Fig. 5).

4.4 Extramaxillary Approach

The extramaxillary approach consisted of a supra crestal incision similar to the one described by Stella, allowing the visualization of the maxillary anatomical structures and zygoma bases. A spherical or a Lindemann bur is used to perforate the alveolar crest, emerging on the vestibular face of alveolar ridge, drilling until the base of the zygoma body. The drilling osteotomy is progressively widened according to the zygomatic implant protocol. No antrostomy is performed on the extramaxillary approach [30] (Fig. 6).

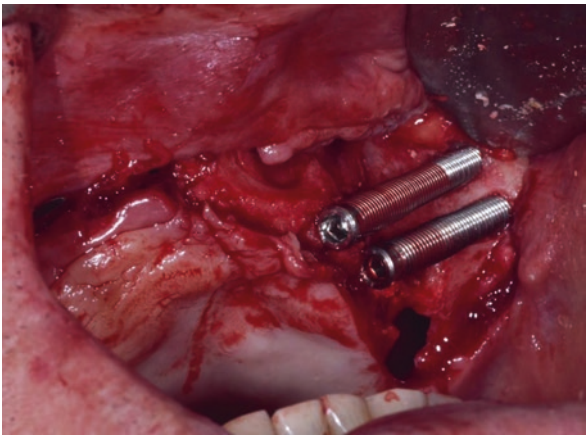

Fig. 6 The extramaxillary approach does not require antrostomy; the ZI passes external to the sinus lateral wall directly to the zygoma bases. This approach provides a more lateral position of the implant head, compensating for the lateral alveolar resorption that usually occurs in severely atrophic maxilla

In majority of cases, the decision of a slot or extramaxillary technique is related to the anatomy of maxilla and zygoma, because severe atrophy results in the palatal dislocation intensifying the zygomatic buttress curvature. An extramaxillary approach is preferred in such cases to obtain a better implant head position. On the other hand, in the cases with smooth maxillary zygomatic curvature, the implant path may require a slot for membrane protection, drilling visualization and irrigation.

4.5 Minimally Invasive Approach

Several authors refer to the use of guided surgery as minimally invasive surgery. However, the incision, reflection, and drilling are exactly the same as the conventional approach, the only one difference being the use of a guide cast in order to orient the drill direction. The concept of minimally invasive procedure relies on the significant reduction in the surgical manipulation of the tissues, improving the efficiency of the surgical technique. Arthroscopy is a good example of minimal invasive procedure for the manipulation of soft tissues around a joint, improving the efficiency of the procedure and reducing morbidity. Because the extramaxillary technique does not prioritize the need for palatal anchorage, the visualization of the alveolar crest is not essential for ZI insertion and its success. Hence the incision can be shortened and displaced to the vestibular mucosa without compromising the final result.

In the minimally invasive approach, a small incision (2–4 cm) is made on the jugal mucosa close to the buccal fornix, the maxillary fossa, and zygomatic buttress, and a tunnel is prepared from the alveolar crest to the inferior half of the zygoma body. After the flap reflection, a spherical or a Lindemann bur is used transmucosally, from the planned implant head position, towards the base of the zygoma through the alveolar bone. If necessary, a slot is opened; however, if the drill path passes outside of the sinus, no antrostomy is necessary, resulting in an extramaxillary implant (Fig. 7).

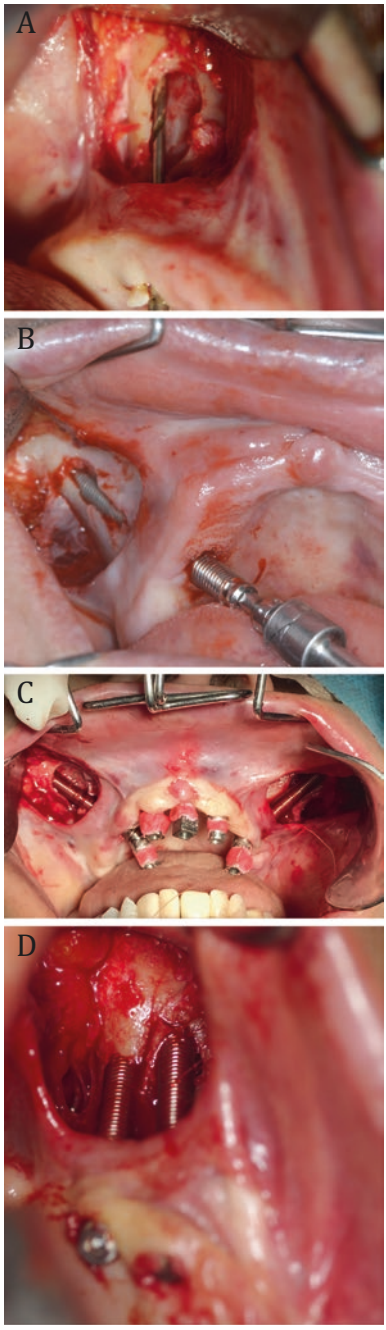

Fig. 7 Minimally invasive approach provided through a tunneling technique, a surgical field very similar to the open classical approach, allowing for the slot osteotomy and membrane detachment (**a**). An access to the zygoma base for the installation of ZI (**b**). The minimally invasive approach can reproduce the advantages of the flapless technique, providing a better soft tissue response and protecting keratinized gum around abutments (**c**). If necessary, the incision can be easily extended for the installation of a second ZI (**d**)

After the determination of the implant entry point on the zygoma base, the implant site is prepared by a widening drill sequence and the implant is inserted through the trans mucosal approach into the drilled path. Despite the excellent visualization provided by the classic approach, it requires an excessive denudation of maxillary bone, with reflection of the vestibular sinusal and palatal mucosa which may compromise the bone vascularization, leading to bone resorption, infection, increasing surgery time, and swelling.

All of the other approaches provide proper visualization of the surgical field. However, the minimally invasive approach allows minimal reflection preserving soft tissues and vascularization. Despite the advantages of soft tissue preservation, namely reduction of pain and swelling, the major advantage of the minimally invasive approach is the preservation of the keratinized gingiva essential for the long-term survival of conventional implants due to the protection of attached gingiva and reduction of peri-implantitis. This factor contributes to the success of ZIs by reducing bleeding and discomfort, and possibly reducing sinus infection, frequent complaints related to ZIs.

Although there are advantages of the minimally invasive approach, it requires a large learning curve for the technique, and demands a profound knowledge of anatomy. Hence it is recommended only for experienced surgeons [36].

4.6 Implant Head Position

Brånemark originally proposed that ZIs should be placed from a palatal alveolar bone position into the zygomatic bone via the maxillary sinus. The palatal approach was supposed to increase implant stability since the implants would be anchored on four bone cortices. Although bone anchorage is crucial for implant survival, other factors must also be considered. The palatinization of ZIs produces a huge volume of the prosthesis, making maintenance of oral hygiene harder, an important factor for the increase of peri-implantitis around ZIs [20, 30, 34]. This results in tongue obstruction, interfering with deglutition and speech. The palatal volume is also an obstruction for the tongue interfering with the speech of some patients. This can be critical in patients with cleft and cancer deformities who already have speech problems.

Stella et al. [24] compared the prostheses in ZIs with the head positioned on the alveolar ridge and on palatal bone, and concluded that the results were superior in the implants positioned on the alveolar ridge. Based on their results, the authors proposed a modification of the original technique, consisting of the insertion of the implants based on the best prosthetic position resulting in an extramaxillary path for the zygomatic insertion of the implant instead of depending on the palatal bone anchor.

The extra sinus technique shows the advantages of improvement in the implant path visualizations and reduction in the frequency of sinus invasion by antrostomy, with a significant reduction in the sinus infection [30, 36, 37].

4.7 Drill Sequence

There are several sets for ZI technique; however, all ZI sets basically follow the instrumentation for the conventional 4.1 mm implants. Obviously, the length of the drills and measurement gauges are adjusted to the alveolar crest/zygoma distances, being longer than conventional implant drills. The first drilling is performed with a perforation drill which is spherical in shape. The perforation drill (a Lindemann or similar can also be used) is used to cross alveolar bone and mark the entry point for the sequential drilling on zygoma.

If the antrostomy drill is available, the blind top is inserted in the zygomatic perforations and a slot is opened with the lateral cutting surface on the maxillary lateral wall. If the set does not provide a specific drill, a spherical or egg drill can be used in order to create the antrostomy and reflect the sinus membrane. After the protection of the sinus membrane (in the intra sinus approach), the drill sequences (drills of 2.3, 2.8 mm, pilot and 3.5 mm) are used in order to widen the implant path perforation.

A crucial challenge of the ZI drilling is irrigation because automatic irrigation is not enough. The cisterns are designed to irrigate the top of the conventional drills but are unable to reach the longer zygomatic drills. In order to achieve proper irrigation, two systems are needed: the conventional mechanical irrigation provided by the drilling system for the crestal area and a manual (with a 20 ml syringe and saline solution) irrigation for the top of the drill.

ZIs can be easily installed with the use of the driller. Due to the high torque provided by the dense zygomatic bone, we recommend the hand approach, at least for the final screwing of the implant. The length of the implants range from 30 to 55 mm (may vary according to the manufacturer). The most common implant lengths are 35 to 45 mm for posterior position and 45 to 47.5 mm in the case of all-on-4 for anterior position [32].

The size selection will vary according to several factors, like ethnic characteristics, patient's size, severity of the atrophy, implant emergence position, and technique adopted (intra or extra sinusal path).

4.8 Postoperative Care

ZIs should preferably receive immediate loading. Patients operated in primary care settings may have to wait for dehospitalization for casting; however, they can be immediately rehabilitated with the provisional fixed acrylic prosthesis. However, metal frameworks (titanium or zirconia) with acrylic teeth may need an extra day for their fabrication in the laboratory but provide a much superior load distribution, reducing bending and twisting forces. After 3–6 months ceramic teeth can be delivered [32].

Immediate loading does not mean immediate stomatognathic functional rehabilitation. Consumption of hard food, speech, muscle and articular proprioception will time for adjust and adapt to the new oral situation. Several factors like atrophy, presurgical prosthesis quality, previous temporomandibular joint or muscle problems, and surgical techniques exclude important factors and use will influence on time needed for the prosthetic reestablishment, physiotherapy, and speech therapy in some patients.

Teeth extraction or alveolar ridge incisions are followed by soft tissue changes in the osseointegration period, causing air escape or food retention, and will require adjustments of the prosthesis. On the other hand, the minimally invasive approach will reduce the soft tissue accommodation, as the incision and reflection is not in the prosthetic area, reducing the postoperative revisions.

ZIs can be placed by a variety of approaches, all with similar success rates ranging from 95% to 100%. A systematic review of 68 studies found a 12 year implant-level cumulative survival rate of 95.21%, which is close to that of conventional implants [4, 7, 17, 21].

5 Complex Cases

ZIs are a valid alternative rehabilitation of edentulous patients with an atrophic maxilla, showing good and predictable results. These results and the experience with maxillectomized patients encourage us in the use of ZIs for complex cases with similar problems or partial edentulism.

5.1 Orosinusal Communications and Zygomatic Implants

Orosinusal communications are surgical sequelae that can occur as a result of ablative procedures or iatrogenic complications. Posterior teeth extraction is the most common cause of orosinusal fistulas. However sinus lift procedures and sinus implant intrusions are recently emerging as orosinusal fistula causes.

Orosinusal fistulas may cause inflammation and infections of the craniomaxillary sinus via oral contamination with the formation of granulation tissue and polyps of the sinus membranes. Fistulas smaller than 5 mm may close spontaneously, but fistulas larger than 5 mm require surgical procedures in order to close the orosinusal communication. These are complex cases for rehabilitation as the bone defect caused by the fistula, and loss of the Schneiderian membrane makes bone graft a very unpredictable procedure. Since the use of ZI is well documented for the rehabilitation of maxillectomized patients [22, 38], with predictable long-term results, it is a valid alternative for the rehabilitation of complex partial maxillary edentulism, sometimes with sequelae to those of ablative surgery, but without the comorbidities of the patients with cancer (Fig. 8).

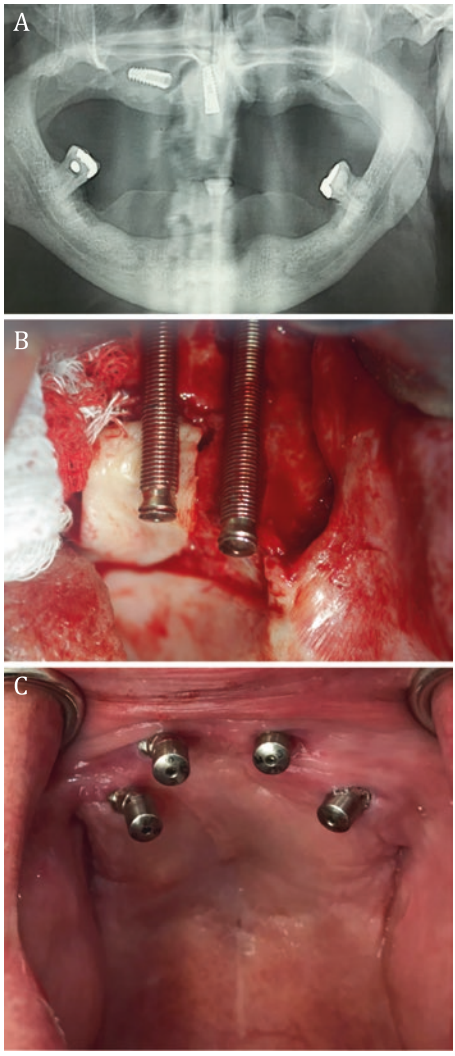

Fig. 8 Orosinusal fistula due to sinus intrusion of implant. The surgeon opened a ridge window while attempting to remove the implant causing an orosinusal fistula (**a**). The implant was removed by a Caldwell Lluc approach and a double flap was performed for the fistula closure with installation of two ZIs (**b**). After 3 months the patient received mandibular implants and a fixed bi-maxillary arch prosthesis (**c**)

The surgical approach for the ZI must be individualized. In cases where there is no alveolar bone, the presence of fibrous tissues due to previous procedures and the need for flap closures with proper vascularization hinder the zygomatic approach and visualization. The minimally invasive approach with a short incision and dissection through the soft tissue into the base of zygomatic bone is the best option for reducing the risk of creating a new fistula. Reinforcement of the flap with Bichat fat pad and the protection of the soft tissue with platelets rich plasma are recommended in such cases.

5.2 Orthognathic Surgery and Zygoma Implants

Although excellent results are reported for ZIsin hypoplastic maxillae, this approach is not able to correct the maxillary skeletal discrepancy and the relationship of the upper and lower arches remains unfavorable to bite force distributions. The rehabilitation of these patients requires prosthetic compensation, generating an anterior cantilever that can lead to failure of the implant or framework [39].

The Le Fort I osteotomy procedure is routinely used to correct maxillomandibular discrepancies. Chiapasco [3] described the use of Le Fort I osteotomies and bone graft to correct maxillary hypoplasia in edentulous patients encouraging several surgeons to perform Le fort I osteotomies with bone grafts for the advancement of the atrophic maxilla.

In order to improve the prognosis and reduce morbidity in the rehabilitation of the severe atrophied maxilla, we adopted the strategy of Le Fort I maxillary reposition with simultaneous ZIs. We planned immediate loading of the ZIs [17] with a rehabilitation period of 3–4 days.

The operation was performed under general anesthesia with nasal endotracheal intubation and local infiltration with xylocaine with epinephrine. The incision was made from the right to the left second bicuspid, and a mucoperiosteal flap was elevated to expose the maxilla and malar prominence. A Le Fort I osteotomy was performed using the piezo surgery device, and the nasal septum and pterygopalatine plate were osteotomized with the septum and curve chisel, respectively. After the osteotomies, the down fracture was gently performed and the maxilla was fixed on the multifunctional guide by screws, and repositioned according to the surgical planning. The anterior plates (Lindorf plates) were fixed on the piriform buttress. With the anterior maxilla properly fixed by miniplates, the intermaxillary fixation was released and the ZIs were installed on the right and left sides. The intermaxillary fixations were done again and the posterior plates, when necessary, were positioned on the zygomatic buttress. The surgical guide is used for reference in the maxillary advancement as well as the guide for the positioning of the implant casting.

The anterior implants (conventional or zygomatic) were installed, and minipillars (abutments) were screwed on the implants for casting. The intermaxillary fixation was released and the surgical wounds sutured by polyglactin 4-0. On the day after the surgery, (add impressions were taken and) the implants were cast at the dental office for prosthodontic finalization. After 24–36 hours the prosthesis was installed (Fig. 9).

6 Conclusion

ZIs require a long learning curve; however, their results, predictability and versatility for ordinary as well as complex maxillary atrophy cases, makes an important tool in the techniques available to the surgeon.

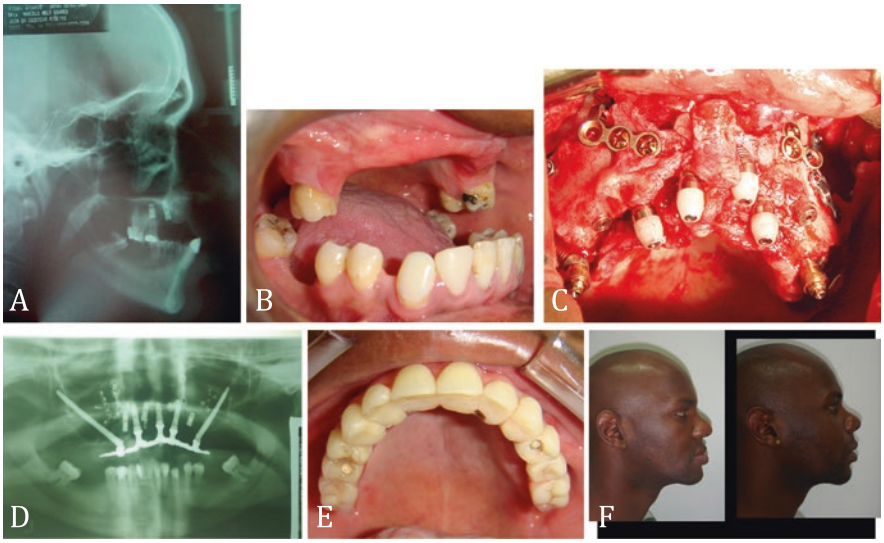

Fig. 9 Male patient presenting with a severe maxillary hypoplasia, with previous maxillary autogenous graft and implant failure (**a**, **b**). In order to reduce the anterior cantilever, and improve esthetic and function, the patient was submitted to Le Fort I advancement osteotomy and ZI installation with immediate loading (**c**, **d**). The prosthesis was installed 3 days after the surgery with ZI repositioned on the repositioned alveolar crest with no anterior cantilever and significant reduction of the prosthetic framework. Figure 8f shows the improvement of the profile and the excellent arch relation, with correction of the naso-labial angle, improvement of nasal alar support, and superior airway space

References

1. Brånemark PI, Grondahl K, Ohrnell LO, Nilsson P, Petruson B, Svensson B, Engstrand P, Nannmark U. Zygoma fixture in the management of advanced atrophy of the maxilla: technique and long-term results. Scand J Plast Reconstr Surg Hand Surg. 2004;38:70–85.
2. Schwartz-Arad D, Herzberg R, Dolev E. The prevalence of surgical complications of the sinus graft procedure and their impact on implant survival. J Periodontol. 2004;75:511–6.
3. Chiapasco M, Brusati R, Ronchi P. Le Fort I osteotomy with interpositional bone grafts and delayed oral implants for the rehabilitation of extremely atrophied maxillae: a 1–9-year clinical follow-up study on humans. Clin Oral Implants Res. 2007;18:74–85.
4. Esposito M, Worthington HV. Interventions for replacing missing teeth: dental implants in zygomatic bone for the rehabilitation of the severely deficient edentulous maxilla. Cochrane Database Syst Rev 2013;(9):CD004151.
5. Higuchi KW. The zygomaticus fixture: an alternative approach for implant anchorage in the posterior maxilla. Ann R Aust Coll Dent Surg. 2000;15:28–33.
6. Parel SM, Brånemark PI, Ohrnell LO, Svensson B. Remote implant anchorage for the rehabilitation of maxillary defects. J Prosthet Dent. 2001;86:377–81.
7. Agliardi EL, Romeo D, Wenger A, Gastaldi G, Gherlone E. Immediate rehabilitation of the posterior maxilla with extensive sinus pneumatization with one axial and one trans-sinus tilted implant: a 3-year clinical report and a classification. J Prosthet Dent. 2015;113:163–8.
8. Cawood JI, Howell RA. A classification of the edentulous jaws. Int J Oral Maxillofac Surg. 1988;17:232–6.

9. Sjostrom M, Sennerby L, Nilson H, Lundgren S. Reconstruction of the atrophic edentulous maxilla with free illiac crest grafts and implants: a 3-year report of a prospective clinical study. Clin Implant Dent Relat Res. 2007;9:46–59.
10. Brånemark P. Surgery and fixture installation: zygomaticus fixture clinical procedures. 1st ed. Goteborg: Nobel Biocare AB; 1998.
11. Miyamoto S, Ujigawa K, Kizu Y, Tonogi M, Yamane GY. Biomechanical three-dimensional finite-element analysis of maxillary prostheses with implants. Design of number and position of implants for maxillary prostheses after hemimaxillectomy. Int J Oral Maxillofac Surg. 2010;39(11):1120–6.
12. Malevez C, Daelemans P, Adriaenssens P, Durdu F. Use of zygomatic implants to deal with posterior resorbed maxillae. Periodontology 2000. 2003;33:82–9.
13. Aparicio C, Manresa C, Francisco K, Claros P, Alández J, González-Martín O, Albrektsson T. Zygomatic implants: indications, techniques and outcomes, and the zygomatic success code. Periodontology 2000. 2014;66:41–58.
14. Bedrossian E. Rehabilitation of the edentulous maxilla with the zygoma concept: a 7-year prospective study. Int J Oral Maxillofac Implants. 2010;25:1213–21.
15. Davo R, Malevez C, Rojas J. Immediate function in the atrophic maxilla using zygoma implants: a preliminary study. J Prosthet Dent. 2007;97(6 Suppl):544–51.
16. Hirsch JM, Öhrnell LO, Henry PJ, Andreasson L, Brånemark PI, Chiapasco M, Gynther G, Finne K, Higuchi KW, Isaksson S, Kahnberg KE, Malevez C, Neukam C, Neukam FW, Sevetz E, Urgell JP, Widmark G, Bolind P. A clinical evaluation of the Zygoma fixture: one year of follow-up at 16 clinics. J Oral Maxillofac Surg. 2004;62:22–9.
17. Soares MM, Ciantelli R. Minimally invasive surgical approach for zygomatic implant placement. Implant News. 2011;8:55–60.
18. Nystrom E, Nilson H, Gunne J, Lundgren S. of the atrophic maxilla with interpositional bone grafting/Lefort I osteotomy and endosteal implants: a 11–16 year follow-up. Int J Oral Maxillofac Surg. 2009;38:1–6.
19. Balshi SF, Wolfinger GJ, Balshi TJ. A retrospective analysis of 110 zygomatic implants in a single-stage immediate loading protocol. Int J Oral Maxillofac Implants. 2009;24:335–41.
20. Davó R, Pons O. 5-year outcome of cross-arch prostheses supported by four immediately loaded zygomatic implants: a prospective case series. Eur J Oral Implantol. 2015;8:169–74.
21. Kuabara MR, Ferreira EJ, Gulinelli JL, et al. Use of 4 immediately loaded zygomatic fixtures for retreatment of atrophic edentulous maxilla after complications of maxillary reconstruction. J Craniofac Surg. 2010;21:803–5.
22. Schmidt BL, Pogrel M, Young CW, et al. Reconstruction of extensive maxillary defects using zygomaticus implants. J Oral Maxillofac Surg. 2004;62:82–9.
23. Peñarrocha M, García B, Martí E, Boronat A. Rehabilitation of severely atrophic maxillae with fixed implant-supported prostheses using zygomatic implants placed using the sinus slot technique: clinical report on a series of 21 patients. Int J Oral Maxillofac Implants. 2007;22:645–50.
24. Stella JP, Warner MR. Sinus slot technique for simplification and improved orientation of zygomaticus dental implants: a technical note. Int J Oral Maxillofac Implants. 2000;15:889–93.
25. Ujigawa K, Kato Y, Kizu Y, Tonogi M, Yamane GY. Three-dimensional finite elemental analysis of zygomatic implants in craniofacial structures. Int J Oral Maxillofac Surg. 2007;36(7):620–5.
26. Kato Y, Kizu Y, Tonogi M, Ide Y, Yamane G. Observation of the internal structures of the zygomatic bone by micro-computed tomography. J Oral Biosci. 2004;46:523–9.
27. Rigolizzo M, Camilli J, Francischone C, Padovani C, Brånemark P. Zygomatic bone: anatomic bases for osseointegrated implant anchorage. Int J Oral Maxillofac Implants. 2005;20:441–7.
28. Rossi M, Duarte LR, Mendonca R, Fernandes A. Anatomical bases for the insertion of zygomatic implants. Clin Implant Dent Relat Res. 2008;10:271–5.
29. Aparicio C, Ouazzani W, Aparicio A, Fortes V, Muela R, Pascual A, Codesal M, Barluenga N, Manresa C, Franch M. Extrasinus zygomatic implants: three year experience from a new

surgical approach for patients with pronounced buccal concavities in the edentulous maxilla. Clin Implant Dent Relat Res. 2010;12:55–61.
30. Malo P, Nobre Mde A, Lopes I. A new approach to rehabilitate the severely atrophic maxilla using extramaxillary anchored implants in immediate function: a pilot study. J Prosthet Dent. 2008;100:354–66.
31. Gross MD, Arbel G, Hershkovitz I. Three-dimensional finite element analysis of the facial skeleton on simulated occlusal loading. J Oral Rehabil. 2001;28:684–94.
32. Nkenke E, Hahn M, Lell M. Anatomic site evaluation of the zygomatic bone for dental implant placement. Clin Oral Implants Res. 2003;14:72–9.
33. Weischer T, Schettler D, Mohr C. Titanium implants in the zygoma as retaining elements after hemimaxillectomy. Int J Oral Maxillofac Implants. 1997;12:211–4.
34. Freedman M, Ring M, Stassen LF. Effect of alveolar bone support on zygomatic implants in an extra-sinus position: a finite element analysis study. Int J Oral Maxillofac Surg. 2015;44:785–90.
35. Wang M, Qu X, Cao M, et al. Biomechanical three-dimensional finite element analysis of protheses retained with or without zygoma implants in maxillectomy patients. J Biomech. 2013;46:1155–61.
36. Stiévenart M, Malevez C. Rehabilitation of totally atrophied maxilla by means of four zygomatic implants and fixed prosthesis: a 6–40-month follow-up. Int J Oral Maxillofac Surg. 2010;39:358–63.
37. Malo P, Nobre M, Lopes A, Francischone C, Rigolizzo M. Three-year outcome of a retrospective cohort study on the rehabilitation of completely edentulous atrophic maxillae with immediately loaded extra-maxillary zygomatic implants. Eur J Oral Implantol. 2012;5:37–46.
38. Esposito M, Balercia A, Barausse C, Pistilli R, Ippolito DR, Felice P. Conventional drills versus piezoelectric surgery preparation for placement of four immediately loaded zygomatic oncology implants in edentulous maxillae: results from 1-year split-mouth randomised controlled trial. Eur J Oral Implantol. 2017;10:147–58.
39. Torrecillas-Martínez L, Monje A, Lin GH, Suarez F, Ortega-Oller I, Galindo-Moreno P, Wang HL. Effect of cantilevers for implant-supported prostheses on marginal bone loss and prosthetic complications: systematic review and meta-analysis. Int J Oral Maxillofac Implants. 2014;29(6):1315–21.

Index

R. S. Chaughule, R. Dashaputra (eds.), *Advances in Dental Implantology using Nanomaterials and Allied Technology Applications*,
https://doi.org/10.1007/978-3-030-52207-0